

IL NUOVO CIMENTO

ORGANO DELLA SOCIETÀ ITALIANA DI FISICA

SOTTO GLI AUSPICI DEL CONSIGLIO NAZIONALE DELLE RICERCHE

VOL. V, N. 1

Serie decima

1° Gennaio 1957

Fermi Coupling and Mass and Charge Spectra of Bosons (*).

B. JOUVET (+)

CERN - Copenhagen

(ricevuto l'8 Settembre 1956)

Summary. — One demonstrates an equivalence theorem between the theory resulting from a scalar Fermi self coupling, and a Yukawa theory postulating a boson coupled with a fermion pair; mass and coupling of this meson have to satisfy equations which are conditions on the meson renormalization constants. It is then shown that the Fermi theory is renormalizable, in the whole. Analysis of the infinities in perturbation theory is given, in view of their subtraction. Effective methods for the treatment of Fermi theory are given; their practical use is exemplified. One discusses finally the magnitude of the boson renormalization constant.

It has been shown in previous works ^(1,2) that a quantum-theoretical treatment of a theory starting with Fermi-type couplings between various elementary spinor fields leads to an equivalent Yukawa-type theory, the bosons being there coupled to the Fermion pairs.

(*) This paper was presented at the International Congress on Fundamental Constants, Turin, September 1956. For this reason many points which are not essential for the understanding of the theory were only briefly mentioned. The author has the intention to develop more fully some of these points later on. Also this paper treats two connected subjects which might have been presented separately, namely the Fermi coupling treatment and the magnitude of the renormalization constants.

(+) CERN, Theoretical Study Division at the Institute for Theoretical Physics, University of Copenhagen. In absence from Institut Henri Poincaré, Paris.

⁽¹⁾ B. JOUVET: *Compt. Rend. Ac. Sci.*, **237**, 1642 (1953); *Journ. de Math.*, **33**, 201 (1954) or *Thèse de doctorat*, Paris (1954).

⁽²⁾ B. JOUVET: *Suppl. Nuovo Cimento*, **2**, 941 (1955); *Reports Pisa Conf., Suppl. Nuovo Cimento* (in print) (1956).

However, neither the masses nor the coupling constants of the bosons thus obtained were determined, as they depended on the cut-off used to eliminate the divergences which arose. Further, one was led to the apparent paradox that the Fermi theory, which is known to be non-renormalizable ⁽³⁾, was identical to a Yukawa one, which is renormalizable.

Here, we shall first determine under what conditions these two types of theory can be made equivalent. This leads us to show that

1) the masses and the mesic charges of the bosons are effectively determined by the Fermi theory, and

2) that the Fermi theory is renormalizable, though of course not in a perturbation expansion.

1. - Equivalence Theorem.

Let us consider the simplest example of a scalar Fermi self-coupling ⁽⁴⁾. Let L_F be the Fermi lagrangian, in terms of unrenormalized quantities:

$$(1) \quad L_F = L_{\text{fermion}}(\psi_0, m_0) + (g_0/2)(\bar{\psi}_0\psi_0)(\bar{\psi}_0\psi_0)$$

and let S_F be the corresponding S -matrix.

Let, on the other hand,

$$(2) \quad L_Y = L_{\text{fermion}}(\psi_0, m_0) + L_{\text{boson}}(A_0, \mu_0) + G_0 A_0 \bar{\psi}_0 \psi_0$$

a Yukawa Lagrangian, also in unrenormalized form; we assume m_0 and ψ_0 to be the same as in the Fermi theory, and we leave arbitrary the constants G_0 and μ_0 . We assume that the Matthews term is nul:

$$(3) \quad \lambda_0 G_0^4 A_0^4 = 0, \quad \text{i.e.} \quad \lambda_0 = 0.$$

Let $(S_Y)_{0m}$ be the S -matrix elements of the Yukawa theory for no real mesons.

By comparing these elements of $(S_Y)_{0m}$ proportional to G_0^{2N} with those of S_F of order g_0^N , we see that we would have

$$(4) \quad S_F = (S_Y)_{0m}$$

if

$$(5) \quad g_0 = \frac{G_0^2}{p^2 + \mu_0^2}.$$

⁽³⁾ A. SALAM: *Phys. Rev.*, **84**, 427 (1951).

⁽⁴⁾ B. JOUVET: *Nuovo Cimento*, **3**, 1133 (1956).

This relation can only hold if

$$(6) \quad G_0^2 = \text{infinite}, \quad \mu_0^2 = \text{infinite}, \quad G_0^2/\mu_0^2 = g_0.$$

Thus the contact Fermi interaction is equivalent to that resulting from the exchange of mesons with infinite mass and coupling. It must be remembered, however, that these parameters are the unrenormalized, and hence unobservable, ones.

The proof that (6) implies equality (4) requires some caution since g_0 enters in divergent expressions. Let us make a cut-off $\Lambda^2 > |p^2|$ on the fermion momenta, modifying the free propagator

$$(7) \quad S_c(p, m_0) = (i\gamma + m_0)^{-1} \quad \text{to} \quad S_A(p, m_0) = S_c(p, m_0)F(|p^2|/\Lambda^2), \quad F(0) = 1,$$

F is a sufficiently rapid cut-off function, say $\exp[-|p^2|/\Lambda^2]$. We can see that if

$$(8) \quad G_0^2(\Lambda) = \infty, \quad \mu_0^2(\Lambda) = \infty \quad \text{and} \quad G_0^2(\Lambda)/\mu_0^2(\Lambda) = g_0,$$

then

$$(9) \quad (S_V(\Lambda))_{0m} = S_F(\Lambda).$$

Let us consider this equality in terms of renormalized quantities. The renormalized mass μ and the mesic charge G are connected, respectively, with the pole and the residue which appear in the S -matrix element for two Fermions scattering in Yukawa theory. By (9) S_F has the same residue and pole, hence μ and G are functions of m_0 , g_0 and Λ . On the other hand, the renormalized constants are related to the unrenormalized ones in Yukawa theory by

$$(10) \quad G_0^2 = G^2 \cdot Z_1^2/Z_2^2 \cdot Z_3; \quad \mu_0^2 = \mu^2 + (\delta\mu^2/Z_3); \quad m_0 = m + (\delta m/Z_2); \quad \lambda_0 = \lambda Z_4.$$

(The prescription of Kroll-Ruderman has been followed for the charge renormalization).

The renormalization constants, Z_i , $\delta\mu^2$ and δm , can be expressed in terms of the renormalized quantities and the cut-off alone (G^2 , μ^2 , m , Λ). The conditions (8) are thus fulfilled if the renormalized constants μ^2 and G^2 (which are finally functions of Λ , m , and g_0), satisfy the equations

$$(11) \quad Z_3(\Lambda, G^2(\Lambda), \mu^2(\Lambda), m) = 0,$$

$$(12) \quad \delta\mu^2(\Lambda, G^2(\Lambda), \mu^2(\Lambda), m) = G^2(\Lambda)(Z_1/Z_2)^2/g_0.$$

The observable constants are the limits, if any, of the renormalized func-

tions $\mu^2(A)$ and $G^2(A)$ as $A \rightarrow \infty$. It may be recalled that the equation $Z_3 = 0$ means, in perturbation theory, that the series of counter-terms for the Lagrangian of the renormalized boson field, $L_{\text{Boson}}(A, \mu^2)$, which consists of finite terms when there is a cut-off, compensates the Lagrangian away. Then, while it may be useful to employ the infinite unrenormalized constant G_0 , it has no physical sense.

The condition $\lambda_0 = 0$, which we have imposed and which is required for the proof of (9) (because otherwise terms of the type M , containing four-vertices closed loops, would be different in the two theories), can be interpreted in the following manner. We denote by $G^4\lambda$ the value, as determinable experimentally, of the S -matrix scattering matrix element for two zero momentum and mass mesons, and let $\lambda G^4 A^4$ be the Matthews term in the renormalized Yukawa lagrangian. In calculating corrections to the meson-meson scattering, we must add to this lagrangian counter-terms of the form $(\delta(\lambda G^4) A^4)$ in each order in G^2 and λ . These terms are determined as functions of G^2 , m , μ^2 and λ , and of the cut-off of fermion and boson fields by the renormalization prescription that, after the subtraction, each subgraph and each divergent graph M vanish when the four-momenta at the vertices are null. Then the total scattering matrix element is λG^4 , under the same conditions. The sum of all the terms in A^4 in the total lagrangian can be written as $\lambda G^4 Z_4 (Z_1/Z_2)^4 A^4$, which can be expressed as a function of unrenormalized quantities such as $\lambda_0 G_0^4 A_0^4$. The condition $\lambda_0 = 0$ then means that $\lambda Z_4 = 0$, that is that the constant λ is determined by the equation

$$(13) \quad Z_4(\lambda, m, \mu^2, G^2) = 0.$$

This implies that the sum of counter-terms $\sum (\delta(\lambda G^4)) A^4$ equals $(-\lambda G^4) A^4$. One can also show that this is equivalent to the omission in L_Y of the terms $\lambda G^4 A^4$ together with keeping in S_Y all the M -parts, divergent or not, whose series must sum to a finite value λG^4 .

If one assumes S_F to be unitary, the equality (4) implies that

$$(14) \quad S_Y | \text{meson} \rangle = 0.$$

This occurs if the meson is unstable, having a mass $\mu > 2m$ ⁽²⁾. Certain modifications of the Yukawa theory formalism are then required ⁽⁵⁾. The constants Z_3 and $\delta\mu^2$ must be defined, in perturbation theory, as the real

⁽⁵⁾ I am very indebted to Dr. V. GLASER for many interesting discussions on the unstable particles problem that he treated in detail in the case of Lee Model (Colloquium, October 31st, 1955, Copenhagen).

part of the quantities ordinarily calculated ⁽⁶⁾; the Bose field can then be expressed in terms of the fermion ones. There being no incoming or outgoing boson free waves at infinities, the matrix $S_Y = (S_Y)_{0m}$ can be obtained directly from a lagrangian no longer containing L_{boson} , and having instead of the coupling $G_0 A_0 J_0$, the « action-at-a-distance » ⁽⁷⁾ coupling

$$(15) \quad (G_0^2/2) J_0(X) \int \bar{D}_{\mu_0^2}(X - X') \cdot J_0(X') d^4 X', \quad J_0 = \bar{\psi}_0 \psi_0,$$

$\bar{D}_{\mu_0^2}(X - X')$ having a Fourier transform $\propto P(1/(p^2 + \mu_0^2))$.

2. - Renormalizability of Fermi Theory.

Let us now examine the problem of the renormalizability of the Fermi theory. The identity (8) or (4) shows that the divergences of S_F can be compensated. One must see, however, whether this compensation can be made by way of scale changes of the observable Fermi quantities only, namely g_F , m , ψ . To see this, we shall show that $(S_Y)_{0m}$ can be expressed as a function of these quantities only, multiplied by renormalization constants containing the divergences. Let us first define the renormalized Fermi constant, g_F , as the value of S_Y for the scattering of two zero energy fermions, under the exchange of a single meson,

$$(16) \quad i g_F = \frac{i G^2 / \mu^2}{1 + (i G^2 / \mu^2) K_R^{\mu^2}(p^2 = 0)},$$

$K_R^{\mu^2}(p^2)$ is the renormalized vacuum polarization operator of the boson. It is pure imaginary at $p^2 = 0$, and satisfies the renormalization conditions:

$$(17) \quad \text{Im} (K_R^{\mu^2}(-\mu^2)) = 0; \quad \left[\text{Im} \left(\frac{d}{dp^2} K_R^{\mu^2}(p^2) \right) \right]_{p^2 = -\mu^2} = 0.$$

It can then be seen ⁽⁸⁾ that $(S_Y)_{0m}$ can be expressed as a functional of the operators ψ_0 , $\bar{\psi}_0$, $S_c(m_0) = (i\gamma p + m_0)^{-1}$ and of the operator

$$(18) \quad Y_0 = i G_0^2 A'_{F0} = \frac{i G_0^2 (p^2 + \mu_0^2)}{1 + [i G_0^2 / (p^2 + \mu_0^2)] K_0(p^2)},$$

⁽⁶⁾ These prescriptions were also given independently by H. UMEZAWA, Y. TOMOZAWA, M. KONUMA and S. KAMEFUCHI: *Nuovo Cimento*, **3**, 772 (1956).

⁽⁷⁾ J. A. WHEELER and R. P. FEYNMAN: *Rev. Mod. Phys.*, **21**, 425 (1949).

⁽⁸⁾ One can see that for instance in perturbation theory, by summing all the vacuum polarization effects on every internal boson lines.

(Δ'_{F_0} is the Dyson function in terms of u.r. constants), in which K_0 is the unrenormalized polarization operator; it is itself expressible as a functional of $S_c(m_0)$ and Y_0

$$(19) \quad K_0(p^2) = K_0(p^2; [S_c(m_0)]; [Y_0]) .$$

Symbolically K_0 is represented by the series of graphs

$$(20) \quad K_0(p^2) = \text{---} \text{---} + \text{---} \text{---} + \text{---} \text{---} + \text{---} \text{---} + \text{---} \text{---} + \dots$$

p is the momentum of the pair; to each straight line corresponds a function $S_c(m_0)$, and to each wavy one Y_0 . One gets this symbolic series of diagrams from the known series defining $K_0(p^2)$ in terms of S_c and Δ_c (represented by fermion, respectively boson lines) by replacing every boson line by a wavy one (substituting Y_0 to $G^2\Delta_c$), and suppressing every graph with vacuum polarization effects on the internal boson lines (the latter being already included in Y_0).

Expressing the unrenormalized quantities in terms of the renormalized ones ⁽⁹⁾, we have

$$(22) \quad Y_0 = \frac{iG^2/(p^2 + \mu^2)}{1 + [iG^2/(p^2 + \mu^2)]K_R^{\mu^2}(p^2)} \cdot \frac{\{Z_1\}^2}{\{Z_2\}} = Y_R \cdot (Z_1/Z_2)^2 .$$

The fermion renormalization constants can be considered as functionals of Y_R , (and so of Y_0) and of m :

$$(23) \quad Z_1, Z_2, \delta m = \text{functionals of } (Y_0, m) .$$

From (16) and (22) follows

$$(24) \quad Y_0 = \frac{ig_F}{1 + ig_F(K_R^{\mu^2}(p^2) - K_R^{\mu^2}(0) + (1/iG^2)p^2)} (Z_1/Z_2)^2 ,$$

while (18) and (22) lead to

$$(25) \quad K_R^{\mu^2}(p^2) - K_R^{\mu^2}(0) + (1/iG^2)p^2 = (Z_1/Z_2)^2(K_0(p) - K_0(0)) + (Z_3/iG^2)p^2 ;$$

thus

$$(26) \quad Y_0 = \frac{ig_F(Z_1/Z_2)^2}{1 + ig_F(Z_1/Z_2)^2(K_0(p^2) - K_0(0)) + p^2 Z_3(g_F/G^2)} .$$

⁽⁹⁾ Using for instance: $\Delta'_{F_0} \equiv \langle P(A_0(x), A_0(x')) \rangle_0 = Z_3 \langle P(A(x), A(x')) \rangle_0 \equiv Z_3 \Delta'_{FR}$.

As a result we see from (19), (23) and (26) that Y_0 (and so $(S_Y)_{0m}$) is a function only of m and g_F if $Z_3 = 0$.

Under that condition (26) can be written as

$$(27) \quad Y_0 = \frac{ig_0}{1 + ig_0 K_0(p^2)},$$

with

$$(28) \quad \begin{cases} ig_0 = \frac{ig_F(Z_1/Z_2)^2}{1 - ig_F(Z_1/Z_2)^2 K_0(0)} = ig_F \cdot Z \cdot (Z_1/Z_2)^2, \\ Z = 1 + ig_0 K_0(0) = \frac{1}{1 - ig_F(Z_1/Z_2)^2 K_0(0)}. \end{cases}$$

By (19) we can regard (27) as an integral equation which determines Y_0 as a function of g_0 and m_0 . The matrix $(S_Y)_{0m}$ thus expressed in terms of g_0 and m_0 is obviously S_F . Expressing the unrenormalized fermion quantities in terms of the renormalized ones, we arrive at the renormalized Fermi Lagrangian ⁽¹⁰⁾

$$(29) \quad L_F = Z_2 \cdot L_{\text{Fermion}}(\psi, m) + \delta m \cdot \bar{\psi}\psi + (\tfrac{1}{2})g_F Z \cdot (Z_1)^2 (\bar{\psi}\psi)(\bar{\psi}\psi).$$

The renormalized function Y_R , defined by (22), can be expressed as

$$(30) \quad Y_R = iG^2 A'_{FR} = \frac{ig_F}{1 + ig_F K_{RF}(p^2)},$$

where A'_{FR} is the renormalized Dyson function for boson, and the renormalized Fermi polarization operator K_{RF} is defined by

$$(31) \quad \begin{cases} K_{RF}(p^2) = K_{R(\psi, I)}(p^2) - K_{R(\psi, I)}(0); & K_{RF}(0) = 0 \\ K_{R(\psi, I)}(p^2) = (Z_1/Z_2)^2 K_0(p^2). \end{cases}$$

$K_{R(\psi, I)}$ is the polarization operator of the bosons in the Yukawa theory, but renormalized only with respect to the vertices and the Fermion

$$(32) \quad K_{R(\psi, I)}(p^2) \propto \int \text{Tr} \{ S'_{FR}(k) \gamma S'_{FR}(p+k) \Gamma_R(k, p+k) \} d^4k,$$

S'_{FR} denotes the renormalized Dyson function for fermions, and Γ_R the renormalized vertex function; in the scalar case γ is 1.


⁽¹⁰⁾ The constant $Z_1^2 \cdot Z$ was called Z_F in ref. ⁽⁴⁾.

It may also be noted that equation (12) is equivalent to equation (16), which is simpler in form; this can be seen from (18), (22) and (28).

3. - The Infinities in S_F .

We can now compare this general proof of renormalizability of S_F with the perturbation theory.

There are three types of infinities encountered by this method:

3.1 The fictitious infinities. - These are the ones compensated when one includes higher and higher order terms in g_F ; for example, it is sufficient to insert at each vertex of the divergent graph  an arbitrary number of loops (which have been rendered finite) and to sum all these graphs to notice such a compensation ⁽¹⁾. This compensation occurs in general, because the total series of terms has the effect of bringing in at each vertex, not g_F but instead the kernel Y_R which vanishes as $1/p^2$ at infinity, but whose development in powers of g_F would yield stronger and stronger divergences. One can connect the appearance of such infinities in the formal development of S_F in powers of g_F with the fact that g_F has dimension M^{-2} and is thereby not an expansion parameter. What is found to play such a role is the dimensionless « parameter » $ig_F K_{RF}(p^2)$, which depends on p^2 . Thus, whenever there occurs a sum over virtual states, this « parameter » becomes greater than unity, the critical value μ^2 of $-p^2$ being that for which

$$(33) \quad -ig_F K_{RF}(-\mu^2) = 1.$$

For this value, there is a pole corresponding to the boson. Beyond it, the expansion of Y_R in powers of $ig_F K_{RF}$ (or of g_F), is no longer valid.

3.2 The renormalization infinities (*). - As a result of the compensation of the fictitious infinities, the divergences of the vertex-parts (without exchange of pairs between the different Fermions) can be absorbed by the one constant Z_1 , and those carried by the Fermion lines are absorbed by δm and Z_2 .

⁽¹⁾ N. HU: *Phys. Rev.*, **80**, 1109 (1950); S. KAMEFUCHI: *Prog. Theor. Phys.*, **11**, 273 (1954).

It must be noted that the Fermi theories are different from the other non-renormalizable theories with regard to the objection of LEHMANN to the HU method (H. LEHMANN: *Nuovo Cimento*, **11**, 342 (1954)); indeed, contrarily to the other theories, there is no free meson propagator, since there is no given meson.

(*) For graphical illustration and syntetic view of the following discussion the reader is referred to the figure at the end of this paper.

Among the two kinds of infinities of Fermion closed loops which remain after subtraction of Z_1 , Z_2 and δm -parts from the closed loops (true divergences), the quadratically divergent terms, which in Yukawa theory are absorbed by $\delta\mu^2$, are here split off by the renormalization condition $K_{FF}(0) = 0$, and absorbed in Z .

3.3. *The fundamental infinities.* — The logarithmic divergence, however, which comes in, multiplied by p^2 , (as does Z_3 in Yukawa theory) can at first be separated from the finite part by specifying a renormalization condition, such as

$$(34) \quad K'_{FF}(0) = \left[\frac{d}{dp^2} K_{FF}(p^2) \right]_{p^2=0} = C,$$

where C is some given constant which is related to the value of the derivative of the Fermi interaction at $p^2 = 0$. But these infinities cannot be absorbed by any change of scale of the fermion quantities (g_F , m , ψ). One can, however, remove them by suitable « counter-interactions » in L_F . This is equivalent to the choice of a « counter-interaction »

$$(35) \quad Z(p^2, C) = \frac{1}{1 - ig_F [K_{R(\psi, \Gamma)}(0) + p^2 (K'_{R(\psi, \Gamma)}(0) - C)]},$$

instead of the simple constant Z .

It is then an essentially new statement in the Fermi theory that *the sum of all the counter-interactions must vanish*. This means that C must be chosen such that

$$(36) \quad C_0 \equiv C + \delta C \equiv C - K'_{R(\psi, \Gamma)}(0) = 0 \quad \text{whence} \quad Z(p^2, C) \rightarrow Z.$$

Since $K_{R(\psi, \Gamma)}(0)$ is obtained in general as a series of divergent terms depending on m , g_F and C , equation (36) determines the constant C in the same fashion as the equation $Z_3 = 0$ determines $G = G(\mu, m)$ ⁽¹²⁾.

The M -divergences are also fundamental infinities. One can treat them in the same manner as in the Yukawa theory. The term $\lambda(g_F)^4(J)^4$ is added to L_F ; the M -divergent part is separated from the convergent one by the corresponding prescriptions, and is cancelled by counter-terms of the form $\delta(\lambda g_F^4)(J)^4$. The total Matthews term in L_F is then

$$(37) \quad \lambda(g_F)^4 \cdot Z^4 \cdot Z_4(Z_1)^4(J)^4 \quad J = \bar{\psi}\psi$$

⁽¹²⁾ One can deduce from the theorem of Gell-Mann and Low ⁽¹⁴⁾ that, if $Z_3 = 0$, one should have $(p^2 A'_{FF})_{p^2 \rightarrow \infty} = 0$, and then according to (30) $(K_{FF}(p^2)/p^2)_{p^2 \rightarrow \infty} \rightarrow 0$; this condition must be equivalent to the equations (11) and (36).

which can be expressed as $\lambda_0(g_0)^4 \cdot (J_0)^4$. The constant λ is still determined by

$$(38) \quad Z_4(\lambda, g_F, m, C(g_F, m)) = 0$$

if it is supposed that λ_0 is null, as in the lagrangian of formula (1).

4. - Practical Methods.

We conclude from this analysis that a practical method of treating S_F might be:

- 1) to avoid introducing the fictitious infinities;
- 2) to avoid treating the fundamental infinities.

The two methods which are sketched below suppress the first difficulty, but only bypass the second in the following sense. In analogy to the treatment of the M -divergences in Yukawa theory, we introduce two arbitrary constants C and λ . One can then calculate any desired effect to any order as a function of g_F , m , C and λ . But the constants C and λ are, in principle, determined as functions of g_F and m , by the condition that the infinite approximation leads to the true Fermi theory in which $C_0 = 0$ and $\lambda_0 = 0$; this is equivalent to the condition that certain series of divergent terms must have a given value.

The first method starts from L_F , written in the form:

$$(39) \quad L_F = Z_2 L_{\text{fermion}}(\psi, m) + \delta m \bar{\psi} \psi + (g_F/2)(Z_1)^2 \cdot Z \cdot J J + \lambda(g_F)^4 \cdot Z_4 \cdot Z_1^4 \cdot J^4$$

and uses for Z formula (35):

$$(40) \quad \begin{aligned} Z &= \frac{1}{1 - ig_F \{ K_{R(\psi, I)}(0) + p^2 [K'_{R(\psi, I)}(0) - C] \}} \\ &= \left(\frac{1}{1 + ig_F C p^2} \right) \cdot \left[1 + \frac{ig_F}{1 + ig_F C p^2} (K_{R(\psi, I)}^{(0)} + p^2 K_{R(\psi, I)}^{(0)}) + \dots \right] \\ &= X + X \frac{ig_F X \cdot [K_{R(\psi, I)}^{(0)} + p^2 K'_{R(\psi, I)}(0)]}{1 - ig_F X \cdot [K_{R(\psi, I)}^{(0)} + p^2 K'_{R(\psi, I)}(0)]} = X + \delta X, \end{aligned}$$

with $X = X(p^2) = 1/(1 + ig_F C p^2)$.

The Fourier transform of L_F may be written as

$$(41) \quad \begin{aligned} L_F &= L_{\text{fermion}}(\psi, m) + (ig_F/2) J(p) X(p^2) J(-p) + \\ &+ \lambda(ig_F)^4 \iiint J(p_1) J(p_2) J(p_3) J(p) X(p_1^2) X(p_2^2) X(p_3^2) X(p^2) \cdot \\ &\cdot \delta(p_1 + p_2 + p_3 + p) d^4 p_1 \cdot d^4 p_2 \cdot d^4 p_3 + \text{Counter-terms} . \end{aligned}$$

The interaction terms are represented by the graphs

$$(\text{---}\text{---}) + 16\lambda \left(\begin{array}{c} \diagup \quad \diagdown \\ \times \\ \diagdown \quad \diagup \end{array} \right); \quad \text{where } (\text{---}\text{---}) \text{ means the interaction } (ig_F/2)X.$$

The counter-terms are such that all the infinities are subtracted to each order in « X » and λ , in such a way that the calculated observable value of m , g_F , ψ , C , and λ remain unchanged. These counter-terms have the effect to modify in L_F the preceding quantities to their unrenormalized values. But according to (36) and (38) the constants C and λ have to be chosen in such a way that in the infinite approximation the constants C_0 and λ_0 are zero.

Another possible method consists of treating (30), say by variational methods, by cutting off at some order in Y_R the series (20) which yields the kernel $K(Y_R)$. The renormalization conditions which are imposed in the course of the calculation of K_{RP} , (on the vertices, the Fermion self-energies and the M -parts and on K_{RT} and its derivative at $p^2 = 0$) are equivalent to the subtraction of counter-terms in L_F .

Of course the different methods will yield unequal results at a finite stage of approximation.

However, the practical usefulness of these methods lies in the hope that the comparison of the theory with experiment (which gives the μ and the G of the bosons) will permit one to determine a significant law for C and λ , which are known to be functions of m and g_F .

In previous attempts ^(1,2) these constants were introduced by the regularization of closed loops; further instead of suppressing the infinities by counter-terms which modify the constants, one has only «normalized» at each order the kernels K , without caring about the counter-terms this procedure implied in L_F ; apart from these differences the results are alike.

We were then able to show ⁽¹⁾ that electrodynamics follows from a neutral vector Fermi coupling between electron and neutrino pairs; there appear then two fundamental constants of type C (one for each fermion type of closed loop), which are determined by experiment; with the present method these constants are, in principle, given by equations of the type (11) and (12), and in particular α , the fine structure constant, must be the solution of the equation $Z_3(\alpha) = 0$ in the electrodynamics ⁽⁴⁾.

The case of triangular p.s. Fermi coupling

$$\begin{array}{c} \text{(np)} \\ \diagup \quad \diagdown \\ \text{(ev)} \text{ --- } \text{(\mu\nu)} \end{array}$$

involves more constants, as the equivalent Yukawa theory contains three bosons of different masses and couplings, the lightest of which can be iden-

tified with π^\pm . The properties of π^\pm -meson that may desintegrate into leptons and that are coupled to the nucleons, permit the deduction of a qualitative law for $C(m)$, ($C(m) \rightarrow \infty$ if $m \rightarrow 0$), in accordance with the values obtained from the photon. Taking this law into account, the properties of the pions, in particular the existence of isotopic spin, can be deduced from the given couplings ⁽²⁾:

$$(42) \quad g_F[\{(\bar{n}n) - (\bar{p}p)\}\{\text{Neutral lepton pairs}\} + (\bar{n}p)\{(\bar{e}\nu) + (\bar{\mu}\nu)\}].$$

5. - The Equation $Z_3 = 0$.

The main point of our proof of the equivalence theorem rests on the hypothesis that one of the fundamental equations which determine the mesic charge and mass, namely $Z_3(A, G^2(A), \mu^2(A)) = 0$, has a solution for every value of A which tends to infinity. Thus it is essential to study this question in the light of the works done on the renormalization constants. We shall be mainly concerned here with the case of electrodynamics. Various arguments have been put forward, based on the formula of Källén ⁽¹³⁾

$$(43) \quad \left\{ \begin{array}{l} 1/Z_3 = 1 + \int_0^\infty \frac{\Pi(-a)}{a} da, \\ \Pi(p^2) = \lim_{r \rightarrow \infty} \frac{V}{-3p^2} \sum'_{p^{(2)}=p} |\langle 0 | j_\nu | z \rangle|^2 (-1)^{N_z} = \text{Sum of positive terms}, \end{array} \right.$$

in which one tried to show that the constant Z_3 is identically zero, which if true would destroy any hope of finding a solution to our equation. We therefore consider now the value of these arguments.

5.1. *In perturbation theory* ⁽¹⁴⁾. - We take a cut-off A on the fermion momenta and use the calculations ⁽¹⁵⁾ of the first terms of the development of the function $\Pi(p^2)$ in powers of α , the fine structure constant. We get to second order in α

$$(44) \quad I/Z_3 = I + \alpha(a_0 + b_0 L) + \alpha^2(a_1 + b_1 L + c_1 L^2); \quad L = \log(A^2/m^2)$$

(a, b, c , are geometrical constants).

⁽¹³⁾ G. KÄLLÉN: *Helv. Phys. Acta*, **25**, 417 (1952).

⁽¹⁴⁾ M. GELL-MANN and F. LOW: *Phys. Rev.*, **95**, 1300 (1954).

⁽¹⁵⁾ G. KÄLLÉN: *Dan. Mat. Fys. Medd.*, **29**, no. 17 (1955).

If we let Λ tend to infinity, then evidently $1/Z_3$ tends to infinity for all values of α . However we are not justified in only keeping the first few terms of the series, even as a minorant if each term of the series were positive, unless the series is convergent. But it is clear that on these first few terms the series does not behave like a convergent series; we may confirm this by showing that terms in α^n contain factors which diverge as L^n , and which are no other than the formal development of the function $1/Z_3$ in which one takes Z_3 to have the form

$$(45) \quad Z_3 = 1 - (u_0\alpha + u_1\alpha^2) - (v_0\alpha + v_1\alpha^2)L$$

u_i and v_i are geometrical constants

which have been calculated previously by the method of counter terms ⁽¹⁶⁾. This infinite value of Z_3 contradicts the lemmas of Schwinger and Lehmann ⁽¹⁷⁾ according to which $0 < Z_3 < 1$. But we must note that these lemmas suppose that the integral of the series (43) converges, which is not the case in perturbation theory. The study of the graphs in perturbation theory (α being the renormalized constant) shows that Z_3 would appear to be of the form

$$(46) \quad Z_3 = 1 - u(\alpha) - v(\alpha)L$$

and consequently only exceptional values of α , which give zeros of $v(\alpha)$ or singularities of $u(\alpha)$, can annihilate Z_3 .

Since the two constants v_0 and v_1 are positive, it is not possible to obtain, to second order in α , a compensation of the infinities ⁽¹⁸⁾ or an annihilation of Z_3 for non zero values of α . At present nothing is known of the behaviour of the series defining $u(\alpha)$ and $v(\alpha)$, but it is not improbable that they are asymptotic, which is suggested by the model of $\lambda\varphi^3$ coupling ⁽¹⁹⁾.

5'2. *Other method.* — We shall now discuss the argument of KÄLLÉN ⁽²⁰⁾.

In his words KÄLLÉN starts from «the assumption that all the quantities K , $(1 - L)^{-1}$ and $1/N$ (for notation, cfr. ref. ⁽¹³⁾) are finite or that the integ-

⁽¹⁶⁾ H. UMEZAWA and R. KAWABE: *Prog. Theor. Phys.*, **4**, 443 (1949); R. JOST and J. LUTTINGER: *Helv. Phys. Acta*, **23**, 201 (1950).

⁽¹⁷⁾ J. SCHWINGER; cf. W. PAULI: *Feldquantisierung* (Zürich, 1951); H. LEHMANN: *Op. cit.* ⁽¹¹⁾.

⁽¹⁸⁾ W. PAULI; cf. SCHWEBER *et al.*: *Mesons and Fields* (1955), Vol. I, p. 333.

⁽¹⁹⁾ C. A. HURST: *Proc. Camb. Phil. Soc.*, **48**, 625 (1952); W. THIRRING: *Helv. Phys. Acta*, **26**, 33 (1953); A. PETERMANN: *Phys. Rev.*, **89**, 1160 (1953); R. UTIYAMA and T. IMAMURA: *Prog. Theor. Phys.*, **9**, 431 (1953). I am very indebted to Dr. PETERMANN for numerous enlightening discussions on this question.

⁽²⁰⁾ G. KÄLLÉN: *Dan. Mat. Fys. Medd.*, **27**, no. 12 (1953).

rals (1) converge.» In the notation of the preceding sections, K is the mass renormalization constant for fermions, $1 - L = Z_3$ and $N^2 = Z_1 = Z_2$. The integrals to which he refers are the integral (43) and a similar for fermion renormalization constants. KÄLLÉN's assumption implies that such functions as $\Pi(p^2)$ tend to zero as p^2 tends to $-\infty$. The function $\Pi(p^2)$ consists of a sum of positive terms. For this sum he constructs the following minorant by selecting the state $|z\rangle$ consisting of a pair of Fermions.

$$(47a) \quad \Pi(p^2) > \lim_{v \rightarrow \infty} \frac{v}{-3p^2} \sum'_{q+q'=p} |\langle 0 | j_v | q, q' \rangle|^2.$$

He shows that this inequality can be written in the form

$$(47b) \quad \Pi(p^2) > (\alpha/3\pi) N^4 / Z_3^2,$$

when p^2 tends to $-\infty$.

The right hand side of this inequality is finite according to the assumption of KÄLLÉN. However, to quote KÄLLÉN again, «if all the renormalization constants K , $1/N$ and $1/(1-L)$ are finite, the function $\Pi(p^2)$ cannot approach zero for $-p^2 \rightarrow \infty$. This is an obvious contradiction and the only remaining possibility is that at least one (and probably all) of the renormalization constants is infinite.»

Before discussing this argument, let us complete this calculation by inserting (47b) into (43); we obtain

$$(48a) \quad \frac{1}{Z_3} > 1 + \left(\frac{\alpha}{3\pi} \right) \frac{N^4}{Z_3^2} \int_{m^2}^{\infty} \frac{da}{a} = 1 + \left(\frac{\alpha}{3\pi} \right) \frac{N^4}{Z_3^2} \log \left(\frac{\infty}{m^2} \right).$$

We remark that this result does not give a minorant for $1/Z_3$ but rather an inequality which Z_3 has to satisfy. This inequality does not imply that $1/Z_3$ is infinite, but rather that Z_3 must be complex, which is impossible on physical grounds. The origin of the trouble does not lie in the KÄLLÉN assumption as one might suppose, but rather, for electrodynamics, in the inequality (47a). Here what happens is that, since the photon has no mass, the function is defined by an *infinite* sum of terms for every value of $-p^2 > 4m^2$, because it is always possible to create any number of photons when the energy is greater than $2m$. The inequality (47a) is true only if the series for $\Pi(p^2)$ converges. To make the point clear consider the example $1/(1-X) = 1 + X + X^2 + \dots$; if $X > 1$, then each term of the series is positive, but a single term cannot be said to be a minorant, because the series diverges.

Now we can see that *the series (43) defining $\Pi(p^2)$ in electrodynamics is in*

fact divergent. To show this let us look at the formula (47b) from which we see that $\Pi(p^2)$ depends on the infra-red catastrophe through N^2 ⁽²⁰⁾. In perturbation theory the second member of (47a) is in fact infra-red divergent for every value of $-p^2 > 4m^2$ from the second order in α (the fine structure constant). However it is known that in perturbation series for Z_3 the sum of terms belonging to any order in α is not infra-red divergent. It follows that there cannot be any infra-red divergences in any order of the development of $\Pi(p^2)$ in powers of α ; this was seen by direct computation for the second order in α ⁽¹⁵⁾. Therefore there exist in the series (43) defining $\Pi(p^2)$ terms neglected by KÄLLÉN which cancel the infra-red catastrophes in (47a) and (47b). Since every term of the series (43) is positive, it is necessary that the compensating terms form a divergent series whose sum can be negative.

Let us now examine the case of meson theories. In that case, when p^2 is finite, $\Pi(p^2)$ is defined by a sum of a finite number of terms. As $-p^2$ tends to infinity, the number of terms increases indefinitely, while each term tends to its asymptotic value; now it is essential to remark that the asymptotic form of each term is a *function of the renormalization constants* whether this asymptotic form is finite or not. This is a consequence of the fact that some propagators then reach their asymptotic values, which are related to the values of the renormalization constants, according to the Gell-Mann and Low theorem ⁽¹³⁾; an example is the perturbative calculation of (47a). Finally, for large values of $-p^2$ the function $\Pi(p^2)$ is an explicit function of the renormalization constants. One may then separate the asymptotic part $\Pi_2(p^2)$ of $\Pi(p^2)$ from the rest $\Pi_1(p^2)$ which may also depend on the renormalization constants and which is a series of finite functions which tend to zero as p^2 tends to infinity. Inserting this decomposition into (43) one gets instead of (48a) an equation of the form

$$(48b) \quad \frac{1}{Z_3} = 1 + F_1(G, \mu, m, Z_i, \delta\mu^2, \delta m) + F_2(G, \mu, m, Z_i, \delta\mu^2, \delta m, \infty)$$

(the functions F_1 and F_2 respectively are the contributions of Π_1 and Π_2). If $\int (\Pi(-a)/a) da$ diverges at infinity, then the F_2 part is divergent, but the solution of (48b) for $1/Z_3$ may well be finite, because F_2 contains Z_3 , and may have an arbitrary value depending on the value of the other renormalization constants and of the parameters G, m, μ . As an example suppose that F_2 is of the form $\infty \cdot G_2(Z_3, \alpha)$; then the solution of (48b) is $G_2(Z_3, \alpha) = 0$. Also it may happen that for certain values of the parameters the function F_1 is singular even if the integral converges at infinity (F_2 finite).

The preceding argument applies of course also in the case of electrodynamics discussed above. In that case $Z_1 = Z_3$ and $\mu = 0$ and since there is no infra-red catastrophe in Z_3 , F_1 and F_2 do not depend on Z_1 .

From equation (48b) one also understands why the Schwinger and Lehmann lemmas ⁽¹⁷⁾ do not hold, as we have seen in Sect. 5.1 with perturbative method.

5.3. *With a cut-off.* — Let us now make a cut-off on the momenta of the Fermions, for example by introducing a convergence factor $V(p)$ in the interaction term of the Fermi theory


$$(49) \quad g(\bar{\psi}(p)V(p)\psi(q)V(q))(\bar{\psi}(r)V(r)\psi(s)V(s))\delta^4(p+q+r+s).$$

This implies also the modification of the coupling in the equivalent Yukawa theory

$$(50) \quad G \cdot A(p) \cdot (\bar{\psi}(q)V(q)\psi(s)V(s))\delta^4(p+q+r).$$

We note here that an arbitrary alteration of the usual Yukawa theory (which has linear equations and local coupling) may not always be considered to be a result of a modification of the Fermi theory, although the converse is true: for example we could not obtain a Yukawa theory in which the Hamiltonian of the free mesons has an arbitrary form; in such cases the changed Yukawa theories could not be identical with the Fermi theories, modified or not, except in the limit when the alteration tends towards a definite form or to zero.

With the modifications (49) and (50) the theories no longer give divergences. However a cut-off on the momenta of the fermions does not imply a cut-off on the integral (43), and the series (43) still contains an infinite number of finite terms. Indeed the states with an arbitrary number of mesons are not limited in energy, since the cut-off has no effect except on closed loops, as is seen in the graph

$$\langle 0 | \text{  | z = 3 \text{ mesons} \rangle$$

(cross lines indicate the presence of $V(p)$ cut-off function).

On the other hand the states with a given number of pairs of fermions have an energy which is limited but which increases with the number of pairs.

$$\langle 0 | \text{  | z = 2 \text{ pairs} \rangle$$

Consequently it is not impossible, for certain values of α (in the case of electromagnetism), that on one hand the series (43) might be divergent, and on the other hand that the series, when summed, might furnish a solution which could become singular.

Let us finish by a certain remark:

Suppose that there exists a region of α and A^2 for which the series (43) converges, in which case (47) gives a true minorant; then the inequality (48), where A^2 replaces ∞^2 , implies that, since Z_3 must be real, we have

$$(51) \quad \text{Log } (A^2/m^2) < 3\pi/4\alpha N^4.$$

Several authors, using certain approximations from perturbation theory have met similar inequalities and have interpreted them as an indication of an energy limit to the validity of the theory ⁽²²⁾. We are led on the contrary to interpret this relation as determining a region of possible values of α for which the theory gives no trouble ⁽²¹⁾ when there is a cut-off; then α is not the experimental constant.

The conclusion of this discussion is that none of the arguments advanced to prove that the constant Z_3 is identically zero appear irrefutable. In addition we have seen that it is not impossible that there exist values of charge and mass of the meson for which Z_3 is zero, whether the cut-off is finite or not.

The explicit calculation of charge and mass values and their comparison with experiment for the different existing types of Fermi couplings remains an open question. As far as electrodynamics is concerned, if a vectorial Fermi coupling between electron and neutrino pairs ⁽¹⁾ really exists in Nature, the fine structure constant α , should be the solution of $Z_3 = 0$ for an infinite cut-off; then its value should be of a purely geometrical nature, because it is a zero of a function defined by a series of terms with purely geometrical coefficients. Certain aspects of the method of adiabatic switching on must be therefore revised, because it is no longer possible to consider the observable charge (which is a number) or the non renormalized charge (which is infinite) as parameters variable with time.



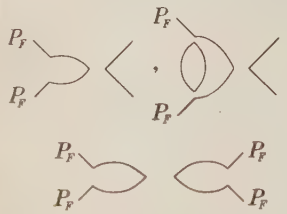



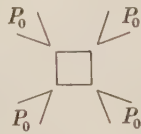
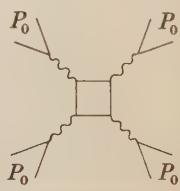
* * *

This work was done under the auspices of CERN, at the Institute for Theoretical Physics, University of Copenhagen. The author wishes to thank Professor MÖLLER for his hospitality; he would also like to acknowledge the helpfulness to this work of many conversations with Drs. S. DESER, V. GLASER, H. LEHMANN, A. PETERMAN and A. VISCONTI. He expresses his thanks to Dr. DESER for his translation of the French manuscript.

⁽²¹⁾ T. D. LEE: *Phys. Rev.*, **95**, 1329 (1954); G. KÄLLÉN and W. PAULI: *Dan. Mat. Fys. Medd.*, **30**, no. 7 (1955); H. UMEZAWA, Y. TOMOZAWA, M. KONUMA and S. KAMEFUCHI: *Nuovo Cimento*, **3**, 772 (1956).

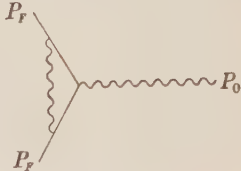
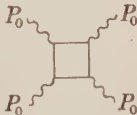
⁽²²⁾ L. D. LANDAU *et al.*: *Dokl. Akad. Nauk SSSR*, **95**, 1177 (1954); S. KAMEFUCHI and H. UMEZAWA: *Nuovo Cimento*, **3**, 1060 (1956).

TABLE I. — We call, as explained in ref. (2), « Realistic theory of meson », the Yukawa theory eq case in which the infinities are of the only type indicated by the graphs (primitive divergences). The momentum has the indicated value; p_0 is nul, p_F is such that $i\gamma p_F + m = 0$ and p_μ such that $p_\mu^2 + \mu^2 = 0$ (or p) for open fermion lines, or with respect to p^2 for closed loops of fermion lines. We indicate only

FERMI COUPLING THEORY				REALIST
	Divergent graphs	Counter terms	Unrenormaliz. quantities	Graphs or equations
Fermion part		$\delta m \bar{\psi} \psi$	$m_0 = m + \frac{\delta m}{Z_2}$	
		$(Z_2 - 1)L(\psi, m)$	$\psi_0 = \psi \sqrt{Z_2}$	
Interaction part		$(Z_1^2 - 1)g_N J^2$	$g_0 = g_F Z \left(\frac{Z_1}{Z_2} \right)^2$	
				equations
		$(Z - 1)g_F J^2$		$\delta \mu^2 = G^2/g_F Z$ or $g_F = G^2 A'_{FE}(0)$
Fundamental part		$(\delta C)p^2 J^2$	equations $C_0 = C + \delta C$ $C_0(C, m, g_F) = 0$	$Z_3(G, \mu, m) = 0$
		$\delta(\lambda g_F^4) J^4$	$\lambda_0 = \lambda + \delta \lambda$ $\lambda_0(\lambda, C, m, g_F) = 0$	$Z_4(\lambda, G, \mu, m) = 0$
				

ent to the Fermi theory, when S_+ is unitary. The counter-terms as given here correspond to the notation p_0, p_F, p_μ , given in the graphs, means that one has to calculate the graph when the external prime in certain graphs means that for these graphs one has to calculate the derivative with respect to the graphs of the realistic theory since it is easy to obtain them from the usual Yukawa theory.

MESON THEORIES

FERMION THEORY		YUKAWA THEORY			
Counter terms		Unrenormaliz. quantities	Counter terms	Divergent graphs	
$\delta m \bar{\psi} \psi$ $(Z_2 - 1)L(\psi, m)$	Fermion part	$m_0 = m + \frac{\delta m}{Z_2}$	$\delta m \bar{\psi} \psi$	$\left(\text{---} \text{---} \text{---} \right)_{P_F}$	Fermion part
		$\psi_0 = \psi \sqrt{Z_2}$	$(Z_2 - 1)L(\psi, m)$	$\left(\text{---} \text{---} \text{---} \right)'_{P_F}$	
$(Z_1^2 - 1) \frac{G^2}{2} J \bar{D} J$	Interaction part	$G_0 = G \frac{Z_1}{Z_2 \sqrt{Z_3}}$	$(Z_1 - 1)GJA$		Interaction part
$\frac{G^2}{2} \sum_{N=1}^{\infty} (\delta \mu^2)^N J \bar{D}^{N-1} J$		$\mu_0^2 = \mu^2 + \frac{\delta \mu^2}{Z_3}$	$\delta \mu^2 A^2$	$\left(\text{---} \text{---} \text{---} , \text{---} \text{---} \text{---} \right)_{P_\mu}$	Boson part
$\frac{G^2}{2} \sum_{N=1}^{\infty} (1 - Z_3)^N J \bar{D} J$		$A_0 = A \sqrt{Z_3}$	$(Z_3 - 1)L(A, \mu^2)$	$\left(\text{---} \text{---} \text{---} \cdot \text{---} \text{---} \text{---} \right)'_{P_\mu}$	
$(Z_4 - 1)\lambda G^8$ $\cdot \bar{D}_1 J_1 \bar{D}_2 J_2 \bar{D}_3 J_3 \bar{D} J_4$		$\lambda_0 = \lambda Z_4$	$(Z_4 - 1)\lambda G^4 A^4$		Interaction part

RIASSUNTO (*)

Si dimostra un teorema d'equivalenza tra la teoria risultante da un autoaccoppiamento di Fermi scalare e una teoria di Yukawa che postula un bosone accoppiato con una coppia di fermioni; massa e accoppiamento di questo mesone debbono soddisfare equazioni che sono condizioni imposte alle costanti di rinormalizzazione. Si dimostra poi che la teoria di Fermi è rinormalizzabile nell'insieme. Si svolge un'analisi delle grandezze infinite che s'incontrano nella teoria delle perturbazioni onde poterle sottrarre. Si indicano metodi efficaci per il trattamento della teoria di Fermi: si danno esempi del loro impiego pratico. Si discute infine la grandezza della costante di rinormalizzazione dei bosoni.

(*) *Traduzione a cura della Redazione.*

On γ -Polarization Effects in Photonuclear Reactions.

A. AGODI

Istituto di Fisica dell'Università, Centro Siciliano di Fisica Nucleare - Catania

(ricevuto 1°8 Settembre 1956)

Summary. — A detailed derivation is given of the most general angular distribution of photonucleons consistent with the conservation principles for angular momentum and parity. Its azimuthal dependence, when photons are linearly polarized, is discussed, with particular emphasis on the physical information obtainable without using any model for the reaction or the nucleus.

1. — The properties of the angular distributions of reaction products, in nuclear reactions of the type

$$A + X \rightarrow B + Y,$$

have been extensively studied by many authors ⁽¹⁾. Some of the general results are also applicable ⁽²⁾ to photonuclear reactions, when the A projectile, impinging on the target nucleus X, is a photon γ . These general results are concerned, particularly, with limitations on the form and complexity of angular distributions in a plane containing the direction of the photon beam.

In recent years some experimental work has been done on azimuthal angular

⁽¹⁾ E. EISNER and R. G. SACHS: *Phys. Rev.*, **72**, 680 (1947); C. N. YANG: *Phys. Rev.*, **74**, 764 (1948); L. WOLFENSTEIN: *Phys. Rev.*, **75**, 1664 (1949); J. M. BLATT and L. C. BIEDENHARN: *Rev. Mod. Phys.*, **24**, 258 (1952); L. C. BIEDENHARN and M. E. ROSE: *Rev. Mod. Phys.*, **25**, 729 (1953).

⁽²⁾ R. J. BLIN-STOYLE: *Proc. Phys. Soc.*, A **64**, 700 (1951); A. SIMON and T. A. WELTON: *Phys. Rev.*, **90**, 1036 (1953); A. SIMON: *Phys. Rev.*, **92**, 1050 (1953); G. R. SATCHLER: *Proc. Phys. Soc.*, A **68**, 1041 (1951).

distributions of photoejected nucleons ⁽³⁾ (e.g. for detecting a supposed linear polarization of the gammas), the most frequently used target nucleus being deuterium.

In the case of D-photodisintegration, the experimental angular distribution of the nucleons can be explained in terms of an electric dipole transition: a well known (perturbative) calculation gives the observed proportionality of the differential cross-section to $\cos^2 \varphi$, φ denoting the azimuthal angle i.e. the angle between the electric vector in the photon beam and the projection of the nucleon momentum on the plane orthogonal to the beam.

Now, it may be of some interest to investigate what can be expected in measuring azimuthal angular distributions of photoejected nucleons from complex nuclei, when photons are linearly polarized, and what kind of information on the polarization of the photon beam as well as on the structure of the target nucleus, can be obtained from observing the azimuthal dependence of the differential cross-section for a (γ, p) or (γ, n) reaction.

In the present paper it will be shown that, on quite general grounds, ^(3 bis) the form and complexity of the azimuthal dependence of the differential cross-section are even more radically limited than commonly expected. To this completely general result some remarks are added, on the possibility of interpreting, in particular cases, the experimental angular distributions without detailed knowledge of the probability amplitudes appearing in the formulas.

2. - The differential cross-section for the general

$$\gamma + X \rightarrow N + Y$$

reaction, induced by linearly polarized photons, in the center of mass reference system, can be written ⁽⁴⁾

$$(1) \quad d\sigma = |\langle NY; \vartheta\varphi | R | \gamma X \rangle|^2 \lambda^2 d\Omega,$$

denoting $2\pi\lambda = k^{-1}$ the wavelength of relative motion in the incidence channel; ϑ, φ the polar and azimuthal angles of the direction defined from the relative motion of the photoejected nucleon N and the residual nucleus Y, in the co-ordinate system whose Oz axis is in the incidence direction of the photon γ on the target nucleus X, and whose Ox axis is in the polarization direction of γ .

⁽³⁾ E.g., K. PHILLIPS: *Phil. Mag.*, **44**, 169 (1953); M. C. TZARA: *Compt. Rend. Ac. Sci.*, **239**, 44 (1954); G. H. WILKINSON: *Phys. Rev.*, **99**, 1347 (1955).

^(3 bis) Only the conservation principles for parity and angular momentum will be used, without making any compound nucleus hypothesis for the reaction.

⁽⁴⁾ J. M. BLATT and L. C. BIEDENHARN: ref. ⁽¹⁾.

We are interested in the angular distribution of the ejected photonucleons, i.e. simply in the function

$$(2) \quad I(\vartheta, \varphi) = |\langle \text{NY}; \vartheta \varphi | R | \gamma \text{X} \rangle|^2.$$

Expanding the photon state in series of electric and magnetic multipole states, and the particle states in series of spin and orbital angular momentum states, gives, if the target nuclei X are unpolarized,

$$(3) \quad I(\vartheta, \varphi) = 8\pi^4 \sum_{m_X m_Y m_N} \sum_{l m L P \pi_Y \pi_X} Y_l^{-m}(\vartheta, \varphi) (i)^{L-l} l m m_X m_Y R(L P \pi_Y \pi_X) (i P)^{\sigma' L \pi_Y} (2L+1)^{\frac{1}{2}} \cdot$$

being π_Y the index giving the parity of the multipole and $P = \pm 1$, $\pi_Y = \pm 1$ the polarization index (a basis of circularly polarized waves is used). $\sigma(L\pi_Y)$ equals zero for magnetic and 1 for electric multipoles. Normalizations and phases are as specified in the appendix.

From (3) and the transformation properties of angular momentum eigenvectors, it can be shown (e.g. following the procedure used by YANG for his first theorem (1)) that, if the superposition principle holds, then R is a rotation invariant operator, this statement being equivalent to the conservation principle for the total angular momentum of an « isolated » system.

As is well known (2) the sums on magnetic quantum numbers in (3) are purely geometric in character, and can be carried out without explicit knowledge of the R matrix elements.

Evaluation of these sums gives (see appendix)

$$(4) \quad I(\vartheta, \varphi) = \sum_{l' L \pi_Y L' \pi_Y'} A_{l'}(L \pi_Y; L' \pi_Y') \{ (i)^{\sigma-\sigma'} [1 + (-)^{L+L'-l'+\sigma'-\sigma}] (l'' | L' 1; L-1) \mathcal{P}_l^0(\cos \vartheta) + (-i)^{\sigma+\sigma'} (\exp[2i\varphi] + (-)^{L+L'-l''-\sigma-\sigma'} \exp[-2i\varphi]) (l'' | L' 1; L1) \mathcal{P}_l^2(\cos \vartheta) \},$$

where $\sigma = \sigma(L\pi_Y)$; $\sigma' = \sigma(L'\pi_Y')$; $\mathcal{P}_l^{m''}(x)$ denotes the normalized Legendre's associated functions of the first kind (5); and the $A_{l'}$ are defined

$$(5) \quad A_{l'}(L \pi_Y; L' \pi_Y') = \sum_{l'' j j' J J'} (4\pi^3) (i)^{L-l'+l''} (l'' | l 0; l' 0) \cdot \\ \cdot \left[(2j+1)(2j'+1)(2L+1)(2L'+1) \frac{(2l+1)(2l'+1)}{2(2l''+1)} \right]^{\frac{1}{2}} \cdot \\ \cdot (2J+1)(2J'+1)(-1)^{1+l-L} (J; l s_N j s_Y \| R(L \pi_Y) \| s_X) (J'; l' s_N j' s_Y \| R(L' \pi_Y') \| s_X)^* \cdot \\ \cdot W(j s_N l'' l'; l j') W(J s_Y l'' j'; j J') W(L s_X l'' J; J' L),$$

the symbols being used as in appendix.

Since $A_{l'}$ is a linear combination of factors $(l'' l' 0; l 0)$, only the terms with $l+l'+l''$ an even integer give a non vanishing contribution to the sum on the r.h.s. of (5). From (4) it follows then that the φ independent term vanishes when either $\sigma \neq \sigma'$ and $L+L'-l''$ is even or $\sigma = \sigma'$ and $L+L'-l''$ is odd; moreover we can have a φ -dependence in $\sin 2\varphi$ when either $\sigma = \sigma'$ and $L+L'-l''$ is odd or $\sigma \neq \sigma'$ and $L+L'-l''$ is even, and a φ dependence in $\cos 2\varphi$ when either $\sigma = \sigma'$ and $L+L'-l''$ is even or $\sigma \neq \sigma'$ and $L+L'-l''$ is odd.

Now let us assume that both the target and residual nuclei are in states of definite parity.

In this case, if a single multipole is responsible for the transition, then l, l' being of the same parity, l'' is even; this implies symmetry of the ϑ angular distribution about $\vartheta = \pi/2$.

Since $L+L'-l'' = 2L-l''$ is even and $\sigma = \sigma'$, it follows that the φ -dependent term in the angular distribution is in $\cos 2\varphi$ and the φ -independent term gives, in general, a non vanishing contribution. Under the same assumption, if two multipoles are responsible for the transition, six cases of mixing are possible, i.e. of two electric or two magnetic multipoles or of an electric and a magnetic one, and in each instance either with the same parity or not. Now, when both multipoles are of the same type ($\sigma = \sigma'$), if they are of the same parity then $l+l', l''$ and $L+L'-l''$ are even; if they are of different parities then $l+l', l''$ are odd, $L+L'-l''$ is even. When the multipoles are of different types ($\sigma \neq \sigma'$), if they are of the same parity then $l+l', l''$ are even, $L+L'-l''$ is odd; if they are of different parities then $l+l', l''$ are odd, $L+L'-l''$ is odd. Concluding, we have always either $\sigma = \sigma'$, $L+L'-l''$ even or $\sigma \neq \sigma'$, $L+L'-l''$ odd, i.e. a φ -dependent term in $\cos 2\varphi$ in addition to a φ -independent term.

If the coefficient of $\cos 2\varphi$ does not vanish, then it follows from (2), obviously, that the φ -independent term must be a non vanishing, positive quantity.

When the residual nucleus is not in a state of definite spin and/or parity, we must write, in the place of (3),

$$(3') \quad \mathcal{I}(\vartheta, \varphi) \sim \sum_{s, \gamma, \gamma'} I^{s, \gamma, \gamma'}(\vartheta, \varphi),$$

being now $I^{s, \gamma, \gamma'}(\vartheta, \varphi)$ the function denoted $I(\vartheta, \varphi)$ in (3). Since for each term in the sum (3') our result holds, its validity is stated in this more general case too.

3. - The results just obtained allow us to state that a measurement of the azimuthal distribution of photoejected nucleons, i.e. of the angular distribution in a plane orthogonal to the incident photon beam, is essentially the determination of α in a function proportional to $F(\alpha, \varphi) = 1 + \alpha \cos 2\varphi$; the (here unimportant) positive proportionality factor could be

determined from a measurement of total cross-section for the observed photoprocess.

Let us now denote with α_0 the value of α in the case of completely polarized incident photon beam: then $\alpha = \varepsilon \alpha_0$ being ε the ratio of polarized to total intensity in the beam, when photons are partially polarized.

From a given experiment α_0 can be determined when both the direction of the polarization vector in the beam ($\varphi = 0$) and ε are known. If this is not the case, then the modulus only of α can be fixed from the given experiment. Since $F(\alpha, \varphi)$ is an essentially non negative quantity we have that, in general, it must be $|\alpha| \leq 1$. Hence,

$$(6) \quad \frac{|\alpha|}{|\alpha_0|} = \varepsilon \geq |\alpha'|;$$

$|\alpha|$ cannot be greater than the ratio ε of polarized to total intensity in the incident photon beam.

With a theoretically determined α_0 , the experiment could give both the direction of the polarization vector in the incident photon beam and ε . Now, in general, α_0 is given, in terms of the $A_{l'}(L\pi_\gamma; L'\pi'_\gamma)$ coefficients, as

$$(7) \quad \alpha_0 = \frac{\sum A_{l'}(L\pi_\gamma; L'\pi'_\gamma)(-i)^{\sigma+\sigma'}(l''|L'1; L1)\mathcal{D}_{l'}^0(0)}{\sum A_{l'}(L\pi_\gamma; L'\pi'_\gamma)(i)^{\sigma-\sigma'}(l''|L'1; L-1)\mathcal{D}_{l'}^0(0)},$$

and the $A_{l'}$ coefficients cannot be calculated without some hypothesis allowing the evaluation of the R matrix elements, i.e. without giving a theory (or, at least, a «model») for the photonuclear reaction.

But the $A_{l'}$ coefficients can also be determined, in some cases, if, for the same photoprocess, one has measured the angular distribution of photonucleons in a plane containing the incidence direction of the photons, in the absence of polarization effects.

The simplest case occurs when a single multipole is responsible for the transition: if the ϑ angular distribution is observed, in absence of polarization effects, then we know the coefficients b_l in the linear combination

$$(8) \quad I_0(\vartheta) = I(\vartheta, \varphi) \Big|_{\varphi = (\pi/4) + m\pi/2} = \frac{1}{2\pi} \int d\varphi I(\vartheta, \varphi) = N \sum_l b_l \mathcal{D}_l^0(\cos \vartheta),$$

m being an integer and N a positive factor that cannot be fixed from an angular distribution measurement.

From (4) and the remarks at the end of the preceding section

$$(9) \quad Nb_l = 2 \sum_{L\pi_\gamma L'\pi'_\gamma} A_{l'}(L\pi_\gamma; L'\pi'_\gamma)(l|L'1; L-1)(i)^{\sigma-\sigma'}$$

and, if a single multipole is responsible for the transition, for every $b_l \neq 0$,

$$(10) \quad \frac{b_l}{(l | L1; L-1)} = \frac{2}{N} A_l(L\pi_\gamma; L\pi_\gamma) = \frac{2}{N} A_l(L\pi_\gamma).$$

Let us consider, e.g. a ϑ angular distribution, in absence of polarization effects, of the type

$$(11) \quad I_0(\vartheta) = N(a_0 + a_2 \cos^2 \vartheta) = N(b_0 \mathcal{P}_0^0 + b_2 \mathcal{P}_2^0(\cos \vartheta)).$$

Such a distribution has been observed for the photoprotons from ^{16}O ⁽⁶⁾, for the photoneutrons from ^{27}Al ⁽⁷⁾, and, as well known, in the photodisintegration of ^2D .

The a_l coefficients in (11) can be expressed in terms of the b_l coefficients in the following way

$$(12) \quad a_0 = \left(\frac{1}{2}\right)^{\frac{1}{2}} [b_0 - \left(\frac{5}{4}\right)^{\frac{1}{2}} b_2]; \quad a_2 = 3\left(\frac{5}{8}\right)^{\frac{1}{2}} b_2.$$

From (7) and (10) we have

$$(13) \quad \alpha_0 = (-)^{\sigma} \frac{(2 | L1; L1)}{(2 | L1; L-1)} \left(\frac{1}{6}\right)^{\frac{1}{2}} \frac{3b_2 \left(\frac{5}{4}\right)^{\frac{1}{2}}}{b_0 - \left(\frac{5}{4}\right)^{\frac{1}{2}} b_2}.$$

Hence, from (12),

$$(14) \quad \alpha_0 = (-)^{\sigma} \frac{(2 | L1; L1)}{(2 | L1; L-1)} \left(\frac{1}{6}\right)^{\frac{1}{2}} \frac{a_2}{a_0}.$$

In the dipole case this reduces to

$$(14') \quad \alpha_0 \Big|_{L=1} = (-)^{\sigma} \frac{a_2}{a_0},$$

and in the quadrupole case to

$$(14'') \quad \alpha_0 \Big|_{L=2} = (-)^{\sigma+1} \frac{a_2}{5a_0}.$$

From (14) the particularly interesting result follows that the sign of α_0 , relative to $((2 | L1; L1)/(2 | L1; L-1))a_2$ distinguishes between electric and magnetic multipole transition (when the multipole order is known) the maxima and minima in the azimuthal angular distribution being interchanged in going from the one case to the other.

⁽⁶⁾ B. M. SPICER: *Phys. Rev.*, **99**, 33 (1955).

⁽⁷⁾ S. A. E. JOHANSSON: *Phys. Rev.*, **97**, 434 (1955).

What has been made for the simple distribution (11) can also be made, obviously, for a general one

$$I_0(\theta) = N \sum a_k \cos^k \theta = N \sum b_l \mathcal{P}_l(\cos \theta)$$

containing even powers only of $\cos \theta$, i.e. admitting an interpretation in terms of a single multipole transition. If odd powers of $\cos \theta$ appear in the angular distribution, then necessarily two or more multipoles are responsible for the transition, and the situation is more complicated: α cannot be given, in general, in terms of what is known from an angular distribution measurement in absence of polarization effects.

* * *

It is a pleasure to thank Prof. M. UINI for many enlightening discussions on the physics of photonuclear reactions, and Prof. R. RICCIO for his kind interest in this work.

APPENDIX

(i) The multipole expansion of the initial photon state is that used by BIEDENHARN and ROSE ⁽⁸⁾, i.e. in the form in which it was given by GOERTZEL ⁽⁹⁾. The $Y_L^M(\theta, \varphi)$ are defined as in CONDON and SHORTLEY ⁽¹⁰⁾.

The vector addition coefficients are identical with those of CONDON and SHORTLEY ⁽¹⁰⁾, with the notational convention

$$(j_1 j_2 m_1 m_2 \mid j_1 j_2 j m) = (j m \mid j_1 m_1 \mid j_2 m_2) = (j \mid j_1 m_1 \mid j_2 m_2),$$

the phase being chosen so that $(j_1 + j_2 \mid j_1 j_1 \mid j_2 j_2) = 1$.

From the just specified choice of the vector addition coefficients it follows that the W coefficients are identical with those of RACAH ⁽¹¹⁾.

The initial and final state expansions have not been normalized; this should be taken in account in defining the matrix elements of the operator R , projection of the Heisenberg transition operator on the subspace of the $NY; m_Y$ vectors in the Dirac space.

It seems that no further details on this subject are needed here.

(ii) For the R matrix elements appearing in (3) we have

$$\langle l m_Y m_X \mid R \mid L P \pi_Y m_X \rangle = \sum_{j_1 j_2} \langle j_1 m_Y \mid J_Y m_Y \rangle \langle j_1 m_Y \mid s_Y m_X \rangle \langle J M \mid s_N j s_Y \mid R \mid L P \pi_Y m_X \rangle.$$

⁽⁸⁾ L. C. BIEDENHARN and M. E. ROSE: ref. ⁽¹⁾; M. E. ROSE: *Multipole Fields* (New York, 1955).

⁽⁹⁾ G. GOERTZEL: *Phys. Rev.*, **70**, 897 (1946).

⁽¹⁰⁾ E. U. CONDON and G. H. SHORTLEY: *Theory of Atomic Spectra* (London, 1935).

⁽¹¹⁾ G. RACAH: *Phys. Rev.*, **62**, 438 (1942); **63**, 367 (1943).

It has been previously pointed out that R is a rotation-invariant operator; consequently the operator $[R LP\pi_\gamma] = R(LP\pi_\gamma)$ operating to the right on the state vectors in terms of which the target nucleus state has been expanded, transforms under D^L , the $(2L + 1)$ -dimensional representation of the 3-dimensional real rotation group. From this and the Eckart theorem ⁽¹²⁾, it follows

$$(A.1) \quad \langle l m m_N m_Y | R | LP\pi_\gamma m_X \rangle = \\ = \sum_{j'} (J | LP; s_N m_N) (J | j m_j; s_Y m_Y) (j | l m; s_N m_N) (J | l s_N j s_Y \| R(LP\pi_\gamma) \| s_X).$$

The reduced matrix elements $(J | l s_N j s_Y \| R(LP\pi_\gamma) \| s_X)$ do not depend on magnetic quantum numbers.

Substitution of (A.1) in (3), and use of the well known

$$Y_l^{-m} Y_{l'}^{m'} = \sum_{l''} \left[\frac{(2l + 1)(2l' + 1)}{4\pi(2l'' + 1)} \right]^{\frac{1}{2}} (l'' | l' 0; l 0) (l'' | l' m'; l - m) Y_{l''}^{m' - m},$$

give

$$(A.2) \quad I(\vartheta, \varphi) = 8\pi^4 \sum (i)^{L-L'+L''} (l'' | l' 0; l 0) Y_{l''}^{m''} (iP)^\sigma (iP')^{-\sigma'} \cdot \\ \cdot \left[(2L + 1)(2L' + 1) \frac{(2l + 1)(2l' + 1)}{4\pi(2l'' + 1)} \right]^{\frac{1}{2}} (J | l s_N j s_Y \| R(LP\pi_\gamma) \| s_X) \cdot \\ \cdot (J' | l' s_Y j' s_Y \| R(LP'\pi_\gamma') \| s_X)^* \left[\sum' (J | j m_j; s_Y m_Y) (j | l m; s_N m_N) (J | LP; s_X m_X) \cdot \right. \\ \cdot (J' | j' m_j'; s_Y m_Y) (j' | l' m'; s_N m_N) (J' | LP'; s_X m_X) (-)^{m'} (l'' m'' | l' m'; l - m) \left. \right]$$

the sum \sum being on $l'l''LP\pi_\gamma PL'\pi_\gamma' P' j j' J J'$ and \sum' on $m_X m_Y m_N m m'$.

For evaluating the sum \sum' let us remember that

$$\sum_{\beta} (e\epsilon | a\alpha; b\beta) (c\gamma | c\epsilon; d\delta) (f\varphi | b\beta; d\delta) = [(2e + 1)(2f + 1)]^{\frac{1}{2}} (c\gamma | a\alpha; f\varphi) W(abcd; ef).$$

By repeated application of this formula we have

$$\sum' (J | j m_j; s_Y m_Y) (j | l m; s_N m_N) (J | LP; s_X m_X) (J' | j' m_j'; s_Y m_Y) (j' | l' m'; s_N m_N) \cdot \\ \cdot (J' | LP'; s_X m_X) (-)^{m'} (l'' m'' | l' m'; l - m) = (-)^{1+l-l'} (2J + 1)(2J' + 1) [(2j + 1) \cdot \\ \cdot (2j' + 1)]^{\frac{1}{2}} (l'' m'' | LP'; L - P) W(j s_N l'' l'; l j') W(J s_X l' j'; j J') W(L s_X l'' J; J' L).$$

From this and being

$$\sum_{P'P''} (l'' m'' | LP'; L - P) (iP)^\sigma (iP')^{-\sigma'} Y_{l''}^{m''} = \sum_{P'} [(l'' | LP'; L - P') (iP')^{\sigma - \sigma'} Y_{l''}^0 + \\ + (l'' | LP'; LP') (-iP')^{\sigma + \sigma'} Y_{l''}^{2P'}] = (i)^{\sigma - \sigma'} [1 + (-)^{L' + L - l'' + \sigma' - \sigma}] \cdot \\ \cdot (l'' | L1; L - 1) Y_{l''}^0 + (-i)^{\sigma + \sigma'} [Y_{l''}^2 + (-)^{L' + L - l'' - \sigma - \sigma'} Y_{l''}^2] (l'' | L1; L1),$$

⁽¹²⁾ C. ECKART: *Rev., Mod. Phys.*, **2**, 305 (1930).

it follows

$$\begin{aligned}
 I(\vartheta, \varphi) = & \left(\frac{1}{2\pi} \right)^{\frac{1}{2}} \sum \left\{ 8\pi^4(i)^{L-L'+L''} (l'' | l' 0; l 0) \left[(2j+1)(2j'+1)(2L+1) \cdot \right. \right. \\
 & \cdot (2L'+1) \frac{(2l+1)(2l'+1)}{4\pi(2l''+1)} \left. \right]^{\frac{1}{2}} (2J+1)(2J'+1)(-1)^{1+L-L'}(J; l s_N j s_N \| R(L\pi_Y) \| s_N) \cdot \\
 & \cdot (J'; l' s_N j' s_N' R(L'\pi_Y' s_N')^* W(j s_N l'' l'; l j') W(J s_N l' j'; j J') W(L' s_N l'' J; J' L) \left. \right\} \cdot \\
 & \cdot \left\{ (i)^{\sigma-\sigma'} [1 + (-1)^{L-L'-L''+\sigma-\sigma'}] (l'' | L' 1; L-1) \mathcal{Q}_{l''}^0(\cos \vartheta) + \right. \\
 & \left. + (-i)^{\sigma+\sigma'} (\exp[2i\varphi] + (-1)^{L+L'-L''-\sigma-\sigma'} \exp[-2i\varphi]) (l'' | L' 1; L 1) \mathcal{Q}_{l''}^2(\cos \vartheta) \right\},
 \end{aligned}$$

the sum being on $l'l''jj'JJ'L\pi_Y L'\pi_Y'$.

(4) and (5) in the text are a transcription of this result.

RIASSUNTO

Viene data in dettaglio la determinazione della più generale distribuzione angolare di fotonucleoni compatibile con i principi di conservazione per il momento angolare e la parità. La sua dipendenza azimutale viene discussa con particolare riguardo alle informazioni fisiche ottenibili senza usare alcun modello per la reazione o per il nucleo.

Integral Equations for Meson Field Theory (*).

R. L. MILLS

Institute for Advanced Study, Princeton, N. J.

(ricevuto il 19 Settembre 1956)

Summary. — A covariant method of approximating the nucleon Green's function S'_p is described, in terms of the solution of a connected sequence of linear integral equations. Explicit expressions for the matrix elements for processes involving only one real nucleon are derived by formal functional differentiation of S'_p with respect to external boson fields. The solution is renormalized, in the sense that its power series expansion in the coupling constant g is the same that obtained by enumerating Feynman diagrams and renormalizing term by term. Closed loops are neglected, though virtual nucleon pairs not corresponding to closed loops are included.

Introduction.

Considerable work has been done with integral equations in trying to deal with the problems of meson field theory ⁽¹⁻¹²⁾. The object of the scheme pre-

(*) Much of this work was performed at Brookhaven National Laboratory, Upton, New York, under the auspices of the U.S. Atomic Energy Commission.

(¹) I. TAMM: *Journ. Phys. (USSR)*, **9**, 449 (1945).

(²) S. M. DANCOFF: *Phys. Rev.*, **78**, 382 (1950).

(³) F. J. DYSON, M. ROSS *et al.*: *Phys. Rev.*, **95**, 1644 (1954); R. H. DALITZ and F. J. DYSON: *Phys. Rev.*, **99**, 301 (1955).

(⁴) M. M. LÉVY: *Phys. Rev.*, **88**, 72, 725 (1952); A. KLEIN: *Phys. Rev.*, **90**, 1101 (1953).

(⁵) E. E. SALPETER and H. A. BETHE: *Phys. Rev.*, **84**, 1232 (1951); M. GELL-MANN and F. LOW: *Phys. Rev.*, **84**, 350 (1951).

(⁶) G. C. WICK: *Phys. Rev.*, **96**, 1124 (1954); E. R. CUTOWSKY: *Phys. Rev.*, **96**, 1135 (1954).

(⁷) M. CINI: *Nuovo Cimento*, **10**, 526, 614 (1953).

(⁸) S. FUBINI: *Nuovo Cimento*, **10**, 851 (1953); M. M. LÉVY: *Phys. Rev.*, **94**, 460 (1954); **98**, 1470 (1955); T. YOSHIMURA: *Progr. Theor. Phys.*, **11**, 224 (1954); S. CHIBA: *Progr. Theor. Phys.*, **11**, 494 (1954).

sented here is to summarize in an unsophisticated way the renormalized contribution of the virtual pion and nucleon fields, neglecting meson-meson interactions and meson self-energy effects, to processes involving only one real nucleon, such as pion-nucleon scattering, pion photoproduction, or the nucleon magnetic moment interaction.

In Sect. 1, a set of unrenormalized linear integral equations describing S_r is set down and discussed, together with the functional differentiation procedure for obtaining the matrix elements of interest. These equations can in fact be formally derived from the original Lagrangian and renormalized, without recourse to perturbation theory: the finiteness and uniqueness of solutions, on the other hand, can only be established for the perturbation expansion. The formal derivation, which is cumbersome and involves a lot of additional notation, is omitted here, and the equations are discussed in terms of an expansion in powers of the coupling constant g . It is, of course, hoped that meaningful solutions may exist where the power series expansion breaks down. In addition to the restriction of neglecting closed loop Feynman diagrams, a further approximation is introduced, consisting of a Tomonaga-like limit on the number of virtual mesons allowed in intermediate states. This reduces the integral equations to a finite sequence.

In Sect. 2 the renormalization procedure is indicated briefly, and the renormalized equations written out. As a result of the further approximation just mentioned, the renormalized integral equations also form a sequence of linear equations, in the sense that the kernel and inhomogeneous term of each equation depend on the solutions of the preceding equations of the sequence, and of the lower-order approximations.

Work along similar lines has been done by ARNOWITT and GASTROWITZ¹², ITABASHI¹³, and H. S. GREEN¹⁴. The method of handling overlapping divergences is similar to that of EDWARDS¹⁵, and is used by GREEN and by ALLCOCK¹⁶.

1. - The Unrenormalized Equations.

In the interest of simplicity, only the case of neutral pseudoscalar mesons will be considered, the extension to the symmetrical theory of charged mesons

¹² R. ARNOWITT and S. GASTROWITZ: *Phys. Rev.*, **95**, 688 (1954); **97**, 824 (1955).

¹³ K. ITABASHI: *Progr. Theor. Phys.*, **11**, 227, 228 (1954).

¹⁴ H. S. GREEN: *Phys. Rev.*, **95**, 548 (1954).

¹⁵ F. E. EDWARDS: *Phys. Rev.*, **97**, 1202 (1955); S. F. EDWARDS and F. E. EDWARDS: *Phys. Rev.*, **101**, 1570 (1956).

¹⁶ S. F. EDWARDS: *Phys. Rev.*, **90**, 284 (1953).

¹⁷ G. R. ALLCOCK: *Bull. Am. Phys. Soc.*, **1**, 208 (1956).

being completely straightforward. The Lagrangian density can be written

$$(1) \quad \mathcal{L} = -\hbar c \left\{ \frac{1}{2} [(\partial_\nu \varphi)^2 + \mu^2 \varphi^2] + \bar{\psi}(\gamma \cdot \partial + m)\psi + i(2\pi)^2 g \bar{\psi} \gamma_5 \psi \varphi \right\}.$$

(The unrenormalized « masses » μ and m , like the « momenta » P and k to be introduced below, have the dimensions of inverse length). The nucleon Green's function is given by the vacuum expectation value of the time-ordered product of the Heisenberg operators ψ and $\bar{\psi}$:

$$(2) \quad S'_F(x_2 - x_1) = \langle (\psi(x_2) \bar{\psi}(x_1))_{+} \rangle \eta(x_{20} - x_{10}),$$

where $\eta(x_0) = x_0 / |x_0|$.

Our procedure will be to seek an approximate form for S'_F , and to express the matrix element of physical interest as a functional derivative of S'_F with respect to a hypothetical external meson field (or an external electromagnetic field in the case of electromagnetic interactions) ⁽¹⁵⁾. In terms of Feynman graphs, this means that the line corresponding to each real boson in the initial or final state is attached in all possible ways to each graph included in S'_F . For meson-nucleon scattering, for example, two functional differentiations are required. The reason for using this procedure is that in a natural way it provides the matrix elements of interest with severable desirable properties which are difficult to obtain in other approximations. For meson-nucleon scattering the crossing theorem of GELL-MANN and GOLDBERGER ⁽¹⁶⁾, governing the low-energy behavior of the matrix element, is satisfied, while for electromagnetic processes, such as photoproduction, the matrix element obtained in this way is gauge invariant. The crossing theorem in particular cannot be satisfied within the framework of a Tamm-Dancoff-like approximation, and while we use such an approximation to obtain S'_F , the functional differentiation procedure takes us outside this framework.

In order to do this functional differentiation, it is clearly not sufficient to know S'_F in the absence of any external field; it is equally clearly not necessary to know S'_F in the presence of an arbitrary field, since only the first few terms of an expansion in powers of the applied field are needed. In the approximation that will be described below, the functional derivatives, taken for vanishing external field, can be expressed in terms of the auxiliary functions used in the calculation of S'_F itself.

⁽¹⁵⁾ The idea of applying functional differentiation techniques to field theory is due to SCHWINGER (*Proc. Natl. Acad. Sci. U. S.*, **37**, 452, 455 (1951), and unpublished material).

⁽¹⁶⁾ M. GOLDBERGER and M. GELL-MANN: *Proceedings of the Rochester Conference* (University of Rochester, Rochester, 1954).

The matrix element for meson-nucleon scattering, say, can be written as

$$(3) \quad M = 4\pi^2(\omega\omega')^{-1/2}g^2\delta^4(P'-P)\bar{u}_f(P-k')\left[S_F^{-1}\frac{\delta^2 S_F'}{\delta g q^*(-k')\delta g q^*(k)}S_F^{-1}\right]u_i(P-k),$$

where u and u_f are spinors describing the initial and final states of the nucleon, normalized so that $u^*u = 1$; and S_F' is the free-nucleon Green's function: $S_F'(p) = -i(\not{p} - m - i\epsilon)^{-1}$. The total four-momentum of the meson-nucleon system is conserved, and is denoted by P .

If the initial approximation is made of ignoring meson-meson interactions, then the function S_F' can be expressed formally as the end result of an infinite sequence of linear integral equations describing certain functions K_n : K_0 is identical to S_F' , and K_n is in general a one-nucleon- n -meson propagator, corresponding to those Feynman graphs which contain no closed loops (17) and which cannot be cut into two separate graphs by a line cutting the nucleon line and fewer than n -meson lines. Such graphs can be constructed by putting end-to-end in all possible ways what may be called «proper» one-nucleon- n -meson graphs. These proper graphs, corresponding to the kernel j_n in the integral equation for K_n , are graphs which cannot be cut into two graphs by a line intersecting the nucleon line and fewer than $n-1$ meson lines. The graph in which there are no interactions at all then contains no parts of the form j_n , and corresponds to a product of free-particle Green's functions, averaged over permutations of the different meson four-momenta. The integral equation will have two terms on the right: one corresponds to the no-interaction graph, and the other, containing j_n explicitly once, and implicitly through K_n itself, corresponds to all the remaining graphs. In a momentum space representation, the integral equation is

$$(4) \quad \begin{aligned} K_n(P; k'_n \dots k'_1, k_n \dots k_1) &= S_F(P - \Sigma k') \Delta_F(k'_n) \dots \Delta_F(k'_1) \cdot \\ &\cdot (n!)^{-1} \sum_{\text{perm.}} \delta^4(k'_n - k_{j(n)}) \dots \delta^4(k'_1 - k_{j(1)}) \cdot \\ &+ S_F(P - \Sigma k') \Delta_F(k'_n) \dots \Delta_F(k'_1) \int (d^4k'')^n j_n(P; k'_n \dots k'_1, k''_n \dots k''_1) \cdot \\ &\cdot K_n(P; k''_n \dots k''_1, k_n \dots k_1). \end{aligned}$$

We have normalized K_n to represent an average rather than a sum over the $n!$ similar Feynman graphs obtained by permuting the meson momentum coordinates.

¹⁷ We shall ignore meson self-energy effects as well as meson-meson interactions, but it will be clear in what follows that any desired approximation to Δ_F' could be used throughout in place of the free-meson Green's function $\Delta_F(k) = i(k^2 - \mu^2 - i\epsilon)^{-1}$.

This equation may be written more briefly by suppressing the meson four-momenta k and the constant total four-momentum P , and by treating the integrations like matrix multiplications. Using also a symmetrizing operator \mathcal{S}_n , defined by

$$(5) \quad (k' | \mathcal{S}_n | k) = (n!)^{-1} \sum_{\text{perm.}} \delta^4(k'_n - k_{j(n)}) \dots \delta^4(k'_1 - k_{j(1)}),$$



Fig. 1. — Structure of the kernel j_n .

Eq. (4) becomes

$$(6) \quad K_n = S_F \Delta_F^n \mathcal{S}_n + S_F \Delta_F^n j_n K_n.$$

Since j_n corresponds to graphs which cannot be cut in fewer than $n+1$ meson lines, it follows that the graphs obtained from j_n by cutting off the first and last interactions along the nucleon line are of the form characteristic of K_{n+1} . This is illustrated in Fig. 1 and described by the equation

$$(7) \quad j_n = (n+1)g^2 \Delta_F^{-n} \gamma_5 K_{n+1} \lambda_5 \Delta_F^{-n}.$$

Written out explicitly, to make clear the integrations involved, this appears as

$$(8) \quad j_n(P; k'_n \dots k'_1, k_n \dots k_1) = (n+1)g^2 \int d^4 k'_{n+1} d^4 k_{n+1} \Delta_F^{-1}(k'_n) \dots \Delta_F^{-1}(k'_1) \cdot \\ \cdot \gamma_5 K_{n+1}(P; k'_{n+1} \dots k'_1, k_{n+1} \dots k_1) \gamma_5 \Delta_F^{-1}(k_n) \dots \Delta_F^{-1}(k_1).$$

As noted above, K_0 is identical to S'_F ; hence j_0 is the same as the usual self-energy function Σ , and is thus described in terms of K_1 .

It must now be admitted that even apart from divergences Eqs. (6) and (7) do not determine S'_F ; in fact, they hardly restrict it in any way, since if $S'_F (= K_0)$ is chosen arbitrarily, then j_0 is determined; but K_1 can be chosen to be consistent with j_0 according to Eq. (7), and successively K_2 , K_3 , etc., can also be made to fit. If, on the other hand, the sequence of equations is cut-off, so that K_N , say, is given, then, apart from the effect of multiple solutions to the integral equations, the functions K_{N-1} , K_{N-2} , ..., $K_0 = S'_F$ are determined. It seems reasonable to suggest that if a crude approximation is made to K_N , where N is sufficiently large, then the resulting function S'_F should be a very good approximation to the true Green's function. The approximation which we shall use is simply to ignore all interactions in K_N , so that

$$(9) \quad K_N^{(N)} = S_F \Delta_F^N \mathcal{S}_N,$$

where \mathcal{S}_N is the symmetrizing operator defined in Eq. (5). This approximation, which we call the approximation $A^{(N)}$, has the effect of restricting the Feynman

graphs corresponding to K_n (and, in particular, S'_p) to those graphs for which no cut intersects in a non trivial way more than N meson lines ⁽¹⁸⁾.

The equations (6) and (7) are the basis for the rest of the development. They are replaced after renormalization by a more complicated set of equations, whose basic features, however, are similar. In particular, the renormalized equations in the approximation $A^{(N)}$ also form a finite sequence of linear integral equations, each of which has a kernel dependent on the solution of the preceding equation in the sequence, and dependent also, together with the inhomogeneous term, on the solutions of the lower-order approximations $A^{(N-1)}$, $A^{(N-2)}$, ..., $A^{(1)}$.

1.1. The Unrenormalized Matrix Element. — The working out of Eq. (3) for the scattering matrix element, using this approximation for S'_p , is much more simply accomplished in terms of the unrenormalized equations (6) and (7), while the basic features are little different when renormalization has been performed. We can ignore the ambiguity associated with the wave function renormalization in Eq. (3), since this can be handled in a standard way, and fix our attention on the factor involving functional differentiation. It is useful for this purpose to consider an inverse function to K_n , defined, since K_n is symmetric in the meson four-momenta k_1, \dots, k_n , by

$$(10) \quad K_n^{-1} K_n = \mathcal{S}_n.$$

(The total four-momentum P is still regarded as a parameter, so that K_n^{-1} is defined for any given value of P .) Eq. (6) can be written in terms of this inverse function:

$$(11) \quad K_n^{-1} = S_F^{-1} \Delta_F^{-n} \mathcal{S}_n - j_n = S_F^{-1} \Delta_F^{-n} \mathcal{S}_n - (n+1) g^2 \Delta_F^{-n} \gamma_5 K_{n+1} \gamma_5 \Delta_F^{-n}.$$

Any functional derivative of K_n can now be expressed in terms of corresponding derivatives of K_{n+1} through differentiation of this equation; and since, in the approximation $A^{(N)}$, K_N is known, the functional derivatives, evaluated for vanishing external field, are determined. The equation satisfied by S_F in the presence of the external field φ^e is

$$(12) \quad i(\gamma \cdot p' + m) S_F(p', p) - g \int d^4 k \varphi^e(k) \gamma_5 S_F(p' - k, p) = \delta^4(p' - p),$$

⁽¹⁸⁾ Other approximations for K_N suggest themselves: one might, for example, let just one of the mesons of K_N be non-interacting, so that K_N would be expressed in terms of K_{N-1} . This leads to non-linear integral equations, but is formally as manageable as the approximation used here.

or briefly,

$$(13) \quad S_F^{-1} = i(\gamma \cdot p + m) \delta^4(p' - p) - g\varphi^e \gamma_5;$$

so that the functional derivative of S_F^{-1} is simply

$$(14) \quad \frac{\delta S_F^{-1}}{\delta g\varphi^e} = -\gamma_5.$$

By differentiating Eq. (10), we obtain the usual results for the derivatives of inverses:

$$(15) \quad \frac{\delta K_n}{\delta g\varphi^e} = -K_n \frac{\delta K_n^{-1}}{\delta g\varphi^e} K_n;$$

$$(16) \quad \begin{aligned} \frac{\delta^2 K_n}{(\delta g\varphi^e)^2} &= K_n \frac{\delta K_n^{-1}}{\delta g\varphi^e(-k')} K_n \frac{\delta K_n^{-1}}{\delta g\varphi^e(k)} K_n + \\ &+ K_n \frac{\delta K_n^{-1}}{\delta g\varphi^e(k)} K_n \frac{\delta K_n^{-1}}{\delta g\varphi^e(-k')} K_n - K_n \frac{\delta^2 K_n^{-1}}{(\delta g\varphi^e)^2} K_n. \end{aligned}$$

These equations, taken together with the equations describing the derivatives of K_n^{-1} (from Eq. (11)),

$$(17) \quad \frac{\delta K_n^{-1}}{\delta g\varphi^e} = -\gamma_5 \Delta_F^{-n} \mathcal{S}_n - (n+1)g^2 \Delta_F^{-n} \gamma_5 \frac{\delta K_{n+1}}{\delta g\varphi^e} \gamma_5 \Delta_F^{-n},$$

$$(18) \quad \frac{\delta^2 K_n^{-1}}{(\delta g\varphi^e)^2} = -(n+1)g^2 \Delta_F^{-n} \gamma_5 \frac{\delta^2 K_{n+1}}{(\delta g\varphi^e)^2} \gamma_5 \Delta_F^{-n},$$

determine the first and second functional derivatives of all the K_n 's (in the approximation $A^{(N)}$), and of $S_F' = K_0$ in particular.

This approach can easily be extended to the case of multiple production (in meson-nucleon collisions), photoproduction, or the nucleon magnetic moment, by means of further functional differentiation. For photoproduction we need in addition a hypothetical external electromagnetic field A_μ^e , so that we can use the relations, for nucleon and meson fields of charge Q ,

$$(19) \quad \frac{\delta S_F^{-1}}{\delta A_\mu^e} = Q\gamma_\mu; \quad \frac{\delta \Delta_F^{-1}}{\delta A_\mu^e} = 2iQk_\mu.$$

This procedure satisfies the requirements of gauge invariance.

2. - Renormalization.

The renormalization procedure is simply an application of the method of Dyson ⁽¹⁹⁾, involving the isolation of primitive divergent parts in any expression, replacing them by finite functions, and finding suitable expressions for the finite functions. The procedure is still consistent in the absence of meson self-energy effects and meson-meson interactions, though the renormalization constants are, of course, different from those of the complete theory. It is neater, though not logically necessary, to go through the renormalization procedure before imposing the approximation $A_{(N)}$, since otherwise the renormalization constants for the lower-order approximations $A^{(N-1)}$, $A^{(N-2)}$, ..., $A^{(1)}$ also become involved and need to be handled properly. The intention here is not to prove anything rigorously about the nature or existence of renormalized solutions, but rather to arrange that the solution be correctly renormalized up to any given finite power of the coupling constant g .

Again we start with Eqs. (6) and (7), and think of the solution as expanded in powers of g . Formally this is not necessary for removing the dependence on the renormalization constants Z , but the procedure can only be justified in terms of the power series expansion. There are three steps, which we shall carry through only sketchily: first, one isolates the primitive divergent vertex and nucleon self-energy parts in the unrenormalized equations; then one finds suitable equations for the primitive divergent parts themselves; and, finally, having expressed the divergent functions as multiples of finite functions one finds appropriate equations for the latter, not involving the divergent renormalization factors.

If K_n is thought of as a sum of products of the functions j_n , then the primitive divergent parts of K_n are all contained in the separate factors j_n , that is, none of the self-energy or vertex graphs lies partly in one j_n -graph and partly in another. If this were not so, in fact, it would be possible to cut such a j_n -graph in one nucleon line and fewer than n meson lines, contrary to their construction. This means that once j_n itself has been renormalized, iteration of the integral equation (6) for K_n will not introduce new divergences.

The procedure for j_n is straightforward, mostly because of the restricted character of the corresponding graphs. If none of the n mesons described by j_n interacts with the nucleon, then the interaction must involve only the nucleon and additional virtual mesons, and contribute only to the nucleon self energy. Such terms in j_n add up to a multiple of $\Sigma(-j_0)$, which fact will enable us to replace S_F by S'_F in the integral equation (6) for K_n . In all other terms of j_n , some of the n mesons interact, and, because of the fact that a

(19) F. J. DYSON: *Phys. Rev.*, **75**, 1736 (1949).

j_n -graph cannot be cut in fewer than $n+1$ meson lines, the two γ_5 vertices appearing in Eq. (7) (see Fig. 1) cannot be part of self-energy diagrams, but must each belong to a separate vertex part Γ_5 .

We find now that the restriction on the graphs included in K_1 is just such

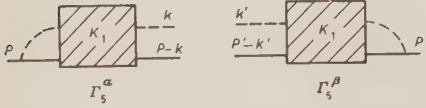


Fig. 2. - Structure of the vertex function Γ_5 .

that if we close off one of the two external meson lines we have the vertex function Γ_5 ; this vertex function includes the same graphs regardless of which end of K_1 is closed off, provided the approximation $A^{(N)}$ has not been imposed on K_1 , so that

while the two corresponding functions for Γ_5 are different, they are closely related. Corresponding to the two cases illustrated in Fig. 2, we define the two functions Γ_5^α and Γ_5^β satisfying the equations

$$(20) \quad \begin{cases} \Gamma_5^\alpha S'_F A_F = \gamma_5 K_1, \\ S'_F A_F \Gamma_5^\beta = K_1 \gamma_5. \end{cases}$$

The relation between them, which holds only in the absence of any approximation (apart from neglecting closed loops), is

$$(21) \quad \Gamma_5^\alpha(P; k) = \Gamma_5^\beta(P'; k') = \Gamma_5^\beta(P - k; -k).$$

The relation (21) breaks down when the approximation $A^{(N)}$ is imposed, and in that case it is still consistent to use both functions in accordance with Eqs. (20).

We can now return to the discussion of the equation (7) for j_n . The structure of K_{n+1} is indeed found to be such that a part of j_n proportional to the nucleon self-energy function Σ can be removed,

$$(22) \quad j_n = \Sigma \Delta_F^{-n} \mathcal{S}_n + J_n,$$

and the remainder J_n can be expressed in terms of the vertex functions Γ_5 ,

$$(23) \quad J_n = (n+1) g^2 \Delta_F^{-n} \Gamma_5^\alpha \bar{K}_{n+1} \Gamma_5^\beta \Delta_F^{-n}.$$

This is of the same form as Eq. (7), with the γ_5 's replaced by the vertex functions Γ_5 , and K_{n+1} replaced by a modified function \bar{K}_{n+1} . This modified function is defined by an equation, not proved here, which describes the structure of K_{n+1} , and from which, on substitution into Eq. (7), the above two equations may be derived:

$$(24) \quad K_{n+1} = (n+1)^{-1} \{ K_1 (\Delta_F^n \mathcal{S}_n) \} + (K_1 S_F'^{-1} \Delta_F^{-1}) \bar{K}_{n+1} (S_F'^{-1} \Delta_F^{-1} K_1).$$

This is illustrated in Fig. 3.

Because of the appearance of the self-energy function Σ in j_n (Eq. (22)), and because of the equation satisfied

by S'_F (Eq. (6), $n = 0$),

$$(25) \quad S'_F = S_F + S_F \Sigma S'_F,$$

it is possible to rewrite Eq. (6) (for $n \neq 0$) in terms of S'_F :

$$(26) \quad K_n = S'_F A_F^n S_n + S'_F A_F^n J_n K_n.$$

(This is trivially true for $n = 0$, since $J_0 = 0$ by Eq. (22).)

Eqs. (23) through (26) now take the place of Eqs. (6) and (7), except that the primitive divergent functions Σ and I_5^β are not yet properly described. The functions I_5^α and I_5^β are defined by Eqs. (20), and can therefore also be described by integral equations related to that satisfied by K_1 (Eq. (26), $n = 1$):

$$(27) \quad \begin{cases} I_5^\alpha = \gamma_5 = I_5^\alpha S'_F J_1 I_1, \\ I_5^\beta = \gamma_5 = J_1 S'_F J_1 I_5^\beta. \end{cases}$$

The self-energy function Σ is described by Eq. (7), $n = 0$, which can be changed, with the aid of Eqs. (20), to involve the I_5^β functions rather than γ_5 :

$$(28) \quad \begin{cases} \Sigma = g^2 \gamma_5 K_1 \gamma_5, \\ \quad = g^2 I_5^\alpha S'_F A_F K_1^{-1} S'_F A_F I_5^\beta, \\ \quad = g^2 I_5^\alpha (S'_F A_F - S'_F A_F J_1 S'_F A_F) I_5^\beta. \end{cases}$$

This form for Σ does in fact remove the overlapping divergences if the subtraction is performed before the final two integrations, leaving only a simple linear divergence, which can be removed by two ordinary subtractions. (This is necessarily true, of course, only up to finite powers of g .)

We can now proceed in the usual way and suppose that the divergent functions we have developed can be expressed as multiples or combinations of certain associated finite functions. In particular, denoting finite quantities by a superscript R , we will suppose that

$$(29) \quad \begin{cases} m = m^R - \delta m, & I_5 = Z_1^{-1} I_5^R, \\ S'_F = Z_2 S'^R_F, & g = Z_1 Z_2^{-1} g^R. \end{cases}$$

The normalization of g is determined by the requirements of finiteness, apart from an arbitrary finite factor with which we are not concerned here. The normalization of I_5^R and S'^R_F is to be determined by conditions imposed on their free-particle behavior:



Fig. 3. - Structure of K_{n+1} .

$$(30) \quad \begin{cases} [(S_F'^R)^{-1}]_F = 0, \\ [-i(\gamma \cdot p + m^R)^{-1}(S_F'^R)^{-1}]_F = 1, \\ [I_5^R]_F = \gamma_5. \end{cases}$$

The notation $[\]_F$ means for $S_F'^R$ that $i\gamma \cdot p + m^R$ is to be set equal to zero, and for $I_5^R(p', p)$ ($= I_5^R(p; p - p')$), that $i\gamma \cdot p' + m^R$ is to be set equal to zero when it appears as a factor on the left, $i\gamma \cdot p + m^R$ is to be set equal to zero when it appears as a factor on the right, and $(p - p')^2$ is to be set equal to zero (or, as an alternative procedure, to $-\mu^2$) wherever it may appear. The covariant form of these functions assures that these conditions do indeed determine an unambiguous free-particle limit independent of p and p' .

It is much more convenient, on the other hand, to normalize in terms of the behavior of S_F' and I_5 for p and p' near zero. On grounds of covariance, we can write

$$(31) \quad \begin{cases} [(S_F'^R)^{-1}]_{p=0} = a, \\ [(\partial/\partial p_\mu)(S_F'^R)^{-1}]_{p=0} = b\gamma_\mu, \\ [I_5^R]_{p'=p=0} = c\gamma_5, \end{cases}$$

where a , b , and c are unknown, but presumably finite, constants. If we use the conditions (31) to normalize $S_F'^R$ and I_5^R , then we can adjust these constants at the end so that the conditions (30) are satisfied.

The functions K_n and J_n are renormalized by the same factors as S_F' and $(S_F')^{-1}$, respectively, while the equations describing them remain unaltered in form. If we make the substitutions (29) into the set of equations (23)-(28) which now describe the problem, and eliminate the constants Z_1 , Z_2 , and δm by means of the conditions (31), we arrive at the corresponding set of renormalized equations. (A_F and μ , of course, require no renormalization.) Rearranging the form of the equations slightly, we have, finally,

$$(32) \quad \begin{cases} K_n^R = S_F'^R A_F^n S_n + S_F'^R A_F^n J_n^R K_n^R; \\ J_n^R = (n+1)(g^R)^2 \Delta_F^{-n} \Gamma_5^{\alpha R} \bar{K}_{n+1}^R \Gamma_5^{\beta R} \Delta_F^{-n}; \\ \bar{K}_{n-1}^R = [(K_1^R)^{-1} S_F'^R A_F] [K_{n+1}^R - (n+1)^{-1} \{K_1^R (A_F^n S_n)\}] S_F'^R A_F (K_1^R)^{-1}; \\ (S_F'^R)^{-1} = a + b\gamma \cdot p - \Sigma_1; \\ \Sigma_1 = \int \{ \Sigma' - [\Sigma']_{p=0} - p_\mu [\partial \Sigma' / \partial p_{\mu}]_{p=0} \}; \\ \Sigma' = (g^R)^2 \Gamma_5^{\alpha R} S_F'^R \Delta_F (K_1^R)^{-1} S_F'^R A_F \Gamma_5^{\beta R} \text{ (not integrated); } \\ I_5^{\beta R} = c\gamma_5 + \int \{ J_1^R S_F'^R A_F I_5^{\beta R} - [J_1^R S_F'^R A_F I_5^{\beta R}]_{p=k=0} \}; \\ I_5^R = c\gamma_5 + \int \{ \Gamma_5^{\alpha R} S_F'^R \Delta_F J_1^R - [\Gamma_5^{\alpha R} S_F'^R \Delta_F J_1^R]_{p=k=0} \}. \end{cases}$$

The explicit appearance of the integral signs is simply to make it clear that the indicated subtractions are to be performed on the integrands, so that the actual integrations may be convergent. This could not be done if the free-particle conditions (30) were used, since the free-particle limit is not defined for the integrands, in which the integration variables appear explicitly. The constants a and b may be eliminated from the equation for $(S'_F)^{-1}$ by using the conditions (30) and the finite function Σ_1 defined above:

$$(33) \quad \begin{cases} (S'_F)^{-1} = i(\gamma \cdot p + m^R) - \Sigma^R, \\ \Sigma^R = \Sigma_1 - [\Sigma_1]_F - (i\gamma \cdot p + m^R)[(\gamma \cdot p + m^R)^{-1}(\Sigma_1 - [\Sigma_1]_F)]_F. \end{cases}$$

The equation for I_5^{NR} (like the one for I_5^{SR}) can be reduced to two ordinary integral equations, one for $I_5^{NR}(0; k)$, and the other for $I_5^{NR}(p; k) - I_5^{NR}(0; k)$. The solution of the latter can be expressed in terms of $I_5^{NR}(0; k)$ and the function K_1 .

2.1. The Approximation $A^{(N)}$. — The effect of the approximation $A^{(N)}$ on these equations can be foreseen in the light of the original description of $A^{(N)}$, as corresponding to those Feynman graphs which cannot be cut (except trivially) in more than N meson lines. The essential modification outside of the fact that J_γ is taken to be zero, is in the equation (24) describing the structure of K_{n+1} in terms of \bar{K}_{n+1} . This becomes, in a natural way,

$$(34) \quad K_{n+1}^{(N)} = (n+1)^{-1} \{ K_1^{(N-n)}(A_F^n S_n) \} + \\ + [K_1^{(N-n)}(S_F^{(N-n-1)})^{-1} \bar{A}_F^{-1} \bar{K}_{n+1}^{(N)} [(S_F^{(N-n-1)})^{-1} \bar{A}_F^{-1} K_1^{(N-n)}],$$

where the lower-order approximations to K_1 and S'_F also enter. The result of this for the renormalized equations (32) is that lower-order approximations to S'_F , I_5^N , I_5^B , and K_1 appear in most of the equations; the appropriate order of approximation follows from the description of $A^{(N)}$. As a result, if the lower-order approximations are presumed solved, then the integral equations which one would have to solve to do the approximation $A^{(N)}$ are each linear, like the original integral equations (6), but unlike the complete set of renormalized equations (32) without approximation.

2.2. The Renormalized Matrix Element. — In order to obtain the renormalized scattering matrix element by means of the technique described earlier, it is convenient to perform the functional differentiations before renormalization, to avoid the irrelevant problem of renormalizing in the presence of the external field. The function $[\delta^2 S'_F / (\delta g q^2)]_{q^2=0}$ can then be renormalized in a manner quite analogous to that just described. Eq. (3) must be modified, however,

to take into account the wave function renormalization, the essential result being that self-energy parts associated with the incoming and outgoing free particles are completely absorbed in the renormalization, and do not appear in the final expression for the matrix element. This means that in Eq. (3) each of the factors S_F^{-1} is simply replaced by $(S_F')^{-1}$, so that

$$(35) \quad M^R = 4\pi^2(\omega\omega')^{-\frac{1}{2}}(g^R)^2 \delta^4(P' - P) \bar{u}_f^R(P - k') \cdot \left\{ (S_F')^{-1} \left[\frac{\delta^2 S_F'}{\delta g q^e (-k') \delta g q^e (k)} \right]_{q^e=0}^R (S_F')^{-1} \right\} u_i^R(P - k).$$

One few feature in the functional differentiation process arises now because the first derivative of $(S_F')^{-1}$ is the vertex function I_5^R , in a different functional form from either I_5^R or I_5^0 . In particular, in the approximation $A^{(N)}$, when the Tamm-Dancoff-like limit is imposed on the number of mesons allowed, the real initial and final mesons represented by the functional differentiations are not counted, so that I_5^R becomes indeed quite different from I_5^R and I_5^0 , and must be renormalized independently. The equations describing $[\delta^2 S_F' / (\delta g q^e)^2]_{q^e=0}^R$ are set down below, and can be derived readily by the sort of procedures already used. In the approximation $A^{(N)}$, the functions S_F' , I_5^R , and K_1 in lower-order approximations will appear in a consistent way.

$$(36) \quad \left\{ \begin{aligned} & \left[\frac{\delta (S_F')^{-1}}{\delta g q^e} \right]_{q^e=0}^R = -I_5^R = -c\gamma_5 + (g^R)^2 \int \left\{ I_5^{\alpha R} S_F'^R \Delta_F \left[\frac{\delta K_1^{-1}}{\delta g q^e} \right]_{q^e=0}^R \right. \\ & \quad \left. + S_F'^R \Delta_F I_5^{\beta R} - \left[I_5^{\alpha R} S_F'^R \Delta_F \left[\frac{\delta K_1^{-1}}{\delta g q^e} \right]_{q^e=0}^R S_F'^R \Delta_F I_5^{\beta R} \right]_{q^e=0} \right\}; \\ & \left[\frac{\delta^2 (S_F')^{-1}}{(\delta g q^e)^2} \right]_{q^e=0}^R = (g^R)^2 I_5^{\alpha R} S_F'^R \Delta_F \left\{ (K_1^R)^{-1} \left[\frac{\delta^2 K_1}{(\delta g q^e)^2} \right]_{q^e=0}^R (K_1^R)^{-1} \right\} S_F'^R \Delta_F I_5^{\beta R}; \\ & \left[\frac{\delta K_n^{-1}}{\delta g q^e} \right]_{q^e=0}^R = -I_5^R \Delta_F^n \mathcal{S}_n - (n+1)(g^R)^2 \Delta_F^n I_5^{\alpha R} S_F'^R \Delta_F; \\ & \quad \cdot \left\{ (K_1^R)^{-1} \left[\frac{\delta}{\delta g q^e} (K_{n+1} - (n+1)^{-1} \{ K_1 (\Delta_F^n \mathcal{S}_n) \}) \right]_{q^e=0}^R (K_1^R)^{-1} \right\} S_F'^R \Delta_F I_5^{\beta R} \Delta_F^n; \\ & \left[\frac{\delta^2 K_n^{-1}}{(\delta g q^e)^2} \right]_{q^e=0}^R = \left[\frac{\delta^2 (S_F')^{-1}}{(\delta g q^e)^2} \right]_{q^e=0}^R \Delta_F^n \mathcal{S}_n - (n+1)(g^R)^2 \Delta_F^n I_5^{\alpha R} S_F'^R \Delta_F; \\ & \quad \cdot \left\{ (K_1^R)^{-1} \left[\frac{\delta^2}{(\delta g q^e)^2} (K_{n+1} - (n+1)^{-1} \{ K_1 (\Delta_F^n \mathcal{S}_n) \}) \right]_{q^e=0}^R (K_1^R)^{-1} \right\} S_F'^R \Delta_F I_5^{\beta R} \Delta_F^n. \end{aligned} \right.$$

Here again, in the equation for I_5^R , an integration symbol appears explicitly to make clear that the subtraction is to be performed before the integration.

In the approximation $A^{(A)}$, the constant c in this equation will differ from that needed to normalize I_5^α and I_5^β .

These equations are based on certain details of the structure of K_{n+1} , described in Eq. (24), which are reasonable but have not been proved here. The rigorous justification of Eq. (21) involves classifying the various permutations involved in the symmetrizing operator \mathcal{S}_n , and is quite complicated. By such a procedure it is possible to obtain for \bar{K}_{n+1} , and for its functional derivatives appearing in Eqs. (36), explicit expressions which reveal the validity of this procedure.

3. - Conclusion.

Little enough can be said about the existence or nature of the solutions to integral equations such as these. The lowest order approximation $A^{(1)}$ can be solved by quadratures ⁽²⁰⁾, and shows nonphysical singularities, or ghosts, in the solution. The approximation $A^{(2)}$ has been examined in some detail ^(*), but without being solved except quite crudely. A reliable approximation for this case would be of considerable interest for comparison with the closely corresponding non-covariant treatment ⁽³⁾. It is almost certain that ghosts will appear in any finite approximation, and the possibility that a limit as $N \rightarrow \infty$ might exist and be ghost-free is not of much practical value. The question of the convergence as $N \rightarrow \infty$ of a Tamm-Dancoff-like approximation is in fact a serious one since if there is no convergence it seems unlikely that the approximation can be good for any value of N . DALITZ and DYSON discuss this matter (Ref. ⁽³⁾, p. 313). We have pointed out above that the power series expansion of the solution is correctly renormalized and finite to any given order in the coupling constant g . This power series may converge for a certain domain of values of g , in which case this would define the solution to the problem, even though there might be a multiplicity of solutions to the equations. Outside this domain of convergence, however, a multiplicity of solutions would leave the true solution indeterminate, and described at best by a finite number of additional parameters. Further physical requirements might, with luck, determine the correct solution unambiguously.

It may still turn out that such difficulties if they do occur may arise because of the unphysical nature of the approximations imposed, and that an approach such as that of Low ⁽¹²⁾, where the natural approximation is itself expressed in terms of physical states of the system, will not be subject to ambiguities and non-physical singularities.

⁽²⁰⁾ K. A. BRUECKNER, M. GELL-MANN and M. GOLDBERGER: *Phys. Rev.*, **90**, 476 (1953).

* * *

The author wishes to express his gratitude to Brookhaven National Laboratory and to Professor J. R. OPPENHEIMER and The Institute for Advanced Study for their generous hospitality; and to Drs. A. KLEIN, M. ROSS, and T. FULTON for helpful discussions.

RIASSUNTO (*)

In termini della soluzione di una sequenza connessa di equazioni integrali lineari si descrive un metodo covariante per l'approssimazione della funzione nucleonica di Green S'_F . Per differenziazione funzionale formale di S'_F rispetto al campo bosonico esterno si ottengono espressioni esplicite per gli elementi di matrice di processi che coinvolgono un solo nucleone reale. Si rinormalizza la soluzione nel senso che il suo sviluppo in serie di potenze della costante d'accoppiamento g è uguale a quello ottenuto enumerando i diagrammi di Feynman e rinormalizzando termine a termine. Si trascurano le anse chiuse, pur includendo coppie virtuali di nucleoni non corrispondenti ad anse chiuse.

(*) Traduzione a cura della Redazione.

Polarization of Nucleons from Photodisintegration of Deuterium.

W. CZYŻ

Physical Institute, Jagellonian University - Kraków, Poland

J. SAWICKI

Institute of Theoretical Physics, University of Warsaw - Warsaw

(ricevuto il 23 Settembre 1956)

Summary. — The polarization of nucleons from the $D(\gamma, n)$ reaction is investigated under the assumption of tensor coupling in the n - p interaction potential. Dipole electric and dipole magnetic transitions are taken into consideration. The polarization is estimated for $\hbar\omega=40$ MeV with the help of recent p - p scattering phase shifts. For sake of illustration the polarization is given for the very singular $\mathbf{L}\cdot\mathbf{S}$ Case and Pais force in Born approximation and for the weak tensor forces of Rarita and Schwinger. The polarization is sensitive to the type of interaction. The general scheme of calculation of the reaction amplitude for tensor forces is given. The quadrupole electric corrections to the polarization are discussed.

1. — Introduction.

Very little is known thus far theoretically and nothing experimentally of the polarization of nucleons in photonuclear reactions. Recently the authors of the present paper gave an outline of calculation of the polarization of photoneutrons for one-particle nuclear models ⁽¹⁾. The polarization effect estimated in ⁽¹⁾ for the ${}^9\text{Be}(\gamma, n){}^8\text{Be}$ reaction was found considerable. Having overcome the experimental difficulties (small yields for the photoreactions) the investigation of polarization might provide new information concerning nuclear interactions.

⁽¹⁾ W. CZYŻ and J. SAWICKI: *Nuovo Cimento*, **3**, 864 (1956).

The aim of the present paper is the investigation of the general features of the polarization effect in photodisintegration of deuterium. The polarization will be expressed in terms of the radial integrals corresponding to different multipole transitions and corresponding phase shifts. The phase shifts are known from the analysis of the nucleon-nucleon scattering. However, unfortunately, no reasonable nucleon-nucleon interaction has been found so far to give a consistent description of the nucleon-nucleon scattering data. Therefore the final state continuum radial wave functions are unknown and this does it impossible to perform exactly the necessary radial integrals. It is hoped that the future analysis of the phase shifts on the methods as suggested by BREIT *et al.* and CLEMENTEL and VILLI ⁽²⁾ will lead to the determination of the interaction potentials and to the radial wave functions. Then the investigation of the polarization in the deuteron photoeffect may be useful in providing a check or some additional information concerning the neutron-proton interaction.

The polarization of nucleons from the $D(\gamma, n)$ reaction was theoretically discussed by L. N. ROZENZWEIG ⁽³⁾. His calculation applies to the zero range approximation and the central n-p forces and is thus confined to low energies. The calculations given below indicate the importance of noncentral forces or spin-orbit forces in some cases in the medium energy range. However, the most important factor causing the polarization of nucleons from the $D(\gamma, n)$ reaction is, as it was indicated in ⁽³⁾, the dipole electric-dipole magnetic interference.

2. — Notation.

J, M_J	the total angular momentum of a final state and its z -axis projection.
L, M_L	the orbital angular momentum of a final state and its z -axis projection.
j, m	the total angular momentum of a initial state and its z -axis projection.
$Y_{L, M_L}(\theta, \varphi)$	the spherical harmonics as defined in ref. ⁽⁴⁾ .
$\mathcal{Q}_{J, L, S}^{UJ}(\theta, \varphi)$	the total angular momentum eigenfunction as defined in ref. ⁽⁴⁾ .
$\chi_{10}^m(\sigma)$	the triplet state spin eigenfunction.
$\chi_0(\sigma)$	the singlet state spin eigenfunction.

⁽²⁾ R. M. THALER and J. BENGSTON: *Phys. Rev.*, **94**, 679 (1954); R. M. THALER, J. BENGSTON and G. BREIT: *Phys. Rev.*, **94**, 683 (1954); G. BREIT and M. H. HULL: *Phys. Rev.*, **97**, 1047 (1955).

⁽³⁾ L. N. ROZENZWEIG: *Žu. Ėksper. Teor. Fiz.*, to be published.

⁽⁴⁾ J. M. BLATT and V. F. WEISSKOPF: *Theoretical Nuclear Physics* (1952).

π	the parity as defined in ref. (5): $(-)^{J+L}$.
η_J	the 3P_J -state phase shift.
δ_s	the 1S_0 -state phase shift.
E	the centre of mass system energy of the relative motion of the n-p system.
k	the n-p system wave vector in the c. m. system ($k = \sqrt{ME/\hbar^2}$).
H'	the time independent part of the interaction of the electromagnetic field with the nucleons.
k_0	the wave vector of the incident photon.
e	the polarization vector of the incident photon.
M	the nucleon mass.
μ_n, μ_p	the magnetic moments of the neutron and the proton (in nuclear magnetons).
σ_n, σ_p	the neutron and the proton spin operators.
$f\chi$	the reaction amplitude: $f\chi = g\chi_0^0 + \sum_{m_s=-1}^1 f_{m_s} \chi_1^{m_s}$.
P	the polarization vector.
$\{...\}_{av}$	denotes averaging over the photon polarizations and the magnetic quantum numbers m of the ground state.
u_0	the 1S_0 -state radial eigenfunction.
u, w	the deuteron ground state radial eigenfunctions (of the S and the D states respectively).
r_J	the radial eigenfunction of the noncoupled ($L = J$) state.
u_J, w_J	the radial eigenfunctions of the coupled ($L = J - 1, L = J + 1$)
$j_i(x), n_i(x)$	the spherical Bessel and Neumann functions.
ε_J	the mixture parameter as defined in ref. (5).

3. - Calculations.

To calculate the polarization one has to determine the reaction amplitude $f\chi$ and use the equation:

$$(1) \quad P = \frac{\{\langle f\chi | \sigma_n | f\chi \rangle\}_{av}}{\{f\chi | f\chi\}_{av}}.$$

The general method of the calculation of $f\chi$ for tensor forces is given in Appendix I. Only the dipole electric and the dipole magnetic transitions from

(5) J. M. BLATT and L. C. BIEDENHARN: *Phys. Rev.*, **86**, 399 (1952).

the $^3S_1 + ^3D_1$ ground state are considered below (the quadrupole electric corrections are considered in Appendix II). Besides the following further simplifications are adopted below: only the dominating dipole magnetic transition to the singlet 1S_0 -state is taken into account and the very small 3F_2 -state admixture to the 3P_2 -state is neglected (see e.g. (6)). Thus we arrive at the only final states: 1S_0 , 3P_0 , 3P_1 , 3P_2 . Thus a similar situation in the calculations is obtained as in the case of a pure $\mathbf{L} \cdot \mathbf{S}$ coupling.

Similarly as in ref. (1) (see also Appendix I) we obtain for the wave function of the n-p system:

$$(2) \quad \Psi(\mathbf{r}, t) \sim f\chi r^{-1} \exp \left[ikr - \frac{iE}{\hbar} t \right],$$

where the reaction amplitude $f\chi = g\chi_0^0 + f_{-1}\chi_1^{-1} + f_0\chi_1^0 + f_1\chi_1^1$. In our simplified (in comparison to that of Appendix I) case we obtain (the unimportant factor $\pi N(E)/k$ being omitted):

$$(3) \quad f\chi = \exp[i\delta_s] \mathcal{Q}_{000}^0 H_{1,m}^{'00} - i(\exp[i\eta_0] \mathcal{Q}_{011}^0 H_{1,m}^{'0,0} + \\ + \exp[i\eta_1] \sum_{M_J=-1}^1 \mathcal{Q}_{111}^{M_J} H_{1,m}^{'1,M_J} + \exp[i\eta_2] \sum_{M_J=-2}^2 \mathcal{Q}_{211}^{M_J} H_{1,m}^{'2,M_J})$$

(the matrix elements $H_{1,m}^{'J,M_J}$ in the brackets correspond to the 3P_J -states). Similarly as in (1) the quantization axis is chosen along the vector $\mathbf{k} \propto \mathbf{k}_0$. In the present approximation H' is proportional to the expression

$$\mathbf{e} \cdot \mathbf{r} + \frac{\hbar}{2Mc} (\mu_n - \mu_p) \left(\frac{\mathbf{k}_0}{k_0} \times \mathbf{e} \right) \cdot (\boldsymbol{\sigma}_n - \boldsymbol{\sigma}_p).$$

On using the same system of reference as in ref. (1) we may write:

$$(4) \quad \mathbf{e} \cdot \mathbf{r} + \frac{\hbar}{2Mc} (\mu_n - \mu_p) \left(\frac{\mathbf{k}_0}{k_0} \times \mathbf{e} \right) \cdot (\boldsymbol{\sigma}_n - \boldsymbol{\sigma}_p) - \left[z + \frac{\hbar}{2Mc} (\mu_n - \mu_p) (\sigma_{nz} - \sigma_{pz}) \right] \cos \varphi + \\ + \left[x - \frac{\hbar}{2Mc} (\mu_n - \mu_p) (\sigma_{nx} - \sigma_{px}) \right] \sin \varphi,$$

where $\varphi = \angle(\mathbf{e}; \mathbf{k} \times \mathbf{k}_0)$. We may express f_{m_s} and g in terms of $\cos \varphi$ and $\sin \varphi$: $f_{m_s} = f_{m_s}^z \cos \varphi + f_{m_s}^x \sin \varphi$, $g = g^z \cos \varphi + g^x \sin \varphi$. In our frame of reference the components P_x and P_y vanish. On using the equation

$$(5) \quad \langle f\chi | \sigma_{nz} | f\chi \rangle = 2 \operatorname{Re} (g^* f_0) + |f_1|^2 - |f_{-1}|^2$$

(6) N. AUSTERN: *Phys. Rev.*, **85**, 283 (1952).

and Eq. (1) we get:

$$(6) \quad P = P_z = \frac{\sum_m [2 \operatorname{Re} (g^{z*} f_0^z) + 2 \operatorname{Re} (g^{z*} f_0^z) + |f_1^z|^2 - |f_{-1}^z|^2]}{\sum_m [|g^z|^2 + |g^z|^2 + \sum_{m_s} (|f_{m_s}^z|^2 + |f_{m_s}^z|^2)]}.$$

After performing the angular integrals, the summations over the magnetic quantum numbers of the final states and the averaging over the magnetic quantum numbers of the initial states we may express P in terms of the radial integrals and phase shifts:

$$(7) \quad P = (\tilde{\sigma})^{-1} \left\{ \frac{1}{2} \left[\frac{1}{3} I_0 I_2 \sin (\eta_0 - \eta_2) + \frac{1}{2} I_1 I_2 \sin (\eta_1 - \eta_2) \right] \sin 2\theta + \right. \\ \left. + \frac{\hbar}{Mc} (\mu_p - \mu_n) I_s I_1 \sin (\eta_1 - \delta_s) \sin \theta \right\},$$

$$(8) \quad \tilde{\sigma} = \frac{\hbar^2}{M^2 c^2} (\mu_n - \mu_p)^2 I_s^2 + \frac{1}{9} I_0^2 + \frac{5}{16} I_1^2 + \frac{73}{144} I_2^2 - \frac{1}{18} I_0 I_2 \cos (\eta_0 - \eta_2) - \\ - \frac{1}{8} I_1 I_2 \cos (\eta_1 - \eta_2) - \\ - \left[\frac{1}{16} I_1^2 + \frac{7}{48} I_2^2 + \frac{1}{6} I_0 I_2 \cos (\eta_0 - \eta_2) + \frac{3}{8} I_1 I_2 \cos (\eta_1 - \eta_2) \right] \cos 2\theta,$$

where

$$I_0 = \int_0^\infty r v_0 (u - 2^{\frac{1}{2}} w) dr, \quad I_1 = \int_0^\infty r v_1 (u + 2^{-\frac{1}{2}} w) dr, \\ I_2 = \int_0^\infty r u_2 \left(u - \frac{1}{5} 2^{-\frac{1}{2}} w \right) dr, \quad I_s = \int_0^\infty u_0 u dr.$$

The expression (8) (excluding the first magnetic term) gives the electric dipole angular distribution of photoneutrons in exact accordance with Eq. (28) of RARITA and SCHWINGER (see (7)).

4. - Discussion and Numerical Results.

As it is seen from Eqs. (7) and (8) the angular dependence of the polarization is of the form:

$$(9) \quad P = \frac{a \sin 2\theta + b \sin \theta}{c + d \sin^2 \theta}.$$

(7) W. RARITA and J. SCHWINGER: *Phys. Rev.*, **59**, 556 (1941).

The first term of the numerator comes from the dipole electric transitions. It is the larger, the larger is the 3P_J -state splitting and vanishes if this splitting is zero. Thus it is zero for low energies of the incident γ -quanta. The second term comes from the electric dipole and the magnetic dipole interference. As it was indicated for low energies by ROZENZWEIG ⁽³⁾ and is shown below, this term is the most important factor causing the polarization. However, in the medium energy range the dipole electric transitions may become most important for the angular dependence and the maximum values of the polarization. The isotropic term in the denominator comes both from the dipole electric and the dipole magnetic transition. It increases seriously in the case of strong 3P_J -states splittings. The second term in the denominator comes from the pure dipole electric transitions. On increasing the 3P_J -states splitting we increase both the maximum values of the nominator and the denominator. If a and b are of the same sign, the contributions from the dipole electric and dipole magnetic transitions add to each other in the region $0 < \theta < \pi/2$ and subtract for $\pi/2 \leq \theta < \pi$. If a and b are of different sign, the situation is reversed: P is small for $0 < \theta < \pi/2$ and large for $\pi/2 \leq \theta < \pi$. Thus a change of sign of a or b shifts the maximum polarization from the forward photonucleon beam to the backward photonucleon beam or conversely.

In the present state of information concerning the nucleon-nucleon interaction only a crude numerical estimation of the radial integrals is possible. Eventually, these integrals may be calculated exactly, but under the assumption of a certain of the up to date known theories of nuclear forces. As is well known, no one of these theories gives satisfactory results. Nevertheless we give below a series of numerical results for several energies in order to investigate the sensitiveness of the polarization to energy and some details of the interactions involved. These examples will also give the view of the order of magnitude of the polarization and the role of different transitions in its creation.

Example 1. — Estimation of $P(\theta)$ was performed for the energy $\hbar\omega=40$ MeV. For this sake we used with the respect to the charge independence of nuclear forces the 3P_J and 1S_0 phase shifts obtained by E. CLEMENTEL and C. VILLI ⁽⁸⁾ satisfactory in description of recent experimental data in the energy range 15 : 260 MeV. The small D -state admixture in the deuteron ground state was neglected. It was assumed that the contributions to the radial integrals corresponding to the region $0 < r < r_c$, where r_c is a quantity of the order of the range of nuclear forces, is small as compared with the contribution coming from the region $r_c < r < \infty$. It seems that this is justified for short-ranged

(⁸) E. CLEMENTEL and C. VILLI: to be published.

singular potentials for energies $\hbar\omega \lesssim 50$ MeV. This «cut-off» procedure was checked for the example of the $\mathbf{L} \cdot \mathbf{S}$ potential of CASE and PAIS ⁽⁹⁾ with the help of the radial wave functions $r_J u_2$ obtained graphically from a differential analyser. The last assumption is equivalent to the assumption of the following expression for I_J :

$$(10) \quad I_J \approx \int_{r_c}^{\infty} r^2 [j_1(kr) \cos \eta_J - \eta_1(kr) \sin \eta_J] u \, dr,$$

where $u = \exp[-\alpha r] - \exp[-\beta r]$ as given e.g. in ref. ⁽⁶⁾. The value $r_c = 2 \cdot 10^{-13}$ cm was used. Such an approximation for $I_s = \int_0^{\infty} u u_0 dr$ is rather too crude and hence I_s was computed on the method given by S. HSIEH ⁽¹⁰⁾. u_0 was adopted in the form $u_0 = \sin(kr + \delta_s)(1 - \exp[-\zeta(r - D_0)])$. The parameters ζ and D_0 were chosen such that u_0 corresponds to the repulsive core of the radius $0.2 \cdot 10^{-13}$ cm, i.e. the core radius as suggested for the 1S_0 -state from the p-p scattering analysis (see e.g. CLEMENTEL and VILLI ⁽¹¹⁾). Finally we obtain:

$$(11) \quad P(\theta) = \frac{0.102 \sin 2\theta - 0.352 \sin \theta}{0.395 + \sin^2 \theta} \quad \text{for } \hbar\omega = 40 \text{ MeV}.$$

The maximum absolute value is: $-P_{\max} = -P_{\hbar\omega=40 \text{ MeV}}(\theta = 149^\circ) = 41.1 \%$

Example 2. — $P(\theta)$ was calculated for different energies $\hbar\omega$ for the $\mathbf{L} \cdot \mathbf{S}$ force of CASE and PAIS ⁽⁹⁾ assumed to act in the 3P_s -states. $P(\theta)$ was calculated in Born approximation (*). In calculations based on Austern's numerical results eventual changes coming from the magnetic dipole transitions corresponding to the corrections from the exchange meson current effects in the n-p system were taken into account. The maximum and minimum values of the magnetic dipole coefficients are given in Table I. It is seen from Table I that these corrections are rather small in the energy range involved. The

⁽⁹⁾ K. M. CASE and A. PAIS: *Phys. Rev.*, **80**, 203 (1950).

⁽¹⁰⁾ S. HSIEH: *Nuovo Cimento*, **4**, 138 (1956).

⁽¹¹⁾ E. CLEMENTEL: private communication.

(*) The values of the radial integrals I_J and I_s , with the taking into account, of the 3D_1 -ground state admixture, and the phases η_J , δ_s were computed from the data given by N. AUSTERN in Born approximation (private communication). These Born approximation calculations may be trusted at least qualitatively.

maximum absolute values of P are given also in Table I.

TABLE I.

$\hbar\omega$ (MeV)	22.4	43.5		61.6	
a	0.049	0.041	0.041	— 0.027	— 0.027
b_{\min}	— 0.066	— 0.045		— 0.032	
b_{\max}	— 0.066		— 0.063		— 0.056
c_{\min}	0.096	0.387		0.925	
c_{\max}	0.096		0.409		0.976
d	1	1	1	1	1
Max. P (%)	$P(160^\circ) =$ — 20.5	$P(149^\circ) =$ — 8.8	$P(149^\circ) =$ — 10.2	$P(46^\circ) =$ — 3.5	$P(46^\circ) =$ — 4.5

Example 3. — $P(\theta)$ was calculated for $\hbar\omega = 17.6$ MeV under the assumption of the weak tensor forces as introduced by RARITA and SCHWINGER (⁷). The results are given in Table II.

TABLE II.

Type of exchange	Symmetrical theory	Charged theory	Neutral theory
a	0.000 ₃	— 0.004	0.029
b	— 0.060	— 0.077	0.032
c	0.022	0.086	0.397
d	1	1	1
Max. P (%)	$P(172^\circ) = -20.5$	$P(23^\circ) = -13.9$	$P(34^\circ) = 6.3$

* * *

The authors are greatly indebted to Dr. N. AUSTERN, Dr. E. CLEMENTEL and Dr. L. ROZENZWEIG for letting them know their unpublished results. One of us (J. S.) thanks Dr. E. CLEMENTEL for an interesting discussion.

Our thanks are due to Professor L. INFELD and Professor H. NIEWODNICZAŃSKI for their kind interest in this work.

APPENDIX I

General Method of Calculation of the Reaction Amplitude for Tensor Forces.

The aim of the present Appendix I is to present the general method of calculation of the $D(\gamma, n)$ reaction amplitude taking account of the tensor forces. The calculation is analogous to the calculation for the spin-orbit forces given in ref. (1). The wave function of the system is of the form:

$$(I.1) \quad \Psi(\mathbf{r}, t) = \left(\sum_E + \int dE' \right) \left\{ \sum_{L, M_L} b_E(L, M_L) \varphi_E(L, M_L) + \sum_{J, M_J, \pi} a_E(J, M_J, \pi) \psi_E(J, M_J, \pi) \right\}.$$

The first sum in the braces applies to the singlet part of the function $\Psi(\mathbf{r}, t)$ and the second sum to the triplet part. q_E and ψ_E are the energy eigenfunction, b_E and a_E — the coefficients of the development will be subsequently calculated in the first approximation of the calculus of perturbations. The reaction amplitude corresponding to the singlet states may be calculated from the first sum in the brackets in Eq. (I.1) with the help of the well known calculations (see e.g. ref. (12)). On the other hand, the triplet part of the amplitude requires the generalized treatment as given below. On adopting the notation of ref. (5) we get three kinds of stationary orthogonal states corresponding to the same quantum numbers E', J, M_J .

$$(I.2) \quad \left\{ \begin{aligned} \psi_E(J, M_J, \pi = +1) &\sim \frac{N(E')}{kr} \sin(kr - \tfrac{1}{2}\pi J + \delta_{J0}) \mathcal{Q}_{J, J+1}^{MJ} \exp \left[-\frac{i}{\hbar} E' t \right], \\ \psi_E^\alpha(J, M_J, \pi = -1) &\sim \frac{M(E')}{kr} \left\{ \cos \varepsilon_J \sin[kr - \tfrac{1}{2}\pi(J-1) + \delta_{J\alpha}] \mathcal{Q}_{J, J-1, 1}^{MJ} + \right. \\ &\quad \left. + \sin \varepsilon_J \sin[kr - \tfrac{1}{2}\pi(J+1) + \delta_{J\alpha}] \mathcal{Q}_{J, J+1, 1}^{MJ} \right\} \exp \left[-\frac{i}{\hbar} E' t \right], \\ \psi_E^\beta(J, M_J, \pi = -1) &\sim \frac{N(E')}{kr} \left\{ -\sin \varepsilon_J \sin[kr - \tfrac{1}{2}\pi(J-1) + \delta_{J\beta}] \mathcal{Q}_{J, J-1, 1}^{MJ} + \right. \\ &\quad \left. + \cos \varepsilon_J \sin[kr - \tfrac{1}{2}\pi(J+1) + \delta_{J\beta}] \mathcal{Q}_{J, J+1, 1}^{MJ} \right\} \exp \left[-\frac{i}{\hbar} E' t \right], \end{aligned} \right.$$

$N(E')$ is the normalization factor. In the first approximation of the calculus

(12) N. F. MOTT and H. S. W. MASSEY: *Theory of Atomic Collisions* (1949).

of perturbations $\Psi(\mathbf{r}, t)$ is of the form:

$$(I.3) \quad \Psi(\mathbf{r}, t) = \left(\sum_{E'} + \int dE' \right) \cdot \left\{ \sum_{J, M_J, \pi} \frac{\exp[(i/\hbar)(E' - E_0 - \hbar\omega)t]}{E' - E_0 - \hbar\omega} H'_{j, m}^{J, M_J, \pi} \psi_{E'}(J, M_J, \pi) \right\},$$

where $H'_{j, m}^{J, M_J, \pi}$ is the matrix element:

$$(I.4) \quad H'_{j, m}^{J, M_J, \pi} = \int \psi_E^*(J, M_J, \pi) H' \psi_{E_0}(j, m) d\tau,$$

$\psi(j, m)$ is the initial state wave function of the binding energy E_0 . The integration over E' in Eq. (I.3) is performed as in ref. (12). On using the asymptotical expressions (I.2) we get:

$$(I.5) \quad \Psi(\mathbf{r}, t) \sim \frac{\pi N(E)}{kr} \exp \left[i \left(kr - \frac{Et}{\hbar} \right) \right] \cdot \sum_{J, M_J} \left[\mathcal{Q}_{J, J+1}^{M_J} H'_{j, m}^{J, M_J, \pi-1} \exp \left[i \left(-\frac{\pi}{2} J + \delta_{J\beta} \right) \right] + H'_{j, m}^{J, M_J, \pi-1, \alpha} \left\{ \cos \varepsilon_J \mathcal{Q}_{J, J-1, 1}^{M_J} \cdot \right. \right. \\ \cdot \exp \left[i \left(-\frac{\pi}{2} (J+1) + \delta_{J\alpha} \right) \right] + \sin \varepsilon_J \mathcal{Q}_{J, J+1, 1}^{M_J} \exp \left[i \left(-\frac{\pi}{2} (J+1) + \delta_{J\alpha} \right) \right] \Big\} + \\ + H'_{j, m}^{J, M_J, \pi=-1, \beta} \left\{ -\sin \varepsilon_J \mathcal{Q}_{J, J-1, 1}^{M_J} \exp \left[i \left(-\frac{\pi}{2} (J-1) + \delta_{J\beta} \right) \right] + \right. \\ \left. + \cos \varepsilon_J \mathcal{Q}_{J, J+1, 1}^{M_J} \exp \left[i \left(-\frac{\pi}{2} (J+1) + \delta_{J\beta} \right) \right] \right\} \Big].$$

The coefficient of the spherical wave in (I.5) is the requested reaction amplitude. This reaction amplitude may be represented in the form of matrix element of H' between the initial and the « final » state ψ_f . On using again the notation of ref. (5) we write:

$$(I.6) \quad \psi_f = \sum_{J, M_J} \left\{ \exp \left[i \left(\frac{\pi}{2} J - \delta_{J\beta} \right) \right] \mathcal{Q}_{J, J+1}^{M_J*}(\vartheta, \varphi) \mathcal{Q}_{J, J+1}^{M_J}(\vartheta', \varphi') \frac{v_J}{r} + \right. \\ + \left(\cos \varepsilon_J \exp \left[i \left(\frac{\pi}{2} (J-1) - \delta_{J\alpha} \right) \right] \mathcal{Q}_{J, J-1, 1}^{M_J*}(\vartheta, \varphi) + \sin \varepsilon_J \exp \left[i \left(\frac{\pi}{2} (J+1) - \delta_{J\alpha} \right) \right] \cdot \right. \\ \cdot \mathcal{Q}_{J, J+1, 1}^{M_J*}(\vartheta, \varphi) \Big) \left(\frac{u_J^\alpha}{r} \mathcal{Q}_{J, J-1, 1}^{M_J}(\vartheta', \varphi') + \frac{w_J^\alpha}{r} \mathcal{Q}_{J, J+1, 1}^{M_J}(\vartheta', \varphi') \right) + \\ + \left(-\sin \varepsilon_J \exp \left[i \left(\frac{\pi}{2} (J-1) - \delta_{J\beta} \right) \right] \mathcal{Q}_{J, J-1, 1}^{M_J*}(\vartheta, \varphi) + \right. \\ + \cos \varepsilon_J \exp \left[i \left(\frac{\pi}{2} (J+1) - \delta_{J\beta} \right) \right] \mathcal{Q}_{J, J+1, 1}^{M_J*}(\vartheta, \varphi) \Big) \cdot \\ \cdot \left(\frac{u_J^\beta}{r} \mathcal{Q}_{J, J-1, 1}^{M_J}(\vartheta', \varphi') + \frac{u_J^\beta}{r} \mathcal{Q}_{J, J+1, 1}^{M_J}(\vartheta', \varphi') \right) \Big\}.$$

One can show that ψ_f has asymptotical form: a plane wave plus a convergent spherical wave. To show this, we first observe that on setting all δ_{J_1} , δ_{J_2} , $\delta_{J\beta}$ equal zero in (I.6) ψ_f becomes asymptotically a plane wave. In fact, on using Eq. (I.2) we obtain:

$$(I.7) \quad \psi_f(\delta_{0,\alpha,\beta} = 0) \sim \sum_{J, M_J, L} \exp \left[i \frac{\pi}{2} L \right] \mathcal{Q}_{J, L, 1}^{M_J*}(\vartheta, \varphi) \mathcal{Q}_{J, L, 1}^{M_J}(\vartheta', \varphi') \frac{1}{r} \sin \left(kr - \frac{\pi}{2} L \right),$$

but

$$\sum_{J, M_J} \mathcal{Q}_{J, L, 1}^{M_J*}(\vartheta, \varphi) \mathcal{Q}_{J, L, 1}^{M_J}(\vartheta', \varphi') = \sum_{M_L, m_s} Y_{L, M_L}^*(\vartheta, \varphi) Y_{L, M_L}(\vartheta', \varphi') \chi_1^{m_s}(\sigma) \chi_1^{m_s}(\sigma'),$$

due to the orthogonality of the vector addition coefficients. On the other hand $\sum_{m_s} \chi_1^{m_s}(\sigma) \chi_1^{m_s}(\sigma') = \chi_1^0(\sigma')$, because $\chi_1^{m_s}(\sigma) = \delta_{m_s, 0}$. On using the addition theorem of spherical harmonics we get:

$$(I.8) \quad \psi_f(\delta_{0,\alpha,\beta} = 0) \sim \sum_L \exp \left[i \frac{\pi}{2} L \right] \frac{2L+1}{4\pi} P_L(\cos \theta) \chi_1^0(\sigma') \frac{1}{r} \sin \left(kr - \frac{\pi}{2} L \right).$$

Thus $\psi_f(\delta_{0,\alpha,\beta} = 0)$ is asymptotically a plane wave. It is easy to ascertain that $\psi_f - \psi_f(\delta_{0,\alpha,\beta} = 0)$ is a spherical convergent wave.

APPENDIX II

Quadrupole Electric Corrections.

On introducing the quadrupole interaction one has to replace the expression (4) by:

$$(II.1) \quad \mathbf{e} \cdot \mathbf{r} + i\mu(\mathbf{e} \cdot \mathbf{r}) \left(\frac{\mathbf{k}_0 \cdot \mathbf{r}}{k_0} \right) + \frac{\hbar}{2Mc} (\mu_n - \mu_p) \left(\frac{\mathbf{k}_0 \times \mathbf{e}}{k_0} \right) \cdot (\boldsymbol{\sigma}_n - \boldsymbol{\sigma}_p) = \\ = \left[z + i\mu zy + \frac{\hbar}{2Mc} (\mu_n - \mu_p^2)(\sigma_{nz} - \sigma_{pz}) \right] \cos \varphi + \\ + \left[x + i\mu xy - \frac{\hbar}{2Mc} (\mu_n - \mu_p^2)(\sigma_{nz} - \sigma_{pz}) \right] \sin \varphi,$$

where $\mu = \frac{1}{4}(\omega/c) - \frac{1}{4}k_0$. For further calculation we neglect the 3D_1 -state small admixture in the deuteron ground state. Since it is known from the phase shifts analysis ⁽¹⁾ that the 3D_J phases are very small, we shall consider these states as free. Under these simplifications, on performing calculations similarly as it was done previously we obtain the following expression for the polariz-

ation with the inclusion of the quadrupole corrections:

$$(II.2) \quad P_q = \left\{ \frac{1}{2} \left[\frac{1}{3} I_0 I_2 \sin(\eta_0 - \eta_2) + \frac{1}{2} I_1 I_2 \sin(\eta_1 - \eta_2) - \right. \right. \\ \left. - \frac{\mu}{6} I_D \cos \theta (5 I_2 \sin \eta_2 - 2 I_0 \sin \eta_0 - 3 I_1 \sin \eta_1) \right] \sin 2\theta + \\ \left. + \frac{\hbar}{Mc} (\mu_n - \mu_p) I_s \left[I_1 \sin(\delta_s - \eta_1) \sin \theta + \frac{1}{2} \mu I_D \sin \delta_s \sin 2\theta \right] \right\} \cdot \\ \cdot \left\{ \tilde{\sigma} + \frac{1}{2} \left[\frac{3}{4} \mu^2 I_D^2 \sin^2 2\theta + \mu I_D \sin \theta \sin 2\theta \left(\frac{1}{3} I_0 \cos \eta_0 + I_1 \cos \eta_1 + \frac{5}{3} I_2 \cos \eta_2 \right) \right] \right\}^{-1},$$

where $I_D = \int_0^\infty r^3 R_D^* u dr$ and R_D is the D -state radial wave function. It is immediately seen that the contribution to the numerator of P_q from the dipole electric — quadrupole electric interference vanishes, when the 3P_J state splitting is zero. The obtained polarization P_q has the angular dependence of the type:

$$(II.3) \quad P_q = \frac{a \sin 2\theta + b \sin \theta + \mu \alpha \cos \theta \sin 2\theta + \mu \beta \sin 2\theta}{c + d \sin^2 \theta + \mu \alpha' \sin \theta \sin 2\theta + \mu^2 \gamma' \sin^2 2\theta}.$$

The terms proportional to μ come from the interference of the quadrupole electric transitions: those $\sim \mu \alpha, \mu \alpha'$ — with the dipole electric and $\sim \mu \beta$ — with the dipole magnetic transitions. The term proportional to μ^2 corresponds to the pure quadrupole transitions. The denominator of the expression for P_q (II.3) gives the angular distribution of the type investigated by SCHIFF⁽¹³⁾ and MARSHALL and GUTH⁽¹⁴⁾. The numerical values of the corrections $\Delta P = P_q - P$ due to the inclusion of the quadrupole electric transitions were estimated for all the discussed examples and found not very important.

(13) L. I. SCHIFF: *Phys. Rev.*, **78**, 733 (1950).

(14) J. F. MARSHALL and E. GUTH: *Phys. Rev.*, **78**, 738 (1950).

RIASSUNTO (*)

Postulando accoppiamento tensoriale nel potenziale d'interazione n-p, si studia la polarizzazione dei nucleoni prodotti nella reazione $D(\gamma, n)$. Si prendono in considerazione transizioni di dipolo elettrico e magnetico. Con l'ausilio dei recenti spostamenti di fase p-p si valuta la polarizzazione per $\omega h = 40$ MeV. A titolo di esempio si dà in approssimazione di Born la polarizzazione per lo specialissimo caso del potenziale $L \cdot S$ di Case e Pais e per le forze tensoriali deboli di Rarita e Schwinger. La polarizzazione risente del tipo di interazione. Si dà lo schema generale di calcolo dell'ampiezza di reazione per le forze tensoriali. Si discutono le correzioni di quadrupolo elettrico da apportare alla polarizzazione.

(*) Traduzione a cura della Redazione.

A Special Representation for the Treatment of a System of two Dirac Particles.

H. JOOS, J. LEAL FERREIRA and A. H. ZIMMERMAN

Instituto de Física Teórica - São Paulo, Brasil

(ricevuto il 23 Settembre 1956)

Summary. — It is shown that in a representation where, besides angular momentum and parity, the radial velocities of two Dirac particles are also diagonal, the radial eigenvalue equations for the energy reduce to a system of four simultaneous differential equations. The usefulness of this representation is shown in the case of the Breit equation.

1. — In the semi-relativistic quantum mechanical treatment of the two body problem without external forces, i.e., a treatment which regards the two particles as relativistic Dirac particles but takes into account only a part of the retardation effects of the interaction, we have an eigen-value equation for the energy, in the center of mass system, of the following form ⁽¹⁾

$$(1) \quad \{c(\alpha^{(2)} - \alpha^{(1)})\mathbf{p} + \beta^{(1)}m_1c^2 + \beta^{(2)}m_2c^2 + \mathcal{I}(\mathbf{r}, \alpha^{(1)}, \alpha^{(2)}, \sigma^{(1)}, \sigma^{(2)}, \dots)\}\psi = E\psi,$$

where \mathbf{p} is the relative momentum, $\beta^{(1)}m_1$ and $\beta^{(2)}m_2$ the rest-mass operators of the two particles.

The interaction operator $\mathcal{I}(\mathbf{r}, \alpha^{(1)}, \alpha^{(2)}, \sigma^{(1)}, \sigma^{(2)}, \dots)$ is an expression built up from the relative distance \mathbf{r} , the Dirac velocity operators of the two particles $\alpha^{(1)}$ and $\alpha^{(2)}$, the corresponding spin matrices $\sigma^{(1)}$ and $\sigma^{(2)}$, etc., which is invariant under rotation and reflection. In the case, e.g., of Coulomb interaction with

⁽¹⁾ I. S. LOWEN: *Phys. Rev.*, **51**, 190 (1937); G. BREIT and G. E. BROWN: *Phys. Rev.*, **74**, 1278 (1948); G. BREIT and R. E. MEYEROTT: *Phys. Rev.*, **72**, 1023 (1947); **75**, 1447 (1949).

its Breit retardation effect we have:

$$\mathcal{J} = \frac{e_1 e_2}{r} \left\{ -1 + \frac{1}{2} \left[\boldsymbol{\alpha}^{(1)} \cdot \boldsymbol{\alpha}^{(2)} + \frac{(\boldsymbol{\alpha}^{(1)} \cdot \mathbf{r})(\boldsymbol{\alpha}^{(2)} \cdot \mathbf{r})}{r^2} \right] \right\}.$$

The wave function ψ is described by a 16-component spinor wave function. It is our purpose to show that the treatment of (1), in a certain representation, leads in a natural way to a reduction to a system of four simultaneous radial equations. This representation may be employed in many problems which usually require an approximate Foldy-Wouthuysen transformation⁽²⁾.

Let us regard eq. (1) in a representation, which is characterized by the simultaneous diagonal form of the following operators:

- (I) The radial distance $r = |\mathbf{r}|$,
- (II) The total angular momentum \mathbf{F} where $\mathbf{F} = \mathbf{r} \wedge \mathbf{p} + (\hbar/2)(\boldsymbol{\sigma}^{(1)} + \boldsymbol{\sigma}^{(2)})$,
- (III) The angular momentum in z -direction F_z ,
- (IV) The parity operator $S = \beta^{(1)}\beta^{(2)}R$, where $R\psi(\mathbf{r}) = \psi(-\mathbf{r})$,
- (V) The radial velocities of the two particles $\alpha_r^{(i)} = (\boldsymbol{\alpha}^{(i)} \cdot \mathbf{r})/r$, $i = 1, 2$,
- (VI) The product q of the Dirac⁽³⁾ pseudo scalars $q_1^{(i)}$, $i = 1, 2$, of the two particles.

From the invariance properties of the operators (I)-(VI) and the commutation rules for the Dirac matrices $[q_v^{(i)}, \sigma_v^{(i')}] = 0$, where $\boldsymbol{\alpha}^{(i)} = q_1^{(i)} \boldsymbol{\sigma}^{(i)}$, $\beta^{(i)} = q_3^{(i)}$, it follows that all these operators commute with each other. The four independent operators S , $\alpha_r^{(i)}$, q have the eigenvalues ± 1 ; the total angular momentum has the eigenvalues $F'(F' + 1)\hbar^2$, $F' = 0, 1, 2, \dots$, and for a given F' the eigenvalues of $(1/\hbar)F_z$ are $(1/\hbar)F'_z = F'$, $(F' - 1), \dots, -F'$. It follows from the completeness of the spherical harmonics and from the fact that labelling with the 16 combinations of the eigenvalues of S , $\alpha_r^{(i)}$, q correspond in a certain way to the 16 wave components of ψ , that the observables (I)-(VI) define a maximal observation.

2. - The choice of this representation for the discussion of (1) leads immediately to a decomposition in 8-component radial equations due to the kinematical constants of motion F^2 , F_z and S . Besides this well known reduction, there follows another simplification from the condition of (V) to be diagonal. In the spherical co-ordinates r , θ , φ in the center of mass system, which are appropriate to our representation, the relative kinetic energy

(2) L. L. FOLDY and S. A. WOUTHUYSEN: *Phys. Rev.*, **78**, 28 (1950).

(3) P. A. M. DIRAC: *Principles of Quantum Mechanics*, third ed. (Oxford, 1947), p. 256; $q_1^{(i)} = \gamma_0^{(i)}$, the interaction matrix of pseudoscalar interaction.

$c(\alpha^{(2)} - \alpha^{(1)}) \cdot \mathbf{p}$ has the form

$$(2) \quad c(\alpha^{(2)} - \alpha^{(1)}) \cdot \mathbf{p} = c \left[(\alpha_r^{(2)} - \alpha_r^{(1)}) p_r + \right. \\ \left. + \frac{1}{r} \left\{ \frac{\alpha_\varphi^{(2)} - \alpha_\varphi^{(1)}}{\sin \theta} p_\varphi + (\alpha_\theta^{(2)} - \alpha_\theta^{(1)}) p_\theta \right\} \right] = c \left[(\alpha_r^{(2)} - \alpha_r^{(1)}) p_r + \frac{1}{r} B \right].$$

The operator $B = ((\alpha_\varphi^{(2)} - \alpha_\varphi^{(1)})/\sin \theta) p_\varphi + (\alpha_\theta^{(2)} - \alpha_\theta^{(1)}) p_\theta$ is represented by a matrix which decomposes for the different eigenvalues of \mathbf{F}^2 , F_z and S , and which is independent of r . The radial part of the kinetic energy $c(\alpha_r^{(2)} - \alpha_r^{(1)}) p_r$ with $p_r \rightarrow (\hbar/i) \partial/\partial r$, is zero for all states with equal radial velocities $\alpha_r^{(2)'} = \alpha_r^{(1)'}$, and therefore (1) decomposes, in the diagonal representation of $\alpha_r^{(1)}$ and $\alpha_r^{(2)}$, into algebraic (« geometric ») and differential (« dynamic ») equations, if we assume that the interaction \mathcal{J} does not contain p_r . The algebraic equations may be used to eliminate half the number of components in the radial equations.

In order to perform this elimination for a general interaction

$$\mathcal{J}(r, \alpha^{(1)}, \alpha^{(2)}, \sigma^{(1)}, \sigma^{(2)}, \dots),$$

we use the projection operators P^γ , $\gamma = \pm 1$, which project on the states with relative velocities $\alpha_r^{(2)'} - \alpha_r^{(1)'} = 0$ or $\gamma' = \alpha_r^{(1)'} \alpha_r^{(2)'} = 1$ and $\alpha_r^{(2)'} - \alpha_r^{(1)'} \neq 0$ or $\gamma' = \alpha_r^{(1)'} \alpha_r^{(2)'} = -1$. Writing $\Omega^{\gamma'\gamma''} = P^{\gamma'} \Omega P^{\gamma''}$ for any operator Ω which appears in (1) and $\psi^{\gamma'} = P^{\gamma'} \psi$ for the corresponding projections of the wave functions, then the following two operator equations are equivalent to (1):

$$(3) \quad \left\{ c(\alpha_r^{(2)} - \alpha_r^{(1)}) p_r + \frac{c}{r} B^{--} + m_1 c^2 \beta^{(1)--} + m_2 c^2 \beta^{(2)--} + \mathcal{J}^{--} \right\} \psi^- + \\ + \left\{ \frac{c}{r} B^{+-} + m_1 c^2 \beta^{(1)+-} + m_2 c^2 \beta^{(2)+-} + \mathcal{J}^{+-} \right\} \psi^+ = E \psi^-,$$

$$(3') \quad \left\{ \frac{c}{r} B^{+-} + m_1 c^2 \beta^{(1)+-} + m_2 c^2 \beta^{(2)+-} + \mathcal{J}^{+-} \right\} \psi^- + \\ + \left\{ \frac{c}{r} B^{++} + m_1 c^2 \beta^{(1)++} + m_2 c^2 \beta^{(2)++} + \mathcal{J}^{++} \right\} \psi^+ = E \psi^+.$$

With the help of the « geometric » relations (3') we eliminate the components ψ^+ , using here that $\beta^{(i)\pm\pm} = B^{++} = 0$, as we point out later in (5)–(7). We get as reduced differential equations

$$[c(\alpha_r^{(2)} - \alpha_r^{(1)}) p_r + K(r)] \psi^- = R \psi^-,$$

where

$$(4) \quad K(r) = \frac{c}{r} B^{--} + \mathcal{J}^{--} + \left\{ m_1 c^2 \beta^{(1)+} + m_2 c^2 \beta^{(1)-} + \frac{c}{r} B^{--} + \mathcal{J}^{--} \right\} \cdot \\ \cdot \{ E - \mathcal{J}^{++} \}^{-1} \left\{ m_1 c^2 \beta^{(1)+} + m_2 c^2 \beta^{(1)-} + \frac{c}{r} B^{++} + \mathcal{J}^{++} \right\},$$

which constitute for a given angular momentum and parity a system of four simultaneous differential equations.

3. - In order to bring these equations to an explicit form, we must know the matrix elements $\langle r', F', F'_z, s', \alpha', \gamma', \varrho' | \Omega | r'', F'', F''_z, s'', \alpha'', \gamma'', \varrho'' \rangle = \langle \xi' | \Omega | \xi'' \rangle$ of the different operators appearing in (4). Using the results given in (4), we can get for them, with the notations $\alpha = \alpha_r^{(1)}$, $\gamma = \alpha_r^{(1)} \alpha_r^{(2)}$, $\bar{s}' = (-1)^{F'} s'$ and $\delta_{\eta' \eta''} = \delta_{F' F''} \delta_{F'_z F''_z} \delta_{s' s''} \delta(\mathbf{r}' - \mathbf{r}'')$:

$$(5) \quad \langle \xi' | B | \xi'' \rangle = -\frac{\hbar}{i} \left\{ \alpha' (1 - \gamma') \left(\delta_{\alpha' \alpha''} - \bar{s}' \frac{1 + \varrho'}{2} \delta_{\alpha' - \alpha''} \right) \delta_{\gamma' \gamma''} - \right. \\ \left. - \frac{\sqrt{F'(F'+1)}}{2} \gamma' \{ (1 + \varrho') - (1 - \varrho') \alpha' \} \delta_{\alpha' \alpha''} \delta_{\gamma', -\gamma''} + \right. \\ \left. + \bar{s}' \{ (1 + \varrho') - (1 - \varrho') \alpha' \gamma' \} \delta_{\alpha' - \alpha''} \delta_{\gamma', -\gamma''} \right\} \delta_{\varrho' \varrho''} \delta_{\eta' \eta''}$$

$$(6) \quad \langle \xi' | \beta^{(1)} | \xi'' \rangle = \frac{1}{2} \{ \alpha' \gamma' - 1 + \varrho' (\alpha' + \gamma') \} \delta_{\alpha' - \alpha''} \delta_{\gamma', -\gamma''} \delta_{\varrho', -\varrho''} \delta_{\eta' \eta''},$$

$$(7) \quad \langle \xi' | \beta^{(1)} | \xi'' \rangle = \frac{1}{2} \{ \varrho' \gamma' (1 + \alpha') + (\alpha' - 1) \} \delta_{\alpha' \alpha''} \delta_{\gamma', -\gamma''} \delta_{\varrho', -\varrho''} \delta_{\eta' \eta''},$$

$$(8) \quad \langle \xi' | Y | \xi'' \rangle = \frac{e^2}{2r} \{ 2\gamma' \delta_{\alpha' \alpha''} + \gamma' \bar{s}' (1 - \varrho' \gamma') \delta_{\alpha' - \alpha''} \} \delta_{\varrho' \varrho''} \delta_{\gamma' \gamma''} \delta_{\eta' \eta''},$$

where Y is the Breit retardation term:

$$\frac{e^2}{2r} \left[\boldsymbol{\alpha}^{(1)} \cdot \boldsymbol{\alpha}^{(2)} + \frac{(\boldsymbol{\alpha}^{(1)} \cdot \mathbf{r})(\boldsymbol{\alpha}^{(2)} \cdot \mathbf{r})}{r^2} \right].$$

Omitting in the representer of the wave function ψ , $(r', F', F'_z, s', \alpha', \varrho')$, the indices of the constants of motion F, F_z, S , as well as γ' (which for components different from zero is equal to -1) we may write (4) in the form

$$(9) \quad \sum_{\alpha'', \varrho''} \left\{ -\frac{2\hbar c}{i} \alpha' \delta_{\alpha' \alpha''} \frac{d}{dr} + (\alpha', \varrho' | K(r) | \alpha'', \varrho'') \right\} (r, \alpha'', \varrho'') = E(r, \alpha'', \varrho''),$$

which constitutes a system of four simultaneous differential equations.

As an application of this scheme, we have calculated in the Breit case,

(4) H. JOOS, J. LEAL FERREIRA and A. H. ZIMMERMAN: to appear in *An. Ac. Bras. Ci.*

$\mathcal{J} = V(r) + Y$, the matrix elements of K , with the help of formulas (5)–(8) by simple algebraic manipulations:

$$\begin{aligned}
 (\alpha', \varrho' | K(r) | \alpha'', \varrho'') = & -\frac{2\hbar c}{i} \left\{ \alpha' \left(\delta_{\alpha' \alpha''} - \frac{1 + \varrho'}{2} \delta_{\alpha', -\alpha''} \right) \delta_{\varrho' \varrho''} + \right. \\
 & + \frac{\sqrt{F'(F'+1)}}{2} (m_1 - \bar{s}' m_2) (\alpha' G_1 \delta_{\alpha' \alpha''} - \varrho' \bar{s}' G_2 \delta_{\alpha', -\alpha''}) \delta_{\varrho', -\varrho''} \Big\} + \\
 & + \left\{ V(r) \delta_{\alpha' \alpha''} - \frac{e^2}{r} \left(\delta_{\alpha' \alpha''} + \frac{1 + \varrho'}{2} \bar{s}' \delta_{\alpha', -\alpha''} \right) + \right. \\
 & + (m_1^2 + m_2^2) c^4 \left[\left(\frac{1 + \varrho'}{2} G_3 + \frac{1 - \varrho'}{2} G_4 \right) \delta_{\alpha' \alpha''} + \bar{s}' \frac{1 + \varrho'}{2} G_5 \delta_{\alpha', -\alpha''} \right] + \\
 & + 2m_1 m_2 c^4 \left[\frac{1 + \varrho'}{2} G_3 \delta_{\alpha' \alpha''} + \left(\bar{s}' \frac{1 + \varrho'}{2} G_5 + \frac{1 - \varrho'}{2} G_4 \right) \delta_{\alpha', -\alpha''} \right] + \\
 & + \frac{\hbar^2 c^2}{r^2} F'(F'+1) [\bar{s}'(1 + \varrho') G_4 + (1 - \varrho') G_6] \Big\} \delta_{\varrho' \varrho''},
 \end{aligned}$$

with

$$\begin{aligned}
 (10) \quad G_1 &= \left[2(E - V) - \frac{e^2}{r} \right] (E - V)^{-1} \left(E - V - \frac{e^2}{r} \right)^{-1}, \\
 G_2 &= \frac{e^2}{r} (E - V)^{-1} \left(E - V - \frac{e^2}{r} \right)^{-1}, \\
 G_3 &= \left(E - V - \frac{e^2}{r} \right) (E - V)^{-1} \left(E - V - \frac{2e^2}{r} \right)^{-1}, \quad G_4 = \left(E - V - \frac{e^2}{r} \right)^{-1}, \\
 G_5 &= \frac{e^2}{r} (E - V)^{-1} \left(E - V - \frac{2e^2}{r} \right)^{-1}, \quad G_6 = (E - V)^{-1}.
 \end{aligned}$$

In order to illustrate the structure of (10), we shall derive from it the first order mass correction to the Rydberg formula for the energy eigenvalues of the hydrogen atom, for states with total angular momentum $F' = 0$ ⁽⁵⁾. For this we put $E = m_1 c^2 + m_2 c^2 + \bar{E}$ and we approximate (10) by neglecting all terms which vanish for $(m_1 + m_2) c^2 \rightarrow \infty$, remarking that, for $F' = 0$, (10) splits into 2-dimensional equations for the two values of ϱ :

$$\begin{aligned}
 (11) \quad \sum_{\alpha'} \Big\{ & -\frac{2\hbar c}{i} \alpha' \left[\left(\frac{d}{dr} + \frac{1}{r} \right) \delta_{\alpha' \alpha''} - \frac{1}{r} \delta_{\alpha', -\alpha''} \right] - \\
 & - \left[\frac{2m_1 m_2}{m_1 + m_2} c^2 + \left(1 + \frac{m_1^2 + m_2^2}{(m_1 + m_2)^2} \right) \left(E - V - \frac{e^2}{r} \frac{(m_1 + \bar{s}' m_2)^2}{(m_1 + m_2)^2} \right) \delta_{\alpha' \alpha''} + \right. \\
 & + \left[\frac{2m_1 m_2}{(m_1 + m_2)^2} (m_1 c^2 + m_2 c^2 + \bar{E} + V) - \right. \\
 & \left. \left. - \frac{e^2}{r} \bar{s}' \left(1 - \frac{(m_1 + \bar{s}' m_2)^2}{(m_1 + m_2)^2} \right) \right] \delta_{\alpha', -\alpha''} \right\} (r, \alpha', +1 |) = 0.
 \end{aligned}$$

⁽⁵⁾ T. ISHIDZU: *Prog. Theor. Phys.*, **6**, 48, 154 (1951).

The wave equation for $q = -1$, in the case $F' = 0$, has no physical meaning because it corresponds to vanishing angular parts.

But these are essentially one particle radial Dirac equations with modified masses and coupling constants, this becoming evident when we make the substitutions

$$(12) \quad \left\{ \begin{array}{l} \psi_1(r) = i[(r, +1, +1|) + (r, -1, +1|)]\delta, \\ E' = \frac{1}{\delta} \bar{E} + Mc^2, \quad M = \frac{m_1 m_2 \sqrt{m_1^2 + m_2^2}}{(m_1 + m_2)^2}, \\ \psi_2(r) = [(r, +1, -1|) - (r, -1, +1|)], \\ V'(r) = \frac{1}{\delta} V(r), \quad \delta = \frac{m_1 + m_2}{\sqrt{m_1^2 + m_2^2}}. \end{array} \right.$$

In this way (11) gives

$$\begin{aligned} \hbar c \frac{d}{dr} \psi_1 - (Mc^2 + E' - V' + Y')\psi_2 &= 0, \\ \hbar c \left(\frac{d}{dr} + \frac{2}{r} \right) \psi_2 + (-Mc^2 + E' - V')\psi_1 &= 0, \end{aligned}$$

with

$$(11') \quad Y' = \delta \frac{e^2}{r} \frac{(1-s')}{2} \left(\frac{m_1 + s'm_2}{m_1 + m_2} - 1 \right),$$

which have the usual form of Dirac radial equations, if we disregard the Y' term. In order to calculate the Rydberg formula, i.e., the lowest order term in $\propto \bar{E}_n$ we can neglect this Y' term. Therefore we get the first order mass correction ($m_1 \rightarrow \infty$) of the Rydberg formula, by making substitution (12) in the classical Rydberg expression for infinite m_1 :

$$(13) \quad \bar{E}_n \approx -\frac{1}{2} \left(1 - 3 \frac{m_2}{m_1} \right) \frac{e^2 m_2}{\hbar^2 n^2}.$$

This differs from the usual non-relativistic reduced mass effect by the appearance of a factor $(1 - 3(m_2/m_1))$ instead of $(1 - (m_2/m_1))$.

4. — We have shown that 16-component wave equations for a system with two Dirac particles can be exactly reduced to 4-component wave equations. From these rather complicated equations, suitable approximations can be derived. These approximations, which correspond to the usual ones, are not

valid for small r , but in this case we can study the analytical form of the exact reduced equations.

For the physical interpretation of the wave function it is advisable to go

TABLE I. — *Table of $2(I, \sigma, \beta^{(1)}, \beta^{(2)}|\gamma, \alpha, \varrho)$.*

$\bar{s}' = (-1)^{F'}$				γ	1	1	1	1	-1	-1	-1	-1
				α	1	-1	1	$\sigma-1$	1	-1	1	-1
L	σ	$\beta^{(1)}$	$\beta^{(2)} \varrho$	1	1	-1	-1	1	1	-1	-1	
F'	0	1	1	0	0	-1	-1	1	1	0	0	
F'	1	1	1	1	-1	0	0	0	0	1	1	
F'	0	-1	-1	0	0	1	1	1	1	0	0	
F'	1	-1	-1	1	-1	0	0	0	0	-1	-1	
$F'-1$	1	1	-1	-b	-b	a	-a	a	-a	b	-b	
$F'+1$	1	1	-1	-a	-a	-b	b	-b	b	a	-a	
$F'-1$	1	-1	1	-b	-b	-a	a	a	-a	-b	b	
$F'+1$	1	-1	1	-a	-a	b	-b	-b	b	-a	a	
$\bar{s}' = -(-1)^{F'}$												
$F'-1$	1	1	1	-b	b	-a	-a	+a	a	-b	-b	
$F'+1$	1	1	1	-a	a	b	b	-b	-b	-a	-a	
$F'-1$	1	-1	-1	-b	b	a	a	a	a	b	b	
$F'+1$	1	-1	-1	-a	a	-b	-b	-b	b	a	a	
F	0	1	-1	0	0	1	-1	1	-1	0	0	
F	1	1	-1	1	1	0	0	0	0	-1	1	
F	0	-1	1	0	0	-1	1	1	-1	0	0	
F	1	-1	1	1	1	0	0	0	0	1	-1	

$$a = \sqrt{\frac{F'}{2F'+1}}, \quad b = \sqrt{\frac{F'+1}{2F'+1}}$$

from our representation to one in which, besides F , F_z and S , the total spin σ , the orbital angular momentum L and the rest mass operators $m_1\beta^{(1)}$ and $m_2\beta^{(2)}$ are also diagonal. For performing this transformation we give in a table below the transition amplitudes $(L, \sigma, \beta^{(1)}, \beta^{(2)} | \gamma, \alpha, \varrho)$ for fixed values of F , F_z and S .

RIASSUNTO (*)

Si dimostra che in una rappresentazione in cui oltre al momento angolare e alla parità, anche le velocità radiali di due particelle di Dirac sono diagonali, le equazioni per gli autovalori radiali dell'energia si riducono a un sistema di quattro equazioni differenziali simultanee. L'utilità di questa rappresentazione è dimostrata per il caso dell'equazione di Breit.

(*) Traduzione a cura della Redazione.

«Dynamical» Lagrangian for the Many Body Problem (*).

J. K. PERCUS and G. J. YEVICK

Walter Kidde Laboratory of Physics, Stevens Institute of Technology - Hoboken, N. J.

(ricevuto il 25 Settembre 1956)

Summary. — A «dynamical» Lagrangian approach to the many body problem in the collective co-ordinate formulation is made possible with the aid of the two-body correlation function. As a consequence, the values of the fictitious masses and frequencies for the collective co-ordinate harmonic oscillators, which represent the physical problem, are dependent on the average motion of the system. Moreover, the introduction of the center of mass and relative co-ordinates for the q_k occasions no difficulty in the present approach. In Part B of the paper, preliminary considerations are presented on the physical extent of the domain of action of q -space; various techniques are utilized to probe its structure. It is found in this way that the «diameter» of q -space is of the order of $N^{\frac{1}{2}}$. Application is made to the speed of sound in a fluid.

Prefatory Remarks.

In two preceding papers (¹), we have presented a simple reformulation of the many body problem using collective co-ordinates. The basic idea is to transform a complicated non-linear system into a set of approximately linear equations. This is accomplished by means of a simple point transformation.

This paper is a continuation of papers I and II in that it pertains to an examination of the foundations of the many body problem and does not em-

(*) Supported in part by the Office of Naval Research.

(¹) G. J. YEVICK and J. K. PERCUS: *A New Approach to the Many Body Problem* and J. K. PERCUS and G. J. YEVICK: *Some Dynamical Considerations in the New Approach to the Many Body Problem* (*Phys. Rev.*, **101**, 1186 (1956), hereafter referred to as papers I and II).

phasize the actual evaluation of immediate, concrete physical phenomena. Our aim is to furnish a sequence of analyses, each more refined and deeper than the preceding. Applications are considered at the conclusion of each major stage of development.

The approximations in I and II can loosely be characterized as kinematical in that the various terms in the Lagrangian are considered and approximated without recourse to the physical motion of the system. The philosophy in this paper can appropriately be regarded as that of a dynamical approach in which all quantities employed are weighted according to their relative importance during the dynamical motion. This constitutes a qualitatively distinct improvement over the kinematical approach for the zero-order theory. Furthermore, as will be shown in a succeeding paper, solution of the zero-order problem permits evaluation of the dynamical weights, thus presenting a self-consistent formulation for all pertinent quantities.

To carry out the program described above, we find it first necessary to enlarge the basic structure of the theory contained in papers I and II by introducing a number of qualitatively new features. These are presented in Part A of the paper. The new ideas comprise the introduction of relative co-ordinates in place of positional co-ordinates in q_k . One can show that many of the difficulties of superfluous surfaces (see paper I) vanish as a result of this simple but significant modification. In addition, the employment of the autocorrelation function for the particle density makes possible the implementation of the dynamical approach described above. This allows a much better physical representation of close-up effects in the zero-order theory. We indicate how the d -function of paper II achieves in this manner a dynamical basis.

In Part B, we present preliminary remarks on the extent of the physical domain of q -space. This problem is a very significant and quite difficult one. The boundary of q -space enters kinematically by the very nature of the point transformation from x -space to q -space. So far, we have been unable to determine the major detailed characteristics of this boundary because of the extreme complexity of the transformation. As discussed in paper I, once $N \geq 2$, the boundary already appears to us as very complicated indeed. These boundaries clearly unite the q 's in some manner, and we should like to ascertain to what extent the coupling of the q 's does or does not occur in the boundary. If, for example, the q 's were to be hopelessly intertwined in the boundary, then we probably have not gained a great deal in our new approach to the many body problem. Perhaps even so, one would be able to apply boundary perturbation methods to such a situation and obtain results approximating closely reality.

Our preliminary remarks on the boundary have been obtained from indirect considerations. First, we find the connection between the average value of q_k^2 and the autocorrelation function which is obtainable from experiment. The

conclusions of this analysis are given further credence by probability considerations utilizing the random walk interpretation of q_k first mentioned in paper I.

Finally, for the case of no internal potential, because of the rectilinearity of the particle motion in real space, we are able to pursue the temporal development of q_k . The results of the calculation show that if there exists an inordinately large value for a specific q_k , due to the motion of the particles, it is rapidly damped down to a « thermal » value of about $N^{\frac{1}{2}}$. The damping action moreover is more rapid the higher the wavenumber k . The effective volume of q -space thus has a diameter far less than the maximum value N , and indeed of the order of $N^{\frac{1}{2}}$. This reduced domain of action has direct consequences with respect to the velocity of sound propagation, and these are briefly considered.

PART A.

An Improved Lagrangian with the Aid of the Correlation Function.

1. — Introduction of Relative Coordinates.

In paper II, we have shown that if the equations of motion of a one-dimensional classical system of N particles in a periodic box of length L , interacting by means of two body potentials, are obtained from the Lagrangian

$$(1) \quad \bar{L}_r = \frac{1}{2} \sum_i m \dot{r}_i^2 - \frac{1}{2} \sum_i \sum_{j \neq i} V(r_i - r_j) - K \left(\sum_i \dot{r}_i \right)^2;$$

then defining

$$(2) \quad q_k = \sum_i \exp [ikr_i],$$

we can replace \bar{L}_r by L_q

$$(3) \quad L_q = \frac{1}{2} \sum_{k \neq 0} f_k (|\dot{q}_k|^2 - \omega_k^2 |q_k|^2) + \frac{1}{2} (N \sum_{k \neq 0} \omega_k^2 f_k - N(N-1)A),$$

where

$$(4) \quad \left\{ \begin{array}{l} A = V_0 \\ K = m/2\alpha N \\ f_k = (m/\alpha N)(d_k/k^2) \\ \omega_k^2 = (\alpha N k^2 V_k)/m \end{array} \right.$$

In (4), N is the number of particles, m their mass; k is an integral multiple of $2\pi/L$, and V_k is given by

$$(5) \quad V_k = \frac{1}{L} \int_{-L/2}^{L/2} V(r) \exp[ikr] dr.$$

The d_k in (4) are Fourier coefficients of the d -function which is an approximation to the Dirac δ -function

$$(6) \quad d(r-r') = (1/L) \left(1 + \sum_{k \neq 0} dk \exp[ik(r-r')] \right)$$

and α is given by

$$(7) \quad \sum_k d_k = \alpha N.$$

Now in (1), we observe that the extra term in \bar{L}_r is $N^2 K \dot{X}^2$ where

$$(8) \quad X = \frac{1}{N} \sum_i r_i,$$

is the position of the center of mass. This suggests that the co-ordinates be chosen such that the term corresponding to the kinetic energy of the center of mass splits off in a natural manner. Such co-ordinates would be e.g. the center of mass itself plus the relative co-ordinates x_i

$$(9) \quad x_i = r_i - X.$$

Instead of (1) we now have

$$(10) \quad L = \frac{1}{2} N m \dot{X}^2 + \frac{1}{2} \sum_i m \dot{x}_i^2 - \frac{1}{2} \sum_i \sum_{j \neq i} V(x_i - x_j),$$

where the K is no longer necessary. Although (10) has $N+1$ degrees of freedom instead of N , this feature will not disturb us in the least. (In A. Bohr's theory⁽²⁾ of the collective motion of the nucleus, this problem presents itself as a serious difficulty). The reason for this is that we shall immediately replace (2) by

$$(11) \quad q_k = \sum_i \exp[ikx_i]$$

and now consider $N-1$ q_k 's together with X (which is itself a collective co-ordinate) as our fundamental independent co-ordinates. From (10), X is ignor-

(2) A. BOHR and B. MOTTELSON: *Kgl. Danske Vidensk. Selskab, Mat.-fys. Medd.*, **27**, No. 16 (1953).

able and we need only the final Lagrangian

$$(12) \quad L_x = \frac{1}{2} \sum_i m \dot{x}_i^2 - \frac{1}{2} \sum_i \sum_{j \neq i} V(x_i - x_j) .$$

Eq. (12) appears to possess N variables, which, according to (9), are not independent. By transforming to the $N-1$ variables of (11), the problem of independence need no longer concern us.

2. — The Two-Body Correlation Function.

We must convert (12) into q -space. In so doing we should like to improve (3), maintaining, however, the simple harmonic oscillator form of (3). For this purpose let us consider the potential energy term

$$(13) \quad V_x = \frac{1}{2} \sum_i \sum_{j \neq i} V(x_i - x_j) .$$

We desire to write (13) as

$$(14) \quad V_q = \frac{1}{2} \sum_{\{k\}} v_k q_k q_k^* + B ,$$

where the set $\{k\}$ consists of any N integral multiples of $k_0 = 2\pi/L$ with the restriction that the presence of k in the set implies that of $-k$; further, we assume $k=0$ to be included in $\{k\}$. B is a constant to be determined.

To ascertain that (14) is appropriate for representing (13), let us transform (14) into x -space.

$$(15) \quad V_q = \frac{1}{2} \sum_i \sum_j \sum_{\{k\}} v_k \exp[ik(x_i - x_j)] + B = \\ = \frac{1}{2} \sum_i \sum_{j \neq i} \sum_{\{k\}} v_k \exp[ik(x_i - x_j)] + B + \frac{N}{2} \sum_{\{k\}} v_k .$$

To identify (15) with (13), it is sufficient that

$$(16) \quad B = -\frac{N}{2} \sum_{\{k\}} v_k ,$$

and

$$(17) \quad V(x_i - x_j) - \sum_{\{k\}} v_k \exp[ik(x_i - x_j)] = 0 .$$

Eq. (16) can be satisfied exactly, whereas (17) can be only approximately valid. There are various methods for approximating (17). These can crudely be divided into the categories of mathematical and physical methods or equi-

valently into those of kinematical and dynamical methods. In paper II, the d -function approach was strictly one of a mathematical or kinematical nature.

At this juncture, we present a dynamical approach to (17) quite different in concept from the d -function of paper II. We shall show, however, that this leads to somewhat similar results.

The basic idea is that we minimize the mean square of (17); the term « mean » signifies, however, not a space averaging, but rather a time average over the dynamical motion of the system. In other words, we seek to minimize the integral,

$$(18) \quad I = \lim_{T \rightarrow \infty} \frac{1}{T} \int_0^T \left\{ V(x_i - x_j) - \sum_{\{k\}} v_k \exp[ik(x_i - x_j)] \right\}^2 dt,$$

where x_i and x_j are the physical positions of two distinct particles.

We now find it convenient to introduce the two-particle correlation function $p(x_i, x_j)$ defined by

$$(19) \quad \lim_{T \rightarrow \infty} \frac{1}{T} \int_0^T g(x_i, x_j) dt = \iint g(x_i, x_j) p(x_i, x_j) dx_i dx_j,$$

where $g(x_i, x_j)$ is an arbitrary function of x_i and x_j ; Eq. (19) is appropriate only for equilibrium or near equilibrium which we henceforth assume. Furthermore, we restrict our analysis to the case of translationally invariant systems. Then we have

$$(20) \quad p(x_i, x_j) = \sigma(x_i - x_j)/L^2,$$

from which it follows that

$$(21) \quad \lim_{T \rightarrow \infty} \frac{1}{T} \int_0^T g(x_i - x_j) dt = \frac{1}{L} \int g(x) \sigma(x) dx.$$

Eq. (18) now becomes

$$(22) \quad I = \frac{1}{L} \int \left\{ V(x) - \sum_{\{k\}} v_k \exp[ikx] \right\}^2 \sigma(x) dx.$$

For minimization of (22), we have

$$(23) \quad \frac{\partial I}{\partial v_k} = \frac{1}{L} \int V(x) \sigma(x) \exp[-ikx] dx - \frac{1}{L} \sum_{\{k\}} v_l \int \exp[i(l-k)x] \sigma(x) dx = 0.$$

Or defining Fourier coefficients as in (5), we have

$$(24) \quad \sum_{\{k\}} \sigma_{k-i} \nu_l = (V\sigma)_k$$

from which the ν_l may be determined. Eq. (24) is the basic equation in this section.

3. - Analysis of Kinetic Energy.

In the preceding section, we utilized the two-particle correlation function to minimize the mean square difference between the exact potential and the « equivalent » harmonic oscillator potential. We now propose to employ a similar process for handling the kinetic energy,

$$(25) \quad T_x = \frac{1}{2} \sum_i m \dot{x}_i^2.$$

We wish to represent (25) as

$$(26) \quad T_q = \frac{1}{2} \sum_{\{k\}} f_k \dot{q}_k \dot{q}_k^*,$$

where the f_k are the fictitious masses of the equivalent harmonic oscillators.

To determine whether (26) is a representation of (25), we transform (26) into x -space:

$$(27) \quad T_q = \frac{1}{2N} \sum_i \sum_j \sum_{\{k\}} \mu_k \exp[ik(x_i - x_j)] \dot{x}_i \dot{x}_j,$$

where

$$(28) \quad \mu_k = N f_k k^2 \quad \text{for } k \neq 0$$

whereas for $k = 0$, μ_k can have any value since $\sum_i \dot{x}_i = 0$ in (27). Eq. (27) would be identical with (25) if we were able to choose

$$(29) \quad \sum_{\{k\}} \mu_k = mN$$

and

$$(30) \quad \sum_{\{k\}} \mu_k \exp[ik(x_i - x_j)] \dot{x}_i \dot{x}_j = 0 \quad \text{for } i \neq j.$$

Eq. (29) can be satisfied exactly, whereas (30) only approximately. Again there are roughly two classes of approximation, kinematical and dynamical. The dynamical approach now consists of minimizing the expression

$$(31) \quad I = \lim_{T \rightarrow \infty} \frac{1}{T} \int_0^T \left\{ \sum_{\{k\}} \mu_k \exp[ik(x_i - x_j)] \dot{x}_i \dot{x}_j \right\}^2 dt.$$

In equilibrium, it is well known from statistical mechanics that in the absence of velocity dependent potentials, \dot{x}_i and \dot{x}_j are independent, identically distributed, stochastic variables and are furthermore independent of the co-ordinates x_n . Utilizing the argument of the previous section (see (19)), (31) may be replaced by the minimization of

$$(32) \quad I = \frac{1}{L} \langle \dot{x}^2 \rangle_{\Delta \tau_0}^2 \int \left\{ \sum_{\{k\}} \mu_k \exp[ikx] \right\}^2 \sigma(x) dx,$$

with the auxiliary condition (29).

Using the lagrange method of multipliers, we have

$$(33) \quad \frac{\partial}{\partial \mu_k} (I + \lambda (\sum_{\{k\}} \mu_k - Nm)) = \lambda + 2 \sum_{\{k\}} \sigma_{k-l} \mu_l = 0.$$

From (33) and (29), it follows that

$$(34) \quad \mu_k = (mN \sum_{\{l\}} \sigma_{kl}^{-1}) / (\sum_{\{l\}\{l'\}} \sigma_{ll'}^{-1}),$$

where σ^{-1} is the inverse matrix to σ defined by

$$(35) \quad \sigma_{kl} = \sigma_{k-l};$$

Eq. (34) is the significant equation for this section.

As we have observed, Eq. (34) effects the minimization of terms which could not in principle be eliminated even with the availability of an infinite number of q_k . Since these terms correspond to transfer of kinetic energy among oscillators, it seems desirable that they be at an absolute minimum, and for this purpose, the wave number distribution $\{k\}$ is at our disposal. One may carry out an analysis which shows that the absolute minimum is achieved when all μ_k are equal to m ; however the corresponding wave number distribution does not have the required properties (see paper II) of separation by k_0 for low k and diffuse separation for higher k .

Fortunately, a minimum is a point of slow variation, and one can show that, with $\mu_k = m$, a satisfactory wave number spectrum may be employed at virtually no expense in efficiency of minimization.

A similar analysis of the correction terms to the potential energy yields a result approximately the same as the above mentioned unpalatable wave number spectrum. Again, however, employment of a more reasonable spectrum, in conjunction with Eq. (24), has little effect on the minimization of the error. This is basically due to the fact that the modified potential $\sigma(x)V(x)$, which plays a predominant role, is well represented by a finite Fourier series.

4. - On the Relation of the d -Function to the Correlation Function.

In this section we shall briefly sketch some plausibility arguments for the connection between papers I and II and the new methods presented in the preceding sections of this paper. A more detailed analytical development pertaining to the relation between the d -function approach and the correlation function method will be presented at a more appropriate time.

The basic idea is the following. Let us assume that the d -function method of papers I and II is valid, i.e., the simple Lagrangian represents to zero-order quite suitably the physical Lagrangian. In other words, with the aid of the d -function, we are able to represent the potential and the kinetic energy satisfactorily. With this assumption, therefore, we are also able to represent averages correctly. Thus, the time average of the squared difference between the actual and approximating potential obtained using the d -function should be very close to a minimum, and hence should yield nearly the same result as the correlation method.

Using now the d -function assumption, let us observe how the results of this paper go over into the results of paper I and II.

In (24) and (34) of this paper, we need to know σ^{-1} , or we wish to solve an equation of the form

$$(36) \quad \sum_{\{l\}} \sigma_{k-l} b_l = a_k.$$

This can be rewritten as

$$(37) \quad \sum_{\{l\}} \frac{1}{L} \int \sigma(x) \exp[i(k-l)x] d_l(b_l \varrho_l) dx = a_k.$$

In (37) we have used the fact that d_l is the reciprocal of ϱ_l and $\varrho_l dl$ is the density of wavenumbers between l and $l + dl$. Because the function $(b_l)(x)$ is a relatively slowly varying function, we can rewrite (37) as follows, making use of the d -function assumption:

$$(38) \quad \int \sigma(x) (b_l \varrho_l)(x) \exp[ikx] dx = a_k.$$

If, in particular, a_k is a constant, the product $\sigma(x)(b_l \varrho_l)(x)$ is a δ -like function, or, since $\sigma(x)$ is extremely small at the origin, $(b_l \varrho_l)(x)$ must be very close to a δ -function. Hence

$$(39) \quad b_l \varrho_l \approx \text{const},$$

or

$$(40) \quad b_l \propto d_l.$$

We, therefore, see that the μ_k in (34) are proportional to d_k , which is the result of papers I and II.

For the solution of (24), the a_k 's of the preceding analysis are not constant, and one can show that this method is inappropriate. However, in this case, we can exhibit the approximate correctness of papers I and II without the assumption of the validity of the d -function. We first note that for a slowly varying function

$$(41) \quad \sum_{\{k\}} b_k = \sum_k b_k q_k,$$

providing that the b 's beyond $|k| > \alpha N/2$ are negligible⁽³⁾. Let us re-write (24) as

$$(1 + \varepsilon)v_k - \sum \bar{\sigma}_{k-l} q_l v_l = (V\sigma)_k = (1 + \varepsilon)V_k - \sum \bar{\sigma}_{k-l} V_l,$$

where $-\bar{\sigma}_k$ is the continuous portion of σ_k :

$$(42) \quad \begin{cases} \sigma_k = (1 + \varepsilon)\delta_{k0} - \bar{\sigma}_k \\ \varepsilon = -\lim_{k \rightarrow 0} \sigma_k \end{cases}$$

and where all sums may be taken for $|k| < \alpha N/2$ (α is assumed large enough so that V_k is negligible for $|k| > \alpha N/2$). Eq. (42) may be written as

$$(43) \quad (1 + \varepsilon)(d_k - 1)V_k = \sum [(1 + \varepsilon)\delta_{k-l} - \bar{\sigma}_{k-l}](V_l - q_l v_l) = \sum \sigma_{k-l}(V_l - q_l v_l)$$

The left hand side of (43) is small inasmuch as $q_k \approx 1$ for low k whereas $v_l \approx 0$ for high k . The solution of (43) is then $V_l = q_l v_l$ or

$$(44) \quad v_l = d_l V_l.$$

Eq. (44) is identical with that used in paper II.

PART B.

Preliminary Remarks on the Extent of the Domain of Action of q -Space.

1. - The Connection between σ_k and q_k .

Because one can determine σ_k experimentally, it is worthwhile to find the relationship between σ_k and q_k and thereby ascertain somewhat crudely the extent of the domain of action of the physical q -space.

⁽³⁾ The symbol α again denotes $(1/N) \sum_{\{k\}} d_k$ and αN roughly represents the extent of k -space utilized.

The instantaneous probability of finding a particle in region dx is clearly given by $p(x)dx$ where

$$(45) \quad p^{\text{inst.}}(x) = (1/N) \sum_i \delta(x - x_i).$$

Correspondingly, let $p(x, y)dx dy$ represent the probability of finding a particle in region dx at x and another in region dy at y ; then

$$(46) \quad p^{\text{inst.}}(x, y) = (1/N(N-1)) \sum_{i \neq j} \delta(x - x_i) \delta(y - x_j).$$

From (20), we may define the Fourier component of the instantaneous correlation function by

$$(47) \quad \sigma_k^{\text{inst.}} = \int p(x, y) \exp[ik(x - y)] dx dy.$$

Rewriting (46) as

$$(48) \quad p^{\text{inst.}}(x, y) = (N/(N-1)) p^{\text{inst.}}(x) p^{\text{inst.}}(y) - (1/N-1) p^{\text{inst.}}(x) \delta(x - y).$$

Recalling the definition of q_k in (11), we have upon substituting (46) into (47)

$$(49) \quad \sigma_k^{\text{inst.}} = (1/N(N-1)) (\langle |q_k|^2 \rangle - N).$$

Averaging (49) over time yields the desired result

$$(50) \quad \sigma_k = (1/N(N-1)) (\langle |q_k|^2 \rangle - N).$$

We now make a few brief remarks concerning (50). Experimentally one knows that σ_k is of the order of $1/N$ for small k and approaches zero for large k . From this we can conclude that $\langle |q_k|^2 \rangle$ is within N of the value of N for small k and approaches N for large k . Results of this type will be encountered frequently in our succeeding analysis.

An instructive, alternative derivation of (50) is as follows:

$$(51) \quad \langle |q_k|^2 \rangle = \left\langle \sum_i \sum_j \exp[ik(x_i - x_j)] \right\rangle$$

where $\langle \rangle$ denotes the time average. Eq. (51) can be written as

$$\begin{aligned} (52) \quad \langle |q_k|^2 \rangle &= \langle N + \sum_i \sum_{j \neq i} \exp[ik(x_i - x_j)] \rangle = \\ &= N + N(N-1) \langle \exp[ik(x - y)] \rangle = \\ &= N + [N(N-1)/L] \int \exp[ikx] \sigma(x) dx = \\ &= N + N(N-1) \sigma_k, \end{aligned}$$

which is identical to (50).

In precisely the same manner, one can show that

$$(53) \quad \langle |\dot{q}_k|^2 \rangle = \left\langle \sum_i \sum_j \exp [ik(x_i - x_j)] k^2 \dot{x}_i \dot{x}_j \right\rangle = Nk^2 \langle \dot{x}^2 \rangle.$$

It is apparent from the method used to obtain (52) and (53) that, if one attempts to find the domain of action of q_k by calculating averages of higher powers, it would be necessary to include many-particle correlations as well. These quantities are not accurately known from experimental data ⁽⁴⁾; hence such a treatment is of dubious value and will not be presented here.

2. - Random Walk Interpretation.

We shall estimate the domain of action by a different mode of analysis suggested by the random walk process first presented in paper I. The idea is simply to consider that the phase angles kx_i in q_k are randomly distributed modulo 2π . For high k , this appears to be quite valid because small displacement of x_i produces a violent change in the value of kx_i modulo 2π . For the case of uniform fluids, this random character extends down to small values of k as well.

We wish, then, to find the probability distribution of the sum of N randomly oriented unit vectors in the complex plane. The orientation of the sum q_k is clearly uniform so that we shall confine our attention to the magnitude of q_k , denoted by Q_k .

Let the angle of q_k be φ_k in the complex plane. We may then write that

$$(54) \quad Q_k = \sum \exp [ik(x_i - \varphi_k)] = \sum \mathcal{R} \exp [ik(x_i - \varphi_k)] = \sum_i r_i.$$

If the number of particles N is very large, then φ_k depends only slightly on any x_i . In such a case we may regard the r_i as uncorrelated identically distributed random variables. The distribution of r_i is readily found to be

$$(55) \quad p(r) = 1/\pi(1 - r^2)^{\frac{1}{2}},$$

with

$$\langle r \rangle = 0,$$

$$\sigma^2(r) = \frac{1}{2}.$$

⁽⁴⁾ If explicit many body correlations are neglected as in J. G. KIRKWOOD and E. M. BOGGS: *Journ. Chem. Phys.*, **10**, 394 (1942), effective many body correlations are obtained in terms of $\sigma(r)$ alone, but the resulting form is not particularly appropriate for computations.

Using the Central Limit Theorem ⁽⁵⁾, it follows at once that Q_k is distributed according to

$$(56) \quad p(Q_k) = (N\pi)^{-\frac{1}{2}} \exp[-Q_k^2/N].$$

Eq. (56) shows again that Q_k is gaussianly distributed with the mean value of Q_k^2 given by N .

3. — Temporal Development of q_k .

We have seen from very general considerations that q_k tends, in magnitude, to spend its time around $N^{\frac{1}{2}}$. The question naturally arises: if q_k is initially given a value greater than $N^{\frac{1}{2}}$, in what manner does it decay into the value $N^{\frac{1}{2}}$? To obtain some insight into this problem, we shall consider a special example.

Let us assume that there are no interactions between the particles, so that we may write

$$(57) \quad x_i(t) = a_i + v_i t$$

and

$$(58) \quad q_k(t) = \sum_{i=1}^N \exp[ika_i + ikv_i t]$$

We now replace the sum by an integral and obtain

$$(59) \quad q_k(t) = \int \exp[ika(i) + ikv(i)t] di + \sum_{j=1}^N R_j,$$

$$R_j = \int_{j-\frac{1}{2}}^{j+\frac{1}{2}} \{ \exp[ik(a(j) + tv(j))] - \exp[ik(a(i) + tv(i))] \} di,$$

where $R = \sum R_j$ is the remainder term.

We first note that R is a sum of N terms, each of order of magnitude unity. After a reasonable length of time, the contributions to R are expected to be independent, so that by the preceding analysis, R will have the value of about $N^{\frac{1}{2}}$, and will represent the irreducible, chaotic behaviour of q_k . We wish to determine how long it takes the integral to dip below this random fluctuation value. To do this we rewrite the integral

$$(60) \quad I_k(t) = N \int \exp[ika(i) + ikv(i)t] \varrho(v) dv,$$

(5) See W. FELLER: *Introduction to Probability Theory* (New York, 1950), p. 192.

where $\varrho(v) = (1/N) di/dv$ is the velocity distribution. The integral (60) can be evaluated under fairly general conditions by the method of stationary phase. This results in a time variation proportional to $t^{-\frac{1}{2}}$. This evaluation, unfortunately, does not apply to small t , or to a case of extreme physical importance, namely, the Maxwell-Boltzmann distribution.

Let us therefore consider separately the Maxwell-Boltzmann distribution:

$$(61) \quad \varrho(v) = (m/2\pi kT)^{\frac{1}{2}} \exp[-mv^2/2kT]$$

and, for simplicity, set $a(i) = 0$. Substituting (61) into (60) and (59), we obtain

$$(62) \quad q_k(t) = N \exp[-(kT/2m)k^2t^2] + R.$$

Here we have chosen the extreme case in which $q_k(t=0) = N$. Eq. (62) shows us that the q_k decay gaussianly in time, and the higher the k the faster the degeneration into chaotic behaviour. Also one easily observes that the rate of degeneration increases with temperature as would be expected.

If the collision time for molecules which do interact is short, then the above analysis also holds in the period of time between collisions. It is only for higher k 's that the period of time between collisions is long enough to allow immediate decay into chaos. For lower k 's the process is undoubtedly slowed down to some extent by the collisions. The decay of the q_k for high k is thus seen to be virtually a kinematical one, independent of the interaction potential.

4. - Probabilistic Approach to the Dynamics of q_k with $V=0$.

In the preceding analysis, we converted a sum into an integral, but thereby encountered difficulty in estimating analytically the remainder. We now re-analyze the temporal dependence of q_k for the case of no internal potential using probabilistic considerations which directly convert the sum into an integral in the sense of expectation values, while the analogue to the remainder term is furnished by the uncertainty, or standard deviation of $q_k(t)$, for which an explicit evaluation may be performed.

It is necessary to consider real quantities. Let

$$(63) \quad c_k(t) = \sum_i \cos kx_i(t) = \sum_i \cos(ka_i + kv_it).$$

(The analysis for $s_k(t) = \sum_i \sin kx_i$ can be performed in the same manner.)

Let $\Omega(a)$ and $Y(v)$ be the assumed probability distributions for initial position and velocity. We note that the x_i are, in reality, constrained so that their

sum is zero. For the large number of particles which are present, we can neglect the correlation resulting from this constraint. First we calculate the mean value of $c_k(t)$,

$$(64) \quad \langle c_k(t) \rangle = \int \dots \int \sum_j \cos(ka_j + k r_j t) \Pi_j \Omega(a_j) \Pi_j Y(r_j) da^N dr^N = \\ = (N/2)(\Omega_k Y_{kt} + \Omega_{-k} Y_{-kt}),$$

where subscripts refer to Fourier coefficients.

We observe that for any non-singular distribution $Y(r)$, the Fourier coefficient Y_{kt} decreases toward zero in time and indeed more rapidly for higher k . Hence the mean value of $c_k(t)$ must fall to zero. However, we must also calculate the spread of $c_k(t)$ about this value as typified by the variance,

$$(65) \quad \sigma^2(c_k(t)) = \langle c_k^2(t) \rangle - \langle c_k(t) \rangle^2 = \\ = (N/2) + (N/4)[\Omega_{2k} Y_{2kt} + \Omega_{-2k} Y_{-2kt}] - (N/4)[\Omega_k Y_{kt} + \Omega_{-k} Y_{-kt}]^2.$$

The initial value of σ^2 could be quite small, but it is clear from (65) that after sufficient time, σ^2 approaches $N/2$. This conclusion is in agreement with the preceding analyses.

A deeper analysis of the problem of the domain of action of q -space is planned for the following paper. The results will be utilized in the study of the superfluid He II.

5. - Application to Sound Velocity.

Neglecting the correlation due to relative co-ordinates, we have for a statistical state

$$(66) \quad \langle \dot{x}_k^2 \rangle = \langle k^2 \sum_i \dot{x}_i \dot{x}_j \sin kx_i \sin kx_j \rangle = Nk^2 kT/2m$$

for an oscillator of frequency given by

$$(67) \quad \omega_k^2 = Nk^2 v_k / \mu_k,$$

this implies an oscillation amplitude of

$$(68) \quad A = \left(\frac{KT}{m} \cdot \frac{\mu_k}{v_k} \right)^{\frac{1}{2}}.$$

Clearly, A grows beyond its « natural bound » of $\sim N^{\frac{1}{2}}$ if k is sufficiently high: thus the oscillator must hit its boundary, and indeed as $v_k \rightarrow 0$ or $A \rightarrow \infty$,

its motion should become linear between its boundary values. (This interpretation is strengthened by the high mean value of \dot{c}_k^2). The result is that the true frequency of motion of c_k , say Ω_k , must differ from ω_k . If one assumes that Ω_k does not have a large spread (despite the possibly rapid thermal absorption for high frequency sound), the effective motion of the boundary and value of Ω_k are readily obtained.

Suppose that the boundary of c_k space for a given transit of c_k is b ; then for an assumedly constant quarter period τ , we must have

$$(69) \quad b = \tau \dot{c}_k, \quad \Omega_k = \pi/2\tau.$$

Now a boundary distribution $f(b)$ (due to the motion of the other $N-1$ co-ordinates not explicitly taken into account) coupled with a constant velocity during a transit yields a co-ordinate distribution

$$(70) \quad \varrho(c_k) = \int_{c_k}^{\infty} \frac{1}{b} f(b) db;$$

since, except for normalization, we have seen that

$$(71) \quad \varrho(c_k) = \exp[-c_k^2/N]$$

it follows that

$$(72) \quad f(b) = b^2 \exp[-b^2/N].$$

To the extent that (72) is kinematic, it should be valid for all k . The determination of τ is immediate: from Eq. (69) and (72), we have

$$(73) \quad \langle \dot{c}_k^2 \rangle = 3N/2\tau^2,$$

and so, from Eq. (66)

$$(74) \quad \tau = \frac{1}{k} \left(\frac{3m}{KT} \right)^{\frac{1}{2}}.$$

We note for future reference that the same result would follow for the mean value of τ^{-2} if we choose a constant boundary

$$(75) \quad b = \left(\frac{3}{2}\right)^{\frac{1}{2}} N^{\frac{1}{2}}.$$

Since q_k is the k -th Fourier component of particle density, the group velocity of sound at low wave number is certainly

$$(76) \quad c = \partial \Omega_k / \partial k;$$

for higher wave number, the discreteness of the particles causes q_{nk} to be excited by a density distribution of nominal wave number k , and indirectly lower q_k 's as well. However, aside from the resulting energy degeneration, (76) should remain valid. Now at low k , ν_k is generally high and so A of (68) is low; for assumed constant Ω_k , the boundary is never hit, whence $\Omega_k = \omega_k$, or from (67)

$$(77) \quad c = (N\nu_k/\mu_k)^{\frac{1}{2}} + k \partial(N\nu_k/\mu_k)^{\frac{1}{2}}/\partial k.$$

At very high k , we have from (69) and (74)

$$(78) \quad c = (\pi/\sqrt{12})(kT/m)^{\frac{1}{2}} = .908(kT/m)^{\frac{1}{2}}$$

corresponding quite well to the known $c = (kT/m)^{\frac{1}{2}}$.

The intermediary range commences when the harmonic oscillation terminus is just at the boundary; this occurs when

$$(79) \quad \langle A^2 \rangle = \langle b^2 \rangle$$

or

$$\omega_k/k = \sqrt{\frac{2}{3}}(kT/m)^{\frac{1}{2}}.$$

For larger k , we proceed as in the limiting case of (69) to (74); Eq. (69) must of course be replaced by

$$(80) \quad b = A \sin \omega_k \tau$$

for amplitude A of the hypothetical full oscillation of c_k ; then, over a quarter cycle

$$(81) \quad \langle c_k^2 \rangle = A^2 \omega_k^2 \int_0^{\tau} \cos^2 \omega_k t \, dt / \tau,$$

so that utilizing

$$\frac{3}{2}N = \langle b^2 \rangle = \sin^2 \omega_k \tau \langle A^2 \rangle$$

together with (66),

$$(82) \quad k^2 \sin^2 \omega_k \tau / \omega_k^2 = (3m/KT) \int_0^{\tau} \cos^2 \omega_k t \, dt / \tau.$$

Solving, for $\Omega_k > \omega_k$

$$(83) \quad \Omega_k = \frac{\pi}{2\tau} = \frac{k\pi}{\sqrt{12}} \sqrt{\frac{KT}{m}} \left(1 - \frac{1}{10} \left(\frac{\omega_k}{k} \right)^4 \left(\frac{m}{KT} \right)^2 + \dots \right),$$

from which c may be determined. Since Ω_k/k varies only from $\sqrt{\frac{2}{3}}(kT/m)^{\frac{1}{2}}$ to $\pi/\sqrt{12}(kT/m)^{\frac{1}{2}}$ in this region, wide variations in c are not to be expected.

The preceding results are of course, model-dependent; thus, if retaining (74), we fix \hat{c}_k at the value given by (66) and then use the mean oscillation period to compute sound velocity, we obtain (in addition to an absorption coefficient) instead of (78)

$$(84) \quad c = (\pi^3/32)^{\frac{1}{2}}(kT/m)^{\frac{1}{2}} = .984(kT/m)^{\frac{1}{2}}.$$

Eq. (84) has, however, no greater theoretical justification in the light of the present crude analysis.

RIASSUNTO (*)

L'attacco del problema di più corpi nella formulazione con coordinate collettive per mezzo di un lagrangiano « dinamico » è reso possibile ricorrendo alla funzione di correlazione di due corpi. Come conseguenza i valori delle masse e delle frequenze fittizie per gli oscillatori armonici delle coordinate collettive che rappresentano il problema fisico dipendono dal moto medio del sistema. Inoltre, l'introduzione del centro di massa e delle relative coordinate per i q_k non offrono alcuna difficoltà in questo procedimento. Nella parte B del lavoro si espongono considerazioni preliminari sull'estensione fisica del dominio d'azione dello spazio q ; si utilizzano varie tecniche per saggiare la sua struttura. In tal modo si trova che il « diametro » dello spazio q è dell'ordine di $N^{\frac{1}{2}}$. Se ne fa un'applicazione alla velocità del suono di un fluido.

(*) Traduzione a cura della Redazione.

Further Development of a New Approximate One-Velocity Theory of Multiple Scattering.

C. C. GROSJEAN (*)

*Interuniversitair Instituut voor Kernwetenschappen
Centrum van de Rijksuniversiteit Gent - Belgium*

(ricevuto l'8 Ottobre 1956)

Summary. — In two preceding papers, dealing with a new approach for solving one-velocity multiple scattering problems in infinite homogeneous media, approximations for the particle density and current have been derived and studied in detail. Within the framework of the same formalism, the present article concerns the calculation of five further terms in the spherical harmonics expansion of the angular density. From a complete spherical harmonics analysis of the well-known transport equation (carried out in the Appendix), three rigorous continuity conditions relating the unknown coefficients to the density and the current components are derived. In the special case of an isotropic point source, these equations reduce to one single equation and the propounded problem can be solved without great difficulty due to the existing symmetry properties. The solution is then generalized to the case of a given distribution of isotropic sources and both the « direct beam » and the « scattered » contributions to the various coefficients are calculated. The results have all been obtained in the case of slightly non-isotropic scattering, which evidently includes isotropic scattering as a special case. They are finally introduced in the expansions of the scattered particle density and the total density. These formulae will play an important role in a further extension of the new formalism to finite medium problems.

1. — Introduction.

In two preceding papers ⁽¹⁾, we have developed and studied in detail a new high accuracy approximation for solving one-velocity multiple scattering

(*) On leave of absence to Princeton University, under the sponsorship of the Francqui Foundation, Brussels, Belgium. Address: Palmer Physical Laboratory, Princeton University, Princeton, N. J., U.S.A.

⁽¹⁾ C. C. GROSJEAN: *Nuovo Cimento*, **3**, 1262 (1956); **4**, 582 (1956).

problems in infinite homogeneous media. The first article concerned the derivation of the scalar particle density $\varrho(\mathbf{r})$, whereas in the second, we derived the current density vector $\mathbf{j}(\mathbf{r})$. In the present paper, we wish to proceed one step further and derive the next five terms in the spherical harmonics expansion of the angular density $\varrho(\mathbf{r}, \mathbf{\Omega})$. Again we are not interested in exact formulae for the five terms involved, but we wish to obtain their appropriate expressions implied by the approximate density $\varrho(\mathbf{r})$ and the approximate current $\mathbf{j}(\mathbf{r})$ within the framework of the formalism. This will be carried out without introducing any further approximation in the theory. The reason for calculating these additional five terms is not only that they will enable us to represent the angular density $\varrho(\mathbf{r}, \mathbf{\Omega})$ by the sum of the first nine terms instead of the first four terms in its spherical harmonics expansion, but also that the results obtained here will play an important role in the extension of the formalism to finite medium problems where accurate boundary conditions have to be set up. We keep as much as possible the same symbols as those used in our previous articles.

2. - Theoretical Development.

Let $S(\mathbf{r})d\mathbf{r}$ describe an arbitrary given distribution of isotropic sources present in an infinite homogeneous medium. Let us consider at once the case of slightly non-isotropic scattering, in which the angular distribution of the ω secondaries emitted after a collision is described by the following probability function:

$$(1) \quad p(\gamma) \frac{\sin \gamma d\gamma}{2} = (1 + 3 \overline{\cos \gamma} \cos \gamma) \frac{\sin \gamma d\gamma}{2}.$$

As we know, this constitutes the most general case of non-isotropic scattering with rotational symmetry around the incoming direction, which can be introduced in the theory under its present form.

Let $Oxyz$ be the given fixed frame of reference. We shall represent the angular density in any point A at the position \mathbf{r} by $\varrho(\mathbf{r}, \theta, \varphi)$, being the number of particles per unit volume and unit solid angle moving in the direction described by the angles θ and φ . These angles are the usual polar co-ordinates measured with respect to a local frame of reference with its origin in A , obtained by pure translation of the given frame $Oxyz$. In each point of space, the angular density can be expanded in a series of spherical harmonics of the type:

$$(2) \quad \varrho(\mathbf{r}, \theta, \varphi) = \sum_{l=0}^{\infty} a_{l,0}(\mathbf{r}) P_l(\cos \theta) + 2 \sum_{l=1}^{\infty} \sum_{m=1}^l a_{l,m}(\mathbf{r}) P_l^m(\cos \theta) \cos m\varphi + \\ + 2 \sum_{l=1}^{\infty} \sum_{m=1}^l b_{l,m}(\mathbf{r}) P_l^m(\cos \theta) \sin m\varphi,$$

in which

$$(3) \quad \left. \begin{aligned} a_{l,m}(\mathbf{r}) \\ b_{l,m}(\mathbf{r}) \end{aligned} \right\} = \frac{2l+1}{4\pi} \frac{(l-m)!}{(l+m)!} \int_0^\pi P_l^m(\cos \theta') \sin \theta' d\theta' \int_0^{2\pi} \varrho(\mathbf{r}, \theta', \varphi') \frac{\cos m\varphi'}{\sin m\varphi'} d\varphi'.$$

It follows directly from these formulae that

$$(4) \quad \left\{ \begin{aligned} a_{0,0}(\mathbf{r}) &= \frac{1}{4\pi} \varrho(\mathbf{r}), & a_{1,0}(\mathbf{r}) &= \frac{3}{4\pi v} j_z(\mathbf{r}), \\ a_{1,1}(\mathbf{r}) &= \frac{3}{8\pi v} j_x(\mathbf{r}), & b_{1,1}(\mathbf{r}) &= \frac{3}{8\pi v} j_y(\mathbf{r}). \end{aligned} \right.$$

2.1. *The rigorous continuity conditions.* — In order to calculate the five coefficients for which $l=2$, we need to know the proper equations relating them to density and current. These equations can be obtained by making the appropriate spherical harmonics analysis of the well-known transport equation. This has been carried out in detail in the Mathematical Appendix even for a much more general case than the one considered here. Applying the results (69), (70) and (71) obtained in this appendix to the present case (infinite homogeneous medium, distribution of isotropic sources), we get the following equations:

$$(5) \quad \frac{6}{5} \left(\frac{\partial a_{1,2}}{\partial x} + \frac{\partial b_{2,1}}{\partial y} \right) + \frac{2}{5} \frac{\partial a_{2,0}}{\partial z} + \frac{\partial a_{0,0}}{\partial z} = -\frac{a_{1,0}}{\lambda} (1 - \omega \cos \gamma),$$

$$(6) \quad \frac{12}{5} \left(\frac{\partial a_{2,2}}{\partial x} + \frac{\partial b_{2,2}}{\partial y} \right) + \frac{6}{5} \frac{\partial a_{2,1}}{\partial z} + \frac{\partial a_{0,0}}{\partial x} - \frac{1}{5} \frac{\partial a_{2,0}}{\partial x} = -2 \frac{a_{1,1}}{\lambda} (1 - \omega \cos \gamma),$$

$$(7) \quad \frac{12}{5} \left(\frac{\partial b_{2,2}}{\partial x} - \frac{\partial a_{2,2}}{\partial y} \right) + \frac{6}{5} \frac{\partial b_{2,1}}{\partial z} + \frac{\partial a_{0,0}}{\partial y} - \frac{1}{5} \frac{\partial a_{2,0}}{\partial y} = -2 \frac{b_{1,1}}{\lambda} (1 - \omega \cos \gamma).$$

These equations and the rest of the calculations in this article appear to be considerably simplified by the introduction of the following symmetric tensor of the second rank:

$$(8) \quad \left\{ \begin{aligned} k_{xx}(\mathbf{r}) \\ k_{xy}(\mathbf{r}) = k_{yx}(\mathbf{r}) \\ k_{yy}(\mathbf{r}) \end{aligned} \right\} = \int_0^\pi \int_0^{2\pi} \sin^3 \theta' d\theta' \int_0^{2\pi} \varrho(\mathbf{r}, \theta', \varphi') \frac{\cos^2 \varphi'}{\sin^2 \varphi'} d\varphi'$$

$$\left\{ \begin{aligned} k_{xz}(\mathbf{r}) = k_{zx}(\mathbf{r}) \\ k_{yz}(\mathbf{r}) = k_{zy}(\mathbf{r}) \end{aligned} \right\} = \int_0^\pi \cos \theta' \sin^2 \theta' d\theta' \int_0^{2\pi} \varrho(\mathbf{r}, \theta', \varphi') \frac{\cos \varphi'}{\sin \varphi'} d\varphi'.$$

$$\left\{ \begin{aligned} k_{zz}(\mathbf{r}) \end{aligned} \right\} = \int_0^\pi \cos^2 \theta' \sin \theta' d\theta' \int_0^{2\pi} \varrho(\mathbf{r}, \theta', \varphi') d\varphi'.$$

In fact, we shall consider the components of this tensor as the new unknowns of the problem. There are five simple relations expressing the coefficients $a_{2,0}$, $a_{2,1}$, $b_{2,1}$, $a_{2,2}$ and $b_{2,2}$, whose definitions are included in (3), in terms of the tensor components and the density ϱ . One easily finds:

$$(9) \quad \left\{ \begin{array}{lll} a_{2,0} = \frac{5}{8\pi} (3k_{zz} - \varrho), & a_{2,1} = \frac{5}{8\pi} k_{xz}, & b_{2,1} = \frac{5}{8\pi} k_{yz}, \\ a_{2,2} = \frac{5}{32\pi} (k_{xx} - k_{yy}), & b_{2,2} = \frac{5}{16\pi} k_{xy}. \end{array} \right.$$

As there were originally five unknowns in our problem and we went over to six new unknowns, there must necessarily exist a relation involving some of the tensor components. Indeed, by contraction we know that we must get an invariant and by the use of the definitions, we find:

$$(10) \quad k_{xx} + k_{yy} + k_{zz} = \int_0^\pi \sin \theta' d\theta' \int_0^{2\pi} \varrho(\mathbf{r}, \theta', \varphi') d\varphi' = \varrho.$$

Furthermore, introducing the relations (9) and (4) into the equations (5), (6) and (7), the latter are transformed into three new equations involving the tensor components and the current vector:

$$(11) \quad \left\{ \begin{array}{ll} \frac{\partial k_{xz}}{\partial x} + \frac{\partial k_{yz}}{\partial y} + \frac{\partial k_{zz}}{\partial z} = -\frac{(1 - \omega \cos \gamma)}{\lambda v} j_z, & (\text{from (5)}), \\ \frac{\partial k_{xx}}{\partial x} + \frac{\partial k_{yy}}{\partial y} + \frac{\partial k_{zz}}{\partial z} = -\frac{(1 - \omega \cos \gamma)}{\lambda v} j_x, & (\text{from (6)}), \\ \frac{\partial k_{xy}}{\partial x} + \frac{\partial k_{yy}}{\partial y} + \frac{\partial k_{zz}}{\partial z} = -\frac{(1 - \omega \cos \gamma)}{\lambda v} j_y, & (\text{from (7)}), \end{array} \right.$$

or briefly

$$(11') \quad \frac{\partial k_{\alpha\beta}}{\partial x_\alpha} = -\frac{(1 - \omega \cos \gamma)}{\lambda v} j_\beta, \quad (\alpha, \beta = 1, 2, 3),$$

if the indices 1, 2, 3 stand for x, y, z and the co-ordinates x_1, x_2, x_3 for x, y, z . From the point of view of tensor calculus, it is not surprising that differentiation followed by contraction leads to a vector. Comparing the set of equations (11) with the system (5, 6, 7), it is completely evident that a large simplification has been introduced.

The remaining problem is, of course, to obtain the explicit mathematical forms of the six tensor components, knowing the approximations for density and current presented in our previous papers.

2'2. *Solution of the problem in the case of an isotropic point source.* — Let us choose a frame of reference whose origin contains the point source. Due to the spherical symmetry, we can introduce a density function only depending on two parameters, namely

$$(12) \quad \varrho(r, \eta) dV \frac{\sin \eta d\eta}{2},$$

being the number of particles present in dV at a distance r from the source and moving in a direction making an angle between η and $\eta + d\eta$ with the position vector of the considered point in space (Fig. 1). It is now possible to expand $\varrho(r, \eta)$ in a series of Legendre polynomials and this leads us to

$$(13) \quad \varrho(r, \eta) = \sum_{l=0}^{\infty} C_l(r) P_l(\cos \eta)$$

in which

$$(14) \quad C_l(r) = \frac{2l+1}{2} \int_0^\pi \varrho(r, \eta') P_l(\cos \eta') \sin \eta' d\eta',$$

so that

$$(14') \quad C_0(r) = \varrho(r) \quad \text{and} \quad C_1(r) = \frac{3}{r} j_r(r).$$

Now we have to find the connection between these new quantities and those appearing in the preceding paragraph. Let us therefore consider a point A with position vector \mathbf{r} and polar co-ordinates r , ξ and ζ (Fig. 1). In this point, let a direction be characterized by the polar angles θ and φ with respect to Oxy . According to our first description, the number of particles in dV moving in the elementary solid angle $d\Omega$ around the direction (θ, φ) , can be denoted as

$$(15) \quad \varrho(\mathbf{r}, \theta, \varphi) dV d\Omega.$$

According to (12), however, the same quantity can be written as

$$(16) \quad \varrho(r, \eta) dV \frac{d\Omega}{4\pi},$$

in which

$$\eta = \text{Arc cos} [\cos \xi \cos \theta + \sin \xi \sin \theta \cos (\zeta - \varphi)].$$

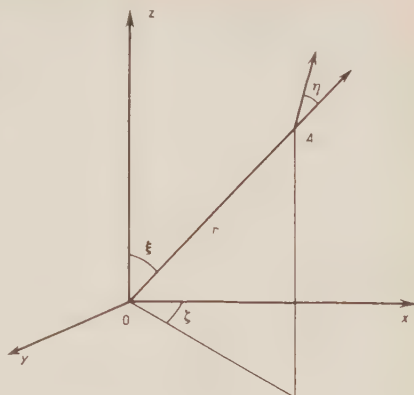


Fig. 1.

This means that we may write

$$\varrho(\mathbf{r}, \theta, \varphi) = \frac{1}{4\pi} \sum_{l=0}^{\infty} C_l(r) P_l(\cos \eta),$$

and making use of the addition theorem for Legendre polynomials

$$\begin{aligned} (17) \quad \varrho(\mathbf{r}, \theta, \varphi) &= \frac{1}{4\pi} \sum_{l=0}^{\infty} C_l(r) \left[P_l(\cos \xi) P_l(\cos \theta) + \right. \\ &\quad \left. + 2 \sum_{m=1}^l \frac{(l-m)!}{(l+m)!} P_l^m(\cos \xi) P_l^m(\cos \theta) \cos m(\zeta - \varphi) \right] = \\ &= \frac{1}{4\pi} \sum_{l=0}^{\infty} [(C_l(r) P_l(\cos \xi))] P_l(\cos \theta) + \\ &\quad + \frac{2}{4\pi} \sum_{l=1}^{\infty} \sum_{m=1}^l \left[\frac{(l-m)!}{(l+m)!} C_l(r) P_l^m(\cos \xi) \cos m\zeta \right] P_l^m(\cos \theta) \cos m\varphi - \\ &\quad + \frac{2}{4\pi} \sum_{l=1}^{\infty} \sum_{m=1}^l \left[\frac{(l-m)!}{(l+m)!} C_l(r) P_l^m(\cos \xi) \sin m\zeta \right] P_l^m(\cos \theta) \sin m\varphi. \end{aligned}$$

Comparing this with (2), we see that in the special case of an isotropic point source, we have

$$(18) \quad \begin{cases} a_{l,0}(\mathbf{r}) = \frac{1}{4\pi} C_l(r) P_l(\cos \xi), \\ a_{l,m}(\mathbf{r}) = \frac{1}{4\pi} \frac{(l-m)!}{(l+m)!} C_l(r) P_l^m(\cos \xi) \cos m\zeta, \\ b_{l,m}(\mathbf{r}) = \frac{1}{4\pi} \frac{(l-m)!}{(l+m)!} C_l(r) P_l^m(\cos \xi) \sin m\zeta, \end{cases}$$

in which

$$(19) \quad \begin{cases} \cos \xi = \frac{z}{r}, & \sin \xi = \frac{(r^2 - z^2)^{\frac{1}{2}}}{r} = \frac{(x^2 + y^2)^{\frac{1}{2}}}{r}, \\ \cos \zeta = \frac{x}{(x^2 + y^2)^{\frac{1}{2}}}, & \sin \zeta = \frac{y}{(x^2 + y^2)^{\frac{1}{2}}}. \end{cases}$$

In particular, we can write for the first nine coefficients:

$$(20) \quad \begin{cases} a_{0,0}(\mathbf{r}) = \frac{1}{4\pi} C_0(r) = \frac{1}{4\pi} \varrho(r); & a_{1,0}(\mathbf{r}) = \frac{z}{4\pi r} C_1(r) = \frac{3z}{4\pi r} j_r(r); \\ a_{1,1}(\mathbf{r}) = \frac{x}{8\pi r} C_1(r) = \frac{3x}{8\pi r} j_r(r); & b_{1,1}(\mathbf{r}) = \frac{y}{8\pi r} C_1(r) = \frac{3y}{8\pi r} j_r(r); \\ a_{2,0}(\mathbf{r}) = \frac{1}{4\pi} P_2\left(\frac{z}{r}\right) C_2(r) = \frac{3z^2 - r^2}{8\pi r^2} C_2(r); & a_{2,1}(\mathbf{r}) = \frac{xz}{8\pi r^2} C_2(r); \\ b_{2,1}(\mathbf{r}) = \frac{yz}{8\pi r^2} C_2(r); & a_{2,2}(\mathbf{r}) = \frac{x^2 - y^2}{32\pi r^2} C_2(r); & b_{2,2}(\mathbf{r}) = \frac{xy}{16\pi r^2} C_2(r). \end{cases}$$

When one replaces these nine coefficients by their corresponding expressions according to this table, in the equations (5), (6) and (7), one finds after some elaborate calculations that each of these equations leads to the same new relation between $\varrho(r)$, $j_r(r)$ and $C_2(r)$, namely

$$(21) \quad \frac{2}{5r^3} \frac{d}{dr} [r^3 C_2(r)] = - \frac{3(1-\omega \cos \gamma)}{\lambda v} j_r(r) - \frac{d\varrho(r)}{dr}.$$

This equation enables us to calculate the desired approximation for $C_2(r)$ directly, knowing that in our formalism density and radial current around an isotropic point source are given by

$$(22) \quad \varrho(r) \cong \frac{S_0}{4\pi v r^2} \left\{ \exp \left[-\frac{r}{\lambda} \right] + \frac{\omega K^2}{1-\omega} \frac{r}{\lambda} \exp \left[-K \frac{r}{\lambda} \right] \right\},$$

$$(23) \quad j_r(r) \cong \frac{S_0}{4\pi r^2} \left\{ (1-\omega) \exp \left[-\frac{r}{\lambda} \right] + \omega \left(1 + K \frac{r}{\lambda} \right) \exp \left[-K \frac{r}{\lambda} \right] \right\},$$

in which

$$(24) \quad K \equiv \left(\frac{3(1-\omega)(1-\omega \cos \gamma)}{2-\omega + (1-\omega)^2 \cos \gamma} \right)^{\frac{1}{2}},$$

S_0 : represents the total source strength.

With these quantities introduced in (21) and the integration performed, say from 0 to r , $C_2(r)$ can easily be obtained. The result will be completely determined apart from a term C/r^3 containing a constant of integration C , actually representing the value of $[r^3 C_2(r)]_r=0$. Fortunately, the exact theory of multiple scattering from a point source is sufficiently well known⁽²⁾ to write down the rigorous formula for $C_2(r)$:

$$(25) \quad C_2(r) = \frac{5S_0}{4\pi v r^2} \left\{ \exp \left[-\frac{r}{\lambda} \right] + \frac{\omega r}{\pi \lambda} \int_0^{\infty} \mathcal{F}(u) j_{\frac{3}{2}} \left(\frac{r}{\lambda} u \right) du \right\},$$

in which

$$\mathcal{F}(u) = \frac{\left[\operatorname{arctg} u + \frac{3(1-\omega) \cos \gamma}{u} \left(1 - \frac{\operatorname{arctg} u}{u} \right) \right] \cdot \left[\operatorname{arctg} u - \frac{3}{u} \left(1 - \frac{\operatorname{arctg} u}{u} \right) \right]}{u - \omega \operatorname{arctg} u - \frac{3\omega(1-\omega) \cos \gamma}{u} \left(1 - \frac{\operatorname{arctg} u}{u} \right)},$$

$$j_{\frac{3}{2}}(x) = \sqrt{\frac{\pi x}{2}} J_{\frac{3}{2}}(x) = \frac{3 \sin x}{x^2} - \frac{3 \cos x}{x} - \sin x.$$

⁽²⁾ See e.g., C. C. GROSJEAN: *Verhand. Kon. Vl. Acad. Wet. (België)*, **13**, n. 36 (1951); *Nuovo Cimento*, **11**, 11 (1954).

With the aid of this formula it is possible to study the behaviour of $C_2(r)$ for small values of r . It turns out that the second term between the braces in (25) becomes proportional to r in an infinitely close neighbourhood of $r = 0$. This leads to the conclusion that

$$(26) \quad [r^3 C_2(r)]_{r=0} = 0.$$

Therefore our approximation for $C_2(r)$ should not contain any $1/r^3$ -term. Dropping C/r^3 from the result after the integration, we obtain as final expression for $C_2(r)$:

$$(27) \quad C_2(r) \cong \frac{5S_0}{4\pi v r^2} \left\{ \exp \left[-\frac{r}{\lambda} \right] - \frac{\omega \lambda}{2r} (1 + (1 - \omega) \cos \gamma) \left[3 \left(1 + \frac{r}{\lambda} \right) \exp \left[-\frac{r}{\lambda} \right] - \left(3 + 3K \frac{r}{\lambda} + K^2 \frac{r^2}{\lambda^2} \right) \exp \left[-K \frac{r}{\lambda} \right] \right] \right\}.$$

Now that the approximations for the three coefficients $C_0(\varrho)$, $C_1(3/\varrho)j(r)$ and C_2 are known, let us calculate the «direct beam» and the «scattered» contributions to the density $\varrho(r)$, the current $j(r)$ and the tensor $\mathbf{k}(r)$.

Returning to expression (12), we can write

$$(28) \quad \varrho(r, \eta) dV \frac{\sin \eta d\eta}{2} = [\varrho_d(r, \eta) + \varrho_s(r, \eta)] dV \frac{\sin \eta d\eta}{2}.$$

The direct beam contribution to the angular density at A consists of particles all moving in the direction OA (Fig. 1). Therefore:

$$(29) \quad \varrho_d(r, \eta) dV \frac{\sin \eta d\eta}{2} = \frac{S_0}{4\pi v r^2} \exp \left[-\frac{r}{\lambda} \right] \delta(\eta) dV d\eta,$$

in which the point of discontinuity of the Dirac δ -function must be regarded as an inside point of the interval $0 < \eta < \pi$. Expanding (29) in a series of Legendre polynomials, we get

$$(30) \quad \varrho_d(r, \eta) = \frac{S_0 \exp[-r/\lambda]}{4\pi v r^2} [1 + 3P_1(\cos \eta) + 5P_2(\cos \eta) + \dots].$$

Putting the expressions for C_0 , C_1 and C_2 into (13) and subtracting (30), we see that the contribution of the scattered particles to the angular density can be written as follows:

$$(31) \quad \varrho_s(r, \eta) \cong \frac{S_0 \omega}{4\pi v r^2} [f_0(r) + 3f_1(r)P_1(\cos \eta) + 5f_2(r)P_2(\cos \eta) + \dots],$$

in which

$$(32) \quad f_0(r) = \frac{K^2}{1-\omega} \frac{r}{\lambda} \exp\left[-K \frac{r}{\lambda}\right],$$

$$(33) \quad f_1(r) = -\exp\left[-\frac{r}{\lambda}\right] + \left(1 + K \frac{r}{\lambda}\right) \exp\left[-K \frac{r}{\lambda}\right],$$

$$(34) \quad f_2(r) = \frac{\lambda}{2r} [1 + (1-\omega) \cos \gamma] \left\{ -3 \left(1 + \frac{r}{\lambda}\right) \exp\left[-\frac{r}{\lambda}\right] + \right. \\ \left. + \left(3 + 3K \frac{r}{\lambda} + K^2 \frac{r^2}{\lambda^2}\right) \exp\left[-K \frac{r}{\lambda}\right] \right\}.$$

Now, in analogy with (13) and (14'), we can write directly:

$$(35) \quad \varrho_d(r) = \frac{S_0 \exp[-r/\lambda]}{4\pi r r^2}, \quad \varrho_s(r) \cong \frac{S_0 \omega}{4\pi r r^2} f_0(r),$$

$$(36) \quad \mathbf{j}_d(r) = (j_d)_r \mathbf{1}_r = \frac{S_0 \exp[-r/\lambda]}{4\pi r^2} \mathbf{1}_r, \quad \mathbf{j}_s(r) = (j_s)_r \mathbf{1}_r \cong \frac{S_0 \omega}{4\pi r^2} f_1(r) \mathbf{1}_r.$$

Finally, to calculate the coefficients of the tensors \mathfrak{k}_d and \mathfrak{k}_s , one can deduce the five coefficients $a_{2,0}$, $a_{2,1}$, $b_{2,1}$, $a_{2,2}$ and $b_{2,2}$ from (20) in which $C_2(r)$ has to be replaced

$$\text{firstly by } \frac{5S_0 \exp[-r/\lambda]}{4\pi r r^2},$$

$$\text{secondly by } \frac{5S_0 \omega}{4\pi r r^2} f_2(r),$$

and afterwards, the six components of each tensor can be found solving the system formed by the five relations (9) and the equation (10). The final results are:

$$(37) \quad \begin{cases} k_{xx}^d = \frac{S_0 \omega^2}{4\pi r r^4} \exp\left[-\frac{r}{\lambda}\right], & k_{yy}^d = \frac{S_0 \omega^2}{4\pi r r^4} \exp\left[-\frac{r}{\lambda}\right], & k_{zz}^d = \frac{S_0 \omega^2}{4\pi r r^4} \exp\left[-\frac{r}{\lambda}\right], \\ k_{xy}^d = \frac{S_0 \omega^2 y}{4\pi r r^4} \exp\left[-\frac{r}{\lambda}\right], & k_{xz}^d = \frac{S_0 \omega^2 z}{4\pi r r^4} \exp\left[-\frac{r}{\lambda}\right], & k_{yz}^d = \frac{S_0 \omega^2 z}{4\pi r r^4} \exp\left[-\frac{r}{\lambda}\right], \end{cases}$$

or in tensor notation

$$(37') \quad k_{\alpha\beta}^d = \frac{S_0 \omega^2 x_\alpha x_\beta}{4\pi r r^4} \exp\left[-\frac{r}{\lambda}\right];$$

$$(38) \quad \begin{cases} k_{xx}^s \cong \frac{S_0 \omega}{4\pi r r^2} \left[\frac{f_0(r)}{3} - \frac{f_2(r)}{3} + \frac{r^2 f_2(r)}{r^2} \right], & k_{yy}^s \cong \dots, & k_{zz}^s \cong \dots, \\ k_{xy}^s \cong \frac{S_0 \omega x y}{4\pi r r^4} f_2(r), & k_{xz}^s \cong \dots, & k_{yz}^s \cong \dots, \end{cases}$$

or in tensor notation

$$(38') \quad k_{\alpha\beta}^s \cong \frac{S_0 \omega}{4\pi v r^2} \left\{ \frac{x_\alpha x_\beta}{r^2} f_2(r) + \frac{1}{3} [f_0(r) - f_2(r)] \delta_{\alpha\beta} \right\}.$$

This solves the problem in the case of an isotropic point source.

2'3. Solution of the problem in the case of a given distribution of isotropic sources. — Let us return to the more general case in which the isotropic source distribution is described by $S(\mathbf{r})d\mathbf{r}$. It is now an easy matter to generalize the final results of the preceding paragraph to this case. We find immediately — for the direct beam contributions:

$$(39) \quad \varrho_d(\mathbf{r}) = \frac{1}{4\pi v} \iiint_{-\infty}^{\infty} S(\mathbf{r}') \frac{\exp[-|\mathbf{r} - \mathbf{r}'|/\lambda]}{|\mathbf{r} - \mathbf{r}'|^2} d\mathbf{r}',$$

$$(40) \quad \mathbf{j}_d(\mathbf{r}) = \frac{1}{4\pi} \iiint_{-\infty}^{\infty} S(\mathbf{r}') \frac{(\mathbf{r} - \mathbf{r}') \exp[-|\mathbf{r} - \mathbf{r}'|/\lambda]}{|\mathbf{r} - \mathbf{r}'|^3} d\mathbf{r}',$$

$$(41) \quad k_{\alpha\beta}^d(\mathbf{r}) = \frac{1}{4\pi v} \iiint_{-\infty}^{\infty} S(\mathbf{r}') \frac{(x_\alpha - x'_\alpha)(x_\beta - x'_\beta) \exp[-|\mathbf{r} - \mathbf{r}'|/\lambda]}{|\mathbf{r} - \mathbf{r}'|^4} d\mathbf{r}';$$

— for the contributions due to scattered particles:

$$(42) \quad \varrho_s(\mathbf{r}) \cong \frac{\omega}{4\pi v} \iiint_{-\infty}^{\infty} S(\mathbf{r}') \frac{f_0(|\mathbf{r} - \mathbf{r}'|)}{|\mathbf{r} - \mathbf{r}'|^2} d\mathbf{r}',$$

$$(43) \quad \mathbf{j}_s(\mathbf{r}) \cong \frac{\omega}{4\pi} \iiint_{-\infty}^{\infty} S(\mathbf{r}') \frac{(\mathbf{r} - \mathbf{r}') f_1(|\mathbf{r} - \mathbf{r}'|)}{|\mathbf{r} - \mathbf{r}'|^3} d\mathbf{r}',$$

$$(44) \quad k_{\alpha\beta}^s(\mathbf{r}) \cong \frac{\omega}{4\pi v} \iiint_{-\infty}^{\infty} S(\mathbf{r}') \frac{(x_\alpha - x'_\alpha)(x_\beta - x'_\beta) f_2(|\mathbf{r} - \mathbf{r}'|)}{|\mathbf{r} - \mathbf{r}'|^4} d\mathbf{r}' + \\ + \frac{\omega \delta_{\alpha\beta}}{12\pi v} \iiint_{-\infty}^{\infty} S(\mathbf{r}') \frac{f_0(|\mathbf{r} - \mathbf{r}'|) - f_2(|\mathbf{r} - \mathbf{r}'|)}{|\mathbf{r} - \mathbf{r}'|^2} d\mathbf{r}'.$$

The direct beam contributions are quantities which have to be calculated by straightforward integration in (39), (40) and (41), as soon as $S(\mathbf{r})$ is given explicitly. The density $\varrho_s(\mathbf{r})$ can either be obtained in the same way using (42)

or as a solution of a second order partial differential equation, namely

$$(45) \quad \nabla^2 \varrho_s(\mathbf{r}) - \frac{K^2}{\lambda^2} \varrho_s(\mathbf{r}) + \frac{\omega K^2 S(\mathbf{r})}{(1 - \omega) v \lambda} = 0,$$

in which K is given by (24). This was shown in our first paper on the approximate formalism. In our second article, we have seen that the current vector $\mathbf{j}_s(\mathbf{r})$ can be simply expressed in terms of some of the previously mentioned quantities. Indeed, we found:

$$(46) \quad \mathbf{j}_s(\mathbf{r}) \cong -\omega \mathbf{j}_d(\mathbf{r}) - \frac{[2 - \omega + (1 - \omega)^2 \cos \gamma] \lambda v}{3(1 - \omega \cos \gamma)} \nabla \varrho_s(\mathbf{r}).$$

In practice, this simplifies the calculation of the current a great deal. As it can be expected that a similar formula may exist, by which $k_{\alpha\beta}^s$ can be expressed in terms of the direct beam contributions and ϱ_s , we wish to establish this formula. This can be carried out on the basis of the expressions (39) to (44). As an example and at the same time as a verification, let us proceed with the re-derivation of \mathbf{j}_s on the basis of the integral expressions. Suppose we take the first partial derivative of ϱ_s with respect to x . We find:

$$(47) \quad \frac{\partial \varrho_s}{\partial x} \cong \frac{\omega K^2}{4\pi(1 - \omega)v\lambda} \frac{\partial}{\partial x} \int \int \int_{-\infty}^{\infty} S(\mathbf{r}') \frac{\exp[-K|\mathbf{r} - \mathbf{r}'|/\lambda]}{|\mathbf{r} - \mathbf{r}'|} d\mathbf{r}' \\ \cong \frac{\omega K^2}{4\pi(1 - \omega)v\lambda} \int \int \int_{-\infty}^{\infty} \frac{S(\mathbf{r}')}{|\mathbf{r} - \mathbf{r}'|^3} (x - x') \left(1 + K \frac{|\mathbf{r} - \mathbf{r}'|}{\lambda} \right) \exp[-K|\mathbf{r} - \mathbf{r}'|/\lambda] d\mathbf{r}'.$$

Taking into account the definition of $f_1(r)$, we can write

$$\frac{\partial \varrho_s}{\partial x} \cong -\frac{\omega K^2}{4\pi(1 - \omega)v\lambda} \int \int \int_{-\infty}^{\infty} \frac{S(\mathbf{r}')}{|\mathbf{r} - \mathbf{r}'|^3} (x - x') \{f_1(|\mathbf{r} - \mathbf{r}'|) + \exp[-|\mathbf{r} - \mathbf{r}'|/\lambda]\} d\mathbf{r}',$$

so that, comparing with (43) and (40),

$$\frac{\partial \varrho_s}{\partial x} \cong -\frac{K^2}{(1 - \omega)v\lambda} (j_s)_x - \frac{\omega K^2}{(1 - \omega)v\lambda} (j_d)_x.$$

From this, we get directly:

$$(j_s)_x \cong -\omega (j_d)_x - \frac{(1 - \omega)\lambda v}{K^2} \frac{\partial \varrho_s}{\partial x},$$

which is the first of the three scalar equations contained in (46).

Let us now apply the same method to the calculation of $k_{\alpha\beta}^s$. We can start with the second partial derivative of q_s with respect to x :

$$(48) \quad \frac{\partial^2 q_s}{\partial x^2} \simeq - \frac{\omega K^2}{4\pi(1-\omega)v\lambda} \int_{-\infty}^{\infty} \int_{-\infty}^{\infty} \frac{S(\mathbf{r}')}{|\mathbf{r}-\mathbf{r}'|^3} \cdot \left\{ \left(1 + K \frac{|\mathbf{r}-\mathbf{r}'|}{\lambda} \right) - \frac{(x-x')^2}{|\mathbf{r}-\mathbf{r}'|^2} \left(3 - 3K \frac{|\mathbf{r}-\mathbf{r}'|}{\lambda} + K^2 \frac{|\mathbf{r}-\mathbf{r}'|^2}{\lambda^2} \right) \right\} \exp \left[-K \frac{|\mathbf{r}-\mathbf{r}'|}{\lambda} \right] d\mathbf{r}'.$$

By a careful analysis, one can prove that the integral on the right hand side is still perfectly convergent notwithstanding the relatively high powers of $|\mathbf{r}-\mathbf{r}'|$ in the denominators.

Taking into account that

$$\left(3 - 3K \frac{r}{\lambda} + K^2 \frac{r^2}{\lambda^2} \right) \exp \left[-K \frac{r}{\lambda} \right] = \left[1 - (1-\omega) \cos \gamma \right] \lambda + 3 \left(1 + \frac{r}{\lambda} \right) \exp \left[-\frac{r}{\lambda} \right],$$

we have

$$\begin{aligned} \frac{\partial^2 q_s}{\partial x^2} \simeq & \frac{\omega K^2}{2\pi(1-\omega)[1-(1-\omega)\cos\gamma]r\lambda^2} \int_{-\infty}^{\infty} \int_{-\infty}^{\infty} \frac{S(\mathbf{r}')}{|\mathbf{r}-\mathbf{r}'|^2} \left(\frac{(x-x')^2}{|\mathbf{r}-\mathbf{r}'|^2} - \frac{1}{3} \right) f_2(|\mathbf{r}-\mathbf{r}'|) d\mathbf{r}' \\ & + \frac{3\omega K^2}{4\pi(1-\omega)v\lambda} \int_{-\infty}^{\infty} \int_{-\infty}^{\infty} \frac{S(\mathbf{r}')}{|\mathbf{r}-\mathbf{r}'|^3} \left(\frac{(x-x')^2}{|\mathbf{r}-\mathbf{r}'|^2} - \frac{1}{3} \right) \left(1 + \frac{|\mathbf{r}-\mathbf{r}'|}{\lambda} \right) \exp \left[-\frac{|\mathbf{r}-\mathbf{r}'|}{\lambda} \right] d\mathbf{r}' \\ & + \frac{\omega K^4}{12\pi(1-\omega)v\lambda^3} \int_{-\infty}^{\infty} \int_{-\infty}^{\infty} \frac{S(\mathbf{r}')}{|\mathbf{r}-\mathbf{r}'|} \exp \left[-K \frac{|\mathbf{r}-\mathbf{r}'|}{\lambda} \right] d\mathbf{r}', \end{aligned}$$

and by comparison with (44) and (42):

$$(49) \quad \frac{\partial^2 q_s}{\partial x^2} \simeq \frac{2K^2}{(1-\omega)[1+(1-\omega)\cos\gamma]\lambda^2} k_{xx}^s \frac{[(1+\omega) - (1-\omega)^2 \cos\gamma]K^2}{3(1-\omega)[1-(1-\omega)\cos\gamma]\lambda^2} q_s(\mathbf{r}) + \frac{\omega K^2}{4\pi(1-\omega)v\lambda} \int_{-\infty}^{\infty} \int_{-\infty}^{\infty} \frac{S(\mathbf{r}')}{|\mathbf{r}-\mathbf{r}'|^3} \left(3 \frac{(x-x')^2}{|\mathbf{r}-\mathbf{r}'|^2} - 1 \right) \left(1 + \frac{|\mathbf{r}-\mathbf{r}'|}{\lambda} \right) \exp \left[-\frac{|\mathbf{r}-\mathbf{r}'|}{\lambda} \right] d\mathbf{r}'.$$

Comparing the last term in this formula with (39), (40) and (41), we see that it may perhaps be transformed into a simple expression containing q_a and k_{ax}^d , but not $(j_a)_x$ since the first power of $(x-x')$ does not appear in the numerator. On the other hand, a combination of q_a and k_{ax}^d alone does not suffice to represent this term properly. Therefore, let us calculate the first

partial derivative of $(j_a)_x$ with respect to x :

$$(50) \quad \frac{\partial(j_a)_x}{\partial x} = \frac{1}{4\pi} \int \int_{-\infty}^{\infty} \frac{S(\mathbf{r}')}{|\mathbf{r} - \mathbf{r}'|^3} \left[1 - \frac{(x-x')^2}{|\mathbf{r} - \mathbf{r}'|^2} \left(3 + \frac{|\mathbf{r} - \mathbf{r}'|}{\lambda} \right) \right] \exp \left[-\frac{|\mathbf{r} - \mathbf{r}'|}{\lambda} \right] d\mathbf{r}' =$$

$$- \frac{1}{4\pi} \int \int_{-\infty}^{\infty} \frac{S(\mathbf{r}')}{|\mathbf{r} - \mathbf{r}'|^3} \left(3 \frac{(x-x')^2}{|\mathbf{r} - \mathbf{r}'|^2} - 1 \right) \exp \left[-\frac{|\mathbf{r} - \mathbf{r}'|}{\lambda} \right] d\mathbf{r}' - \frac{r'_x}{\lambda} \frac{r'_x}{\lambda}.$$

(39), (41) and (50) can now be suitably combined to yield the last term in (49). This combination is

$$(51) \quad \frac{\omega K^2}{(1-\omega)\lambda^2} \left[2k_{xx}^d - \frac{\lambda}{v} \frac{\partial(j_a)_x}{\partial x} - \varrho_a \right].$$

Therefore, our final result for k_{xx}^s takes the following form:

$$(52) \quad k_{xx}^s \cong \frac{(1-\omega)[1 + (1-\omega) \cos \gamma] \lambda^2}{2K^2} \frac{\partial^2 \varrho_s}{\partial x^2} + \frac{(1+\omega) - (1-\omega)^2 \cos \gamma}{6} \varrho_s +$$

$$+ \frac{\omega[1 + (1-\omega) \cos \gamma]}{2} \left[\varrho_a + \frac{\lambda}{v} \frac{\partial(j_a)_x}{\partial x} - 2k_{xx}^d \right].$$

A completely similar calculation can be carried out for the tensor components with two different indices. For k_{xy}^s , it leads to the following result:

$$(53) \quad k_{xy}^s \cong \frac{(1-\omega)[1 + (1-\omega) \cos \gamma] \lambda^2}{2K^2} \frac{\partial^2 \varrho_s}{\partial x \partial y} +$$

$$\frac{\omega[1 + (1-\omega) \cos \gamma]}{2} \left[\frac{\lambda}{v} \frac{\partial(j_a)_x}{\partial y} - 2k_{xy}^d \right].$$

In tensor notation, the complete result is given by

$$(54) \quad k_{\alpha\beta}^s \cong \frac{\omega[1 + (1-\omega) \cos \gamma]}{2} \left[\varrho_a \delta_{\alpha\beta} + \frac{\lambda}{v} \frac{\partial(j_a)_\alpha}{\partial x_\beta} - 2k_{\alpha\beta}^d \right] +$$

$$+ \frac{(1-\omega)[1 + (1-\omega) \cos \gamma] \lambda^2}{2K^2} \frac{\partial^2 \varrho_s}{\partial x_\alpha \partial x_\beta} + \frac{(1+\omega) - (1-\omega)^2 \cos \gamma}{6} \varrho_s \delta_{\alpha\beta}.$$

Various verifications can be carried out, such as e.g. checking the equations (10) and (11).

The final phase of the calculations which we had in mind, is the introduction of the new results in the spherical harmonics expansion of the angular densities $\varrho_s(\mathbf{r}, \theta, \varphi)$ and $\varrho(\mathbf{r}, \theta, \varphi)$. To do this, we first have to transform the

sum of the first nine terms in an expansion of the form (2). This can be worked out without any difficulty using the relations (4), (9) and (10). If we represent the unit vector in the direction (θ, φ) by Ω , and if we call $\Omega_1, \Omega_2, \Omega_3$ resp. the x -, y -, and z -component of this vector, we get the following result:

$$(55) \quad \varrho(\mathbf{r}, \Omega) = \frac{1}{4\pi} \left\{ \varrho(\mathbf{r}) + \frac{3}{r} \Omega \cdot \mathbf{j}(\mathbf{r}) + 5 \frac{[3\Omega_\alpha \Omega_\beta k_{\alpha\beta}(\mathbf{r}) - \varrho(\mathbf{r})]}{2} + \dots \right\},$$

in which only the terms with $l = 0, 1$ and 2 have been transformed.

Now, let us introduce into (55) the various terms due to the scattered particles. Taking into account that

$$\Omega_\alpha \Omega_\beta \frac{\partial^2}{\partial x_\alpha \partial x_\beta} \equiv (\Omega \cdot \nabla)^2,$$

and

$$\Omega_\alpha \Omega_\beta \frac{\partial (j_a)_\alpha}{\partial x_\beta} = (\Omega \cdot \nabla)(\Omega \cdot \mathbf{j}_a),$$

we get as final result for the angular density:

$$(56) \quad \varrho_s(\mathbf{r}, \Omega) \cong \frac{1}{4\pi} \left\{ \varrho_s(\mathbf{r}) - 3\Omega \cdot \left[\frac{\omega \mathbf{j}_a}{v} + \frac{(1-\omega)\lambda}{K^2} \nabla \varrho_s \right] + \right. \\ \left. + \frac{5}{4} [1 + (1-\omega) \cos \gamma] \cdot \left[3\omega \left(\varrho_a + \frac{\lambda}{v} (\Omega \cdot \nabla)(\Omega \cdot \mathbf{j}_a) - 2\Omega_\alpha \Omega_\beta k_{\alpha\beta}^a \right) + \right. \right. \\ \left. \left. + 3 \frac{(1-\omega)\lambda^2}{K^2} (\Omega \cdot \nabla)^2 \varrho_s - (1-\omega)\varrho_s \right] + \dots \right\}.$$

Adding the expansion of $\varrho_a(\mathbf{r}, \Omega)$ to (56), we find for the total angular density:

$$(57) \quad \varrho(\mathbf{r}, \Omega) \cong \frac{1}{4\pi} \left\{ \varrho(\mathbf{r}) + 3(1-\omega)\Omega \cdot \left[\frac{\mathbf{j}_a}{v} - \frac{\lambda}{K^2} \nabla \varrho_s \right] + \right. \\ \left. + \frac{5}{4} [3\omega - 2 + 3\omega(1-\omega) \cos \gamma] \varrho_a + \frac{15}{2} (1-\omega)(1-\omega \cos \gamma) \Omega_\alpha \Omega_\beta k_{\alpha\beta}^a + \right. \\ \left. + \frac{5}{4} [1 + (1-\omega) \cos \gamma] \cdot \left[3 \frac{\omega\lambda}{v} (\Omega \cdot \nabla)(\Omega \cdot \mathbf{j}_a) + 3 \frac{(1-\omega)\lambda^2}{K^2} (\Omega \cdot \nabla)^2 \varrho_s - (1-\omega)\varrho_s \right] + \dots \right\}.$$

The formulae (56) and (57) will appear particularly useful in further extensions of our formalism.

* * *

We are indebted to the Institut Interuniversitaire des Sciences Nucléaires and to Prof. Dr. J. L. VERHAEGHE for his interest in this research work.

APPENDIX

In this appendix, we wish to carry out a complete spherical harmonics analysis of the steady-state transport equation of multiple scattering, not only in the rather simple case considered in the present paper, but at once in a much more general case.

Let $Oxyz$ be the given fixed frame of reference and consider any point \mathbf{r} inside an arbitrary scattering medium (not necessarily infinite), in which particles emitted by a given steady-state source distribution $S(\mathbf{r}, \theta, \varphi)$ (per unit volume and unit solid angle) and always moving with the same velocity v , undergo multiple scattering. The angle θ and φ , characterizing a direction at \mathbf{r} , are the usual polar coordinates measured with respect to a local frame of reference with its origin at \mathbf{r} and obtained by pure translation of $Oxyz$. Let us further denote by

- $\lambda(\mathbf{r})$: the total mean free path at \mathbf{r} ;
 $\omega(\mathbf{r})$: the average number of secondaries emitted after a collision at \mathbf{r} ;
 $p(\gamma, \mathbf{r}) \frac{\sin \gamma d\gamma}{2}$: the elementary probability that in a collision at \mathbf{r} , an emitted secondary would move in a direction making an angle between γ and $\gamma + d\gamma$ with the direction of motion of the incident particle;
 $\varrho(\mathbf{r}, \theta, \varphi)$: the angular density at \mathbf{r} .

Note that the scattering medium need not be homogeneous, since λ , ω and $p(\dots)$ are allowed to depend on the space coordinates.

The well-known steady-state transport equation satisfied by the angular density can be written as follows:

$$(58) \quad \mathbf{v} \cdot \text{grad } \varrho(\mathbf{r}, \theta, \varphi) = -\frac{v}{\lambda(\mathbf{r})} \varrho(\mathbf{r}, \theta, \varphi) + \\ + \frac{v\omega(\mathbf{r})}{4\pi\lambda(\mathbf{r})} \int_0^{2\pi} \int_0^\pi \varrho(\mathbf{r}, \theta', \varphi') p(\gamma, \mathbf{r}) \sin \theta' d\theta' d\varphi' + S(\mathbf{r}, \theta, \varphi),$$

in which

$$\cos \gamma = \cos \theta \cos \theta' + \sin \theta \sin \theta' \cos (\varphi - \varphi').$$

Let us now introduce into this equation the spherical harmonics expansion of the angular density, namely (2), and a similar expansion for the source distribution, namely:

$$(59) \quad S(\mathbf{r}, \theta, \varphi) = \sum_{l=0}^{\infty} c_{l,0}(\mathbf{r}) P_l(\cos \theta) + 2 \sum_{l=1}^{\infty} \sum_{m=1}^l c_{l,m}(\mathbf{r}) P_l^m(\cos \theta) \cos m\varphi + \\ + 2 \sum_{l=1}^{\infty} \sum_{m=1}^l s_{l,m}(\mathbf{r}) P_l^m(\cos \theta) \sin m\varphi,$$

in which

$$(60) \quad \left. \begin{matrix} c_{l,m} \\ s_{l,m} \end{matrix} \right\} = \frac{2l+1}{4\pi} \frac{(l-m)!}{(l+m)!} \int_0^\pi P_l^m(\cos \theta') \sin \theta' d\theta' \int_0^{2\pi} S(\mathbf{r}, \theta', \varphi') \frac{\cos m\varphi'}{\sin m\varphi'} d\varphi'.$$

Let us also introduce the Legendre expansion of the arbitrary non-isotropic angular distribution $p(\gamma, \mathbf{r})$, namely

$$(61) \quad p(\gamma, \mathbf{r}) = \sum_{l=0}^{\infty} A_l(\mathbf{r}) P_l(\cos \gamma),$$

in which

$$(62) \quad A_l(\mathbf{r}) = \frac{2l+1}{2} \int_0^\pi p(\gamma', \mathbf{r}) P_l(\cos \gamma') \sin \gamma' d\gamma' = (2l+1) [\overline{P_l(\cos \gamma)}]_{\mathbf{r}}.$$

The last equality is a consequence of the fact that

$$\int_0^\pi p(\gamma', \mathbf{r}) \frac{\sin \gamma' d\gamma'}{2} = 1,$$

$p(\gamma, \mathbf{r}) \sin \gamma d\gamma/2$ being a probability distribution.

Making use of the well-known addition theorem for Legendre polynomials to work out the double integral, one can easily show that the right hand side of eq. (58) becomes

$$(63) \quad \sum_{l=0}^{\infty} \left\{ c_{l,0} - \frac{v a_{l,0}}{\lambda} \left[1 - \frac{\omega A_l}{2l+1} \right] \right\} P_l(\cos \theta) + 2 \sum_{l=1}^{\infty} \sum_{m=1}^l \left\{ c_{l,m} - \frac{v a_{l,m}}{\lambda} \left[1 - \frac{\omega A_l}{2l+1} \right] \right\} \cdot P_l^m(\cos \theta) \cos m\varphi + 2 \sum_{l=1}^{\infty} \sum_{m=1}^l \left\{ s_{l,m} - \frac{v b_{l,m}}{\lambda} \left[1 - \frac{\omega A_l}{2l+1} \right] \right\} P_l^m(\cos \theta) \sin m\varphi.$$

On the other hand, making use of the addition formulae for the sine and the cosine function, we find for the left hand side of the transport equation:

$$(64) \quad r \sum_{l=0}^{\infty} \left(\frac{\partial a_{l,0}}{\partial x} \sin \theta \cos \varphi + \frac{\partial a_{l,0}}{\partial y} \sin \theta \sin \varphi + \frac{\partial a_{l,0}}{\partial z} \cos \theta \right) P_l(\cos \theta) + \\ r \sum_{l=1}^{\infty} \sum_{m=1}^l \left\{ \frac{\partial a_{l,m}}{\partial x} \sin \theta [\cos (m+1)\varphi + \cos (m-1)\varphi] + \right. \\ \left. + \frac{\partial a_{l,m}}{\partial y} \sin \theta [\sin (m+1)\varphi - \sin (m-1)\varphi] + 2 \frac{\partial a_{l,m}}{\partial z} \cos \theta \cos m\varphi \right\} P_l^m(\cos \theta) + \\ + v \sum_{l=1}^{\infty} \sum_{m=1}^l \left\{ \frac{\partial b_{l,m}}{\partial x} \sin \theta [\sin (m+1)\varphi + \sin (m-1)\varphi] + \right. \\ \left. + \frac{\partial b_{l,m}}{\partial y} \sin \theta [\cos (m-1)\varphi - \cos (m+1)\varphi] + 2 \frac{\partial b_{l,m}}{\partial z} \cos \theta \sin m\varphi \right\} P_l^m(\cos \theta).$$

The terms in the expressions (63) and (64) cannot readily be identified one with the other, because the series (64) is not a spherical harmonics expansion. However, it can be brought in this form without any difficulty. Let us first rewrite (64) as follows:

$$\begin{aligned}
 (65) \quad v \sum_{l=0}^{\infty} \left(\frac{\partial a_{l,0}}{\partial x} \sin \theta \cos \varphi + \frac{\partial a_{l,0}}{\partial y} \sin \theta \sin \varphi - \frac{\partial a_{l,0}}{\partial z} \cos \theta \right) P_l(\cos \theta) + \\
 + v \sum_{l=1}^{\infty} \sum_{m=0}^{l-1} \left(\frac{\partial a_{l,m+1}}{\partial x} + \frac{\partial b_{l,m+1}}{\partial y} \right) \sin \theta P_l^{m+1}(\cos \theta) \cos m\varphi + \\
 + v \sum_{l=2}^{\infty} \sum_{m=1}^{l-1} \left(\frac{\partial b_{l,m+1}}{\partial x} - \frac{\partial a_{l,m+1}}{\partial y} \right) \sin \theta P_l^{m+1}(\cos \theta) \sin m\varphi + \\
 + v \sum_{l=1}^{\infty} \sum_{m=2}^{l+1} \left(\frac{\partial a_{l,m-1}}{\partial x} - \frac{\partial b_{l,m-1}}{\partial y} \right) \sin \theta P_l^{m-1}(\cos \theta) \cos m\varphi + \\
 + v \sum_{l=1}^{\infty} \sum_{m=2}^{l+1} \left(\frac{\partial b_{l,m-1}}{\partial x} + \frac{\partial a_{l,m-1}}{\partial y} \right) \sin \theta P_l^{m-1}(\cos \theta) \sin m\varphi + \\
 + 2v \sum_{l=1}^{\infty} \sum_{m=1}^l \frac{\partial a_{l,m}}{\partial z} \cos \theta P_l^m(\cos \theta) \cos m\varphi + \\
 - 2v \sum_{l=1}^{\infty} \sum_{m=1}^l \frac{\partial b_{l,m}}{\partial z} \cos \theta P_l^m(\cos \theta) \sin m\varphi .
 \end{aligned}$$

Now, we have to make use of the following relations between Legendre functions:

$$(66) \quad \left\{ \begin{aligned} \cos \theta P_l(\cos \theta) &= \frac{l}{2l+1} P_{l-1}(\cos \theta) + \frac{l+1}{2l+1} P_{l+1}(\cos \theta), \quad (l=0,1,2,\dots), \\ \sin \theta P_l(\cos \theta) &= \frac{1}{2l+1} [P_{l+1}^1(\cos \theta) - P_{l-1}^1(\cos \theta)], \quad (l=0,1,2,\dots; P_{-1} \equiv 0), \\ \cos \theta P_l^m(\cos \theta) &= \frac{l-m}{2l+1} P_{l-1}^m(\cos \theta) + \frac{l+m+1}{2l+1} P_{l+1}^m(\cos \theta), \\ &\quad (l=0,1,2,\dots; m=0,1,2,\dots,l), \\ \sin \theta P_l^{m-1}(\cos \theta) &= \frac{1}{2l+1} [P_{l+1}^m(\cos \theta) - P_{l-1}^m(\cos \theta)], \\ &\quad (l=0,1,2,\dots; m=1,2,\dots,l+1; P_{-1} \equiv 0), \\ \sin \theta P_l^{m+1}(\cos \theta) &= \frac{(l+m)(l+m+1)}{2l+1} P_{l-1}^m(\cos \theta) - \\ &\quad \frac{(l-m)(l-m+1)}{2l+1} P_{l+1}^m(\cos \theta), \quad (l=1,2,3,\dots; m=0,1,2,\dots,l-1). \end{aligned} \right.$$

These relations enable us to transform (65) into a spherical harmonics ex-

pansion. We find:

$$\begin{aligned}
 (67) \quad & v \sum_{l=1}^{\infty} \sum_{m=1}^l \frac{1}{2l-1} \left(\frac{\partial a_{l-1,m-1}}{\partial x} - \frac{\partial b_{l-1,m-1}}{\partial y} \right) F_l^m(\cos \theta) \cos m\varphi - \\
 & - v \sum_{l=1}^{\infty} \sum_{m=1}^l \frac{1}{2l+3} \left(\frac{\partial a_{l+1,m-1}}{\partial x} - \frac{\partial b_{l+1,m-1}}{\partial y} \right) F_l^m(\cos \theta) \cos m\varphi + \\
 & + v \sum_{l=1}^{\infty} \sum_{m=1}^l \frac{1}{2l-1} \left(\frac{\partial b_{l-1,m-1}}{\partial x} + \frac{\partial a_{l-1,m-1}}{\partial y} \right) F_l^m(\cos \theta) \sin m\varphi - \\
 & - v \sum_{l=1}^{\infty} \sum_{m=1}^l \frac{1}{2l+3} \left(\frac{\partial b_{l+1,m-1}}{\partial x} + \frac{\partial a_{l+1,m-1}}{\partial y} \right) F_l^m(\cos \theta) \sin m\varphi + \\
 & - r \sum_{l=0}^{\infty} \sum_{m=0}^l \frac{(l+m-1)(l+m+2)}{2l+3} \left(\frac{\partial a_{l-1,m-1}}{\partial x} + \frac{\partial b_{l-1,m-1}}{\partial y} \right) F_l^m(\cos \theta) \cos m\varphi - \\
 & - r \sum_{l=2}^{\infty} \sum_{m=0}^{l-2} \frac{(l-m-1)(l-m)}{2l-1} \left(\frac{\partial a_{l-1,m-1}}{\partial x} - \frac{\partial b_{l-1,m-1}}{\partial y} \right) F_l^m(\cos \theta) \cos m\varphi - \\
 & + r \sum_{l=1}^{\infty} \sum_{m=1}^l \frac{(l-m-1)(l-m+2)}{2l+3} \left(\frac{\partial b_{l-1,m-1}}{\partial x} - \frac{\partial a_{l-1,m-1}}{\partial y} \right) F_l^m(\cos \theta) \sin m\varphi - \\
 & - r \sum_{l=2}^{\infty} \sum_{m=1}^{l-2} \frac{(l-m-1)(l-m)}{2l-1} \left(\frac{\partial b_{l-1,m-1}}{\partial x} + \frac{\partial a_{l-1,m-1}}{\partial y} \right) F_l^m(\cos \theta) \sin m\varphi + \\
 & + v \sum_{l=0}^{\infty} \frac{l+1}{2l-3} \frac{\partial a_{l+1,0}}{\partial z} P_l(\cos \theta) + 2v \sum_{l=1}^{\infty} \sum_{m=1}^l \frac{l+m+1}{2l+3} \frac{\partial a_{l+1,m}}{\partial z} F_l^m(\cos \theta) \cos m\varphi + \\
 & + v \sum_{l=1}^{\infty} \frac{l}{2l-1} \frac{\partial a_{l-1,0}}{\partial z} P_l(\cos \theta) + 2v \sum_{l=2}^{\infty} \sum_{m=1}^{l-1} \frac{l-m}{2l-1} \frac{\partial a_{l-1,m}}{\partial z} F_l^m(\cos \theta) \cos m\varphi + \\
 & + 2v \sum_{l=1}^{\infty} \sum_{m=1}^l \frac{l+m+1}{2l+3} \frac{\partial b_{l+1,m}}{\partial z} F_l^m(\cos \theta) \sin m\varphi + \\
 & + 2v \sum_{l=2}^{\infty} \sum_{m=1}^{l-1} \frac{l-m}{2l-1} \frac{\partial b_{l-1,m}}{\partial z} F_l^m(\cos \theta) \sin m\varphi,
 \end{aligned}$$

in which $b_{l,0} \equiv 0$ ($l = 0, 1, 2, \dots$).

Putting this expression equal to the right hand side of the transport equation, namely (63), and taking into account the orthogonality properties of the spherical harmonics, it is now possible to deduce an infinite system of simultaneous equations expressing rigorous relations between the various coefficients which enter the problem.

In this paper, we are only interested in the first four equations which can be obtained by identifying respectively the coefficients of $P_0(\cos \theta)$, $P_1(\cos \theta)$, $P_1^1(\cos \theta) \cos \varphi$ and $P_1^1(\cos \theta) \sin \varphi$ on both sides with each other. We find:

$$(68) \quad \frac{v}{3} \left[2 \left(\frac{\partial a_{1,1}}{\partial x} + \frac{\partial b_{1,1}}{\partial y} \right) + \frac{\partial a_{1,1}}{\partial z} \right] = c_{e,0} - \frac{v(1-\omega)}{\lambda} a_{e,0},$$

$$(69) \quad r \left[\frac{6}{5} \left(\frac{\partial a_{2,1}}{\partial x} + \frac{\partial b_{2,1}}{\partial y} \right) + \frac{2}{5} \frac{\partial a_{2,0}}{\partial z} + \frac{\partial a_{1,1}}{\partial z} \right] - c_{1,0} - \frac{v}{\lambda} \left(1 - \frac{\omega A_1}{3} \right) a_{1,0},$$

$$(70) \quad v \left[\frac{12}{5} \left(\frac{\partial a_{2,2}}{\partial x} + \frac{\partial b_{2,2}}{\partial y} \right) + \frac{6}{5} \frac{\partial a_{2,1}}{\partial z} + \frac{\partial a_{0,0}}{\partial x} - \frac{1}{5} \frac{\partial a_{2,0}}{\partial x} \right] = 2 \left[c_{1,1} - \frac{v}{\lambda} \left(1 - \frac{\omega A_1}{3} \right) a_{1,1} \right],$$

$$(71) \quad v \left[\frac{12}{5} \left(\frac{\partial b_{2,2}}{\partial x} - \frac{\partial a_{2,2}}{\partial y} \right) + \frac{6}{5} \frac{\partial b_{2,1}}{\partial z} + \frac{\partial a_{0,0}}{\partial y} - \frac{1}{5} \frac{\partial a_{2,0}}{\partial y} \right] = 2 \left[s_{1,1} - \frac{v}{\lambda} \left(1 - \frac{\omega A_1}{3} \right) b_{1,1} \right].$$

Taking into account the physical meaning of the coefficients $a_{0,0}$, $a_{1,0}$, $a_{1,1}$ and $b_{1,1}$ expressed by (4), and realizing that

$$c_{0,0} = \frac{1}{4\pi} \int_0^\pi \sin \theta' d\theta' \int_0^{2\pi} S(\mathbf{r}, \theta', \varphi') d\varphi' = \frac{S(\mathbf{r})}{4\pi},$$

where $S(\mathbf{r})$ represents the total strength of the non-isotropic source (per unit volume) at the point \mathbf{r} , the first equation namely (68) simply becomes

$$\nabla \cdot \mathbf{j} = S(\mathbf{r}) - v(1 - \omega) \varrho(\mathbf{r}) / \lambda.$$

This is the well-known continuity equation valid in any point of a scattering medium, in the most general case of non-isotropic scattering and with any non-isotropic source present.

The other three equations constitute the desired starting point for the calculations carried out in the present article.

RIASSUNTO (*)

In due lavori precedenti su un nuovo modo per risolvere i problemi di scattering multipli a velocità unica in mezzi omogenei infiniti, si sono ottenute e studiate in dettaglio approssimazioni per la densità e la corrente di particelle. Nel quadro dello stesso formalismo, nel presente articolo si calcolano cinque ulteriori termini nello sviluppo della densità angolare in armoniche sferiche. Da una completa analisi in armoniche sferiche della ben nota equazione del trasporto (sviluppata nell'Appendice) si derivano tre condizioni rigorose di continuità che legano i coefficienti incogniti alle componenti della densità e della corrente. Nel caso speciale di una sorgente puntiforme isotropica, queste equazioni si riducono a una sola e il problema proposto si risolve senza gravi difficoltà date le proprietà di simmetria esistenti. Si generalizza poi la soluzione al caso di una data distribuzione di sorgenti isotropiche e si calcolano i contributi ai vari coefficienti dovuti sia al « raggio diretto » che al « raggio che ha subito lo scattering ». I risultati si sono tutti ottenuti per il caso di scattering leggermente non isotropico che evidentemente comprende come caso speciale quello dello scattering isotropico. I risultati si introducono infine negli sviluppi della densità delle particelle scatterate e della densità totale. Queste formule avranno grande importanza in una prossima estensione del nuovo formalismo a problemi in un mezzo finito.

(*) Traduzione a cura della Redazione.

Possible Forms of Non Linear Mesodynamics.

A. BORGARDT

Department of Theoretical Physics, State University of Dnepropetrovsk, USSR

(ricevuto il 13 Ottobre 1956)

Summary. — Some principles of construction of non linear equations of meson fields are considered. The wave equations obtained are more general than those of SCHIFF. Asymptotic solutions in static approximation at small distances are found in the case of pseudoscalar mesodynamics. The saturation condition for these non-linear potentials is discussed.

All basic works on nonlinear mesodynamics are bounded chiefly with Schiff's equation (1),

$$(\square^2 - k_0^2 - \lambda\psi^2)\psi = \varrho$$

that gives only one aspect in describing nonlinear fields.

This work is based on the matrix formalism proposed by KEMMER (2). The latest viewpoint seems to be more effective for the pure physical analysis of some non linear phenomena.

1. - Wave Equations, Conservation Laws and Self-Action Specialization.

We use the following non linear wave equations for a free meson field

$$(1) \quad \beta_\lambda \partial\psi/\partial x_\lambda + k_0\psi + \lambda\beta'\psi \cdot \psi^+\beta''\psi = 0,$$

$$(1') \quad -\beta_\lambda^T \partial\psi^+/\partial x_\lambda + k_0\psi^+ + \lambda\beta'^T\psi^+ \cdot \psi^+\beta''\psi = 0,$$

(1) L. SCHIFF: *Phys. Rev.*, **84**, 1 (1951).

(2) N. KEMMER: *Proc. Roy. Soc., A* **173**, 94 (1939).

where

$$(2) \quad \beta_\mu \beta_\nu \beta_\rho + \beta_\rho \beta_\nu \beta_\mu - \beta_\mu \delta_{\nu\rho} - \beta_\rho \delta_{\nu\mu} = 0$$

and the charge-conjugate under ψ^+ is defined by

$$(3) \quad \psi^+ = \psi^* R_4 \quad (R_\mu = 2\beta_\mu^2 - 1).$$

In the above β' and β'' are included in the full group of β -s. The non linear term must contain a Lorentz-invariant contraction over the co-ordinate indices of β' and β'' . Non linearities of higher order than ψ^3 can be introduced in analogous way. It must be noticed that this case may be even simpler than (1) because of the relations between the tensor, vector and scalar densities of the meson field ⁽³⁾ analogous to those of V. Fock ⁽⁴⁾ for the spinor field.

The basic equation are gauge invariant in respect to the transformations of the electromagnetic potential and therefore the usual \mathcal{D} -formalism is available.

$$(4) \quad \beta_\lambda \mathcal{D}_\lambda \psi + k_0 \psi + \lambda \beta' \psi \cdot \psi^+ \beta'' \psi = 0,$$

$$(4') \quad -\beta_\lambda^T \mathcal{D}_\lambda^+ \psi^+ + k_0 \psi^+ + \lambda \beta'^T \psi^+ \cdot \psi^+ \beta'' \psi = 0.$$

Charge conservation is guaranteed by the same sign of λ in (1) and (1') and by the form of charge conjugated non linear term.

Conservation of the action-current, of the quantity inserted at first in (3) is governed by the equation

$$(5) \quad \partial s_\lambda / \partial x_\lambda - (1/c) \psi^+ R_5 \psi - (\lambda/2k_0 c |s|) \psi^+ \{R_5 \beta'\} \psi \cdot \psi^+ \beta'' \psi = 0,$$

where

$$(6) \quad s_\mu = (-\frac{1}{2} k_0 c) \psi^+ R_5 \beta_\mu \psi$$

and

$$(7) \quad R_5 = \prod_{\mu=1}^4 R_\mu.$$

According to

$$(8) \quad S = \int s_\lambda d\sigma_\lambda,$$

the equation (5) is the Hamilton-Jacobi equation for a non linear mesonic field ⁽⁵⁾.

⁽³⁾ A. BORGARDT: *Žu. Eksper. Teor. Fiz.*, **24**, 284 (1953).

⁽⁴⁾ V. FOCK: *Zeits. f. Phys.*, **57**, 261 (1929).

⁽⁵⁾ H. FREISTADT: *Phys. Rev.*, **97**, 1158 (1955).

For obtaining the energy-momentum conservation, the use of supplementary equations is necessary. The multiplication of (1) and (1') by the matrix operators $\beta_\sigma \beta_\mu \mathcal{D}_\sigma$ and $(\beta_\sigma \beta_\mu)^T \mathcal{D}_\sigma^+$ gives respectively

$$(8) \quad (\mathcal{D}_\mu - \beta_\sigma \beta_\mu \mathcal{D}_\sigma)(\psi + \lambda(NL)/k_0) - (ie/2\mathcal{E}_0)F_{\sigma\lambda}(\beta_\sigma \beta_\mu \beta_\lambda + \delta_{\mu\sigma} \beta_\lambda)\psi = 0,$$

$$(8') \quad (\mathcal{D}_\mu - (\beta_\sigma \beta_\mu)^T \mathcal{D}_\sigma^+)(\psi^+ + \lambda(NL)^+/k_0) - (ie/2\mathcal{E}_0)F_{\sigma\lambda}\psi^+(\beta_\lambda \beta_\mu^T \beta_\sigma + \delta_{\mu\sigma} \beta_\lambda^T) = 0$$

((NL) nonlinear term).

From (4) (4') and supplementary equation (8) (8') the conservation law for non linear energy-momentum tensor (symmetrized) follows

$$(9) \quad \partial T_{\mu\lambda}^{(NL)}/\partial x_\lambda = \lambda(\psi^+ \beta' \partial(\psi \cdot \psi^+ \beta'' \psi)/\partial x_\mu + \partial(\psi^+ \beta'' \psi \cdot \psi^+)/\partial x_\mu \cdot \beta' \psi)/k_0 + F_\mu,$$

where

$$(10) \quad T_{\mu\nu}^{(NL)} = T_{\mu\nu}^{(L)} + (\lambda/k_0)\psi^+(\beta_\nu \beta_\mu \beta' + \beta' \beta_\mu \beta_\nu)\psi \cdot \psi^+ \beta'' \psi$$

and

$$(11) \quad F_\mu = (ie/\mathcal{E}_0)F_{\mu\lambda}\psi^+ \beta_\lambda \psi.$$

This indicates that conservation occurs only when $\beta' = \beta''$ or when

$$(12) \quad (NL) = \frac{1}{2}(\beta' \psi \cdot \psi^+ \beta'' \psi + \beta'' \psi \cdot \psi^+ \beta' \psi).$$

In the last case will be

$$(13) \quad T_{\mu\nu}^{(NL)} = T_{\mu\nu}^{(L)} + (\lambda/2k_0)\psi^+(\beta_\nu \beta_\mu \beta' + \beta' \beta_\mu \beta_\nu)\psi \cdot \psi^+ \beta'' \psi + \\ + (\lambda/2k_0)\psi^+(\beta_\nu \beta_\mu \beta'' + \beta'' \beta_\mu \beta_\nu)\psi \cdot \psi^+ \beta' \psi - (3\lambda/2k_0)\delta_{\mu\nu}\psi^+ \beta' \psi \cdot \psi^+ \beta'' \psi.$$

It must be noticed as an interesting result that in a non linear field a rest mass of free particles is only partly determined by constant $k_0 = \mathcal{E}_0/\hbar c$. The self-energy density related to a free field, can be introduced by the equation (3),

$$(14) \quad \mathcal{E}_0(x) = (T_{4\mu})^{\frac{1}{2}}$$

(for a linear electromagnetic field we get, for example

$$\mathcal{E}_0 = (\frac{1}{4}(\mathbf{H}^2 - \mathbf{E}^2) + (\mathbf{E}, \mathbf{H})^2)^{\frac{1}{2}}.$$

For the simplest self-action with $\beta' = \beta'' = I$ we obtain

$$(15) \quad \mathcal{E}_0^{(NL)} = \mathcal{E}_0^{(L)}(1 + \lambda\psi^+ \psi).$$

In other variants of the nonlinear theory that may not be the case. By means of the field equations of type (1) without the mass term $k_0\eta'$ particles of non-vanishing rest-mass can be probably described.

2. - Pseudoscalar Fields.

Pseudoscalar fields are of the greatest interest for the theory. The consequences obtained in this problem are essential for all the nuclear physics. The initial task in this field is the problem of the static potential of the point source. The applicability of such a potential in the nuclear theory is defined by its behavior at small distances from the source. The small distance approximation is equivalent to $k_0 \rightarrow 0$, which restricts the equations of motion (1) in one sense: no more singularities must arise by the limiting process $k_0 \rightarrow 0$. This condition can be fulfilled by modification of λ (by means of multiplying λ , in difficult cases by k_0).

Lorentz-covariance of the whole formalism leads to the fact that β' and β'' can differ only by the diagonal multiples including obviously operators of co-ordinate reflections

$$(16) \quad \beta' = R'\beta, \quad \beta'' = R''\beta.$$

It follows from the foregoing considerations that R' and R'' can be developed on the basis of I and R_5 .

Operators $\frac{1}{2}(I \pm R_5)$ are necessary for splitting a wave function under η into potentials and field strengths in covariant manner.

Matrices β of group \mathcal{G}_{126} are divided into two parts

$$(A) \quad (I \pm R_5)\beta(I \mp R_5) = 0,$$

$$(B) \quad (I \pm R_5)\beta(I \pm R_5) = 0.$$

All the sixteen operators of the ground physical quantities are also divided into two groups

$$(A) \quad I, \quad \{\beta_\mu\beta_\nu\}, \quad [\beta_\mu\beta_\nu], \quad \beta_{(\mu}\beta_\nu\beta_0\beta_\tau) = \beta_5,$$

$$(B) \quad \beta_\mu, \quad \beta_5\beta_\mu.$$

The self-action with $\{\beta'_\mu\beta'_\nu\}$ is nearly equivalent to weak self-actions of the gravitational type and will be omitted. The self-actions with $[\beta'_\mu\beta'_\nu]$ and $\beta'_5\beta'_\mu$ are vanishing for pseudoscalar fields. The electromagnetic self-action with $\beta' \cdot \beta'_\mu$ vanishes for neutral fields and differs slightly for charged fields from the self-action with $\beta = R_5\beta_\mu$.

We leave thus only two versions

$$(A) \quad \beta = I, R_5,$$

$$(B) \quad \beta = R_5 \beta_\mu.$$

as a keystone of the following investigation.

In R' , R'' operators we limit ourselves with the cases:

$$1) \quad R' = R'' = I,$$

$$2) \quad R' = R'' = \frac{1}{2}(I + R_5),$$

$$3) \quad R' = R'' = \frac{1}{2}(I - R_5),$$

$$4) \quad R' = \frac{1}{2}(I \pm R_5), \quad R'' = \frac{1}{2}(I \mp R_5).$$

The variants A_1 , A_2 are equivalent to each other in static approximation by $k_0 \rightarrow 0$ and contain equations the integration of which is hard. Potentials corresponding to them can oscillate at small distances from a source.

The variant A_3 gives in the same asymptotical approximation the non-linear equation of Schiff

$$(17) \quad \nabla^2 \varphi - \lambda \varphi^3 = 0$$

considered by many authors ⁽⁶⁻⁹⁾.

Other variants are by $k_0 \rightarrow 0$

$$(18) \quad \nabla^2 \varphi - \lambda \varphi (\nabla \varphi)^2 = 0,$$

$$(19) \quad \nabla^2 \varphi - \lambda \varphi (\nabla \varphi)^2 / (1 + \lambda \varphi^2) = 0,$$

$$(20) \quad \nabla^2 \varphi - 2\lambda \varphi (\nabla \varphi)^2 / (1 + \lambda \varphi^2) = 0,$$

where

$$(21) \quad \varphi = (1/k_0) \prod_{\mu=1}^4 \frac{1}{2}(I + R_\mu) \psi$$

is the pseudoscalar potential of the field.

⁽⁶⁾ L. SCHIFF: *Phys. Rev.*, **84**, 395 (1952).

⁽⁷⁾ B. MALENKA: *Phys. Rev.*, **85**, 686 (1952).

⁽⁸⁾ W. THIRRING: *Zeits. f. Naturf.*, **7a**, 63 (1952).

⁽⁹⁾ R. FORNAGUERA: *Nuovo Cimento*, **1**, 132 (1955).

3. Asymptotical Solutions at Small Distances and Their Behavior.

The equations (19)-(21) may be integrated without essential difficulties.

According to the theorem proved in ⁽¹⁰⁾ the solutions of these equations are functions of the solutions of the correspondent linear problem q_L , i.e. the solutions of Laplace equation. Employing this fact one can therefore rewrite (19)-(21) in the form

$$(22) \quad d^2\varphi/d\varphi_L^2 - \lambda f(\varphi)(d\varphi/d\varphi_L)^2 = 0$$

and obtain, after a formal integration

$$(23) \quad \int_0^{q_L} d\xi' \exp \left[-\lambda \int_0^{\xi'} d\xi f(\xi) \right] = \varphi_L(\mathbf{x}),$$

(it follows from boundary condition that $\varphi_L \rightarrow 0$ by $x \rightarrow \infty$ so that the non linear potential also tends to zero by $x \rightarrow \infty$).

The solutions obtained are namely for (19), (20) and (21)

$$(24) \quad \int_0^{\varphi} \exp [-\lambda \xi^2/2] d\xi = \varphi_L(\mathbf{x}),$$

$$(25) \quad \varphi(\mathbf{x}) = (1/\sqrt{\lambda}) \sinh (\sqrt{\lambda} \varphi_L(\mathbf{x})),$$

$$(26) \quad \varphi(\mathbf{x}) = (1/\sqrt{\lambda}) \operatorname{tg} (\sqrt{\lambda} \varphi_L(\mathbf{x})).$$

respectively. We now see that when $\lambda \rightarrow 0$ (signs of λ and k_a coincide) all the three potentials have a moving singularity $x_0 = x_0(g, \lambda)$. When for example the spherically symmetric potential φ_L is adopted then

$$(27) \quad x_0 \sim g\sqrt{\lambda}.$$

By $x < x_0$ in virtue of (24)-(26) it is seen that: 1) there does not exist any potential solution (24); 2) there is a potential which oscillates with increasing frequency when x tends to zero and remains finite (solution (25)) or is divergent (solution (26)). By $\lambda = 0$ we obtain an usual linear potential; the same occurs at small q_L far from a source. By $\lambda < 0$ we obtain the relatively weakly divergent potential in a source or in the case (26) the finite value of φ , $\varphi_0 = \lambda^{-1/2}$.

Taking as a linear potential the solution of the Laplace equation with the

⁽¹⁰⁾ K. BECHERT: *Mathem. Nachr.*, **6**, 271 (1952).

bipolar symmetry $\varphi_L(\mathbf{x}) = f\boldsymbol{\sigma}, \mathbf{x}/x^3$ ($\boldsymbol{\sigma}$ a spin of the nucleon) we obtain the dipole nonlinear potential. It must be noticed that the knowledge of a spherically symmetric potential is not enough for evaluating a dipole potential by means of differentiating on co-ordinates. The latter method is based on a superposition principle and fails in a non linear theory. The paper ⁽¹¹⁾ contains some error in this point.

When dipole potentials are used in the above, the position of the moving singularity depends on a direction of tending to the source.

The presence of oscillations in potentials when $\lambda > 0$ is the consequence of non-linearity in equations connecting field strengths and potentials i.e., $\frac{1}{2}(I - R_1)R' = 0$. The same complication occurs in S -functions of fields as was stated by HEISENBERG ⁽¹²⁾.

We now shall attempt to apply the preceding theory to a nucleus. This expansion contains no difficulties due to the superposition of q_L . The mesic field in a nucleus of N slowly moving nucleons with co-ordinates $\mathbf{x}_1, \mathbf{x}_2, \dots, \mathbf{x}_N$ and spins $\boldsymbol{\sigma}_1, \boldsymbol{\sigma}_2, \dots, \boldsymbol{\sigma}_N$ is described by the potential

$$\varphi = \varphi(f \sum_{i=1}^N (\boldsymbol{\sigma}_i, \mathbf{x} - \mathbf{x}_i) / |\mathbf{x} - \mathbf{x}_i|^3).$$

One can expect that saturation effects appear only for the potentials restricted by the condition

$$(28) \quad \varphi(n\varphi_L) < n\varphi(\varphi_L).$$

Interaction energy of a nucleon pair is to be now calculated from pure field considerations

$$(29) \quad U_{12}(\mathbf{x}_1, \mathbf{x}_2) = \int (\mathcal{E}_{12}(\mathbf{x}_1, \mathbf{x}_2, \mathbf{x}) - \mathcal{E}_1(\mathbf{x}_1, \mathbf{x}) - \mathcal{E}_2(\mathbf{x}_2, \mathbf{x})) d\mathbf{x},$$

where

$$(30) \quad \mathcal{E}_i = T_{44i}^{(NL)}.$$

The change of this expression when $(\mathbf{x}_1 - \mathbf{x}_2) \rightarrow 0$ cause the applicability of nonlinear potential in the deuteron problem. Regarding the solutions (24)-(26) from this viewpoint we see now that the saturation condition is true for (24) and (26) when $\lambda < 0$ and for (15) when $\lambda > 0$. A rigorous analysis of (29) is hard for the solution (25) due to oscillations with unlimited frequency while tending to the source. For the potential (26) when $\lambda < 0$ the dipole catastrophe vanishes because of the regularity of the potential at all points of space. The

⁽¹¹⁾ F. ČAP: *Phys. Rev.*, **95**, 287 (1954).

⁽¹²⁾ W. HEISENBERG: *Zeits. f. Naturf.*, **9a**, 292 (1954).

potential (30) also works. In fact

$$(31) \quad \mathcal{E} \sim (d\varphi/d\varphi_L)^2 (\nabla\varphi_L)^2$$

but

$$(32) \quad d\varphi/d\varphi_L(\mathbf{x} - \mathbf{x}_i) = \exp[-\lambda\varphi^2(\mathbf{x} - \mathbf{x}_i)/2]$$

this function is a strong regulator which compensates the divergence of ∇q_L .

4. - Some Concluding Remarks.

The generalization of the non linear theory developed in 1-2 to the region of vector fields demands a transition to the non linear Klein equation from the system (1) or (4). This transition in a vector case seems to be more complicated than in a pseudoscalar one because of the presence of the Lorentz condition.

Splitting the equations of a field by the projection operators $\frac{1}{2}(I \pm R_5)$ into the equations of motion and supplementary equations defining the field strength by potentials, we obtain ($\beta' = \beta'' = \beta$ for a simplicity)

$$(33) \quad \beta_\lambda^{(+)} \partial\psi^{(1)}/\partial x_\lambda + \psi^{(11)} + (\lambda/2k_0)(1 + R_5)\beta^{(+)}\psi \cdot \psi^+ \beta^{(+)}\psi = q^{(11)}$$

$$(34) \quad \beta_\lambda^{(+)} \partial\psi^{(11)}/\partial x_\lambda + k_0^2\psi^{(1)} + (\lambda/2k_0)(1 - R_5)\beta^{(+)}\psi \cdot \psi^+ \beta^{(+)}\psi = q^{(1)}$$

and the charge conjugate.

In this version we employ a reducible sixteen-rowed representation of Kemmer algebra (it can be formed of two commuting reducible representations of Dirac algebra of the same rank $\beta_\mu^{(+)} = \frac{1}{2}(\gamma_\mu + \bar{\gamma}_\mu)$) with the undor of the second rank ψ as a wave function and the undor q as a source density distribution (*).

Excluding the strength part of ψ , $\psi^{(11)}$, we found a preliminary form of the Klein equation. A perfect form of it follows from the introduction of the Lorentz condition. The latter may be formulated in matrix form with another representation of $\beta - s$, $\beta_\mu^{(-)}$ orthogonal to $\beta_\mu^{(+)}$

$$(35) \quad \beta_\mu^{(-)}\beta_\mu^{(+)} = 0 \quad (\text{no summation!})$$

where

$$(36) \quad \beta_\mu^{(-)} = \frac{1}{2}(\gamma_\mu - \bar{\gamma}_\mu).$$

(*) About the connection between these two representations see author's paper on the rôle of the generalized Larmor transformation in the meson theory, *Dokl. Akad. Nauk SSSR*, **78**, 1113 (1951).

The application of $\beta_\lambda^{(-)} \partial / \partial x_\lambda$ to (34) leads to the Lorentz condition of the form

$$(37) \quad \beta_\lambda^{(-)} \partial \psi^{(1)} / \partial x_\lambda = k_0^{-2} \beta_\lambda \partial q^{(1)} / \partial x_\lambda - \lambda k_0^{-2} \beta_\lambda^{(-)} \beta^{(+)} \psi \partial (\psi^+ \beta^{(+)} \psi) / \partial x_\lambda.$$

Supposing a conservation of the source density q we see that the Lorentz condition includes no terms in the right hand side when

$$(38) \quad \beta_\lambda^{(-)} \beta^{(+)} \psi \cdot \partial (\psi^+ \beta^{(+)} \psi) / \partial x_\lambda = 0.$$

In the relatively simple case $\beta' = \beta'' = \dots$ this is true for transverse plane waves and static fields with spherical symmetry only (by $\Psi \equiv 0$).

The integration of the proposed nonlinear equations for waves may be fulfilled in elliptical functions. An approximate solution is obtained by using the perturbation theory and regarding λ as a parameter of the power expansion ⁽¹³⁾.

The same method is applicable to a calculation of the S -functions and is absolutely wrong in the case of static fields (every term of such a power expansion diverges when $\mathbf{x} \rightarrow 0$).

Exact solutions of the static equations given above, without $k_0 = 0$, may be obtained in the five-dimensional theory. The introduction of the fifth coordinate excludes a mass term from the wave equations

$$(39) \quad \beta_\lambda \partial \psi / \partial x_\lambda + \beta_5 \partial \psi / \partial x_5 + \lambda R' \beta \psi \cdot \psi^+ R'' \beta \psi = 0$$

where β_μ, β_5 must form a five-dimensional representation of Kemmer algebra investigated by LUBANSKI and ROSENFELD ⁽¹⁴⁾.

The technique of resolving the above mentioned equations due to the disappearance of a mass term approaches that of the (19)-(21).

⁽¹³⁾ A. BORGARDT: *Hauñn. zapiski Dneprop. univ.*, **42**, 1954.

⁽¹⁴⁾ J. LUBANSKI and L. ROSENFELD: *Physica*, **9**, 117 (1942).

RIASSUNTO (*)

Si esaminano alcuni principi per la impostazione di equazioni non lineari dei campi mesonici. Le equazioni d'onda ottenute sono più generali di quelle di Schiff. Nel caso della mesodinamica pseudoscalare, si trovano soluzioni asintotiche in approssimazione statica a brevi distanze. Si discute la condizione di saturazione per questi potenziali non lineari.

(*) Traduzione a cura della Redazione.

On the Λ -Nucleon Force and the Binding Energy of the Light Hyperfragments (*).

N. DALLAPORTA and F. FERRARI

Istituto di Fisica dell'Università - Padova

Istituto Nazionale di Fisica Nucleare - Sezione di Padova

(ricevuto il 13 Ottobre 1956)

Summary. — The problem of the binding of a Λ -particle in nuclear matter is considered, assuming that the force acting between Λ and nucleon is due not only to the K-field but also to the π -field; the interaction schemes are: $\Lambda \rightarrow N + \bar{K}$, $N \rightarrow \Lambda + K$, $N \rightarrow N + \pi$, $\Lambda \leftrightarrow \Sigma + \pi$. The calculations are done assuming the d'Espagnat and Prentki hamiltonian, with both scalar and pseudovector coupling (spin of the Λ and the Σ equal $\frac{1}{2}$). A good fit to the experimental values for the binding energy of the Λ in light hyperfragments is obtained, if one assumes that the interaction constants for both the π and K-forces are of the same order of magnitude as the coupling constant of the ordinary nuclear forces: with this assumption the π -force turns out to be the more important for the binding.

1. — It is well known that the unstable fragments observed in ever increasing numbers in different kinds of nuclear disintegrations may generally be interpreted by assuming that they are due to a Λ -particle which remains bound in the nuclear matter of the fragment and disintegrates after a time comparable with its proper mean life, that is $\sim 10^{-10}$ s. This fact provides a good opportunity for studying the forces that act between Λ 's and nucleons, and already different authors ⁽¹⁾ have tried to calculate the binding energy of the Λ for some specific cases. In these approaches however the binding has been practically always attributed to an exchange force between Λ and

(*) Presented at the Torino Conference, September 1956.

⁽¹⁾ E. DIANA and F. DUIMIO: *Nuovo Cimento*, **2**, 370 (1955); K. NISHIJIMA: *Prog. Theor. Phys.*, **14**, 527 (1955); G. WENTZEL: *Phys. Rev.*, **101**, 835 (1956); R. GATTO: *Nuovo Cimento*, **3**, 499 (1956).

nucleon, operating through K-meson exchange. The possibility of an interaction through the pion force has been pointed out by DALITZ⁽²⁾; a reason why this had not previously been considered may perhaps be found in the fact that interactions between nucleons and Λ 's through exchange of a single pion imply only the elementary reaction

$$(1) \quad \Lambda \rightarrow \Lambda + \pi^0$$

through the neutral pion field, which is not charge independent, owing to the fact that the isotopic spin of the Λ is zero: the Λ -neutron and the Λ -proton forces would then be of opposite sign, a consequence that would not seem to fit either with actual theoretical ideas about elementary particles, or with the scanty experimental evidence concerning the binding energies of hyperfragments having higher atomic weights. Therefore one is led to consider two-pion reactions of the kind

$$(2) \quad \Lambda \rightarrow \Lambda + \pi^+ + \pi^-$$

as the lowest order interactions that have to be taken into account; hence this more complex situation is probably the reason for the preferential consideration that has been given so far to the K-force.

We think however that the preceding reasons are by no means an argument that should induce one to consider a priori that the pion forces are less effective in binding the Λ to the nucleon. First of all, we know from ordinary theory of nuclear forces that two-meson interaction terms are generally as strong or even much stronger than one-meson interaction terms. Secondly, the range of a two π -meson force is still larger than the range of the one-K-meson force. Moreover, if we consider that while we know as yet very little of the mechanism of the K-nucleon interaction, more definite predictions may be made if we use our knowledge of some properties of the pion field, we see that it may appear safer to consider, as a first approach to the problem, to what extent the phenomena connected with unstable fragments might be interpreted through the pion interaction between Λ 's and nucleons. Therefore we propose in this paper to examine this question in some detail: in Sect. 2 the general criteria for the choice of the interactions will be given together with the assumptions on the nature of the forces; in Sect. 3 the explicit calculation of the interaction terms considered will be deduced, and the resulting potentials calculated; in Sect. 4 the binding energy of the Λ in light hyperfragments will be calculated and the relative strength of the pion and K forces discussed.

(²) R. H. DALITZ: *Phys. Rev.*, **99**, 1551 (1956).

2. — According to the preceding considerations, we assume that both the pion field and the K field are effective in the nuclear interaction of the Λ (with relative strengths that should be weighted in order to agree with the experimental data). The elementary reactions to be considered are in the first case:

$$(3) \quad N \rightarrow N + \pi$$

$$(3') \quad \Lambda \rightarrow \Sigma + \pi, \quad \Sigma \rightarrow \Lambda + \pi$$

reaction (1) being excluded as it does not preserve charge independence; and in the second case:

$$(4) \quad N \rightarrow K + \Lambda, \quad \Lambda \rightarrow \bar{K} + N.$$

The interaction terms of the hamiltonian may then be written in the simplest way according to D'ESPAGNAT and PRENTKI ⁽³⁾ as:

$$g \int d^3x \sum_i \psi_N^\dagger \gamma_5 \tau_i \varphi_i \psi_N + g_\Lambda \int d^3x \psi_\Lambda^\dagger \sum_i \Gamma_\Lambda \varphi_i \psi_{\Sigma i} + g_\Lambda \int d^3x \sum_i \psi_{\Sigma i}^\dagger \Gamma_\Lambda \varphi_i \psi_\Lambda + \\ + g_K \int d^3x \psi_\Lambda^\dagger \Gamma_K \chi^+ \psi_N + g_K \int d^3x \psi_N^\dagger \Gamma_K \chi \psi_\Lambda,$$

where $\varphi_i \chi \chi^+$ are the π and K fields, $\psi_N \psi_\Lambda \psi_\Sigma$ the wave functions of nucleons, Λ and Σ , $gg_\Lambda g_K$ the coupling constants for the different interactions and $\Gamma_\Lambda \Gamma_K$ operators that will depend on the type of interaction assumed.

Recent theoretical work ⁽⁴⁾ has shown that the spin of the Λ must be $\leq \frac{3}{2}$; we shall therefore assume as the simplest case that the spin of the Λ is $\frac{1}{2}$. Nothing being known about the spin of the Σ , we shall assume for simplicity that it is also $\frac{1}{2}$. Neither is anything actually known concerning the parity of the hyperons. As for K-mesons, experimental evidence ⁽⁵⁾ concerning τ decay seems to favour spin 0; however owing to doubt if the θ and τ are, or are not, the same particle ⁽⁶⁾, nothing definite can be said about the parity to be attributed to them. In conclusion, the most natural assumption will be to assume spin 0 for the K, and try both scalar and pseudoscalar coupling for both reactions (3') and (4) which should cover all possible cases

⁽³⁾ B. D'ESPAGNAT and J. PRENTKI: *Nuclear Physics*, **1**, 38 (1956).

⁽⁴⁾ M. RUDERMAN and R. KARPLUS: *Phys. Rev.*, **102**, 247 (1956).

⁽⁵⁾ A. BONETTI, M. BALDO CEOLIN, D. GREENING, S. LIMENTANI, M. MERLIN and G. VANDERHAEGE: *Torino Conference*, September 1956 (in course of publication on *Suppl. Nuovo Cimento*).

⁽⁶⁾ T. D. LEE and C. N. YANG: *Phys. Rev.*, **102**, 290 (1956).

of relative parity for the interacting particles. Since in our problem we are only interested in the non-relativistic limit, the pseudoscalar terms may be transformed by a similar transformation to that of DYSON⁽⁷⁾, provided we assume the same mass for the two types of interacting fermions. ($M_\Sigma = M_\Lambda$ in case (3') and $M_N = M_\Lambda$ in case (4)). The interaction terms of interest in the present case turn out to be

$$\begin{aligned} & \frac{g_\Lambda}{2M} \int d^3x \psi_\Lambda^\dagger \sum_i \sigma \cdot \text{grad } \varphi_i \psi_{\Sigma i} + \text{conj.} + \frac{g_\Lambda^2}{2M} \int d^3x \psi_\Lambda^\dagger \beta \varphi^2 \psi_\Lambda + \\ & + \frac{g_K}{2M} \int d^3x \psi_\Lambda^\dagger \sigma \cdot \text{grad } \chi \psi_N + \text{conj.} + \frac{g_K^2}{2M} \int d^3x \psi_N^\dagger \chi \bar{\chi} \psi_N + \frac{g_K^2}{2M} \int d^3x \psi_\Lambda^\dagger \chi \bar{\chi} \psi_\Lambda. \end{aligned}$$

As in the case of ordinary nucleon interaction, the first term is the ordinary pseudovector coupling, and the second is a two-meson term which for the pion interaction corresponds to the interaction scheme (2) already proposed by DALITZ.

3. — For both fields we have now to consider all terms up to a given order which may be of importance in evaluating the Λ -nucleon interaction. This is obviously the same problem as that of the ordinary nuclear forces, and one is faced with the same difficulties. Our aim of course is not to solve these difficulties in our case, but to develop a formalism which follows exactly the same lines as a selected theory of nuclear forces, in order that our predictions for hyperfragments could be compared to the predictions for the deuteron problem in this theory, independently in some respect of the main difficulties of the formalism which in both cases are avoided in the same way. For this purpose we have chosen the BRUECKNER and WATSON⁽⁸⁾ theory, and we shall now discuss the terms that have to be considered for both interaction fields.

Let us first consider the pion interaction with pseudoscalar coupling. The great similarity between this case and that of the nuclear forces suggests that we should follow the discussion of BRUECKNER and WATSON step by step and consider all interaction terms up to two mesons in the intermediate states. The V_2 term of interaction will be excluded by charge independence arguments, while the V_4 term will contain the same terms as in B.W.: V_σ (Fig. 1a; these are the customary two-meson exchange terms, with and without crossing of the meson lines), $V(1)$ (Fig. 1b, 1c) and $V(2)$ (Fig. 1d).

(7) F. J. DYSON: *Phys. Rev.*, **73**, 929 (1948); L. L. FOLDY: *Phys. Rev.*, **84**, 168 (1951); S. S. SCHWEBER, H. BETHE and F. HOFFMANN: *Meson and Fields*, I, (New York, 1955), p. 446.

(8) K. A. BRUECKNER and K. W. WATSON: *Phys. Rev.*, **92**, 1023 (1953). Indicated in the following as B.W.

We have assumed that the bare baryon intermediate states have not to be considered (as is also generally done for normal nuclear forces in the adiabatic approximation). However KLEIN ⁽⁹⁾ has shown that they ought to be

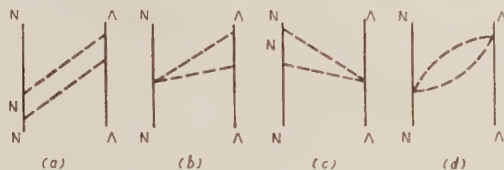


Fig. 1.

considered for the V_4 term as the non-adiabatic correction to the V_2 term. These bare nucleon terms should give a repulsive contribution to the central force of the triplet state, which does not fit the experimental evidence. Therefore B.W. have tried to eliminate them by showing that their contribution becomes small when they are calculated with the true wave functions of the adiabatic potential instead of plane waves. According to our program of proceeding in a parallel way to this theory we also have considered it more suitable to omit them.

Further, we may consider the Klein and Levy terms $V(1)$ and $V(2)$ to be strongly damped so that in our case also the chief term will be V_9 , which will be assumed to be effective down to a distance of about $0.3 \cdot 10^{-13}$ cm when a hard core is supposed to be present.

In the scalar case, since no second order term is allowed and since the two meson terms $V(1)$ and $V(2)$ do not exist, the only term will be the fourth order V_9 , for which the same assumptions will be made as in the preceding case.

Let us now consider the K interaction: here the second order term V_3 is present and corresponds to the simple schemes (Fig. 2a, 2b). The range of this K force is already somewhat smaller than the two-pion force range, but as it decreases somewhat slower with distance than the two pion force it may very well compete with it. The fourth order terms of the K interactions, however, are of much shorter range and are expected to be efficient only in the hard core region. Therefore we assume that they are included in the hard core, and need not be calculated explicitly.

We shall now give the results for the calculation of the terms according to the preceding discussion.



Fig. 2.

⁽⁹⁾ A. KLEIN: *Phys. Rev.*, **94**, 195 (1954); E. A. POWER: *Nuovo Cimento*, **3**, 323 (1954).

Pion interaction: pseudoscalar case [$x = (\mu c/\hbar)r$; $x' = (\mu_K/\mu)x$]

$$(5) \quad V_{g\pi} = -\mu \frac{g^2}{4\pi} \frac{g_\Lambda^2}{4\pi} \frac{\mu^2}{4M_N^2} \frac{\mu^2}{4M_\Lambda^2} \frac{1}{x^3} \frac{2}{\pi} \left\{ 3 \left[\frac{4 + 4x + x^2}{x} \exp[-x] K_1(x) + \right. \right. \\ \left. \left. + (2 + 2x + x^2) K_0(x) \exp[-x] \right] - 2\sigma_1 \sigma_2 \left[6K_0(2x) + \frac{6 + 4x^2}{x} K_1(2x) \right] + \right. \\ \left. + 2\sigma_1 \sigma_2 \left[K_0(x) \exp[-x] (1 + x) + \frac{2 + 2x + x^2}{x} K_1(x) \exp[-x] \right] + \right. \\ \left. + \frac{1}{3} S_{12} \left[36K_0(2x) + \frac{45 + 12x^2}{x} K_1(2x) - \right. \right. \\ \left. \left. - 3 \left\langle (1 + x) K_0(x) \exp[-x] + \frac{5 + 5x + x^2}{x} K_1(x) \exp[-x] \right\rangle \right] \right\},$$

$$(6) \quad V(1)_\pi = \mu \frac{g^2}{4\pi} \frac{g_\Lambda^2}{4\pi} \left[\left(\frac{\mu}{2M_N} \right)^2 \frac{\mu}{2M_\Lambda} + \left(\frac{\mu}{2M_\Lambda} \right)^2 \frac{\mu}{2M_N} \right] 3\lambda \left(\frac{1 + x}{x^2} \right)^2 \exp[-2x],$$

$$(7) \quad V(2)_\pi = -\mu \frac{\mu}{2M_N} \frac{\mu}{2M_\Lambda} \frac{g^2}{4\pi} \frac{g_\Lambda^2}{4\pi} 3\lambda \frac{2}{\pi} \frac{1}{x^2} K_1(2x),$$

(λ is the damping coefficient introduced by B.W.).

Scalar case:

$$(8) \quad V = V_{g\pi} = 6\mu \frac{g^2}{4\pi} \frac{g_\Lambda^2}{4\pi} \frac{\mu^2}{4M_N^2} \frac{2}{\pi} \frac{1}{x} \left(1 + \frac{1}{x} \right) K_1(x) \exp[-x],$$

K interaction: pseudoscalar case

$$(9) \quad V = V_{2K} = \frac{1}{3} \mu_K \frac{\mu_K}{2M_N} \frac{\mu_K}{2M_\Lambda} \frac{g_K^2}{4\pi} \left[\sigma_1 \sigma_2 + \frac{3 + 3x' + x'^2}{x'^2} S_{12} \right] \frac{\exp[-x']}{x'},$$

scalar case:

$$(10) \quad V = V_{2K} = -\mu_K \frac{g_K^2}{4\pi} \frac{\exp[-x']}{x'}.$$

As was to be expected there is no dependence of the forces on isotopic spin; only the pseudoscalar interactions depend on ordinary spin while the scalar ones do not.

It may be remarked that the pion scalar interaction is always repulsive and the pion pseudoscalar interaction always attractive either for the triplet or singlet states—the singlet being somewhat lower—while the K force is attractive for singlet and repulsive for triplet; the scalar K force always attractive. Thus unless we assume the coupling constants to be very different from each other, we may disregard the scalar pion force and consider the

binding between nucleon and Λ to be due to a pseudoscalar two-pion force combined with a K-meson force that can be either scalar or pseudoscalar. The choice of the pseudoscalar case for the K-meson force should increase the spin dependence of the resultant Λ -nucleon force.

We shall assume in our calculation that all interactions are pseudoscalar, and that $g_\Lambda = g_K = g$.

In this case the lower energy level in the interaction Λ -nucleon is the singlet state. The calculated

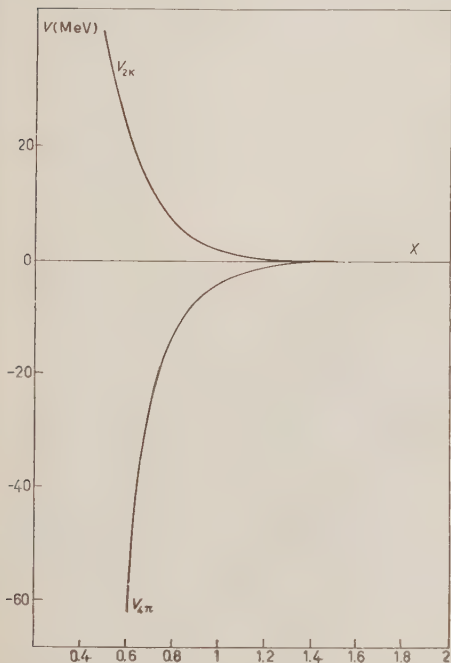


Fig. 4. - The calculated Λ -nucleon triplet potentials for $g = g_K = g_\Lambda$.

force what are the consequences which concern the binding energy of the Λ in light hyperfragments.

Experimental data on hyper-fragments are up to now rather scanty, as only a few examples of each type are available. Practically, the only cases in

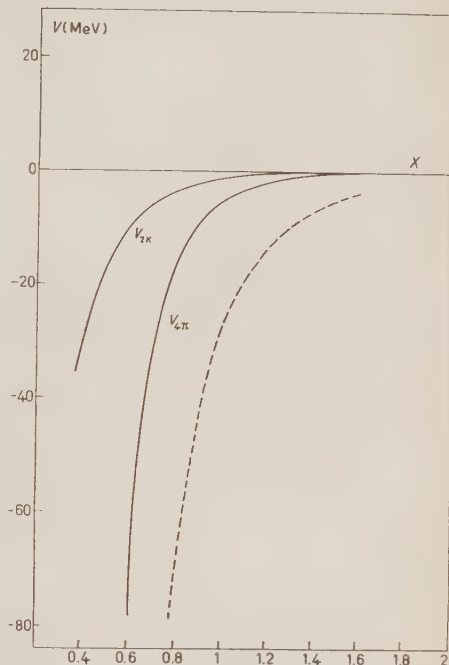


Fig. 3. - The calculated π -nucleon singlet potentials for $g = g_K = g_\Lambda$. The dotted line is the triplet (central plus tensor) nucleon-nucleon potential.

Λ -nucleon potential is plotted in Figs. 3 and 4. In Fig. 3 we have also reported as comparison the triplet (central and tensor) nucleon-nucleon potential (dotted line).

4. - Let us now try to deduce from our assumption about Λ^0 -N

which a sufficient number of events allows one to give a significant mean value for the binding energy, are the light hyperfragments, ${}^3\text{H}^\Lambda$, ${}^4\text{H}^\Lambda$, ${}^4\text{He}^\Lambda$, ${}^5\text{He}^\Lambda$ ⁽¹⁰⁾. It is noticeable that no case of either ${}^2\text{H}^\Lambda$ or ${}^3\text{He}^\Lambda$ have been recorded, so that it appears rather probable that these fragments do not exist. This evidence, together with some other indications from heavier hyperfragments, suggests the following as a suitable approach to our problem: If we assume that the nucleon-nucleon force is stronger than the Λ -nucleon force (which, in fact also follows from our calculation), then the nucleons will constitute a kind of nuclear core of the fragment, to which the Λ will be bound. Further, in this picture, it is to be expected that the only hyperfragments which can exist will be those in which the core alone is a normal nucleus, since the Λ -nucleon force is not strong enough to effect binding in a core which would not be stable by itself. This is consistent with the observed facts and the known four light hyperfragments would then be interpreted as

$${}^3\text{H}^\Lambda \rightarrow {}^2\text{H} + \Lambda, \quad {}^4\text{H}^\Lambda \rightarrow {}^3\text{H} + \Lambda, \quad {}^4\text{He}^\Lambda \rightarrow {}^3\text{He} + \Lambda, \quad {}^5\text{He}^\Lambda \rightarrow {}^4\text{He} + \Lambda$$

with cores corresponding to the only known stable light nuclei. Instead

$${}^3\text{He}^\Lambda \rightarrow {}^2\text{He} + \Lambda$$

is not observed; and ${}^2\text{H}^\Lambda \rightarrow \text{P} + \Lambda$ which would be due to the pure Λ -nucleon force is probably non-existent, because the nucleon-nucleon force gives already a very weak binding energy for the deuteron, and the weaker Λ -nucleon force would not be able by itself to bring about binding.

According to this picture, if we indicate the configuration of a given hyperfragment by the symbol (j, j_1) , where j denotes the total angular momentum of the fragment and j_1 the angular momentum of the nuclear core, the states of these hyperfragments will be given by:

$${}^2\text{H}^\Lambda \rightarrow (0, \tfrac{1}{2}), \quad {}^3\text{H}^\Lambda = (\tfrac{1}{2}, 1), \quad {}^4\text{H}^\Lambda \text{ and } {}^4\text{He}^\Lambda = (0, \tfrac{1}{2}), \quad {}^5\text{He}^\Lambda = (\tfrac{1}{2}, 0).$$

For the three-baryon case, the assignment $j_1 = 1$, implies an isotopic spin for the nucleons $T_1 = 0$, so that ${}^3\text{He}^\Lambda$ and ${}^3\text{n}^\Lambda$ are excluded. We can now calculate the binding energy of the Λ as a two body problem in which the potential acting on the Λ is the resultant of the potentials of all the nucleons of the nuclear core. Let us indicate with $Y_s(r)$ and $Y_T(r)$ the Λ -nucleon potential corresponding to the singlet and triplet states (we assume the damping

⁽¹⁰⁾W. FRY: *Seminar at Columbia University* (New York, Aprile 1956).

constant $\lambda = 0$ for the $V(1)_\pi$ and $V(2)_\pi$ terms, according to B. W.). Then:

$$(11) \quad \begin{cases} Y_s = V_{\pi s}^{DS} + V_{2KS}^{DS}, \\ Y_T = V_{\pi T}^{DS} + V_{2KTS}^{DS}. \end{cases}$$

The mean value of the potential that a nucleon will exert on the Λ independently of the spin orientation will be:

$$(12) \quad Y(r) = \frac{3}{4}\bar{Y}_T(r) + \frac{1}{4}Y_s(r),$$

where $Y_T(r)$ is the value of the triplet potential averaged over all angles.

Then, if we indicate by $\varrho(r)$ the nucleon density in the core we obtain the potential for the Λ in the four hyperfragment cases:

$$(13) \quad \begin{cases} {}^5\text{He}^\Lambda & V = \int 4 Y(r-r') \varrho_{\text{He}^\Lambda}(r') d\mathbf{r}', \\ {}^4\text{He}^\Lambda & V = \int [2\bar{Y}(r-r') + Y_s(r-r')] \varrho_{\text{He}^\Lambda}(r') d\mathbf{r}', \\ {}^4\text{H}^\Lambda & V = \int [2\bar{Y}(r-r') + Y_s(r-r')] \varrho_{\text{H}^\Lambda}(r') d\mathbf{r}', \\ {}^3\text{H}^\Lambda & V = \int 2 Y_s(r-r') \varrho_{\text{H}^\Lambda}(r') d\mathbf{r}'. \end{cases}$$

Obviously, the extra nucleon in the ${}^4\text{He}^\Lambda$ and ${}^4\text{H}^\Lambda$ cases and the two nucleons in the ${}^3\text{He}^\Lambda$ case are assumed to interact with the Λ -particle through the singlet state. It is interesting to note that in the case of ${}^5\text{He}^\Lambda$ according to (9) and (12) the contribution of the K force cancels out exactly, so that in this approximation the binding is due exclusively to the pion force. This fact shows clearly the oversimplification of the theories considering only the 2nd order K force and is important as the binding energy of ${}^5\text{He}^\Lambda$ may be used to get the value for the g_Λ constant.

The density factors which give the nucleon distribution in the core are assumed to be of gaussian form:

$$(14) \quad \varrho(r) = \varrho_0 \exp \left[-\frac{1}{2} \frac{r^2}{R^2} \right],$$

where the values of the constant R are given in the following Table I. For ${}^4\text{He}$, the value of the constant R is directly assumed from the experimental work of HOFSTADTER *et al.* (11) on high-energy electron scattering. As no direct

(11) R. HOFSTADTER *et al.*: *Proc. Sixth Annual Rochester Conference*, 1956.

TABLE I.

	$r \cdot m \cdot s \cdot 10^{13} \text{ cm}$	$R \cdot 10^{13} \text{ cm}$
${}^4\text{He}$	1.61	1.32
${}^3\text{He}$	1.83	1.5
${}^3\text{H}$	1.83	1.5
D	1.73	1.42

experimental evidence is available for the other cases, they have been derived from the following consideration. For the deuteron, HOFSTADTER *et al.* ⁽¹²⁾

give the density distribution assuming a square well. According to scattering theory one can from this distribution go back to the form factor in the scattering formula, and find the equivalent gaussian distribution that fits this factor; in this way the figure for the deuteron has been obtained. For ${}^3\text{H}$ and ${}^3\text{He}$, no experimental data of any kind are available; one can then assume that the distribution for both these nuclei is the same, and that the difference in binding energy between them is due only to the Coulomb repulsion between the two protons in ${}^3\text{He}$; then the gaussian shape that gives the observed difference may be calculated and yields the values of R given in Table I.

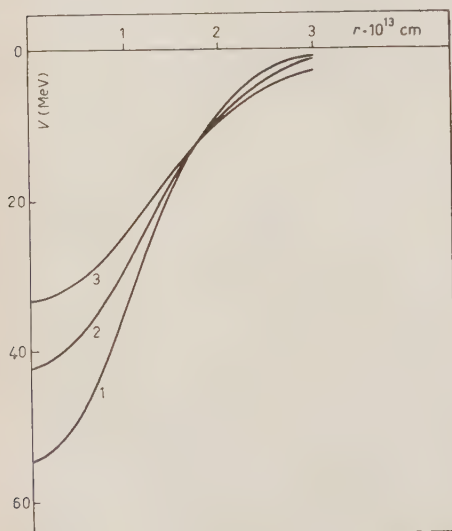


Fig. 5. Λ -nucleon potential: (1) HHe_M^Λ ; (2) He_M^Λ and H_M^Λ ; (3) H_M^Λ .

With these assumptions, the potentials (6) turn out to be given by

$$(15) \quad V(r) = \frac{4\pi R^2}{r^2} \varrho_0 \exp \left[-\frac{r^2}{2R^2} \right] \int_0^\infty Y(\varrho) \exp \left[-\frac{\varrho^2}{2R^2} \right] \varrho \sinh \frac{\varrho r}{R^2} d\varrho.$$

As already stated, the Λ -nucleon potentials are cut-off at the hard core radius, which according to the B.W. values, has been assumed equal to $0.33 \cdot 10^{-13} \text{ cm}$.

The potentials so obtained are given in Fig. 5. They may be well approx-

⁽¹²⁾ R. HOFSTADTER *et al.*: *Proc. Fifth Annual Rochester Conference* 1955.

imated by a gaussian curve:

$$V(r) = A \exp \left[-\frac{r^2}{a^2} \right],$$

with the following values for the parameters A , a .

TABLE II.

	A [MeV]	$a \cdot 10^{13}$ cm	
${}^5\text{He}^\Lambda$	54.6	1.45	(curve 1)
${}^4\text{He}^\Lambda$	43.2	1.60	(curve 2)
${}^4\text{H}^\Lambda$	43.2	1.60	(curve 2)
${}^3\text{H}^\Lambda$	35.7	1.79	(curve 3)

The calculation of the binding energy of the Λ has been done by the Ritz variational method, assuming as a trial function an exponential

$$u = \frac{x^3}{a^3} \exp \left[-\frac{x}{a} \right],$$

with α as the parameter to be varied. The results are given in the Table III.

TABLE III.

	α	E [MeV]	E_t [MeV]	E_{exp} [MeV]
${}^5\text{He}^\Lambda$	0.533	-2.44	—	-2.4 \pm 0.4
${}^4\text{He}^\Lambda$	0.490	-1.44	-0.78	-1.5 \pm 0.4
${}^4\text{H}^\Lambda$	0.490	-1.44	-0.78	-1.25 \pm 0.2
${}^3\text{H}^\Lambda$	0.457	-0.68	—	-0.2 \pm 0.3
${}^2\text{H}^\Lambda$	1.225	-0.07	—	~ 0

The first column shows the value of α which minimizes the binding energy E . The second column gives the binding energy E , the third the result of the same calculation made for two cases assuming the triplet state instead of the singlet state interaction between the Λ and the extra nucleon, and the fourth column gives the experimental data on binding energies. The results for the excited deuteron are also given, calculated directly from the Λ -nucleon potential.

The general agreement is excellent; the hyperdeuteron results hardly bound at all, while the calculated values in the other cases are well comprised within the errors of the experimental data. If this should be considered as an indication that our assumptions are true, then we could deduce from it the relative

parities of the different heavy particles considered. In fact, it has been shown by DALITZ ⁽¹³⁾ from an analysis of the reaction ${}^4\text{H}^\Lambda \rightarrow {}^4\text{He} + \pi$ that the parity of the ${}^4\text{H}^\Lambda$ is $(-1)^j$ where j is its spin. In our assumptions, the spin of ${}^4\text{H}$ turns out to be 0, its parity $-$, and this can be obtained with a Λ of spin $\frac{1}{2}$ when the parity is $-$. It then follows from our other assumptions that the Σ has also parity $-$; while the K should have parity $-$ if we assume a PS interaction as we have done. It may happen that the results will not be very different if we assume a scalar interaction for the K force which would give a $-$ parity for the K; we consider that this point should await further evidence.

Before however any definite conclusions may be drawn it remains to be seen if as good an agreement might also be obtained with other values of the g constants, to what extent the fit might be achieved in each case by changing the value of the hard core radius and what might be the effect of considering other interactions terms in the potentials. It is considered to examine these points more accurately in the near future.

Note added in proof.

After this work was presented at the Turin conference, we came to know a paper from D. LICHTENBERG and M. ROSS [*Phys. Rev.*, **103**, 1131 (1956)] who considers the same problem as we do starting from the same assumptions; the results however are different owing to the fact that these authors consider the graphs related with the bare baryon intermediate states for the calculation of the potential, which we have omitted.

⁽¹³⁾ R. H. DALITZ: *Proc. Sixth Annual Rochester Conference 1956; Seminar at Padua University*, May 1956.

RIASSUNTO

Si studia l'energia di legame delle Λ in materia nucleare, supponendo che l'interazione Λ -nucleone sia dovuta non solo al campo K ma anche al campo π ; le reazioni considerate sono $\Lambda \rightarrow N + \bar{K}$, $N \rightarrow \Lambda + K$, $N \rightarrow N + \pi$, $\Lambda \leftrightarrow \Sigma + \pi$. I calcoli sono stati eseguiti assumendo l'hamiltoniano di d'Espagnat e Prentki, con accoppiamento sia scalare sia pseudovettore (spin della Λ e della Σ uguale a $\frac{1}{2}$). L'energia di legame della Λ è in buon accordo con i dati sperimentali se si fa l'ipotesi che le costanti di interazione per le forze π e K siano dello stesso ordine di grandezza della costante di accoppiamento delle ordinarie forze nucleari: in questo caso la forza π risulta prevalente rispetto alla forza K.

Nuclear Scattering of K^+ -Mesons in the Energy Region of 80 MeV.

N. N. BISWAS, L. CECCARELLI-FABBRICHESI, M. CECCARELLI (*),
K. GOTTSTEIN (+), N. C. VARSHNEYA and P. WALOSCHEK (-)

Max-Planck-Institut für Physik - Göttingen

(ricevuto il 18 Ottobre 1956)

Summary. — The scattering of K^+ -mesons by nuclei of photoemulsion has been investigated in the 60 to 100 MeV region. Data on 27 collisions of K^+ -mesons with hydrogen nuclei, collected from various laboratories, are also presented. The angular distribution of the elastic scatterings is compared with curves calculated by COSTA and PATERGNANI for an optical model of the nucleus. The inelastic scattering data are, instead, compared with the results of a calculation performed with the Monte Carlo method, for a Fermi-gas nuclear model. Experimental evidences, such as the frequent occurrence of small angle elastic scatterings and the rarity of large energy losses, argue in favour of a repulsive nuclear potential acting on the K^+ -meson. The angular distribution of the K^+ -p collisions is then satisfactorily described assuming a predominant s -wave scattering for energies lower than ~ 50 MeV in the center of mass system. The data on the K^+ -nuclei inelastic scattering are shown instead to be well described, on the basis of the Fermi model, with the assumption that the K -nucleon cross-section is peaked backwards or is energy dependent. The influence of the two isotopic spin states which intervene in the K -nucleon scattering is discussed.

1. — Introduction.

The study of the interactions of K^+ -mesons with complex nuclei ⁽¹⁾ is at present of interest because it allows to gain information on the elementary

(*) On leave from Padua University.

(+) At present at the University of California, Berkeley.

(-) On leave from the Argentine Comisión Nacional de la Energía Atómica.

⁽¹⁾ J. E. LANNUTTI, W. CHUPP, G. GOLDBABER, S. GOLDBABER, E. HELMY, E. L. ILOFF, A. PEVSNER and D. RITSON: *Phys. Rev.*, **101**, 1617 (1956). See also the results

processes between nucleons and heavy mesons. As soon as the K^+ -proton and K^+ -neutron cross-sections will be known independently, K^+ -nuclei interactions may, moreover, become a valuable tool for studying the properties of nuclei, because the positive heavy mesons have rather small total cross-section, are not absorbed and can be easily identified after the scattering.

In this paper we present some data on a number of events in which artificially produced K^- -mesons with energies around 80 MeV were scattered by the nuclei of photoemulsion. We have attempted to gather information on the elastic scatterings by the nucleus as a whole and on the elementary scattering with single nucleons. We expect to present in another paper some data on the determination of the total cross-sections for scattering and charge exchange and their dependence on energy.

2. - Experimental Details.

The track scanning procedure was the same as described in a letter by BISWAS *et al.* ⁽²⁾. The straggling in the range of K^+ -mesons of a given nominal momentum is approximately ± 4.0 mm which leads to an error in the energy of ± 7 MeV for mesons at a residual range corresponding to 60 MeV and of ± 4 MeV for those of 100 MeV. The values of the nominal energies have been determined for the various plates by using K -mesons which stop in the stack without having suffered interactions. In the case of the second stack that we have used the occasional occurrence of low energy K -mesons has been found. These low energy tracks can be easily discriminated by grain counting.

In the course of scanning all interactions with a projected scattering angle greater than 10° , for nominal energies between 50 and 115 MeV, have been recorded. Out of ~ 450 K -meson collisions observed, 221 with nuclei different from hydrogen have been selected which obey the following criteria:

- a) Nominal energy between 60 and 100 MeV,
- b) Grain density of the primary consistent with the nominal energy,
- c) Projected scattering angle $\geq 10^\circ$,
- d) K -meson stopping in the stack and
- e) clearly identified by its decay.

of the European Laboratories reported by N. DALLAPORTA at the Sixth Rochester Conference 1956. and at the Turin Conference 1956.

⁽²⁾ N. N. BISWAS, L. CECCARELLI-FABBRICHESI, M. CECCARELLI, M. CRESTI, K. GOTTSTEIN, N. C. VARSHNEYA and P. WALOSCHEK: *Nuovo Cimento*, **3**, 1481 (1956).

The proportion of K-mesons which stop without showing any decay product has been assumed to be the same for scattered and non-scattered particles, and has been found to be 14 %. This has been taken into account in correcting the value of the total track length followed, which results then to be 105 m in the 60 to 100 MeV region. This value may, however, still be subject to some slight variation as a consequence of the difficulties in estimating the contamination by background tracks.

Two events showing all the five previous characteristics have been excluded because the last two conditions were fulfilled only due to the occurrence of a second process (a second scattering and a decay in flight) so that otherwise the K-meson would have left the stack. Moreover, four events in which the meson left the stack from side or back have been included for reasons which will appear later.

Assuming now the two stacks to be sheets of infinite size and with thicknesses of 39 and 60 mm respectively and the mesons to be isotropically scattered around their direction of motion, a correction coefficient ≥ 1 for each event has been computed which is a function of the secondary range, the angle of scattering, and the depth of the event in the stack. This coefficient corresponds to the number of events of the same type which one would expect to observe if the conditions (c) and (d) were eliminated. In the following we shall always use these corrected numbers for the distributions, and the effective numbers for the computation of the statistical errors.

For each event the primary energy has been calculated from the nominal energy curves and from its position in the stack, and the secondary energy from the range of the outgoing meson. This method permits an accurate determination of the energy of the scattered meson and is less likely to cause systematic errors than an energy determination by the measurement of ionization and scattering.

In Table I are listed the events for which the projected angle is $\geq 12^\circ$ and the true scattering angle θ is $\geq 20^\circ$ (*). The columns (except the first) correspond to equal intervals of solid angle, namely to $\Delta \cos \theta = 0.2$. The rows correspond to the percentage energy loss $(E_{\text{prim}} - E_{\text{sc}})/E_{\text{prim}}$. The numbers without parenthesis are, as mentioned before, the corrected numbers of events; those in parenthesis are the effective numbers.

In a number of events, prongs emerging out of the point of collision have been observed; their presence has, however, not been taken into account for classifying the events, except in explicitly mentioned cases.

The energies of the primaries are nearly uniformly distributed between

(*) We indicate with θ the scattering angle in the laboratory system and with χ the angle in the center of mass of the K-nucleon system.

60 and 100 MeV. For the calculations we shall usually consider our events to have a single primary energy, namely 80 MeV.

3. - Elastic and Slightly Inelastic Scatterings.

In Fig. 1 the distribution of the relative energy losses $\Delta E/E$ is shown for all events of Table I. One sees that there do not exist two clearly separated classes of events which might be called elastic and inelastic.

As to the definition of elastic collisions we have not found it satisfactory, to classify the events using an arbitrary cut-off value of the energy loss, or by

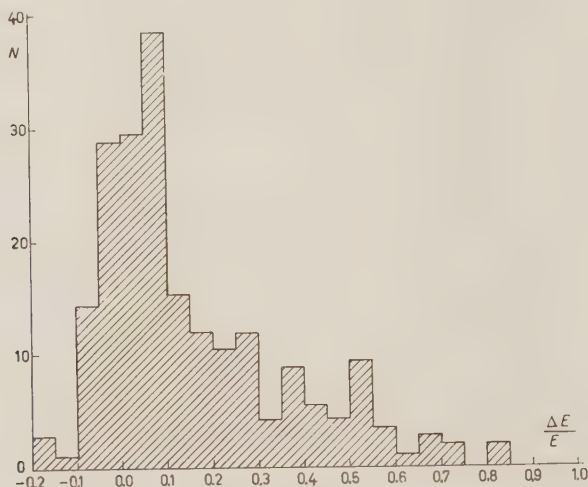


Fig. 1. Distribution of the relative energy losses.

imposing the condition of absence of additional prongs at the point of collision, which may, in fact, occur also in an unpredictable number of inelastic events. The only unbiased procedure seems to be the one first applied by MINGUZZI *et al.* ⁽³⁾, in which one considers as due to the elastic events that part of the energy loss distribution which is symmetrical around the value of the energy (E_{recoil}) kinematically transferred to the recoiling nucleus. In this way, however, only about one half of the events in each angular interval are used.

⁽³⁾ A. MINGUZZI, G. PUPPI and A. RANZI: *Nuovo Cimento*, **11**, 697 (1954).

Up to a K-meson scattering angle θ smaller than $\arccos 0.4$, a separation between collisions with light and heavy nuclei is unreliable under our experimental conditions. We have, therefore, calculated the energy of the recoiling nucleus emitted in this small angle region on the assumption that the nucleus has on the average a value of A equal to 75. The value chosen for the target mass is not very important as the energy transferred to the recoiling nucleus

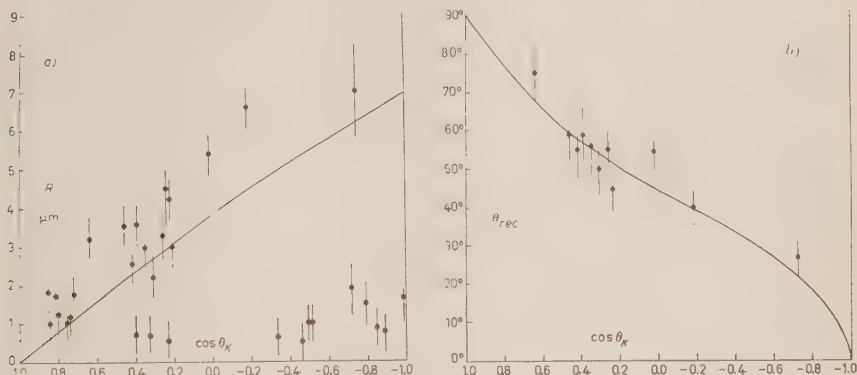


Fig. 2. — a) Range of the recoiling nucleus versus the scattering angle of the K-meson; b) Emission angle of the recoiling nucleus versus the scattering angle of the K-meson.

is very small. In case of larger values of the angle θ , the elastic scatterings on light nuclei can be identified on account of the rather long range of the recoil. In Figs. 2a and 2b are shown the expected distributions for the range ⁽⁴⁾ and for the emission angle for a nitrogen nucleus elastically hit by a K-meson of 80 MeV, as a function of the angle of the scattered meson. The points in Fig. 2 represent all events in which the energy loss is less than 20 MeV and a single blob is emitted in a direction consistent with that to be expected for an elastic collision. The data on the angular distribution of the recoils having a range greater than $2 \mu m$ are presented in Fig. 2b. The experimental points which lie around the curve of Fig. 2a, represent very probably the collisions of a K-meson with a light nucleus as a whole. Such an analysis is, however, inefficient for detecting the cases where some nuclear excitation of the target nucleus has occurred. We shall show subsequently that such a possibility should be taken into account.

We have assumed the distribution of the energy losses ΔE for the elastic events to be around the recoil energy (E_{recoil}). The number of the elastic events within each angular interval has then been taken to be twice the number of

⁽⁴⁾ The range energy relation for nitrogen has been taken from H. L. REYNOLDS and A. ZUCKER: *Phys. Rev.*, **96**, 393 (1954).

cases in the same interval for which $\Delta E - E_{\text{recoil}} \leq 0$. The case of heavy and light nuclei have been treated separately, as has been explained before, and the two contributions have then been added.

Among the elastic events, also the scattering with θ between 10° and 20° have been included. These events, in order not to decrease too much the statistical weight of the points in this important region of the angular spectrum, have all been considered elastic, provided the quantity $\Delta E/E$ is smaller than 0.2. The fact that the ΔE distribution for these events is very well centered around zero proves that this procedure is substantially correct.

For these small angle scattering events the geometrical correction coefficient has not been computed for each event individually, but for each group of events in the same angular interval.

In our experiment the mean free path for elastic scattering with angles larger than 20° comes out to be 1.0 m. If we compare this value with the results of a calculation made by COSTA and PATERGNANI ⁽⁵⁾ for the optical

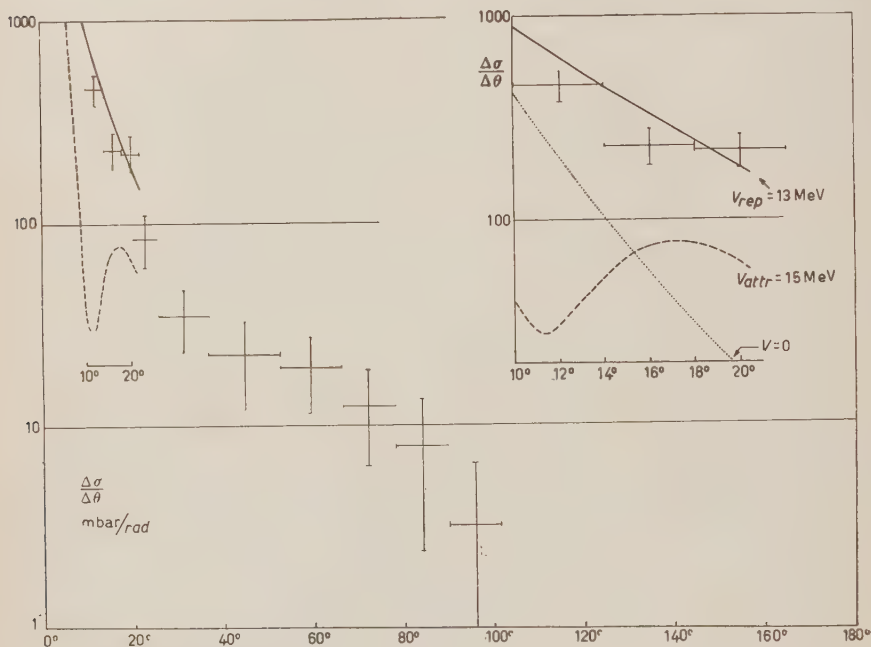


Fig. 3. — Angular distribution of the elastic events. The curves correspond to the cases of interference between the Coulomb field and: — a repulsive nuclear potential of 13 MeV; ---- an attractive nuclear potential of 15 MeV.

(5) G. COSTA and G. PATERGNANI: reported at the Turin Conference, 1956.

model of the nucleus, we find that it is consistent with either of the two alternative assumptions: a Coulomb field interfering with a nuclear repulsive potential of about 12 MeV or with a nuclear attractive potential of about 20 MeV.

In Fig. 3 the differential angular distribution of our elastic events is shown together with two curves also derived from the work of COSTA and PATERGNANI. These represent the expected angular distributions in cases of repulsive and attractive nuclear potentials for the primary energy spectrum of our experiment. As first pointed out by OSBORNE, it may be seen that this method of discrimination between the two signs of the potential is very sensitive for certain intervals of scattering angle. Our experimental data seem to favour definitely the repulsive nuclear potential.

It can be seen from Fig. 3 that in apparent disagreement with the results of other experiments (*) there is no significant contribution of large angles. This has induced us to search for possible sources of systematic errors due to the use of different methods in ascertaining the energies of the incoming and outgoing mesons. In principle, some errors might have been introduced by the fact that the mesons coming out of the nuclear collisions generally have a geometry different from that of the non-scattered K -mesons, which have been used for the determination of the nominal energy spectrum. Effects such as uneven thickness of plates, distortion of the emulsion, etc., might play a role due to this difference of geometry. In order to check this, we have studied the π secondaries, from a number of τ -mesons, having widely different geometries in the stacks. From the comparison of the Q -values calculated from the range of secondaries with different geometrical conditions we are able to exclude that the energy determination of the scattered K -mesons may involve a systematic error of more than 1 MeV.

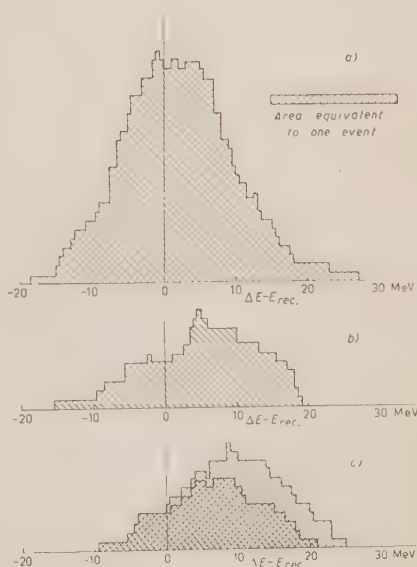


Fig. 4. — Distribution of the $(\Delta E - E_{\text{recoll}})$ smaller than 20 MeV for the cases: a) all events with scattering angles between 20° and 30° ; b) scatterings on light nuclei with $\theta \geq \arccos 0.4$; c) scatterings on heavy nuclei with $\theta \geq 90^\circ$.

(*) See the Padua group results of ref. (1).

The fact that the large angle scatterings are often accompanied by a slight excitation of the target nucleus is indicated by Fig. 4 where the distributions of $\Delta E - E_{\text{recoil}}$ are shown for the cases:

- a) all events with scattering angles between 20° and 30° ,
- b) elastic collisions with light nuclei, having $\theta \geq \arccos 0.4$,
- c) all remaining collisions having $\theta \geq 90^\circ$ and $\Delta E - E_{\text{recoil}} \leq 20$ MeV, assuming the target to be a heavy nucleus.

The positions of the maxima, particularly in the last two distributions, are seen to be markedly shifted towards the right. The doubly hatched part of figure *c* corresponds to the events kinematically inconsistent with collisions with a free nucleon of less than 20 MeV energy. A number of events is thus found to lie in a region intermediate between that of elastic scattering and that of collision with a single nucleon. The interpretation of these events as being due to nuclear excitation seems to be reasonable (⁷).

In Fig. 5 is given the integral distribution of the ratios of the elastic events

to the total as a function of the scattering angle. Our ratios seem to be slightly lower than those obtained by other authors; this effect can be explained by the different methods in estimating the elastic contribution.

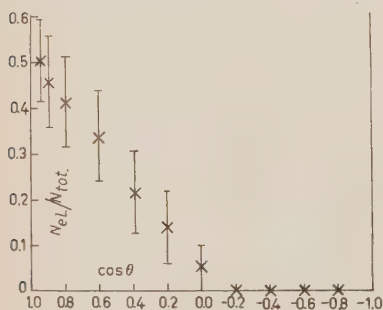


Fig. 5. — Integral distribution of the ratios of the elastic to the total events as a function of the scattering angle.

4. — The Inelastic Scatterings.

4.1. *Comparison with a nuclear Fermi gas model.* — Due to the difficulties in separating the inelastic scattering which may be attributed to collisions with single nucleons from the elastic scatterings and from those of «small inelasticity», only the events of Table I in which the quantity $\Delta E/E$ is larger or equal to 0.2 have been considered in this section. This cut-off is largely

(⁷) Similar effects in case of p-nuclei collisions have been extensively studied by K. STRAUCH and F. TITUS: *Phys. Rev.*, **104**, 191 (1956).

outside the elastic part for the majority of the events. In addition, two events with the proper energy loss (marked with asterisc in Table I) have been excluded because it seems kinematically impossible that they are due to a single collision with a nucleon inside the Fermi momentum sphere.

The experimental distribution of the scattering angles for these inelastic events is shown by the points of Fig. 6*a*; in Fig. 6*b* is instead shown the experimental distribution of the quantity $\Delta E/E$. The same points of Fig. 6*a* are also drawn in Figs. 7*a* and 8*a*, and those of Fig. 6*b* in Figs. 7*b* and 8*b*. In Fig. 9 are plotted the values of the average relative energy loss for the different scattering angle intervals.

In order to compare these data with some nuclear collision model, a Monte-Carlo calculation (*) has been performed assuming that each event can be considered to be due to a single collision with a nucleon and that the nucleons form a completely degenerate Fermi gas. The first hypothesis seems to be tenable due to the small nuclear cross-section of the K^+ -mesons. The calculation has been done for a total of 800 collisions, including those forbidden by the Pauli exclusion principle or eliminated by the conventions of $\theta > 20^\circ$ and $\Delta E/E > 0.2$. In Figs 6 : 9, curves have been drawn trying a best fit to the Monte-Carlo points (+).

The curves in Figs. 6*a* and 6*b* correspond to the cases of an isotropic distribution of the scattering angles in the center of mass of the K-nucleon system and to:

- 1) primary energy of 80 MeV; repulsive potential of 20 MeV,
- 2) primary energy of 80 MeV; repulsive potential of 10 MeV,
- 3) primary energy of 80 MeV; no potential,
- 4) primary energy of 70 MeV; attractive potential of 10 MeV.

The Coulomb potential is included in these values and the total cross-section has been assumed to be independent of energy. The values indicated are those of the primary energy outside the nucleus. In case 1), the refraction of the particle at the nuclear surface has been taken into account and the angles modified by this effect have been used in drawing the corresponding curve in Fig. 6*a*. The changes due to this effect have, however,

(*) Details on this calculation are given in the Appendix.

(+) It should be remembered that the Monte-Carlo points have also statistical errors which in our case are about $\frac{1}{3}$ of those attached to the experimental points. Due, however, to the fact that often various curves have been derived from a same set of Monte-Carlo configurations, as explained in the Appendix, even rather small relative displacements of the curves may be taken to have some significance.

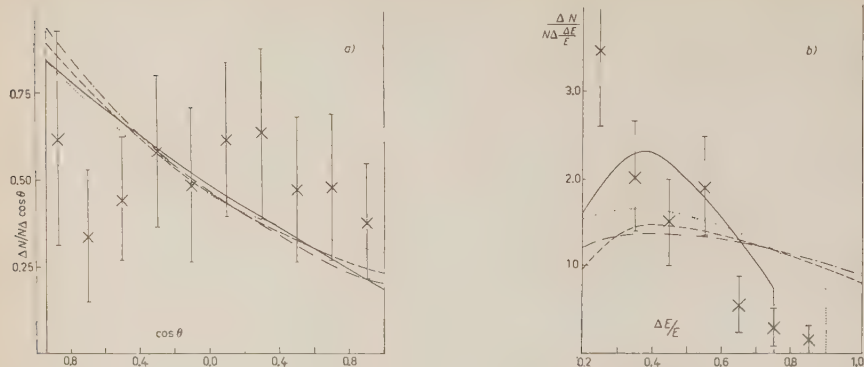


Fig. 6a and 6b. — Effect of the nuclear potential. The curves correspond to Monte-Carlo calculations assuming isotropic angular distribution in the center of mass system, σ_{tot} independent of the energy and: — 20 MeV repulsive potential; ···· 10 MeV repulsive potential; ----- no potential; - · - · - 10 MeV attractive potential.

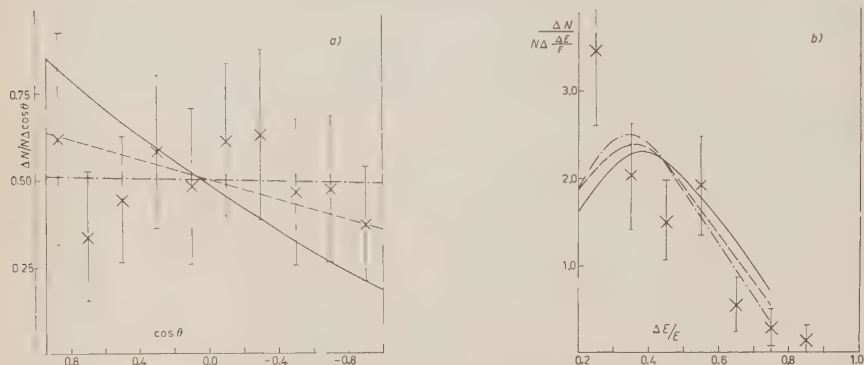


Fig. 7a and 7b. — Effect of the energy dependence of the total cross-section. The curves correspond to Monte-Carlo calculations assuming isotropic angular distribution in the center of mass system, 20 MeV repulsive potential and: — E^0 ; ----- $\sigma_{\text{tot}} \propto E^{-1/2}$; - · - · - $\sigma_{\text{tot}} \propto E^{1/2}$.

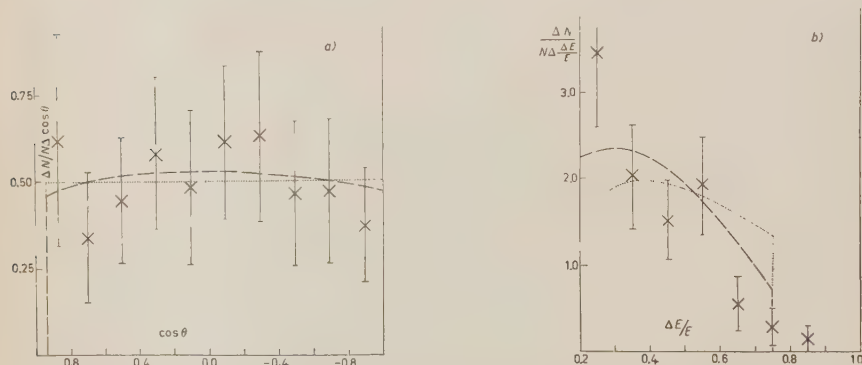


Fig. 8a and 8b. — Effect of the shape of the angular distribution in the center of mass system. The curves correspond to Monte-Carlo calculations assuming σ_{tot} independent of energy, 20 MeV repulsive potential and: ···· $\sigma_{\text{diff}} \propto 1.5 - 0.5 \cos \chi$; ----- isotropic for $E_{\text{C.M.S.}} < 50$ MeV and $\sigma_{\text{diff}} \propto 2.5 - 1.5 \cos \chi$ for $E_{\text{C.M.S.}} > 50$ MeV.

been found to be not very important and so we have not considered it necessary to extend this calculation to the other cases.

Among the four curves of Fig. 6a the best agreement is with that corresponding to the maximum repulsive potential. This agreement is more clearly seen in the representation of Fig. 9, in which the average relative energy loss is plotted as a function of the scattering angle; this function is substantially independent of the shape of the angular distribution in the center of mass of the K-nucleon system.

A common feature of the curves of Fig. 6a is that the Monte-Carlo angular distributions based on the hypothesis of an isotropic cross-section in the center of mass system show a tendency to give more forward scattering than that observed in the experiment. This disagreement can be removed by assuming that the cross-section depends on the energy of the K-meson in the center of mass system. (In this connection, it should be remembered that the energy in the center of mass system for a K-meson colliding with a Fermi gas nucleon spreads over a wide range. For a K-meson of 80 MeV, energies in the center of mass system from 10 to 70 MeV can be found).

In Figs. 7a and 7b the experimental points are again compared with two new Monte-Carlo calculations. A repulsive potential of 20 MeV has been taken and the total K-nucleon cross-section has been assumed to be proportional to $E^{\frac{1}{2}}$ and E^1 . It is seen that a weak dependence of the cross-section on the energy, such as $\sigma \propto E^{\frac{1}{2}}$, may lead to a better agreement with the experimental points.

If, alternatively, one assumes that the cross-section in the center of mass system rises in the backward direction, an agreement can be easily obtained between the Monte-Carlo and the experimental angular distributions. The results of a calculation for a cross-section of the form $1.5 - 0.5 \cos \chi$ is shown in Fig. 8a. Such a cross-section, however, does not predict very satisfactorily the frequent occurrence of the low energy loss events, as can be seen from Fig. 8b. The agreement with the experimental data is improved by assuming that the cross-section is isotropic at low energies in the center of mass system

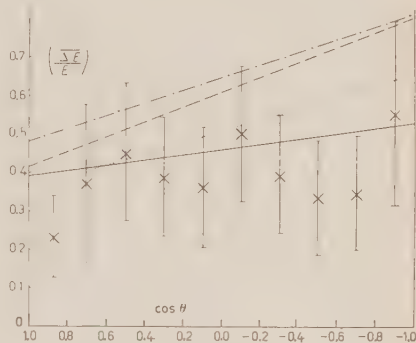


Fig. 9. — Average energy loss of inelastic events with $\Delta E/E > 0.2$ as a function of the scattering angle. The curves correspond to Monte-Carlo calculations with the same assumptions as those of Fig. 6 and have been indicated by the same symbols.

and rises backward at higher energies. The results of a Monte-Carlo calculation with a σ isotropic up to an energy of 40 MeV in the center of mass system and of the form $2.5 - 1.5 \cos \chi$ at higher energies are also shown in Figs. 8a and 8b. The value of the total cross-section has been here assumed to be independent of energy.

For the sake of convenience we have considered in this section only a very simple dependence of σ on χ and E , though realizing their little physical meaning.

4.2. *Discussion of other possible nuclear models.* — There are reasons to believe that the independent particle model is only an approximate picture of the nucleus; it has therefore been considered to be of little use to try a much better description of the experimental data by considering, in the Monte-Carlo calculation, more complicated angular distributions and energy dependences of the elementary cross-section.

As an indication of the limitations of the Fermi gas model, we may for instance recall the occurrence of backward scattering (see Fig. 4c) in which the energy loss is too small to be explained as due to a single collision with a Fermi sphere nucleon but too large to be attributed to elastic scattering.

This type of events could be understood assuming a nuclear model with high momentum nucleons; it is then easy to predict qualitatively that a contribution to the scattering will result from the collisions with nucleons moving rapidly towards the incoming K-particle and that these collisions will give rise to scatterings preferentially in the backward direction in the laboratory system, and with small energy losses.

Another way to solve the above mentioned difficulty could be to assume that a fraction of the collisions have occurred not with isolated nucleons but with groups of nucleons⁽⁸⁾. This could be the case if the nucleons inside the nucleus were not statistically distributed in space but were clogged in groups with energies comparable with that of the incident K-mesons. Collisions with systems of high mass will generally cause smaller energy losses and also lead to rather large angles of scattering in the laboratory system. To assume that nucleons are partly grouped together would also help to bring a better agreement between the value of the K^+p cross-section obtained from the observed hydrogen collisions and that of the K^+ -nucleon cross-section derived from the mean free path in nuclear matter^(9,10).

(8) An indication in this sense is given by the occurrence of the reaction $K^+ + {}^{12}\text{C} \rightarrow K^+ + {}^3\text{He}$, recently found by F. ANDERSON, D. KEEFE, A. KERNAN and J. LOSTY: *Nuovo Cimento*, **4**, 1198 (1956) and by N. N. BISWAS, L. CECCARELLI-FABBRICHESI, M. CECCARELLI, K. GOTTSTEIN, N. C. VARSHNEYA and P. WALOSCHKE: *Nuovo Cimento*, **4**, 1201 (1956).

(9) J. E. LANNUTTI *et al.*, see ref. (1).

(10) On this argument see the discussion in ref. (2).

If the collisions with aggregates of nucleons were frequent processes, then all our conclusions on K-nuclei collisions would have to be revised. The independent particles model seems, indeed to be well supported by the correctness of its prediction, particularly for the scattering of slow π -mesons ⁽¹¹⁾. In this case, however, the occasional occurrence of collisions with nuclear clusters may not be easily detected due to the smallness of the pion mass. For the K-meson scattering, the influence of the mass of the target is greater.

5. - Results on K^+ -Proton Scatterings.

We have collected from various laboratories data on the K^+ -proton collisions found in nuclear emulsion. So far 27 events having a scattering angle θ larger than 10° ($\chi \gtrsim 16^\circ$ in center of mass system) and energies lower than 150 MeV ($E \lesssim 60$ MeV in center of mass system) are known to us. These events have been found by following a total K-track length of about 600 m; the total cross-section turns out to be of 14 ± 3 mb.

In Fig. 10 is shown the distribution of the scattering angles χ of these events. The histograms represent the distributions expected for s -wave scattering considering the interference with the Coulomb field, the total cross-section being 14 mb. These histograms are the mean of a number of distributions corresponding to the energies over which the collisions were observed.

It appears from this figure that, for a repulsive nuclear potential, the assumption of a predominant s -wave scattering in the $T=1$ state is satisfactory for explaining the experimental results. This assumption is also supported by the fact that the cross-section for K^+ -proton scattering does

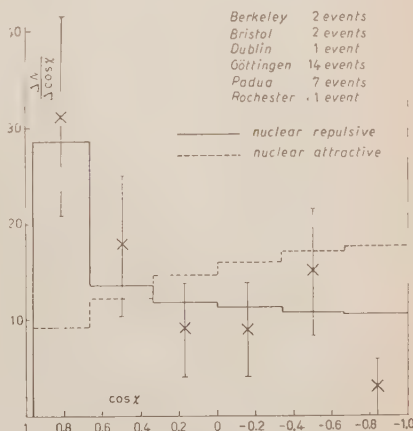


Fig. 10. - Distribution of the angles χ for 27 K-p collisions. The curves correspond to the cases of interference between the Coulomb field and: — a repulsive nuclear potential; - - - an attractive nuclear potential.

⁽¹¹⁾ See ref. ⁽³⁾ and also: V. BORELII, L. FERRETTI, R. GESSAROLI, L. LENDINARA, A. CHIARINI, A. TOMASINI, G. QUARENI, A. RANZI and G. PUPPI: *Report of the Turin Conference*, 1956.

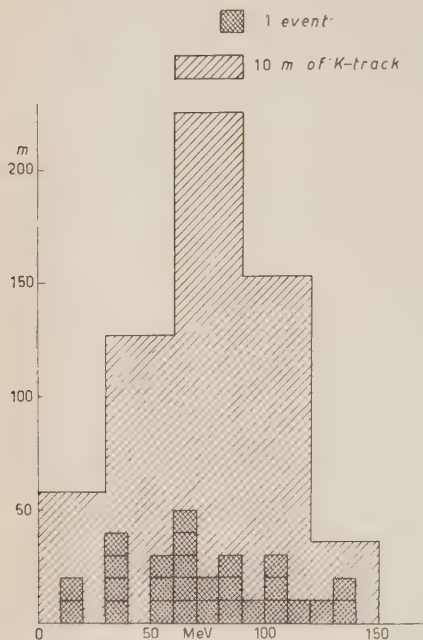


Fig. 11. — Distribution of the primary energy of 27 K-p collisions and of the K-track length observed in various energy intervals.

b) The differential cross-section rises backward with increasing energies, its total value remaining constant.

The present experimental data on the variation of the K-nuclei cross-section with energy are not sufficient to lead to a definite preference for one of these two hypotheses. A slight increase of the inelastic K-nuclei cross-section with energy, which seems to be indicated by some experimental results⁽¹²⁾, could merely be due to the influence of the Pauli principle and to the reflecting effect of the repulsive potential barrier and may not imply such a behaviour for the elementary K-nucleon cross-section.

The presence of an important backward scattering term of the isotopic spin state $T=1$ seems to be unlikely at present, at energies in center of mass system lower than ~ 50 MeV, as discussed in the preceding section. If therefore a backward scattering term would be found to be necessary for expla-

not seem to be strongly dependent on energy, as can be seen from Fig. 11 where the energy spectrum of the primary K-mesons is plotted together with the track-length followed in the various intervals.

6. — Conclusion.

The existence of a nuclear repulsive field of about 15 MeV acting on the K^+ -meson seems to be well established by the various evidences presented in this paper. On this basis and utilizing the Fermi gas model we may interpret the K^+ -nucleus scattering data by postulating for the K-nucleon cross-section either of the following two extreme behaviours:

a) The differential cross-section remains substantially isotropic in the center of mass system but its total value increases with energy.

⁽¹²⁾ See the report of N. DALLAPORTA at the Turin Conference 1956.

ining the K-nuclei scattering data, the present evidence would favour the hypothesis either that this term occurs, in the $T=1$ state, at energies larger than ~ 50 MeV in the center of mass system, or that the scattering in the $T=0$ state is not negligible and is dominated by the p -wave, as discussed by Cocconi *et al.* ⁽¹³⁾. The kinematical consequences of these two hypotheses are very similar, so that the present experiment can not decide between them.

* * *

We are grateful to Prof. W. HEISENBERG and to Drs. G. COSTA, K. NISHIJIMA, G. QUARENI and G. SALANDIN for the very useful discussions, and to the scanning team of our Institute for their efficient work.

Without the kind co-operation of Drs. E. J. LOFGREN, R. W. BIRGE, D. H. STORK and their collaborators at the Radiation Laboratory in Berkeley who arranged the exposure of the emulsions to the K⁺-beam this investigation would not have been possible. We are also particularly indebted to Drs. R. CESTER, M. CRESTI, G. GOLDBERGER, J. E. HOOPER, D. KEEFE and G. QUARENI who have very kindly sent us the data on the K-proton collision events and the length of track followed in their laboratories.

N. N. B. thanks the Government of India, M. C. the Max-Planck-Gesellschaft and N. C. V. the Alexander v. Humboldt Stiftung for their maintenance grants.

The Deutsche Forschungsgemeinschaft has supported our work by the purchase of microscopes.

APPENDIX

Details of the Monte-Carlo Calculation.

The inelastic collision of a K^+ -meson with a nucleus has been tentatively represented by the following model:

- i) The K-meson traverses the surface of the nucleus, with a modification of its momentum due to the nuclear potential;
- ii) it interacts with a nucleon and then escapes from the nuclear surface without suffering further collisions;
- iii) at the point of exit it undergoes a change in momentum as in i).

⁽¹³⁾ G. COCCONI, G. PUPPI, G. QUARENI and A. STANGHELLINI: Turin Conference, 1956.

The interaction ii) of the K-meson with a nucleon is defined by the following parameters:

- a) energy of the meson inside the nucleus,
- b) energy of the target nucleon,
- c) angle between the momenta of the two colliding particles,
- d) angle between the plane of collision and the plane of scattering,
- e) angle of scattering in the center of mass system.

As usual in the Monte-Carlo calculations a number of collision configurations has been constructed by assigning to some of the parameters determined values and to others random values. For the energy of the K-meson inside the nucleus was taken a value depending on the primary energy and on the nuclear potential which has been postulated to act on the particle.

The nucleons inside the nucleus have been assumed to form a completely degenerate Fermi gas. The momentum sphere, assumed to have a radius of 200 MeV c , has been divided into 1000 equal probability intervals, namely: ten for parameter b), twenty for c) and twenty for d). The values of these three parameters were then assigned at random.

The parameter e) has instead been varied regularly. The angular distribution of scattering has been assumed to be isotropic in the center of mass system and the whole range of the scattering angle has been divided into twenty equally probable intervals. Corresponding to each one of these intervals, an equal number of collision configurations has been constructed for different sets of the other parameters. We were in this way not limited only to an isotropic angular distribution; it was indeed possible, without further construction of new collision configurations, to obtain distributions corresponding to any desired angular dependence. This could be done simply by attributing proper weights to the configurations corresponding to the different angular intervals.

The calculations have been carried out graphically, in the classical approximation, and in three dimensions with a mechanical device. The precision of the calculation has been proved to be sufficient for our purposes.

A number of configurations out of the total has been eliminated, namely: those forbidden by the Pauli exclusion principle (about 25%, for σ isotropic) and those for which the scattering angle is smaller than 20° or the energy loss is smaller than 20% (for comparing the Monte-Carlo calculation with the experimental results).

The relative velocity of the K-meson with respect to the target nucleon was also computed for each configuration. By grouping them into various intervals of this parameter, and giving to each group a proper weight, it was possible to take into account any energy dependence of the elementary scattering cross-section as well as any variation of the probability of collision as a function of the relative velocity.

The variation of momentum at the entrance and exit of the nucleus has been computed, for a given point and angle of impact, attributing to the nuclear matter a refractive index which depends on the potential supposed

to act on the meson. The point of entrance has been chosen at random; that of exit has been chosen, for a given angle of scattering, by taking at random the position of the K -nucleon collision.

RIASSUNTO

Nel presente lavoro sono presentati i risultati di una esperienza sulla diffusione di mesoni K^+ d'energia compresa fra 60 e 100 MeV da parte dei nuclei della emulsione fotografica. Si riportano anche dati relativi a 27 esempi di collisione tra un mesone K^- ed un nucleo d'idrogeno, raccolti tra diversi laboratori. La distribuzione sperimentale degli angoli di diffusione elastica viene paragonata con curve calcolate da COSTA e PATERGNANI per il modello ottico del nucleo. I dati sulla diffusione inelastica sono paragonati invece con i risultati di un calcolo, eseguito con il metodo di Monte-Carlo, per un modello nucleare a gas di Fermi. Alcuni fatti sperimentali, e cioè l'elevato numero di diffusioni elastiche a piccolo angolo e la scarsità di collisioni fortemente inelastiche, suggeriscono che il potenziale nucleare agente sul mesone K^+ sia repulsivo. La distribuzione angolare delle collisioni K^- -protone può essere allora descritta in modo soddisfacente supponendo che, al disotto d'energie di circa 50 MeV nel baricentro, l'onda s sia dominante. I dati sulla diffusione inelastica K^- -nucleo si lasciano invece meglio descrivere, sulla base del modello a gas di Fermi, qualora si supponga che la sezione d'urto dell'interazione K^- -nucleone abbia una distribuzione angolare lievemente diretta all'indietro o dipenda dall'energia. Viene discussa la possibile influenza dei due stati di spin isotopico che intervengono in questa interazione.

On the Paramagnetic Resonance Spectrum of Triphenylmethyl.

P. BROVETTO and S. FERRONI

Istituto di Fisica dell'Università - Torino

Istituto Nazionale di Fisica Nucleare - Sezione di Torino

(ricevuto il 19 Ottobre 1956)

Summary. — In this work the paramagnetic resonance of the triphenylmethyl radical has been investigated. The hyperfine structure spectrum is deduced using the Slater-Pauling theory. The agreement with the existing experimental data is satisfactory. The usefulness of paramagnetic resonance measurements as an investigation method in valence theory is stressed.

1. — Introduction.

Recently, in the paramagnetic resonance spectrum of a diluted solution of some organic radicals, the hyperfine structure due to the coupling of the electron and nuclear spin has been observed.

The theoretical interpretation of such spectra involves considerable difficulties, since it requires the accurate knowledge of the molecular wave function in the ground state. In this paper the theoretical spectrum of triphenylmethyl is calculated using the wave function of the $2p_z$ electrons obtained by the Slater-Pauling method.

As it is well known such a method provides a rather simple and reasonably good approximation for the energy of the ground state ⁽¹⁾. One can assume, therefore, that the wave function is accurate enough to provide a good estimate for the hyperfine structure of the radical spectrum.

⁽¹⁾ L. PAULING and G. WELAND: *Journ. Chem. Phys.*, **1**, 362 (1933).

2. - Theory.

As is well known Pauling's model assigns four L -electrons to every carbon atom of the molecule $(\text{C}_6\text{H}_5)_3\text{C}\cdot$. Three of them are used in σ -type trigonal bindings sp^2 with the hydrogen atom and the neighbouring carbon atoms, while the fourth one is in the $2p_z$ state whose axis is orthogonal to the molecular plane.

The paramagnetism of the radical depends on the 19 $2p_z$ -electrons (π -electrons) present in the three benzene-rings and in the methylic carbon. The wave function $|\Psi, S_z\rangle$ which describes the state of such electrons is therefore sufficient for our purposes. The index $S_z = \pm \frac{1}{2}$ refers to the two components of the electronic spin. One can construct, by means of the 19 π -electrons, 44 valence bond wave functions q, S_z related to spin $\frac{1}{2}$ structures in which one paramagnetic electron and 9 bindings of π type appear between neighbouring carbon atoms.

Let us separate the functions $|\varphi, S_z\rangle$ into three groups, associated with the positions of the paramagnetic electron. To these three groups belong the 8, 12, 24 independent wave functions for the paramagnetic electron in the methylic carbon, and in the para and ortho position of the benzene ring respectively. In Fig. 1 three diagrams are shown one for each of these groups. In the following we shall distinguish these three groups with the indices 1, 2, 3 respectively.

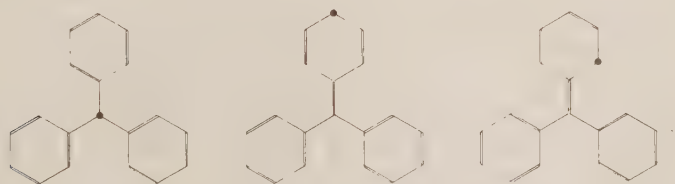


Fig. 1. - These three diagrams correspond to a function $|\varphi, S_z\rangle$ belonging to the groups 1, 2, 3 respectively.

All functions related to Dewar structures will be neglected. $|\Psi, S_z\rangle$ can be expressed as a linear combination of the q, S_z functions which will be chosen in such a way as to minimize the energy of the 19 π -electrons. In this linear combination, for symmetry reasons, we shall assume that the coefficients of the functions q, S_z belonging to the same group are identical. Therefore we have:

$$(1) \quad |\Psi, S_z\rangle = \sum_i c_i \sum_r |\varphi_{ir}, S_z\rangle$$

The hamiltonian for the system of the π electrons is:

$$(2) \quad \mathcal{H} = \mathcal{H}_1 + \mathcal{H}_2$$

$$\mathcal{H}_1 = \mathcal{H}_0 + g\beta \left(\mathbf{H} \cdot \sum_{\lambda} \mathbf{S}_{\lambda} \right),$$

$$\mathcal{H}_2 = g\beta g_N \beta_N \sum_{\lambda\mu} \left[\frac{(\mathbf{S}_{\lambda} \cdot \mathbf{I}_{\mu})}{r_{\lambda\mu}^3} + 3 \frac{(\mathbf{r}_{\lambda\mu} \cdot \mathbf{S}_{\lambda})(\mathbf{r}_{\lambda\mu} \cdot \mathbf{I}_{\mu})}{r_{\lambda\mu}^5} \right] + \frac{8\pi}{3} g\beta g_N \beta_N \sum_{\lambda\mu} (\mathbf{S}_{\lambda} \cdot \mathbf{I}_{\mu}) \delta(\mathbf{r}_{\lambda\mu}).$$

\mathcal{H}_0 is the term which depends on the kinetic energy and the Coulomb potential; \mathbf{S}_{λ} , \mathbf{I}_{μ} are the spin operators of the electrons and nuclei; β , β_N are the nuclear and electronic magnetons respectively and g , g_N the gyromagnetic ratios; $\mathbf{r}_{\lambda\mu}$ is the distance between the λ -electron and the μ -proton; \mathbf{H} the magnetic field.

Let us now take into account only the term \mathcal{H}_1 ; \mathcal{H}_2 which is responsible for the hyperfine structure will be introduced later as a perturbation (*).

2'1. *Fine structure term and evaluation of the wave function* $|\Psi, S_z\rangle$. — The secular equation for our problem is:

$$(3) \quad \text{Det} \left| \sum_{i,j} \left(\langle \varphi_{ir}, S_z | \mathcal{H}_1 | \varphi_{js}, S'_z \rangle - \langle \varphi_{ir}, S_z | \varphi_{js}, S_z \rangle W \right) \right| = 0.$$

The matrix elements of the operator \mathcal{H}_1 and the overlap integrals can be easily calculated as usual by means of the superposition of the patterns which represent the functions $|\varphi, S_z\rangle$. We have (2):

$$(4) \quad \langle \varphi_{ir}, S_z | \mathcal{H}_1 | \varphi_{js}, S'_z \rangle = \frac{1}{2^{n-h}} \left[Q + \Sigma' \alpha - 2 \Sigma'' \alpha - \frac{1}{2} \Sigma''' \alpha \right] \delta_{S_z, S'_z} +$$

$$+ S_z \langle \varphi_{ir}, S_z | \varphi_{js}, S'_z \rangle g\beta H,$$

$$(4') \quad \langle \varphi_{ir}, S_z | \varphi_{js}, S'_z \rangle = \frac{1}{2^{n-h}} \left[1 + \Sigma' \Delta - 2 \Sigma'' \Delta + \frac{1}{2} \Sigma''' \Delta \right] \delta_{S_z, S'_z},$$

where:

n = number of bindings;

h = number of closed contours in the superposition pattern;

Q = Coulomb integral;

α = simple exchange integral;

Δ = simple overlap integral;

(*) The contact term of the hamiltonian \mathcal{H}_2 is not too exact, since the electric field around the proton does not have spherical symmetry because of the neighbouring carbon atom. However the approximation is sufficient for our purposes.

(2) C. A. COULSON: *Valence* (Oxford, 1952); B. PULLMAN and A. PULLMAN: *Les théories électroniques de la chimie organique* (Paris, 1952).

\sum', \sum'' are the sums performed on orbitals belonging to the same open or closed contour and separated respectively by an odd or even number of bindings;

\sum''' is the sum performed on orbitals belonging to different open or closed contours.

From the equations (4), (4') we can see at once that:

$$(5) \quad \langle \varphi_{ir}, S_z | \mathcal{H}_1 | \varphi_{js}, S'_z \rangle - \langle \varphi_{ir}, S_z | \varphi_{js}, S'_z \rangle W = \\ = \langle \varphi_{ir}, S_z | \mathcal{H}_0 | \varphi_{js}, S'_z \rangle - \langle \varphi_{ir}, S_z | \dot{\varphi}_{js}, S'_z \rangle (W - S_z g \beta H).$$

And if W_0 is any eigenvalue of \mathcal{H}_0 :

$$(6) \quad W = W_0 + S_z g \beta H.$$

In other words the resonance of the molecule among several structures does not change the spin levels of the electron. Furthermore it appears evident from equations (4), (4'), (5) that the secular equation (3) can be factorized into two identical terms associated with the spin states and depending only on the Hamiltonian \mathcal{H}_0 . The problem of the triphenylmethyl radical in a magnetic field is therefore reduced to the problem of the radical without magnetic field. We shall here neglect the simple exchange integrals belonging to non-contiguous atoms, the multiple exchange integrals and the overlap integrals Δ . We shall suppose, moreover that all exchange integrals are identical. The groups of matrix elements which appear as terms of the determinant (3) can be easily calculated, using the rules given by PAULING and WHELAND, on the matrix elements, of the phenylmethyl radical (For this calculations see appendix (I)). In this way equation (3) reduces to:

$$\begin{vmatrix} (Q - W_0) \frac{125}{8} + \alpha \frac{1425}{16} & (Q - W_0) \frac{75}{8} + \alpha \frac{585}{8} & (Q - W_0) \frac{375}{16} + \alpha \frac{675}{4} \\ (Q - W_0) \frac{75}{8} + \alpha \frac{585}{8} & (Q - W_0) \frac{180}{8} + \alpha \frac{1017}{8} & (Q - W_0) \frac{225}{8} + \alpha \frac{3285}{16} \\ (Q - W_0) \frac{375}{16} + \alpha \frac{675}{4} & (Q - W_0) \frac{225}{8} + \alpha \frac{3285}{16} & (Q - W_0) \frac{1125}{16} + \alpha \frac{14625}{32} \end{vmatrix} = 0$$

from which we deduce for W_0 the values:

$$W_0 = Q + 6.8078\alpha$$

$$W'_0 = Q + 3.5858\alpha$$

$$W''_0 = Q + 2.8064\alpha$$

in which $\alpha = -1.4$ eV. The coefficients which determine the wave function of the ground state W_0 are:

$$c_1 = 0.068\,341$$

$$c_2 = 0.060\,338$$

$$c_3 = 0.067\,630.$$

The wave functions of the levels W'_0, W''_0 are of no interest for our problem.

2.2. Hyperfine structure terms. — It has been shown by S. I. WEISSMAN⁽³⁾ that the dipole interaction for the hyperfine structure gives a vanishing contribution for molecules in a dilute solution. This is due to the fact that the molecules undergo fast tumblings, therefore the hamiltonian \mathcal{H}_2 has to be averaged over all possible orientations, with uniform spherical distribution. This time-average is reliable if during the precession period of the nuclear spin around the electron spin the orientation of the molecule varies so fast as to assume a large number of positions uniformly distributed on the sphere. Hence the hyperfine structure depends only on the contact terms of the hamiltonian \mathcal{H}_2 , that is on the overlapping of the wave functions of the π -electrons and of the protons of the benzene rings. It is easy to see that the contact interaction between a proton and an electron in a $2p_z$ orbital not belonging to the contiguous carbon atom is negligible. To this purpose we wish to point out that the C—H length in the benzene-rings is 1.08 \AA while the distance between a carbon and the proton bond to the contiguous carbon atom is 2.15 \AA . Let us assume for the radial factor of the $2p_z$ orbitals the Zeener functions. It follows that the charge density of a π electron becomes about 10^2 times smaller when the distance from the carbon atom (to which the orbital of the electron is bound) is increased from 1.08 to 2.15 \AA . The matrix elements of \mathcal{H}_2 are therefore:

$$(10) \quad \langle \varphi_{ir}, S_z | \mathcal{H}_2 | \varphi_{js}, S_z \rangle = \frac{8\pi}{3} g\beta_N \beta_N S_z \frac{A}{2^{n-h}} \sum_{\mu=0,1,2,\dots} (-1)^\mu I_{z,\mu},$$

where A is the factor which depends on the spatial part of the $2p_z$ orbitals. The sum over μ is performed on the spin operators of the protons contiguous to the carbon atoms which enter into the open contour of the superposition pattern associated with the functions $|\varphi_{ir}, S_z\rangle, |\varphi_{js}, S_z\rangle$.

Taking into account the equation (10) we are able now to construct an hamiltonian independent of the orbitals related to the π electrons. This hamiltonian reduces the determination of the hyperfine structure levels to

⁽³⁾ S. I. WEISSMAN: *Journ. Chem. Phys.*, **22**, 1378 (1954).

the calculation of the eigenvalues of a linear combination of the operator $I_{z,\mu}$. Such a linear combination is:

$$(11) \quad \langle \Psi, S_z | \mathcal{H}_2 | \Psi, S_z \rangle = \sum_{ij} c_i c_j \sum_{rs} \langle \varphi_{ir}, S_z | \mathcal{H}_2 | \varphi_{js}, S_z \rangle.$$

The sums over r, s can be easily evaluated using a recipe similar to the one shown in the appendix I for the analogous sums related to the operator \mathcal{H}_0 (see Appendix II).

In such a way, if I_{zo}, I_{zm}, I_{zp} are the sums of the operators $I_{z\mu}$ corresponding to the protons in position ortho, meta, para, the equation (11) becomes (4):

$$(12) \quad \langle \Psi, S_z | \mathcal{H}_2 | \Psi, S_z \rangle = \frac{8\pi}{3} g\beta g_N \beta_N S_z A \cdot \\ \cdot [0.18227 I_{zp} - 0.10382 I_{zm} + 0.20008 I_{zo}].$$

The eigenvalues of (12) give at once the hyperfine structure levels; imposing the selection rules for the paramagnetic resonance $\Delta S_z = 1$, $\Delta I_{z\mu} = 0$ the values of the magnetic field corresponding to the transitions are:

$$(13) \quad H = \frac{\hbar\omega}{g\beta} - \frac{8\pi}{3} g_N \beta_N A [0.18227 I_{zp} - \\ - 0.10382 I_{zm} + 0.20008 I_{zo}].$$

In this equation ω is the frequency of the absorbed electromagnetic field, I_{zp} varies from $+\frac{3}{2}$ to $-\frac{3}{2}$ and I_{zm}, I_{zo} from -3 to $+3$. The intensities of the lines are clearly proportional to the statistical weights of the components I_{zp}, I_{zm}, I_{zo} . A spectrum symmetrical with respect to the value of the magnetic field $H = \hbar\omega/g\beta$ is



Fig. 2. - Paramagnetic resonance spectrum of the triphenylmethyl for $H > \hbar\omega/g\beta$ ($8\pi g_N \beta_N A/3$ units).

(4) This is substantially the operator proposed by M. H. L. PRYCE for this kind of problem. See: *Proc. Phys. Soc.*, A **63**, 25 (1950), eq. (17).

TABLE I. — *Position of the spectral line and their relative intensities as functions of the magnetic field ($8\pi g_N \beta_N A/3$ units) for the different values of I_{zp} , I_{zm} , I_{zo} .*

I_{zp}	I_{zm}	I_{zo}	$-3H/8\pi g_N \beta_N A$	Intensity
$+\frac{1}{2}$	-3	-2	0.00243	18
$-\frac{1}{2}$	+1	+1	0.00512	675
$-\frac{1}{2}$	-1	0	0.01268	900
$-\frac{3}{2}$	+3	+3	0.01537	1
$-\frac{1}{2}$	-3	-1	0.02024	45
$-\frac{3}{2}$	+1	+2	0.02293	90
$-\frac{3}{2}$	-1	+1	0.03049	225
$-\frac{3}{2}$	-3	0	0.03805	20
$+\frac{3}{2}$	+2	0	0.06576	120
$+\frac{3}{2}$	0	-1	0.07332	300
$+\frac{3}{2}$	-2	-2	0.08088	36
$+\frac{1}{2}$	+2	+1	0.08357	270
$+\frac{1}{2}$	0	0	0.09113	1200
$+\frac{1}{2}$	-2	-1	0.09869	270
$-\frac{1}{2}$	+2	+2	0.10138	108
$-\frac{1}{2}$	0	+1	0.10894	900
$-\frac{1}{2}$	-2	0	0.11650	360
$-\frac{3}{2}$	+2	+3	0.11919	6
$-\frac{3}{2}$	0	+2	0.12675	120
$-\frac{3}{2}$	-2	+1	0.13431	90
$+\frac{3}{2}$	+3	+1	0.16202	15
$+\frac{3}{2}$	+1	0	0.16958	300
$+\frac{3}{2}$	-1	-1	0.17714	225
$+\frac{1}{2}$	+3	+2	0.17983	18
$+\frac{3}{2}$	-3	-2	0.18470	6
$+\frac{1}{2}$	+1	+1	0.18739	675
$+\frac{1}{2}$	-1	0	0.19495	900
$-\frac{1}{2}$	+3	+3	0.19764	3
$-\frac{1}{2}$	-3	-1	0.20251	45
$-\frac{1}{2}$	+1	+2	0.20520	270
$-\frac{1}{2}$	-1	+1	0.21276	675
$-\frac{1}{2}$	-3	0	0.22032	60
$-\frac{3}{2}$	+1	+3	0.22301	15
$-\frac{3}{2}$	-1	+2	0.23057	90
$-\frac{3}{2}$	-3	+1	0.23813	15
$+\frac{3}{2}$	+2	+1	0.26584	90
$+\frac{3}{2}$	0	0	0.27340	400
$+\frac{3}{2}$	-2	-1	0.28096	90
$+\frac{1}{2}$	+2	+2	0.28365	108
$+\frac{1}{2}$	0	+1	0.29121	900
$+\frac{1}{2}$	-2	0	0.29877	360
$-\frac{1}{2}$	+2	+3	0.30146	18
$-\frac{1}{2}$	0	+2	0.30902	360
$-\frac{1}{2}$	-2	+1	0.31658	270
$-\frac{3}{2}$	0	+3	0.32683	20
$-\frac{3}{2}$	-2	+2	0.33439	36
$+\frac{3}{2}$	+3	+2	0.36210	6
$+\frac{3}{2}$	+1	+1	0.36966	225

TABLE I (continued).

I_{zp}	I_{zm}	I_{z0}	$-\zeta H/8\pi g_N \beta_N A$	Intensity
$+\frac{3}{2}$	-1	0	0.37722	300
$+\frac{1}{2}$	+3	+3	0.37991	3
$+\frac{3}{2}$	-3	-1	0.38478	15
$+\frac{1}{2}$	+1	+2	0.33747	270
$+\frac{1}{2}$	-1	+1	0.39503	675
$+\frac{1}{2}$	-3	0	0.40259	60
$-\frac{1}{2}$	+1	+3	0.40529	45
$-\frac{1}{2}$	-1	+2	0.41284	270
$-\frac{1}{2}$	-3	+1	0.42040	45
$-\frac{3}{2}$	-1	+3	0.43065	15
$-\frac{3}{2}$	-3	+2	0.43821	6
$+\frac{3}{2}$	+2	+2	0.46592	36
$+\frac{3}{2}$	0	+1	0.47348	300
$+\frac{3}{2}$	-2	0	0.48104	120
$+\frac{1}{2}$	+2	+3	0.48373	18
$+\frac{1}{2}$	0	+2	0.49129	360
$+\frac{1}{2}$	-2	+1	0.49885	270
$-\frac{1}{2}$	0	+3	0.50910	60
$-\frac{1}{2}$	-2	+2	0.51666	108
$-\frac{3}{2}$	-2	+3	0.53447	6
$+\frac{3}{2}$	+3	+3	0.56218	1
$+\frac{3}{2}$	+1	+2	0.56974	90
$+\frac{3}{2}$	-1	+1	0.57730	225
$+\frac{3}{2}$	-3	0	0.58486	20
$+\frac{1}{2}$	+1	+3	0.58755	45
$+\frac{1}{2}$	-1	+2	0.59511	270
$+\frac{1}{2}$	-3	+1	0.60267	45
$-\frac{1}{2}$	-1	+3	0.61292	45
$-\frac{1}{2}$	-3	+2	0.62048	18
$-\frac{3}{2}$	-3	+3	0.63829	1
$+\frac{3}{2}$	+2	+3	0.66600	6
$+\frac{3}{2}$	0	+2	0.67356	120
$+\frac{3}{2}$	-2	+1	0.68112	90
$+\frac{1}{2}$	0	+3	0.69137	60
$+\frac{1}{2}$	-2	+2	0.69893	108
$-\frac{1}{2}$	-2	+3	0.71674	18
$+\frac{3}{2}$	+1	+3	0.76982	15
$+\frac{3}{2}$	-1	+2	0.77738	90
$+\frac{3}{2}$	-3	+1	0.78494	15
$+\frac{1}{2}$	-1	+3	0.79519	45
$+\frac{1}{2}$	-3	+2	0.80275	18
$-\frac{1}{2}$	-3	+3	0.82056	3
$+\frac{3}{2}$	0	+3	0.87364	20
$+\frac{3}{2}$	-2	+2	0.88120	36
$+\frac{1}{2}$	-2	+3	0.89901	18
$+\frac{3}{2}$	-1	+3	0.97746	15
$+\frac{3}{2}$	-3	+2	0.98502	6
$+\frac{1}{2}$	-3	+3	1.00283	3
$+\frac{3}{2}$	-2	+3	1.08128	6
$+\frac{3}{2}$	-3	+3	1.18510	1

therefore obtained. This spectrum has 196 lines. In Table I the positions of the spectral lines are given as functions of the values of $I_{z\nu}$, I_{zm} , I_{zo} apart from the factor $-(8\pi/3)g_N\beta_N A$ and their relative intensities.

In Fig. 2 we plot the upper part of the spectrum corresponding to values of H larger than $\hbar\omega/g\beta$.

3. - Conclusions.

The derivative of the paramagnetic resonance spectrum of the triphenylmethyl has been experimentally determined by JARRET and SLOAN⁽⁵⁾. The measurement has been performed at room temperature at frequency $\omega/2\pi = 24$ GHz. At a molar concentration 0.1 they observed a spectrum symmetrical around $H = 8450$ G consisting of 21 groups of unresolved lines. At larger dilutions (0.001 molar) 18 equally spaced groups appear, resolvable into four or more spectral lines. The intensities of these groups of lines decrease considerably if the magnetic field becomes different from the central value $H = 8450$ G.

The theoretical spectrum calculated in this paper can be divided into 21 groups of lines, whose centers are practically equally spaced. The intensities of the external groups are very small as compared to those of the central ones. Moreover at both ends of the spectrum there are four lines too weak to be observed. Practically all the features of the experimental spectrum can be found in the theoretical one. We can therefore deduce that the Slater-Pauling method is in good agreement with experiment also with regard to the form of the wave function. From the comparison between the experimental⁽⁵⁾ and the theoretical spectrum spread, the value of the hyperfine structure constant A , which is practically the probability density of finding the π -electron on the proton, turns out to be $1.3 \cdot 10^{-23}$ cm⁻³. This value is somewhat larger than the one deduced using Zeener's atomic orbitals of the carbon atom, and describing the proton by means of a harmonic oscillator wave function.

In conclusion the comparison between the organic radical spectra obtained from the paramagnetic resonance experiments and the theoretical results provides a method of great efficiency in testing the reliability of the theoretical model postulated for the problem. In a later paper the same problem will be discussed with the molecular orbital method.

(⁵) H. S. JARRET and C. J. SLOAN: *Journ. Chem. Phys.*, **22**, 1783 (1954).

APPENDIX I

In the phenylmethyl radical three groups of valence functions χ, S_z are possible. To these groups belong 2, 1, 2 functions which correspond to the paramagnetic electron in the methyl carbon or in the para, ortho position in the benzene-ring respectively. We shall label such groups of functions with indices $i, j = 1, 2, 3$ respectively.

Let us put:

$$(14) \quad \sum_{rs} \langle \chi_{ir}, S_i | \mathcal{H}_0^{(1)} | \chi_{js}, D_z \rangle = k_{ij} Q + a_{ij} \alpha,$$

where $\mathcal{H}_0^{(1)}$ is the Hamiltonian for the phenylmethyl radical and the sums are performed on the valence functions belonging to each group. The coefficients k_{ij}, a_{ij} can be easily evaluated with the diagram superposition method. One finds:

$$\begin{aligned} k_{11} &= \frac{5}{2}; & k_{12} &= \frac{1}{2}; & k_{13} &= \frac{5}{4}; & k_{22} &= 1; & k_{23} &= 1; & k_{33} &= \frac{5}{2}; \\ a_{11} &= \frac{19}{4}; & a_{12} &= 2; & a_{13} &= \frac{17}{4}; & a_{22} &= 1; & a_{23} &= \frac{5}{2}; & a_{33} &= 4. \end{aligned}$$

In the same way we have for the triphenylmethyl:

$$(15) \quad \sum_{rs} \langle \varphi_{ir}, S_z | \mathcal{H}_0 | \varphi_{js}, S_z \rangle = K_{ij} Q + A_{ij} \alpha.$$

Using the relations proposed by PAULING, the coefficients of equation (15) can be expressed by means of those of equation (14).

One gets:

$$\begin{aligned} K_{11} &= k_{11}^3; & K_{12} &= 3k_{11}^2 k_{12}; & K_{13} &= 3k_{11}^2 k_{13} \\ K_{22} &= 3k_{11}^2 k_{22} + 6k_{11} k_{12}^2; & K_{23} &= 3k_{11} k_{23} + 6k_{11} k_{12} k_{13} \\ K_{33} &= 3k_{11}^2 k_{33} + 6k_{11} k_{13}^2 \\ A_{11} &= 3a_{11} k_{11}^2 \\ A_{12} &= 6a_{11} k_{11} k_{12} + 3k_{11}^2 a_{12} \\ A_{13} &= 6a_{11} k_{11} k_{13} + 3k_{11}^2 a_{13} \\ A_{22} &= 6a_{11} k_{11} k_{22} + 3k_{11}^2 a_{22} + 6a_{11} k_{12}^2 + 12k_{11} k_{12} a_{12} \\ A_{23} &= 6a_{11} k_{11} k_{23} + 3k_{11}^2 a_{23} + 6a_{11} k_{12} k_{13} + 6k_{11} a_{12} k_{13} + 6k_{11} k_{12} a_{13} \\ A_{33} &= 6a_{11} k_{11} k_{33} + 3k_{11}^2 a_{33} + 6a_{11} k_{13}^2 + 12k_{11} k_{13} a_{13}. \end{aligned}$$

Using these relations we can get the K_{ij} and A_{ij} coefficients of eq. (15).

APPENDIX II

We are now concerned as in Appendix I with the phenylmethyl radical. The sums:

$$\sum_{rs} \langle \chi_{ir}, S_z | \mathcal{H}_2^{(1)} | \chi_{js}, S_z \rangle,$$

where $\mathcal{H}_2^{(1)}$ is the hyperfine structure hamiltonian for the phenylmethyl radical, can be readily evaluated by means of equation (10). One finds in such a way the following expressions:

$$(16) \quad \left\{ \begin{array}{l} \sum_{rs} \langle \chi_{1r}, S_z | \mathcal{H}_2^{(1)} | \chi_{1s}, S_z \rangle = 0 \\ \sum_{rs} \langle \chi_{1r}, S_z | \mathcal{H}_2^{(1)} | \chi_{2s}, S_z \rangle = g\beta g_N \beta_N S_z A \frac{1}{4} [2\mathbf{I}_{zp}^{(1)} - \mathbf{I}_{zm}^{(1)} + \mathbf{I}_{zo}^{(1)}] \\ \sum_{rs} \langle \chi_{1r}, S_z | \mathcal{H}_2^{(1)} | \chi_{3s}, S_z \rangle = g\beta g_N \beta_N S_z A \frac{1}{4} [\mathbf{I}_{zp}^{(1)} - \mathbf{I}_{zm}^{(1)} + 3\mathbf{I}_{zo}^{(1)}] \\ \sum_{rs} \langle \chi_{2r}, S_z | \mathcal{H}_2^{(1)} | \chi_{2s}, S_z \rangle = g\beta g_N \beta_N S_z A \mathbf{I}_{zp}^{(1)} \\ \sum_{rs} \langle \chi_{2r}, S_z | \mathcal{H}_2^{(1)} | \chi_{3s}, S_z \rangle = g\beta g_N \beta_N S_z A \frac{1}{2} [2\mathbf{I}_{zp}^{(1)} - \mathbf{I}_{zm}^{(1)} + \mathbf{I}_{zo}^{(1)}] \\ \sum_{rs} \langle \chi_{3r}, S_z | \mathcal{H}_2^{(1)} | \chi_{3s}, S_z \rangle = g\beta g_N \beta_N S_z A \frac{1}{2} [\mathbf{I}_{zp}^{(1)} - \mathbf{I}_{zm}^{(1)} + 3\mathbf{I}_{zo}^{(1)}]. \end{array} \right.$$

In these equations the operator $\mathbf{I}_{zp}^{(1)}$ refers to the proton in the para position, while $\mathbf{I}_{zm}^{(1)}$, $\mathbf{I}_{zo}^{(1)}$ are the sums of the operators related to the meta and ortho-protons respectively. For the triphenylmethyl the sums:

$$\sum \langle \varphi_{ir}, S_z | \mathcal{H}_2 | \varphi_{js}, S_z \rangle,$$

can be expressed as functions of (16) through the following relations:

$$(17) \quad \left\{ \begin{array}{l} \sum_{rs} \langle \varphi_{1r}, S_z | \mathcal{H}_2 | \varphi_{1s}, S_z \rangle = 0 \\ \sum_{rs} \langle \varphi_{1r}, S_z | \mathcal{H}_2 | \varphi_{2s}, S_z \rangle = k_{11}^2 \sum_1^3 \sum_{rs} \langle \chi_{1r}, S_z | \mathcal{H}_2^{(0)} | \chi_{2s}, S_z \rangle = \\ \quad = g\beta g_N \beta_N S_z A \frac{25}{16} [2\mathbf{I}_{zp} - \mathbf{I}_{zm} + \mathbf{I}_{zo}] \\ \sum_{rs} \langle \varphi_{1r}, S_z | \mathcal{H}_2 | \varphi_{3s}, S_z \rangle = k_{11}^2 \sum_1^3 \sum_{rs} \langle \chi_{1r}, S_z | \mathcal{H}_2^{(0)} | \chi_{3s}, S_z \rangle = \\ \quad = g\beta g_N \beta_N S_z A \frac{25}{16} [\mathbf{I}_{zp} - \mathbf{I}_{zm} + \mathbf{I}_{zo}] \\ \sum_{rs} \langle \varphi_{2r}, S_z | \mathcal{H}_2 | \varphi_{2s}, S_z \rangle = k_{11}^2 \sum_1^3 \sum_{rs} \langle \chi_{2r}, S_z | \mathcal{H}_2^{(0)} | \chi_{2s}, S_z \rangle + \\ \quad + 4k_{11}k_{12} \sum_1^3 \sum_{rs} \langle \chi_{1r}, S_z | \mathcal{H}_2^{(0)} | \chi_{2s}, S_z \rangle = \\ \quad = g\beta g_N \beta_N S_z A \frac{5}{4} [7\mathbf{I}_{zp} - \mathbf{I}_{zm} + \mathbf{I}_{zo}] \end{array} \right.$$

$$\begin{aligned}
 (17) \quad & \left\{ \begin{aligned}
 \sum_{rs} \langle \varphi_{2r}, S_z | \mathcal{H}_2 | \varphi_{3s}, S_z \rangle &= k_{11}^2 \sum_{\varrho} \sum_{rs} \langle \chi_{2r}, S_z | \mathcal{H}_2^{(\varrho)} | \chi_{3s}, S_z \rangle + \\
 &+ 2k_{11}k_{12} \sum_{\varrho} \sum_{rs} \langle \chi_{1r}, S_z | \mathcal{H}_2^{(\varrho)} | \chi_{3s}, S_z \rangle + \\
 &+ 2k_{11}k_{13} \sum_{\varrho} \sum_{rs} \langle \chi_{1r}, S_z | \mathcal{H}_2^{(\varrho)} | \chi_{2s}, S_z \rangle = \\
 &= g\beta g_N \beta_N S_z A \frac{5}{16} [32 I_{zp} - 17 I_{zm} + 21 I_{zo}] \\
 \sum_{rs} \langle \varphi_{3r}, S_z | \mathcal{H}_2 | \varphi_{3s}, S_z \rangle &= k_{11}^2 \sum_{\varrho} \sum_{rs} \langle \chi_{3r}, S_z | \mathcal{H}_2 | \chi_{3s}, S_z \rangle + \\
 &+ 4k_{11}k_{13} \sum_{\varrho} \sum_{rs} \langle \chi_{1r}, S_z | \mathcal{H}_2 | \chi_{3s}, S_z \rangle = \\
 &= g\beta g_N \beta_N S_z A \frac{25}{4} [I_{zp} - I_{zm} + 3 I_{zo}].
 \end{aligned} \right.
 \end{aligned}$$

In the equations (17) the sums over ϱ are meant to be performed on the three phenylic groups of the triphenylmethyl; the operators I_{zp} , I_{zm} , I_{zo} are the sums of the spin operators for the para, meta, ortho protons on the three phenylic groups.

RIASSUNTO (*)

In questo lavoro si studia la risonanza paramagnetica del radicale trifenilmetile. Lo spettro di struttura iperfine è dedotto usando la teoria di Slater-Pauling; l'accordo coi dati sperimentali esistenti è soddisfacente. Si mette in rilievo l'utilità delle misure di risonanza paramagnetica come metodo di indagine nella teoria della valenza.

(*) Traduzione a cura della Redazione.

General Relativistic Interpretation of Some Spinor Wave Equations.

F. GÜRSEY

Theoretical Physics Department, University of Istanbul

(ricevuto il 20 Ottobre 1956)

Summary. — The non-linear conform-invariant spinor wave equation proposed in an earlier paper is given a simple geometrical interpretation within the frame of general relativity. At each point of a conformal space-time manifold, an orthogonal frame of reference is defined, this frame being associated with a 4-spinor ψ . It is shown that if the contracted torsion tensor A_α relative to the frame vanishes (as in the case of a co-ordinate transformation) and the pseudo-vector L_α derived from the same torsion tensor remains constant and space-like, then the associated 4-spinor ψ satisfies just the above mentioned wave equation which, in turn, determines the orthogonal frame of reference at every space-time point to within a conformal transformation of the co-ordinate system. In particular, if the pseudo-vector L_α also vanishes one obtains Dirac's equation for a particle of rest mass zero. In a discussion of the physical meaning of the orthogonal frame of reference, the time-like basis vector and one of the space-like basis vectors are respectively related to the current density and the spin density 4-vectors associated with the wave equation.

1. — Introduction.

In a previous paper ⁽¹⁾ (referred to as I) a modified form of Heisenberg's generalization ⁽²⁾ of Dirac's equation was suggested as a possible basis for a unitary field theory of fundamental particles. The equation proposed was a non linear 4-spinor equation invariant with respect to conformal transformations. Another approach to unified field theories is by way of general rela-

⁽¹⁾ F. GÜRSEY: *Nuovo Cimento*, **3**, 988 (1956).

⁽²⁾ W. HEISENBERG: *Physica*, **19**, 897 (1953).

tivity⁽³⁾ where certain tensor equations define the geometrical structure of possible space-time manifolds. These tensor equations are then interpreted as equations for known physical fields like the gravitational, electromagnetic or mesonic fields. If (as it seems unavoidable in quantum field theory) a spinor equation has to be used for the unitary description of all physical fields, the only possibility for incorporating it in the scheme of general relativity would be to try to describe the space-time structure by means of spinor (instead of tensor) equations which thereby would allow a geometrical interpretation. Thus the way would be open to regard a basic spinor equation (like the one proposed by HEISENBERG) as a purely geometrical equation defining a certain space-time model so that the two methods used in the quest of a unitary field theory might at last be made to converge.

How can we introduce a spinor field in general relativity? The answer follows from the work of several authors⁽⁴⁻⁸⁾. The essential fact is that whenever we have an orthogonal frame of reference, a 4-spinor (Einstein's semi-vector) can be associated with it, each basis vector of the frame being a quadratic homogeneous function of the 4-spinor components. The explicit and detailed way of constructing that 4-spinor (or the corresponding 2×2 matrix) from four mutually orthogonal 4-vectors has been given in two previous papers^(9,10). The basis vectors of an orthogonal frame defined at each point of a Riemannian space-time manifold are called Beingrößen (EINSTEIN) and said to form an ennuple or tetrad. Such tetrads are introduced in affine theories of distant parallelism⁽¹¹⁾ as well as in Riemannian geometry when the structure of the manifold is defined by linear Pfaff forms⁽¹²⁾. If we restrict in any way the properties of the above considered tetrad field we implicitly define a 4-spinor field with corresponding properties.

In this paper we derive certain differential equations obeyed by the basis vectors of the tetrad field and find the spinor field which corresponds to this space-time model. More precisely our purpose is to show that, starting from an affine conformal space-time, a set of 8 equations obeyed by the Beingrößen

(3) For a review see: C. KILMISTER and G. STEPHENSON: *Suppl. Nuovo Cimento*, **11**, 91 (1954).

(4) V. FOCK: *Zeits. f. Phys.*, **57**, 261 (1929).

(5) H. WEYL: *Proc. Nat. Acad. Sci.*, **15**, 323 (1929).

(6) E. SCHRÖDINGER: *Preuss. Akad. Wiss. Berlin*, 105 (1932).

(7) A. EINSTEIN and W. MAYER: *Preuss. Akad. Wiss. Berlin*, 522 (1932).

(8) J. HELLER and P. G. BERGMANN: *Phys. Rev.*, **84**, 665 (1951).

(9) F. GÜRSEY: *Rev. Fac. Sci. Univ. Istanbul*, A **20**, 149 (1955).

(10) F. GÜRSEY: *Rev. Fac. Sci. Univ. Istanbul*, A **21**, 33 (1956).

(11) A. EINSTEIN: *Preuss. Akad. Wiss. Berlin*, 217, 224 (1928).

(12) See for instance E. CARTAN: *Leçons sur la Géométrie des Espaces de Riemann* (Paris, 1951).

can be translated into a conform-invariant spinor equation (of the type proposed in I) which thereby acquires a geometrical meaning. The equivalent tensor equations that the basis vectors satisfy are generalized from the identities satisfied by the unit vectors associated with a conformal transformation in flat space-time.

In Sect. 2 we define the basis vectors of the conformal affine space-time and derive the two fundamental vectors L and A . Sect. 3 deals with the 2×2 matrix associated with a complex combination of L and A and the results are applied to the conformal case in Sect. 4. Sect. 5 contains the derivation of 4-spinor equations characterizing different conformal space-time models.

Sect. 6 is devoted to the discussion of the physical meaning of the fundamental vectors and of the determinant of the 2×2 matrix, associated with the wave function.

2. - The Affine Space-Time. The Torsion 4-Vector A and the Torsion Pseudo-vector L .

Let the basis vectors of a local frame of reference in space-time be denoted by E_α ($\alpha = 0, 1, 2, 3$), so that the fundamental displacement vector is defined by

$$(2.1) \quad dX = E_\alpha dx^\alpha.$$

The vectors E_α can be analyzed into components by means of fixed cartesian unit vectors $I_{(\beta)}$. We have

$$(2.2) \quad E_\alpha = {}^\beta t_\alpha I_{(\beta)}.$$

The left index β ($\beta = 0, 1, 2, 3$) is used for the numbering of the four invariant Pfaff forms

$$(2.3) \quad \sigma^{(\beta)} = {}^\beta t_\alpha dx^\alpha \quad ,$$

which characterize the space-time manifold. Indices between brackets have the same character as left indices and, unlike right indices, do not indicate covariant or contravariant behaviour. Left (or bracketted) indices are raised and lowered by means of the metric tensor $\gamma_{(\mu\nu)}$ of special relativity defined by

$$(2.4) \quad \gamma_{(00)} = -\gamma_{(11)} = -\gamma_{(22)} = -\gamma_{(33)} = 1, \\ \gamma_{(\mu\nu)} = 0 \quad \text{if} \quad \mu \neq \nu,$$

while the tensor

$$(2.5) \quad g_{\mu\nu} = {}^\beta t_\mu \cdot {}^\beta t_\nu$$

serves to raise and lower right indices. The summation convention is employed both for left and right indices.

The line element is given by

$$(2.6) \quad ds^2 = \gamma_{(\mu\nu)} \sigma^{(\mu)} \sigma^{(\nu)} = g_{\alpha\beta} dx^\alpha dx^\beta,$$

so that the Riemannian metric tensor is $g_{\alpha\beta}$. By means of the invariant Pfaff forms the displacement (2.1) may be written in the equivalent form

$$(2.7) \quad dX = I_{(\mu)} \sigma^{(\mu)}.$$

The metric covariant derivative is defined by

$$(2.8) \quad \Delta_\alpha A_\mu = \partial_\alpha A_\mu - \left\{ \begin{matrix} \nu \\ \alpha\mu \end{matrix} \right\} A_\nu, \quad \left(\partial_\alpha = \frac{\partial}{\partial x^\alpha} \right),$$

where $\left\{ \begin{matrix} \nu \\ \alpha\mu \end{matrix} \right\}$ is the Christoffel symbol (symmetrical in α and μ) derived from the tensor $g_{\alpha\beta}$.

The displacement law for the basis vectors E_α is

$$(2.9) \quad dE_\beta = (\partial_\alpha E_\beta) dx^\alpha = \Gamma_{\alpha\beta}^\gamma E_\gamma dx^\alpha,$$

where $\Gamma_{\alpha\beta}^\gamma$ denote the coefficient of the affine connection. We have

$$(2.10) \quad \Gamma_{\alpha\beta}^\gamma = \mu_{\beta'} \cdot \partial_\alpha (\mu_{\beta'})^\gamma.$$

The parallel displacements of a vector A^α is defined by

$$d(E_\alpha A^\alpha) = 0,$$

or, using (2.9),

$$(2.11) \quad dA^\gamma = -\Gamma_{\alpha\beta}^\gamma A^\beta dx^\alpha.$$

If we define *affine derivation* by the symbol

$$(2.12) \quad w_e A_\alpha = \partial_e A_\alpha - \Gamma_{e\alpha}^\gamma A_\gamma,$$

then, in a parallel displacement, the affine derivatives of a vector vanish.

We have identically

$$(2.13) \quad w_e E_\alpha = 0$$

and

$$(2.14) \quad \Delta_e g_{\alpha\beta} = 0.$$

The integrability conditions of the Pfaff forms (2.3) are expressed by the equations

$$(2.15) \quad \partial_\alpha E_\beta - \partial_\beta E_\alpha = 0,$$

or

$$(2.16) \quad A_{\alpha\beta}^\gamma = 0,$$

where

$$(2.17) \quad A_{\alpha\beta}^\gamma = A_{\alpha\beta}^{\cdot\cdot\gamma} = \frac{1}{2}(\Gamma_{\alpha\beta}^\gamma - \Gamma_{\beta\alpha}^\gamma)$$

is a tensor (the so called torsion tensor) antisymmetrical in the indices α and β .

The difference between the coefficients of the affine connection and the Christoffel symbols gives rise to the Ricci coefficients of rotation ⁽¹³⁾ defined by

$$(2.18) \quad B_{\alpha\beta}^{\cdot\cdot\gamma} = \Gamma_{\alpha\beta}^\gamma - \left\{ \begin{matrix} \gamma \\ \alpha\beta \end{matrix} \right\}.$$

Taking the covariant derivatives of the covariant and contravariant basis vectors we obtain

$$(2.19) \quad \Delta_\alpha E_\beta = B_{\alpha\beta}^{\cdot\cdot\gamma} E_\gamma$$

and

$$(2.20) \quad \Delta_\alpha E^\gamma = -B_{\alpha\beta}^{\cdot\cdot\gamma} E^\beta.$$

We can also write

$$(2.21) \quad B_{\alpha\beta}^{\cdot\cdot\gamma} = {}_\mu t^\gamma \cdot \Delta_\alpha ({}^\mu t_\beta).$$

The Ricci coefficients can be expressed in terms of the torsion tensor by means of the formula

$$(2.22) \quad B_{\alpha\beta\gamma} = \Delta_{\alpha\beta\gamma} - \Delta_{\beta\gamma\alpha} + \Delta_{\gamma\alpha\beta},$$

which shows that they form a tensor antisymmetrical with respect to its last two covariant indices, i.e.

$$(2.23) \quad B_{\alpha\beta\gamma} = -B_{\alpha\gamma\beta}.$$

In flat space (2.16) is satisfied, the torsion tensor and therefore the Ricci

⁽¹³⁾ See for instance L. P. EISENHART: *Non-Riemannian Geometry* (New York, 1927).

tensor vanish. Hence in this case we have

$$(2.24) \quad \begin{cases} A_{\varepsilon} E_{\alpha} = 0 \\ A_{\varepsilon} g_{\alpha\beta} = 0. \end{cases}$$

In metric Riemannian space we have

$$(2.25) \quad \begin{cases} A_{\varepsilon} E_{\alpha} = B_{\varepsilon\alpha}{}^{\gamma} E_{\gamma} \\ A_{\varepsilon} g_{\alpha\beta} = 0. \end{cases}$$

After reviewing these well-known definitions and properties we introduce two four-vectors which can be derived from the fundamental torsion tensor (2.17). The first, that we call the *torsion 4-vector* is just the contracted torsion tensor

$$(2.26) \quad A^{\varepsilon} = A_{\varepsilon}{}^{\alpha\alpha},$$

and the second, that we call the *torsion pseudo-vector*, namely

$$(2.27) \quad L^{\varepsilon} = \frac{1}{4} k^{\varepsilon\alpha\beta\gamma} A_{\alpha\beta\gamma}$$

is proportional to the dual of the completely antisymmetrized torsion tensor. The factor $\frac{1}{4}$ is included for convenience and the completely antisymmetrical tensor with four indices equals $\pm k$ according as $(\varepsilon\alpha\beta\gamma)$ is an even or odd permutation of $(0\ 1\ 2\ 3)$, k being defined by

$$k = \sqrt{-\text{Det}(g_{\alpha\beta})}.$$

Replacing A by B in (2.26) and (2.27) we could also define a contracted Ricci tensor and the dual of the completely antisymmetrized Ricci tensor, but these give nothing new, since

$$(2.28) \quad B^{\varepsilon} = B_{\varepsilon}{}^{\alpha\alpha} = 2A^{\varepsilon},$$

and

$$(2.29) \quad k^{\varepsilon\alpha\beta\gamma} B_{\alpha\beta\gamma} = k^{\varepsilon\alpha\beta\gamma} A_{\alpha\beta\gamma} = 4L^{\varepsilon}$$

in virtue of the relation (2.22).

The torsion 4-vector was considered by EINSTEIN ⁽¹¹⁾ and tentatively interpreted by him as the electromagnetic potential, an interpretation which he later discarded. The introduction of the torsion pseudo-vector in unitary field theory seems to be new.

Contracting the first equation (2.25) we obtain

$$(2.30) \quad \Delta_\alpha E^\alpha = k^{-1} \partial_\alpha (k E^\alpha) = B_\alpha E^\alpha = 2\Delta_\alpha E^\alpha.$$

In flat space the vanishing of the torsion tensor also implies the vanishing of Λ^e and L^e , that is, of their complex combination

$$(2.31) \quad K^e = \Lambda^e + iL^e = \Lambda_{\alpha\beta}^{\alpha\beta} + \frac{i}{4} k^{\alpha\beta\gamma} \Lambda_{\alpha\beta\gamma}.$$

The reverse is, of course, not true. We can have a curved space-time in which K^e vanishes. The vector K with contravariant components K^e is defined by

$$(2.32) \quad K = E_e K^e.$$

or, when referred to the cartesian basis vectors $I^{(\alpha)}$,

$$(2.33) \quad K = I^{(\alpha)} K_{(\alpha)},$$

where

$$(2.34) \quad K_{(\alpha)} = {}_\alpha t^\mu K_\mu$$

denote four complex invariants which certainly vanish in the Euclidian case, but may or may not vanish in curved space time. We shall see in the following sections that the eight real (or four complex) equations

$$K = 0$$

are equivalent to the Dirac equation for a particle of zero rest mass.

3. - 2×2 Matrix Expression of the Complex 4-Vector K .

Following the notations of I we now associate with the fundamental vectors E_α hermitian 2×2 matrices that we denote by the same symbols. The adjoint matrices being indicated by a bar, we have from (2.5)

$$(3.1) \quad E_\alpha \bar{E}_\beta + E_\beta \bar{E}_\alpha = 2E_\alpha \cdot \bar{E}_\beta = 2g_{\alpha\beta}.$$

Here the dot product is defined by (I, 2.28). The fundamental displacement vector (2.1) is also represented by a hermitian matrix which gives

$$\text{Det } (dX) = dX d\bar{X} = g_{\alpha\beta} da^\alpha d\bar{a}^\beta = ds^2.$$

The first equation (2.25) can also be read as a 2×2 matrix equation. Multiplying both sides by $E^\alpha \bar{E}^\beta$ we obtain the matrix

$$(3.2) \quad E^\alpha \bar{E}^\beta A_\alpha E_\beta = E^\alpha \bar{E}^\beta E^\gamma B_{\alpha\beta\gamma}.$$

We now use the identity

$$(3.3) \quad \mathcal{H}(A\bar{B}C) = (A \cdot \bar{B})C + (B \cdot \bar{C})A - (A \cdot \bar{C})B$$

valid for any three hermitian 2×2 matrices A, B, C . (See ref. (9) Sect. 2). The symbol on the left hand side stands for « hermitian part » and is defined as in ref. (9) by

$$\mathcal{H}(Q) = \frac{1}{2}(Q + Q^\dagger).$$

From (3.3) we derive

$$(3.4) \quad \mathcal{H}(E^\alpha \bar{E}^\beta E^\gamma) = g^{\alpha\beta} E^\gamma + g^{\beta\gamma} E^\alpha - g^{\alpha\gamma} E^\beta$$

with the help of (3.1). Using the antisymmetry property (2.23) we obtain

$$(3.5) \quad \mathcal{H}(E^\alpha \bar{E}^\beta E^\gamma B_{\alpha\beta\gamma}) = 2B_{\alpha\gamma}^{\alpha\gamma} E^\gamma = 4A^\gamma E_\gamma,$$

where we have employed (2.28).

The second identity we need refers to the antihermitian part of the matrix product $A\bar{B}C$. It reads

$$\mathcal{A}(A\bar{B}C) = -iI_{(\alpha)} A^{(\alpha)} = -i\delta_{0123}^{\varepsilon\alpha\beta\gamma} \bar{I}_{(\varepsilon)} A_{(\alpha)} B_{(\beta)} C_{(\gamma)},$$

where the determinants $I^{(\alpha)}$ are defined by means of the cartesian components of A, B, C as in ref. (9) Sect. 2, and δ is the completely antisymmetrical Kronecker symbol, so that the above matrix expression is orthogonal to A, B , and C separately. It follows that the antihermitian part of $E^\alpha \bar{E}^\beta E^\gamma$ is proportional to the covariant vector E_ε , the indices $\alpha, \beta, \gamma, \varepsilon$ being all different, that is,

$$\mathcal{A}(E^\alpha \bar{E}^\beta E^\gamma) = \mu E_\varepsilon.$$

Dot multiplication by \bar{E}^ε gives (see ref. (9) Sect. 2)

$$\mu = \text{Det}(\bar{E}^0 E^1 \bar{E}^2 E^3) = i \text{Det}(\alpha_{\beta}^t) = ik,$$

so that we get

$$(3.6) \quad \mathcal{A}(E^\alpha \bar{E}^\beta E^\gamma) = ik^{\varepsilon\alpha\beta\gamma} E_\varepsilon,$$

where we have used the completely antisymmetrical tensor defined in the preceding section. Therefore we obtain

$$(3.7) \quad \mathcal{A}(E^\alpha \bar{E}^\beta E^\gamma B_{\alpha\beta\gamma}) = i k^{\varepsilon\alpha\beta\gamma} B_{\alpha\beta\gamma} E_\varepsilon = 4iL^\varepsilon E_\varepsilon$$

in virtue of (2.29).

It follows from the combination of (3.5) and (3.6) and from the definition (2.31) that

$$(3.8) \quad \frac{1}{4} E^\alpha \bar{E}^\beta E^\gamma B_{\alpha\beta\gamma} = (\Lambda^\varepsilon + iL^\varepsilon) E_\varepsilon = K,$$

that is, the invariant matrix (3.2) is just four times the matrix which represents the complex vector K of the preceding section.

We now proceed to study the effect of the rotation of the fundamental tetrad at each point of space-time. Such a rotation is represented by a Lorentz transformation specified by a 2×2 unimodular matrix ξ which is a function of the co-ordinates. Denoting the new basis vectors by primed letters we have

$$(3.9) \quad E_\beta = \xi^\dagger E'_\beta \xi,$$

with the notation of I, so that

$$(3.10) \quad E_\alpha \cdot \bar{E}_\beta = E'_\alpha \cdot \bar{E}'_\beta = g_{\alpha\beta}.$$

The matrices defined by

$$(3.11) \quad \omega_\alpha = (\partial_\alpha \xi) \bar{\xi}$$

are traceless since

$$(3.12) \quad \xi \bar{\xi} = \text{Det}(\xi) = 1.$$

On the other hand, ξ being invariant we have

$$\Delta_\alpha \xi = \partial_\alpha \xi,$$

and, consequently,

$$(3.13) \quad \Delta_\alpha E_\beta = \xi^\dagger \Delta_\alpha E'_\beta \xi + E'_\beta \bar{\xi} \omega_\alpha \xi + \xi^\dagger \omega_\alpha^\dagger \bar{\xi}^\dagger E_\beta.$$

At this point we need the identities

$$(3.14) \quad \bar{E}^\beta E_\beta = 4$$

and

$$(3.15) \quad \bar{E}^\beta \Omega E_\beta = 0$$

where Ω is an arbitrary traceless 2×2 matrix. Using (2.2) we obtain

$$\bar{E}^\beta E_\beta = (\mu t^\beta)({}^\nu t_\beta) \bar{I}^{(\mu)} I_{(\nu)} = \bar{I}^{(\mu)} I_{(\mu)},$$

since

$$(\mu t^\beta)({}^\nu t_\beta) = \delta_\mu^\nu.$$

It may be directly verified (see ref. (9) identity (3.7)) that

$$\bar{I}^{(\mu)} I_{(\mu)} = \frac{1}{2} \text{Tr} (\bar{I}^{(\mu)} I_{(\mu)}) = 4,$$

which proves (3.14).

In the same way (3.15) follows from the identity

$$\bar{I}^{(\mu)} \Omega I_{(\mu)} = 0$$

proved in ref. (9) (identity (3.7)).

Now, using (3.14) and (3.15) we get the following matrix expression for the complex vector K

$$(3.16) \quad K = \frac{1}{4} E^\alpha \bar{E}^\beta \Delta_\alpha E_\beta = \xi^\dagger (K' + E'^\alpha \omega_\alpha) \xi,$$

or, using (3.11),

$$(3.16') \quad K = \xi^\dagger (K' \xi + E'^\alpha \partial_\alpha \xi),$$

where

$$(3.17) \quad K' = \frac{1}{4} E'^\alpha \bar{E}'^\beta \Delta_\alpha E'_\beta.$$

4. - The Conformal Case.

In the case of conformal space-time we have

$$(4.1) \quad ds^2 = f^2 d\tau^2 = f^2 [(dx^0)^2 - (dx^1)^2 - (dx^2)^2 - (dx^3)^2],$$

that is,

$$(4.2) \quad g_{\alpha\beta} = f^2 \gamma_{(\alpha\beta)},$$

where the metric tensor of special relativity (2.4) is used. Therefore the basis vectors E_α are mutually Lorentz orthogonal and their representative matrices have the form

$$(4.3) \quad E_\alpha = f \xi^\dagger I_{(\alpha)} \xi,$$

where ξ is a unimodular matrix. Thus we can choose

$$(4.4) \quad E'_\alpha = f I_{(\alpha)}$$

with which are associated the contravariant vectors

$$(4.5) \quad E'^\alpha = f^{-1} I^{(\alpha)}.$$

The matrix invariant K' defined by (3.17) can easily be calculated from the torsion tensor associated with E'_α , that is

$$(4.6) \quad A'_{\alpha\beta}{}^{\gamma} = \frac{1}{2} (\tau_\alpha \delta_\beta^\gamma - \tau_\beta \delta_\alpha^\gamma),$$

where

$$(4.7) \quad \tau_\alpha = \partial_\alpha \log f.$$

We thus obtain

$$L'_\alpha = 0 \quad \text{and} \quad A'_\alpha = \frac{3}{2} \tau_\alpha,$$

so that

$$K' = (A'_\alpha + i L'_\alpha) E'^\alpha = \frac{3}{2} E'^\alpha \tau_\alpha.$$

Inserting this into (3.16') we get

$$K = \xi^\dagger E'^\alpha (\partial_\alpha \xi + \frac{3}{2} \tau_\alpha \xi),$$

or, with the help of (4.7) and (4.5),

$$(4.8) \quad K = f^{-\frac{3}{2}} \xi^\dagger I^{(\alpha)} \partial_\alpha (f^{\frac{3}{2}} \xi).$$

Now, if we define a new matrix Φ by

$$(4.9) \quad \Phi = f^{\frac{3}{2}} \xi,$$

we have

$$(4.10) \quad \Phi^{-1} = f^{-\frac{3}{2}} \bar{\xi}$$

and

$$(4.11) \quad f = (\Phi \bar{\Phi})^{\frac{1}{3}}.$$

On the other hand, since the cartesian basis vectors $I^{(\alpha)}$ are represented by the unit matrix and the three Pauli matrices, using the notation (I, 2.29)

we can write

$$(4.12) \quad D = I^{(\alpha)} \partial_\alpha = \partial_0 + \sigma_1 \partial_1 + \sigma_2 \partial_2 + \sigma_3 \partial_3$$

for the matrix associated with the gradient operator. Using the definitions (4.9) and (4.12) we can put the complex vector K (4.8) in the form

$$(4.13) \quad K = (\Phi \bar{\Phi})^{-\frac{1}{2}} (\bar{\Phi}^\dagger)^{-1} D \Phi.$$

From (4.3) it is clear that if the unit vectors $I^{(\alpha)}$ are subjected to a constant Lorentz transformation specified by the constant unimodular matrix Q ,

$$I^{(\alpha)} \rightarrow Q^\dagger I^{(\alpha)} Q,$$

then, ξ transforms according to the spinor law

$$(4.14) \quad \xi \rightarrow Q \xi$$

which also holds for the spinor matrix Φ .

The matrix Φ can be given a simple geometrical meaning by noting that a three-dimensional surface element $d\Sigma$ has the form

$$d\Sigma = -i\mathcal{A}(\delta X \delta \bar{Y} \delta Z),$$

where δX , δY , δZ denote the matrix expressions of three linearly independent space-like displacements. More explicitly we have

$$d\Sigma = -i\mathcal{A}(E^\alpha \bar{E}^\beta E^\gamma) [\delta x_\alpha \delta y_\beta \delta z_\gamma] = k E^\epsilon d\Sigma_\epsilon,$$

or, with the help of (4.3) and (4.9),

$$(4.15) \quad d\Sigma = \Phi^\dagger dS \Phi$$

where

$$(4.16) \quad dS = -i\mathcal{A}[I^{(\alpha)} \bar{I}^{(\beta)} I^{(\gamma)}] \delta x_\alpha \delta y_\beta \delta z_\gamma = I^{(\alpha)} dS_{(\alpha)}$$

is the cartesian surface element.

5. Various Space-Time Models Characterized by 4-Spinor Equations.

A simple space-time model can be found by assuming a conformal manifold in which both the vectors M and L derived from the torsion tensor vanish as in flat space-time. In such a model the surface element is

$$(5.1) \quad d\Sigma = \Phi^\dagger I^{(\alpha)} \Phi dS_{(\alpha)},$$

and the line element is given by (4.1), i.e.

$$(5.2) \quad ds^2 = (\Phi \bar{\Phi})^{\frac{1}{2}} d\tau^2,$$

where we have used (4.11) and (4.15-16). Furthermore the complex vector K is identically zero, that is

$$(5.3) \quad K = A + iL = 0.$$

This invariant equation is equivalent to the eight real tensor equations

$$(5.4) \quad A_e = 0$$

$$(5.5) \quad L_e = 0.$$

or to the 2×2 matrix equation

$$(5.6) \quad D\Phi = 0$$

obtained by equating to zero the matrix expression (4.13) of the complex vector K . To the equations (5.1), (5.2) and (5.6) which characterize this space-time model we must also add the condition

$$\text{Det}(\Phi) = \Phi \bar{\Phi} = \text{real},$$

which follows from the definition (4.9).

In particular Eq. (5.6) must be satisfied in flat space-time where Φ becomes the transformation factor of the surface element in a conformal transformation. This has already been shown directly in I (Eq. (2.32)). When the matrix equation (I, 2.32) continues to hold in curved space-time we obtain the special type of conformal manifold introduced above.

We have shown in I that Eq. (5.6) is equivalent to a 4-spinor equation. Let φ be the 4-spinor associated with the 2×2 matrix Φ by means of the formula (I, 3.9). Then (5.6) is equivalent to

$$(5.7) \quad (\partial_0 + \alpha_1 \partial_1 + \alpha_2 \partial_2 + \alpha_3 \partial_3) \varphi = 0$$

where α_1 , α_2 and α_3 denote the 4×4 Dirac matrices. The transformation (4.14) also induces the correct transformation law for the 4-spinor φ (See ref. ⁽¹⁰⁾, (2.23-24)). We have thus proved that the tensor equations (5.4-5) which are purely geometrical in character are equivalent to the Dirac equation (5.7) for a particle of zero rest mass.

We note that the scalar

$$\bar{\varphi} \varphi = \Phi \bar{\Phi},$$

which is interpreted as the particle number per unit proper volume in the Dirac theory has the dimensions of an inverse volume so that $\bar{q}\mathcal{T}d\tau$ ($d\tau$ being the rest volume element) must be invariant. This is in accordance with (5.1) since the left hand side $d\Sigma$ is invariant.

Now we proceed to introduce a wider class of conformal space-time models by relinquishing the condition (5.5) but keeping (5.4). In such a manifold the four conservation equations

$$(5.8) \quad \partial_\epsilon(kE^\epsilon) = 0 \quad \text{or} \quad \partial_\epsilon(k^\alpha \bar{t}^\epsilon) = 0$$

which follow from (2.30) continue to hold just as in the Euclidean case. This implies that the property

$$(5.9) \quad \oint d\Sigma = 0$$

of flat space is still valid in the curved model. It follows from (5.4) that the matrix invariant K must be antihermitian. We have

$$K = -iL$$

and, using (4.13), we find that Φ must satisfy the equation

$$(5.10) \quad D\Phi = i(\Phi\bar{\Phi})^\dagger\bar{\Phi}^\dagger L.$$

Now we further assume that L is a constant vector, that is

$$(5.11) \quad \partial_\epsilon L = 0$$

which is equivalent to say that its covariant components L_ϵ obey the parallel displacement law (2.11). A second assumption concerning L is that it is space-like. Under these two assumptions we can write the hermitian matrix representing L in the canonical form (see I, (7.8-9))

$$(5.12) \quad L = \lambda\eta^\dagger\sigma_3\eta,$$

where σ_3 is the third Pauli matrix, λ a real scalar and η a constant unimodular matrix. This simply means that we can find a Lorentz transformation specified by η which brings the vector L in a rest frame where its only non-vanishing component is along the Oz axis and has the value λ . No preference for the Oz axis is implied since replacement of σ_3 by any other Pauli matrix results in a new choice for η .

Putting

$$(5.13) \quad \Psi = \Phi \bar{\eta}$$

we obtain for the new 2×2 matrix Ψ the equation

$$(5.14) \quad D\Psi - \lambda i(\Psi \bar{\Psi})^{\frac{1}{2}} \bar{\Psi}^{\dagger} \sigma_3 = 0$$

which is the same as the conform-invariant wave equation (I, 1.3) proposed in I, in its matrix form (I, 3.18). Again Ψ satisfies the condition

$$(5.15) \quad \text{Det}(\Psi) = \Psi \bar{\Psi} = R(\Psi \bar{\Psi}) = \text{real}.$$

Translated into 4-spinor language this implies that the pseudo-invariant

$$\omega_2 = \bar{\psi} \gamma_5 \psi$$

must vanish. Here ψ is the 4-spinor associated with the matrix Ψ .

The equation (5.14) does not determine Ψ uniquely since it is invariant with respect to conformal transformations.

6. - Discussion.

We have seen that, if we consider a curved conformal space-time model in which the contracted torsion tensor vanishes and the torsion pseudo-vector is constant and space-like, then the orthogonal frame of reference which serves to characterize the space-time structure is determined at each point (to within a conformal transformation) by a non linear conform-invariant spinor equation which is a generalization of Dirac's equation for a free particle.

Now let us examine the condition that the determinant of Ψ must be real. If the three-dimensional surface element is given by (5.1) we note that (5.1) is invariant against the phase transformation

$$(6.1) \quad \Phi' = \Phi e^{i\alpha} = f^{\frac{1}{2}} e^{i\alpha} \xi,$$

where ξ is a unimodular matrix and f, α are real scalars. We then have

$$\Phi' \bar{\Phi}' = f^3 e^{2i\alpha}$$

and

$$\Phi' \bar{\Phi}' / \Phi \bar{\Phi} = e^{2i\alpha},$$

the bars denoting the absolute value of the scalar between them. Hence we obtain

$$(6.2) \quad \bar{\Phi} = f^{\frac{1}{2}} \bar{\xi} = \Phi' \sqrt{|\Phi' \bar{\Phi}'|/|\Phi' \bar{\Phi}'|}$$

and

$$(6.3) \quad \Phi \bar{\Phi} = |\Phi' \bar{\Phi}'|.$$

Now if we replace Φ by its value (6.2) we get the equation obeyed by a transformation matrix Φ' with arbitrary phase. This new equation is invariant against the phase transformation (6.1) which in spinor language reads

$$(6.4) \quad \varphi' = e^{i\alpha} \varphi.$$

A second point worth discussing is the connection between the present theory and the scalar theory of gravitation. We have already shown elsewhere⁽¹³⁾ that the scalar gravitational potential is given by f if the conformal metric has the form (4.1). According to (4.11) the gravitational potential is then

$$f = (\Psi \bar{\Psi})^{\frac{1}{2}},$$

so that the field equation (5.14) can be written as

$$(6.5) \quad D\Psi - m\bar{\Psi}^{\dagger}i\sigma_3 = 0,$$

where

$$(6.6) \quad m = \lambda f$$

is the variable mass in a gravitational potential expressed in natural units. But (6.5) is just the Dirac equation (in matrix form) for a particle in a scalar potential.

The rest energy density of the field is therefore determined by the contracted Einstein tensor associated with the metric (4.1), that is (ref. (14), Eq. (12)),

$$(6.7) \quad R = 6f^{-3} \square f = 6(\Psi \bar{\Psi})^{-1} \square (\Psi \bar{\Psi})^{\frac{1}{2}}.$$

In the third part of our discussion we make some remarks about the physical interpretation of the basis vectors of the orthogonal frame. The equation (5.8) reads

$$(6.8) \quad \partial_{\alpha}(\Psi^{\dagger} I^{(\lambda)} \Psi) = 0$$

⁽¹⁴⁾ F. GÜRSEY: *Proc. Camb. Phil. Soc.*, **49**, 285 (1953).

and is equivalent to the 4 divergence equations

$$(6.9) \quad D \cdot (\Psi \Psi^\dagger) = 0$$

$$(6.10) \quad D \cdot (\Psi \sigma_1 \Psi^\dagger) = 0$$

$$(6.11) \quad D \cdot (\Psi \sigma_2 \Psi^\dagger) = 0$$

$$(6.12) \quad D \cdot (\Psi \sigma_3 \Psi^\dagger) = 0$$

where $\sigma_1, \sigma_2, \sigma_3$ are the Pauli matrices. (6.9) is just the conservation equation for the current-density 4-vector and (6.12) expresses the conservation of the spin density 4-vector (See ref. ⁽¹⁰⁾ Sect. 5). We have

$$(6.13) \quad J = \Psi \Psi^\dagger = I^{(v)} (\Psi^\dagger \cdot \bar{I}_{(v)} \Psi) = f^2 I^{(v)} {}^0 t_v, \quad \Psi \sigma_n \Psi^\dagger = f^2 I^{(v)} {}^n t_v \quad (n = 1, 2, 3).$$

Thus ${}^0 t_v$ and ${}^3 t_v$ are respectively proportional to the current vector and the spin density pseudo-vector. The complex vector ${}^1 t_v + i^2 t_v$ is proportional to the de Broglie vector (ref. ⁽¹⁰⁾ Sect. 5) connected with the 4-spinor wave equation.

We are now in a position to give a possible interpretation of the assumptions made about the torsion pseudo-vector L . In his theory of a relativistic fluid, SYNGE ⁽¹⁵⁾ defines the vorticity 4-vector by the relation

$$(6.14) \quad \omega^\varepsilon = \frac{1}{4} \delta^{\varepsilon\alpha\beta\gamma}_{0123} \lambda_\gamma (\partial_\alpha \lambda_\beta - \partial_\beta \lambda_\alpha),$$

where λ_α denotes the velocity vector of the fluid and δ is the completely anti-symmetrical Kronecker symbol. In our definition of the torsion pseudo-vector (2.27) we have, remembering (2.10) and (2.17)

$$(6.15) \quad L^\varepsilon = \frac{1}{8} k \delta^{\varepsilon\alpha\beta\gamma}_{0123} t_{\mu\gamma} [\partial_\alpha ({}^\mu t_\beta) - \partial_\beta ({}^\mu t_\alpha)].$$

A summation is implied over μ . The first term corresponding to $\mu = 0$ gives a contribution which is proportional to ω^ε , since ${}^0 t_\alpha$ can be interpreted as the velocity vector λ_α according to (6.13). Accordingly the torsion pseudo-vector is closely connected with the vorticity vector of a fluid the stream-lines of which are along the time-like basis vector ${}^0 t_\alpha$ of the fundamental orthogonal frame. It follows that the constancy and the time-like character of the torsion pseudovector correspond in some way to the fact that the associated fluid has constant (and space-like) vorticity. It is then not surprising that the spinor equation which describes this space-like model is a field equation for particles of constant spin.

⁽¹⁵⁾ J. L. SYNGE: *Proc. London Math. Soc.*, **43**, 376 (1937).

RIASSUNTO (*)

Si ha una semplice interpretazione geometrica nel quadro della relatività generale dell'equazione d'onda spinoriale non lineare conformemente invariante proposta in un precedente lavoro. In ogni punto di un universo spazio-temporale conforme si definisce un sistema di riferimento ortogonale associato con un 4-spinore ψ . Si dimostra che il tensore torsionale contratto A_α si annulla (come nel caso di una trasformazione di coordinate) e il pseudovettore L_α derivato dallo stesso tensore torsionale rimane costante e spaziale, il 4-spinore ψ associato soddisfa esattamente la suddetta equazione d'onda che, a sua volta, determina in ogni punto dello spazio-tempo, a meno di una trasformazione conforme, il sistema ortogonale di riferimento. In particolare, se anche il pseudovettore L_α si annulla, si ottiene l'equazione di Dirac per una particella di massa a riposo nulla. In una discussione del significato fisico del sistema ortogonale di riferimento, il vettore base temporale e uno dei vettori base spaziali sono rispettivamente in rapporto con la densità di corrente e i 4-vettori di densità spinoriale associati con l'equazione d'onda.

(*) Traduzione a cura della Redazione.

K^+ -Meson Interaction with Nucleons and Nuclei.

G. COCCONI, G. PUPPI, G. QUARENI and A. STANGHELLINI

Istituto di Fisica dell'Università - Bologna

(ricevuto il 29 Ottobre 1956)

Summary. — The results obtained in several Laboratories on the nuclear interaction of the K^+ -mesons of energy between 40 and 150 MeV have been analyzed. It is assumed that all K^+ -mesons have identical interaction properties and that Gell-Mann's scheme is correct. The main results are the following: 1) The total cross-section for the process $K^+ + p$ (isotopic spin state $T=1$) is $\sigma_0 = 14 \pm 3$ mb. The corresponding differential cross-section may be described essentially with S -wave and coulombian constructive interference. 2) The isotopic spin state $T=0$ is not negligible compared to $T=1$. P -wave should be important in the $T=0$ state. 3) To explain the K^+ -meson interaction with nuclei, a nuclear repulsive potential $V \simeq 10$ MeV should be added to the coulombian potential. With these assumptions we can describe: *a*) The elastic scattering in terms of the optical model. *b*) The inelastic scattering, by considering the interaction due to single collisions of the K^+ -mesons with the nucleons (which are considered as independent particles of a Fermi-gas). 4) The K^+ -nucleon interaction in the $T=1$ state may be described by a central potential equivalent to a hard-core of radius $a = 0.8(\hbar/m_K c)$.

1. — Introduction.

The results obtained in the last year in several European and American Laboratories about the interaction of artificially produced K^+ -mesons in nuclear emulsions are by now numerous enough to allow a detailed analysis of the phenomenon.

Such an analysis is attempted in the present paper, utilizing the results obtained in the following Laboratories:

- 1) Max-Planck Institut für Physik, Göttingen.
- 2) Istituto di Fisica dell'Università, Padova.
- 3) Physics Department, University of California, Berkeley.
- 4) H. H. Wills Physical Laboratory, University of Bristol, Bristol.
- 5) Istituto di Fisica dell'Università, Bologna.

The available experimental evidence suggests that all the K⁺-mesons produced by collisions of accelerated protons with nuclei have the same physical properties independently of their mode of decay. We shall therefore assume in our analysis that these K⁺-mesons are all identical, at least as far as their interaction with nucleons and nuclei is concerned. If further evidence shall disprove this assumption, the results of our analysis have to be considered as describing the average properties of the various K-mesons in the beam.

2. - Experimental Results.

a) All the available examples of (K⁺+nucleus) interactions (~ 200 cases obtained in the Laboratories quoted in Sect. 1, plus many more in other Laboratories) indicate that the Gell-Mann selection rules always hold. We consider this as the justification for taking the Gell-Mann scheme as the basis for our analysis.

The isospin of the K⁺-mesons is then $T=\frac{1}{2}$, and the possible interactions with nucleons (at energies below the threshold for π -meson production) can take place in the states with isospin 1 and 0 with the following relative probabilities:

	$T=1$	$T=0$
$K^+ + p \rightarrow K^+ + p$ (elastic scattering)	$\frac{4}{6}$	0
$K^+ + n \rightarrow K^+ + n$ (elastic scattering)	$\frac{1}{6}$	$\frac{1}{2}$
$K^+ + n \rightarrow K^0 + p$ (charge exchange)	$\frac{1}{6}$	$\frac{1}{2}$

b) Of the two elementary interactions (K⁺+p) and (K⁺+n), the first can be observed in emulsion, where the hydrogen content is of $3 \cdot 10^{22}$, atoms cm⁻³. Unfortunately, the number of cases thus far observed is too small for an accurate determination of the total cross-section, σ_p , and of the differential

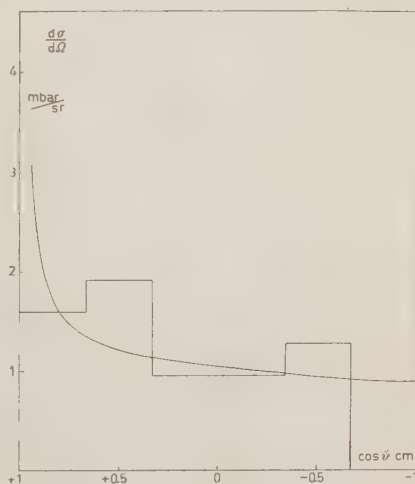


Fig. 1. - Differential cross-section of the reaction $K^+ + p = K^+ + p$. The histogram gives the experimental results. The curve is the result of the model of Section 5, assuming for the radius of the core the value $0.8 r_K$.

cross-section, $d\sigma_p/d\Omega$. Using all available cases for K^+ -mesons in the energy range between 50 and 150 MeV one obtains:

$$\sigma_p = (14 \pm 3) \text{ mb}$$

and $d\sigma_p/d\Omega$ (center of mass system) as given in Fig. 1. Forward scattering seems more probable than backward scattering.

c) The interactions of K^+ -mesons with the nuclei in the emulsion (C, N, O, Br, Ag) can be divided in 3 categories: elastic scatterings (E); inelastic scatterings (I); and charge exchange (C.E.).

The classification of the observed events in the three categories often is a tough experimental problem. As far as the scatterings are concerned, the determinations of the K^+ energy before and after the collision is usually affected by an error seldom smaller than 10%. The separation between elastic and inelastic scatterings is therefore uncertain whenever the fractional energy loss, $\Delta E/E$, is of this order of magnitude. For this reason, we have taken into consideration only those inelastic scatterings for which $\Delta E/E \geq 0.20$.

For these events and for scattering angles, ϑ , larger than 20° , we have obtained:

$$\sigma_I = 5 \text{ mb/nucleon}$$

$$\left(\vartheta \geq 20^\circ, \frac{\Delta E}{E} \geq 0.20 \right).$$

The differential cross-section, $d\sigma/d\Omega$ (L-system), is given in Fig. 2a.

These results refer to events pro-

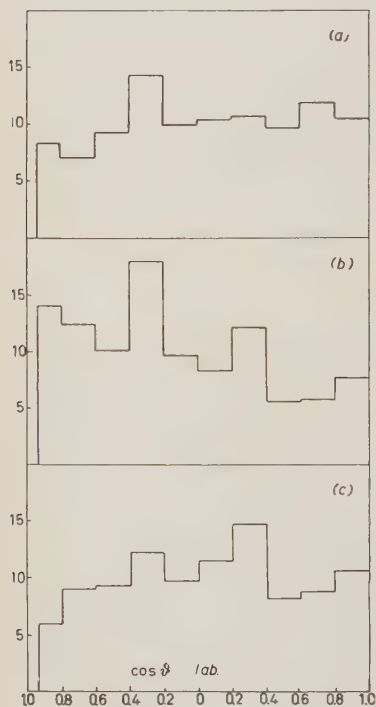


Fig. 2. — Differential cross-section of the inelastic collisions of K^+ -mesons against the nuclei of the emulsion. The ordinates represent percent of the events. a) Experimental results. b) Results of the first Monte-Carlo calculation (elementary cross-section equal to that of Fig. 1). c) Results of the second Monte-Carlo calculation (elementary cross-section equal to that of Fig. 5).

duced by K⁺-mesons of energies between 60 and 130 MeV (average energy ~ 90 MeV) (*).

If the inelastic scatterings are interpreted as the result of collisions of the K⁺-mesons with the single nucleons in the nucleus, the differential cross-section of Fig. 2 suggests that in the nuclei the average (K⁺ + nucleon) cross-section is mostly backwards in the center of mass system.

We have also analysed the inelastic scattering according to the energy lost by the K⁺-mesons. In Fig. 3a and 3a' we have plotted the energy losses for the K⁺-mesons scattered forward and backward, respectively. The lack of large energy losses for backward scattered mesons is quite unexpected. In fact in the elementary (K⁺ + nucleon) collisions the large angle scatterings are always accompanied by large energy losses.

These facts suggest, as we shall discuss later, that K⁺-mesons feel in the nuclei a strong repulsive potential.

d) An event is classified as a charge exchange, whenever no K⁺-meson is emitted after the collision. This interpretation is justified, as stated before, by the fact that in all cases observed, the visible excitation of the nucleus is much smaller than that expected if the K⁺-meson were absorbed.

A difficulty in the interpretation of these events arises in the cases of pure «stops», i.e. whenever there is no visible excitation of the nucleus. Some of these cases in fact can be decays in flight, in which the track of the secondary particles is not easily

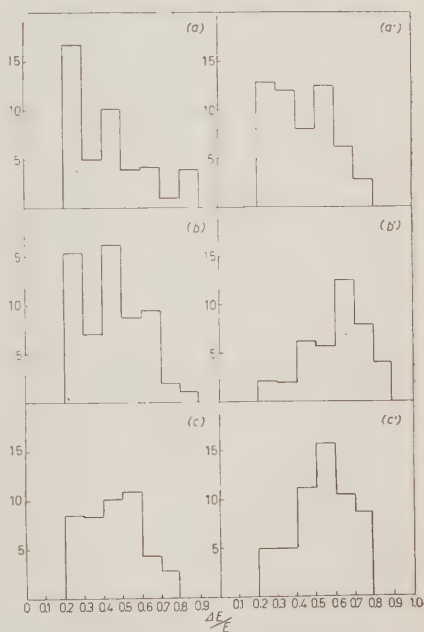


Fig. 3. — Distribution of the energy losses of K-mesons scattered by nuclei forwards (a, b, c) and backwards (a', b', c') in the Laboratory. The ordinates are percent of events. a, a') Experimental results. b, b') Results of the first Monte-Carlo calculation c, c') Results of the second Monte-Carlo calculation.

(*) It would be desirable to subdivide the events in energy intervals, to study the energy dependence of the cross-sections. Unfortunately, the available data are too meagre to warrant this. We have always tried a subdivision into 2 energy groups, and have found no meaningful difference between them,

visible. In principle, one could evaluate the probability of this phenomenon. However, the number of « stops » thus far observed is too small to make the correction worthwhile.

If one takes into account only the charge exchange with visible excitation, produced by K^+ -mesons of energies between 40 and 150 MeV, one obtains the lower limit for the charge exchange cross-section,

$$\frac{\sigma_{C.E.}}{\sigma_I} \sim \frac{1}{5}.$$

It could be very interesting to know the energy dependence of this ratio. The data at our disposal seem to indicate that it increases as the K^+ -energy increases. However, the total number of cases is so small (12 events) that any conclusion is premature.

From the sum $\sigma_I + \sigma_{C.E.}$, one can deduce that the total cross-section for non-elastic collision is of 6 mb.

e) Our analysis of the elastic scatterings is limited to the events with scattering angle $\vartheta \geq 20^\circ$ (L-system). This is because only for such events the scanning efficiency in the experiments whose data we are using was close to unity.

We have considered as elastic all the events for which $\Delta E/E \leq 0.10$. As

we shall see, the Monte-Carlo analysis of the inelastic K^+ -collisions indicates that inelastic scattering with $\Delta E/E \leq 0.10$ is very improbable.

The average total cross-section for the nuclei present in the emulsion (hydrogen excluded) is:

$$\sigma_h(\vartheta \geq 20^\circ) = (216 \pm 20) \text{ mb.}$$

The corresponding differential cross-section is plotted in Fig. 4.

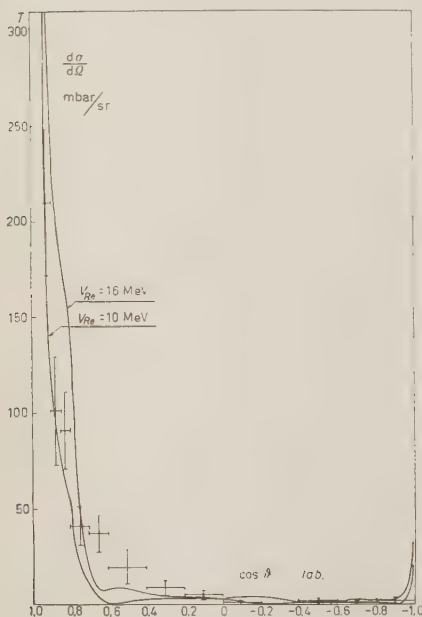


Fig. 4. - Differential cross-section of K^+ -mesons scattered elastically by the nuclei of the emulsion. The crosses represent the experimental results. The two curves are the results of the optical model of Sect. 4, for two values of the real part of the nuclear potential.

RIUNIONI DI FISICA IN ITALIA NEL 1957

- 11-15 Giugno – **Venezia**, Fondazione « G. Cini ».
Terza conferenza internazionale sui fenomeni di ionizzazione nei gas, organizzata dalla Società Italiana di Fisica.
Segretario generale: prof. U. FACCHINI, Laboratori Cise, Via Procaccini, 1, Milano.

- 21-26 Giugno – **Varenna**, Villa Monastero.
Conferenza internazionale sugli aspetti astrofisici dei problemi relativi alla radiazione cosmica, organizzata dall'Unione Internazionale di Fisica pura ed applicata d'intesa con la Società Italiana di Fisica.
Segretario generale: prof. B. ROSSI, Department of Physics, Massachusetts Institute of Technology, Cambridge 39 (Mass., U.S.A.).

- 14 Luglio-3 Agosto – **Varenna**, Villa Monastero.
Corso internazionale sulla Fisica dello stato solido, organizzato, sotto gli auspici del Ministero della Pubblica Istruzione e del Consiglio Nazionale delle Ricerche, della Società Italiana di Fisica.
Direttore del Corso: prof. F. FUMI, Istituto di Fisica dell'Università, Via Archirafi, 36, Palermo.

- 11-15 Settembre – **Varenna**, Villa Monastero.
Convegno internazionale sugli stati condensati di sistemi semplici, organizzato, sotto gli auspici dell'Unione Internazionale di Fisica pura ed applicata e del Consiglio Nazionale delle Ricerche, dalla Società Italiana di Fisica.
Segretario generale: prof. G. CARERI, Istituto di Fisica dell'Università, Via Marzolo, 8, Padova.

- 17-20 Settembre – **Roma**, Accademia Nazionale dei Lincei.
Nona Assemblea generale dell'Unione Internazionale di Fisica pura ed applicata.
Segretario generale: prof. P. FLEURY, 3, Boulevard Pasteur, Paris XV.

- 22-27 Settembre – **Venezia**, Fondazione « G. Cini »; Padova, Università.
Convegno internazionale sui mesoni e le particelle recenti, organizzato sotto gli auspici dell'Unione Internazionale di Fisica pura ed applicata e del Consiglio Nazionale delle Ricerche, dalla Società Italiana di Fisica; *XLIII Congresso Nazionale di Fisica*, organizzato, sotto gli auspici del Consiglio Nazionale delle Ricerche, dalla Società Italiana di Fisica.
Segretario generale delle due riunioni: prof. A. ROSTAGNI, Istituto di Fisica dell'Università, Via Marzolo, 8, Padova.

MEETINGS ON PHYSICS IN ITALY IN 1957

- June 11th-15th – **Venice**, Fondazione «G. Cini»,
Third International Conference on the Ionization Phenomena in Gases, organized by the Italian Physical Society.
Secretary General: prof. U. FACCHINI, Laboratori Cise, Via Procaccini 1, Milano.

- June 21st-26th – **Varenna**, Villa Monastero.
International Conference on the Astrophysical Aspects of Problems relative to the Cosmic Radiation, organized by the International Union of Pure and Applied Physics in agreement with the Italian Physical Society.
Secretary General: prof. B. ROSSI, Departement of Physics, Massachusetts Institute of Technology, Cambridge 39 (Mass., U. S. A.).

- July 14th-August 3rd – **Varenna**, Villa Monastero.
International Course on Solid State Physics, organized by the Italian Physical Society, under the auspices of the International Union of Pure and Applied Physics and the National Research Council.
Director of the Course: prof. F. FUMI, Istituto di Fisica dell'Università, Via Archirafi 36, Palermo.

- September 11th-15th – **Varenna**, Villa Monastero.
International Meeting on the Condensed States of the Simple Systems, organized by the Italian Physical Society under the auspices of the International Union of Pure and Applied Physics and the National Research Council.
Secretary General: prof. G. CARERI, Istituto di Fisica dell'Università, Via Marzolo 8, Padova.

- September 17th-20th – **Rome**, Accademia Nazionale dei Lincei.
Ninth General Meeting of the International Union of Pure and Applied Physics.
Secretary General: prof. P. FLEURY, 3, Boulevard Pasteur, Paris XV.

- September 22nd-27th – **Venice**, Fondazione «G. Cini»; Padua, University.
International Meeting on Mesons and Recent Particles, organized by the Italian Physical Society, under the auspices of the International Union of Pure and Applied Physics and the National Research Council; *43rd National Congress of Physics*, organized by the Italian Physical Society, under the auspices of the National Research Council.
Secretary General of the two meetings: prof. A. ROSTAGNI, Istituto di Fisica dell'Università, Via Marzolo 8, Padova.

3. - Monte-Carlo Analysis of Inelastic Collisions.

For the interpretation of the inelastic events we have made the assumption that the collision between a K-meson and a nucleus is equivalent to the collision of the K-meson with *one* nucleon of the Fermi gas of nucleons constituting the nucleus.

The main justification for this assumption rests on the facts that the nuclear cross-section of the K-mesons is much smaller than geometrical, and that the De Broglie wave length of the mesons at the energies considered here is of the order of $\frac{1}{2}r_0$. Furthermore, it is known that models of this kind give satisfactory results in the interpretation of the collisions with nuclei of low energy π -mesons, where the situation is much less favourable than in our case.

The model has been treated with the Monte-Carlo method. Thus far we have developed the calculation for collisions produced by K⁺-mesons of 85 MeV, the average energy used in the experiments considered. Because of the qualitative nature of this analysis, in the calculation we have not taken into account:

a) double scatterings. This is justified by the smallness of the elementary cross-section;

b) the effects of both the Coulomb and the average nuclear potentials on the incoming and outgoing waves. We believe that our results for the angular distribution on the K⁺-mesons are not strongly affected by this simplification. The effect of the potentials on the kinetic energy of the mesons has been taken into account by summing the potential energy to the meson kinetic energy far from the nucleus.

The fraction $(1 - \eta)$ of collisions forbidden by the Pauli principle can be deduced from our analysis. However, these collisions belong to the category of the elastic events, and cannot be further analyzed by the Monte-Carlo method.

A first calculation has been carried out using for the (K⁺-nucleon) collisions a differential cross-section of the same shape as that observed for the (K⁺-p) collisions (Fig. 1).

The fraction of collisions forbidden by the Pauli principle turned out to be $(1 - \eta_1) = 0.35$.

The results obtained for the angle and energy distributions are plotted in Figs. 2b, 3b and 3b'. These distributions are in strong disagreement with the experimental data (see Figs. 2a, 3a and 3a'). In fact, the calculated angular distribution is much more forward than the experimental one, while as expected, the energy distribution of the mesons scattered backwards is excessively rich in particles that underwent strong energy losses.

A better agreement for the angular distribution can be achieved by using

an elementary cross-section more peaked backwards than that of Fig. 1. Such a modification however, would not improve the situation as far as the energy losses are concerned, since these depend in our model only on the scattering angle.

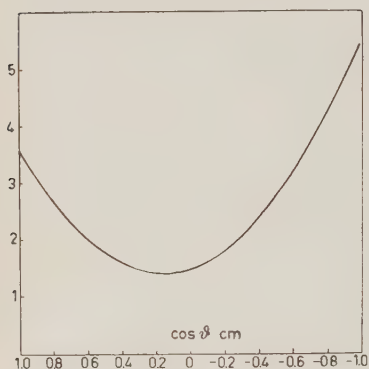


Fig. 5. - Average differential cross-section per nucleon utilized in the second Monte-Carlo calculation. Ordinates in arbitrary units. A shape of this kind is necessary in order to reproduce the observed angular distribution of the K^- -mesons scattered inelastically by the nuclei (see Fig. 2). The curve can be described by the following equation:

$$d\sigma/d\Omega \propto 1.5 - \cos \beta + 3 \cos^2 \theta.$$

In fact, if a repulsive potential is effective, the percent energy losses of the low energy mesons are strongly reduced and many more cases fall in the small $\Delta E/E$ region, where most of the discrepancy stays.

The fraction of collisions forbidden by the Pauli principle turned out to be, in this calculation, $1 - \eta_2 = 0.26$.

If one is willing to accept Fig. 5 as representative of the average cross-section of K^- -mesons for collisions on protons and neutrons, one may deduce information about the $(K^+ + n)$ cross-section by subtracting from it the $(K^+ + p)$ cross-section of Fig. 1. In the limiting case, where all the forward quadrant and the isotropic part of the backward quadrant is assigned to the protons, the $(K^+ + n)$ cross-section should be essentially backwards. For the neutron then the effect of the Pauli principle should be practically negligible ($\eta_3 \sim 1$)

The most plausible way out of this difficulty consists in assuming that the K^+ -mesons feel in the nuclei a strong repulsive potential, besides the Coulomb potential.

A second calculation was performed introducing for the $(K^+ + \text{nucleon})$ collisions the differential cross-section plotted in Fig. 5, which produces the angular distribution of Fig. 2c, in good agreement with the experimental one of Fig. 2a. In Figs. 3c and 3c' we have plotted the forward and backward energy distributions calculated assuming that the average nuclear potential felt by the K^+ -mesons is repulsive and equal to 10 MeV (added to the Coulomb potential (*)). The agreement with experiments is appreciably improved, though Fig. 3c' is still quite different from Fig. 3a'. This could in part be due to the fact that our calculations refer to a monochromatic beam of K^+ -mesons, while the experiments were performed in the energy range $60 \div 130$ MeV.

(*) Because of the addition of the 10 MeV-nuclear potential, Figs. 2c, 3c and 3c', refer to K^+ -meson of average energy of 95 MeV (not 85 as before), in the L-system.

and the ratio $\alpha = \sigma_n/\sigma_p = 0.37$, where σ_n is the total cross-section ($K^+ + n$), charge exchange excluded.

The average K^+ inelastic cross-section per nucleon in the nucleus can then be expressed as follows:

$$\sigma_I = \frac{Z\sigma_p\eta_1 + N\sigma_n\eta_3}{Z + N} = \sigma_p \frac{Z\eta_1 + N\alpha\eta_3}{Z + N} \simeq 7 \text{ mb}$$

in satisfactory agreement with the observed value of 5 mb. If this interpretation is correct, one is led to believe that the ($K^+ + \text{nucleon}$) interaction in the state $T = 1$ is practically isotropic, and that the state $T = 0$ is responsible for the destructive interference in the case of the neutrons.

4. - Elastic Scattering.

As pointed out in Sect. 3, the Monte-Carlo analysis gives no information about elastic scattering.

These events have been treated with the formalism of the optical model, utilizing the results obtained for the inelastic collisions.

The average K^+ inelastic cross-section of 6 mb/nucleon corresponds to a mean path in nuclear matter of:

$$\lambda = \frac{4\pi}{3} \frac{r_0^3}{\sigma_I} \simeq 16 r_0, \quad \text{where} \quad r_0 = \frac{\hbar}{m_\pi c}.$$

which indicates an imaginary potential.

$$V_{\text{Im}} = -\frac{1}{2} \frac{r_K}{\lambda} \beta_K m_K c^2 \simeq 2 \text{ MeV}, \quad \text{where} \quad r_K = \frac{\hbar}{m_K c}.$$

The total potential felt by the K^+ -mesons in a nucleus is then:

$$V = V_{\text{Re}} + iV_{\text{Im}},$$

with

$$V_{\text{Re}} \simeq 10 \text{ MeV} \quad \text{and} \quad V_{\text{Im}} \simeq 2 \text{ MeV}.$$

The differential cross-section for elastic scattering can be determined by solving the Klein-Gordon equation ⁽¹⁾

$$(E - V)^2 \psi = (p_K^2 c^2 + m_K^2 c^4) \psi,$$

⁽¹⁾ K. M. GATHA and R. J. RIDDEL: *Phys. Rev.*, **86**, 1035 (1952).

where V satisfies the following condition:

$$V = \frac{Ze^2}{r} \quad \text{for } r > R$$

$$V = V_{\text{Re}} + iV_{\text{Im}} + \frac{Ze^2}{R} \left[\frac{3}{2} - \frac{1}{2} \left(\frac{r}{R} \right)^2 \right] \quad \text{for } r < R,$$

R being the nuclear radius. This equation has been solved in the WKB approximation, which is legitimate because $kR \ll 1$ (k is the wave number) for both the heavy and the light nuclei present in the emulsion. The calculations were developed for K -mesons of 80 MeV, separately for a light nucleus ($Z = 7$, $N = 7$) and for a heavy nucleus ($Z = 42$, $N = 54$).

The results for the «average nucleus» in emulsion are plotted in Fig. 4 for $V_{\text{Re}} = +10$ and $+16$ MeV.

The real potential needed to interpret the experimental results is $V_{\text{Re}} \simeq +10$ MeV, possibly slightly larger.

The results on inelastic events discussed in the previous section also suggest the presence of a repulsive potential of the same order of magnitude.

5. - A Possible Model for $(K^+ + p)$ Collisions.

In this section we shall present a model for the interpretation of the $(K^+ + \text{nucleon})$ interaction in the isospin state $T = 1$. The value of this model comes from the fact that it is very simple, and allows definite prediction to be compared with experimental data.

The fundamental facts to be interpreted are the following:

- a) an elementary total $(K^+ + \text{proton})$ cross-section of ~ 14 mb, practically energy independent in the energy range of 50 to 150 MeV;
- b) an angular distribution slightly forwards, but not too different from isotropic;
- c) a real $(K^+ + \text{nucleus})$ potential of about $+10$ MeV, probably not strongly energy dependent.

Our model consists in assuming that the $(K^+ + \text{nucleon})$ interaction in the $T = 1$ state can be described with a central potential equivalent to a hard core of radius:

$$a = 0.8r_K = 0.8 \frac{h}{m_K c}.$$

This gives, for K⁺-mesons of 80 MeV colliding with protons the angular distribution represented by the full line of Fig. 1, and the angular dependence of the total cross-section of Fig. 6.

Both are in agreement with the experimental evidence.

The real part of the (K+nucleus) potential can be calculated with the model. Let

$$f(0) = \frac{Zf_p(0) + Nf_n(0)}{Z + N},$$

be the forward scattering amplitude averaged over the protons and the neutrons in the state $T=1$, in the laboratory system. Then in the optical model the connection between $f(0)$ and the real potential in the nucleus is given by the expression:

$$\frac{V(V-2E)}{2m_K c^2} = -\frac{3\hbar^2}{2r_0^3 m_K} f(0),$$

which gives $V_{\text{re}} \sim -12$ MeV. This result is not strongly modified by taking into account the possible interference effect with the $T=0$ state.

One reaches therefore the conclusion that the repulsive average nuclear potential is essentially due to the $T=1$ state. Most of the characteristics of the interaction of K⁺-mesons with nucleons and nuclei can thus be explained by the simple model considered in this section in which the nucleons for the $T=1$ state are equivalent to hard cores.

As far as the isospin state $T=0$ is concerned, its existence is certainly suggested by the experimental evidence. More precise measurements are needed to reach quantitative conclusions. However it seems likely as discussed in Sect. 3, that the scattering cross-section on neutrons is peaked backward. If this is true, a large P wave is needed in the $T=0$ state. As a consequence, a large energy dependence for the contribution to the total cross-section of the $T=0$ state is expected. Simple considerations on isospin conservation lead to expect that the angular distribution of charge exchange scatterings is roughly symmetrical to the non charge exchange scattering, in respect to 90° , i.e. strongly forward. Notwithstanding the large value for the charge exchange in the elementary cross-section that would follow, the charge exchange cross-section on nuclei would be quite small, because strongly reduced by the Pauli principle. Moreover, it is expected that the excitation of the nucleon after

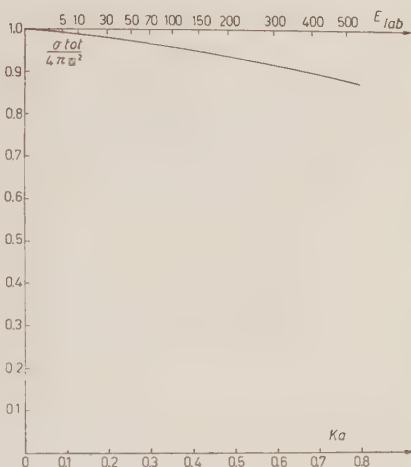


Fig. 6. - Total cross-section of K⁺-mesons of energy E and wave number k colliding with a hard sphere of radius $a = 0.8r_K$.

a charge exchange is small and the number of observed «stops» appreciable. This is not in disagreement with the scanty experimental evidence accumulated thus far.

* * *

We feel very grateful to the Laboratories that gave us the experimental results on which our analysis was based and we want to thank Dr. M. CECARELLI, Prof. N. DALLAPORTA and Dr. A. SALANDIN with whom we frequently corresponded on the subject.

RIASSUNTO

Sono stati analizzati i risultati ottenuti in diversi Laboratori sull'interazione nucleare dei mesoni K^+ di energia tra 40 e 50 MeV. Si assume che tutti i mesoni K^+ abbiano identiche proprietà e che lo schema di Gell-Mann sia valido. I principali risultati sono i seguenti: 1) La sezione d'urto totale del processo $K^+ + p$ (stato di spin isotopico $T=1$) è $\sigma_p = 14 \pm 3$ mb. La corrispondente sezione d'urto differenziale si può descrivere con un'onda S e l'interferenza coulombiana costruttiva. 2) Lo stato di spin isotopico $T=0$ non è trascurabile rispetto a $T=1$. Nello stato $T=0$ sarebbe importante un'onda P . 3) I nuclei presentano un potenziale nucleare repulsivo $V \simeq 10$ MeV da aggiungersi a quello coulombiano. Con queste assunzioni si può rendere conto dell'interazione elastica considerando l'interazione dovuta a collisioni singole dei mesoni K^+ con i nucleoni costituenti un gas di particelle indipendenti. 4) L'interazione K^+ -nucleone nello stato $T=1$ può essere descritta da un potenziale centrale equivalente ad una sfera rigida di raggio $a = 0.8(\hbar/m_K c)$.

On the Problem of the Static Helium Film.

II - Effects Due to the Smallness of One Dimension.

S. FRANCHETTI

Istituto di Fisica dell'Università - Firenze

(ricevuto il 29 Ottobre 1956)

Summary. — Some aspects of the thermodynamical behaviour of certain fluids when they are made to occupy very flat spaces (their density being held constant) are investigated. The zero point energy change of liquid ^4He (a problem first considered by K. R. ATKINS) is studied in Sect. 2 on the basis of two different models. The changes in the internal energy and in the free energy of two types of Bose-Einstein perfect gases in a state of partial condensation are analyzed in Sect. 3.

1. $\frac{1}{2}$ - Introduction.

The effects dealt with in the present paper should not be confused with any ordinary surface effect. They are purely quantum phenomena (that is ones that would disappear by having \hbar tend to zero), arising from the fact that one dimension of the system under consideration is no longer sufficiently large compared with some « natural length » inherent to the system.

This, however, is not to be taken to mean that the « small dimension », say t , and the « natural length », say l , are to be of the same order of magnitude. In the problems treated here, the ratio l/t is at most of the order 10^{-2} . These conditions are however sufficient to make it necessary to carry out directly certain summations appearing in some statistical formulae, the usual substitution of integrals in their place being no longer allowed if accurate values are to be obtained. This is how the effects in question are brought into play analytically. (With the exception of the case in Sect. 2'2) where the mechanism is different).

In Sect. 2'1 we consider the zero point energy E_0 of liquid ^4He , assimilating it to that of a system of longitudinal Debye waves. In Sect. 2'2 the same problem is treated on the basis of an entirely different model taking explicitly into account the atomic structure of the fluid and the result is shown to be essentially the same. In the first treatment the natural length is the Debye cut-off wavelength, while in the second it is the width of the « individual cell » in which any atom is prevalently moving about. The two lengths are of course of the same order of magnitude.

In Sect. 3 we deal with two types of ideal Bose-Einstein gases in a state of partial condensation. In Sect. 3'1 the gas is assumed to be one of « material particles », that is particles whose energy is proportional to the square of momentum. In Sect. 3'2 the energy is assumed to depend linearly on momentum (phonons). The natural length for the first case turns out to be

$$\Lambda = h(8\pi\mu kT)^{-\frac{1}{2}},$$

μ being the mass of the particles. In the second case the natural length is

$$\lambda = hC(2kT)^{-1}$$

where C is the velocity of (ordinary) sound.

2. — The Zero Point Energy Change.

2'1. *The Zero Point Energy of a Debye Wave System in a Thin Sheet.* — As was already mentioned in a previous paper ⁽¹⁾ ATKINS was the first to point out a dependence of the zero point energy per atom of liquid ^4He from the dimensions of the sample (at constant density) ⁽²⁾.

Following ATKINS, the zero point energy (E_0) of liquid helium will be assimilated to that (E^0) of a Debye system of harmonic oscillators. (An alternative treatment not based on this assumption is sketched in Sect. 2'2). That gives for ordinary, *macroscopic* samples the well known formula for E^0

$$(1) \quad E^0 = \frac{9N}{v_D^3} \int_0^{v_D} \frac{h\nu}{2} \nu^2 d\nu = \frac{9N}{8} h\nu_D = \frac{9}{8} R_D,$$

⁽¹⁾ S. FRANCHETTI: *Nuovo Cimento*, **4**, 1504 (1956).

⁽²⁾ K. R. ATKINS: *Canad. Journ. Phys.*, **32**, 347 (1954); *Conférence de Physique des Basses Températures*, Paris 1955, p. 100.

where ν_D is the maximum allowed frequency and Θ_D is known from specific heat measurements ⁽³⁾ to be about 27.4 °K.

It must be noted that this way of describing E_0 , though currently accepted, is not altogether obvious. Indeed, there can be no doubt—since LANDAU's work—that low frequency phonons are an essential feature of liquid ⁴He at low temperatures. However, the model of linear oscillators is well justified only for mutual atom displacements small compared to the atomic inter-distance, a condition of which it is not easy to say to what extent it is fulfilled in liquid helium at high frequencies. (Note that according to (1), two thirds of the total value of E^0 are contributed by the region $\nu > 0.76\nu_D$). Since, however, the alternative method proposed in Sect. 2'2 is not itself free from uncertainties and on the other hand the subject may be of some interest in itself, we feel justified in reconsidering the argument even if it contains some assumption whose applicability to the problem of helium does not look—at least *a priori*—entirely objection-free.

Expression (1) for E^0 is valid for macroscopic samples. We have to find out how E^0 will change when one dimension of the sample is no longer very large in comparison of the Debye wavelength $\lambda_D = C/\nu_D$, with C the velocity of sound. (We shall however assume that it is still of the order of, say, $10^2\lambda_D$). For simplicity's sake let us suppose C to be independent of frequency and direction ⁽⁴⁾ of the wave.

The effect pointed out by ATKINS is essentially due to the necessity of replacing the integral in (1) by a sum, when one of the dimensions is small. (A graphical method equivalent to a summation is employed here for convenience).

We take the sample to be a square sheet of the liquid, having thickness t (along the x -axis) and sides L , L (along the y - and z -axes). In accordance with the nature of the medium under consideration, only *longitudinal* waves in the sheet will be considered. We shall

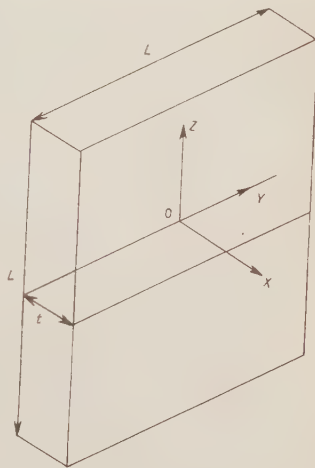


Fig. 1.

⁽³⁾ H. C. KRAMERS, J. WASSCHER and C. J. GORTER: *Physica*, **18**, 329 (1952).

⁽⁴⁾ The contrary hypothesis of C depending on direction may appear singular for a liquid. But in the particular case aimed at, namely helium films, a certain amount of uniaxicity would arise because the film is subject to strong forces normal to the wall. (See for instance the graph of density versus distance in Fig. 5, of ref. ⁽¹⁾). We come back to this point at the end of the section.

assume moreover the simplest boundary conditions by taking the amplitude of the oscillations to be zero on the walls of the sheet. Each stationary wave in the sheet will be characterized by three positive integers n_x , n_y , n_z (with minimum value 1) on which the frequency will depend through the formula

$$(2) \quad \nu^2 = \frac{C^2}{4} \left[\frac{n_x^2}{t^2} + \frac{1}{L^2} (n_y^2 + n_z^2) \right].$$

In a space where n_x , n_y , n_z are co-ordinates, the representative points of the waves form a cubic lattice with volume density 1. The points corresponding to waves having frequencies not exceeding a given ν will belong to the volume bounded by the ellipsoid

$$(2') \quad \frac{n_x^2}{t^2} + \frac{n_y^2}{L^2} + \frac{n_z^2}{L^2} = \frac{4}{C^2} \nu^2 = 4K^2$$

K being the wave number.

It will be convenient to transform this ellipsoid by choosing as co-ordinates

$$(3) \quad \eta_x = \frac{L}{t} n_x, \quad n_y, \quad n_z.$$

The ellipsoid (2') then becomes a *sphere* of radius $2LK$:

$$(4) \quad \eta_x^2 + n_y^2 + n_z^2 = \frac{4L^2\nu^2}{C^2},$$

while

$$(5) \quad \frac{t}{L},$$

is the new density of representative points.

Reverting for a moment to the quasi-continuous case (i.e. t not small) we now wish to introduce a notion which is peculiar of the present treatment, namely that in the isotropic case, the Debye criterion⁽⁵⁾ of fixing a cut-off frequency ν_D makes the zero-point energy a *minimum*. This is almost self-evident.

Indeed, the Debye condition will simply state that the representative points

(5) In a liquid, the Debye cut-off condition is still applicable, while Brillouin's condition is not, requiring as it does a strict periodicity of the medium, without which a minimum wavelength cannot be determined.

shall fill the positive octant of a *sphere*, whose radius

$$(6) \quad R = 2LK_D$$

is such that the total number of enclosed points is $3N$. That is:

$$(6') \quad \frac{1}{8} \frac{4}{3} \pi (2LK_D)^3 \frac{t}{L} = 3N.$$

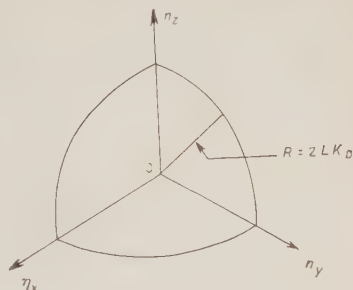


Fig. 2.

This statement can be justified by noting that each wave vector corresponds to *one* linear oscillator (longitudinal waves only) and hence introduces *just one* quantum number. We should expect, however, for reasons of correspondence to have as many quantum numbers as there are degrees of freedom in the system, that is $3N$. This leads to (6').

Introducing a spherical co-ordinate system in place of the rectangular one defined by (3), the radius vector ϱ will be given (because of (4)) by

$$(6'') \quad \varrho = 2LK = 2L \frac{v}{c},$$

and the Debye condition takes the form

$$(7) \quad 3N = \frac{t}{L} \int_0^{\pi/2} d\varphi \int_0^{\pi/2} \sin \theta d\theta \int_0^R \varrho^2 d\varrho = \frac{1}{3} \frac{t}{L} \int_0^{\pi/2} d\varphi \int_0^{\pi/2} R^3 \sin \theta d\theta.$$

With the same notations the zero point energy will be

$$E^0 = \frac{t}{L} \int_0^{\pi/2} d\varphi \int_0^{\pi/2} \sin \theta d\theta \int_0^R \frac{\hbar \nu}{2} \varrho^2 d\varrho,$$

or, by (6'')

$$(8) \quad E^0 = \frac{\hbar Ct}{16L^2} \int_0^{\pi/2} d\varphi \int_0^{\pi/2} R^4 \sin \theta d\theta.$$

To show that this expression is a minimum (under condition (7)), let R vary with the direction instead of being constant, as the Debye condition requires. For simplicity's sake let the variation $\delta R(\theta)$ be dependent only on θ . Clearly,

the variation of (7) must be taken zero, giving, to the 2-nd order of δR

$$(7') \quad 0 = \int_0^{\pi/2} [R \delta R + (\delta R)^2] \sin \theta d\theta.$$

Similarly

$$(8') \quad \delta E^1 = \frac{h C t}{4 L^2} \frac{\pi}{2} R^2 \int_0^{\pi/2} \left[R \delta R + \frac{3}{2} (\delta R)^2 \right] \sin \theta d\theta.$$

Combining the two relations we get

$$(9) \quad \delta E^0 = \frac{\pi}{8} \frac{h C t}{L^2} R^2 \int_0^{\pi/2} \frac{1}{2} (\delta R)^2 \sin \theta d\theta \geq 0.$$

The sign of δE^0 shows that E^0 would always be larger than in the Debye case of a spherical boundary ($\delta R = 0$).

This result is satisfactory, since E^0 is the energy of a quantum system in its fundamental state and should therefore be expected to show minimum properties.

Of course, the variation considered here, amounting to change the boundary of the Debye distribution of representative points without altering its density,

is a very special one. It has been chosen because it leads to eq. (9) which will be useful in a moment. The property $\delta E \geq 0$, however, holds quite generally.

We now revert to the case of t so small that we cannot any longer integrate in the space of representative points, or better, we cannot do so along the η -axis on which successive points lie at a distance L/t apart.

The representative points, in this case, will occupy a space formed by piling up (in the positive octant) quarters of flat cylinders having thickness L/t (whose sections with the $n_y n_z$ plane are represented in Fig. 3).

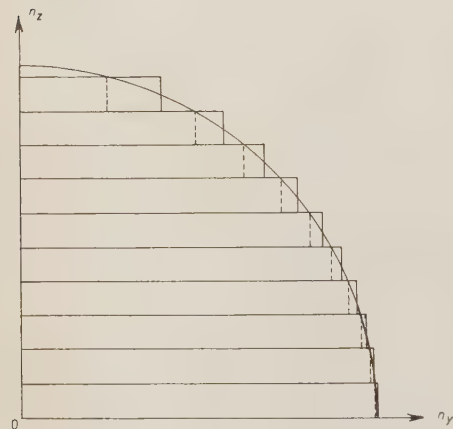


Fig. 3.

We have to choose «in the best manner» the radii of these cylinders (which can legitimately be considered as continuous variables).

In the light of the result just reached, the «best manner» appears to be that which makes the outer surface of the cylinders approach most closely that of a sphere. Of course, the smaller is t the less the surface will satisfy the required condition, so that E^0 should be a minimum for $t = \infty$, and increase as t decreases.

An approximate solution, which however we deem very likely to be accurate enough, is obtained by drawing the profile of the cylinders as shown in Fig. 3 (full line) where the vertical sides are made to cut the circle of radius R in their middle points⁽⁶⁾. In this way $\delta R(\theta)$ is a continuous function with derivative discontinuous at a finite number of points, oscillating about an average zero value.

For L/t sufficiently smaller than R , which, because of (6) means t sufficiently larger than λ_D ⁽⁷⁾, δR can be taken to vary linearly between δ_0 and $-\delta_0$ with $\delta_0 = (L/2t) \cos \theta$ (fig. 4). This gives

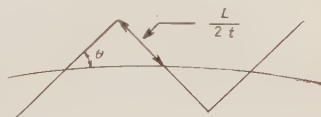


Fig. 4.

$$\overline{\delta R^2} = \frac{1}{12} \frac{L^2}{t^2} \cos^2 \theta.$$

From this, (9) and (6) one gets

$$\delta E^0 = \frac{1}{24} \frac{\pi}{6} h C t^{-1} L^2 R_D^2$$

and since $L^2 t = V$ (the volume of the sample),

$$\delta E^0 = \frac{1}{24} \frac{\pi}{6} h C V K_D^2 t^{-2}.$$

Combining with (8), which can be written

$$E^0 = \frac{\pi}{2} h C V K_D^4,$$

one gets the final result

$$(10) \quad \frac{\delta E^0}{E^0} = \frac{1}{72} (t K_D)^{-2} = \frac{1}{72} \left(\frac{\lambda_D}{t} \right)^2.$$

⁽⁶⁾ ATKINS' procedure translated into the present scheme, would amount to choose the cylinders *inscribed* in the circle (Fig. 3, broken line) and then increase the radius R so that the volume still encloses the prescribed number of points. It is visible that this choice makes the surface more different from a sphere.

⁽⁷⁾ The thickness t of helium films, to which these considerations are to be applied, is—in current experiments—of the order $10^2 \lambda_D$ (corresponding to $t \approx$ some 10^{-6} cm).

This is about half the value of the corresponding term as calculated by ATKINS, by neglecting the minimum properties of E^0 ⁽⁸⁾.

The cut-off wavelength turns out to be (eq. (6'))

$$(10') \quad \lambda_D = 4.0 \cdot 10^{-8} \text{ cm.}$$

Combining this datum and that for Θ (27.4 °K) we obtain from (1) and (10) for the change $\delta\mathcal{E}^0$ of the zero point energy *per atom*

$$(10'') \quad \delta\mathcal{E}^0 = \frac{1}{72} \mathcal{E}^0 \left(\frac{\lambda_D}{t} \right)^2 = 0.94 \cdot 10^{-31} t^{-2} \text{ erg.}$$

Among the assumptions leading to eq. (10) for the zero point energy change, that concerning the velocity of sound C , namely the absence of any dependence of this quantity on ν and θ , is surely not very restrictive. Indeed, any dependence of this kind, would make the calculations more cumbersome ⁽⁹⁾, but is unlikely to affect the final result substantially, at least as far as $C(\nu, \theta)$ is a smoothly varying function of its arguments and thus can be replaced by a suitable average in the integrals. Indeed, we should always expect a minimum energy surface to exist in the ν_1, ν_2, ν_3 space and this leads for δE^0 to an expression of type (9) ⁽¹⁰⁾.

However, since we cannot know *a priori* how faithfully the picture by a system of linear oscillators will represent the properties of the zero point energy of liquid helium, it appears desirable to check the result contained in eq. (10) or (10'') by some independent procedure.

2.2. *Alternative treatment.* – The obvious difficulty we meet in abandoning the picture based on Debye waves is that any other model for a liquid is more intricate. It turns out, however, that, with some simplifying assumptions the model proposed by the Author ⁽¹¹⁾ yields, without difficulty a formula in good agreement with (10'').

⁽⁸⁾ In ATKINS' treatment a *negative* term in λ_D/t appears in the expression for the zero point energy, besides the $(\lambda_D/t)^2$ term, as for instance in eq. (19) of *Canad. Journ. Phys.*, ref. (2)). That would not be consistent with a minimum of E^0 for $t = \infty$. In fact, the sign should be *positive*, the error arising from having inadvertently started with $n_s = 0$ (instead of $n_s = 1$) the summation leading to eq. (16). The term in question disappears altogether by taking into account the minimum properties of E^0 , as has been done here.

⁽⁹⁾ In particular, the minimum surface would of course not be a simple sphere.

⁽¹⁰⁾ The minimum condition for E^0 should supplement in the anisotropic case the Debye condition giving the volume occupied by the representative points.

⁽¹¹⁾ S. FRANCHETTI: *Nuovo Cimento*, **12**, 743 (1954); **2**, 1127 (1955).

First of all, we note that the dependence of E_0 on the *size* of the sample, apart from any density change, suggests that the potential energy is not concerned and we have to do with a typical quantum effect on the kinetic energy of the atoms.

In the Author's model the eigenfunction for the fundamental state of an atom in a sample of liquid ^4He containing N atoms is taken to be (12)

$$(11) \quad \psi(\mathbf{r}) = A \sum_{i=1}^N \varphi(\mathbf{r} - \mathbf{r}_i),$$

where the vectors \mathbf{r}_i define a lattice in the space occupied by the liquid. A is a normalization factor and φ is a « local » eigenfunction (Fig. 5) describing the motion of the atom in its own « cell », that is in the field of its neighbours, *corrected for the effect of correlations*. Of course, the zero point energy in such a model is essentially that associated with the « local » motion, that is with the eigenfunction φ .

A numerical evaluation has given for the kinetic energy per atom associated with the local motion the value $\mathcal{E}_c \approx 17 \cdot 10^{-6}$ erg (ref. (11), 1-st, eq. (3')). The eigenfunction (11) however corresponds to a somewhat lower kinetic energy which turns out to be $\mathcal{E}_0 \approx 14 \cdot 10^{-6}$ erg in the case of an *unlimited* sample (ref. as above, eq. (12)).

There is a simple though not rigorous way to see how the kinetic energy can vary in such a manner that (in the fundamental state) it has the value \mathcal{E}_c when the atom is confined to a single cell, while it tends to \mathcal{E}_0 when the size of the sample is made to tend to ∞ . This is to approximate the eigenfunction (11) by a linear combination $\psi = \alpha\varphi + \beta\psi_f$ of anyone of the « local » eigenfunctions $\varphi(\mathbf{r} - \mathbf{r}_i)$ and the fundamental eigenfunction ψ_f for a particle free to move in the interior of the sample (the sheet, fig. 1). For simplicity's sake we may assume all the functions and constants to be real. The kinetic

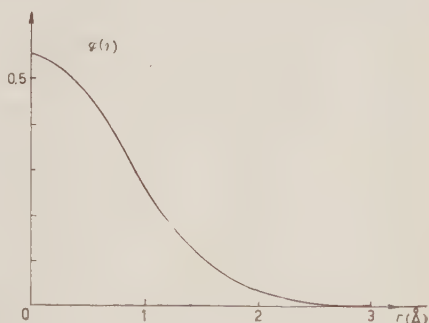


Fig. 5.

(12) It would obviously be impossible to assume the *same* eigenfunction for any atom if these were to obey Fermi-Dirac statistics. The considerations that follow, valid for ^4He , would therefore not apply to ^3He .

energy will then be given by

$$\mathcal{E} = \alpha^2 \mathcal{E}_c + \beta^2 \frac{\hbar^2}{8\mu} \left(\frac{1}{t^2} + \frac{2}{L^2} \right) + 2\alpha\beta \int \varphi \langle \mathcal{E} \rangle_{0z} \psi_f d^3\mathbf{r},$$

where μ is an effective mass.

In our condition $2/L^2$ will be negligible with respect to $1/t^2$ and so we get

$$\mathcal{E} = \alpha^2 \mathcal{E}_c + \beta^2 \frac{\hbar^2}{8\mu} \frac{1}{t^2} + 2\alpha\beta \frac{\hbar^2}{8\mu t^2} \int \varphi \psi_f d^3\mathbf{r}.$$

The ratio of the 3-rd term to the 2-nd is of the order

$$\frac{2\alpha}{\beta} \int \varphi \psi_f d^3\mathbf{r} \approx \frac{2\alpha}{\beta} \sqrt{\frac{V_c}{V}},$$

where V_c is the volume of a cell and V that of the sample. Unless β is vanishingly small, which is not the case—as we shall presently see—the 3-rd term can therefore be neglected, and we are left with

$$(12) \quad \mathcal{E} = \alpha^2 \mathcal{E}_c + \beta^2 \frac{\hbar^2}{8\mu t^2}.$$

Assuming α^2 to be practically independent of t , we can determine its value from the limiting condition $\mathcal{E} = \mathcal{E}_0 = 14 \cdot 10^{-16}$ erg for $t \rightarrow \infty$. This gives

$$\alpha^2 = \frac{\mathcal{E}_0}{\mathcal{E}_c} \approx \frac{14}{17} = 0.82.$$

We thus have $\beta^2 = 0.18$ and finally

$$(12') \quad \delta\mathcal{E} = 0.18 \frac{\hbar^2}{8\mu} t^{-2}.$$

Numerical computation has given

$$(12'') \quad \mu = 12.5 \cdot 10^{-24} \text{ g}, \quad (13)$$

so that

$$(12''') \quad \delta\mathcal{E} = 0.79 \cdot 10^{-31} t^{-2} \text{ erg}$$

(13) In ref. (11 1-st), the value of μ is given as $14 \cdot 10^{-24}$ through a numerical slip in the computation.

in fair agreement with (10'') as anticipated, the difference in the numerical coefficient being hardly surprising, in view of the many uncertainties affecting the two calculations.

It may be noted that the agreement between (10'') and (12'') seems to point out that the *mutual* displacements of the atoms are indeed small even at high frequencies. This means strong correlations between the movements of next neighbours. The assumption of strong correlations is actually at the basis of the determination of $\varphi(r)$. (Ref. (11 1-st)).

3. The Free Energy of a Bose-Einstein Gas (Partially Condensed) Confined to a Very Flat Space.

3'1. « Quadratic » Case. — In this section we consider an ideal Bose-Einstein gas enclosed in a space as in Fig. 1 and we shall investigate the internal and free energy changes taking place when t is made sufficiently small, the volume L^2t being however held *constant*.

It will be assumed that the energy of the molecules depends *quadratically* on momentum. Explicitly

$$(13) \quad \epsilon_{n_x n_y n_z} = A^2 kT \left(\frac{n_x^2}{t^2} + \frac{n_y^2 + n_z^2}{L^2} \right),$$

with

$$(13') \quad A^2 = \frac{h^2}{8\mu} \frac{1}{kT},$$

where μ is the mass of a molecule and n_x, n_y, n_z are integers (14).

There seem to be no reasons, in the conditions under consideration, which would invalidate the ordinary law for occupation numbers

$$n_s = \frac{1}{A \exp[\epsilon_s / kT] - 1}.$$

It will therefore be used throughout this and the following section, with $A = 1$, according to the assumption of partial condensation, or indeterminate number of particles.

The internal energy will therefore be given by (*)

$$(14) \quad U = \sum_{n_x=1}^{\infty} \sum_{n_y=1}^{\infty} \sum_{n_z=1}^{\infty} \frac{A^2 kT \left(\frac{n_x^2}{t^2} + \frac{n_y^2 + n_z^2}{L^2} \right)}{\exp \left[A^2 \left(\frac{n_x^2}{t^2} + \frac{n_y^2 + n_z^2}{L^2} \right) \right] - 1}.$$

(14) The order of magnitude for A is $5.6 \cdot 10^{-8} T^{-\frac{1}{2}} \text{ cm}$, with μ as in the foregoing Section (eq. (12'')).

(*) Let it be noted that the state $n_x = n_y = n_z = 1$ is not considered as the fundamental one. The fundamental state (whose energy is taken as zero) is one in which

Strictly speaking, since we have in view to apply these considerations to liquid helium where the moving elements are supposed to possess the character of Bloch waves, the upper limits in the sum should not be ∞ , but t/l_0 and L/l_0 respectively, where l_0 is a parameter of the order of the atomic interdistance. The correction arising from this fact has been worked out in detail. Since however it turns out to be of very limited importance, we shall disregard it, omitting the lengthy calculations it involves ⁽¹⁵⁾. The final correction itself is, however, given in eqs. (22') and (22'').

For t sufficiently small, the first sum in (14) cannot be replaced by an integral as usual. We shall assume however that this is possible for the two other summations. (Going to polar co-ordinates in the $n_x/L, n_z/L$ plane, eq. (14) yields

$$U = \frac{\pi}{4} L^2 k T \sum_{n_x=1}^{\infty} \int_0^{\infty} \frac{A^2(n_x^2/t^2) + A^2 q^2}{\exp[A^2(n_x^2/t^2) + A^2 q^2] - 1} 2q \, dq.$$

By putting

$$(15) \quad q = A^2 q^2$$

the above expression can be transformed in

$$(16) \quad U = \frac{\pi}{4} L^2 k T \left\{ \frac{1}{t^2} \sum_{n=1}^{\infty} n^2 \int_0^{\infty} \frac{dq}{\exp[A^2(n^2/t^2) + q] - 1} + A^{-2} \sum_{n=1}^{\infty} \int_0^{\infty} \frac{q \, dq}{\exp[A^2(n^2/t^2) + q] - 1} \right\}.$$

We have therefore to evaluate

$$(17) \quad \left\{ \begin{aligned} \Sigma_1 &= \sum_{n=1}^{\infty} n^2 \int_0^{\infty} \frac{dq}{\exp[bn^2 + q] - 1} = - \sum_{n=1}^{\infty} n^2 \ln(1 - \exp[-bn^2]) \\ \Sigma_2 &= \sum_{n=1}^{\infty} \int_0^{\infty} \frac{q \, dq}{\exp[bn^2 + q] - 1}, \end{aligned} \right.$$

with

$$b = \frac{A^2}{t^2}.$$

$p=0$ (at least for macroscopic samples. And the film is to be considered as such, under this respect, apart from the small correction dealt with in Sect. 2.2). For the justification of this assumption see ref. ⁽¹¹⁾.

⁽¹⁵⁾ These amount to the evaluation of a number of sums and have been performed partly by the method described below and partly by use of the Euler-MacLaurin summation formula.

The method employed in evaluating these sums is the very elegant one described by MACFARLANE ⁽¹⁶⁾. Although it does often lead only to « asymptotic » expressions, the accuracy is more than sufficient in the cases treated below. In particular we shall make use of the formula

$$(18) \quad \sum_{n=0}^{\infty} f(n+1) = \frac{1}{2\pi i} \int_{\gamma-i\infty}^{\gamma+i\infty} F(s) \zeta(s) ds,$$

where the right hand side is a Mellin inversion integral, $F(s)$ is the Mellin transform of $f(x)$ and $\zeta(s)$ the Riemann ζ -function.

The Mellin transform for the first sum is

$$F_1(s) = - \int_0^{\infty} x^{s+1} \ln(1 - \exp[-bx^2]) dx = \frac{b^{-(s/2)-1}}{s+2} \int_0^{\infty} \frac{y^{(s/2)+1}}{e^y - 1} dy.$$

That for the second sum is

$$F_2(s) = \int_0^{\infty} x^{s-1} dx \int_0^{\infty} \frac{q dq}{\exp[bx^2 + q] - 1}.$$

And employing the well known expansion

$$(19) \quad \int_0^{\infty} \frac{q^x dq}{\exp[q] - 1} = \Gamma(x+1) \sum_{n=1}^{\infty} \frac{\exp[-nc]}{n^{x+1}},$$

one gets easily

$$F_1(s) = \frac{b^{-(s/2)-1}}{s+2} \Gamma\left(\frac{s}{2} + 2\right) \zeta\left(\frac{s}{2} + 2\right),$$

$$F_2(s) = \sum_{m=1}^{\infty} \frac{1}{m^2} \int_0^{\infty} \exp[-mbx^2] x^{s-1} dx = \frac{1}{2} b^{-s/2} \Gamma\left(\frac{s}{2}\right) \zeta\left(\frac{s}{2} + 2\right).$$

Taking these expressions into (18), the integrals can be evaluated by summing the residua. (For Σ_1 we have poles at $s = 1$ and $s = 2$, while for Σ_2 the poles are at $s = 1$, $s = 0$ and $s = -2$). The result is

$$\Sigma_1 = \frac{1}{3} b^{-\frac{3}{2}} \Gamma\left(\frac{5}{2}\right) \zeta\left(\frac{5}{2}\right) + 2 \zeta'(-2)$$

$$\Sigma_2 = \frac{1}{2} b^{-\frac{1}{2}} \Gamma\left(\frac{1}{2}\right) \zeta\left(\frac{5}{2}\right) + \zeta(2) \zeta(0) - 2b \zeta'(-2).$$

⁽¹⁶⁾ G. G. MACFARLANE: *Phil. Mag.*, **40**, 188 (1949).

Inserting numerical values ⁽¹⁷⁾ and taking into eq. (16) one gets

$$(20) \quad U = \frac{\pi}{4} V k T A^{-3} [1.782 - 0.822 A t^{-1}],$$

where V replaces $L^3 t$.

To get the free energy $F = U - TS$ the formula

$$(21) \quad F = -T \int_0^t \frac{U}{T^2} dT,$$

may be used, yielding (eq. (20) and (13'))

$$(22) \quad F = F_\infty + \frac{2\pi}{h^2} V \mu (kT)^2 0.822 t^{-1},$$

with

$$(22a) \quad F_\infty = -1.341 \frac{(2\pi\mu)^{\frac{3}{2}}}{h^3} V (kT)^{\frac{3}{2}},$$

or

$$(23) \quad F = F_\infty (1 - 0.692 A t^{-1}).$$

(The subscript ∞ characterizes the limiting case $t \rightarrow \infty$).

The correction for the finiteness of the minimum wavelength would amount to the following substitution of the factor 0.822 in eq. (22)

$$(22') \quad 0.822 \rightarrow 0.822 + \Sigma$$

with

$$(22'') \quad \Sigma = \sum_{m=1}^{\infty} \frac{\exp[-(A/l_0)^2 m]}{m^2} \left(1 - \exp \left[-0.273 \left(\frac{A}{l_0} \right)^2 m \right] \right),$$

l_0 being of the order of 3 Å.

Eqs. (22) and (23) show that there is an increase of the free energy beyond its ordinary value when the «small dimension» t is no longer very large with respect to A , the relative increase being of the order A/t .

In applying this result to the exciton gas in helium films, it will combine

⁽¹⁷⁾ Values for the ζ -function sufficiently accurate for the present purpose can be found in E. JAHNKE and F. EMDE: *Tables of Functions* (New York, 1945), p. 273. Values for the derivative ζ' may be obtained from the Hurwitz formula, which is to be found, for instance, in E. T. WHITTAKER and G. N. WATSON: *Modern Analysis* (Cambridge, 1946), p. 269.

with the density change already studied in the preceding paper (ref. (1)), causing terms of order higher than 1-st in Λ/t to enter the expression of F .

It must however be noted that the foregoing result cannot be employed as it stands for « quadratic » excitons in liquid helium, since it is well known that the simple model considered here does not give results in quantitative agreement with experiment. The way of introducing the necessary corrections will be dealt with in a paper to follow, where the results of this and the preceding paper shall be applied to the theory of helium films.

3.2 « Linear » Case. — We now consider the same problem as in the foregoing section, in the assumption of a linear (instead of quadratic) dependence of the particle energy on momentum (phonon gas).

The boundary being always as in Fig. 1, the energy of a single phonon will be given by

$$(24) \quad E = h\nu = \frac{hC}{2} \left| \frac{n_x^2}{t^2} + \frac{1}{L^2} (n_y^2 + n_z^2) \right|^{\frac{1}{2}},$$

where n_x, n_y, n_z are integers. Putting

$$(25) \quad \frac{hC}{2kT} = \lambda \quad (18)$$

(not to be confused with a wavelength) the internal energy of the gas can be written (19)

$$U = \sum_{n_x=1}^{\infty} \sum_{n_y=1}^{\infty} \sum_{n_z=1}^{\infty} \frac{\lambda kT [(n_x^2/t^2) + (1/L^2)(n_y^2 + n_z^2)]^{\frac{1}{2}}}{\exp [\lambda \{ (n_x^2/t^2) + (1/L^2)(n_y^2 + n_z^2) \}^{\frac{1}{2}}] - 1}.$$

Supposing, as usual, $L \gg \lambda$, we replace the summations, except the first, by integrations, getting

$$U = \frac{\pi}{2} L^2 kT \sum_{n_x=1}^{\infty} \int_0^{\infty} \frac{\lambda [(n_x^2/t^2) + \varrho^2]^{\frac{1}{2}}}{\exp [\lambda \{ (n_x^2/t^2) + \varrho^2 \}^{\frac{1}{2}}] - 1} d\varrho.$$

By putting

$$\lambda \left(\frac{n_x^2}{t^2} + \varrho^2 \right)^{\frac{1}{2}} = q,$$

(18) Numerically, with $C = 2.37 \cdot 10^4$ cm s⁻¹, one has $\lambda = 5.68 \cdot 10^{-7} T^{-1}$ cm.

(19) The effect of the finiteness of the upper limits in the sums (see preceding Section) turns out to be entirely negligible in the conditions of interest, that is for application to phonons in liquid ⁴He below, say, 3 °K. This of course is due to the fact that the Debye temperature is much higher (about 27.5 °K).

the above expression transforms into

$$(26) \quad U = \frac{\pi}{2} L^2 k T \lambda^{-2} \sum_{n=1}^{\infty} \int_{\lambda n/t}^{\infty} \frac{q^2}{e^q - 1} dq.$$

The sum can be handled by the method of Mellin transforms. With

$$f(x) = \int_{\lambda x/t}^{\infty} \frac{q^2}{e^q - 1} dq,$$

we get for the Mellin transform

$$F(s) = \int_0^{\infty} x^{s-1} dx \int_{\lambda x/t}^{\infty} \frac{q^2}{e^q - 1} dq.$$

Integrating by parts with respect to x one finds without difficulty

$$F(s) = \left(\frac{\lambda}{t}\right)^3 s^{-1} \int_0^{\infty} \frac{x^{s+2} dx}{\exp[\lambda x/t] - 1}$$

and utilizing eq. (19)

$$F(s) = \left(\frac{t}{\lambda}\right)^3 s^{-1} \Gamma(s+3) \zeta(s+3),$$

with ζ the Riemann zeta-function.

Making use of this result and of eq. (18) one gets for the sum in eq. (26)

$$\sum_{n=1}^{\infty} \int_{\lambda n/t}^{\infty} \frac{q^2}{e^q - 1} dq = \sum \text{Res} \left\{ \left(\frac{t}{\lambda}\right)^3 s^{-1} \Gamma(s+3) \zeta(s+3) \right\},$$

which yields without difficulty (poles at $s=1$, $s=0$, $s=-3$)

$$\sum_{n=1}^{\infty} \int_{\lambda n/t}^{\infty} \frac{q^2}{e^q - 1} dq = 6.494 \frac{t}{\lambda} - 1.202 + 0.00139 \left(\frac{t}{\lambda}\right)^{-3}.$$

⁽²⁰⁾ Both U and S decrease by decreasing t and this is easily comprehensible, since the energy levels get more separated (formulae (13) and (24)) and thus the particles tend to crowd in the lower (less displaced) levels, thus giving a smaller average energy and a smaller spread in the μ -Raum.

From this and (26), noting that $L^2 t = V$ and dropping the 3-rd order term (which would at most be significant only below 0.1 °K) we have

$$(27) \quad U = 3.247 \pi V k T \lambda^{-3} \left(1 - 0.185 \frac{\lambda}{t} \right)$$

and by use of (21), remembering (25)

$$(28) \quad F = F_{\infty} + \frac{3.774}{h^3 C^2} V (kT)^{3/2} t^{-1},$$

with

$$(28a) \quad F_{\infty} = - \frac{27.20}{h^3 C^3} V (kT)^4.$$

Or else

$$(29) \quad F = F_{\infty} (1 - 0.277 \lambda t^{-1}).$$

In this, as in the case treated in the preceding section, there is a *decrease* in the internal energy (with respect to the normal case $t \rightarrow \infty$) and an *increase* of the free energy, showing the prevailing effect of the entropy term ⁽²⁰⁾.

* * *

The Author wishes to express his gratitude to Prof. G. SANSONE for having kindly clarified some mathematical points in connection with the present work.

APPENDIX A

On a Semiclassical Formula.

, In a preliminary survey (ref. ⁽¹¹⁾, 2-nd) the problem dealt with in Sect. 3.1 was treated in a semiclassical way by use of the partition function in the μ -Raum, that is on the basis of the formula

$$\mathcal{F} = -kT \ln \frac{e}{N} \sum_{n_x=1}^{\infty} \sum_{n_y=1}^{\infty} \sum_{n_z=1}^{\infty} \exp \left[-A^2 \left(\frac{n_x^2}{t^2} + \frac{n_y^2}{L^2} + \frac{n_z^2}{L^2} \right) \right],$$

for the free energy per atom. (Same notation as in Sect. 3.1). This formula can be treated like that in eq. (14) (the only «true» sum being that in n_x)

with the result

$$\mathcal{F} = -kT \ln \frac{e}{N} \frac{\pi}{4} A^{-2} L^2 \sum_{n=1}^{\infty} \exp \left[-\frac{A^2}{t^2} n^2 \right].$$

The sum can be handled by the method of Mellin transforms yielding

$$\sum_{n=1}^{\infty} \exp \left[-\frac{A^2}{t^2} n^2 \right] = \frac{1}{2} \left(\sqrt{\pi} \frac{t}{A} - 1 \right) \quad (21).$$

Hence

$$L^2 \Sigma = L^2 t \frac{1}{2} \left(\frac{\sqrt{\pi}}{A} - t^{-1} \right) = V \frac{\sqrt{\pi}}{2A} \left(1 - \frac{A}{\sqrt{\pi}} t^{-1} \right).$$

We have therefore

$$\mathcal{F} = -kT \ln \frac{e}{N} \frac{\pi^{\frac{3}{2}}}{8} V A^{-3} \left(1 - \frac{A}{\sqrt{\pi}} t^{-1} \right),$$

from which, characterizing by the subscript ∞ the limiting case $t \rightarrow \infty$:

$$\mathcal{F} - \mathcal{F}_{\infty} = -kT \ln \left(1 - \frac{A}{\sqrt{\pi}} t^{-1} \right),$$

which is just eq. (7) of the above reference, and gives

$$\mathcal{F} - \mathcal{F}_{\infty} = kT \frac{A}{2\pi} t^{-1} + \text{terms of higher order}.$$

From eq. (22) of the present paper, dividing by the number of particles belonging to excited states, that is

$$N_n = \frac{2.612}{h^2} V (2\pi\mu kT)^{\frac{3}{2}},$$

one gets for $\mathcal{F} - \mathcal{F}_{\infty}$ the corresponding (under the assumptions, rigorous) expression

$$0.629 kT \frac{A}{\sqrt{\pi}} t^{-1},$$

somewhat smaller than the above one. This is hardly surprising in view of the strong degeneration preventing to attain rigorous results by a semiclassical method.

⁽²¹⁾ The asymptotic character of this result is evident. However, a check by the more tedious method of the Euler-MacLaurin summation formula shows that the approximation is quite good in the conditions of interest (that is $t/A \approx 10^2$).

APPENDIX B

On the Calculation of the Effective Mass.

The value for the effective mass μ ($12.5 \cdot 10^{-24}$ g) employed in Sect. 2.2 has been computed by the formula

$$\mu = \frac{\hbar^2}{4\pi^2 a^2 (I - \sigma \mathcal{C}_c)}$$

established in previous work (ref. (11), 1-st). Here we wish only to give some details about the calculation of the quantities σ and I , which, together with next-neighbour number and distance (a) determine μ . These quantities are defined as

$$(B.1) \quad \left\{ \begin{array}{l} \sigma = 2\pi \int_0^\infty \int_0^\pi \varphi(\varrho) \varphi(\varrho') \varrho^2 \sin \theta \, d\varrho \, d\theta, \\ I = 2\pi \int_0^\infty \int_0^\pi [E - V(\varrho)] \varphi(\varrho) \varphi(\varrho') \varrho^2 \sin \theta \, d\varrho \, d\theta. \end{array} \right.$$

Here: $\varphi(\varrho)$ is the «local» eigenfunction studied in the above mentioned paper and recalled in Sect. 2.2 (Fig. 5); ϱ , ϱ' , θ are defined in Fig. 6, where O and A are neighbouring nodes of an appropriate lattice (22); $V(\varrho)$ is the *effective potential*, that is the average increase of potential energy when an atom is at a distance x from its «equilibrium position», proper account being taken of the *correlations* between the displacements of neighbouring atoms; E is the lowest eigenvalue in the spherical potential well $V(\varrho)$. (No attempt was made to determine $V(\varrho)$ theoretically. Instead a simple trapezoidal well was chosen so as to give the appropriate value for the zero point energy and a reasonable one for μ . This potential well is the only «adjusted» element introduced so far into the theory).

Since the main contribution to the integrals (B.1) comes from the region midway between O and A , the approximation

$$\varrho' \approx \varrho + \frac{a^2}{2\varrho} - a \cos \theta$$

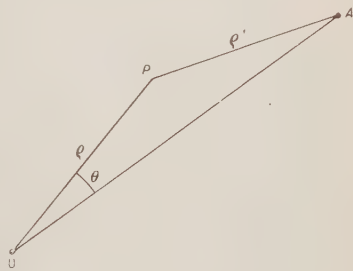


Fig. 6.

(22) The nodes of the lattice are thought to be «equilibrium positions» for the atoms, but the distribution $\varphi^2(\varrho)$ around the node is rather widely spread. (Compare OA , which is about 3 Å, with the abscissa scale in Fig. 5).

(amounting to neglect $|q' - q|$ against $2q$) may be used to transform σ in

$$\sigma = \frac{2\pi}{a} \int_0^{\infty} \varphi(q) q^2 dq \int_{q+a^2/2q-a}^{q+a^2/2q+a} \varphi\left(q + \frac{a^2}{2q} - a \cos \theta\right) d\left(q + \frac{a^2}{2q} - a \cos \theta\right).$$

By putting

$$\Phi(x) = \int_0^x \varphi(q) dq,$$

since the upper limit in the 2-nd integral can be replaced by ∞ , one gets

$$(B.2) \quad \sigma = \frac{2\pi}{a} \int_0^{\infty} \left[\Phi(\infty) - \Phi\left(q + \frac{a^2}{2q} - a\right) \right] \varphi(q) q^2 dq.$$

Integral I requires only to introduce a further factor $E - V(q)$ in the integrand of (B.2). In both cases the remaining integrations can easily be performed numerically.

There is of course some incertitude due to the imperfect knowledge of liquid helium structure. In ref. (11, 1-st) the data of REECKIE and HUTCHINSON (23) for next neighbour number and distance were used. Recent data (24) are somewhat different. One may however hope in some compensation because of the introduction of the «adjusted» potential well mentioned above (25).

Another source of incertitude regarding μ is due to exchange effects (ref. (11) Sec. 6). They were neglected in the calculation leading to the value (12''). This value might therefore be good enough for use in connection with the *fundamental* state (as in Sec. 2'2), exchange being absent in that case, while being somewhat in error for *excited* states.

(23) J. REECKIE and T. S. HUTCHINSON: *Phys. Rev.*, **92**, 827 (1953).

(24) D. G. HURST and D. G. HENSHAW: *Phys. Rev.*, **100**, 994 (1955).

(25) No attempt was made to perform again the lengthy calculations leading to φ and μ on the basis of the new values.

RIASSUNTO

Vengono studiati certi aspetti del comportamento termodinamico di alcuni fluidi quando siano costretti in spazi laminari sufficientemente piatti. In particolare vengono prese in considerazione: a) la variazione dell'energia di zero dell' ^4He (problema considerato per la prima volta da K. R. ATKINS); b) le variazioni di energia interna e di energia libera di due tipi di gas ideali di Bose-Einstein (differenti per lo spettro energetico) in stato di parziale condensazione.

On the Physical Significance of the Redundant Solutions of the Low Equation.

R. HAAG (*)

Max-Planck-Institut für Physik - Göttingen

(ricevuto il 5 Novembre 1956)

Summary. — Some arguments are given which indicate that only one solution of the Low equation is acceptable from the physical point of view. The arguments stem from a comparison with the general scattering theory of non-relativistic quantum mechanics. A short study of the situation in a relativistic field theory is attached.

1. — Introduction.

In recent years the idea of formulating Quantum Field Theory directly in terms of renormalized quantities has met with a certain amount of success. Thus the work of LEHMANN, SYMANZIK and ZIMMERMANN ⁽¹⁾ showed—among other things—how to obtain the usual renormalized power series expansions from basic equations which do not contain any infinite constants. LOW ⁽²⁾, starting from similar equations, but using a different procedure of approximation, obtained some interesting results in meson physics ⁽³⁾. The characteristic feature of these schemes is that they do not work with a specific form of the Hamiltonian given explicitly in terms of canonical variables, but instead use a system of integral equations for quantities closely connected with the *S*-matrix elements. This departure from the straightforward canonical scheme seems

(*) On leave of absence from the Institut für Theoretische Physik der Universität München.

⁽¹⁾ H. LEHMANN, K. SYMANZIK and W. ZIMMERMANN: *Nuovo Cimento* **1**, 205 (1955), in the following quoted as LSZ.

⁽²⁾ F. E. LOW: *Phys. Rev.*, **97**, 1392 (1955).

⁽³⁾ G. F. CHEW and F. E. LOW: *Phys. Rev.*, **101**, 1570 (1956).

to be inevitable if infinite quantities are to be avoided ⁽⁴⁾. The weakness of the LSZ scheme on the other hand is that the integral equations do not contain all the information corresponding to a specific model. This may be different for a complete system of equations of the type considered by Low, but still nothing is known about the manifold of solutions of such a system. In this connection it is of interest that CASTILLEJO, DALITZ and DYSON ⁽⁵⁾ were able to carry through a complete mathematical analysis of the approximate Low scattering equation in some simple cases. They found infinitely many solutions which differ in the number and location of zeros of the Low function $h(\omega)$ (see below) on the energy axis. The particular solution taken by CHEW and Low in their discussion of π -N-scattering is the one in which h has no zeros. It was not clear whether the multitude of solutions found by CDD reflects a corresponding multitude of different models, all leading to the same Low equation, or whether the redundant CDD solutions have no physical significance.

In the present analysis we shall give some arguments which indicate that the latter alternative is the correct one, i.e. that only the Chew-Low-solution is acceptable. The arguments mentioned stem from a comparison between the Low equation and general scattering theory in non-relativistic quantum mechanics. Thus, as a first indication, one may note that the number of zeros of h determines the difference $\delta(0) - \delta(\infty)$ between the scattering phase shift for zero energy and that for infinite energy. It is, however, a rather general result of quantum mechanics that $\delta(0) - \delta(\infty) = m\pi$ (m being the number of bound states). This will be discussed in Sect. 2. A more detailed analysis of the non-relativistic Low equation is given in Sect. 3. Of course by the non-relativistic approximation one important feature of the Low equation is lost (the crossing theorem) and this affords a serious objection against our arguments. What will be shown, however, is the following: Starting from a frame in which we have a unique correspondence between Low function and Hamiltonian the CDD solutions still all formally exist but only one solution is acceptable, the others leading to a system of energy eigenfunctions which is not linearly independent.

Sect. 4 contains a few remarks about the field theoretical case. This is attached for two reasons: to bring out the points of analogy with the discussion in Sect. 3 and to dispel a misunderstanding which appears to be rather widespread, namely that for the establishment of the Low equations no knowledge

⁽⁴⁾ R. HAAG: *Dan. Mat. Fys. Medd.*, **29**, Nr. 12 (1955); A. S. WIGHTMAN: *Quantum Field Theory in Terms of Vacuum Expectation values II*, *Phys. Rev.*, to be published.

⁽⁵⁾ L. CASTILLEJO, R. H. DALITZ and F. Y. DYSON: *Phys. Rev.*, **101**, 453 (1956). To be quoted as CDD.

of the model is necessary except that the field operators satisfy the casual commutation relations. In order to escape all complications which are not essential to the main points under discussion we shall consider in Sects. 2 and 3 only the scattering of a scalar, neutral particle of zero angular momentum by a fixed center of force according to the 1-meson approximation. Then the Low equation reads (⁵)

$$(1) \quad h^+(\omega) = \sum A_i \left(\frac{1}{\omega_i - \omega} + \frac{1}{\omega_i + \omega} \right) + \\ + \frac{1}{\pi} \int_{\mu}^{\infty} v(k') k' |h^+(\omega')|^2 \left[\frac{1}{\omega' - \omega - i\gamma} + \frac{1}{\omega' + \omega} \right] d\omega'.$$

Here $v(k)$ is the cut-off function of the theory; $v(0)=1$, $v(\infty)=0$. $k=\sqrt{\omega^2-\mu^2}$ is the momentum, ω the energy, μ the rest mass of the particle. The ω_i are the bound state energies, A_i positive constants. The limit $\gamma \rightarrow 0$ is to be understood in the first integral on the right hand side. The physical significance of the Low-function $h^+(\omega)$ is

$$(2) \quad h^+(\omega) = \frac{e^{i\delta} \sin \delta}{k v(k)},$$

δ being the scattering phase shift. In the non-relativistic approximation we put

$$(3) \quad \omega = E + \mu; \quad E = k^2$$

and replace the terms with the large energy denominators by a (positive) constant c . Thus

$$(4) \quad h^+(E) = \sum \frac{A_i}{E_i - E} + \frac{1}{\pi} \int_0^{\gamma} v(k') k' |h^+(E')|^2 \frac{dE'}{E' - E - i\gamma} + c.$$

2. - The Difference $\delta(0) - \delta(\infty)$.

If we define the function of the complex variable z

$$(5) \quad h(z) = \sum \frac{A_i}{E_i - z} + \frac{1}{\pi} \int_0^{\gamma} v(k') k' |h^+(E')|^2 \frac{dE'}{E' - z} + c,$$

then $h^+(E)$ is the limit of $h(z)$ as z tends towards E from the upper half plane.

The integral equation (4) may be replaced by stating a few properties of the function $h(z)$ ^(3,5):

1) $h(z)$ is an analytic function in the z -plane cut along the real axis from 0 to ∞ . It is regular everywhere in the cut plane save for the simple poles on the negative real axis corresponding to the bound states. $h(\infty) = c$.

2) $h(z^*) = h^*(z)$.

3) On the upper lip of the cut real axis

$$\text{Im } h(E) = k \cdot v(k) |h(E)|^2.$$

Further important properties which may be directly read off from equation (5) are

4) $\text{Im } h(z) \geq 0$ for $\text{Im } z \geq 0$.

5) $dh(z)/dz > 0$ for real $z < 0$.

Thus, zeros of h , if they exist, must all lie on the real axis and in the neighbourhood of such a zero the function h has the form $a(z - \tau)$ with positive a .

The general solution of (4) is readily obtained by considering the function $H(z) = 1/h(z)$. This function has analytic properties similar to h but instead of 3) we now have

6) $\text{Im } H^+(E) = -kr(k)$.

Therefore by Cauchy's theorem

$$(7) \quad H(z) = \frac{1}{c} + \sum_k \frac{a_k}{z - \tau_k} - \frac{1}{\pi} \int_{E'} \frac{k' r(k')}{z} dE'.$$

The a_k must be positive, the τ_k real and furthermore these constants must be chosen so that the zeros of H are just the bound state energy levels E_i .

Since the expression (7) has properties analogous to 4) and 5) the zeros of H may be put in the right position without seriously restricting the arbitrariness of the constants a_k, τ_k .

Now consider the integral

$$\int \frac{H'(z)}{H(z)} dz,$$

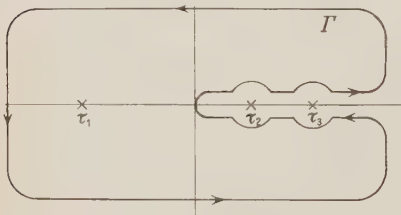


Fig. 1.

around the closed contour Γ . The contribution of the infinite circle vanishes if $H(z) \rightarrow (1/c) + (b/z)$ for $z \rightarrow \infty$, that is if the cut-off function decreases more strongly than k^{-3} at infinity. Remembering that $\text{Im } \ln H^+ = -\delta$ we get

$$(8) \quad \delta(0) - \delta(\infty) = \pi(m - N).$$

Here m is the number of bound states (zeros of H), N the number of zeros of h . In quantum mechanics on the other hand one has in general

$$(8a) \quad \delta(0) - \delta(\infty) = m\pi.$$

The reason for the relation (8a) may be seen by a simple qualitative argument. The phase shift may be defined by

$$\delta(k) = \lim_{n \rightarrow \infty} (n\pi - kr_n),$$

where r_n is the n -th node of the radial wave function. Then, for interactions which are not too singular, one may expect $\delta(\infty) = 0$ because for infinite kinetic energy the effect of the interaction upon the wave function is negligible. To discuss the behaviour of δ for very small energy let us suppose that a range R of the interaction may be defined. Then, if the wave length is large compared to R we have

$$\delta = Z\pi; \quad Z = \begin{cases} l \\ l+1 \end{cases} \quad \text{if} \quad \begin{cases} \psi'(R) > 0 \\ \psi(R) < 0 \end{cases}.$$

Here l is the number of nodes of the zero energy wave function *within the interaction range*. The connection of Z with the number of bound states is plausible again in consequence of the orthogonality relations. In any case $Z \geq 0$.

A mathematical proof of the relation (8a) has been given for the case of an ordinary potential⁽⁶⁾. Here we have to deal with the Schrödinger equation

$$(9) \quad \psi'' + k^2\psi = V(r)\psi.$$

Let $g(k, r)$ be that solution of (9) which tends asymptotically towards $\exp[ikr]$ and consider the function $g(k) = g(k, 0)$ for complex argument k in the upper half plane. JOST shows that

- a) $g(k)$ is an analytic function, regular in the entire half plane. $g(\infty) = 1$.
- b) The zeros of g in the half plane correspond uniquely to the bound states.
- c) $g^*(k) = g(-k^*)$.
- d) On the positive real axis g determines the scattering phase shift by

$$\frac{g(k)}{|g(k)|} = \exp[-i\delta(k)].$$

⁽⁶⁾ N. LEVINSON: *Dan. Mat. Fys. Medd.*, **25**, No. 9 (1949). See also R. JOST: *Helv. Phys. Acta*, **2**, 256 (1947). The potential is required to vanish more strongly than $1/r^3$ for $r \rightarrow \infty$ and to have no stronger singularity than $1/r$ at the origin. The function $g(k)$ used below equals $f(-k)$ in the paper of Jost.

From these properties (8a) follows immediately. One could carry the comparison of (4) with potential scattering still a step further. Remembering that the upper half plane of k corresponds to the whole cut E -plane one can deduce from the listed properties of the functions H and g that

$$(10) \quad H(k) = (1/c) \cdot g(\bar{k}),$$

which implies that H should have no poles. However, the result (10) cannot be regarded as more than an analogy because a velocity independent potential is not the type of interaction with which (4) should be compared.

To close this section we shall write down the relation which replaces (8) in the case of the «relativistic» equation (1). For a cut-off vanishing rapidly enough at infinity we get

$$(8b) \quad \delta(0) - \delta(\infty) = (m - (N/2) - 1).$$

The factor 1/2 appears because the zeros of h now lie symmetrically with respect to the origin.

3. - The Low Equation in a Non-relativistic Scattering Problem.

In this section we consider the S -wave scattering according to non-relativistic quantum mechanics for an arbitrary interaction V . Following the ideas of WICK⁽⁷⁾ we establish the analogue to the Low equation. In the special case of an interaction which is factorized in the momentum representation this equation reduces to the form (4) previously considered. We shall then discuss the uniqueness of the scheme. For the sake of simplicity we assume that there are no bound states.

Let H_0 be the kinetic energy, $H = H_0 + V$ the total Hamiltonian, $|k\rangle$ the eigenstate of H_0 to the energy $E = k^2$ and $|\bar{k}\rangle$ the eigenstate of H to the same energy, normalized so as to satisfy the asymptotic condition⁽⁸⁾

$$(11) \quad \lim_{t \rightarrow +\infty} \exp[iH_0 t] \exp[-iHt] |\bar{k}\rangle \rightarrow |k\rangle.$$

Then we define the vectors T_k and χ_k^\pm by

$$(12) \quad T_k = V|k\rangle; \quad \chi_k^\pm = |\bar{k}\rangle \mp |k\rangle$$

⁽⁷⁾ G. C. WICK: *Rev. Mod. Phys.*, **27**, 339 (1955).

⁽⁸⁾ The plus and minus signs here have just the opposite meaning to that in ref⁽⁷⁾ and⁽³⁾.

and find (3.7)

$$(13) \quad \chi_k^+ = -\frac{1}{H - k^2 + i\gamma} T_k,$$

$$(14) \quad \langle k^+ | T_k \rangle = \langle k^+ | V | k \rangle = -\frac{k}{2i} (S(k) - 1) = -\frac{2k}{\pi} \exp[i\delta] \sin \delta.$$

Now

$$\langle k^+ | T_k \rangle = \langle \chi_{k'}^+ | T_k \rangle + \langle k' | V | k \rangle$$

Or, by (13), using the completeness of the $|k^+ \rangle$:

$$(15) \quad \langle k^+ | T_k \rangle = - \int \frac{\langle k^+ | T_{k'} \rangle^* \langle k^+ | T_k \rangle}{E' - E - i\gamma} dk' + \langle k' | V | k \rangle.$$

This is as near to the Low equation as we can get without knowing any specific properties of the interaction V . The special feature of equation (4) is that it gives a relation for S -matrix elements alone, i.e. only the elements of T on the energy shell appear. This simplification results—as in the field theoretical case—if and only if T factorizes so that it may be written ⁽⁹⁾

$$(16) \quad \langle k^+ | T_k \rangle = t(k') \frac{u(k)}{u(k')}.$$

This implies in turn that the interaction has the special form

$$(17) \quad \langle k' | V | k \rangle = A u^*(k') u(k).$$

Substituting (16) and (17) into (15) and (14) we come indeed back to (4) and (2) if we introduce the definitions

$$(18) \quad h(k) = -\frac{\pi t(k)}{[u(k)]^2}; \quad |u(k)|^2 = 2k^2 v(k).$$

Let us first consider the general case of equation (15). It is clear that, given the function $T(k'; k) = \langle k' | T_k \rangle$ we can reconstruct the complete model.

⁽⁹⁾ This factorization of T is a common feature of those semi-relativistic models which try to approximate a local field theory by suppressing virtual pair creation effects and use a cut-off function instead (Chew-model, Lee-model with cut-off). In the completely non-relativistic limit this is equivalent to an interaction of the type (17), i.e. V is then a projection operator onto a single state u . One should not believe, of course, that the special form (17) has any physical significance beyond the statement that the interaction is confined to a small region in space corresponding to the extension of the state u in the position representation. In the present paper we are, however, not concerned with the physical basis of the Chew-Low scattering equation itself but only with the discussion of the manifold of its solutions.

Equation (15) itself may be regarded as the definition of the interaction energy in terms of the function T . From (13) we obtain

$$\vec{k}' \chi_{k'} - \delta(k - k') - \vec{k} \cdot k' = - \frac{1}{E - E' + i\gamma} \langle \vec{k} | T_{k'} \rangle.$$

Thus the energy eigenfunctions are given by ⁽¹⁰⁾

$$(19) \quad \langle \vec{k}' | \vec{k} \rangle = \delta(k - k') + \frac{1}{E - E' - i\gamma} \langle \vec{k} | T_{k'} \rangle^*.$$

Alternatively, if V is given, then (15) may have many solutions T . This has been demonstrated in the case of the special interaction (17). But only one of these solutions can be acceptable. The failure of the others must show up if one looks at the eigenfunctions (19). Let us check the completeness and orthogonality relations of these functions. The former reduce to

$$A(k'; k) = A(k; k')^* \\ A(k'; k) = \langle \vec{k}' | T_k \rangle + \int \frac{\langle \vec{k}'' | T_{k'} \rangle^* \langle \vec{k}'' | T_k \rangle}{E'' - E' - i\gamma} dk''.$$

The orthogonality relations may be written

$$B(k'; k) = B(k; k')^* \\ B(k'; k) = \langle \vec{k} | T_{k'} \rangle^* + \int \frac{\langle \vec{k}' | T_{k''} \rangle \langle \vec{k} | T_{k''} \rangle^*}{E' - E'' + i\gamma} dk''.$$

Since T shall be a solution of (15) the completeness relations are satisfied due to the fact that V is hermitian. One may therefore expect that for the redundant solutions the orthogonality relations will fail, or, in other words, that the eigenfunctions (19) will not be linearly independent. This guess is easily verified in the special case (16), (17) which has been the subject of our previous discussion. Here

$$B(k'; k) = - \frac{u(k)u^*(k')}{\pi} \left[h^*(k) - \frac{1}{\pi} h(k') h^*(k) \int \frac{k'' v(k'') dk''}{E' - E'' + i\gamma} \right].$$

⁽¹⁰⁾ If we forget the original definition (12) of the T -function, keeping in mind only the integral equation (15) and the interpretation (14), then the rest of the scheme (including (19)) follows. The proof is omitted since this question does not seem to be of particular interest in our context.

Recalling the general solution (7) the bracket on the right hand side equals

$$h^*(k) - h(k')h^*(k) \left(H(k') - \frac{1}{e} - \sum_{E'} \frac{a_i}{E' - \tau_i} \right) = h(k')h^*(k) \left(\frac{1}{e} + \sum_{E'} \frac{a_i}{E' - \tau_i} \right).$$

This is hermitian only if all the a_i vanish. A more direct way to see the significance of the condition that h should have no zeros is the following. By (19) we have

$$\begin{aligned} \bar{k}'; k \rangle &= \delta(k - k') + \psi(k'; k) \\ \psi(k'; k) &= - \frac{1}{\pi(E - E' - i\gamma)} u(k) u^*(k') h^*(k). \end{aligned}$$

Using the Low equation (4) we find

$$\int \psi^*(k''; k) \langle k'; \bar{k} \rangle^+ dk = - \psi(k'; k'').$$

If $h(k)$ has a zero for $k = k_0$, then

$$\int \psi^*(k_0; k) \langle k'; \bar{k} \rangle^+ dk = 0$$

showing that the system $\langle \bar{k} \rangle$ is not linearly independent.

4. - The Field Theoretical Case.

The simplest method of deriving a complete system of Low equations is the LSZ formalism (1). However, in order to illustrate both the parallels and the differences between the scheme discussed in the last section and the case of field theory we shall use a somewhat different nomenclature. To keep the formulas simple we consider the model of references (1) and (4) in which only one type of particle exists and we have to deal with only one scalar field $A(x)$. We shall establish the complete system of Low equations for this case (equation (24)) to see explicitly how the details of the model are accounted for.

The first difference from Sect. 3 is that we cannot make use of the « unperturbed » Hamiltonian H_0 and its system of eigenfunctions (4). We can, however, still introduce a system of states satisfying a condition analogous to (11). For this purpose we first consider the complete orthogonal system n of eigenstates of H . The $+$ sign signifies as before that these states have a simple

physical meaning with respect to observations at $t = +\infty$ ⁽¹¹⁾. Next we define the operators

$$a_q^\dagger = \int \left[E_q A(\mathbf{x}, 0) - i \frac{\partial A}{\partial t}(\mathbf{x}, 0) \right] \exp[i\mathbf{q}\mathbf{x}] d\mathbf{x}, \quad E_q = \sqrt{\mathbf{q}^2 + m^2}$$

and the states

$$|n; q\rangle = a_q^\dagger |\vec{n}\rangle.$$

Without interaction a_q^\dagger would be the creation operator of a particle with momentum q . Then, if we accept the asymptotic condition in the form given by LSZ we have

$$\lim_{t \rightarrow +\infty} \exp[i(H - E_n - E_q)t] |n; q\rangle = |n; q\rangle, \quad |n; q\rangle = a_q^{\dagger \text{out}} |\vec{n}\rangle.$$

Obviously the states $|n; q\rangle$ do not form an orthogonal system, but apart from this fact we can proceed as in the last section. Thus we define

$$(20) \quad \chi_{n,q}^\dagger = |n; q\rangle - |n; q\rangle; \quad T_{n,q} = (H - E_n - E_q) |n; q\rangle$$

and obtain

$$(21) \quad \chi_{n,q}^\dagger = - \frac{1}{H - E_n - E_q + i\gamma} T_{n,q}.$$

Again $\langle \vec{n}' | T_{n,q} \rangle$ for $E_n + E_q = E_{n'}$ is the S -matrix element for the process $n \rightarrow q = n'$ if n is a single particle state. For processes with more than 2 initial particles the connection between the S -matrix elements and the T -functions is more involved ⁽¹²⁾.

From (20) and (21) we obtain

$$(22) \quad \langle \vec{n}' | p | T_{n,q} \rangle = - \left\langle T_{n',p} \left| \frac{1}{H - E_{n'} - E_p - i\gamma} \right| T_{n,q} \right\rangle + B$$

$$B = \langle \vec{n}' | a_p (H - E_n - E_q) a_q^\dagger | \vec{n} \rangle.$$

⁽¹¹⁾ The states $|\vec{n}\rangle$ are obtained by repeated application on the vacuum of the creation operators derived from A_{out} .

⁽¹²⁾ A complete system of equations supplementing the Low equation and different from ours has been given by N. FUKUDA and J. S. KOVACS: *Phys. Rev.*, to be published. Instead of our states $|n; q\rangle \dots a_q^\dagger |\vec{n}\rangle$ they use the states $a_{q_1}^\dagger a_{q_2}^\dagger \dots |1\rangle$, where $|1\rangle$ is a physical 1-particle state.

In their scheme the S -matrix elements for all processes are given by the T -functions on the energy shell. The disadvantage is, however, that besides the T -functions a second set of functions is required which makes the system of equations more complicated.

In the case of quantum mechanics B was the matrix element of the interaction. The analogue of (22) was our final equation (15). Here, B may be split up in the following manner. We introduce the operators

$$\varrho(x) = (\square - m^2)A(x) : \quad \varrho(\mathbf{p}) = \frac{1}{\sqrt{2E_p}} \int \varrho(\mathbf{x}, 0) \exp[-i\mathbf{p}\mathbf{x}] d\mathbf{x}.$$

Then by the definition of the a_p^\dagger and their hermitian conjugates a_p

$$[a_p^\dagger H] + E_p a_p^\dagger = -\varrho(-\mathbf{p}) = -\varrho^\dagger(\mathbf{p})$$

$$[a_p H] - E_p a_p = \varrho(\mathbf{p}).$$

Thus

$$T_{n,q} = \varrho(-\mathbf{q})|n\rangle$$

and

$$(H - E_q - E_n)a_q|\dot{n}\rangle = -\varrho(\mathbf{q})|\dot{n}\rangle = -T_{n,-q}.$$

Considering the boundary condition (13)

$$\lim_{t \rightarrow \infty} \exp[i(H - E_n - E_q)t]a_q|\dot{n}\rangle = 0$$

we have

$$a_q|\dot{n}\rangle = -\frac{1}{H + E_q - E_n + i\gamma} T_{n,-q}.$$

Therefore

$$\begin{aligned} B &= \langle \dot{n}' | a_p \varrho(-\mathbf{q}) | \dot{n} \rangle = \langle \dot{n}' | [a_p \varrho_{-q}] | \dot{n} \rangle + \langle \dot{n}' | \varrho_{-q} a_p | \dot{n} \rangle = \\ &= \left\langle T_{n',-q} \left| \frac{1}{H + E_p - E_n + i\gamma} T_{n,-p} \right. \right\rangle + \langle \dot{n}' | K_{p,q} | \dot{n} \rangle, \\ (23) \quad \langle \dot{n}' | K_{p,q} | \dot{n} \rangle &= \langle \dot{n}' | [a_p \varrho_{-q}] | \dot{n} \rangle. \end{aligned}$$

(13) We assume for the sake of simplicity that the configuration n does not contain a particle of momentum q .

We have then finally the system of Low equations ⁽¹⁴⁾

$$(24) \quad \langle n'; p | T_{n,q} \rangle = - \sum_{n''} \frac{\langle n'' | T_{n',p} \rangle^* \langle n'' | T_{n,q} \rangle}{E'' - E_{n'} - E_p - i\gamma} + \\ + \frac{\langle n'' | T_{n',-q} \rangle^* \langle n'' | T_{n,-p} \rangle}{E'' - E_n - E_p - i\gamma} + \langle n' | K_{n,q} | n' \rangle.$$

The specific character of the interaction is now expressed by the system of functions K . In the case of causal commutation relations we can say that the K -functions depend only on the difference $(p - q)$. But only in the Chew model (fixed source meson theory with an interaction energy linear in the meson field) all the K -functions vanish. The question as to the uniqueness of the solutions of the general Low scheme is thus reduced to the following: Is it possible that for two different models all the commutator functions (23) may be identical? We shall not attempt to answer this question here but merely point out that among the local theories usually considered different models lead to different K .

Note Added in Proof.

F. J. DYSON (private correspondence) has drawn the author's attention to the fact that there exist models which are not in disagreement with any known principle and yet lead to a Low function with zeros. An example is the Glaser-Källén-model ⁽¹⁵⁾ (Lee-model with an instable V -particle). To avoid incorrect conclusions it is therefore important to stress that two restrictions have been tacitly assumed in the previous discussion:

1) The underlying theory is of the «normal type» i.e. the basic variables are not more numerous than the asymptotic observables. In other words, there shall be no part in the Hilbert space which is annihilated by the operator $\lim_{t \rightarrow \infty} \exp[iHt] \exp[-iH_0t]$. This restriction appears to be sensible in our context since ordinary meson theory and the Chew-model are of this type (if one disregards the instability of the meson which has nothing to do with our problem). The Glaser-model on the other hand is not of this type. It may be of interest to note that relation (8a) is easily generalized to cover also models of the Glaser type. In this case the number m on the right hand side

⁽¹⁴⁾ It is clear that the usefulness of the scheme (24) is limited to models in which $K_{p,q}$ vanishes (i.e. essentially the Chew model). In other cases K will not be free from renormalization constants nor is it simple to choose a set of K -functions which is in accordance with all consistency requirements.

⁽¹⁵⁾ V. GLASER and G. KÄLLÉN: *Nuclear Physics*, to be published.

signifies the difference between the number of states which may be observed asymptotically and the number of states entering in the Hamiltonian scheme.

2) We consider always the complete set of Low equations i.e. one equation for the amplitude of each reaction which is possible according to the theory.

Then I propose to assert that this set of equations is sufficient to determine the S -matrix. The information 1) may be used to obtain a criterion which selects the appropriate solution of the scheme. The discussion in Sect. 3 shows that this statement is true in quantum mechanics. For the case of field theory we have no proof of the statement but the arguments in Sect. 4 seem to make it plausible.

RIASSUNTO (*)

Si espongono alcuni argomenti a sostegno del fatto che solo una soluzione dell'equazione di Low è accettabile dal punto di vista fisico. L'argomentazione è basata sul confronto con la teoria generale dello scattering in meccanica quantistica non relativistica. È aggiunto un breve studio della situazione che si determina in una teoria relativistica dei campi.

(*) *Traduzione a cura della Redazione.*

Demostration of the Existence of the Σ^0 Hyperon and a Measurement of its Mass (*).

R. PLANO and N. SAMIOS

Columbia University - New York, N.Y.

M. SCHWARTZ and J. STEINBERGER (+)

Brookhaven National Laboratory - Upton, Long Island, N.Y.

(ricevuto il 12 Novembre 1956)

Summary. — Three events, demonstrating the existence of the Σ^0 hyperon, have been found in a propane bubble chamber. The Q -value for the decay $\Sigma^0 \rightarrow \Lambda^0 + \gamma + Q$ has been measured to be (73.0 ± 3.5) MeV.

A neutral hyperon, completing an isotopic triplet with the Σ^- and Σ^{++} particles, forms an integral part of current theoretical views on the scheme of elementary particles (¹). The Σ^0 is expected to decay in a time of the order of $(1/\alpha) \times$ « nuclear time », or $\sim 10^{-20}$ s, into a Λ^0 and γ . In this time the path of the Σ^0 is too short to permit observation, and the Σ^0 will be recognized by its decay into Λ^0 and γ with a « Q » such that its mass is similar to those of Σ^- and Σ^+ .

So far, no conclusive simultaneous observation of Λ^0 and γ from such a decay has been found. There is considerable experimental evidence favoring the Σ^0 , but it is chiefly of a somewhat negative sort. A number of observ-

(*) Research supported in part by the joint program of the Office of Naval Research and Atomic Energy Commission.

(+) On leave from Columbia University.

(¹) T. NAKANO and K. NISHIJIMA: *Prog. Theor. Phys.*, **10**, 581 (1953); M. GELL-MANN and A. PAIS: *Proc. of the Glasgow Conference*.

(²) W. B. FOWLER, R. P. SHUTT, A. M. THORNDIKE and W. L. WHITEMORE: *Phys. Rev.*, **98**, 121 (1954).

ations (^{2,4}) are reported in which a Λ^0 is observed but with energy and direction inconsistent with the kinematics of direction production. If it is assumed, however, that the Λ^0 is the daughter of a Σ^0 , both production angle and energy have a continuous range and the observations can be reconciled.

We report here three events, in which both decay products of the Σ^0 , as well as the θ^0 produced in association, are observed. These events are from exposure of a 12" diameter, 8" deep propane bubble chamber to π^- beams of various energies at the Brookhaven National Laboratory. The chamber was in a magnetic field of 13.4 kG.

The first two events are clearly consistent with the interactions taking place in Hydrogen: $\pi^- + p \rightarrow \Sigma^0 + \theta^0$, $\Sigma^0 \rightarrow \Lambda^0 + \gamma + Q$. It is therefore possible to check the interpretation in detail and to exclude other possible explanations of the events. The existence of the Σ^0 can be clearly established and the Q value of the decay can be measured.

Of these two events, both obtained in the 1.15 GeV kinetic energy beam, the one shown in Fig. 1 permits the most accurate momentum measurements. The three V's associated with the stopped beam particle are interpreted as θ^0 , Λ^0 and γ -ray as indicated. The measured kinematical quantities are given in Tables I and II. The momenta have been corrected for ionization loss, and in the case of the electron-positron pair it was necessary to make an additional correction of $(1.5 \pm .75)^\circ$ for radiation loss. The beam energy was measured as in Ref. (⁴).

Calculated angles and momenta for the process $\pi^- + p \rightarrow \Sigma^0 + \theta^0$; $\Sigma^0 \rightarrow \Lambda^0 + \gamma$ have also been entered into the tables. In performing the calculation, the four center of mass system production and decay angles are free parameters

TABLE 1. - Angular Measurements (in degrees).

Angle	Measurement	Expected
$\pi^-_{inc}-\theta^0$	59 ± 4	558
$\pi^-_{inc}-\Lambda^0$	$11.6 \pm .3$ (*)	11.6
$\pi^-_{inc}-\gamma$	$19.1 \pm .2$	19.1
$\pi^-_{\theta}-\theta^0$	59 ± 5	65
$\pi^-_{\theta}-\theta^0$	41 ± 2	43
$\pi^-_{\Lambda}-\Lambda^0$	$4.8 \pm .2$	4.6
$p-\Lambda^0$	$1.8 \pm .2$	1.8

(*) From measurements on the proton and π^- .

(³) W. WALKER and W. SHEPARD: *Phys. Rev.*, **101**, 1810 (1955).

(⁴) R. BUDDE, M. CHRETIEN, J. LEITNER, N. SAMIOS, M. SCHWARTZ and J. STEINBERGER: *Phys. Rev.*, **103**, 1827 (1956).

TABLE II. — *Momentum Measurements* (in MeV/c).

Particle	Measured			Expected
	Component along beam	Component transverse to beam and field	Total	
π_{inc}^-	1277 ± 25 (*)	—	1277 ± 25 (*)	1277
π_0^-	-37 ± 7	$+180 \pm 32$	217 ± 38	185
π_0^+	$+263 \pm 18$	$+57 \pm 5$	226 ± 19	232
π_Λ^-	$+266 \pm 27$	-79 ± 8	278 ± 30	279
p	$+730 \pm 73$	-126 ± 13	740 ± 75	717
γ	$+146 \pm 7$	-51 ± 3	154.6 ± 8	—

Net longitudinal momentum (29 ± 75) MeV/cTotal transverse momentum (19 ± 35) MeV

(*) Determined as in Ref. (4).

which were chosen to give the best agreement. The Σ^0 mass was chosen to fit the γ -ray energy exactly. The agreement between experiment and kinematical prediction is satisfactory. This agreement can hardly be fortuitous if it is considered that the number of independently measured parameters is greatly in excess of the free parameters of the process.

The « Q » of the process $\Sigma^0 \rightarrow \Lambda^0 + \gamma + Q$ follows directly from the Λ^0 momentum and γ -ray energy, and is $Q = (69.7 \pm 5)$ MeV. The error is primarily due to the uncertainty in the momentum of the γ -ray and secondarily to the uncertainty in initial beam energy. The corresponding Σ^0 mass is $(2317 \pm 10) m_e$.

The second event is very similar, but the tracks of the component of the pair are too short for good momentum measurement. It is however still possible to demonstrate the nature of this event and to obtain a measure of the « Q » using the observed production angles. The Q arrived at by this means is (82 ± 15) MeV. The corresponding Σ^0 mass is $(2341 \pm 30) m_e$.

The third event is from an exposure at 850 MeV kinetic energy. This event is interpreted as taking place in Carbon. One can assume that the Λ^0 and γ originate from a Σ^0 and calculate the « Q » knowing the energies of both secondaries and the angle between them. The proton from the Λ^0 stops in the chamber and its range is measured to be $(15.2 \pm .1)$ cm, yielding an energy of $(97.6 \pm .5)$ MeV. The Λ^0 opening angle is 66.8 ± 1.0 . This yields a momentum for the Λ^0 of (502 ± 1) MeV/c. The angle between the Λ^0 and γ is measured to be $23.6^\circ \pm .5^\circ$. The γ momentum, after correction for ionization

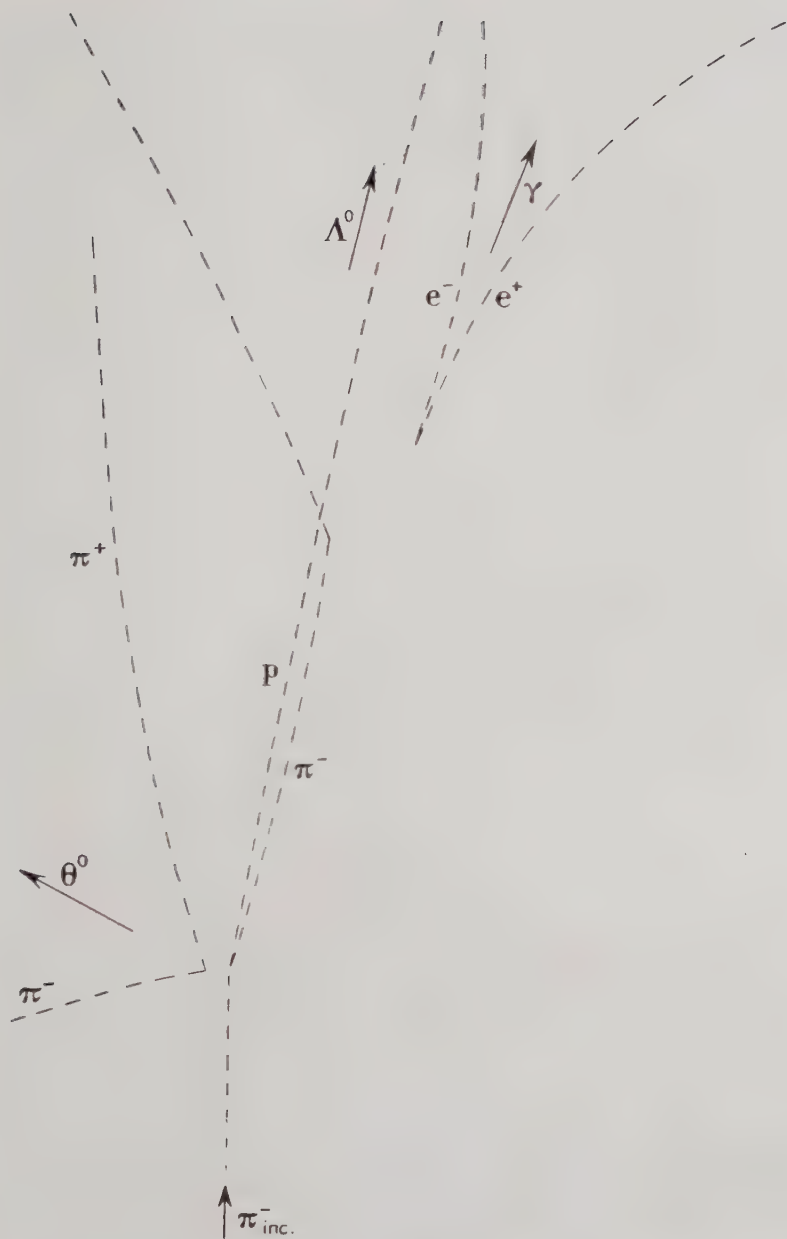
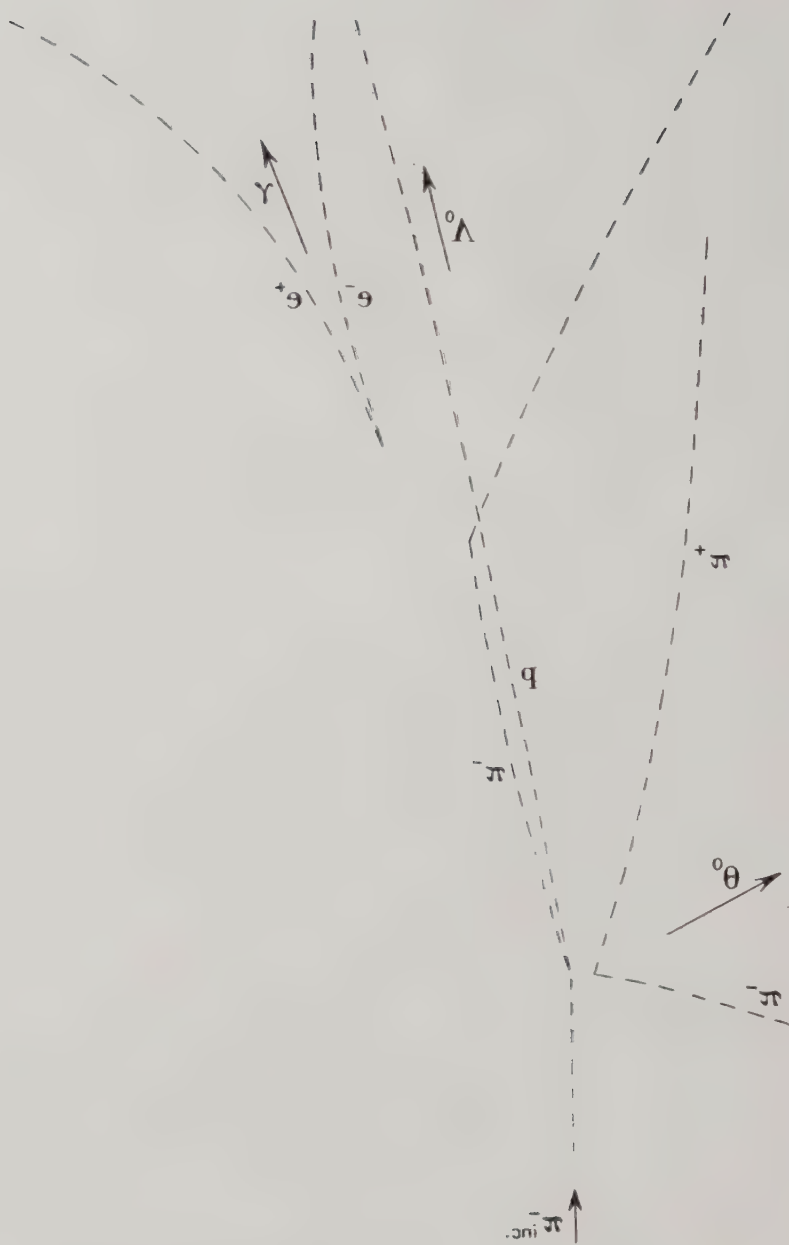


Fig. 1. $\pi^- + p \rightarrow \Sigma^0 + \theta^0$; $\Sigma^0 \rightarrow \Lambda^0 + \gamma$. Lines of flight of various components are indicated.

Fig. 1. $\pi^- \rightarrow \pi^- + b \rightarrow \pi^- + \theta_0$; $\pi^- \rightarrow V_0 + \gamma$. Lines of flight of various components are indicated.





and radiation loss, as in the first event, is measured to be (115 ± 6) MeV/c. This yields a $\langle Q \rangle$ of (75.3 ± 5) MeV. The corresponding Σ^0 mass is (2328 ± 10) m.e.

Combining these three measurements we obtain $Q = (73.0 \pm 3.5)$ MeV and $M_{\Sigma^0} = (2323 \pm 7)$ m.e.

The three masses compare as follows:

$$M_{\Sigma^+} = 2327 \pm 3 \quad (3)$$

$$M_{\Sigma^0} = 2323 \pm 7$$

$$M_{\Sigma^-} = 2341 \pm 5 \quad (4,6).$$

* * *

We wish to express our gratitude to the staff of the Cosmotron Department at the Brookhaven National Laboratory for its friendly and effective co-operation.

(5) M. CECCARELLI, M. GRILLI, M. MERLIN, A. SALANDIN and B. SECHI: *Pisa Conference*, 1955.

(6) W. W. CHUPP, G. GOLDBABER, S. GOLDBABER and F. B. WEBB: *Pisa Conference*, 1955.

RIASSUNTO (*)

In una camera a bolle a propano si sono trovati tre eventi che dimostrano l'esistenza dell'iperone Σ^0 . Il valore di Q per il decadimento $\Sigma \rightarrow \Lambda^0 + \gamma + Q$ è risultato (730 ± 3.5) MeV.

(*) Traduzione a cura della Redazione.

Proprietà elettromagnetiche del protone e rinormalizzazione della costante d'accoppiamento.

L. TENAGLIA

Istituto di Fisica dell'Università - Bari

(ricevuto il 16 Novembre 1956)

Riassunto. — Sono riportati dei calcoli sull'interazione fra protone, campo mesonico pseudoscalare e sorgenti statiche di campo elettrico e magnetico, secondo la teoria perturbativa relativistica ad accoppiamento debole. Vieni mostrato come un procedimento di rinormalizzazione che elimini solo i termini divergenti degli elementi di matrice (di 1° e di 2° ordine) non è sufficiente onde ottenere risultati fisicamente accettabili.

Introduzione.

La densità di carica e di corrente del campo pionico circondante un nucleone si possono calcolare più correttamente con la teoria a sorgente fissa ⁽¹⁾ che non mediante il calcolo perturbativo relativistico ad accoppiamento debole.

Infatti è dubbio che il metodo perturbativo sia applicabile al calcolo degli elementi di matrice dell'operatore di scattering per un nucleone interagente con un campo mesonico virtuale e con un campo elettromagnetico esterno. È però sembrato utile riportare alcuni risultati ottenuti in prima approssimazione con il metodo ad accoppiamento debole. Da questi viene messo in evidenza come il momento magnetico del protone ed il potenziale elettrostatico che si stabilisce fra tale particella ed una distribuzione statica di carica dipende dalla natura del campo esterno agente sul protone. Soprattutto, viene mostrato come sia necessario rinormalizzare sia i termini divergenti che quelli finiti degli elementi di matrice dell'operatore di scattering, se si attribuisce a questi un reale significato di valori approssimati.

⁽¹⁾ H. MIYAZAWA: *Phys. Rev.*, **101**, 1564 (1956); S. FUBINI: *Nuovo Cimento*, **3**, 1425 (1956).

1. - Potenziale elettrico e momento magnetico del protone.

1.1. *Potenziale elettrostatico del protone: sorgente puntiforme.* — Il metodo perturbativo relativistico fu applicato da molti autori a problemi riguardanti il comportamento elettromagnetico dei nucleoni. Per brevità ci si riferisce al procedimento di FRIED⁽²⁾, con opportuni adattamenti del caso: questo autore ha calcolato infatti il momento magnetico del neutrone ed il potenziale medio di interazione neutrone-elettrone. Gli elementi di matrice dell'operatore di Feynmann-Dyson che tengono conto dell'interazione tra il protone ed i due campi e ne permettono il calcolo in prima approssimazione, sono dovuti ai due grafici riportati in Fig. 1.



Fig. 1.

Ivi, k_0 e k_+ sono gli autovalori di energia-impulso per il campo mesonico neutro e positivo rispettivamente: le altre lettere hanno il significato convenzionale. Manca un grafico « chiuso » che non contribuisce all'interazione, come accade anche nel caso neutronico. I simboli usati nel seguito sono equivalenti a quelli adottati da FRIED.

Nel caso protonico, l'elemento di matrice totale è:

$$(1) \quad M = -(M_{II} - \frac{1}{2}M_I),$$

perchè — rispetto ai grafici analoghi a quelli di Fig. 1, ma relativi al neutrone — M_{II} ha segno opposto ed M_I ha valore dimezzato⁽³⁾. È poi:

$$(2) \quad M = [2(D_{II} + E_{II} - 2B_{II} + \frac{1}{2}A_{II}) - \frac{1}{2}(E_I + D_I - \frac{1}{2}D_I q^2) - (C_{II} - \frac{1}{2}C_I)] \gamma_\mu a'_\mu + \frac{1}{2}[(D_{II} + E_{II} - 2B_{II} + \frac{1}{2}A_{II}) - \frac{1}{2}(D_I + E_I)] 2\sigma_{\mu\nu} a'_\nu q_\mu = P\gamma a + Q(\sigma_{\mu\nu} a'_\nu q_\mu)$$

se il potenziale elettromagnetico è dato dalla relazione

$$A_\mu(\mathbf{x}) = (2\pi)^{-4} \int a_\mu(q) \exp[i\mathbf{q}\mathbf{x}] d^4q.$$

Nella formula (2) tutti gli elementi sono funzioni di q : i fattori C_I e C_{II} divergono logaritmicamente, qualunque sia la forma di $a(q)$. Rinormalizzando

⁽²⁾ B. FRIED: *Phys. Rev.*, **88**, 1144 (1952); K. CASE: *Phys. Rev.*, **76**, 1 (1949); S. NAKABAYASHI e I. SATO: *Prog. Theor. Phys.*, **6**, 252 (1951).

⁽³⁾ K. CASE: cfr. cit. ⁽²⁾.

questi termini nel modo consueto ⁽⁴⁾ (mediante sottrazione) si ha:

$$(3) \quad - (C_{II}(q^2) + \frac{1}{2}C_I(q^2) - C_{II}(0) - \frac{1}{2}C_I(0)) = \\ = \int_0^1 x dx dy [\lg(1 + A_1 q^2) + \frac{1}{2} \lg(1 + A_2 q^2)],$$

ove si è posto:

$$A_1 = x^2 y (1 - y) [\eta x + (1 - x)^2]^{-1} \\ A_2 = x^2 y (1 - y) [\eta (1 - x) + x^2]^{-1}.$$

Si supponga ora il potenziale esterno dovuto ad un elettrone fisso a distanza $r = |\mathbf{x} - \mathbf{x}'|$, ($x_4 = x'_4$) e quindi in luogo di A_μ si introduca nella (2)

$$(4) \quad V_0(r) = \frac{-2e}{(2\pi)^2} \int \frac{\exp[i\mathbf{q}\mathbf{r}]}{q^2} d^3\mathbf{q}.$$

Conviene misurare q in unità κ (inverso della lunghezza d'onda Compton del mesone π) ed r in unità κ^{-1} . Il nuovo elemento di matrice che si ottiene introducendo nella (2) la V in luogo di A ed integrando in q è la funzione $M'(r)$, data dall'equazione

$$(2') \quad M'(r) = -e^2 g^2 \kappa \int d\mathbf{x}' \cdot \\ \cdot u_1^\dagger \{P + Qq^{-1}(\boldsymbol{\sigma} \wedge \mathbf{q} - i\boldsymbol{\alpha}\mathbf{q})\} \frac{\exp[i\mathbf{q}\mathbf{r}]}{q^2} d^3\mathbf{q} \cdot \exp[i(\mathbf{p} - \mathbf{p}_1)\mathbf{x}'] \cdot u,$$

u_1^\dagger , u sono gli operatori di creazione-distruzione per le funzioni d'onda iniziale e finale del protone: la (2') è analoga alla formula (36) di Fried. Da un confronto con le comuni espressioni per l'interazione elettromagnetica, riportate da FRIED, è immediato dedurre che il potenziale elettrostatico che si stabilisce tra protone ed elettrone tramite il campo mesonico è proporzionale a P ove si trascuri il termine di interazione spin-orbita $Qq^{-1}\boldsymbol{\alpha}\mathbf{q}$: precisamente l'energia potenziale ad esso proporzionale è:

$$(5) \quad V_1(r) = -e^2 g^2 \kappa \int P(q) \exp[i\mathbf{q}\mathbf{r}] q^{-2} d^3\mathbf{q}.$$

⁽⁴⁾ Ad esempio, in H. A. BETHE, DE HOFFMAN e S. SCHWEBER: *Meson and Fields* (New York, 1954), pag. 298, vol. I. Trattandosi di una divergenza « vertex part » si devono rinormalizzare le costanti d'accoppiamento, non senza una certa ambiguità: vedi G. KÄLLÉN: *Nuovo Cimento*, **12**, 217 (1954).

Per il calcolo di $V_1(r)$ conviene effettuare la trasformata di Fourier del secondo membro nella (5): $P(q)$ consta dei termini entro la prima parentesi a destra nella relazione (2) (tenuto conto della (3)). Essi sono noti dal lavoro di FRIED. Le trasformate di Fourier ⁽⁵⁾ dei singoli gruppi di termini della equazione (5) sono riportati nella tabella che segue:

TABELLA I.

termini	trasformate: $(2\pi r)^{-1} \int_0^{\infty} x dx dy$
$2(D_{II} + E_{II} - 2B_{II} + \frac{1}{2} A_{II})$	$2[1 - 2xy(2 - x)][\eta x + (1 - x)^2]^{-1}(1 - \exp[-rX_1])$
$-\frac{1}{2}(D_I + E_I)$	$-2x^2y[x^2 + \eta(1 - x)]^{-1}(1 - \exp[-rX_2])$
$\frac{1}{4}D_I q^2$	$x^2y[x^2 + \eta(1 - x)]^{-1} \exp[-rX_2]$
$-(C_{II} + \frac{1}{2}C_I)$	$-2[Ei(-rX_1) + \frac{1}{2} Ei(-rX_2)]$

È: $X_1 = A_1^{-\frac{1}{2}}$, $X_2 = A_2^{-\frac{1}{2}}$, $E_i(z)$ indica la funzione integral-logaritmo.

Dei quattro gruppi di termini, i due ultimi sono singolari nell'origine, i primi sono ivi nulli. Per r molto grande gli esponenziali e le funzioni $Ei(z)$ sono trascurabili: ne viene l'espressione asintotica

$$(6) \quad V_{1as}(r) = -\frac{g^2 e^2}{4\pi} 0.218 \cdot \frac{1}{r},$$

se r è ora misurato in unità c.g.s. Con $g^2/4\pi \simeq 7.33$ si ha un'energia potenziale ovunque maggiore (in modulo) di quella coulombiana, e negativa: essa è decisamente inammissibile.

Il calcolo perturbativo ad accoppiamento debole dà in genere risultati molto grossolani: ciò è noto in particolare dal calcolo del momento magnetico del neutrone e del protone. La (6) però è decisamente inammissibile, sia per il segno di V_{1as} , sia per il modulo. Nè si può sperare che i termini superiori modifichino sostanzialmente un risultato in così forte contrasto con i dati presumibili.

Seguendo l'idea originaria di KRAMERS ⁽⁶⁾, si rinormalizzi M' eliminando da esso i termini privi di significato fisico. Come tali sono generalmente intesi quei termini che corrispondono ad una variazione nulla dell'energia-impulso delle particelle reali, diffuse da un campo di forze. Sostituendo ad $M'(q^2)$ il nuovo elemento di matrice

$$(7) \quad M''(q^2) = M'(q^2) - M'(0),$$

⁽⁵⁾ W. GRÖBNER e N. HOFREITER: *Integraltafeln* (Wien-Innsbruck, 1950), Vol. II, pag. 127 e 150.

⁽⁶⁾ H. A. BETHE *et al.*: cit. ⁽⁴⁾, pag. 274.

da esso si deduce un potenziale accettabile sia per il suo segno, sia per la dipendenza da r . Precisamente, in luogo di $V_1(r)$ dalla (7) si ha un potenziale V dato dall'equazione:

$$(8) \quad V(r) = \frac{g^2 e^2}{2\pi r} \int_0^1 dx dy \left\{ [x - 2x^2 y(2-x)][\eta x + (1-x)^2]^{-1} \exp[-zX_1] - \right. \\ \left. \frac{1}{2} x^2 y(3-y)[x^2 + \eta(1-x)]^{-1} \exp[-zX_2] - x \left[Ei(-zX_1) + \frac{1}{2} Ei(-zX_2) \right] \right\},$$

ove: $z = \kappa r$. V è sensibile entro un intorno di alcun lunghezze Compton κ^{-1} : esso diverge nell'origine come r^{-2} . Va rilevato che la rinormalizzazione effettuata nella (7) non altera l'ultimo termine della Tabella 2: ciò è evidente conseguenza della (3). Posto

$$(8') \quad V(r) = \frac{g^2 e^2}{4\pi r} F(z),$$

$F(z)$ è una funzione rapidamente decrescente, i cui valori sono riportati nella Tabella 2), (si è preso $\eta^{\frac{1}{2}} = 0.151$). Un confronto tra la densità di carica responsabile del potenziale V e quella che si ha dalla

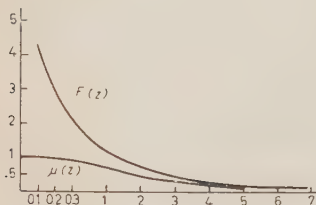


Fig. 2.

TABELLA II.

z	$F(z)$	z	$F(z)$
0.1	4.330	3	0.458
0.2	2.782	4	0.296
0.3	2.098	5	0.205
1	1.098	6	0.141
2	0.702	7	0.09

teoria a sorgente fissa (nella one-meson approximation) mette in evidenza una differenza sensibile soprattutto per r piccolo. Secondo il calcolo ad interazione debole (in prima approssimazione) la carica elettrica viene ad essere maggiormente diffusa e lontana nello spazio, attorno al protone (?), rispetto a quanto si ha con i metodi ad accoppiamento forte. In Fig. 2 sono riportati $F(z)$ e la densità di momento magnetico $\mu(z)$ (vedi Sez. 3) reso unitario in $r = 0$.

(?) Questo fatto è comprensibile, ove si tenga conto che, nel calcolo perturbativo, campo elettromagnetico e mesonico sono introdotti simultaneamente e trattati « alla pari » nonostante i diversi valori di e e di g . Per campi carichi circondanti il protone (Fig. 1) si può in un certo senso ripetere le considerazioni che SCHWINGER (*Phys. Rev.*, **76**, 790 (1949), appendice) fa a proposito del potenziale dovuto alla polarizzazione del vuoto; tale potenziale e il $V(r)$ — formula (8) — hanno andamento simile.

1.2. *Potenziale del protone nell'atomo di idrogeno.* — Si supponga ora il protone soggetto al potenziale dovuto ad un elettrone (non relativistico) nello stato s . Misurando le distanze in unità a_0 (raggio dell'orbita fondamentale di Bohr) la densità di carica elettronica ed il potenziale da essa prodotti sul protone (nell'origine del sistema di riferimento) sono:

$$(9) \quad \varrho(r) = -4e \cdot \exp[-2r] \quad V_0(r) = 4e \int \exp[i\mathbf{q}\mathbf{r}] d\mathbf{q} (q^2 + 4)^{-1}.$$

Il calcolo va sviluppato come nel caso precedente (sorgente puntiforme): posto $a = (a_0\kappa)^{-1}$ si ottiene dalla (2'):

$$(10) \quad V' = -\frac{4a_0}{r} e^2 g^2 2\pi \int_0^1 dx dy \int_0^\infty \frac{\sin qr}{q^2 + 4} dq \cdot q \left[\frac{\varphi_i}{\alpha_i + \beta_i q^2 a^2} + \frac{q q^2}{\alpha + \beta q^2 a^2} \right] + \\ + \psi \left[\lg(1 + \gamma a^2 q^2) + \frac{1}{2} \lg(1 + \gamma_1 q^2 a^2) \right],$$

ove le α_i , β_i , α , β , γ_i , φ_i e ψ sono funzioni solo di x e di y . L'ultimo termine (proporzionale a ψ) è ottenuto dalla differenza che compare nell'equazione (3), già normalizzata. La integrazione di tale fattore dà:

$$-\pi E i(-\kappa a_0 r \cdot \gamma^{-\frac{1}{2}})$$

ed un ulteriore termine, inferiore al precedente. Esso quindi, come nel caso di sorgente puntiforme, dà un fattore di V' senz'altro accettabile, e che ha un raggio di azione di qualche lunghezza d'onda Compton. Questo risultato è dovuto alla rinormalizzazione preliminare effettuata nella (3). Anche il termine proporzionale a q ha un valore apprezzabile solo nell'intorno di qualche κ^{-1} .

Il primo gruppo di fattori nella (10) (termini in q_i) dà invece un'espressione inammissibile: infatti dall'eguaglianza

$$\int_0^\infty \frac{\sin qr \cdot q dq}{(q^2 + 4)(\alpha_i + \beta_i a^2 q^2)} = \frac{\pi}{2(\alpha_i - 4\beta_i a^2)} (\exp[-2r] - \exp[-\kappa a_0 r(\alpha_i/\beta_i)^{\frac{1}{2}}]),$$

tenendo conto che l'integrazione in x ed y non altera sensibilmente gli ordini di grandezza, si rileva immediatamente che entro un largo intervallo (di qualche a_0) — $V'(r)$ è negativo e maggiore (a parte il segno) del potenziale coulombiano prodotto dalla densità elettronica definita nell'equazione (9). La rinormalizzazione dell'elemento di matrice secondo l'equazione (7) porta all'eliminazione di tale inconveniente: si ottiene per tale via un potenziale sensibile

entro un intervallo di alcuni α^{-1} . Una valutazione alquanto grossolana mostra che esso si scosta sensibilmente da quello dovuto ad un elettrone fisso in un punto: all'incirca, per un fattore 2. Si può quindi verificare un fatto comprensibile ed intuitivo: nel calcolo perturbativo, il comportamento elettromagnetico dipende in modo rimarchevole dalla forma del campo esterno.

Per potenziali dovuti ad elettroni in altri stati idrogenici le cose non vanno diversamente, come è immediato verificare. Non è quindi difficile stabilire che le difficoltà che esigono, nel calcolo perturbativo, la rinormalizzazione (7), sono generali a tutta questa categoria di problemi.

1.3. *Protone soggetto al campo magnetico di un dipolo puntiforme.* — Nell'elemento di matrice (2'), il secondo fattore a destra (proporzionale a Q) corrisponde al noto termine d'interazione magnetica nell'equazione non relativistica di Dirac:

$$(11) \quad \mu(\boldsymbol{\sigma}\mathbf{H} - i\boldsymbol{\alpha}\mathbf{E}) .$$

Una particella dotata di momento magnetico \mathbf{s} e fissa, produce (classicamente) in un punto a distanza r un potenziale $\mathbf{A}(r)$ dato da:

$$(12) \quad -\mathbf{s} \wedge \text{grad } r^{-1} = \frac{\mathbf{s} \wedge \mathbf{n}}{2\pi^2} \int_0^\infty i(\mathbf{n}\mathbf{q}) \exp[i\mathbf{q}\mathbf{r}] q^{-2} d\mathbf{q} ,$$

(con $\mathbf{n} = \text{vers } r$) e quindi un campo magnetico:

$$\mathbf{H} = \frac{i}{2\pi^2} \int_0^\infty (\mathbf{n}\mathbf{q})^2 q^{-2} \exp[i\mathbf{q}\mathbf{r}] d\mathbf{q} \quad (\mathbf{i} = \mathbf{n} \wedge (\mathbf{s} \wedge \mathbf{n})) .$$

Introducendo tale campo nella (2') si ha un nuovo elemento di matrice:

$$(13) \quad M_i = u_1^\dagger \left\{ \int B(\mathbf{n}\mathbf{q})^2 \exp[i\mathbf{q}\mathbf{r}] q^{-2} d\mathbf{q} \int i\boldsymbol{\sigma} \exp[i(\mathbf{p} - \mathbf{p}_1)\mathbf{x}'] d^4\mathbf{x}' \right\} u .$$

Con i simboli di Fried è

$$(14) \quad B = -\frac{M}{2} \frac{eg^2}{8\pi} Q$$

(Q è definito nell'eq. (2)). Il momento magnetico responsabile dell'interazione (11) come si ottiene con la sostituzione dei valori per le singole grandezze e in

unità magnetoni di Bohr del protone) ha perciò densità

$$(15) \quad \mu(z) = -\frac{g^2}{4\pi} \pi^2 \int_0^1 dx dy [\eta x + (1-x)^2]^{-1} \cdot \\ \cdot \{2x(x^2y - 2xy + \frac{1}{2})(1 - \exp[-zX_1]) - (1-x)^2y(1 - \exp[-zX_2])\},$$

(X_1 ed X_2 sono definite in precedenza, dopo l'equazione (3)). Il segno di $\mu(z)$ è errato, quindi la (15) è inammissibile. Effettuando la rinormalizzazione (7) $\mu(z)$ riesce positivo: si ha in particolare

$$\mu(0) = 0.113 \, x^2 g^2 / 4\pi$$

e cioè un valore circa metà di quello sperimentale. L'andamento di $\mu(z)$ è decrescente a partire da $z = 0$, e si discosta assai fortemente da quello che si deduce con la tecnica di Miyazawa, almeno per $z \simeq 1$ (vedasi Fig. 2: in scala, $\mu(0)$ è preso unitario).

Il momento μ calcolato per il potenziale A degli elettroni idrogenici presenta caratteristiche analoghe a quelle che si hanno per un potenziale esterno dovuto ad un dipolo fisso. Dunque anche nel caso magnetico è necessaria la rinormalizzazione degli elementi di matrice definita dalla relazione (7). Per quanto riguarda i termini superiori dello sviluppo perturbativo, analoga necessità si presenta certamente per alcuni grafici riportati da NAKABAYASI (²), e probabilmente per tutti. Il problema della rinormalizzazione di tutti gli elementi, finiti o divergenti, dell'operatore di scattering è dunque generale nei calcoli perturbativi riguardanti le proprietà elettromagnetiche dei nucleoni.

2. - Conclusione.

I risultati che precedono, pur essendo limitati all'ordine più basso della teoria delle perturbazioni, conducono a ritenere che il procedimento di rinormalizzazione della carica elettrica, univocamente definito nel caso di interazione fra un campo materiale (spinoriale o bosonico) (⁸) e il campo elettromagnetico quantizzato, sia essenzialmente valido anche quando sorgenti del campo elettromagnetico siano più campi di qualunque tipo in interazione fra loro. In questo caso la carica elettrica, rinormalizzata, sarà funzione anche delle costanti di accoppiamento che caratterizzano l'interazione fra i campi non elettromagnetici considerati.

(⁸) P. T. MATTHEWS e ABDUS SALAM: *Rev. Mod. Phys.*, **33**, 311 (1951); F. DYSON: *Phys. Rev.*, **75**, 486, 1736 (1949); P. T. MATTHEWS e A. SALAM: *Phys. Rev.*, **94** 185 (1954).

Il procedimento qui usato, basato sulla sottrazione dall'elemento di matrice per un dato processo della parte che corrisponde a trasferimento nullo di impulso e di energia fra sorgente e campo elettromagnetico equivale precisamente alla ridefinizione della carica elettrica rinormalizzata all'ordine più basso in g^2 .

* * *

Ringrazio sentitamente il prof. M. CINI per aver corretto e rivisto il manoscritto di questa nota.

SUMMARY (*)

The author reports calculations on the interaction between proton, pseudoscalar mesonic field and static sources of the electric and magnetic field, following the relativistic perturbation theory for weak coupling. He shows that a renormalization method which eliminates only the divergent terms of the matrix elements (of 1-st and 2-nd order) is not sufficient to obtain physically consistent results.

(*) *Editor's translation.*

Struttura del protone o scattering elettrone-protone.

L. TENAGLIA

Istituto di Fisica dell'Università - Bari

(ricevuto il 16 Novembre 1956)

Riassunto. — Si calcola, a partire dalla teoria a sorgente fissa, la densità di carica e di momento magnetico della nuvola pionica che circonda il protone. Tali densità permettono di determinare con sufficiente approssimazione la sezione d'urto per elettroni di 188 MeV, diffusi elasticamente dal protone.

Introduzione.

Le recenti esperienze ⁽¹⁾ sullo scattering di elettroni d'elevata energia (da 150 a 550 MeV) da parte del protone sono uno dei dati di maggior interesse per la determinazione del comportamento elettromagnetico di questa particella. Il risultato sperimentale più notevole consiste in una sensibile diminuzione della sezione d'urto, ad angoli elevati rispetto alla direzione d'incidenza, in relazione alla curva di Mott-Rutherford. Una prima interpretazione di tale fatto è stata data da HOFSTADTER e McALLISTER ⁽¹⁾ i quali, ammessa la carica ed il momento magnetico del protone distribuiti uniformemente in una sfera di raggio r_0 , mostrarono che dev'essere $r_0 \simeq 7.8 \cdot 10^{-14}$ cm. Una trattazione precedente di ROSENBLUTH ⁽²⁾, basata sul calcolo perturbativo ad accoppiamento debole fra protone, campo mesonico ed elettromagnetico, diede risultati errati. Il problema fu ripreso recentemente da SALZMAN ⁽³⁾ per elettroni

⁽¹⁾ R. HOFSTADTER e R. MACALLISTER: *Phys. Rev.*, **93**, 217 (1955); R. HOFSTADTER e D. YENNIE: *Proceedings of the Sixth Annual Rochester Conference* (New York, 1955), pag. 162 e segg.; E. E. CHAMBERS e R. HOFSTADTER: *Phys. Rev.*, **103**, 1454 (1956).

⁽²⁾ M. ROSENBLUTH: *Phys. Rev.*, **79**, 615 (1950).

⁽³⁾ G. SALZMAN, non ancora pubblicato: ringrazio il prof. CINI che concesse in visione questa nota.

di 188 MeV, partendo dal calcolo delle densità di carica e di corrente del campo pionico virtuale che circonda il protone, secondo il metodo di Chew e Low ⁽⁴⁾ (one-meson approximation) per l'ampiezza di scattering mesone-protone. Nel lavoro, assai breve, non sono riportati i valori delle densità di carica e di corrente, nè sono discussi i contributi della sorgente.

Le densità di carica e di momento sono state calcolate dalla teoria mesonica a sorgente fissa, seguendo il metodo sviluppato di recente da CINI ⁽⁵⁾ e FUBINI e, indipendentemente, da MIYAZAWA ⁽⁶⁾. Da queste grandezze si è determinato la sezione d'urto differenziale, in prima approssimazione di Born, per lo scattering elastico d'elettroni di 188 MeV. Per energie assai elevate dell'elettrone diffuso ed angoli di scattering grandi, si verifica un fatto interessante: una notevole parte del campo pionico non contribuisce allo scattering. Questa parte del campo occupa una porzione rilevante del range comunemente usato nella teoria della sorgente fissa per calcolare le densità di carica e di momento magnetico. Essendo presumibilmente ancora applicabili i risultati della teoria a sorgente fissa, si può stabilire un'espressione di facile uso pel calcolo della sezione d'urto ad energie elevate.

1. - Calcolo delle densità di carica e di momento magnetico.

Partiamo dalle espressioni ⁽⁷⁾ della densità di carica e della densità di corrente della nuvola mesonica:

$$(1) \quad \varrho(\mathbf{x}) = \frac{2\tau_z}{\pi^3} \int_0^\infty dk \int_0^\infty dk' \frac{v(k)v(k')k^3k'^3j_1(kr)j_1(k'r)}{k^2 - k'^2} [R_2(\omega_k) - R_2(\omega_{k'})],$$

$$(1') \quad \mathbf{j}(\mathbf{x}) = -\frac{2\tau_z \mathbf{r} \wedge \boldsymbol{\sigma}}{\pi^3 r^2} \int_0^\infty dk \int_0^\infty dk' \frac{v(k)v(k')k^3k'^3j_1(kr)j_1(k'r)}{k^2 - k'^2} \left[\frac{R_3(\omega_k)}{\omega_k} - \frac{R_3(\omega_{k'})}{\omega_{k'}} \right].$$

Tutti i simboli sono spiegati nella ref. ⁽⁷⁾.

Per calcolare queste grandezze conviene semplificare le formule precedenti, integrando in una delle variabili. Per definizione, $R_2(\omega_k)$, $R_3(\omega_k)$ ed $R_3(\omega_k)/\omega_k$ sono funzioni analitiche regolari per ogni valore di k e tali che

$$\lim_{k \rightarrow \infty} \omega_k R_i(\omega_k) \quad (i = 2, 3)$$

⁽⁴⁾ G. SALZMAN: *Phys. Rev.*, **99**, 973 (1956); G. CHEW e F. LOW: *Phys. Rev.*, **101**, 1570 (1956) e lavori precedenti ivi citati.

⁽⁵⁾ M. CINI e S. FUBINI: *Nuovo Cimento*, **3**, 764 (1956); *Phys. Rev.*, **102**, 1379 (1956); M. CINI, S. FUBINI e A. STANGHELLINI: *Nuovo Cimento*, **3**, 1379 (1956).

⁽⁶⁾ H. MIYAZAWA: *Phys. Rev.*, **101**, 1564 (1956).

⁽⁷⁾ S. FUBINI: *Nuovo Cimento*, **3**, 1425 (1956).

sono termini finiti: in più, le R_i sono derivabili, e

$$(3) \quad \frac{dR_i}{dk}, \quad \frac{d}{dk} \frac{R_i}{\omega_k},$$

sono pur esse grandezze finite. Nella (1) si può calcolare a parte l'integrale in k' :

$$(4) \quad \int_{-\infty}^{\infty} \frac{v(k') k'^3 j_1(k'r)}{k^2 - k'^2} [R_2(\omega_k) - R_3(\omega_k)] dk'.$$

Il fattore di convergenza $v(k')$ è di per sé funzione del modulo di k' : la funzione integranda è dunque pari e l'integrale (dividendo per 2) può estendersi ai limiti $-\infty, \infty$. Per k' molto grande, la funzione integranda (regolare e finita) è proporzionale a $v(k') j_1(k'r)$, e quindi converge a zero. Introducendo in luogo di k' una nuova variabile complessa z , nel piano complesso l'integrale (4) si può calcolare lungo il cammino $\Delta + \Delta_1$, segnato in Fig. 1, tenendo conto ⁽⁸⁾ che

$$(4') \quad \int_{\Delta_1} \frac{\sin z}{z} dz = 0.$$

(L'integrazione nel semipiano inferiore può portare a delle difficoltà per l'integrale (4') ove si supponga solo $v(z)$ finito in $z \rightarrow \infty$). La (4) quindi si riduce al calcolo del residuo in $k + k' = 0$: essendo $k \geq 0$, si ha in effetti un solo polo. Le medesime considerazioni si possono fare per la determinazione di $\mathbf{j}(\mathbf{x})$ (o del momento magnetico), tenendo conto che $R_3 \omega_k$ è pur essa derivabile e finita ovunque.

Integrando le (1) e (1') in k' ed introducendo, in luogo di $v(k)$, una funzione a gradino di range K_0 , la densità di carica e di corrente che si ottengono sono coincidenti con le grandezze omonime calcolate con la tecnica di Miyazawa (come è mostrato nell'Appendice I). La densità di corrente della nuvola mesonica è data da:

$$(5) \quad \left\langle \left| \int \varrho(k, r) dk \right| \right\rangle = \frac{16f^2}{3\pi^2 m^2} \int_0^{K_0} j_1^2(kr) \frac{k^6 dk}{\omega_k^3} - \frac{1}{3\pi^4} \int_0^{K_0} \frac{k^6 dk}{\omega_k} j_1^2(kr) \int_0^\infty \frac{\sigma'(E) dE}{(E + \omega_k)^2 (E^2 + m^2)^{\frac{1}{2}}},$$

⁽⁸⁾ R. COURANT: *Differential and Integral Calculus* (London, 1949), pag. 554.

(m indica la massa pionica, k è misurato in unità m , si è posto $h = 1$, $c = 1$).

Integrando in r si ottiene la carica totale q_m della nuvola pionica: precisamente è, in unità e ,

$$(6) \quad \begin{cases} q_m = 0.551 & \text{per } K = 5 m, \\ = 0.856 & = 6 m. \end{cases}$$

I valori delle densità di carica $\varrho(r)$ della nuvola mesonica (ove r è la distanza dalla sorgente, misurata in unità $\lambda_{\pi} = 1.42$ fermi) sono stati calcolati per $K_0 = 5 m$ e $K_0 = 6 m$, prendendo $f^2 = 0.08$, σ^+ dai dati sperimentali di ANDERSON⁽⁹⁾ ed altri, riportati al sistema baricentrale.

Il medesimo procedimento si è seguito per la determinazione del momento magnetico $\mu(r)$: i valori di $\varrho(r)$ e di $2\pi\mu(r)$ per $K_0 = 5 m$, $K_0 = 6 m$ sono riportati nella Tabella I, e ivi indicati rispettivamente con ϱ_1 , ϱ_2 , μ_1 , μ_2 (*). La scelta di K_0 altera sensibilmente le densità di carica e di momento magnetico solo in un intorno non molto esteso di $r = 0.5$. Nella Fig. 2 sono tracciati i grafici di $10\varrho_1$, $10\varrho_2$, μ_1 e μ_2 .

TABELLA I.

r	ϱ_1	ϱ_2	μ_1	μ_2
0,0	0.014	0.015	0.056	0.075
0.2	0.035	0.440	0.186	0.234
0.3	0.050	0.050	0.362	0.520
0.4	0.075	0.091	0.518	0.612
0.5	0.078	0.091	0.620	0.760
.6	0.068	0.075	0.645	0.734
0.8	0.037	0.38	0.544	0.564
1	0.023	0.025	0.436	0.466
1.2	0.017	0.018	0.350	0.366
1.4	0.0095	0.0102	0.284	0.292
1.6	0.0089	0.0095	0.0228	0.236
1.8	0.0070	0.0072	0.186	0.194
2	0.0056	0.0057	0.150	0.158
2.5	0.0038	0.0038	0.110	0.116
3	0.0013	0.0013	0.060	0.060
3.5	—	—	0.200	0.020

(⁹) H. L. ANDERSON, W. C. DAVIDON e U. E. KRUSE: *Phys. Rev.*, **100**, 339 (1956).

(*) Il momento magnetico è notoriamente un vettore assiale. Le densità μ_1 e μ_2 sono integrate nella coordinata φ : il momento magnetico totale μ_m della nuvola mesonica è dato da

$$\mu_m = -2 \int \mu_i(r) r^2 dr \int_0^{\pi/2} \cos \vartheta \sin \vartheta d\vartheta \quad \text{con } i = 1, 2.$$

Per quanto riguarda il contributo della sorgente alla carica e al momento magnetico totali, sarebbe possibile calcolarli, dalle espressioni dei valori medi di τ_z e di σ_z . Per esempio, l'equazione (18b) della ref. (17) dà per τ_z l'espressione (coincidente con quella deducibile dalle eq. (25) e (26) di Miyazawa):

$$(7) \quad \langle \tau_z \rangle = \left(\frac{1}{Q^2} \right)^2 - \frac{m^2}{f_0^2 2\pi} \int_0^\infty \frac{\sigma^+ - \sigma^-}{\omega_k} dk = 0.256.$$

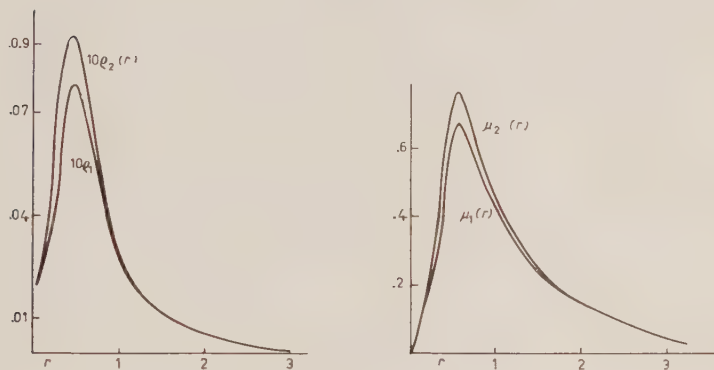


Fig. 2.

Tuttavia, i valori medi τ_z e σ_z non si possono consistentemente calcolare per tale via: nelle equazioni che li definiscono (come la (7)) mancano quei fattori di convergenza che, nelle espressioni dei valori medi degli operatori del campo mesonico, rendono trascurabile il contributo alle elevate energie. Questo problema è stato trattato chiaramente da CINI e FUBINI (5,7).

Per di più, non c'è da aspettarsi che la teoria a sorgente fissa descriva correttamente le proprietà della sorgente, che fisicamente sono le proprietà degli strati più interni del protone, dove predominano fenomeni di tipo più complesso (formazioni di coppie nucleone-antinucleone, interazione con mesoni K, ecc.). La teoria della sorgente fissa è adatta, essenzialmente alla descrizione dei fenomeni pionici, ad energie dell'ordine della massa (*) del mesone π . Essi dipendono dalle sezioni d'urto dello scattering pione-nucleone, per energie limitate superiormente, all'incirca, da $E_0 = M$, con M massa protonica.

Per questo motivo il risultato più importante della teoria a sorgente fissa è quello di una descrizione presumibilmente corretta della densità di carica e di momento magnetico della nuvola mesonica. Esse, del resto, sono le uniche

(*) Vedasi anche osservazione in fine.

grandezze che intervengono nel calcolo della sezione d'urto di scattering per elettroni d'energia dell'ordine di 200 MeV.

2. - Calcolo della sezione d'urto.

La sezione d'urto di scattering, $\sigma(\theta)$, è stata calcolata in approssimazione di Born, ammesso che fra protone esteso ed elettrone avvenga lo scambio di un solo fotone del campo elettromagnetico quantizzato, per mezzo del quale le due particelle interagiscono. Si trascurano le correzioni radiative elettromagnetiche e i termini d'ordine superiore di Born, perchè il loro apporto a $\sigma(\theta)$ è irrilevante. L'elemento di matrice, relativo al grafico di Feynmann che interessa, è $(2,1)$

$$(8) \quad eF_1\gamma_\mu + \mu_0 F_2\sigma_{\mu\nu}q_\nu ;$$

F_1 ed F_2 sono fattori che tengono conto dell'estensione della carica protonica: è

$$(9) \quad F_1 = \int \varrho_p(r) \exp[i\mathbf{q}\cdot\mathbf{r}] d\mathbf{r}, \quad F_2 = \int \mu_0(r) \exp[i\mathbf{q}\cdot\mathbf{r}] d\mathbf{r},$$

$\varrho_p(r)$ indica la densità di carica del protone fisico, μ_0 è la parte anomala del momento magnetico di questo nucleone e $\mu_0(r)$ è la densità di μ_0 ; infatti della interazione fra particella di Dirac di momento magnetico unitario e campo elettromagnetico tien già conto il primo termine della (8).

A causa della comparsa di μ_0 nell'elemento di matrice d'interazione, il secondo termine della (8) sembra a prima vista introdurre nel calcolo della sezione d'urto, un momento che non è quello della nuvola mesonica. Infatti, secondo la teoria a sorgente fissa, il momento magnetico di tale nuvola non coincide con la parte anomala del momento protonico.

Per chiarire questo punto, si può osservare che presumibilmente al momento magnetico totale del protone, oltre a quello pionico, contribuiscono altri (*) campi dovuti a particelle di massa superiore a quella del pione. In approssimazione statica, le dimensioni della zona di spazio in cui sono addensati gli elementi di questi campi sarà dell'ordine di grandezza della lunghezza d'onda Compton (+) di tali particelle. Poichè le particelle che possono interagire

(*) Un'ipotesi del genere, per quanto riguarda il momento magnetico del neutrone, è stata proposta da G. SANDRI: *Phys. Rev.*, **101**, 1616 (1956); vedasi anche osservazione in fine.

(+) Va osservato in proposito che, oltre ai risultati sopra dati, relativi alla distribuzione di carica mesonica, un fatto del genere si manifesta per la densità di carica e corrente di polarizzazione del vuoto che, in approssimazione statica dà luogo al noto potenziale di Schwinger (J. SCHWINGER: *Phys. Rev.*, **75**, 651 (1949), pag. 661) e ciò nonostante il valore assai diverso delle costanti di accoppiamento mesonica ed elettromagnetica.

fortemente col protone (o col neutrone) sono presumibilmente di massa maggiore di quella del pione, la zona in cui è sensibile la loro distribuzione sarà piccola rispetto alle dimensioni medie della nuvola pionica. (Ciò si può dire a maggior ragione del contributo dato, al momento magnetico totale, da processi più interni, come quello di creazione di coppie nucleone-antinucleone). L'apporto di tali campi al momento magnetico totale del protone può compensare la differenza con il momento magnetico pionico, in modo che questo nucleone si può ancora pensare una particella di Dirac normale. Se così è si può cercare quale effetto abbia sullo scattering di elettroni di lunghezza d'onda paragonabile con λ_π , la presenza di una nuvola pionica, di una distribuzione di momento entro una zona di dimensioni assai più limitate e inne del « core » considerato come una particella spinoriale di momento magnetico unitario.

Nel calcolo della sezione d'urto in approssimazione di Born intervengono i due fattori F_1 ed F_2 dell'equazione (9) in cui $[q_z \mathbf{dr}]$ e $[\mu(r) \mathbf{dr}]$ danno la carica totale del protone fisico e la parte anomala del suo momento. Per lunghezze d'onda dell'elettrone dell'ordine di λ_π negli integrali l'esponentiale si può sviluppare in serie di potenze e, arrestando tale sviluppo ai primi termini, l'errore commesso è trascurabile. Ciò posto

$$(10) \quad \begin{cases} F_1 = \sum_{(2n-1)!} q^{2n} (-1)^n \int q_0 r^{2n} \mathbf{dr}, \\ F_2 = \frac{1}{\mu_0} \sum \frac{q^{2n}}{(2n+1)!} (-1)^n \int \mu_0(r) r^{2n} \mathbf{dr}. \end{cases}$$

Nelle ipotesi fatte, che cioè a μ_0 contribuisca, oltre alla nuvola pionica, una distribuzione di carica e corrente di dimensioni molto piccole rispetto a λ_π , e quindi alla lunghezza d'onda dell'elettrone incidente, si ha

$$\mu_0 \simeq \int \mu(r) \mathbf{dr}, \quad \int \mu_0 r^{2n} \mathbf{dr} \simeq \int \mu(r) r^{2n} \mathbf{dr},$$

in cui $\mu(r)$ è la densità di carica mesonica. Analogamente, per $q_0(r)$ si può introdurre in F_1 la densità di carica della nuvola pionica calcolata in precedenza.

Va rilevato che il procedimento di approssimazione seguito è certamente giustificabile dalle considerazioni di carattere intuitivo fatte prima per energie sino a 200 MeV dell'elettrone diffuso (tenuto conto del possibile contributo di mesoni K). È presumibile che con elettroni di energia molto maggiore (ad esempio di 1000 MeV) le cose vadano diversamente per la possibilità che si renda sensibile l'esistenza di distribuzioni di carica non pionica.

Va però tenuto conto di una limitazione assai più notevole alla interazione

fra elettrone e campo pionico virtuale, derivante dalla natura analitica di $\varrho(r)$ e di $\mu(r)$. Riseriviamo le equazioni (1) e (5) per la densità di carica nella forma:

$$(11) \quad \varrho(r) = \int_0^{K_0} \varrho'(k) j_1^2(kr) dk,$$

ove $\varrho'(k)$ è la parte dipendente solo da k della densità di carica $\varrho(k, r)$, facilmente deducibile dall'equazione (5). Con la posizione (11), la F_1 diviene

$$(12) \quad F_1 = \int_0^{K_0} \varrho'(k) dk \int_0^\infty j_1^2(kr) \exp[iq\mathbf{r}] d\mathbf{r} = \frac{2\pi^2}{q} \int_0^{K_0} \varrho'(k) \frac{dk}{k} \int_0^\infty \sin qr J_{\frac{3}{2}}^2(kr) dr,$$

avendo introdotto (previa inintegrazione nella parte angolare di \mathbf{r}) le funzioni di Bessel $J_{1+\frac{1}{2}}(kr)$ in luogo delle funzioni sferiche di Bessel ($j_n(kr) = (\pi/2kr)^{\frac{1}{2}} J_{n+\frac{1}{2}}(kr)$).

L'ultimo integrale nella (12) è noto ⁽¹⁰⁾: per $q > 0$ si ha

$$(13) \quad \int_0^\infty \sin qr J_{\frac{3}{2}}^2(kr) dr = (2k)^{-1} (1 - q^2/2k^2) \quad q < 2k$$

$$= 0 \quad q > 2k$$

(il caso $q = 0$ evidentemente non interessa). Dalla (13), integrando la (12) si ricava

$$(14) \quad F_1 = \frac{\pi^2}{q} \int_{q/2}^{K_0} \varrho' \frac{dk}{k^2} \left(1 - \frac{q^2}{2k^2} \right).$$

Una formula analoga si ha esprimendo $\mu(r)$ con una posizione del tipo (11). Se q è piccolo rispetto ad m (perchè k è misurato in unità m) le equazioni (14) e (10) (in cui ci si arresti al termine $n = 1$) praticamente coincidono: per q elevato la cosa cambia. Ad esempio per elettroni di 500 MeV, ad un angolo di scattering di 140° si ha $q/2 = 2.78 m$. Ci si può chiedere se l'eliminazione d'una parte così notevole del range K_0 d'integrazione sia ammissibile con un uso corretto della teoria a sorgente fissa.

A proposito di ciò va osservato che la limitazione espressa dalla (11) non è legata al fatto che, alle basse energie, lo scattering mesone-nucleone è in netta prevalenza dovuto a mesoni nello stato p : infatti si ha in

genere ⁽¹⁰⁾)

$$(15) \quad \int_0^{\infty} \sin qr J_{n+\frac{1}{2}}^2(kr) = (2k)^{-1} P_n(1 - q^2/2k^2) \quad q < 2k$$

$$= 0 \quad q > 2k$$

con $P_n(z)$ polinomi di Legendre di grado n . In più integrando la (11) in \mathbf{r} , da

$$\int_0^{K_0} \varrho(r) d\mathbf{r} - 2\pi^2 \int_0^{K_0} \varrho' \frac{dk}{k^2} = q_m,$$

si rileva subito che nel calcolo di F_1 non sono introdotti colla (14) fattori che possono alterare la convergenza dell'integrale (14) rispetto al calcolo usuale di F_1 : anzi il termine additivo (in $q^2/2k^2$) rende più plausibile il cut-off alle elevate energie.

Si può spiegare la forte riduzione di F_1 e di F_2 alle elevate energie dell'elettrone diffuso come conseguenza di un fenomeno d'interferenza: per essa, non possono contribuire allo scattering dell'elettrone i mesoni d'impulso minore di $q/2$, se q è l'impulso (nel sistema del laboratorio) che l'elettrone può ricevere dal protone.

Il calcolo dei fattori F_1 ed F_2 a partire dalla (11) e da una posizione analoga per la densità di momento magnetico, riesce abbastanza comodo e forse più attendibile, ad energie elevate, di quello che si può fare integrando numericamente le equazioni (9) nelle coordinate spaziali. Questo perchè anche piccoli errori nel valore di $\varrho(r)$ e di $\mu(r)$, a distanze piccole, possono portare ad errori sensibili. È già in corso la determinazione della sezione d'urto per elettroni d'energie comprese fra i 300 e i 1000 MeV integrando la (14).

Per elettroni di 188 MeV il calcolo della sezione d'urto è stato effettuato dallo sviluppo (11) arrestato al terzo termine; $\sigma(\vartheta)$ cade entro i limiti degli errori

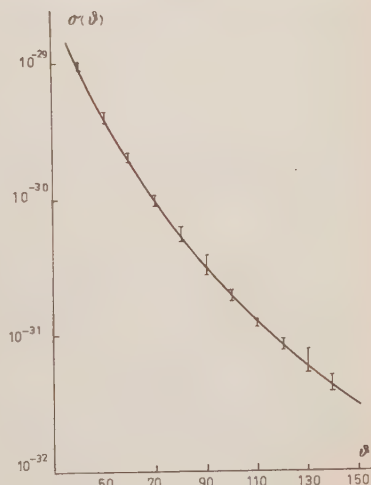


Fig. 3.

⁽¹⁰⁾ A. ERDÉLYI (editor): *Tables of Integral Transforms* (New York, 1954), vol. I, pag. 102, num. 23.

sperimentali. La sezione d'urto per l'elemento di matrice (8) è

$$\sigma(\vartheta) = \sigma_{MR} \left[F_1^2 + \frac{q^2}{4M^2} (2[F_1 + \mu_0 F_2]^2 \operatorname{tg}^2 \frac{\vartheta}{2} + \mu_0^2 F_2^2) \right],$$

con: σ_{MR} sezione d'urto di Mott-Rayleigh, corretta per il recoil del protone

q è la variazione d'impulso della particella incidente (nel sistema baricentrale),

M indica la massa protonica.

I risultati sono sintetizzati nel grafico della Fig. 3: ivi sono anche riportati i dati sperimentali di McALLISTER e HOFSTADER.

Osservazione. — CLEMENTEL e VILLI (*Nuovo Cimento*, **4**, 1207 (1956)) hanno recentemente comunicato che i dati della teoria a sorgente fissa non sono sufficienti per un calcolo preciso della sezione d'urto di elettroni la cui energia E sia superiore ai 200 MeV. L'errore rilevato da questi autori (del 35% ad angoli elevati, per $E = 550$ MeV) è forse eccessivo: però, anche il metodo precedente — più preciso di quello usato dai predetti autori — non dà risultati soddisfacenti per 200 MeV. CLEMENTEL e VILLI propongono di tener conto di un termine additivo al potenziale coulombiano del protone, sensibile a distanze molto piccole dal protone. Presumibilmente l'errore in questione può essere eliminato tenendo conto del contributo che il campo mesonico K dà all'interazione fra campo elettromagnetico e protone: ciò, almeno, fino ad $E = 800$ MeV.

* * *

Ringrazio sentitamente il prof. M. CINI per le discussioni e gli utili schiarimenti fornitimi sul problema trattato.

APPENDICE I

La tecnica di MIYAZAWA porta a risultati coincidenti a quelli dati da FUBINI per le espressioni di $\varrho(\mathbf{r})$, $\mathbf{j}(\mathbf{r})$ e $\mu(\mathbf{r})$.

Si indichi con

$$(A.1) \quad \varphi_{km}(\mathbf{r}) = N(k) j_1(kr) Y_1^m(\vartheta, \varphi)$$

la generica funzione d'onda del campo mesonico pseudoscalare. k indica l'impulso del mesone, m ($= \pm 1, 0$) è ora il numero quantico magnetico: la teoria a sorgente fissa usa solo le onde del campo pionico per cui è $l = 1$, e tale

numero quantico è sottinteso. Gli operatori di campo sono in corrispondenza alla (A.1):

$$(A.2) \quad \begin{cases} \varphi(\mathbf{r}) = \sum_{k,m} \varphi_{km}(\mathbf{r}) (2\omega_k)^{-\frac{1}{2}} [a_{km} + (-1)^m b_{k-m}^*] \\ \pi(\mathbf{r}) = \sum_{k,m} \varphi_{km}^*(\mathbf{r}) (\omega_k/2)^{\frac{1}{2}} [a_{km}^* - (-1)^m b_{k-m}], \end{cases}$$

essendo a_{km}^* , b_{km}^* operatori di creazione dei campi pionici positivo e negativo rispettivamente.

Usando, — con MIYAZAWA — la particolare diagonalizzazione di Sachs ⁽¹¹⁾ si ottiene, per la densità di corrente, l'espressione (a meno del fattore e , carica del protone):

$$(A.3) \quad \varrho(\mathbf{r}) = i[\pi^* \varphi^* - \pi \varphi] = \sum_{km} N^2 j_1^2(kr) Y_1^m(\Gamma_1^m)^* [a_{km}^* a_{km}^* - b_{km}^* b_{km}].$$

Dalle proprietà del sistema ortonormale di funzioni d'onda (del continuo) $j_1(kr)$ è noto che $N^2 = 2k^2/\pi$.

I valori medi

$$(A.4) \quad \langle a_{km}^* a_{km} \rangle, \quad \langle b_{km}^* b_{km} \rangle,$$

con $m = \pm 1$ sono noti dal lavoro di MIYAZAWA. Per quanto riguarda i termini (A.4) con $m = 0$, nella hamiltoniana d'interazione protone-pione, i coefficienti di $a_{k0}^* a_{k0}$, $b_{k0}^* b_{k0}$ sono

$$(A.5) \quad \tau_- \sigma_3 \cdot \tau_+ \sigma_3, \quad \tau_+ \sigma_3 \cdot \tau_- \sigma_3$$

rispettivamente.

Tali fattori (coefficienti di Clebsch-Gordon) sono simmetrici in σ e τ , per cui

$$\tau_i \sigma_k \cdot \tau_e \sigma_k = \sigma_i \tau_k \cdot \sigma_e \tau_k.$$

I coefficienti (A.5) sono, nell'hamiltoniana d'interazione, fattori dei termini $c_{k1}^* c_{k1}$ e $c_{k-1}^* c_{k-1}$ rispettivamente (c_{km}^* sono operatori di creazione del campo pionico neutro). Per tale motivo $a_{k0}^* a_{k0}$ e $b_{k0}^* b_{k0}$ si possono calcolare dai valori medi $\langle c_{k1}^* c_{k1} \rangle$ e $\langle c_{k-1}^* c_{k-1} \rangle$. In tal modo si ottiene, con le espressioni date da MIYAZAWA per i valori medi dei diversi prodotti di operatori di creazione-distruzione, la formula (5) per $\varrho(r)$. L'espressione della densità di momento magnetico è deducibile direttamente da quella del momento, data da MIYAZAWA.

⁽¹¹⁾ G. SACHS: *Phys. Rev.*, **87**, 1100 (1952); G. SACHS e S. TREIMAN: *Phys. Rev.*, **103**, 435 (1956).

APPENDICE II

Recentemente ⁽¹²⁾ MÖLLERING, ZEMACH, KLEIN e LOW, studiando la struttura iperfina dello spettro idrogenico, sono riusciti a stabilire che se $f(r)$ è una funzione di distribuzione (radiale) del momento magnetico protonico e se

$$(B.1) \quad \int f(r) dr = 1,$$

allora è possibile determinare con dati spettroscopici l'estensione media del momento magnetico del protone. Infatti da questi dati risulta che

$$(B.2) \quad r = \int r f(r) dr \leq 2.5 \hbar / Mc$$

(\hbar / Mc è la lunghezza d'onda Compton del protone).

Nella (B.2) si può sostituire la densità di momento magnetico pionico, omettendo il contributo di campi prossimi all'origine. La (B.2) diviene

$$(B.3) \quad r = \frac{1}{2.793} \int \mu(r) r dr \simeq 1.21 \lambda_\pi.$$

I dati della struttura iperfine coincidono come ordine di grandezza con quelli calcolati in precedenza: secondo il calcolo fatto a partire dai dati della Tabella I, il fattore 2.5 nella (B.2) andrebbe maggiorato di un fattore ~ 3 . Va però osservato che il calcolo di MÖLLERING *et al.* non può essere molto esatto. D'altra parte, r è circa costante sia che si calcoli da $\mu_1(r)$ che da $\mu_2(r)$; la medesima cosa si può dire del momento magnetico totale μ_m della nuvola protonica che, calcolato dai dati della Tabella I (integrando numericamente), fornisce i seguenti risultati:

$$(B.4) \quad \begin{cases} \mu_m = 1.61 & K_0 = 5 m \\ - 1.69 & K_0 = 6 m. \end{cases}$$

Anche il calcolo di μ_m fatto da MIYAZAWA dà oscillazioni non indifferenti. Per quanto riguarda la (B.3) è però possibile asserire un netto disaccordo fra il risultato di MÖLLERING e quello che si può avere dalla teoria a sorgente fissa.

⁽¹²⁾ W. M. MÖLLERING, A. C. ZEMACH, A. KLEIN e F. LOW: *Phys. Rev.*, **100**, 441 (1955).

SUMMARY

Starting from the fixed source theory we calculate the charge density of the pion cloud surrounding the proton and its magnetic moment. These densities enable one to determine the differential cross-section for electrons scattered elastically from the proton. That is done for 188 MeV electrons. For higher energy electrons a useful formula is given, taking into account that, in this case, a little part only of the pion field contributes to the scattering.

Fast Neutron Component in Photonuclear Reactions (*).

F. FERRERO, L. GONELLA, R. MALVANO, C. TRIBUNO and A. O. HANSON (+)

Istituto di Fisica dell'Università - Torino

Istituto Nazionale di Fisica Nucleare - Sezione di Torino

(ricevuto il 22 Novembre 1956)

Summary. — In this work are given preliminary results about the fast photoneutron component in many elements with special attention to Al, Cu, Ag, Ba, Au and Bi.

The study of photonuclear reactions, except for the case of deuterium and berillium, where the threshold is particularly low, developed together with the development of the electron accelerators (betatron, synchrotron, linear accelerator, etc.) which yield rather intense beams of bremsstrahlung X-rays whose energy is easily variable from few MeV to their maximum values.

The preliminary experimental results, clearly demonstrated an extraordinary similarity in the behaviour of the different nuclides: all of them present a certain opacity to the electromagnetic radiations limited to a rather narrow region of the γ -ray spectrum (giant resonance) the characteristics of which change continuously with the mass number A .

Besides these preliminary experimental results seemed to support the assumption that also photonuclear reactions should be described by a two step process, as proposed by N. BOHR for the other types of nuclear reactions: the giant resonance should be explained on the basis of a γ -ray absorption by a collective nuclear motion which results in a general nuclear heating and subsequent decay via the statistical model of the nucleus.

(*) Work presented at the Conference of the Ital. Physical Society (Turin, 6-12 September, 1956).

(+) University of Illinois (U.S.A.).

For the validity of such an explanation of the giant resonance, the following three conditions, concerning the reaction products, should have, however, to be satisfied:

- 1) the reaction products should come out isotropically;
- 2) the ratio between the proton and neutron yields should be particularly low, specially for heavy nuclei;
- 3) the neutron spectrum in the heavy elements should have only an extremely low fraction of fast neutrons ($> 5 \div 6$ MeV).

In this case the experimental study of the photonuclear reactions would consist only in the measurement of the absorption cross-sections as a function of the γ -ray energy and of the nuclear parameters A , N , Z ; directly or through the measurement of the yields of the reaction products which would come in only as experimental means to investigate the behaviour of the absorption cross-sections.

Experimental results indicated, however, that the proton-neutron yield ratio is many orders of magnitude greater than required by the evaporation theory; besides the angular distribution and the spectrum of the reaction products disagree markedly from the above stated conditions. *In particular the fast neutron group has been found to be rather important and coming out anisotropically* ^(1,2).

To overcome these difficulties, more recent theoretical work has been done where the giant resonance is considered as arising from the enhanced electric dipole transitions from the upper shell states to unfilled states in the continuum ⁽³⁾.

In order to see if this point of view is born out experimentally we tried to answer, at least qualitatively, the following questions which were not clearly answered in earlier experimental work.

— Has the fast neutron group the same giant resonance as that for the total neutron spectrum?

— Is the angular distribution of the fast neutrons consistent with that expected in the single particle model?

— Is the observed fraction of fast neutrons consistent with the assumption that the absorption of the photons results in a single particle transition?

We shall see from our experimental results, which we shall briefly comment, that these three questions can be answered, with some qualifications, in the affirmative.

(1) B. A. PRICE: *Phys. Rev.*, **93**, 1279 (1954).

(2) F. FERRERO: A. O. HANSON, R. MALVANO and C. TRIBUNO: *Nuovo Cimento*, **4**, 418 (1956).

(3) D. H. WILKINSON: *Nuclear Photodisintegration, International Conference on Nuclear Reactions*, Amsterdam (1956).

Experimental Method and Results.

Cylinders, 2 cm in diameter and 2 cm thick, of the elements under investigation were placed in a collimated X-ray beam from a 31 MeV B.B.C. betatron. The spread of the electron energy is estimated to be of the order of 0.3 MeV. The beam was monitored by a parallel plate ionization chamber connected to an electrometer, with about 5 cm of aluminium converter in front of the chamber.

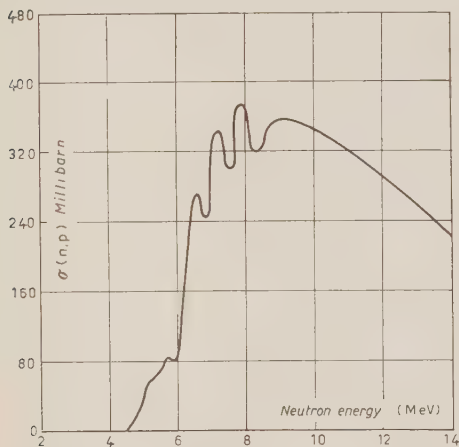


Fig. 1.

The fast photoneutron flux was measured by the neutron induced activity in silicon samples placed near the irradiated element. In this work it was found to be convenient to use the silicon samples in powder form and to pour the powders, immediately after the irradiation, into the jacket of a Geiger

counter adapted for counting liquids. The observed activity is the 2.4 min activity from the $^{28}\text{Si}(n, p)^{26}\text{Al}$ reaction, which has an effective threshold of about 5 MeV. The measured silicon (n, p) cross-section is shown in Fig. 1.

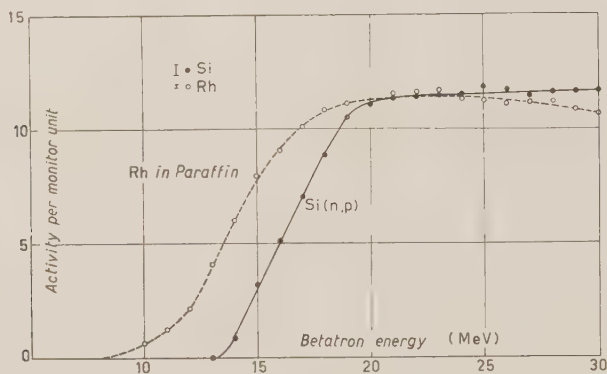


Fig. 2.

Fig. 2 shows the excitation functions for bismuth in which may be seen the total neutron excitation function measured with a rhodium slow neutron

detector as well as the (n, p) detector yield curve. It can be easily seen that the knees of the total neutron and of the fast neutron yields are placed quite at the same energy.

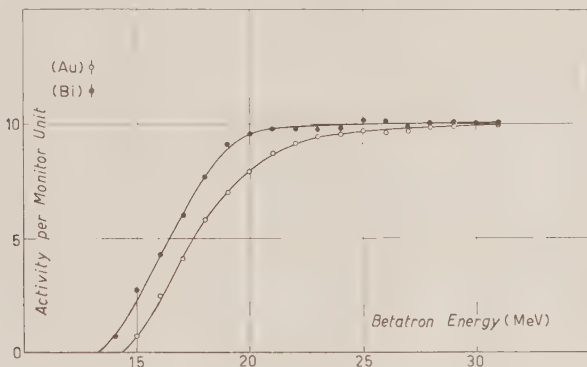


Fig. 3.

Fig. 3 shows the fast neutron yield of gold, as measured by Si, compared with the one of bismuth; Fig. 4 shows these same curves for the case of barium and silver. One can easily see the different width of the giant resonances of bismuth and barium compared with gold and silver respectively. As a matter

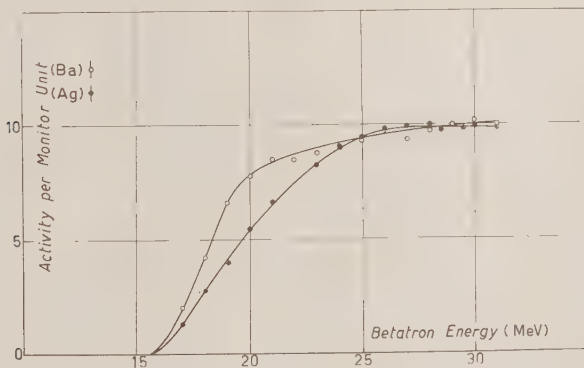


Fig. 4.

of fact the latter elements are magic in neutron number while the former are not. This experimental evidence was already known and has been further emphasized by our measurements. However, we note the different behaviour of barium and bismuth after the knees of the fast neutron yield curves: in

barium we have a continuous increase of the neutron yield while in bismuth the excitation function stays quite constant.

This increase of the fast neutron yield outside the giant resonance is clearly shown also by copper, whose excitation function is given in Fig. 5 together

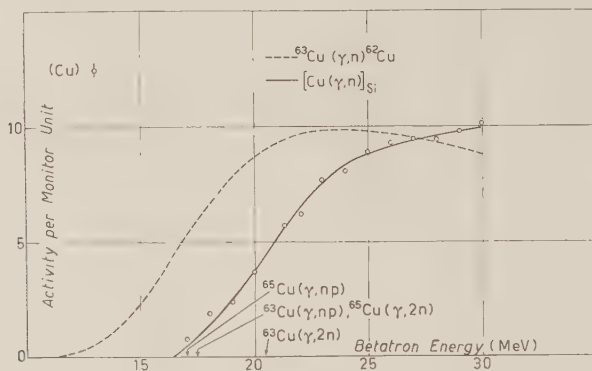


Fig. 5.

with the residual activity yield in the $^{63}\text{Cu}(\gamma, n)^{62}\text{Cu}$ photonuclear reaction. Fig. 6, finally, presents the aluminum case where the knee of the curve may scarcely be identified. The slope of the fast neutron yield in the region of the

giant resonance is not very much greater than that above this region.

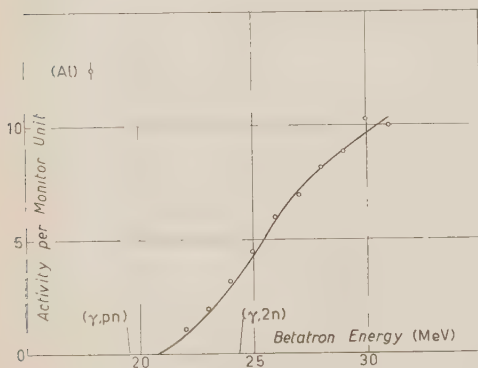


Fig. 6.

The excitation functions we have shown indicate that the fast neutrons are produced predominantly by photons in the region of the giant resonance giving further experimental evidence that the giant resonance can be attributed to strong individual particle transitions rather than a collective type of photon absorption. The same excitation functions indicate,

however, that a certain fraction (greater for low A) of fast neutrons are produced outside the giant resonance by a somewhat different direct process (for example the quasi deuteron model).

Fig. 7 shows a typical angular distribution of fast neutrons observed in bismuth. This experimental angular distribution can be represented, also in

the other elements we have studied, by a function of the type $1 + a \sin^2 \theta + b \cos \theta$, where b (much smaller than a) describes a small forward component, the existence of which is now very well established, but not clearly understood.

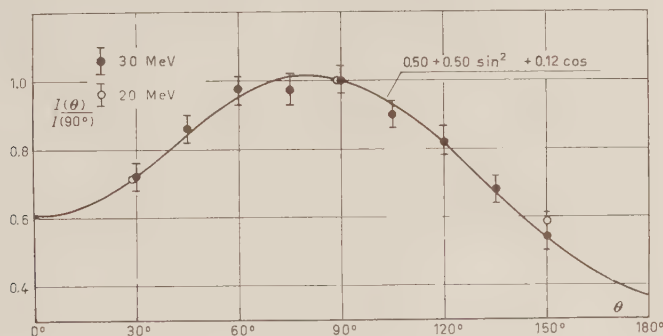


Fig. 7.

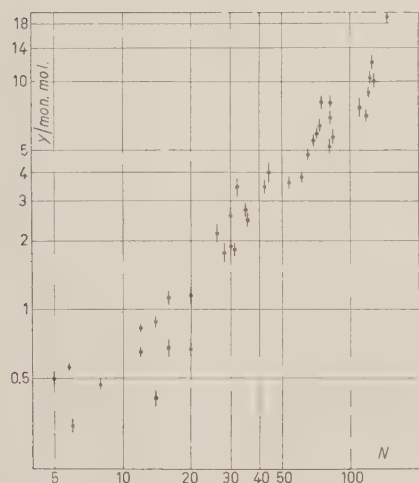


Fig. 8.

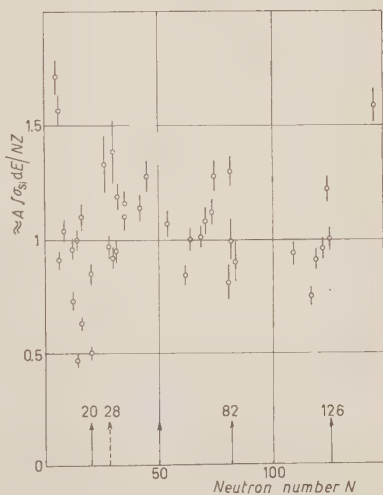


Fig. 9.

Fig. 8 presents the fast neutron yields, at 30 MeV, of about 40 elements plotted against their neutron number. A rough proportionality between the above two quantities is clearly detectable. Deriving from the yields the integrated cross-sections, normalized to the «sum rule» factor NZ/A , we get Fig. 9, where these quantities are plotted as a function of the neutron number. These values seem to be rather constant throughout the entire table

of the elements, rising however in the neighborhood of the neutron magic numbers 50, 82, 126. For very light elements this regularity is less evident.

To account for the fast neutron yields in the framework of the single particle model, we point out, limiting the discussion to medium and heavy nuclei, that only the electric dipole transitions from the upper neutron shells are effective, since directly excited protons have very small probability of penetrating the coulomb barrier and contribute only to the evaporative process.

The fraction of neutrons escaping directly without interaction with the rest of the nucleus can be expressed as $F = \Gamma_n / (\Gamma_n + \Gamma_a)$ where Γ_n is the width for neutron emission and Γ_a is the corresponding width for the absorption of the simple neutron state into a general excitation of the nucleus. As a rough approximation for Γ_n one may use the relation $3\hbar v T_{1n}/R$, where v is the neutron velocity, R is the conventional nuclear radius and T_{1n} is the transmission of

the angular momentum barrier. Γ_a is calculated with the quasi optical model taking into account the dependence of the imaginary part of the complex potential on the excitation above the Fermi energy.

The calculations for the specific case of bismuth and the values obtained for the fraction of fast neutrons F and for the anisotropy parameter a in the angular distribution are given in a previous work. These same calculations have been done for Al, Cu, Zr, Ag, Ba and Ta and the values of the fraction F as a function of the neutron number are given in

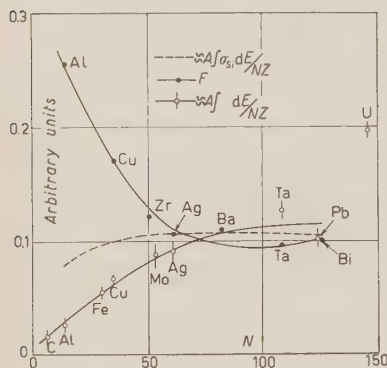


Fig. 10.

Fig. 10 together with the normalized integrated cross-sections from the work of TERWILLIGER and JONES⁽⁴⁾. The product of the above two quantities, i.e. the calculated fast neutron integrated cross-sections (normalized), is given as a dotted line. It seems to describe quite well, the average behaviour of the experimental values given in Fig. 9.

⁽⁴⁾ L. W. JONES and K. M. TERWILLIGER: *Phys. Rev.*, **91**, 699 (1953).

RIASSUNTO

In questo lavoro si riportano alcuni risultati preliminari sulla componente neutronica veloce nelle reazioni fotonucleari studiata in molti elementi ed in special modo nell'Al, Cu, Ag, Ba, Au e Bi.

NOTE TECHICHE

Level Flights with Expansible Balloons.

J. E. LABY, Y. K. LIM and V. D. HOPPER

Physics Department, University of Melbourne

(ricevuto il 6 Settembre 1956)

Summary. — Single rubber or neoprene ballons have been used to obtain level flights at altitudes in the region 80 000 – 105 000 feet to expose nuclear emulsion plates to cosmic radiation. String operated valves have been developed and a comparison is made of the performance of various sizes of rubber and neoprene ballons. On some flights a clock released a load after the balloon had levelled off and for these the new ceiling height has been investigated.

1. — Introduction.

The main object of these flights was to expose nuclear emulsion plates to cosmic rays, the pay load being of the order of 2 kg. The ideal flight is one in which the balloon rises rapidly to a high altitude which it maintains for a known time.

Methods available include the use of large non-expansible plastic balloons (General Mills ⁽¹⁾, DAVIES and FRANZINETTI ⁽²⁾), multiple balloons (sometimes as a combination of expansible and non expansible ones) (DEMERS ⁽³⁾) and single expansible balloons fitted with a valve mechanism (DARBY *et al.* ⁽⁴⁾, BARFORD *et al.* ⁽⁵⁾). The last method was used as most suitable for the project as flights could then be carried out at least expense by a small group.

Flights have been made with rubber and neoprene balloons of various sizes. On some of these two packets of plates were flown, one packet being jettisoned

⁽¹⁾ GENERAL MILLS AERONAUTICAL LABORATORIES: *Technical Data* (1951).

⁽²⁾ J. DAVIES and C. FRANZINETTI: *Nuovo Cimento*, **12**, 480 (1954).

⁽³⁾ P. DEMERS: *Can. Journ. Phys.*, **31**, 366 (1953).

⁽⁴⁾ J. F. DARBY, V. D. HOPPER, J. E. LABY and A. R. W. WILSON: *Austr. Journ. Phys.*, **6**, 471 (1953).

⁽⁵⁾ N. C. BARFORD, G. DAVIS, A. J. HERZ, R. M. TENNENT and D. A. TIDMAN: *Journ. Atm. Terr. Phys.*, **5**, 219 (1954).

after a predetermined time chosen to give a good chance of recovery, the other remaining with the balloon which then ascended to a new level, thus getting additional exposure but with less chance of recovery.

The principle of the method for obtaining level flights has been described previously (DARBY *et al.* ⁽⁴⁾, BARFORD *et al.* ⁽⁵⁾). It consists of a string

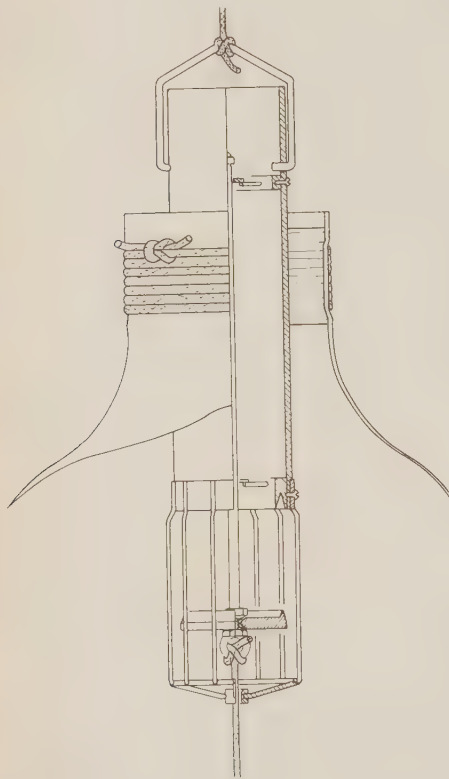


Fig. 1-a. - Recent design of valve for use with 800 g - 2400 g rubber or neoprene balloon.

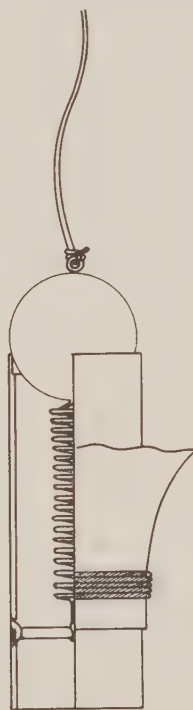


Fig. 1-b. - Simple valve used with 300-800 g balloons.

operated mechanical valve fitted in the neck of the balloon which is opened to release excess gas at a predetermined diameter. One end of the string is attached to the lid of the valve and the other end connected to a rubber cork fixed inside the balloon diametrically opposite the neck. When the balloon is at ground level the excess string is loosely wound around the neck of the valve. Two recent designs of valves are shown in Fig. 1a and Fig. 1b. The wire cage shown in Fig. 1a prevents the string from catching under the bevelled edge of the valve lid. This type of valve is preferred for large balloons where a long length of string is required.

2. - Principle of Method.

The heights at which the valve opens and the balloon levels can be estimated. Assuming the gas law, the pressure p_1 (gwt cm⁻²) at the height h_1 (cm) corresponding to the first opening of the valve is given by (BARFORD *et al.* (5)).

$$(1) \quad p_1 = \frac{G_1}{(\rho_A - \rho_g)} \frac{T_1}{T_g} \frac{p_g}{V_h} \quad p_g,$$

where G_1 is the gross lift (gwt) (sum of weight of balloon, free lift and pay load).

ρ_A and ρ_g are the densities of air and gas in balloon at ground level, (g cm⁻³).

T_1 , T_g the temperatures of the gas inside the balloon at height h_1 and at ground level respectively (°K).

p_g the atmospheric pressure at ground level (gwt cm⁻²).

V_h the volume of the balloon at height h_1 (cm³).

p_g the excess pressure inside the balloon at pressure p_1 (gwt cm⁻²).

After the valve opens the balloon continues to rise to the height h_2 , where the valve closes and the balloon levels. The new gross lift G_2 at the level height is equal to the weight of the balloon plus pay load and also

$$G_2 = G_1 + F,$$

where F is the free lift given to the balloon at ground level.

The pressure p_2 of the air at the level height h_2 is given by

$$(2) \quad p_2 = \frac{G_2}{G_1} p_1 \quad (*)$$

(*)

$$G_1 = V_h \rho_A^1 - m_1$$

$$G_2 = V_h \rho_A^{11} - m_2$$

where ρ_A^1 , ρ_A^{11} are the densities of air at heights h_1 and h_2 (g cm⁻³);

m_1 , m_2 are the masses of the gas in the balloon at ground level and height h_2 respectively (g).

But

$$\frac{\rho_A^1}{\rho_A^{11}} = \frac{p_1 T_2^1}{p_2 T_1^1}$$

where T_1^1 and T_2^1 are the external temperatures of the air at heights h_1 and h_2 , and

$$\frac{m_2}{m_1} = \frac{T_1 (p_2 + p_g)}{T_2 (p_1 + p_g)},$$

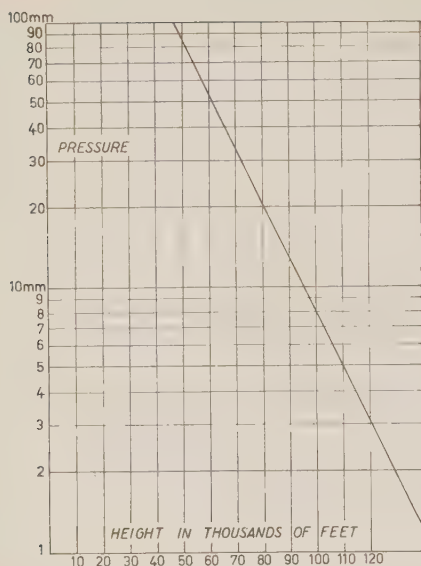
T_1 and T_2 being the temperatures of the gas in the balloon at heights h_1 and h_2 .

From these

$$G_2 = G_1 \frac{T_1^1}{T_2^1} \frac{p_2}{p_1} + V_g \rho_g \left\{ \frac{p_2 T_1^1}{p_1 T_2^1} - \frac{T_1 (p_2 + p_g)}{T_2 (p_1 + p_g)} \right\},$$

The second term on the right hand side of this equation is usually small and can be neglected. Also as T_1^1 and T_2^1 are approximately equal, then

$$p_2 = \frac{G_2}{G_1} p_1.$$



From the value of p_1 we can obtain the height h_1 at which the valve opens from the altitude-pressure curve (Fig. 2). Similarly the height at which the balloon levels is obtained from p_2 of equation (2). We see that using a string of length just below the bursting diameter of the balloon, the height h_2 of level flight is greater than the bursting height ($\sim h_1$) of a similarly loaded balloon without valve but having the same initial free lift. This is due to the fact that with the valve operated

Fig. 2. — Altitude pressure curve used for heights above 50000 ft (Data to 80000 ft from BROMBACKER⁽⁶⁾ extrapolated to higher altitudes).

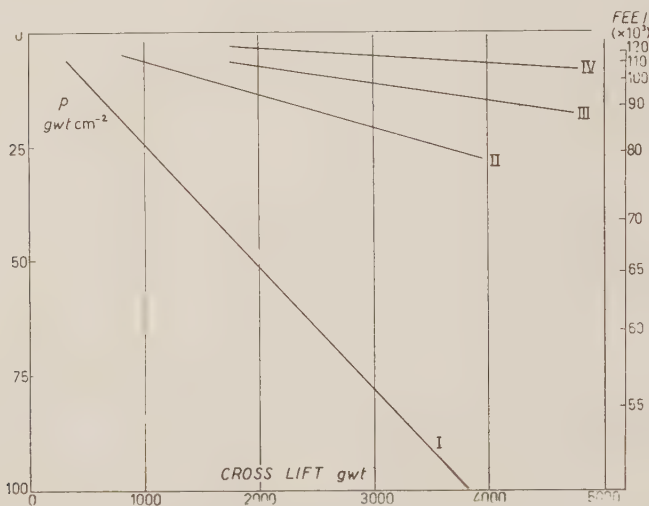


Fig. 3. — Graphs showing heights reached by balloons for varying gross lifts.

- I 300 g balloon with 3.8 m (12'6") string
- II 800 g balloon with 6.1 m (20') string
- III 1750 g balloon with 7.6 m (25') string
- IV 1750 g balloon with 9.8 m (32') string.

⁽⁶⁾ W. G. BROMBACKER: *National Advisory Committee for Aeronautics*, Report No. 538 (1938).

balloon, the gas which provided the free lift has escaped enabling the balloon to rise to a greater altitude for the same diameter. The increase in height from h_1 to h_2 is greatest for small balloons with low loads (see Fig. 3) when, it is noted, F does not vary greatly for fixed rate of ascent, with size of balloon. The valve method is thus suitable for cosmic ray studies which involve high altitude level flights and where the load is limited to one or two kilograms. For general meteorological studies such as wind velocity determinations the valve operated balloon is useful particularly when it is remembered that the rate of ascent can be increased without affecting the ceiling height. Thus on days when there may be jet winds, a greater amount of gas can be used to provide the free lift provided the valve has been suitably chosen.

Finally, if some of the load included in G_2 is removed so as to reduce the gross lift to G_3 , the balloon will ascend to a new pressure level p_3 given by:

$$p_3 = \frac{G_3}{G_2} p_2.$$

This result is important as it predicts the new height reached by the balloon when part of the apparatus is jettisoned by clock-work after a predetermined time of flight.

3. - Measurement of T_1 and p_σ .

To determine p_1 (from equation (1)) and hence p_2 (from equation (2)) it is necessary to know T_1 the internal temperature of the gas in the balloon when the valve opens and also the excess pressure p_σ . These were determined as follows:

An estimate of T_1 was made by BARFORD *et al.* ⁽⁵⁾ from a laboratory experiment and it was concluded that T_1 was about 270 °K. It was however possible to measure T_1 directly during a flight. To do this, a resistance element of a radiosonde was placed in the neck of the valve of the balloon. When the valve opened during flight the temperature of the gas issuing from the balloon was thus measured. The results of two separate flights made recently in conjunction with the Commonwealth Meteorological Branch at latitude 38° are given in Table I.

TABLE I.

Flight	Date	Time valve opened (h)	h_1 (ft)	T_1 (°K)	T_1^1 (°K)
1	5-7-56	16 15	70 000	228	216
2	19-7-56	12 40	90 000	238	226

T_1 has been corrected for adiabatic cooling (order of 1 °K) and T_1^1 for the influence of solar radiation on the radiosonde temperature reading.

A series of measurements of the excess pressure p_σ inside various rubber and neoprene balloons have been made during inflation in the laboratory.

Curves relating the measurements of excess pressure with balloon diameter are shown in Fig. 4. It will be noted that the excess pressure p_σ inside a neoprene balloon for a certain diameter is much less than that for a rubber balloon of the same diameter.

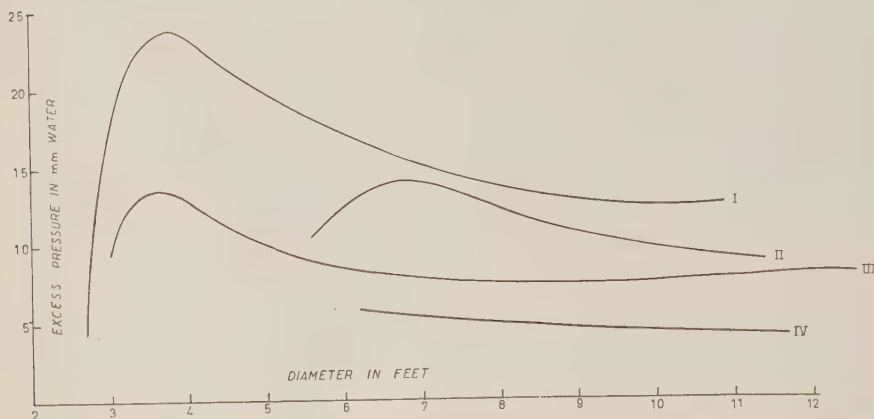


Fig. 4. — Excess pressure inside balloons during inflation. I Rubber 350 g; II Rubber 1250 g; III Neoprene 300 g; IV Neoprene 800 g.

4. — Results of Flights.

Assuming the following values

$$\begin{aligned}
 p_\sigma &= 1.035 \text{ gwt cm}^{-2}, \\
 T_1 &= 233^\circ \text{K} & \epsilon_A &= 1.22 \cdot 10^{-3} \text{ g cm}^{-3}, \\
 T_g &= 290^\circ \text{K} & \epsilon_B &= 8.5 \cdot 10^{-5} \text{ g cm}^{-3},
 \end{aligned}$$

equation (1) gives

$$p_1 = (14.1 \cdot 10^5 G_1/d^3) - p_\sigma \text{ (gwt cm}^{-2}\text{)},$$

where d cm is the length of the string used.

Actual performances of two neoprene balloons types J8-18-800 and J7-24-1750 (Darex) are shown in Fig. 5 and compared with calculated performances (see Table II). Also included in Table II are the pressure levels reached by a valve operated 300 g neoprene balloon.

Reasonably close agreement between the calculated and measured results was obtained considering the assumptions made. In the case of the 300 g balloon, the balloon would need to attain a diameter of 20 feet to reach the height of 95 000 feet if no valve was used and this is well above the normal bursting diameter of such balloons. Thus using valve operated 300 g balloons and radar, one can determine wind velocities up to altitudes of 95 000 feet. On clear days when theodolites can be used and the radar target is no longer necessary, heights of the order of 102 000 feet should be reached. The simple

light valve, shown in Fig. 1*b*, spring loaded so that it remains closed even when inverted and weighing only 60 g, has been devised for this purpose. It

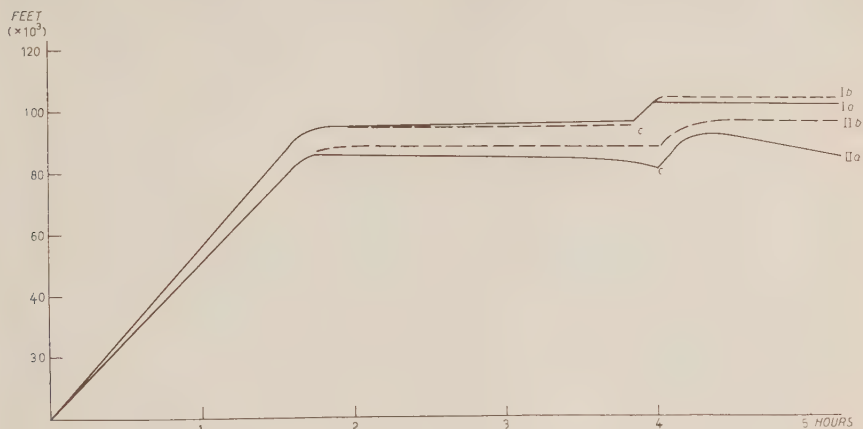


Fig. 5. — Comparison of calculated and observed performances by balloons.

Ia Observed record for 1750 g neoprene balloon with 7.6 m (25') string.

Ib Calculated curve for flight.

IIa Observed record for 800 g neoprene balloon with 6.1 m (20') string.

IIb Calculated curve for flight: at *C* the clock released 1 kg load and balloon rose to new level.

TABLE II. — Pressure levels reached by valve operated balloons.

Weight of balloon kg . .	0.30	0.80	1.75
<i>d</i>	3.8 m (12'6")	6.10 m (20')	7.6 m (25')
p_{σ} gwt cm ⁻²	0.8	0.4	0.4 "
G_1 kg	1.75	3.8	4.75
G_2 kg	0.60	2.8	3.75
G_3 kg	—	1.8	2.75
p_1 (calc.) gwt cm ⁻² . . .	43.8	23.1	15.2
p_2 { (calc.) gwt cm ⁻² . . .	15.1	17.0	12.0
(obs.) gwt cm ⁻² . . .	11.1	19.5	12.9
p_3 { (calc.) gwt cm ⁻² . . .	—	11.8	8.3
(obs.) gwt cm ⁻² . . .	—	14.3	8.9
h_1 (calc.) feet	68 000	82 000	91 000
h_2 { (calc.) feet	92 000	89 000	96 000
(obs.) feet	95 000	86 000	95 000
h_3 { (calc.) feet	—	98 000	105 000
(obs.) feet	—	93 000	103 000

consists of a $1\frac{1}{2}$ " diameter aluminium tube 4" long inserted in the neck of the balloon. The valve top consists of a ping pong ball which is held against the edge of the aluminium tube by a light spring. With the neoprene balloons (Darex) a flaw is sometimes seen in the rubber at the point opposite the neck.

It has been the practice to connect the cork so as to cover this flaw as occasionally a hole occurs in this rough section when the balloon is placed in hot water prior to flight. If a hole occurs at this point the rubber is then tied

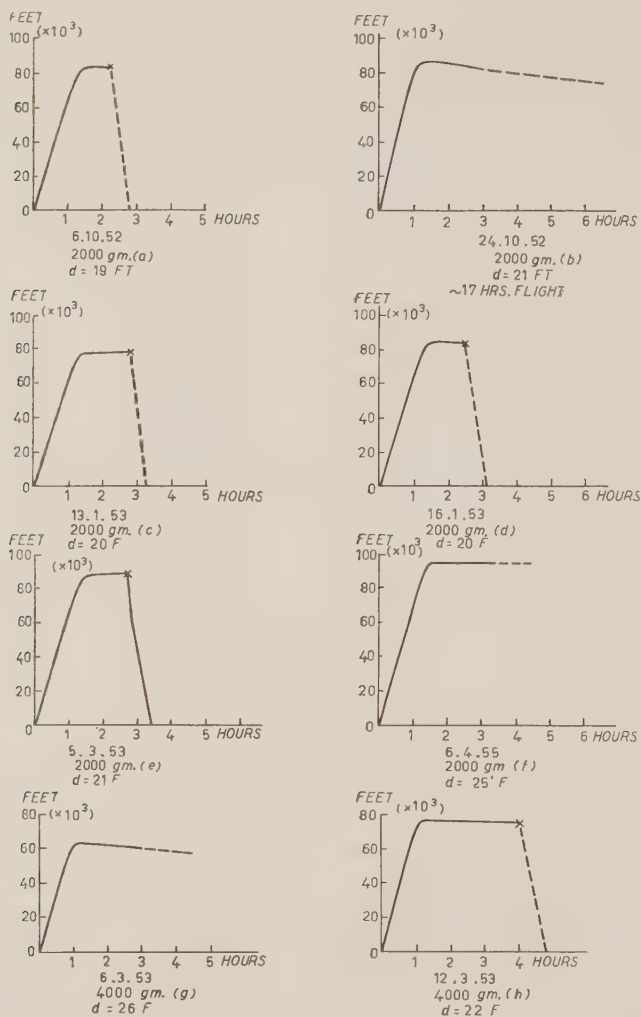


Fig. 6. - Record of level flights using 2000 and 4000 g rubber balloons.

together above the cork. Balloons treated in this way behave normally as the damaged or weak section does not undergo strain during flight.

A number of flights have been made with rubber and neoprene balloons and simultaneous observations were taken whenever possible using two theo-

dolites separated by a base line of about 4 miles. Some of these flights are shown in Figs. 6 and 7. It will be observed that the rubber balloons often burst within two hours of levelling. Of 29 rubber balloons flown, thirteen did

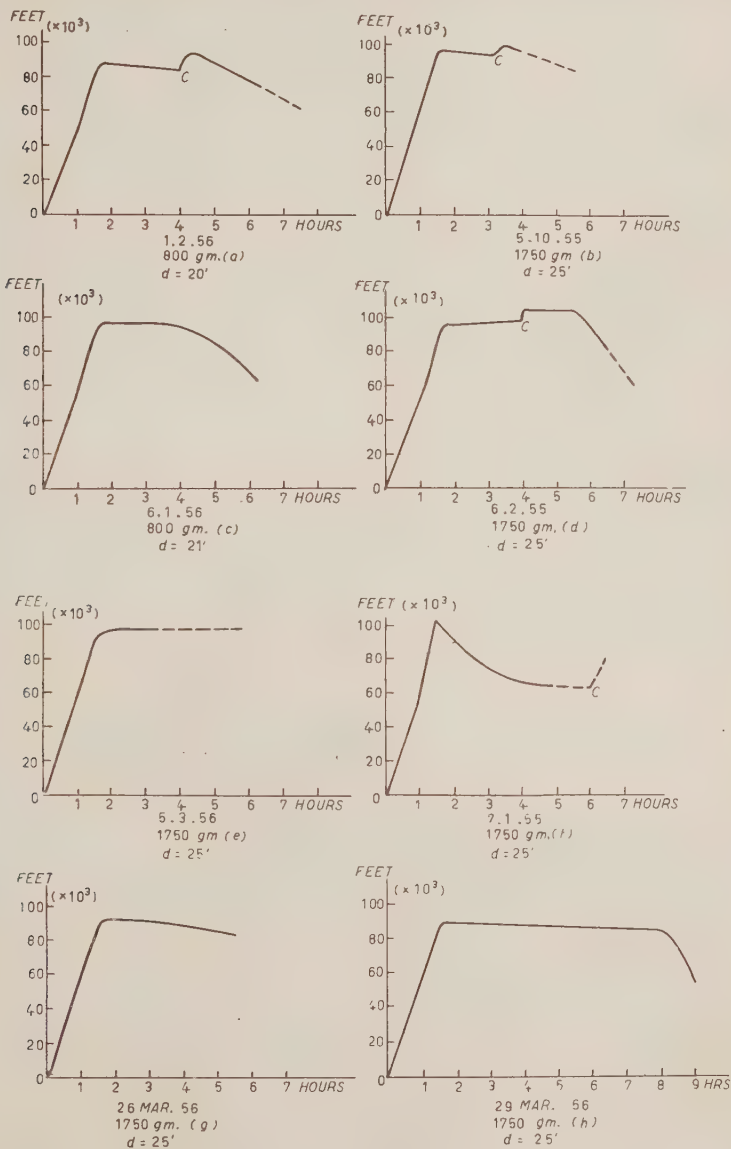


Fig. 7. — Record of level flights using neoprene balloons. At C a clock released part of the load.

not reach their levelling height which was set at about 90 000 feet. Of 20 neoprene balloons, only three burst before levelling. For these the levelling height was pre-set at about 100 000 feet and they reached heights of 105 000, 97 000 and 103 000 feet respectively. The reason for the low height of the 4000 g rubber balloon (Fig. 6g) was probably due to the string becoming entangled and operating the valve at a much smaller length than the 26 feet set.

Using an earlier type of valve, a number of balloons descended immediately after reaching their maximum height and this effect was either due to the balloon overshooting the levelling height and thus letting out too much gas or due to the valve not sealing effectively. Later valves were designed to give a greater rate of escape of gas during operation as well as more effective seating when the ceiling height was reached, and these flights were more successful. An interesting feature was observed in some of these earlier flights and is best illustrated by the flight shown in Fig. 7f. After reaching a maximum height, the balloon started to fall at a velocity of 500 feet min^{-1} , but this rate of descent decreased with time and was almost zero at 65 000–70 000 feet. Other neoprene balloon flights showed a less marked but definite decrease in rate of descent with height. This could be attributed to a gradual rise of temperature of the gas in the balloon. All level flights that have been studied near sunset show that at about this time the balloon starts to descend due to the temperature of the gas in the balloon cooling to the external temperature.

In some cases, see Figs. 7a and 7b, the balloon descended slowly after a few hours at level height and then on jettisoning the first packet of plates went to a new ceiling height, but soon descended at about the same rate as previously. A possible explanation of this behaviour is that holes had developed in the balloon as on some recovered balloons circular holes have been observed.

A summary of the flights using the valve technique is given in Table III where a comparison is made of the 2000 g rubber, the 800 g neoprene, and the 1750–2400 g neoprene balloon flights.

TABLE III. — *Comparison of balloon performances.*

	Rubber (*) 2000 g	Neoprene (×) 800 g	Neoprene (×) 1750-2400 g
Total number of observed flights . .	29	7	13
Level flights exceeding 2 hours . . .	3	3	6
Level flights not exceeding 2 hours .	6	0	0
Number reaching levelling height but descending soon afterwards with ve- locity > 250 ft/min	7	2	4
Number bursting before levelling . .	13	2	1
Flights without valve	0	0	2
Mean level flight height	82 000'	97 000'	95 000'
Mean string length	22'	20'	25'
Mean payload	2 kg	2 kg	2 kg
Mean maximum height	80 000'	98 000'	98 000'
Number recovered	21	4	11

(*) Beritex rubber balloons (Guide Bridge Co. Bury, England).

(×) Darex neoprene balloons (Demey e Almy, Mass., U.S.A.).

This comparison shows that using this valve method rubber balloons are less reliable than neoprene ones for the following reasons:

1) A large proportion burst before reaching levelling height which in any case was set much lower than for neoprene balloons.

2) Of the few that did reach levelling height the majority burst after an hour or two of level flight, whereas all the neoprene balloons that reached levelling height survived until observations ceased, usually several hours later. This difference in behaviour may be due to the lower excess pressure inside the neoprene balloons as compared with rubber ones under the same conditions.

We conclude from this investigation that it is possible with comparatively cheap valve operated neoprene balloons to obtain flights exceeding four or five hours at 90 000 to 100 000 feet. All the long flights described in this paper were observed with a pair of theodolites at a fixed base and this limited the duration of observations to a maximum of nine hours, but for several flights the total time at high altitude was considerably longer than this as was deduced from the recovery points of balloons.

* * *

We wish to acknowledge the help of Mr. W. L. THOMAS, Mr. G. BRIANT and other members of the laboratory who have assisted with balloon flights. Members of the Commonwealth Meteorological Branch and the Supply Department have readily assisted when required. This research has been supported by a grant from the Nuffield Foundation.

RIASSUNTO (*)

Si sono usati palloni isolati di gomma o di isoprene per eseguire voli orizzontali ad altezze fra gli 80 000 ÷ 105 000 piedi onde esporre alla radiazione cosmica pacchi di emulsioni nucleari. Si sono messe a punto valvole a comando funicolare e si fa un confronto del comportamento dei palloni di gomma e di isoprene di differenti dimensioni. In alcuni voli un orologio liberava un peso dopo di che il pallone si era stabilizzato in quota e si è ricercato per questi la nuova quota di plafond.

(*) Traduzione a cura della Redazione.

Arrêt de la diffusion des radio-éléments dans les émulsions nucléaires par exposition a basse température.

M. DEBEAUVAIS (*), E. PICCIOTTO et S. WILGAIN

Laboratoire de Physique Nucléaire - Université Libre de Bruxelles

(ricevuto il 17 Ottobre 1956)

Resumé. — On montre que la diffusion des radioéléments dans les émulsions nucléaires peut être arrêtée par l'action de la basse température. On n'observe plus d'effet de diffusion du Radon à -85°C et du Tn à -36°C . A ces températures respectives, la répartition observée entre étoiles et traces simples correspond à la répartition théorique. Cette méthode permet d'utiliser le phénomène caractéristique de la formation des étoiles pour mesure de très faibles quantités de radioéléments.

1. — Introduction.

Une propriété caractéristique de la technique des émulsions photographiques nucléaires est la possibilité d'enregistrer les désintégrations successives d'un seul atome, sous la forme d'une « étoile » de trajectoires issues d'un même point ⁽¹⁾. Ce phénomène peut être utilisé pour la mesure de très faibles quantités de certains radio-éléments, notamment du Thorium ^(2,3). La probabilité de formation d'étoiles de particules α d'une multiplicité donnée en fonction du temps d'exposition a été calculée pour tous les nuclides radioactifs naturels par SENFTLE *et al.* ⁽⁴⁾ et par d'autres auteurs pour des cas plus particuliers ^(1,5,6).

(*) En congé de l'Institut de Physique, Université de Strasbourg.

(1) H. J. TAYLOR and V. D. DABHOLKAR: *Proc. Ind. Acad.*, **3**, 265 (1936).

(2) E. PICCIOTTO et S. WILGAIN: *Nature*, **173**, 632 (1954).

(3) F. KOCZY, E. PICCIOTTO, G. POULAERT et S. WILGAIN: à paraître dans *Geochim. et Cosmochim. Acta*.

(4) F. E. SENFTLE, T. A. FARLEY et L. A. STIEFF: *Geochim. et Cosmochim. Acta*, **6**, 197 (1954).

(5) R. WESTOO: *Ark. f. Mat., Astr. och Fys.*, **34** B, no. 22, 1 (1947).

(6) R. FLAMENT: *Bull. Centre Phys. Nucl. Univ. Libre Bruxelles*, no. 3 (1948).

Les fréquences des divers types d'étoiles prévues par la théorie ne sont généralement pas confirmées par l'observation à cause de la diffusion des atomes radioactifs dans l'émulsion, amenant la dissociation d'une étoile donnée en étoiles de multiplicité inférieure. Après les premières observations de TAYLOR et DABHOLKAR ⁽¹⁾, plusieurs auteurs ^(5,7-13) ont mis en évidence la diffusion du Rn et Tn et, à un degré moindre, celle de la plupart des membres des trois familles radioactives. Les effets les plus importants sont, comme on peut s'y attendre, dus au Radon qui peut migrer à de grandes distances et sortir de l'émulsion avant de se désintégrer ⁽¹¹⁻¹³⁾.

Ces phénomènes de diffusion soulèvent de grandes difficultés dans les mesures radioactives basées sur la formation d'étoiles. Nous montrons dans le présent travail qu'il est possible de surmonter ces difficultés et d'arrêter toute diffusion des radio-éléments en maintenant les émulsions photographiques à basse température suivant la technique développée par l'un de nous ⁽¹⁴⁾.

Notre but était principalement de mettre au point, dans le cadre de la technique de la double émulsion ⁽¹⁵⁾, la mesure de très faibles quantités de Radium et de Radiothorium en mettant à profit la formation d'étoiles à 4 et à 5 branches à partir de ces nuclides. La principale difficulté de cette mesure réside dans la dissociation de ces étoiles, due à la diffusion du Radon et du Thoron.

2. — Procédés expérimentaux.

On a étudié les étoiles formées à partir du Ra pur et du Th en équilibre. On a utilisé une solution de RaBr₂ récemment purifié contenant $6 \cdot 10^{-11}$ g de Ra et 10^{-5} g de BaCl₂ par ml; le Radon a été chassé par barbotage d'air avant l'emploi. Pour le Th, on a employé une solution de (NO₃)₄Th vieux de plus de 50 ans; la solution contenait par ml, $1,7 \cdot 10^{-8}$ g de Th en équilibre avec tous ses descendants. Les 2 solutions étaient en milieu citrique à pH 7.

A l'aide d'une microseringue, on a déposé des gouttes calibrées de $2 \cdot 10^{-3}$ ml de ces solutions sur des émulsions Ilford C2 et G5 de 100 μ m d'épaisseur, coulées sur un support d'acétate de cellulose pour résister aux basses températures ⁽¹⁴⁾. Après 2 h de séchage, les gouttes de solution ont été recouvertes d'une goutte d'émulsion liquide Ilford. Cette seconde couche d'émulsion a été séchée en

⁽⁷⁾ M. BLAU et H. WAMBACHER: *Sitzber. Akad. Wiss. Wien, Math. naturw. Klasse, Abt. II a*, **145**, 9, 605 (1936).

⁽⁸⁾ P. DEMERS: *Phys. Rev.*, **72**, 536 (1947).

⁽⁹⁾ H. YAGODA: *Radioactive Measurements with Nuclear Emulsions* (New York, 1949).

⁽¹⁰⁾ G. G. EICHHOLZ et F. C. FLACK: *Journ. Chem. Phys.*, **19**, no. 3, 363 (1951).

⁽¹¹⁾ E. FROTA-PESSOA: *An. Acad. Bras. Ciencias*, **25**, no. 4, 337 (1953).

⁽¹²⁾ W. SCHNEIDER et T. MATITSCH: *Sitzber. österr. Akad. Wiss. Math. naturw. Klasse, Abt. II a*, **161**, 4, 131 (1952).

⁽¹³⁾ L. VIGNERON, R. CHASTEL et J. GENIN: *Compt. Rend.*, **236**, 2053 (1953); *Proc. of the Science and Appl. of Photography*, **445** (1954); *Journ. Phys. Radium*, **14**, 28 (1953); *Compt. Rend.*, **240**, 1423 (1955).

⁽¹⁴⁾ M. DEBEAUVAIS-WACK: *Nuovo Cimento*, **10**, 1590 (1953).

⁽¹⁵⁾ E. PICCIOTTO: *Compt. Rend.*, **228**, 2020 (1949).

quelques heures. Les plaques ont été ensuite maintenues à des températures contrôlées à $\pm 1^\circ\text{C}$, variant de -85°C à 18°C . Après des expositions de 6 à 27 jours, les plaques ont été développées dans un révélateur à l'amidol et à l'acide borique suivant la méthode à deux températures ⁽¹⁶⁾.

Toutes les trajectoires d' α émises dans le volume délimité par la double couche d'émulsion ont été comptées.

3. - Résultats.

On a calculé d'après ⁽¹⁾ les nombres théoriques de traces simples et d'étoiles, ces nombres ont été comparés aux nombres observés pour chaque température d'exposition.

3.1. *Radium*. - Les résultats concernant le Ra sont reportés aux tableaux I et II. Le nombre de désintégrations du Ra est donné par la somme des traces simples et des étoiles à 4 branches, quels que soient les effets de la diffusion du Rn.

Dans les émulsions exposées à $+18^\circ$, 0° et -25° , on constate par rapport aux prévisions théoriques, un excès de traces simples et d'étoiles à 3 branches et un défaut d'étoiles à 4 branches. Cette situation est clairement expliquée

TABLEAU I. - *Radium* - Répartition théorique des traces simples et des étoiles et répartitions observées aux diverses températures d'exposition. Temps d'exposition: 7 jours.

Température	— 85°	— 25°	0°	+ 18°
Nombre de désintégrations du Ra	1 218	532	571	2 177
$\alpha \begin{cases} \text{th} \\ \text{ob} \end{cases}$	$\begin{matrix} 738 \\ 758 \end{matrix}$	$\begin{matrix} 277 \\ 447 \end{matrix}$	$\begin{matrix} 296 \\ 485 \end{matrix}$	$\begin{matrix} 1\,132 \\ 1\,863 \end{matrix}$
$E_2 \begin{cases} \text{th} \\ \text{ob} \end{cases}$	$\begin{matrix} 0 \\ 0 \end{matrix}$	$\begin{matrix} 0 \\ 7 \end{matrix}$	$\begin{matrix} 0 \\ 4 \end{matrix}$	$\begin{matrix} 0 \\ 12 \end{matrix}$
$E_3 \begin{cases} \text{th} \\ \text{ob} \end{cases}$	$\begin{matrix} 0 \\ 12 \end{matrix}$	$\begin{matrix} 0 \\ 173 \end{matrix}$	$\begin{matrix} 0 \\ 113 \end{matrix}$	$\begin{matrix} 0 \\ 128 \end{matrix}$
$E_4 \begin{cases} \text{th} \\ \text{ob} \end{cases}$	$\begin{matrix} 480 \\ 460 \end{matrix}$	$\begin{matrix} 255 \\ 85 \end{matrix}$	$\begin{matrix} 274 \\ 86 \end{matrix}$	$\begin{matrix} 1\,045 \\ 314 \end{matrix}$

α = traces simples
 E_n = étoile de multiplicité n

th = théorique
ob = observé

⁽¹⁶⁾ C. C. DILWORTH, G. OCCHIALINI et L. VERMAESEN: *Bull. Centre Phys. Nucl. Univ. Libre Bruxelles*, no. 13 a (1950).

par la diffusion du Rn amenant la dissociation de l'étoile à 4 branches: Ra - Rn - Ra A - (Ra B - Ra C -) Ra C' - Ra D en une trace simple et une étoile à 3 branches. On trouve également quelques étoiles à 2 branches dont la probabilité de formation est théoriquement nulle; elles sont généralement accompagnées, à quelques microns de distance, d'une trace simple ou d'une autre étoile à 2 branches. La combinaison $E_2 + \alpha$ correspond à la dissociation de E_3 par diffusion du RaB ou du RaC (¹¹). La combinaison $E_2 + E_2$ ne peut s'expliquer que par la diffusion du RaA, malgré la courte durée de vie de ce nucléide. Rappelons que DEMERS (⁸) a observé la diffusion du ThA dont la période est encore plus courte.

Dans les émulsions exposées à -85° , la situation est toute différente; la concordance est excellente entre les prévisions théoriques et l'expérience. Le léger excès d'étoiles à 3 branches qui subsiste peut être attribué au Rn incomplètement chassé et aux diffusions qui ont eu lieu pendant le séchage et le développement.

On peut en conclure qu'à -85°C , la diffusion du Radon et des autres éléments est complètement arrêtée.

De la comparaison des résultats théoriques et expérimentaux, on peut estimer les proportions de Rn fixé, déplacé et sorti de l'émulsion; elles sont présentées au Tableau II.

TABLEAU II. — Sort des atomes de Radon produits et désintégrés pendant le temps d'exposition.

	-85°	-25°	0°	18°
% Rn non déplacé	> 96	33	31	30
% Rn déplacé de moins de $50\ \mu\text{m}$	0	27	8	2
% Rn déplacé de plus de $50\ \mu\text{m}$	< 2	40	35	12
% Rn sorti de l'émulsion	0	0	26	56

A $+18^\circ$, 0° et -25° , une fraction constante (environ 30%) du Rn produit et désintégré pendant l'exposition ne diffuse pas ou migre de moins de $1\ \mu\text{m}$. VIGNERON *et al.* (¹³) trouvent le même ordre de grandeur tandis que FROTA-PESSOA (¹¹) ne trouve que 4%. SCHNEIDER et MATITSCH (¹²) trouvent que 78% du Rn ne diffuse pas dans des émulsions traitées à l'alcool. La proportion du Rn fixé doit dépendre fortement de l'état de la gélatine de l'émulsion (¹³).

Les résultats du Tableau II montrent que l'amplitude de la migration est de plus en plus réduite lorsque la température est abaissée et qu'elle devient pratiquement nulle à -85° .

3.2. *Thorium*. — Les résultats concernant le Thorium en équilibre sont reportés au Tableau III. Le nombre théorique de chaque type d'événement a été calculé d'après la quantité de Th présent.

Dans les émulsions exposées à $+18^\circ$ et 0° , on remarque une discordance considérable entre la théorie et l'observation. Cette discordance est principalement due à la diffusion du Thoron amenant la scission des étoiles à 5 branches du RdTh en étoiles à 2 et à 3 branches. On a également observé, mais

beaucoup plus rarement, les diffusions d'autres radioéléments signalées par DEMERS (*). Cette diffusion est pratiquement arrêtée à -36° . Des essais plus rapides conduits à -85° montrent les mêmes résultats qu'à -36° .

TABLEAU III. — *Thorium. Répartition théorique et observée des étoiles.*

Température	-36°	0°	$+18^\circ$
Exposition	27 jours	27 jours	9 jours
$x \begin{cases} \text{th} \\ \text{ob} \end{cases}$	<div>397 419</div>	<div>430 473</div>	<div>481 562</div>
$E_2 \begin{cases} \text{th} \\ \text{ob} \end{cases}$	<div>0 4</div>	<div>0 130</div>	<div>0 63</div>
$E_3 \begin{cases} \text{th} \\ \text{ob} \end{cases}$	<div>0 7</div>	<div>0 164</div>	<div>4 129</div>
$E_4 \begin{cases} \text{th} \\ \text{ob} \end{cases}$	<div>74 85</div>	<div>80 56</div>	<div>163 110</div>
$E_5 \begin{cases} \text{th} \\ \text{ob} \end{cases}$	<div>256 239</div>	<div>278 140</div>	<div>141 67</div>

On peut déduire du Tableau III que 45 % du Tn produit à 18° et à 0° ont subi un déplacement perceptible ($> 1 \mu\text{m}$) tandis que moins de 2 % du Tn produit à -36° s'est déplacé.

On peut aussi montrer que la migration du Tn dans les émulsions à 0° et $+18^\circ$ est insuffisante pour permettre au Tn de s'échapper de l'émulsion avant de se désintégrer.

En conclusion, nous avons confirmé que toute méthode de dosage basée sur la formation d'étoiles doit tenir compte des effets de diffusion des radioéléments, principalement du Rn et du Tn (*). *Il est possible d'arrêter complé-*

(*) Dans la publication de FROTA-PESSOA ⁽¹¹⁾, on lit que des méthodes de titration basées sur la formation d'étoiles ont été utilisées dans un travail de BEGEMAN *et al.* ⁽¹⁷⁾, sans tenir compte des effets de diffusion. Les faits auxquels se réfère FROTA-PESSOA occupent 4 lignes dans un travail de 34 pages consacré à un tout autre sujet, et concernent l'estimation d'un ordre de grandeur d'une contamination en Ra.

Il semble difficile de désigner cette estimation sous le terme de « titration ». De plus, nous avons approximativement tenu compte des pertes par diffusion, mais le sujet était trop accessoire pour insister sur des détails connus de tous les chercheurs familiarisés avec la technique des émulsions nucléaires. (Note de E.P.).

⁽¹⁷⁾ F. BEGEMAN, H. V. BUTTLAR, F. HOUTERMANS, N. ISAAC et E. PICCIOTTO: *Bull. Centre Phys. Nucl. Univ. Libre Bruxelles*, no. 37 (1952); *Geochim. et Cosmochim. Acta*, **4**, 21 (1953).

tement la diffusion du Rn en exposant les émulsions à -85° tandis que le Tn est pratiquement immobilisé à -36° . Les applications au microdosage du Th seront publiées prochainement.

On pourrait se baser sur la diffusion du Rn et du Tn pour étudier les variations des propriétés de la gélatine en fonction de la température suivant la méthode utilisée par EICHHOLZ et FLACK⁽¹⁰⁾. Notons cependant que le modèle utilisé par ces auteurs semble trop simplifié. Le fait que les proportions d'atomes formés, ayant diffusé de moins de $1\text{ }\mu\text{m}$, sont du même ordre pour le Rn et le Tn (dans les mêmes conditions expérimentales), alors que leur vie moyenne est dans un rapport de $5 \cdot 10^3$, confirme que tous les atomes de Rn ne sont pas dans les mêmes conditions, et, qu'une fraction n'est pas libre de diffuser et reste fixée dans l'émulsion⁽¹¹⁻¹³⁾ par un processus encore mal défini.

Note ajoutée en cours d'impression.

Alors que cet article était sous presse, nous avons pris connaissance d'une nouvelle détermination de la période du ^{232}Th par R. L. MACKLIN et H. S. POMERANCE (*Journ. Nucl. Energy*, 2, 243 (1956)). Ces auteurs trouvent $T = 1.45 \cdot 10^{10}$ ans avec une incertitude de $\pm 3.5\%$.

RIASSUNTO (*)

Si mostra come la diffusione dei radioelementi alle emulsioni nucleari può essere arrestata dall'azione della bassa temperatura. Non si osserva più alcun effetto di diffusione del Radon a -85°C e del Tn a -36°C . A tali temperature la ripartizione osservata tra stelle e tracce semplici corrisponde alla ripartizione teorica. Questo metodo permette d'utilizzare il fenomeno caratteristico di formazione delle stelle per la misura di debolissime quantità di radioelementi.

(*) Traduzione a cura della Redazione.

Apparato per misure standard di scambio isotopico del deuterio fra idrogeno e vapor d'acqua a pressione atmosferica e a 100 °C.

M. SILVESTRI e N. ADORNI

Laboratori CISE - Milano

(ricevuto il 22 Ottobre 1956)

Riassunto. — Si descrive un apparato per la misura dello scambio isotopico del deuterio fra idrogeno e vapor d'acqua, particolarmente previsto per prove di lunga durata sui catalizzatori. Si sono prese precauzioni per evitare il più possibile l'inquinamento del gas e dell'acqua e si sono adottati vari accorgimenti per rendere sicuro il funzionamento ed evitare una continua sorveglianza. Le misure della concentrazione del deuterio nell'idrogeno possono essere eseguite in due modi: per termoconduttività, direttamente sul gas, oppure col metodo del galleggiante sull'acqua ottenuta dalla combustione dell'idrogeno con ossigeno. La frazione di equilibrio raggiunta (β) è presa come misura della capacità scambiante del catalizzatore ed è determinata con una precisione dell'ordine di $\pm 5\%$.

1. — Premessa.

Da alcuni anni nei nostri Laboratori usiamo apparati per esperienze standard di scambio isotopico fra idrogeno e vapor d'acqua, particolarmente previsti per prove di lunga durata sui catalizzatori che sono efficaci per promuovere tale reazione di scambio, in modo da poterne seguire il comportamento nel tempo ⁽¹⁾.

Ci sembra interessante fare oggetto della presente nota la descrizione dell'ultima versione di tale apparecchiatura da noi realizzata, la quale dati i vari accorgimenti adottati, è adatta a funzionare continuamente anche per parecchie centinaia di ore richiedendo solo saltuariamente l'intervento degli operatori per le misure, la ricarica dell'acqua di alimentazione e la sostituzione di tubi di assorbimento a silicagel, e conserva il più possibile puri fino allo scambio isotopico l'acqua ed il gas impiegati.

⁽¹⁾ B. BRIGOLI e E. CERRAI: *Proc. Symp. Heavy Water Prod.* (Roma, 1955), p. 99.

2. - Fondamenti teorici.

È ben noto che, quando una reazione di scambio del deuterio fra idrogeno gas e vapor d'acqua coinvolge concentrazioni in deuterio sufficientemente basse come quelle sempre da noi impiegate ($< 2 : 3\%$) si possono considerare praticamente assenti le specie molecolari D_2 e D_2O e l'unica reazione di scambio praticamente presente è descritta dall'equazione:



La cui costante di equilibrio è

$$(2) \quad K_1 = \frac{Q_{HDO} Q_{H_2}}{Q_{H_2O} Q_{HD}},$$

in cui le Q sono le funzioni di ripartizione delle specie molecolari indicate.

K_1 è variabile con la temperatura e il suo valore alle varie temperature è noto ⁽²⁾.

Tutte le espressioni da noi usate sono in concentrazione equivalente (trasferendo cioè le molecole HDO e HD in D_2O e D_2); si sono indicate con X le concentrazioni nel vapore e con X' quelle nel gas.

Se lo scambio avviene totalmente fino all'equilibrio l'equazione del bilancio isotopico è

$$(3) \quad yX'_0 + X_0 = yX'_e + X_e,$$

in cui gli indici 0 e e si riferiscono rispettivamente alle concentrazioni prima dello scambio e a quelle all'equilibrio, e y è il rapporto molare fra idrogeno e vapore

$$(4) \quad y = \frac{\text{Moli}_{(gas)}}{\text{Moli}_{(vapore)}}$$

Se invece lo scambio avviene solo parzialmente e non si raggiunge l'equilibrio:

$$(5) \quad yX'_0 + X_0 = yX' + X.$$

Come termine rappresentativo dell'*efficienza dello scambio* si è assunto il rapporto β fra la quantità di isotopo realmente trasferita e quella da trasferire per raggiungere l'equilibrio. Nel nostro caso, usando come alimentazioni acqua deuterata ed idrogeno a concentrazione in deuterio quasi nulla, il trasferimento di isotopo avviene nel senso di arricchire l'idrogeno, per cui

$$(6) \quad \beta = \frac{X' - X'_0}{X' - X_0}$$

⁽²⁾ E. CERRAI, C. MARCHETTI, R. RENZONI, L. ROSEO, M. SILVESTRI e S. VILLANI: *Chem. Eng. Prog. Symp. Series* 50 (1954), p. 271.

L'efficienza dello scambio β può quindi essere presa anche come misura della capacità scambiante di quel dato campione di catalizzatore nelle condizioni della prova; essa viene da noi determinata misurando le concentrazioni prima dello scambio X'_0 e X_0 e quella dell'idrogeno dopo lo scambio X' .

La concentrazione del gas all'equilibrio X'_e è calcolabile dalla (3) e dalla espressione di K_1 :

$$(7) \quad K_1 = \frac{X_e(1 - X'_e)}{(1 - X_e)X'_e}$$

L'espressione che lega l'efficienza ai dati sperimentali è

$$(8) \quad \beta = \varrho(K_1 + y) \frac{(1 - \varepsilon/\varrho)}{1 - \varepsilon K_1 + K_1(K_1 - 1)X_0(1 + \varepsilon y)^2/(K_1 + y)^2},$$

in cui

$$\varrho = \frac{X'}{X_0}; \quad \varepsilon = \frac{X'_0}{X_0}.$$

Con le basse concentrazioni da noi impiegate e con l'idrogeno prima dello scambio a concentrazione assai prossima a zero, tutto il termine frazionario differisce dall'unità di pochi per cento.

3. - Condizioni sperimentali.

L'idrogeno che viene mandato allo scambio con portate dell'ordine di 2 M/h proviene da un elettrolizzatore in equilibrio isotopico, alimentato con acqua a concentrazione naturale per cui anche l'idrogeno si può considerare a concentrazione dell'acqua naturale ($X'_0 \cong 0.015\%$).

L'acqua che viene immessa nel serbatoio che alimenta l'apparato è a concentrazione prossima all'1%, misurata ogni volta che si effettua una carica. Le portate di alimentazione sono attorno a 2 M/h.

Il rapporto molare fra idrogeno e vapore, y , è ottenuto facendo il rapporto delle portate del gas e dell'acqua che vanno allo scambio.

La temperatura della camera di reazione è di 100 °C, essendo termostata ad acqua bollente ($K_1 = 2.55$).

La concentrazione dell'idrogeno dopo lo scambio X' è misurata in modo continuo ⁽³⁾ in due modi: o misurando con il metodo del galleggiante ⁽⁴⁾ la concentrazione dell'acqua prodotta bruciando il gas con ossigeno, in lieve eccesso rispetto alle proporzioni stechiometriche (10 ÷ 15%), oppure direttamente mediante un analizzatore per termoconduttività ⁽⁵⁾.

⁽³⁾ I. KIRSHENBAUM: *Physical Properties and Analysis of Heavy Water* (New York, 1951), first edition, p. 292 e segg.

⁽⁴⁾ E. CERRAI, C. MARCHETTI e M. SILVESTRI: *Nuovo Cimento*, **9**, 530 (1952).

⁽⁵⁾ M. SILVESTRI e N. ADORNI: *Rev. Sci. Instr.*, **27**, 388 (1956).

4. - Apparato.

Lo schema dell'apparato è rappresentato in Fig. 1, mentre la Fig. 2 ne mostra la realizzazione pratica.

L'idrogeno proveniente dall'elettrolizzatore (elettrolito: soluzione di KOH al 20% — 3 celle in serie — 35 A - 300 W), depurato dalla potassa trascinata,

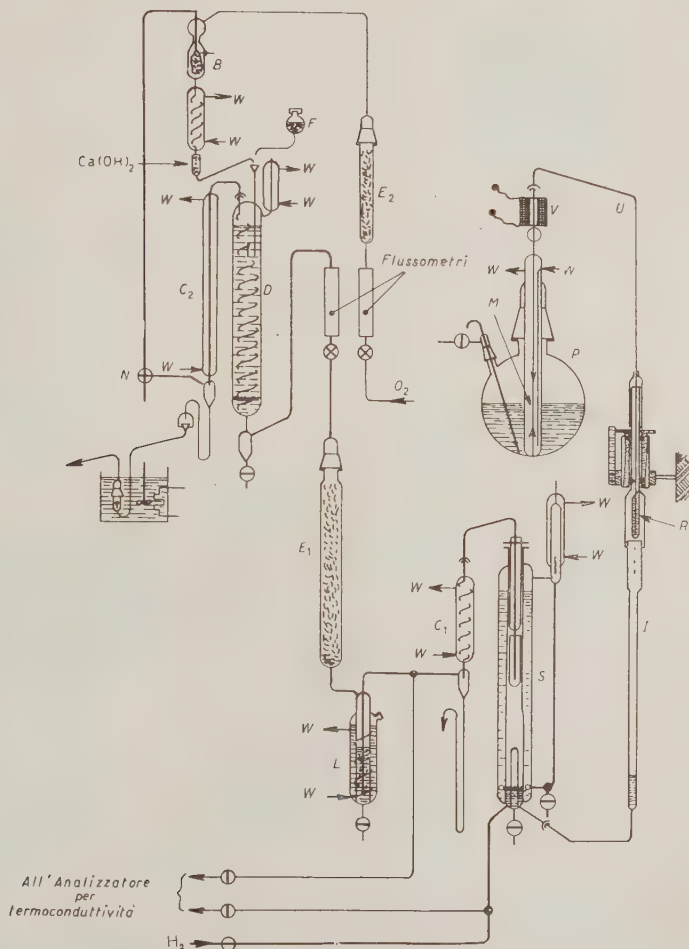


Fig. 1. - Schema dell'apparato: *B*, bruciatore. *C*₁-*C*₂, condensatori. *D*, distillatore. *E*₁-*E*₂, assorbitori a silicagel. *F*, serbatoio con ugello di scarico. *L*, colonnina stabilizzatrice di pressione. *M*, tubo capillare. *N*, rubinetto commutatore. *P*, serbatoio dell'acqua di alimentazione. *R*, tubetto spostabile verticalmente per la regolazione della portata. *S*, elemento scambiante. *T*, tubo di entrata dell'aria in *P*. *U*, sifone. *V*, valvola elettromagnetica.

dalla CO_2 , dall'ossigeno, essiccato con trappola a ghiaccio secco, è condotto all'elemento scambiante *S* con tubi di politene. L'ingresso all'apparecchiatura avviene attraverso un rubinetto di vetro ingrassato con grasso minerale da vuoto.

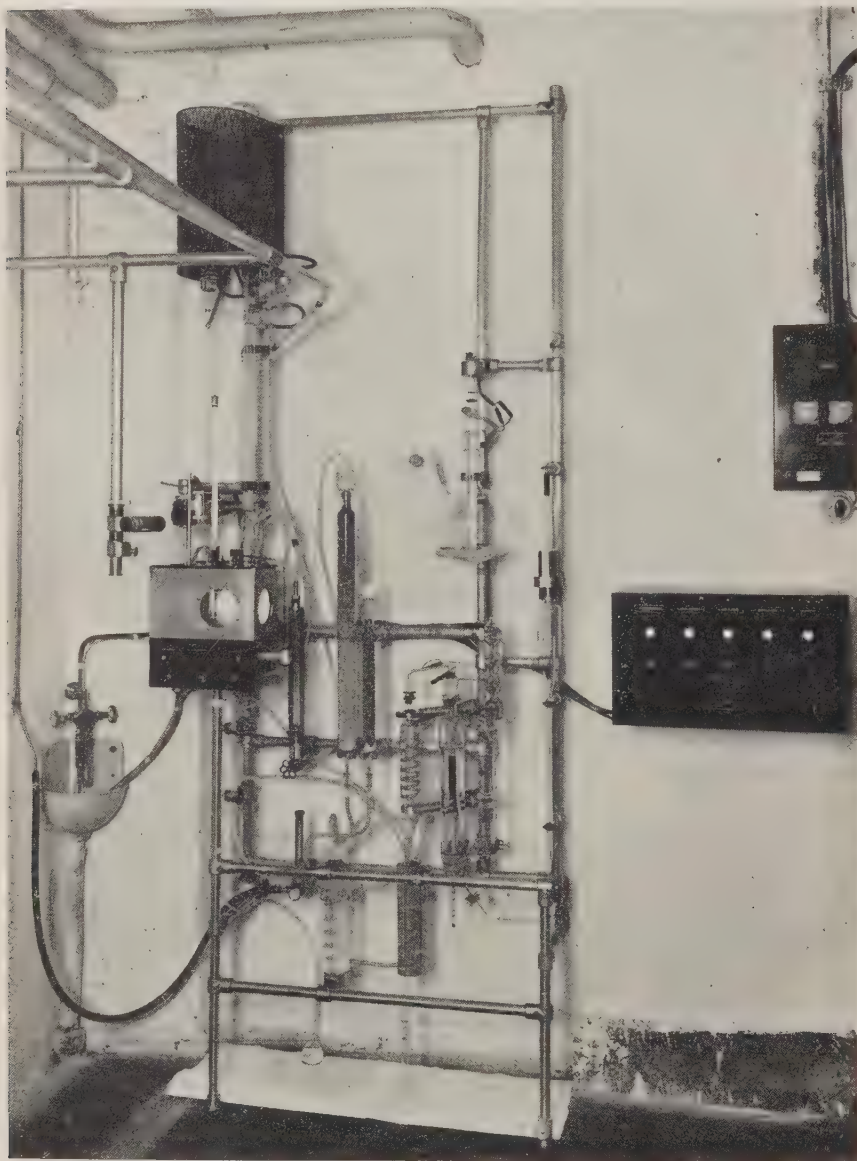


Fig. 2. - L'apparato come è realizzato in pratica.

Immediatamente a monte dell'elemento scambiante, una derivazione, pure di politene, chiusa da un rubinetto identico al precedente, permette d'inviare un piccolo flusso di gas ($\sim 1 \text{ cm}^3/\text{s}$) all'analizzatore per termoconduttività come gas di riferimento. La portata di gas che va allo scambio viene variata e misurata variando e misurando la corrente nell'elettrolizzatore, per controllo si è però inserito nell'apparecchiatura anche un flussimetro.

L'acqua di alimentazione proviene dal pallone *P* (capacità $\sim 3000 \text{ cm}^3$) ed esce attraverso il capillare *M* termostato con camicia ad acqua corrente, che si trova nell'interno del pallone, ed è saldato al cono di chiusura di *P*. Ad *M*, mediante giunto sferico è collegato il tubo *U* la cui estremità pesca in un piccolo recipiente *R* ($\sim 15 \text{ cm}^3$) a forma di provetta; l'acqua da questo tracima nell'imbuto *I* collegato all'elemento scambiante *S* mediante un secondo giunto sferico. *R* può essere alzato ed abbassato e così si può variare la portata: i valori ottenibili, riferiti ad una scala graduata solidale con *R* sono riportati nel grafico di Fig. 3. Si fa notare che la portata non è influenzata dal livello dell'acqua nel pallone poiché esso comunica con l'atmosfera mediante il tubo pescante *T*.

Il caricamento dell'acqua si fa, tolto il tubo *T*, dal cono che collega *T* al pallone.

Il tratto del dispositivo di regolazione della portata in cui l'acqua viene a contatto con l'atmosfera è protetto dal pulviscolo con due campane di vetro.

L'elemento di scambio *S* di vetro pyrex rappresentato in Fig. 4 è costituito da un tubo chiuso nella parte inferiore e termostato con una camicia d'acqua bollente riscaldata da una resistenza immersa, e munita di condensatore a ricadere.

Alla parte inferiore del tubo costituente il saturatore, arrivano l'acqua e l'idrogeno per formare la miscela che deve scambiare.

Nella parte più bassa si è previsto uno scarico chiuso da una sferetta di acciaio inossidabile magnetico posta in una sede conica smerigliata direttamente nel vetro. L'apertura dello scarico è effettuata dall'esterno sollevando la sferetta con un magnete.

La parte superiore di *S* termina con una piccola flangia e la chiusura è effettuata da una seconda flangia che porta, nella parte verso l'interno la camera di reazione di circa 25 cm^3 con diametro 18 mm, e nella parte verso l'esterno un tubo, terminante con giunto sferico, dal quale esce la miscela che ha scambiato. La tenuta è assicurata ingrassando le flange con grasso da vuoto al silicone.

Il tubo di uscita è surriscaldato da una resistenza per evitare condensazioni che potrebbero bagnare il catalizzatore.

Per quanto riguarda la saturazione è da notarsi che l'elemento scambiante

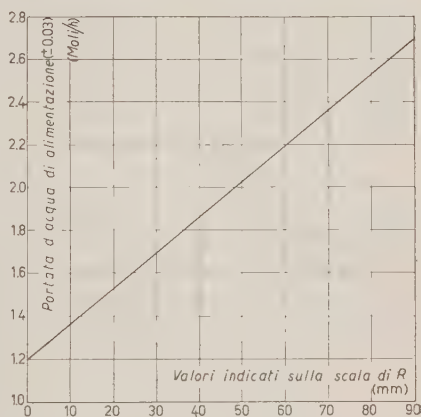


Fig. 3. - Grafico di taratura del dispositivo per la regolazione della portata d'acqua di alimentazione.

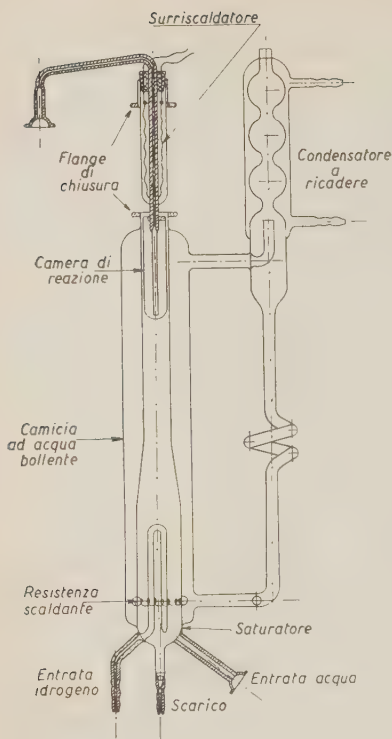


Fig. 4. — Disegno costruttivo dell'elemento scambiante.

una diminuzione della portata d'acqua vale il ragionamento opposto.

Analoghe considerazioni portano a concludere che l'acqua nel saturatore ha un livello di regime per ogni valore della portata dell'acqua di alimentazione e per ogni valore della portata di idrogeno quantunque a quest'ultima il livello sia molto meno sensibile. In pratica con le varie portate da noi impiegate le variazioni di livello sono dell'ordine del centimetro.

La concentrazione isotopica nel vapore, quando il saturatore è a regime, risulta naturalmente eguale a quella di alimentazione.

Il condensatore C_1 (Fig. 1), raffreddato con acqua corrente a 15°C e collegato ad S mediante giunto sferico, effettua la separazione dell'acqua dall'idrogeno dopo lo scambio: l'acqua viene scaricata all'esterno e recuperata, il gas passa attraverso una colonnina stabilizzatrice di pressione L che svincola la pressione nell'elemento di scambio dalle variazioni delle perdite di carico negli apparecchi a valle, viene essiccato in un tubo d'assorbimento a silicagel E_1 , e dopo passaggio attraverso un rotometro attraversa il distillatore D in cui si satura in contro-corrente con l'acqua di combustione proveniente dal ricombinatore B , acqua che condensa in C_2 e sgocciola direttamente nella cameretta per la misura di concentrazione e di qui viene scaricata al-

regola per sua natura automaticamente la portata di acqua evaporata in modo da mantenerla uguale a quella di alimentazione. Ciò avviene mediante il seguente meccanismo: se S è funzionante da un tempo sufficientemente lungo alimentato da due determinate portate di acqua e di gas, l'acqua nel saturatore si troverà ad un certo livello costante ed avrà una certa temperatura alla quale corrisponde per la miscela satura idrogeno-vapore che si forma alla pressione di funzionamento, un rapporto molare y tale da smaltire esattamente la portata di alimentazione. Se ora si varia — per esempio si aumenta — la portata dell'acqua di alimentazione, in un primo tempo vi sarà accumulo in S , e quindi un aumento di livello. Ciò avviene fino a che, aumentando in tal modo la superficie di contatto fra la camicia riscaldante e l'acqua nel saturatore, questa può ricevere una maggior quantità di calore ed aumentare la sua temperatura ad un valore tale da fornire una nuova composizione della miscela satura idrogeno-vapore con un valore di y diverso e al quale corrisponde una portata di vapore uguale alla nuova alimentazione.

Da questo punto, S funziona ad un nuovo regime in cui sono variati y ed il livello dell'acqua nel saturatore. Per

l'esterno e recuperata mentre il gas prosegue per *B* in cui si ricombina con ossigeno di bombola preventivamente essiccato su silicagel in *E*₂.

Prima della distillazione l'acqua di ricombinazione viene fatta passare su $\text{Ca}(\text{OH})_2$ per neutralizzare l'acido nitrico formatosi nella combustione a causa delle tracce d'azoto contenute nell'ossigeno.

Un rubinetto commutatore *N* permette di eseguire agevolmente le manovre di accensione e spegnimento del bruciatore, il cui innescio viene effettuato dalla scarica di un Tesla.

Per determinare la concentrazione isotopica dell'acqua di alimentazione e per fare di tanto in tanto lo zero del galleggiante con acqua naturale è previsto un piccolo serbatoio *F* di circa 50 cm³ da riempire con l'acqua da misurare, munito di scarico con capillare che versa nel distillatore *D* con portata abbastanza bassa per evitare l'accumulo.

In tal caso il bruciatore deve essere spento oppure l'acqua di combustione deve essere deviata fuori dal distillatore, ciò che si ottiene facilmente ruotando il tubetto contenente l'idrato di calcio.

Tutta l'apparecchiatura è munita di sicurezze:

— Contro la mancanza di tensione, che provocando il raffreddamento dell'elemento scambiante porterebbe all'accumularsi in esso dell'acqua di alimen-

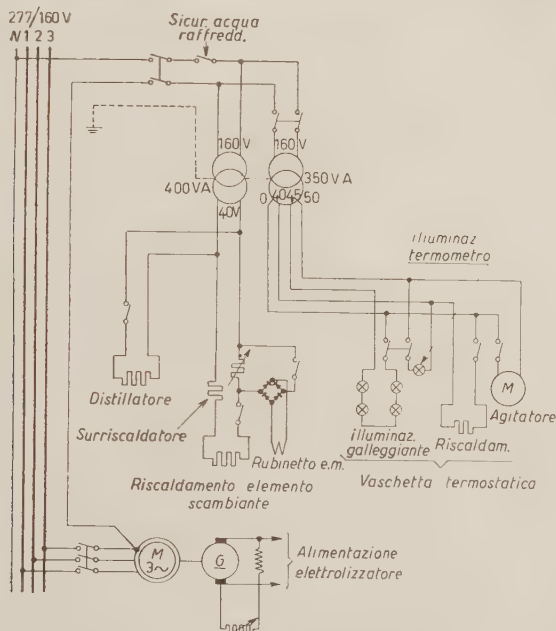


Fig. 5. — Schema elettrico con le protezioni relative.

tazione, è prevista all'uscita del pallone una valvola elettromagnetica *V* il cui avvolgimento è in serie con la resistenza scaldante dell'elemento di scambio.

L'elettromagnete è infilato esternamente al tubo di uscita del pallone; lo

spillo di chiusura è costituito da una sferetta uguale a quella usata per lo scarico di fondo dell'elemento *S*, appesantita da un cilindretto di nichel (~ 4 g). La sede è pure conica smerigliata nel vetro.

— Contro la mancanza o insufficienza dell'acqua di raffreddamento, mediante un interruttore a bulbo di mercurio posto sullo carico.

— Contro la mancanza di idrogeno che porterebbe all'accumulo dell'acqua nell'elemento scambiante e che può avvenire solo per mancanza di tensione all'elettrolizzatore, non prevedendo la possibilità di guasti, è sufficiente la stessa protezione per il caso di mancanza di tensione.

Nella Fig. 5 è rappresentato lo schema elettrico dell'apparecchiatura e le relative protezioni.

Per diminuire al massimo le possibilità di inquinamento dell'acqua e del gas nell'apparato:

— L'acqua, dal pallone che la contiene fino allo scarico dopo lo scambio, viene a contatto solamente con vetro pyrex e con le due valvole di acciaio inossidabile e nichel descritte precedentemente.

I giunti sferici non sono ingrassati e la tenuta viene affidata al velo d'acqua.

Una volta caricata nel pallone l'acqua viene a contatto con l'aria atmosferica nel pallone stesso, nel quale l'aria entra a bolle dal tubo immerso *T*, e nel sistema di alimentazione *R-I*.

Il cono di chiusura del pallone e quello dal quale entra il tubo *T* sono ingrassati con grasso minerale da vuoto con il quale l'acqua non viene mai a contatto.

— Il gas fino allo scambio passa solo in vetro e tubi di politene, dopo lo scambio invece sono tollerati anche tubi di cloruro di polivinile. Tutti i rubinetti sono ingrassati con grasso minerale da vuoto.

5. — Precisione.

Le incertezze nelle misure sono:

— Sulle concentrazioni $\pm 0.01\%$.

— Sulle portate tanto per l'acqua che per l'idrogeno ± 0.03 M/h.

— Sul valore di $K_1 \pm 0.01$.

Con queste incertezze e con i valori di portate e concentrazioni indicati in precedenza, l'incertezza su β è dell'ordine di ± 0.05 .

SUMMARY

An apparatus for the measurement of the isotopic exchange of deuterium between hydrogen and water vapour is described. It is particularly arranged for catalyst life tests. Precautions were taken in order to prevent contamination of the gas and of the water, and some constructive devices were chosen in order to obtain safety and to avoid continuous watching. Measurements of the deuterium concentration in hydrogen can be made in two ways: by thermal conductivity directly on the gas, or by a float method on the water obtained by combustion of hydrogen with oxygen. The fraction of conversion (β) is chosen as the measure of operational efficiency of the catalyst. Accuracy on β is of the order of $\pm 5\%$.

Metodi di comando rapido di rivelatori di tracce (*).

S. FOCARDI, C. RUBBIA e G. TORELLI

Istituto di Fisica dell'Università - Pisa
Sottosezione di Pisa dell'Istituto Nazionale di Fisica Nucleare

F. BELLA

Istituto di Fisica dell'Università - Roma

(ricevuto il 21 Novembre 1956)

Riassunto. — Il presente lavoro consta di due parti. La prima parte è uno studio sul funzionamento dei contatori piani. Nella seconda vengono presentati alcuni nuovi circuiti di coincidenza veloci. Il lavoro nel suo insieme è un contributo al problema di ottenere con estrema prontezza impulsi di alta tensione in corrispondenza al passaggio di una particella ionizzante attraverso un opportuno rivelatore. Tale problema ha interesse pratico in connessione con la necessità, che talvolta si presenta (per esempio in esperienze di fisica nucleare) di poter sottoporre ad un intenso campo elettrico una regione di spazio subito dopo che essa è stata attraversata da una particella ionizzante. La cosa si può esemplificare pensando al caso di una camera odoscopica ⁽¹⁾ o di una camera a bolle ⁽²⁾ comandata.

1. — Contributo allo studio dei contatori piani.

Come rivelatori sono stati usati contatori piani del tipo descritto da BELLA e FRANZINETTI ⁽³⁾. Essi sono formati da due elettrodi paralleli di rame aventi le dimensioni di 10×3 cm², posti ad una distanza di 2 mm e racchiusi in un involucro di pirex riempito di argon alla pressione di 36 cm Hg con l'aggiunta di 4 cm Hg di alcool etilico.

(*) Presentato da C. RUBBIA al XLII Congresso Nazionale della Società Italiana di Fisica (Torino, Settembre 1956).

⁽¹⁾ M. CONVERSI e A. GOZZINI: *Nuovo Cimento*, **2**, 189 (1955); M. CONVERSI *et al.*: *CERN Symp.*, Giugno 1956 (2^a settimana).

⁽²⁾ G. MARTELLI: *CERN Symp.*, Giugno 1956 (2^a settimana).

⁽³⁾ F. BELLA e C. FRANZINETTI: *Nuovo Cimento*, **10**, 1460 (1953).

Come è ben noto, se tra i due elettrodi di un contatore piano si stabilisce una differenza di potenziale opportuna (nel nostro caso ~ 3 kV), il passaggio di una particella ionizzante tra i due elettrodi produce una scintilla. L'impulso di tensione che così si ottiene può, con i contatori da noi usati, raggiungere i 3 kV.

Per avere impulsi di tensione rettangolari di durata e forma ben definita, si è fatto uso di linee di ritardo secondo lo schema di Fig. 1, dove la linea L è un cavo coassiale di impedenza pari a Z_c e lunghezza opportuna ed R è una resistenza di carico il cui valore (che si aggira sui 10 M Ω) va determinato in modo da garantire lo spengimento del contatore (^{3,4}).

L'impulso agli estremi di Z_c (osservato mediante un sincroscopio Tetrax 517) ha l'andamento mostrato dalla Fig. 2. La forma particolare del fronte dell'impulso si può interpretare pensando che la resistenza interna del contatore, η , non sia costante nel tempo.

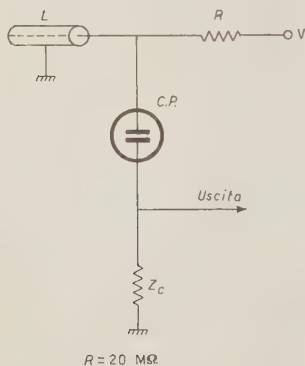


Fig. 1. - Schema di utilizzazione di un contatore piano (C.P.) controllato da una linea di ritardo (L). Z_c è la resistenza caratteristica della linea; R è la resistenza (> 10 M Ω) per la carica della linea; V è la tensione di lavoro (~ 3 kV) di C.P.

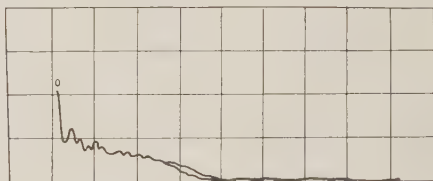


Fig. 2. - Impulso di tensione fornito da un contatore piano montato secondo lo schema della Fig. 1. Valori usati: $Z_c = 75 \Omega$; $R = 10$ M Ω ; sovratensione = 800 V. Scala delle ascisse: 50 μ s/quadr.; Scala delle ordinate: 500 V/quadr. L'origine dell'impulso è il punto 0.

Se chiamiamo c_∞ la differenza di potenziale che si stabilirebbe ai capi di Z_c qualora la resistenza η fosse trascurabile rispetto a Z_c si ha

$$(1) \quad \eta(t) = 2Z_c \left(\frac{1}{\varrho(t)} - 1 \right),$$

avendo posto $\varrho(t) = v(t)/v_\infty$.

Come si vede dalla Fig. 2 è ragionevole scegliere per c_∞ il valore che assume la $v(t)$ dopo un tempo di $\sim 0.2 \mu$ s dall'inizio dell'impulso, in quanto il valore della tensione così raggiunto rimane costante per tutta la durata dell'impulso della linea, qualunque ne sia la lunghezza.

(4) R. W. PIDD and L. MADANSKY: *Phys. Rev.*, **75**, 1175 (1949).

Le varie curve della Fig. 3 sono ottenute in corrispondenza a vari valori di Z_c facendo uso della (1): $i(t)$ dipende probabilmente dalla sovratensione, definita come differenza tra tensione di lavoro e tensione di soglia, ma non è stato possibile precisare questa dipendenza nell'intervallo di valori investigato ($0 \div 1500$ V) a causa degli errori relativamente grandi, riportati in Fig. 3.

Tali errori sono dovuti alle oscillazioni che si notano nella prima parte dell'impulso (v. Fig. 2). Queste dipendono non dal meccanismo della scintilla, bensì dalle induttanze e capacità distribuite nel circuito, come risulta dal fatto che l'aggiunta di piccole capacità (~ 2 pF) nel circuito esterno del contatore modifica profondamente la loro forma.

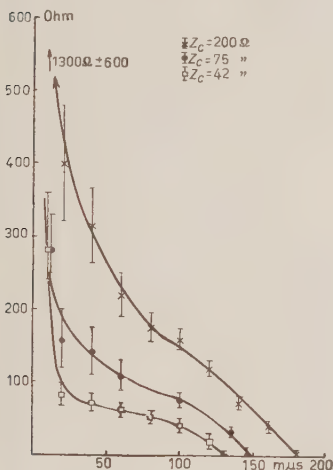


Fig. 3. - Andamento della resistenza interna di un contatore piano usato in un circuito del tipo di Fig. 1, per vari valori* di Z_c .

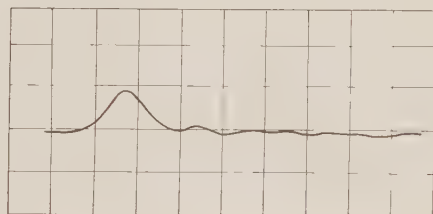


Fig. 4. - Impulso ricavato con il montaggio di Fig. 5 per $R = 20$ M Ω ; $R_1 = 20$ Ω ; $Z_{L_1} = -Z_{L_2} = 75$ Ω ; sovratensione = 500 V; scale: ascisse: 10 μ s/quadr.; ordinate: 500 V/quadr.

Impulsi di forma definita e di durata inferiore ai 50 μ s (vedi Fig. 4) si ottengono con lo schema illustrato in Fig. 5, dove la linea L_2 (di lunghezza minore di L_1) ha lo scopo di modellare l'impulso, e le resistenze R_1 ed R_2 assicurano che la linea sia correttamente caricata.

Per avere qualche informazione sul ritardo proprio dei contatori piani abbiamo applicato agli elettrodi di un primo contatore (CP1) un impulso rettangolare della durata di ~ 1 μ s, il cui fronte di salita ha l'andamento indicato in Fig. 6. Tale impulso è fornito da un modulatore per radar comandato da un secondo contatore piano (CP2) posto immediatamente sopra al primo, secondo lo schema di Fig. 7. Il ritardo aggiuntivo introdotto dal modulatore è

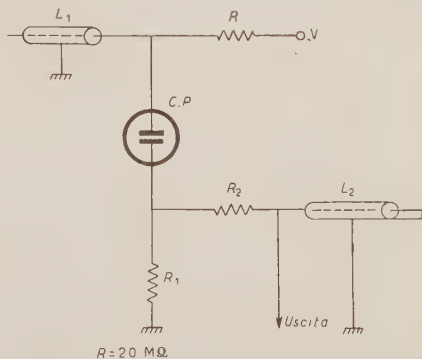


Fig. 5. - Circuito con linea modellatrice di impulsi.

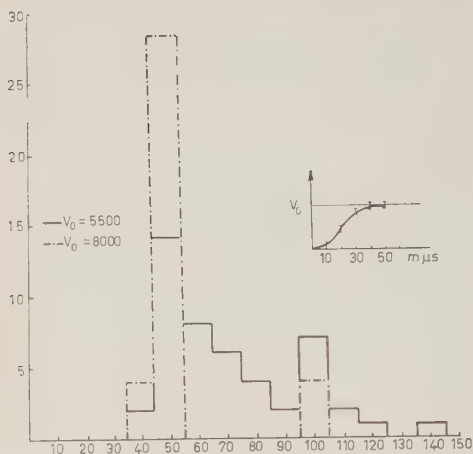


Fig. 6. - Distribuzione dei ritardi nelle accensioni di un contatore CP1 (avente tensione di soglia 2550 V), operato impulsivamente con il montaggio di Fig. 7. In alto a destra è riportata la forma del fronte dell'impulso (di $\sim 1 \mu s$) applicato a CP1.

lita, relativamente grande, dell'impulso applicato a CP1. Infatti durante il tempo di salita, gli elettroni prodotti in CP1 migrano, per effetto del campo elettrico, verso posizioni più sfavorevoli per la formazione della valanga. Inoltre gli elettroni più vicini al catodo, che sono i più favoriti per la formazione della valanga, possono essere catturati da questo nel tempo intercorrente tra il passaggio della particella e l'insorgere dell'impulso applicato a CP1. Anche un breve difetto di parallelismo delle lastre potrebbe comportare conseguenze analoghe. Peraltro non sembra possibile decidere, senza ulteriori mi-

$\sim 40 \mu s$. Nella stessa Fig. 6 è riportata la distribuzione dei ritardi intercorrenti tra l'inizio del fronte dell'impulso applicato al contatore (CP1) e l'inizio della scintilla in esso presumibilmente provocata dalla stessa particella che ha attraversato il contatore (CP2). Naturalmente il tempo così misurato è maggiore del ritardo proprio del contatore, dato il lungo tempo di salita (circa $50 \mu s$) dell'impulso a questo applicato (vedi Fig. 6).

In accordo con KEUFFEL ⁽⁵⁾ e con quanto prevedibile teoricamente ⁽³⁾, le fluttuazioni nei ritardi di un contatore piano diminuiscono al crescere della sovratensione. Tuttavia esse risultano, nelle nostre misure, molto più grandi di quelle trovate da KEUFFEL ⁽⁵⁾ ed altri ⁽⁶⁾. È possibile che la causa di questa discrepanza risieda nel tempo di sa-

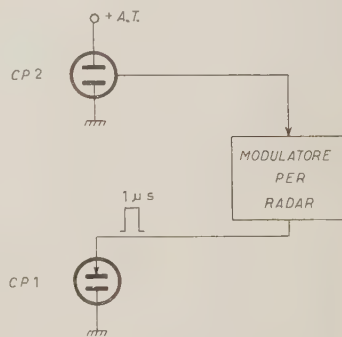


Fig. 7. - Schema a blocchi dell'impulsatore usato per la misura del ritardo proprio di un contatore piano. Il contatore CP2 (alimentato con tensione continua ed « acceso » casualmente da particelle ionizzanti dei raggi cosmici) comanda un modulatore per radar. Questo fornisce gli impulsi ad alta tensione che alimentano (per $\sim 1 \mu s$) il contatore CP1.

⁽⁵⁾ J. W. KEUFFEL: *Rev. Scient. Instr.*, **20**, 202 (1949).

⁽⁶⁾ E. ROBINSON: *Proc. Phys. Soc.*, A **66**, 73 (1956).

sure, quale di queste od altre eventuali cause sia responsabile dei risultati ottenuti. Lo stesso dicasi per il picco che si riscontra intorno ai 100 m μ s in Fig. 6; esso non è certamente dovuto ad accensioni spurie del contatore, come si vede dalla Fig. 8, dove, accanto alla curva caratteristica di un contatore piano montato secondo lo schema di Fig. 1, è riportata (per lo stesso contatore) la probabilità di accensione spuria quando ai suoi elettrodi del contatore una tensione rettangolare di 1 μ s della tensione indicata in ascisse.

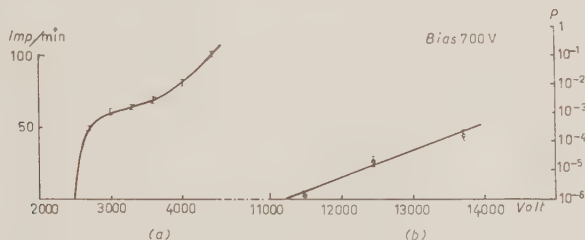


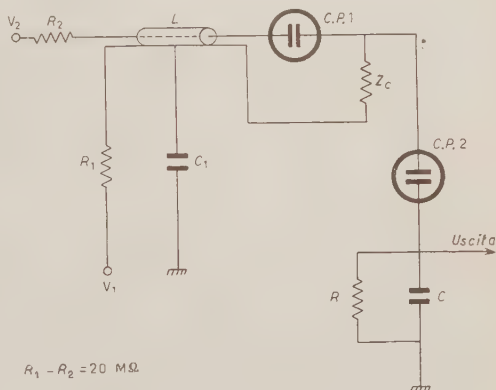
Fig. 8. — *a*) Plateau di un contatore piano montato secondo lo schema di Fig. 1; *b*) probabilità P di accensione spuria per lo stesso contatore alimentato da un impulso di 1 μ s, avente fronte di salita come riportato in Fig. 6 e l'ampiezza indicata in ascisse. (La curva è stata ottenuta mantenendo tra gli elettrodi del contatore una tensione continua di 700 V di segno concorde al segno dell'impulso).

Dal complesso di tali misure emerge la possibilità di utilizzare i contatori piani con comando impulsato, per esempio in sincronismo con il fascio di particelle di una macchina acceleratrice, a tensioni notevolmente maggiori delle usuali tensioni di lavoro continue. Ciò può permettere di ridurre notevolmente le fluttuazioni nei ritardi, attesa la forte dipendenza di queste dalla sovratensione (⁵⁻⁷).

2. — Coincidenze rapide.

2.1. — In Fig. 9 è riportato lo schema di una coincidenza veloce fra due contatori piani. Il contatore CP1, i cui elettrodi si trovano ad una differenza di

Fig. 9. — Schema di coincidenze doppie con contatori piani in serie. $R_1 = R_2 = 20$ M Ω ; $R = 2$ k Ω ; $Z_c = 75$ Ω ; $C = 100$ pF; $C_1 = 1000$ pF.



(⁷) C. FRANZINETTI: comunicazione privata.

potenziale pari a $V_2 - V_1$, è in condizioni di funzionamento, mentre il contatore CP2 è normalmente ad una tensione inferiore alla soglia. Il passaggio di una particella ionizzante attraverso il contatore CP1 e la conseguente scintilla che in esso ha luogo, genera ai capi della resistenza Z_c una d.d.p. $(V_2 - V_1) \varrho(t)/2$.

Si stabilisce allora fra gli elettrodi del contatore CP2 una d.d.p., $V_2(t)$, pari a

$$(2) \quad V_2(t) = V_1 + \frac{V_2 - V_1}{2} \varrho(t) \frac{C_p}{C + C_p}.$$

dove C_p è la capacità del contatore piano. I valori delle costanti che compaiono nell'espressione (2) sono scelti in maniera tale che, dopo un tempo brevissimo ($10 \div 20$ mps) dall'inizio dell'impulso del contatore CP1, $V_2(t)$ sia sufficiente a porre il contatore CP2 in « plateau ». Se una particella ionizzante ha attraversato ambedue i contatori ai capi di C si ottiene così un impulso di tensione approssimativamente uguale a V_1 . Se invece solo il contatore CP1 ha funzionato, l'ampiezza dell'impulso in uscita è

$$\frac{V_2 - V_1}{2} \varrho(t) \frac{C_p}{C + C_p}.$$

Una opportuna scelta dei parametri ($C_p \ll C$ e $(V_2 - V)/2 < V_1$) permette una ottima separazione tra impulsi singoli e impulsi di coincidenza.

Il ritardo tra l'impulso di coincidenza e l'impulso fornito dal contatore CP1 fluttua tra 10 e 20 mps quando la d.d.p. applicata agli elettrodi del contatore CP1 supera di 800 V la sua tensione di soglia. Ciò è in accordo coi risultati di KEUFFEL ⁽⁵⁾.

Le curve riportate nella Fig. 10, che mostrano la dipendenza del rendimento della coincidenza dalla tensione V_2 per vari valori di V_1 , sono state calcolate in base ai risultati sperimentali, riportati da BELLA e FRANZINETTI ⁽³⁾, sulla dipendenza del rendimento di un contatore piano dalla sovratensione.

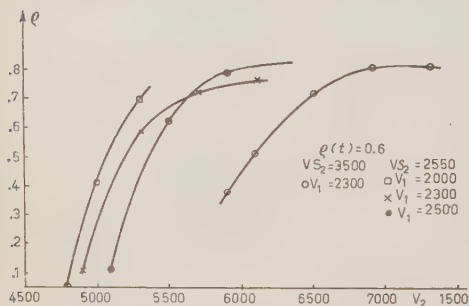


Fig. 10. - Rendimento del circuito di coincidenze di Fig. 9 in funzione di V_2 per vari valori di V_1 (V_{s2} indica la tensione di soglia di CP2).

vissimi rispetto al passaggio della particella attraverso i contatori piani, è stato realizzato impiegando una valvola 715 B.

I due contatori sono collegati alla griglia controllo ed alla griglia schermo della valvola; le due griglie sono normalmente mantenute ad un potenziale negativo in modo che un solo impulso non è sufficiente a porre la valvola in regime di conduzione. Si può così ottenere un impulso di coincidenze avente

2.2. - Un altro circuito di coincidenze rapide capace di fornire impulsi di tensione con ampiezza fino a 15 kV e con ritardi bre-

le seguenti caratteristiche: ritardo rispetto agli impulsi di comando ~ 50 μ s; tempo di salita ~ 20 μ s; durata dipendente dalla durata delle linee di ritardo adattate ai contatori.

2.3. — Un potere risolutivo τ più elevato può essere raggiunto utilizzando un sistema di coincidenze del tipo proposto da WELLS⁽⁸⁾ e BELL⁽⁹⁾ (Fig. 11). τ è determinato dalla lunghezza della linea L_5 ($< L_1, < L_2$) e può ridursi o 20 μ s. In questo caso però la durata dell'impulso di coincidenza è al massimo uguale a τ .

Impulsi di durata maggiore, si ottengono con lo schema di Fig. 12. In tal caso

$$\tau = t_\tau + t_{L_3} + t_{L_4}.$$

se t_τ è il tempo di salita degli impulsi e t_{L_3}, t_{L_4} sono i tempi di transito caratteristici delle linee L_3, L_4 . La durata degli impulsi di coincidenza dipende dalla più breve fra le due linee L_1 e L_3 : L'impulso di coincidenza ottenuto con questo circuito impiegando i nostri contatori piani è dell'ordine di 100 V; esso può essere trasformato in un impulso ad alta tensione mediante un oscillatore bloccato (che utilizzi per esempio una valvola 829) il quale pilota una valvola 715B.

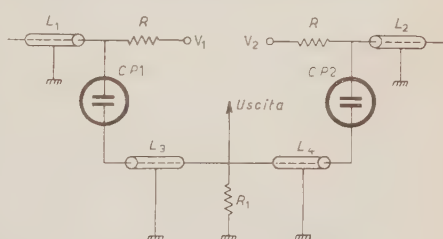
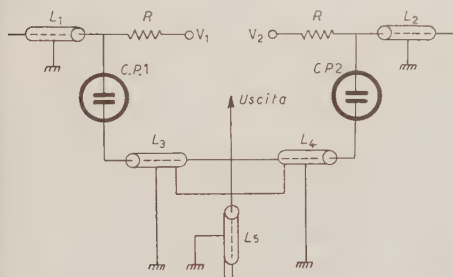


Fig. 11. — Circuito di coincidenze del tipo proposto da WELLS e BELL.

Fig. 12. — Circuito di Fig. 11 modificato.

In tal caso l'impulso in uscita presenta un ritardo di circa $80 \div 100$ μ s rispetto all'impulso fornito dalla coincidenza.

2.4. — Si può relizzare un sistema ultrarapido per il comando di un rivelatore di tracce utilizzando due contatori in opposizione, come indicato in Fig. 13.

Supponiamo per semplicità che sia $V_1 = V_2 = V$ e $L_1 = L_2 = L$ e che un solo contatore sia scaricato. In tal caso agli estremi del rivelatore si ha un

(8) F. H. WELLS: *Brit. Inst. Radio Engrs.*, **2**, 491 (1951).

(9) R. E. BELL, R. L. GRAHAM and H. E. PETCH: *Canad. Soc. Phys.*, (1952).

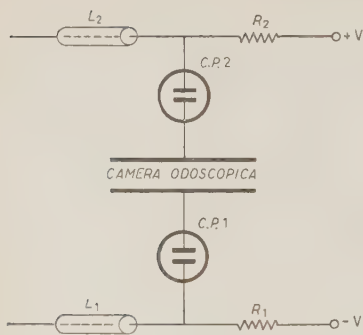


Fig. 13. — Circuito di coincidenze rapide per il comando veloce di un rivelatore di tracce (camera odoscopica).

impulso di tensione $\varrho(t)V/2$ e di durata t_L . Nel caso invece di coincidenza si ha un impulso di ampiezza $V\varrho(t)$ e durata t_L . Il ritardo di questo sistema di comando è costituito dal ritardo proprio dei contatori.

Utilizzando come rivelatore di tracce un insieme (camera odoscopica) di tubi di vetro di 0.6 cm di diametro riempiti con $\text{Ne} + 0.2\%$ di A ⁽¹⁾ alla pressione di 35 cm Hg e posti tra elettrodi piani, si sono ottenuti risultati soddisfacenti con contatori piani funzionanti a 3 kV. In particolare si è trovato che, per campi elettrici impulsivi di durata maggiore di $0.4 \mu\text{s}$ e di valore compreso tra 3 e 10 kV/cm, il rendimento dei tubi usati si mantiene costante.

* * *

Ringraziamo il prof. MARCELLO CONVERSI per averci suggerito questo lavoro e guidato nello svolgimento di esso, ed il prof. CARLO FRANZINETTI per utili discussioni sull'interpretazione dei risultati concernenti i contatori piani.

SUMMARY (*)

The present paper is divided in two parts. The first part studies the working of plane counters. In the second one some new fast coincidence circuits are presented. The paper in the whole is a contribution to the problem of the very fast production of high voltage impulsions at the passage of an ionizing particle through a suitable detector. This problem is of practical interest given the expedience which sometimes arises (for instance in nuclear physics experiments) to be able to submit a given space to an strong electric field immediately after it has been traversed by an ionizing particle. This can be exemplified by a monitored hodoscope- or bubble-chamber.

(*) *Editor's translation.*

LETTERE ALLA REDAZIONE

(La responsabilità scientifica degli scritti inseriti in questa rubrica è completamente lasciata dalla Direzione del periodico ai singoli autori)

The Lifetime of $^3\text{H}_\Lambda$ Hyperfragments.

M. W. FRIEDLANDER

H. H. Wills Physical Laboratory - University of Bristol ()*

(ricevuto il 10 Ottobre 1956)

Since the original observation of BONETTI *et al.* ⁽¹⁾, there have been reported 14 examples of the mesonic decay of $^3\text{H}_\Lambda$ hyperfragments. Most of these fragments decayed after coming to rest, but two of the decays occurred while the fragment was still in flight. We may therefore estimate the lifetime for the mesonic decay of $^3\text{H}_\Lambda$ particles.

Assuming that those hyperfragments which decayed in flight would otherwise have come to rest within the emulsion stacks (and so be identified by their characteristic decay), the best estimate of the lifetime is given by

$$\langle\theta\rangle = \Sigma t_i/N,$$

where t_i are the observed times of flight (moderation times, for those fragments which decay at rest) and N decays in flight were observed. A maximum likelihood calculation for this class of event leads to the same result.

Details of the events which have been published to date are summarised in Table I.

The value obtained for the lifetime is

$$\langle\theta\rangle = 3.7 \cdot 10^{-10} \text{ s.}$$

Since it is based upon only two decays in flight, it is clear that the above value is no more than a guide to the true value. Nevertheless it is considered worth while recording in order to draw attention to the usefulness of reporting such events; as further examples are found, and noted, it will become possible to place narrower limits on the estimate for the mesonic decay of $^3\text{H}_\Lambda$. It is clearly important (see, for example, CHESTON and PRIMAKOFF ⁽²⁾, RUDERMAN and KARPLUS ⁽³⁾ and PRIMAKOFF ⁽⁴⁾) to obtain a measure of the lifetime of the Λ^0 -particle when it is bound within a nucleus, and at present $^3\text{H}_\Lambda$ seems to be the hyperfragment best suited for investigation.

For comparison, the current best estimates of the lifetime of free Λ^0 -part-

(*) Now at Washington University, St. Louis, Mo.

⁽¹⁾ A. BONETTI, R. LEVI SETTI, M. PANETTI, L. SCARSI and G. TOMASINI: *Nuovo Cimento*, **11**, 210 (1954).

⁽²⁾ W. CHESTON and H. PRIMAKOFF: *Phys. Rev.*, **92**, 1537 (1953).

⁽³⁾ M. RUDERMAN and R. KARPLUS: *Phys. Rev.*, **102**, 247 (1956).

⁽⁴⁾ H. PRIMAKOFF: *Nuovo Cimento*, **3**, 1394 (1956).

icles are

$$3.7^{+0.6}_{-0.5} \cdot 10^{-10} \text{ s.},$$

for cosmic-ray events (PAGE⁽⁵⁾), and

$$2.8^{+0.5}_{-0.4} \cdot 10^{-10} \text{ s.}$$

for Λ^0 -particles produced at Brookhaven (BLUMENFELD *et al.*⁽⁶⁾).

TABLE I.

Event	Range of fragment (μm)	Time observed (10^{-10} s)	Reference
1	13 000	2.35	BONETTI <i>et al.</i> ⁽¹⁾
2	1 490	0.51	DEBENEDETTI <i>et al.</i> ⁽⁷⁾
3	520	0.25	DANYSZ ⁽⁸⁾
4	248	0.15	ANDERSON <i>et al.</i> ⁽⁹⁾
5	5 800	1.33	CASTAGNOLI <i>et al.</i> ⁽¹⁰⁾
6	740	0.32	CRUSSARD <i>et al.</i> ⁽¹¹⁾
7	635	0.29	FRY <i>et al.</i> ⁽¹²⁾
8	324	0.18	
9	100	0.07	
10	152	0.11	HASKIN <i>et al.</i> ⁽¹³⁾
11	368	0.19	
12	604	0.27	
13*	44	0.01	SKJEGGESTAD and SØRENSEN ⁽¹⁴⁾
14*	8 340	1.30	BRISBOUT <i>et al.</i> ⁽¹⁵⁾

(*) Decay in flight.

(5) D. I. PAGE: *Phil. Mag.*, **45**, 863 (1954).

(6) H. BLUMENFELD, W. CHINOWSKY, L. LEDERMAN and E. BOOTH: *Phys. Rev.*, **102**, 1184 (1956).

(7) A. DEBENEDETTI, C. M. GARELLI, L. TALONE and M. VIGONE: *Nuovo Cimento*, **12**, 466 (1954).

(8) M. DANYSZ: private communication (1954).

(9) F. ANDERSON, G. LAWLOR and T. E. NEVIN: *Nuovo Cimento*, **2**, 605 (1955).

(10) C. CASTAGNOLI, G. CORTINI and C. FRANZINETTI: *Nuovo Cimento*, **2**, 550 (1955).

(11) J. CRUSSARD, V. FOUCHÉ, G. KAYAS, L. LEPRINCE-RINGUET, D. MORELLET, F. RENARD

It is difficult to estimate the dependence of the hyperfragment lifetime value upon experimental bias. Most fragments, including one of the decays in flight, have been found by area scanning, and this will probably be biased in favour of short tracks, i.e. in favour of double-star events; where the production and decay of the fragment occur in different emulsion strips, they may not be correlated and therefore overlooked, but this should still be unbiased as regards decay in flight or at rest. The Bristol event (decay in flight) was found by following π^- -mesons — also an unbiased method. No correction for bias has been included in the lifetime quoted here.

In confining our attention to a single mode of decay, for which identification and analysis are unambiguous, we have been helped by dealing only with singly charged fragments. For heavier and multiply charged fragments, the situation is at present not as favourable. Generally these fragments are created with very low kinetic energy — the resulting short tracks render identification difficult, ambiguous or impossible, and the lack of momentum balance amongst the charged secondary particles may be evidence for either the emission of neutral secondaries, or the decay in flight of the fragment, or both. It is therefore necessary to be particularly careful in classifying events.

It is a pleasure to thank Drs. R. H. DALITZ and D. KEEFE for helpful discussions and advice.

and J. TREMBLEY: *Pisa Conference Report* (1955), Mimeographed Edition p. 481.

(12) W. F. FRY, J. SCHNEPS and M. S. SWAMI: *Phys. Rev.*, **101**, 1526 (1956).

(13) D. M. HASKIN, T. BOWEN, R. G. GLASSER and M. SCHEIN: *Phys. Rev.*, **102**, 244 (1956).

(14) O. SKJEGGESTAD and S. O. SØRENSEN: *Nuovo Cimento*, **3**, 652 (1956).

(15) F. BRISBOUT, M. W. FRIEDLANDER and P. IREDALE: *Nuovo Cimento*, **4**, 948 (1956).

An Analysis of Rochester $K_{\mu 3}$ and $K_{e 3}$ data.

S. FURUICHI, Y. SUGAHARA, A. WAKASA (*) and M. YONEZAWA

Department of Physics, Hiroshima University - Hiroshima
 (*) *Department of Physics, Kanazawa University - Kanazawa*

(ricevuto il 23 Ottobre 1956)

Basing on the investigation presented by us ⁽¹⁾ we have studied the data of $K_{\mu 3}$ and $K_{e 3}$ which had been reported by CRUSSARD at Rochester Conference ⁽²⁾. Our previous analysis had been done by requiring Lorentz invariance for the interaction (or transition matrix) under the assumption that Fermi interaction ⁽³⁾ is participating in the decays of $K_{\mu 3}$ and $K_{e 3}$.

Although the number of events reported there may be too small even to apply the statistical methods, we have tentatively analyzed the experimental

data to compare with the theoretical distribution by means of χ^2 -test. The solid histograms in Figs. 1 and 2 indicate

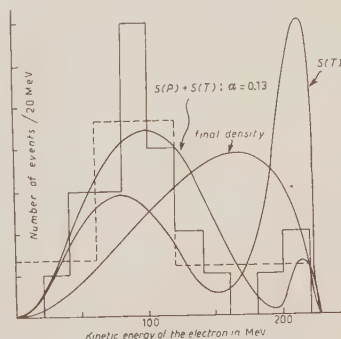


Fig. 1. — Experimental and theoretical distribution for $K_{e 3}$.

⁽¹⁾ For the preliminary report see S. FURUICHI, T. KODAMA, Y. SUGAHARA, A. WAKASA and M. YONEZAWA: *Prog. Theor. Phys.*, **16**, 64 (1956) (L.). The details will soon be published also in *Prog. Theor. Phys.* **17**, No. 1.

⁽²⁾ J. CRUSSARD: *Proceedings of the Sixth Rochester Conference on High Energy Particle*, 1956 (New York, to be published).

Recently reported events, W. A. COOPER, H. FILTHUTH, J. A. NEWTH and R. A. SALMERON: *Nuovo Cimento*, **4**, 390 (1956); R. BIRGE, D. H. PERKINS, J. R. PETERSON, D. H. STORK and M. N. WHITEHEAD: *Nuovo Cimento*, **4**, 834 (1956), are also in favour of our present statement of $K_{e 3}$.

⁽³⁾ Fermi interaction concerned here may be the one realized among $(N, \Delta(\Sigma), \mu(e), \nu)$.

the original Rochester data, while the dashed histograms indicate the reclassified data for the purpose of χ^2 -test. The results of the test are given in Tables I and II. We discuss those data in each case of $K_{\mu 3}$ and $K_{e 3}$.

The features seen in the Rochester (unbiased) $K_{\mu 3}$ data are consistent with those summarized by CRUSSARD *et al.* in

their article (4), if the appropriate consideration about scanning biases is made on the latter data, although they show a large distribution in the low energy

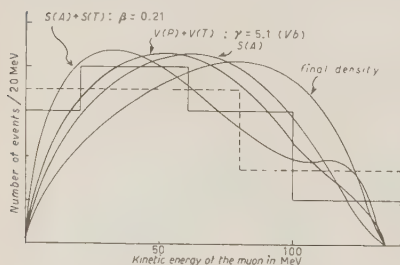


Fig. 2. — Experimental and theoretical distribution for $K_{\mu 3}$.

region (< 50 MeV). The Rochester data give a distribution which is apparently deviated from the final state density distribution to the low energy side. If the comparison is made with each type of

meters of mixing (ratios of effective coupling constants) which give a quite well fit to the present experimental data are given in Table II. The mixing of $S(P)$ and $S(T)$ also gives a curve which is more fitted to the experiment than single $S(A)$ interaction, though the fitness is not so much improved as in the mixture of $S(A)$ and $S(T)$. $S(A)+S(P)$ can not produce better correspondence than single $S(A)$. At first sight the vector $K_{\mu 3}$ does not seem to allow so good a fit. This is the case as long as we are not concerned with the mixing of interactions. However the exhaustive study of mixing can show that a curve with sufficient good correspondence is obtainable. The best fitted curve is constructed by the combination of $V(P)$ and $V(T)$. (This is denoted as Vb in Fig. 1).

$K_{e 3}$. — The feature of the data reported at Rochester is just the same as that of the previously reported data

TABLE I. — χ^2 -probability for various types of interaction of $K_{\mu 3}$ and $K_{e 3}$.

	$S(P)$	$S(A)$	$S(T)$	$V(P)$	$V(A)$	$V(T)$	$V(T)'$	Final state density
$K_{\mu 3}$	0.04	0.66	0.15	0.23	0.12	0.27	0.04	0.25
$K_{e 3}$	$\ll 1 \cdot 10^{-4}$	$3 \cdot 10^{-3}$	$8 \cdot 10^{-3}$	$1 \cdot 10^{-4}$	$\ll 1 \cdot 10^{-4}$	$< 1 \cdot 10^{-4}$	$\ll 1 \cdot 10^{-4}$	$< 1 \cdot 10^{-1}$

distribution, the $S(A)$ (5) interaction gives the best fitting, distinguishing from other types of interaction, and this good correspondence is further improved by mixing with $S(T)$ interaction. The para-

due to systematic surveys on K -particles (6-8). The common feature shown by these data and those of Rochester is the decreasing of the observed events above 100 MeV. As was noted in our previous paper this feature is realized

(4) J. CRUSSARD, V. FOUCHÉ, J. HENNESSY, G. KAYAS, L. LEPRINCE-RINGUET, D. MORELLET and F. RENARD: *Nuovo Cimento*, **3**, 731 (1956).

(5) The notation such as $S(A)$ means scalar K -particle and pseudovector Fermi interaction. As for its explicit form see reference (4). It should also be understood that $S(A)$ does not make any difference from its corresponding one with opposite parity, i.e., $PS(V)$ in our analysis.

(6) G. STACK COLLABORATION: *Nuovo Cimento*, **2**, 1063 (1955).

(7) D. M. RITSON, A. PEVSNER, S. C. FUNG, M. WIDGOFF, G. T. ZORN, S. GOLDHABER and G. GOLDHABER: *Phys. Rev.*, **101**, 1085 (1956).

(8) Reference (4).

TABLE II. — χ^2 -probability for mixed interactions.

$K_{\mu 3}$	combination α		0.36	0.18	0.09
	$S(P)$	$S(T)$	0.68	0.33	0.69
	combination β		0.26	0.21	0.13
	$S(A)$	$S(T)$	0.92	0.99	0.95
	combination γ		3.2	5.1	8.6
	$V(P)$	$V(T)'$	0.78	0.83	0.69
$K_{e 3}$	combination α		0.16	0.13	0.08
	$S(P)$	$S(T)$	0.57	0.73	0.55
	combination β		0.21	0.13	
	$S(A)$	$S(T)$	$8 \cdot 10^{-3}$	0.01	

Parameters of mixing (ratios of effective coupling constants) are given by

$$\alpha = |F^{S(P)}/m_K^2 F^{S(T)}|, \quad \beta = |F^{S(A)}/m_K F^{S(T)}|, \quad \gamma = |F^{V(P)}/F^{V(T)}|.$$

The values of α , β and γ are chosen so as to give curves which are very near to the best fitted curve of each case.

only by the existence of the $S(T)$ type of interaction.

The χ^2 -test does not give so good a result for the $S(T)$ interaction in spite of its apparent resemblance with the form of the experimental distribution, but this is not an unexpected matter, since the classification of data which is restricted by the applicability of the χ^2 -test has not been made so as to characterize the descent of the curve from 90 MeV to 180 MeV. In order to characterize the feature of the distribution shown in

the experiment it is necessary to divide the region 120~240 MeV into more than two or three parts, but this is impossible at present because of the scarcity of data.

However the fitness of the data to the $S(T)$ curve will be improved if there exists strong bias against the scanning of electrons at the high energy end of the region. And this is quite probable as mentioned by CRUSSARD. Unfortunately, however, detailed information about it as not yet been obtained.

Even if the case happens in which

the bias should not be so strongly operative at the high energy side, the situation is still manageable. The mixing of $S(P)$ interaction with $S(T)$ interaction gives a curve which fits sufficiently enough the experimental data. (The mixing $S(T) + S(A)$ does not give such a well corresponding curve as $S(T) + S(P)$). $S(A) + S(P)$ and vector K_{e3} give curves with probability 10^{-4} even if we try to mix the interactions in all possible combinations.

The following statements may be derivable from the present analysis of Rochester data:

a) The spin 1 possibility can so far not be rejected for $K_{\mu 3}$.

b) If the experiment should confirm in future that the distribution from experiment dominates over Vb ⁽⁹⁾ in the low energy region, it would indicate spin 0 for $K_{\mu 3}$.

c) If the situation b) does not occur, the spin determination is hard task. However even in this case it is not impossible to determine the type of interaction for a given spin value, when the experimental distribution is firmly established.

d) K_{e3} seems to be the particle with spin 0 and Fermi interaction of

⁽⁹⁾ Vb is also the curve which has the largest rise in all combinations of interactions in spin 1 $K_{\mu 3}$.

tensor type participates mainly in the decay. An alternative possibility for the decay interaction is the combination of scalar (or pseudoscalar) and tensor types of Fermi interaction, or vector (pseudovector) + tensor type of Fermi interaction owing to the coincidence of $S(P)$ with $S(A)'$.

e) High spin possibility ⁽¹⁰⁾ is very small for K_{e3} .

The fact that K_{e3} seems to have spin 0 is consistent with the observation of the current experiments of θ and τ ⁽¹¹⁻¹³⁾, both or one of which may decay with K_{e3} mode.

In conclusion we wish to note that there exists the possibility that the combination of $S \sim T \sim P$ Fermi interaction may explain both $K_{\mu 3}$ and K_{e3} decay events. This is very interesting in relationship to the universality of «Type» of the Fermi interaction.

* * *

The authors thank Prof. K. SAKUMA and Dr. S. OGAWA for their kindest interest in this work.

⁽¹⁰⁾ The general feature of the distribution by high spin K_{e3} can be well approximated by the final density curve.

⁽¹¹⁾ W. D. WALKER and W. D. SHEPARD: *Phys. Rev.*, **101**, 1810 (1956).

⁽¹²⁾ J. OREAR, G. HARRIS and S. TAYLOR: *Phys. Rev.*, **102**, 1676 (1956).

⁽¹³⁾ L. ALVAREZ: *Proceedings of Sixth Rochester Conference on High Energy Physics*, 1956 (New York, to be published).

On the Decay of ^{141}Ce .

G. B. ZORZOLI

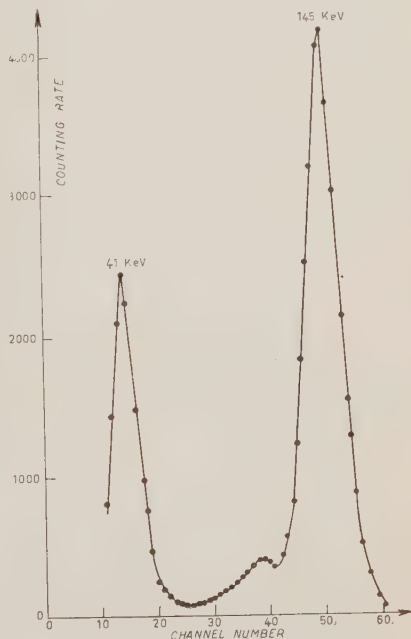
Istituto di Fisica Sperimentale del Politecnico - Milano

(ricevuto il 26 Ottobre 1956)

^{141}Ce decays by β -emission to ^{141}Pr (stable) with a half-life of 32.5 days. Its activity was observed by several investigators ⁽¹⁾, and particularly was found a 145 keV γ -ray classified as a prevailing magnetic dipole transition together with a weak electric quadrupole one ⁽²⁾. By the coulomb excitation with α -particles HEYDENBURG and TEMMER ⁽³⁾ found no E_2 transition. Consequently it seemed worthwhile to measure the conversion coefficient for the K -shell and the rate between K and L electrons for a better determination of the type of transition.

The sample of ^{141}Ce was obtained from the $^{140}\text{Ce}(n, \gamma)^{141}\text{Ce}$ reaction by neutron irradiation of a pure cerium-oxide in the Harwell pile. There was also present the β -emitter ^{143}Pr ($T_{1/2} = 13\text{d}$) with a rather strong activity, and it was necessary to let it decay. The γ - and X-radiations were analysed by means of a twenty-channel pulse analyzer ⁽⁴⁾. A

high transmission intermediate image β -ray spectrometer was used for investigating the β -spectrum ⁽⁵⁾.

Fig. 1. — γ - and X-rays spectrum.

⁽¹⁾ J. M. HOLLANDER, I. PERLAM and G. T. SEABORG: *Rev. Mod. Phys.*, **25**, 469 (1953).

⁽²⁾ E. AMBLER, R. P. HUDSON and G. M. TEMMER: *Phys. Rev.*, **97**, 1212 (1955); M. S. FRIEDMAN and D. W. ENGELKEMEIR: *Phys. Rev.*, **79**, 897 (1950).

⁽³⁾ N. P. HEYDENBURG and G. M. TEMMER: *Phys. Rev.*, **100**, 150 (1955).

⁽⁴⁾ E. GATTI: *Nuovo Cimento*, **11**, 153 (1954).

⁽⁵⁾ G. BOLLA, S. TERRANI and L. ZAPPA: *Nuovo Cimento*, **12**, 875 (1954).

By the scintillation spectrometer it was possible to identify two peaks of 145 and 41 keV (Fig. 1). The first value is in good agreement with previous data for the ^{141}Ce γ -ray energy; the second one corresponds to the KX -rays energy of Pr. The small peak on the left side of the γ -spectrum is to be considered as an impurity, because its intensity in one month (i.e. about one half-life of ^{141}Ce) decreases with a different mean life. The obtained β -spectrum shows two peaks superimposed to the continuous spectrum (K and L conversion electrons). The Fermi-plot may be resolved into two straight lines, with end points at 447 and 591 keV, and intensities respectively of 67 and 33 %. $\log ft$ values are respectively 7.0 and 7.7: therefore the transition should be classified first forbidden ($\Delta I=0.1$: yes).

The intensity measurements of γ and X -spectra were performed in the conventional manner. From the obtained

of course, was corrected for escape peaks and a previous control of the measuring instruments was performed by means of the γ -rays of a Tm standard sample, whose conversion coefficient is well known.

Theoretical conversion coefficients $(^6)$ suggest that the obtained value may account for both M_1 and E_2 transition. But from the β -spectrum it is possible to deduce the intensity of the $L+M$ conversion electron peak, that is practically the L intensity, from which it was deduced

$$\alpha_L = 0.06,$$

that is

$$\frac{K}{L} = 6.2.$$

Theoretical values of K/L for $Z=59$ are

$$\frac{K}{L} = 4 \text{ for } E_2 \text{ trans.}, \quad \frac{K}{L} = 7.5 \text{ for } M_1 \text{ trans.}$$

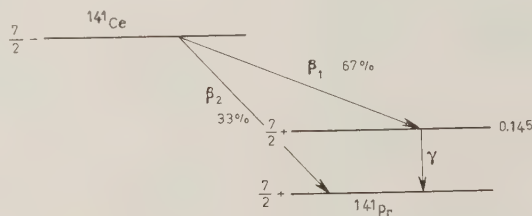


Fig. 2. - Decay scheme.

values of I_γ and I_k it is possible to deduce the conversion coefficient

$$c_k = 0.37.$$

The value did not change within the experimental errors by measurements at different times: it testifies the absence of impurities in the two peaks. Its value,

Therefore it is a reasonable assumption that 145 keV γ -rays arise from a magnetic dipole transition. The absence of E_2 transition agrees with the referred results $(^3)$ by HEYDENBURG and TEMMER.

In Fig. 2 is shown the decay scheme.

$(^6)$ M. E. ROSE in K. SIEGBAHN: *Beta and Gamma Ray Spectroscopy* (Amsterdam, 1955), p. 905.

Mean Free Path of 4.3 GeV π^- -Mesons in Nuclear Emulsions.

A. MARQUES, N. MARGEM and G. A. B. GARNIER

Centro Brasileiro de Pesquisas Físicas - Rio de Janeiro

(ricevuto il 29 Ottobre 1956)

The mean free path for nuclear interactions of 4.3 GeV π^- -meson, from the pion beam of the Berkeley bevatron, was measured in Ilford G-5 emulsions. A value of 33.7 ± 4.7 cm was obtained.

18 482 mm of track were followed and 57 interactions were observed. The events can be thus classified: 4 scatterings at small angles without any change in ionization (assumed to be either shadow or coulomb scatterings); 1 stopping in flight; 46 absorptions in which heavily ionizing prongs were present; 6 absorptions in which only light tracks were present.

The general features of the stars are not essentially different from those observed at 1.5 GeV pion kinetic energy; the average number of visible prongs per star is 10 and the maximum number observed is 31.

One excited ${}^6\text{Li}$ and six unidentified unstable fragments, disintegrating in the emulsion, were observed.

The mean free path measured in this work was converted into an average cross-section for the emulsion nuclei through $\bar{\sigma}_{\text{barn}} = 21/\lambda_{\text{cm}}$. This is compared with results by other workers at different kinetic energies in Fig. 1. The

point of cosmic-ray mesons at intermediate energies corresponds to a pion average kinetic energy of about 350 MeV, calculated from the measured spectrum of those particles. The point at 45 GeV was obtained by the Turin group

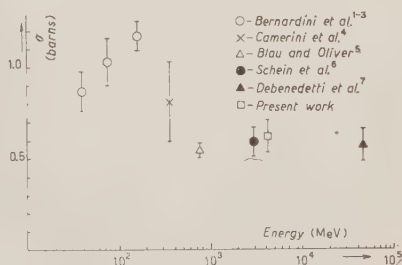


Fig. 1.

and corresponds to the average energy of a group of jet particles having momenta between 1 and 200 GeV/c.

We note that, for energies greater than 750 MeV and up to about 100 GeV, the interaction cross-section seems to be nearly constant and equals the average geometrical cross-section for emulsion nuclei when the value $1.2 \cdot 10^{-13} \text{ A}^{2/3} \text{ cm}^2$ is taken for the nuclear radius.

* * *

We are grateful to Prof. EDWARD LOFGREN for providing the exposures and to prof. M. SCHEIN and Mr. D. HASKIN for their help in obtaining the plates. We are also grateful to professors U.

CAMERINI and H. G. DE CARVALHO for constant assistance and valuable suggestions. To the former we are also indebted for suggesting us the experiment.

(¹) G. BERNARDINI, E. T. BOOTH, L. LEDERMAN and J. TINLOT: *Phys. Rev.*, **8**, 924 (1950).

(²) G. BERNARDINI, E. T. BOOTH, L. LEDERMAN and J. TINLOT: *Phys. Rev.*, **82**, 105 (1951).

(³) G. BERNARDINI, E. T. BOOTH and L. LEDERMAN: *Phys. Rev.*, **83**, 1075 (1951).

(⁴) U. CAMERINI, P. H. FOWLER, W. O.

LOCK and H. MUIRHEAD: *Phil. Mag.*, **41**, 413 (1950).

(⁵) M. BLAU and A. R. OLIVER: *Phys. Rev.*, **102**, 489 (1956).

(⁶) M. SCHEIN, D. M. HASKIN and R. G. GLASSER: *Nuovo Cimento*, **3**, 131 (1956).

(⁷) A. DEBENEDETTI, C. M. GARELLI L. TALONE and M. VIGONE: *Nuovo Cimento*, **4**, (1956) (communicated to us by G. WATAGHIN).

Electron-Photon Cascades of High Energy in Photographic Emulsions.

H. FAY

Max-Planck-Institut für Physik - Göttingen

(ricevuto il 31 Ottobre 1956)

Recently some electron-photon cascades have been described, which deviate markedly from the results of cascade theory⁽¹⁻⁷⁾. Moreover, some authors have found the direct production of electron-pairs (tridents) to be more frequent than to be expected from theory⁽⁸⁻⁹⁾. It appears, therefore, to be of great interest to check experimentally the validity of the relations of quantum electrodynamics at high energies upon which some doubts were cast

by the experimental results mentioned above.

For this purpose 8 cascades produced by single γ -quanta in emulsions have been systematically investigated up to a shower-depth of at least $t = 1.6$ radiation units (1 radiation unit = 29 mm in emulsion). The energy of each shower particle has been determined by relative multiple scattering measurements made between neighbouring tracks according to standard procedure. The energy loss of the electrons by bremsstrahlung has been taken into account. At high energies (> 100 GeV) the separation of the electron-pairs caused by their scattering⁽¹⁰⁾ or the increase in grain-density at the pair origin^(11,15) has been used to estimate the energy of the pairs.

(¹) M. SCHEIN, D. M. HASKIN and R. A. GLASSER: *Phys. Rev.*, **95**, 855 (1954).

(²) A. DEBENEDETTI, C. M. GARELLI, L. TALONE and M. VIGONE: *Nuovo Cimento*, **2**, 220 (1955).

(³) A. JURAK, M. MIĘSOWICZ, O. STANISZ and W. WOLTER: *Bulletin de l'Académie Polonaise des Sciences*, **3**, 369 (1955).

(⁴) A. MILONE: communicated at the Pisa Conference (1955).

(⁵) A. DEBENEDETTI, C. M. GARELLI, L. TALONE, M. VIGONE and G. WATAGHIN: *Nuovo Cimento*, **3**, 226 (1956).

(⁶) M. KOSHIBA and M. F. KAPLON: *Phys. Rev.*, **97**, 193 (1955); **100**, 327 (1955).

(⁷) L. BARBANTI-SILVA, C. BONACINI, C. DE PETRI, J. JORI, G. LOVERA, R. PERILLI-FEDEL and A. ROVERI: *Nuovo Cimento*, **3**, 1465 (1956).

(⁸) M. M. BLOCK and D. T. KING: *Phys. Rev.*, **95**, 171 (1954).

(⁹) L. LOHRMANN: *Nuovo Cimento*, **3**, 820 (1956).

(¹⁰) L. LOHRMANN: *Nuovo Cimento*, **2**, 1029 (1955).

(¹¹) D. H. PERKINS: *Phil. Mag.*, **46**, 1146 (1955).

(¹²) N. ARLEY: *Proc. Roy. Soc., A* **168**, 519 (1938); *Mat. Fys. Medd.*, **17**, 11 (1940).

(¹³) K. PINKAU: *Nuovo Cimento*, **3**, 1156 (1956).

(¹⁴) M. M. BLOCK, D. T. KING and W. W. WADA: *Phys. Rev.*, **96**, 1627 (1954).

(¹⁵) W. WOLTER and M. MIĘSOWICZ: *Nuovo Cimento*, **4**, 648 (1956).

In this way it has been found that 6 of the cascades had a total energy (= energy of the producing γ -quanta) of between 20 and 150 GeV (mean energy 50 GeV), and each of the other two cascades an energy of ~ 300 GeV and ~ 2000 GeV respectively.

Shower-development: In Table I the

of a single cascade on the mean, the mean of only 5 cascades has been taken (crosses), in which the cascade No. 6 has not been taken into account. The drawn curve gives the mean shower development expected from the theory of ARLEY⁽¹²⁾. A good agreement between theory and experiment is

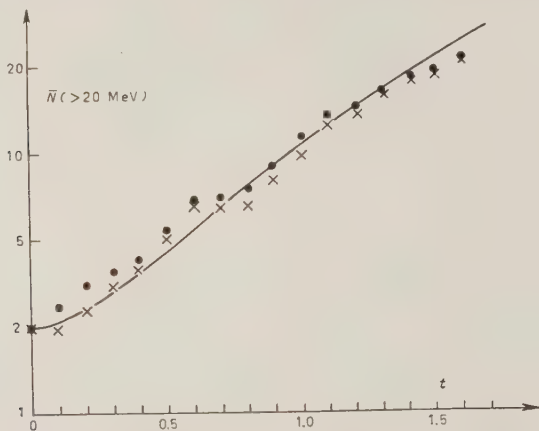


Fig. 1. — The mean number of shower electrons with $E \geq 20$ MeV as a function of shower depth t for the 6 cascades given in Tables I and II.

number of shower particles with energies ≥ 20 MeV is given as a function of the shower-depth for the 6 cascades of energy < 150 GeV. The mean number \bar{N} has been plotted (cf. the points in Fig. 1). To demonstrate the influence

to be noted. The same holds also for the energy spectrum (Fig. 2) of the shower particles at various shower depths. The full curves show the theoretical results normalized for the theoretically expected number of shower particles,

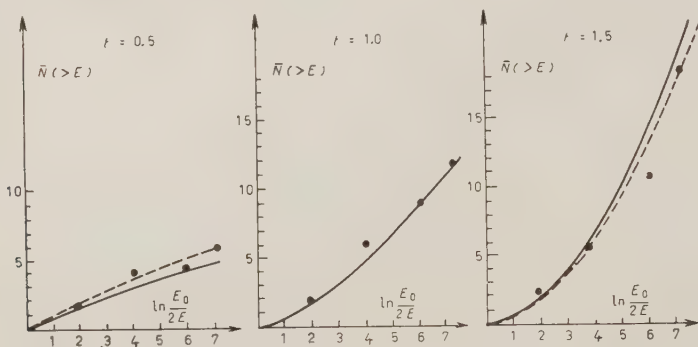


Fig. 2. — The mean energy-spectra of the shower particles for the 6 cascades given in Tables I and II.

TABLE I.

t	Number of cascade						mean \bar{N}
	2	3	4	5	6	8	
0	2	2	2	2	2	2	2
0.1	2	2	2	2	4	2	2.33
0.2	2	4	2	2	6	2	3.00
0.3	3	6	2	2	6	2	3.50
0.4	5	6	3	2	6	2	4.00
0.5	5	9	7	2	8	2	5.50
0.6	7	10	7	4	8	4	6.67
0.7	7	10	7	4	10	4	7.00
0.8	8	10	6	4	12	4	7.34
0.9	8	12	8	6	14	6	9.00
1.0	10	14	10	8	18	8	11.33
1.1	12	19	11	11	18	10	13.50
1.2	15	18	13	11	18	10	14.16
1.3	21	20	12	13	20	12	16.33
1.4	25	19	14	14	22	12	17.67
1.5	25	19	14	14	22	15	18.20
1.6	28	23	18	16	24	17	21.00

Number of shower particles with $E \geq 20$ MeV as a function of shower depth t . As to the energies of the cascades see Table III.

TABLE II.

No. of pair	Number of cascade					
	2	3	4	5	6	8
1	0	0	0	0	0	0
2	0.285	0.126	0.387	0.595	0.090	0.547
3	0.374	0.299	0.447	0.859	0.123	0.894
4	0.460	0.426	0.447	0.920	0.470	0.966
5	0.523	0.447	0.826	0.977	0.606	1.01
6	0.769	0.530	0.957	1.00	0.738	1.25
7	0.972	0.824	1.06	1.05	0.74	1.47
8	1.02	0.901	1.11	1.29	0.888	1.50
9	1.14	1.05	1.17	1.36	0.955	1.60
10	1.19	1.08	1.25	1.57	0.983	
11	1.24	1.10	1.37		1.105	
12	1.29	1.26	1.37		1.22	
13	1.29	1.58	1.56		1.29	
14	1.33	1.59	1.58		1.29	
15	1.50				1.36	
16	1.50				1.54	
17	1.50					

The shower-depth t of the pairs ($E \geq 20$ MeV) created in the 6 cascades with energies between 20 and 150 GeV. As to the energies of the cascades see Table III.

while the dotted curves are normalized for the actually observed number.

In Fig. 3 the mean number of the pairs of energy ≥ 20 MeV created up to a shower depth t has been plotted as a function of t (dotted histogram without cascade No. 6). Fig. 4 shows the energy

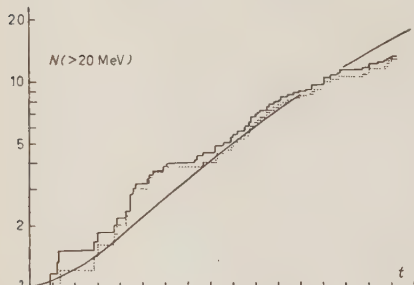


Fig. 3. — The mean number of pairs of energy ≥ 20 MeV created up to a shower depth t as a function of t for the 6 cascades given in Tables I and II.

spectra of these pairs for various values of t . In the figures the full curves give the theoretical results derived from the theory of ARLEY⁽¹²⁾.

The deviations from the theoretically predicted number of pairs at $t \geq 1.3$ are due to the poor detection efficiency for low energetic pairs at these shower depths, since there the shower particles by Coulomb scattering have already spread to a rather wide distribution in space, and pairs of low energy can be lost. All the other deviations at smaller shower depths may probably be considered as statistical fluctuations.

It is to be noted also that the shower curves and the energy spectra of the two cascades with ~ 300 GeV and ~ 2000 GeV are in agreement with the theoretical predictions (Fig. 5a, b; 6a, b).

From these experimental data it can be concluded that the development of the electron-photon cascades up to a total energy of some 1000 GeV is generally in agreement with cascade theory,

and that the theoretical cross-sections for bremsstrahlung and pair-production at high energies apply as well (see also the similar results of K. PINKAU⁽¹³⁾).

Trident-production: The measurement of the m.f.p. of the direct pair-production (tridents) becomes difficult due to bremsstrahlung-pairs (pseudo-tridents), which are produced at so small a distance from the original track that they can be confused with the real tridents within the resolving power of the microscope ($< 0.2 \mu\text{m}$)^(6,8). In order to make the necessary correction in the number of observed tridents, in the present investigation only the two electrons of the

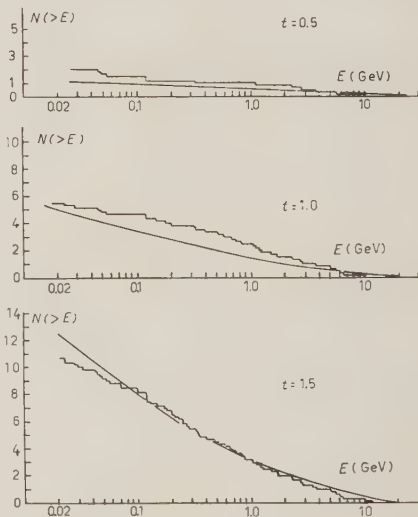


Fig. 4. — The mean energy spectra of pairs created up to a shower depth t for the 6 cascades of Tables I and II.

first pair of each cascade with energy < 150 GeV were used to obtain the m.f.p. of trident production.

The number of pairs of the first generation produced by these 12 primary electron up to $t = 1.0$, is theoretically given as 23.4 (see Table III). Experimentally, one obtains for the total

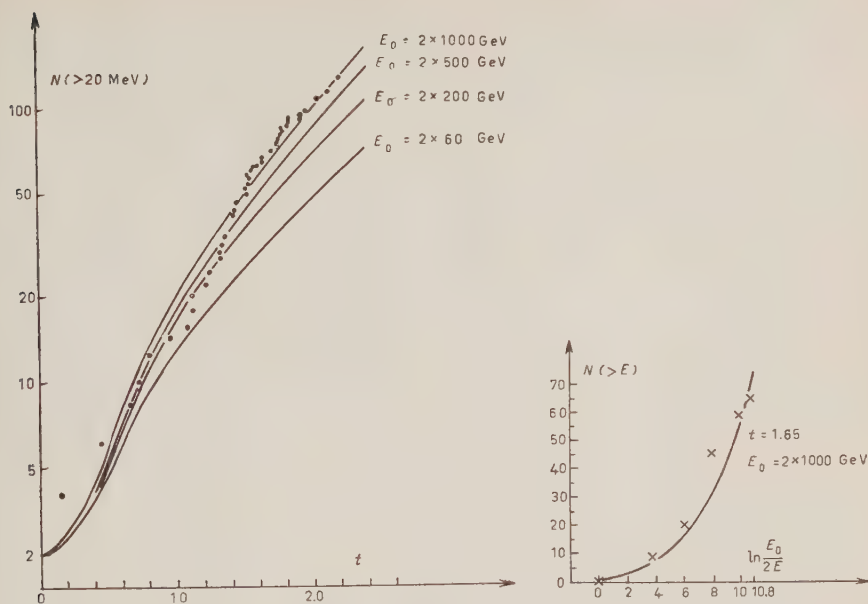


Fig. 5 (a, b). — The number of shower particles vs. shower depth (a) and their energy spectrum (b) for a cascade created by a photon with $E_0 \sim 2000 \text{ GeV}$. The drawn curves represent the theoretical predictions, assuming the energies of the electrons of the first pair to be equal.

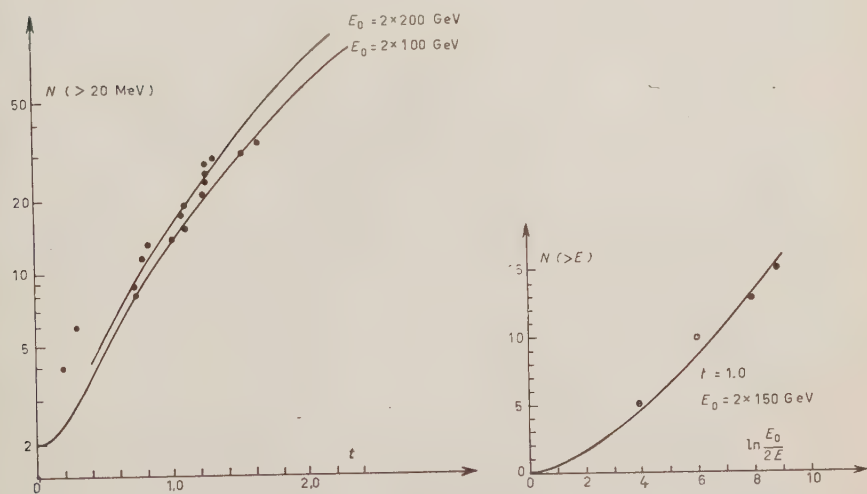


Fig. 6 (a, b). — The number of shower particles vs. shower depth (a) and their energy spectrum (b) of a cascade created by a photon with $E_0 \sim 300 \text{ GeV}$. The drawn curves represent the theoretical predictions, assuming the energies of the electrons of the first pair to be equal.

TABLE III.

1	2	3	4	5	6	7
2	2.5	1.38	0.05	0.069	0.075	0.0364
	30	2.13	0.33	0.703	0.147	0.0863
3	60	2.23	0.46	1.027	0.167	0.1021
	60	2.23	0.46	1.027	0.167	0.1021
4	30	2.13	0.33	0.703	0.147	0.0863
	20	2.01	0.26	0.523	0.133	0.077
5	30	2.13	0.33	0.703	0.147	0.0863
	2.5	1.38	0.05	0.069	0.075	0.0364
6	20	2.01	0.26	0.523	0.133	0.077
	20	2.01	0.26	0.523	0.133	0.077
8	10	1.80	0.17	0.306	0.110	0.0607
	10	1.80	0.17	0.306	0.110	0.0607
23.42				6.48	1.55	0.89

Evaluation of the number of real tridents.

Meaning of the columns:

- 1) Number of cascade.
- 2) Energy of the two primary electrons in GeV.
- 3) Theoretical number of created pairs of the 1-st generation.
- 4) Correction-factor according to KOSHIBA *et al.*
- 5) Number of pseudotridents.
- 6) Number of real tridents according to the theory of Bhabha.
- 7) Number of real tridents according to the theory of Racah.

number of the produced pairs up to $t = 1.0$:

	$x < 0.2 \mu\text{m};$	$x < 5 \mu\text{m};$
N	7	24
	$x < 10 \mu\text{m};$	$x < 200 \mu\text{m},$
N	29	34

where x is the distance of the created pairs from one of the primary electrons. This result is in fair agreement with the theoretical value, if one considers further that to the total number of pairs there is also some contribution from the 2-nd and 3-rd generations.

The number of pseudotridents obtained by means of the correction given by KOSHIBA *et al.* ⁽⁶⁾ is 6.48 as shown in Table III. Therefore, since the theoretical number of real tridents is 0.89, according to RACAH ⁽¹⁴⁾, the total number of real and apparent tridents

should be $6.48 + 0.89 = 7.37 \pm 2.7$, which agrees rather well with the value 7 found experimentally.

Our measurements cannot be considered to corroborate the theoretical value due to their low statistical weights. However, our experimental value agrees better with the theoretical one than with the experimental findings of other authors ^(6,9), in which the trident production is greater by at least a factor of 2.5 than to be expected from the theory of BHABHA.

The author would like to express his thanks to Prof. W. HEISENBERG, Dr. K. GOTTSTEIN and the members of the emulsion group for valuable discussions. He is also grateful for financial aid granted by the Max-Planck-Institut für Physik to carry out this work.

On Parity Conservation and Neutrino Mass.

ABDUS SALAM

St. John's College - Cambridge

(ricevuto il 15 Novembre 1956)

1. — YANG and LEE⁽¹⁾ have recently suggested that present experimental evidence does not exclude the possibility that parity is not conserved in β -decay. If future experiments confirm this, it may be possible to relate parity-violation in neutrino-decays to the vanishing of neutrino mass and self-mass. The argument is as follows: the free neutrino Lagrangian is invariant for the substitution $\psi_\nu \rightarrow \gamma_5 \psi_\nu$ ($\bar{\psi}_\nu \rightarrow -\bar{\psi}_\nu \gamma_5$). If it is further postulated that neutrino interactions produce no self-mass, one way to secure this is to require that the total Lagrangian also remain invariant for the same substitution ⁽²⁾ (so that $\bar{\psi}_\nu \psi_\nu \rightarrow -\bar{\psi}_\nu \psi_\nu$) while other fields (barring degeneracies which we consider later) remain unchanged. In so far as ψ_ν and $\gamma_5 \psi_\nu$ have opposite intrinsic parity, most neutrino interactions would then violate parity conservation.

2. — Some consequences of this invariance are noted:

(a) To all β -decay couplings ⁽³⁾ $[\bar{p}(x)\Omega n(x)][\bar{e}(x)\Omega \nu(x)]$ must be added (non-parity conserving) pseudo-couplings $[\bar{p}(x)\Omega n(x)][\bar{e}(x)\Omega \gamma_5 \nu(x)]$.

(b) The π -decay Lagrangian must read as $\int \bar{\mu}(x) i \gamma \partial \pi(x) (\gamma_5 \nu(x) + \nu(x)) + \text{h.c.}$ and similarly for $K_{\mu\nu}$ decay. The fact that neutrino decay interactions violate parity conservation does not depend on whether the processes are direct or take place through other intermediate fields.

(c) The magnetic moment of the (Dirac) neutrino must vanish. This is because $\bar{\nu}(x)\sigma_{\alpha\beta}\nu(x) \rightarrow -\bar{\nu}(x)\sigma_{\alpha\beta}\nu(x)$. Since $j_\mu = \bar{\nu}(x)\gamma'_\mu \nu(x) \rightarrow +\bar{\nu}(x)\gamma'_\mu \nu(x)$, the neutrino and anti-neutrino are not identical.

⁽¹⁾ C. N. YANG and T. D. LEE. The author is indebted for a pre-print.

⁽²⁾ This is not the mass-reversal transformation discussed by J. TIOMMO (*Nuovo Cimento*, **1**, 226 (1955)) which requires invariance of the total Lagrangian when a substitution $\psi \rightarrow \gamma_5 \psi$, $m \rightarrow -m$ is made for all fields. In this case neutrino self-mass δm_ν need not vanish. In fact $\delta m_\nu \propto m f(m^2)$ and thus $\delta m_\nu \bar{\psi}_\nu \psi_\nu$ does not change sign.

⁽³⁾ We write all field operators with their particle symbols: thus $\pi(x)$ stands for the π -meson field, $\nu(x)$ for the neutrino-field etc.

(d) The conventional μ -decay interactions can be grouped into 2 classes depending on whether two neutrinos or a neutrino and an anti-neutrino are emitted:

$$(A) \quad L_A = \sum_{i=1}^5 g_i [\bar{\mu}(x) \Omega e(x)] [\bar{\nu}(x) \Omega \nu(x)] + \text{h.c.}$$

$$(B) \quad L_B = \sum_{i=1}^5 g_i [\bar{\mu}(x) \Omega e^*(x)] [\bar{\nu}(x) \gamma_4 \Omega \nu(x)] + \text{h.c.}$$

Invariance for the substitution $\nu \rightarrow \gamma_5 \nu$ requires that L_A is a sum of vector and axial-vector, and L_B a sum of scalar, tensor and p.s. interactions. For L_B , the tensor interaction can in fact be excluded if we require further that L_B remain unchanged for the interchange of the two neutrino operators. The Michel parameter has, then, the following unique values, irrespective of the strengths of the couplings involved,

$$L_A: \quad \rho = \frac{3}{4},$$

$$L_B: \quad \rho = 0.$$

3. — For the π , $K_{\mu\nu}$ and neutron decay interactions it is possible to conserve parity as well as make $\delta m_\nu = 0$, by postulating a parity-degeneracy of electrons and μ -mesons. The substitution operation then reads

$$\nu \rightarrow \gamma_5 \nu, \quad \mu_1 \rightarrow \mu_2, \quad e_1 \rightarrow e_2,$$

where the pairs of particles μ_1 , μ_2 and e_1 , e_2 have opposite intrinsic parities. The fact that parity-degeneracy in electrons has never been observed may be attributed to a local preponderance of electrons of one parity (like the local preponderance of negatively charged electrons.) From the present point of view (i.e. with the demand that parity-conservation hold),

(i) a parity-degeneracy for electrons and μ -mesons makes it unnecessary to require parity-degeneracy for K-mesons. There may or may not be two types of K-mesons and $K_{2\pi}$, $K_{3\pi}$ decays are irrelevant so far as neutrino self-mass is concerned.

(ii) Although it is uneconomical to postulate, one may link a parity-degeneracy of K-mesons with the substitution operation $\nu \rightarrow \gamma_5 \nu$, $K_1 \rightarrow K_2$, $e_1 \rightarrow e_2$, $\mu_1 \rightarrow \mu_2$. This in turn must lead to two types of Λ 's and Σ 's if $\delta m_\nu = 0$. The physically observed $K_1 \pi \pi$ and $K_2 \pi \pi \pi$ decays, however, would now give a non-zero self-mass for the neutrino, in so far as they are not substitution invariant.

4. — The alternative is to give up the idea of parity-conservation. There are now two distinct ways in which parity violation occurs, (a) through the requirement that neutrino self-mass vanish; (b) in $K\pi\pi$ and $K\pi\pi\pi$ decays. These decays are unrelated to (a) and do not affect it.

This is unsatisfactory. The ideal would have been to link all parity violations with the « neutrino-gauge » requirement $\delta m_\nu = 0$. The only suggestion that the author can make is the following:

Assume from strong interactions that a parity degeneracy exists for K-mesons

(and for Λ and Σ hyperons) and that the global (strong as well as weak) Lagrangian is invariant for the substitutions $\nu \rightarrow \gamma_5 \nu$, $K_1 \rightarrow K_2$, $\Lambda_1 \rightarrow \Lambda_2$, $\Sigma_1 \rightarrow \Sigma_2$. Parity violation takes place for weak-decays in a specified manner which makes the neutrino self-mass (like the photon self-mass) vanish, while decay times for K_1 , K_2 (or Λ_1 , Λ_2 , or Σ_1 , Σ_2) particles are all the same.

* * *

The author is deeply indebted to Professor PEIERLS who first suggested investigating the consequences of the requirement $\delta m_\nu = 0$. He has profited from discussions with Dr. PURSEY.

Renormalization in Non-Relativistic Field Theories.

(Remarks about the paper by ENZ.)

W. HEITLER

Seminar für theoretische Physik, University of Zürich

(ricevuto il 22 Novembre 1956)

In a recent, very interesting paper published in this journal, ENZ ⁽¹⁾ has developed a non-relativistic quantum-electrodynamics for which he was able to find, under certain conditions, exact solutions. The word non-relativistic is meant in the sense that the charges are attached to heavy, slowly moving, bodies with kinetic energy $p^2/2m$. It was, of course, necessary to introduce an extended source, with radius a , say, in order to avoid infinities. ENZ gave certain renormalization prescriptions, which at first sight, differ widely from the well known renormalization rules of the relativistic theory, namely:

(i) a mass renormalization δm , which renormalizes the mass in $p^2/2m_0$ (m_0 = theoretical mass.)

(ii) no charge renormalization $\delta e = 0$.

(iii) Two kinds of self energies appear which ENZ states to be « independent of the mass renormalization »;

(iiia) a Coulomb self-energy E_{coul} ;

(iiib) a transverse self-energy E_{tr} , say.

E_{coul} is of the order

$$(1) \quad E_{\text{coul}} \simeq \frac{e^2}{a}$$

and

$$(2) \quad \delta m c^2 = \frac{1}{3} E_{\text{coul}} \text{ (exactly).}$$

⁽¹⁾ C. P. ENZ: *Suppl. Nuovo Cimento*, **3**, 363 (1956).

In the case $a \gg e^2/m_0 c^2$ (the only case to be considered below) E_{tr} is of the order

$$(3) \quad E_{tr} \simeq \frac{e^2}{a} \left(\frac{\hbar}{am_0 c} \right) + \text{terms} \sim e^4,$$

(formula (4.10') of Enz). The factor $\frac{1}{a}$ in (2) is familiar from classical theory. It occurs in the self-force ($\sim \dot{v}$), the classical analogue of the mass renormalization.

While reading this paper one feels, that these renormalization prescriptions, if correct, should be derivable from the relativistic theory, at least in certain cases, and it is this question which will be examined below. It is sufficient to do this within the framework of perturbation theory.

In relativistic theory only a mass renormalization exists which also accounts for the self-energies. The non-relativistic approximation to the energy of a single particle is obtained by an expansion according to $1/m_0$,

$$(4) \quad E_0 = m_0 c^2 + \frac{p^2}{2m_0},$$

terms of order $1/m_0^2$ are neglected. (m_0 must be assumed > 0 .) E_0 is the « theoretical energy » (i.e. without interaction with the field). If we renormalize the mass in (4) we obtain the additional energy

$$(5) \quad W = \delta m c^2 - \frac{p^2}{2m_0^2} \delta m.$$

In a non-relativistic theory one may forget the rest energy $m_0 c^2$ but its renormalization supplement $\delta m c^2$ will appear as a self-energy. The second term of (5) renormalizes the mass in the kinetic energy. At first sight it would appear that there must be an exact identity between self-energy and mass renormalization. However, (4) is an expansion according to $1/m_0$ and to be consistent we should expand δm likewise

$$(6) \quad \delta m = \delta m^{(0)} + \delta m^{(1)} + \dots,$$

where $\delta m^{(0)}$ is independent of m_0 , $\delta m^{(1)} \sim 1/m_0$, etc. Accordingly, the expansion of W should be broken off after terms $\sim 1/m_0^2$

$$(7) \quad W = c^2 \delta m^{(0)} + c^2 \delta m^{(1)} - \frac{p^2}{2m_0^2} \delta m^{(0)}.$$

Hence the self-energy $c^2 \delta m^{(1)}$ has no counterpart in the mass renormalization. E_{tr} (3) is of type $\delta m^{(1)}$, and it is therefore consistent that E_{tr} does not appear in δm . The identity of the self-energy and δm is confined to $\delta m^{(0)}$, i.e. the Coulomb energy (1), (2).

Here a genuine discrepancy of Enz's results with the requirement (7) appears, as δm has a factor $\frac{4}{3}$. This discrepancy we shall trace further.

Consider the relativistic expression for the self-energy of a single particle

(spin $\frac{1}{2}$) with momentum \mathbf{p} ⁽²⁾ in the e^2 -approximation:

$$(8) \quad W = \frac{\mu_0 c}{2\tau} \frac{e^2}{\hbar c} \frac{\mu_0 c}{E_0} \int_1^\infty \frac{3\varepsilon^2 - 1}{\varepsilon^3} d\varepsilon, \quad E_0 = c\sqrt{(\mu_0^2 + p^2)} \quad \mu_0 = m_0 c,$$

$$(8') \quad \varepsilon^2 = \frac{(\sqrt{\mu_0'^2 + (\mathbf{p} - \mathbf{k})^2} + k)^2 - p^2}{\mu_0'^2}.$$

A similar formula holds for spin 0, the integrand is then

$$(3\varepsilon^4 + 6\varepsilon^2 - 1)/4\varepsilon^3.$$

ε is an invariant variable, connected with the virtual momentum \mathbf{k} . In order to obtain a non-relativistic limit to W it is, of course, necessary to introduce a cut-off. If, according to the non-relativistic approximation, $k \ll \mu_0$, the cut-off k_0 , say, must be $\ll \mu_0$. Furthermore, if we do not wish to destroy the relativistic form of W the cut-off must be introduced in an invariant manner. (Invariant upper limit to ε). This means that the integral in (8) is independent of \mathbf{p} , and its value can be obtained by putting $\mathbf{p} = 0$ and then limiting k to $k \leq k_0 \equiv \hbar/a$.

Hence $a \gg \hbar/m_0 c$, and unless we assume a charge $e^2/\hbar c \gg 1$ (which would invalidate the use of perturbation theory) we also have $a \gg e^2/m_0 c^2$. (ENZ has also considered the case $a \ll e^2/m_0 c^2$). Expanding then W according to powers of $1/\mu_0$, with $k_0 \equiv \hbar/a \ll \mu_0$, we obtain

$$(9) \quad W = \frac{e^2}{\pi a} \left(1 - \frac{p^2}{2m_0^2} \right) + \frac{e^2}{2\pi a} \left(\frac{\hbar}{am_0 c} \right).$$

Up to this order, the result is the same also for spin 0. (9) agrees indeed with the required form (7). The first term $e^2/\pi a$ and the last term $(e^2/2\pi a)(\hbar/am_0 c)$ agree exactly with ENZ's results, if his cut-off function $u(t)$ is chosen to be $u(t) = 1$, for $t < 1/a$, $u(t) = 0$ for $t > 1/a$ and terms $\sim e^4$ are neglected. (The a in ENZ's paper differs from ours by a factor $2/\pi$). But the factor $\frac{4}{3}$ in the mass renormalization is missing. Actually, it would be consistent to include in (9) also the next term $\sim 1/m_0^2$, as the mass renormalization term is also of this order. This, however, depends on the spin. For spin $\frac{1}{2}$ the term is $-(e^2/2\pi a)(\hbar/am_0 c)^2$, whereas for spin 0 this term vanishes. The latter result also agrees with ENZ, whose theory applies to spin-less particles.

The origin of the factor $\frac{4}{3}$ in the mass renormalization is now easily discerned. The absence of this factor in (9) is due to the relativistic deformation of the source distribution $u(t)$, which is taken into account by our relativistic cut-off. If instead, we assume a «stiff distribution» function, as ENZ has done, we should cut-off at a fixed momentum $k_0 = \hbar/a$, independently of the value of \mathbf{p} . Carrying out the integration in k -space for any \mathbf{p} , (instead of introducing invariant variables) and expanding, as before, according to powers $1/a\mu_0$ and p^2/μ_0^2 we obtain, quite easily,

(²) W. HEITLER: *Quantum Theory of Radiation*, 3-rd ed. (Oxford, 1954), p. 297.

for the first two terms of W :

$$(10) \quad W = \frac{e^2}{2\pi\hbar c} \frac{\mu_0^2}{k_0^2} \int_0^{k_0} dk \int_{-1}^{+1} d \cos \vartheta \left(1 + \frac{(\mathbf{p}\mathbf{k})^2 c^2}{E_0^2 v^2} \right) \rightarrow \frac{e^2}{\pi a} \left(1 - \frac{4}{3} \frac{p^2}{2m_0^2} \right),$$

in agreement with ENZ. But the latter procedure is inconsistent with relativistic requirements.

In a similar manner the charge renormalization can be considered. It is given by ⁽³⁾ the relativistic expression

$$\frac{\delta |e|}{|e|} = -\frac{1}{3\pi} \frac{e^2}{\hbar c} \int_{2\mu_0}^{\infty} \frac{dz}{z^4} (z^2 + 2\mu_0^2) \sqrt{z^2 - 4\mu_0^2}, \quad z = 2\sqrt{\mu_0^2 + \mathbf{p}^2}.$$

where \mathbf{p} is the virtual momentum of the pairs. Limiting the integration likewise to $p < \hbar/a$ one obtains

$$(11) \quad \frac{\delta |e|}{|e|} = -\frac{1}{9\pi} \frac{e^2}{\hbar c} \left(\frac{\hbar}{am_0 c} \right)^3.$$

This is of order $1/m_0^3$, and should therefore be treated as zero in the non-relativistic approximation, in agreement with ENZ. Thus, (ii) and (iii) are correctly obtained as a limiting case from the relativistic theory, but not (i).

The main conclusions that can be drawn from these considerations are the following: The mass renormalization, even in the non-relativistic kinetic energy $p^2/2m$, is a relativistic effect, for which the Lorentz-deformation of the source distribution is essential. A theory using a stiff source distribution of the type developed by ENZ cannot be the limiting case of a relativistic theory, unless the sources are kept fixed altogether, or at least the mass renormalization to $p^2/2m_0$, i.e. terms of order $1/m^2$ in the energy, are also neglected. Similar considerations apply, of course, to any meson theory using an extended source.

⁽³⁾ Loc. cit., p. 323.

Pion-Nucleon Interaction and Strange Particles.

P. BUDINI and L. FONDA

Istituto di Fisica dell'Università - Trieste
Istituto Nazionale di Fisica Nucleare - Gruppo di Trieste

(ricevuto il 26 Novembre 1956)

In a previous paper ⁽¹⁾ we discussed the possibility of ascribing the non localizability of the pion-nucleon interaction to the existence of an intermediate field. In particular a simple model was presented and applied to the problem of pion-nucleon scattering obtaining results equivalent to the well known ones of the extended source theory ^(*). The model had only a mathematical character and the quanta of the internal field had no connection with reality. The purpose of the present note is to propose a more realistic theory in which the internal quanta can be identified with existing particles. At low energy pion-nucleon interactions these particles must be present only in virtual states, thus their rest mass must be higher than the one of the pion. At high energy pion-nucleon collisions they must be apt to be created in real states. We know that K-mesons can be created in such collisions, thus the simplest hypothesis is to take them as quanta of the internal field.

As it is now well known, experimental evidence concerning all phenomena connected with K-mesons indicate that these particles are isospinors ⁽²⁾, while the most reasonable value for their spin seems to be zero. So if we wish an interaction lagrangian linear in the pion field π , it has to be at least quadratic in the K field. Owing to the fact that the pion is pseudoscalar, it is necessary to postulate different parities for the two K wave functions in the interaction term. This possibility seems not to be excluded by reality, as it appears now probable that both parities, — and +, are to be connected with K-mesons ⁽³⁾. Therefore, according to these ideas, the simplest invariant interaction lagrangian between pion and K field is:

$$(1) \quad I_1^{(0)} = -g_{\pi K} [\pi K_s^* \tau K_{ps} + \pi K_{ps}^* \tau K_s]$$

where K_s and K_{ps} represent two isospinor fields of the first kind ⁽⁴⁾, scalar and pseudo-

⁽¹⁾ P. BUDINI: *Nuovo Cimento*, **3**, 1104 (1956).

^(*) It can be shown that such a model is in fact equivalent with some restrictions to a non-local theory of the Pais-Uhlenbeck type (A. PAIS and G. E. UHLENBECK: *Phys. Rev.*, **79**, 145 (1950)).

⁽²⁾ M. GELL-MANN: *Phys. Rev.*, **92**, 833 (1953).

⁽³⁾ T. D. LEE and C. N. YANG: *Phys. Rev.*, **102**, 290 (1956).

⁽⁴⁾ B. D'ESPAGNAT and J. PRENTKI: *Nuclear Physics*, **1**, 33 (1956).

scalar respectively. These fields in turn should interact directly with the nucleon field and, for the corresponding lagrangian, we choose:

$$(2) \quad L_1^{(2)} = -g_s [\bar{\psi}_N \psi_\Lambda K_s + K_s^* \bar{\psi}_\Lambda \psi_N]$$

$$(3) \quad L_1^{(3)} = -ig_{ps} [\bar{\psi}_N \gamma_5 \psi_\Lambda K_{ps} + K_{ps}^* \bar{\psi}_\Lambda \gamma_5 \psi_N],$$

where N refers to nucleons and Λ to isoscalar hyperons (*). The total interaction lagrangian, sum of these, is obviously invariant with respect to the Lorentz group, rotations and reflections in the isobaric space.

The field equations of the K and π fields, supposing equal the masses of the K-particles, are the following:

$$(4) \quad \begin{cases} (\square - m_K^2) K_s = g_s \bar{\psi}_\Lambda \psi_N + g_\pi \boldsymbol{\pi} \cdot \boldsymbol{\tau} K_{ps} \\ (\square - m_K^2) K_{ps} = ig_{ps} \bar{\psi}_\Lambda \gamma_5 \psi_N + g_\pi \boldsymbol{\pi} \boldsymbol{\tau} K_s \\ (\square - m_\pi^2) \boldsymbol{\pi} = g_\pi K_s^* \boldsymbol{\tau} K_{ps} + g_\pi K_{ps}^* \boldsymbol{\tau} K_s. \end{cases}$$

The system can be easily quantized with the usual methods.

From these equations one can eliminate the K fields obtaining an integral equation for the π field. This equation is rather complicated and non linear. If we consider only weak interacting fields, we are justified in eliminating the non linear terms from these equations, which is equivalent to neglecting the reaction of the π field on the K fields and of these on the Λ -N field. Considering besides the π -field only the nucleon field present in the limit $t \rightarrow \pm \infty$, we obtain:

$$(5) \quad (\square - m_\pi^2) \boldsymbol{\pi} = ig_\pi g_s g_{ps} \int \int d^4 x' d^4 x'' \cdot \Delta_K^c(x-x') \Delta_K^c(x''-x) \bar{\psi}_N(x'') [\gamma_5, S_\Lambda^c(x'-x'')] \boldsymbol{\tau} \psi_N(x'),$$

where Δ_K^c and S_Λ^c are the causal Green functions of the K and Λ fields. This equation can be thought of as derived from the lagrangian density:

$$(6) \quad L(x) = L^0 - ig_\pi g_s g_{ps} \int \int d^4 x' d^4 x'' F(x, x', x'') \bar{\psi}_N(x'') \gamma_5 \boldsymbol{\tau} \psi_N(x') \boldsymbol{\pi}(x),$$

with

$$F(x, x', x'') = -2M_\Lambda \Delta_K^c(x-x') \Delta_K^c(x''-x) \Delta_\Lambda^c(x'-x'').$$

Thus the linear approximation of this theory is a non-local covariant form factor theory (5).

Taking this lagrangian as starting point, the self-energy of the nucleon, the nucleon vacuum polarization as well as the other primitive divergent S-matrix

(*) Together with an isoscalar hyperon, one can take an isovector and an isospinor one (Σ , Ξ), the results, apart from numerical factors, are the same; one obtains thus a connection between the K-hyperon and pion-nucleon interactions and a dependence of the corresponding coupling constants.

(5) P. KRISTENSEN and C. MØLLER: *Dan. Mat. Fys. Medd.*, **27**, no. 7 (1952).

elements of the local theory, can be calculated with the Yang-Feldman method ⁽⁶⁾ and result finite.

This model could be tested on the calculation of known experimental data as those on pion-nucleon and K-nucleon scattering, magnetic moment and charge distribution of the nucleon, etc. It implies in particular an influence of the presence of K-mesons in these processes, and should predict the K-production in high energy pion-nucleon collisions.

In order to compare the static approximation of this theory with the pseudovector extended source theory, one has to substitute γ_5 with $\gamma_5 \gamma_\mu$ and K_{ps} with $\nabla_\mu K_{ps}$ in $L_I^{(3)}$ and to insert δ -functions for the sources of the K-fields (this of course will introduce divergences into the theory). We obtain the following equation for the π field:

$$(7) \quad (\nabla^2 - m_\pi^2) \pi_i = -g_\pi g_\pi g_{ps} \tau_i (\boldsymbol{\sigma} \cdot \nabla) \frac{1}{16\pi^2 r^2} \exp[-2m_K r]$$

which can be derived from an extended source pseudovector lagrangian with Fourier transform of the form-factor:

$$(8) \quad v(k) = \frac{2m_K}{k} \arctg \frac{k}{2m_K}.$$

This form-factor has a knee at $k \simeq 2m_K = 1.05 M_N$ which is of the order of magnitude of the cut-offs used in the pion-nucleon scattering theories ⁽⁷⁾. It is to be expected that the r^{-1} singularity of the K fields, which appears at the R.H.S. of (7), will be smoothed down in a dynamical theory, anyway the knee of the form factor (8), which will present a more rapid convergence for $k \rightarrow \infty$, will remain at $\sim 2m_K$.

Some points of this model will be further analyzed in a forthcoming paper.

* * *

We thank Prof. N. DALLAPORTA for an interesting discussion on this subject.

⁽⁶⁾ C. N. YANG and D. FELDMAN: *Phys. Rev.*, **79**, 972 (1950).

⁽⁷⁾ G. C. WICK: *Rev. Mod. Phys.*, **27**, 339 (1955).

Further Measurements on n, p Reactions at 14 MeV.

II — Sulphur, Aluminium, Iron, Copper, Nickel.

L. COLLI and U. FACCHINI

Laboratori CISE - Milano

(ricevuto il 27 Novembre 1956)

In this paper we present the energy distribution of protons emitted by the elements aluminium, sulphur, iron, copper and nickel under 14.5 MeV neutron bombardment.

The measurements reported here have been taken with the same technique and in the same conditions described in our previous papers ⁽¹⁾.

Sulphur.

The spectrum of Fig. 1 represents the energy distributions of protons obtained from sulphur bombarded with 14.5 MeV neutrons. The energy of protons is given in the laboratory system. Two sharp drops are shown rather clearly at ~ 6.5 and ~ 8.6 MeV energy. The isotope ^{32}S has the highest concentration (95.1%) in the natural mixture. ^{34}S has the concentration of 4.2%, ^{33}S 0.7% and ^{36}S 0.016%. The cross section values of the reaction n, p have been measured for ^{32}S and ^{34}S by PAUL and

CLARKE ⁽²⁾. According to their results, ^{32}S has the highest cross-section value. No measurements exist for the other two isotopes, but considering their small concentration they can probably be disregarded. Protons may be attributed to the reactions $^{32}\text{S}(n, p)^{32}\text{P}$ having a Q value of ~ 0.95 MeV. A contribution of protons from the reaction $^{32}\text{S}(n, np)^{31}\text{P}$ may be possible under 5.5 MeV.

We had recently the opportunity to have the results on energy distribution of protons emitted in (n, p) reactions with 14 MeV neutrons obtained by D. L. ALLAN ⁽³⁾. In his experiments ALLAN used nuclear plates as proton detectors and studied separately the different isotopes of aluminium, iron, copper and nickel. In order to compare Allan's and our results, they are both shown on the figures.

⁽¹⁾ L. COLLI and U. FACCHINI: *Nuovo Cimento*, **4**, 671 (1956); C. BADONI, L. COLLI and U. FACCHINI: *Nuovo Cimento* **4**, 1618 (1956).

⁽²⁾ E. B. PAUL and R. L. CLARKE: *Canad. Journ. of Phys.*, **31**, 267 (1953).

⁽³⁾ Private communication and *Proc. Phys. Soc.*

Aluminium.

A good agreement is obtained between Allan's and our results. The energy spectrum shows a peak at ~ 4.2 MeV, superimposed to an exponential descent. In this case ^{27}Al is the only stable isotope. The Q value of the reaction is -1.83 MeV. Protons from

n, np reaction are energetically possible under 6 MeV.

Iron.

In Fig. 3 are shown our results obtained with the natural isotope mixture, and Allan's results obtained separately for ^{54}Fe and ^{56}Fe isotopes. The energy

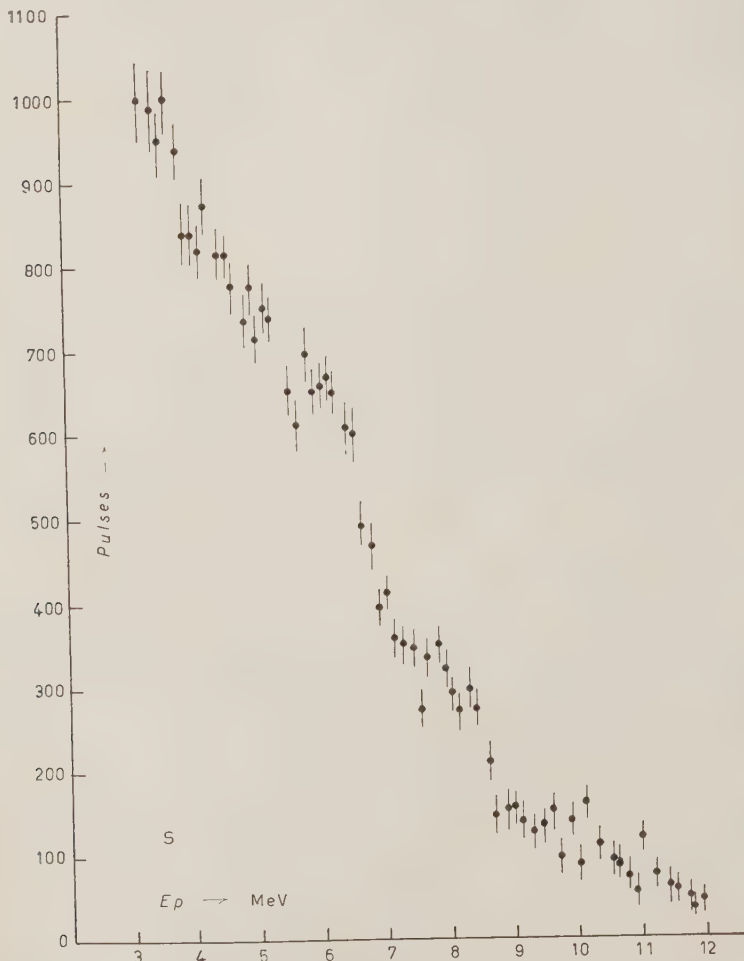


Fig. 1. - Spectrum of protons emitted by sulphur. Abscissae are proton energy in MeV. Ordinates give the number of protons in arbitrary units.

Fig. 2. - Spectrum of protons of aluminium. \bullet results of our measurements; \times Allan's results. Statistical errors, not quoted, are of the order of $\pm 10 \div 20$ percent.

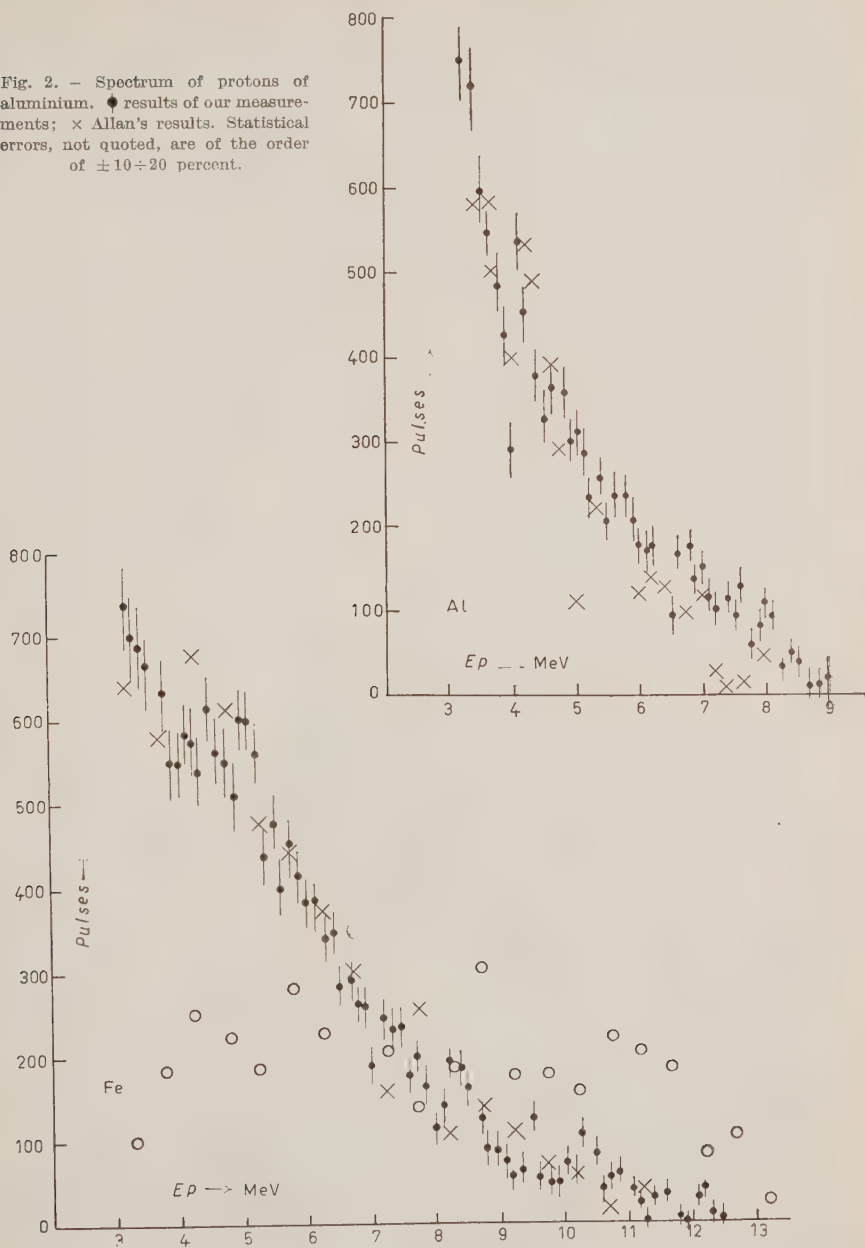


Fig. 3. - Spectrum of protons of iron. \bullet our results; \times Allan's results for ^{54}Fe ; \circ Allan's results for ^{56}Fe .

distribution of protons for ^{54}Fe is in good agreement with ours. On the contrary, ^{56}Fe results disagree notably with ours. The disagreement is quite big, because, on account of Allan's cross-section values and of the isotope concentration of ^{54}Fe and ^{56}Fe , about

tion n, p of copper may be entirely attributed to the isotope ^{63}Cu . Our results are in good agreement with Allan's as shown in Fig. 4. The spectrum shape is a smooth descent, with a small bump at 7.5 MeV, not clearly shown, more pronounced in Allan's results.

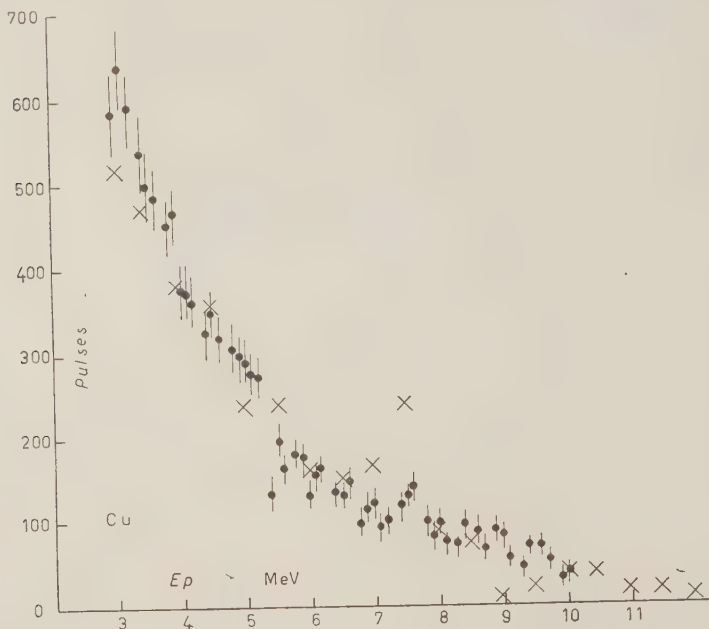


Fig. 4. — Spectrum of protons of copper. \bullet our results; \times Allan's results.

80% of protons from natural iron should be attributed to ^{56}Fe . In these considerations, the two isotopes ^{57}Fe and ^{58}Fe have been disregarded because of their small concentrations (2.2% and 0.33%), but, as their cross-section values are unknown, this may introduce some uncertainties. The reaction $^{56}\text{Fe}(n, p)^{56}\text{Mn}$ has a Q value of -2.9 MeV. The reaction $^{56}\text{Fe}(n, np)^{55}\text{Mn}$ may give protons under 4.1 MeV.

Copper.

According to Allan's results on the cross-section values, protons from reac-

Nickel.

The proton spectrum of nickel is very similar to that of copper. In Fig. 5 Allan's spectra for $^{58}\text{Ni}(n, p)^{58}\text{Co}$ and $^{60}\text{Ni}(n, p)^{60}\text{Co}$ are shown together with our results. The three spectra are in good agreement with one another. The concentrations of the two isotopes ^{58}Ni and ^{60}Ni are respectively 67.76% and 26.16%. The other isotopes have concentrations of a few percentage points. According to Allan's results on cross-section values for ^{58}Ni and ^{60}Ni , protons are mainly due to ^{58}Ni . Cross section

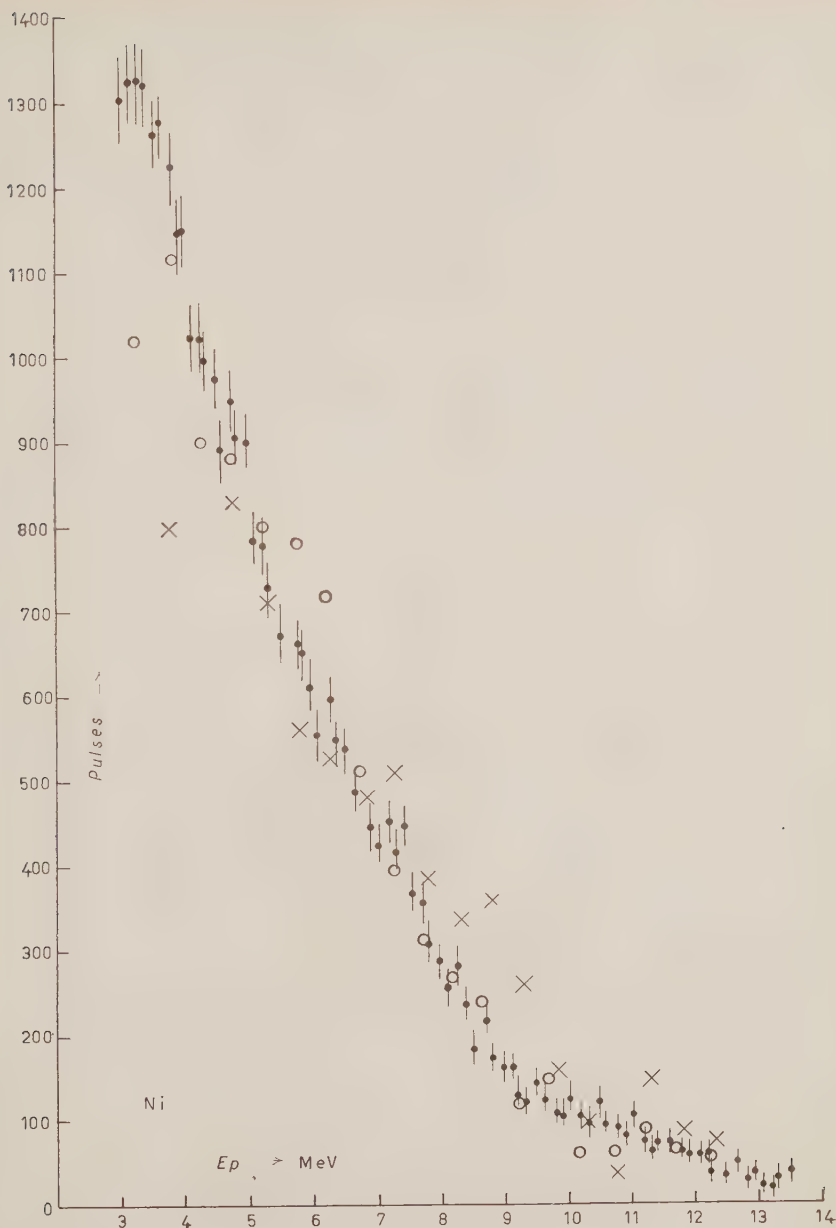


Fig. 5. — Spectrum of protons of nickel. \bullet our results; \times Allan's results for ^{60}Ni ; \circ Allan's results for ^{68}Ni .

values of the other isotopes are not known.

values cannot be used to calculate the absolute values, because the angular distribution of emitted protons is not known for the elements studied.

Table I shows the relative values of

TABLE I. - *Cross section values relative to copper.*

Element	Mg	Al	Si	S	Ca	Fe	Ni	Cu	Zn	Zr
Relative Cross Section at energy > 3 MeV	0.88	0.83	1.79	2.61	4.03	0.97	3.10	1	1.14	0.60

the cross sections of n, p reaction for the ten elements presented in this and in our former paper (¹): copper cross-section is given the value 1.

As our experimental apparatus detects only protons emitted in the forward direction, in an angle between 0 and 60 degrees, our relative cross-section

We sincerely thank Dr. D. L. ALLAN for his permission to refer to his results before publication, and the British Physical Society for the same kind permission. We also thank Mr. T. ROSSINI for his help in the experimental measurements.

Asymmetric Equilibrium Shapes in the Liquid Drop Model.

U. L. BUSINARO

Laboratori CISE - Milano

S. GALLONE

Istituto di Fisica dell'Università e Laboratori CISE - Milano

(ricevuto il 29 Novembre 1956)

In some recent papers ⁽¹⁻³⁾ methods have been given for calculating the potential energy of strongly deformed nuclei under the usual assumptions of the liquid drop model.

These methods have been applied to the calculation of the symmetric saddle shape ⁽²⁾, giving results in good accordance with the ENIAC computations of FRANKEL and METROPOLIS ⁽⁴⁾. Also these computations show ⁽¹⁻³⁾ that sufficiently elongated shapes might be unstable with respect to asymmetric deformations. We will here apply the formulae already derived in ^(1,2) to the problem of the existence and character of asymmetric equilibrium shapes.

Considering deformations of P_2 and P_3 type, only, superimposed on the basic ellipsoid, one may write for the potential energy, in a compact form:

$$(1) \quad \frac{\Delta E}{E_s} = u(y, \alpha_2) + v(y)\alpha_3^2,$$

where, comparing with formula (8) and (12) of ⁽¹⁾, one has:

$$(2) \quad u(y, \alpha_2) = [\bar{A}(y) - 1 + 2x(A(y) - 1)] + \\ + \alpha_2[\bar{B}_2(y) + 2xB_2(y)] + \alpha_2^2[\bar{U}_{22}(y) + 2xU_{22}(y)],$$

⁽¹⁾ U. L. BUSINARO and S. GALLONE: *Nuovo Cimento*, **1**, 629 (1955).

⁽²⁾ U. L. BUSINARO and S. GALLONE: *Nuovo Cimento*, **1**, 1277 (1955).

⁽³⁾ V. G. NOSSOFF: *On the Problem of Asymmetry of Nuclear Fission in Acad. Sci. of the USSR* (unpublished) and *Proceedings of the International Conference on the Peaceful Uses of Atomic Energy*, **2**, 205 (Geneva, 1955).

⁽⁴⁾ S. FRANKEL and J. K. METROPOLIS: *Phys. Rev.*, **72**, 914 (1947).

$$(3) \quad v(y) = \left(\frac{6}{7} \frac{y^2}{5 - 3y^2} \right)^2 ((\bar{C}_{11}(y) + 2xC_{11}(y)) + \frac{6}{7} \frac{2y^2}{5 - 3y^2} (\bar{C}_{13}(y) + 2xC_{13}(y)) + \bar{C}_{33}(y) + 2xC_{33}(y)).$$

The equilibrium shapes are determined by the system of equations:

$$(4) \quad \frac{\partial u}{\partial y} + \frac{\partial v}{\partial y} \alpha_3^2 = 0, \quad \frac{\partial u}{\partial \alpha_2} = 0, \quad \alpha_3 v(y) = 0.$$

This system has solutions of «symmetric» type with $\alpha_3 = 0$, which have already been studied (^{1,2}).

The «asymmetric» solutions are here considered:

$$(5) \quad \alpha_3^2 = - \left(\frac{\partial u}{\partial y} \right) / \left(\frac{\partial v}{\partial y} \right), \quad \frac{\partial u}{\partial \alpha_2} = 0, \quad v(y) = 0.$$

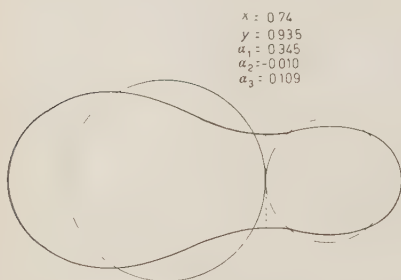


Fig. 1. — The asymmetric equilibrium shape for $x = 0.74$ is shown together with the two tangent spheres discussed in reference (⁴). The fragment mass ratio is about 1:4 for both cases.

librium was guessed for values of x smaller than x_{crit} . The actual behaviour is similar to the one exhibited by the two tangent spheres case of the FRANKEL and METROPOLIS work (⁴), where asymmetric equilibrium shapes exist for $x > x_{\text{crit}} = \sim 0.6$. In Fig. 1 a comparison is made for $x = 0.74$ of the asymmetric equilibrium shapes with the two tangent spheres case.

The energy of the asymmetric shape is greater than that of the symmetric one for the same value of x . Both energies are given in Fig. 2. PRESENT and KNIPP

These solutions are easily computed from the algebraic expressions given in (^{1,2}) of the coefficients A, B, C of formulas (2) and (3). A discussion of (4) shows that for $x < x_{\text{crit}}$ the only solution is the symmetric one, while an asymmetric equilibrium shape also exists for $x_{\text{crit}} < x < \sim 1$; x_{crit} is the value of x for which the symmetric equilibrium shape becomes unstable with respect to asymmetric deformations. In our case $x_{\text{crit}} = 0.47$.

This result is in contrast with the behaviour indicated in Fig. 2b of (¹), where, as generally believed to be plausible, the existence of symmetric shapes of equi-

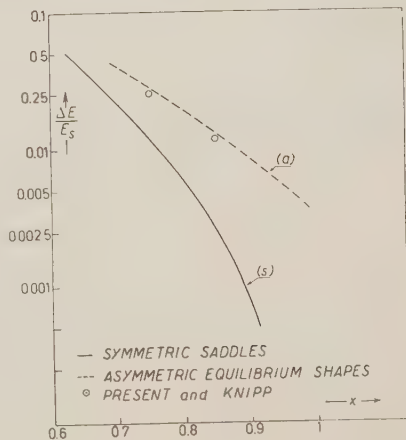


Fig. 2. — The potential energy $\Delta E/E_s$ is given as a function of x both for the symmetric (s) and asymmetric (a) shapes of equilibrium. Also the energy computed by PRESENT and KNIPP (⁶) for two particular asymmetric equilibrium shapes is shown in the figure.

too ⁽⁵⁾ found similar asymmetric shapes, whose energies are indicated in Fig. 2, using an approximate formula. It may be noticed that curve (a) corresponding to the asymmetric shape is less steep than curve (s) corresponding to the symmetric shape.

The experimental dependence of fission threshold upon Z^2/A is also less pronounced than is indicated by curve (s) of Fig. 2. However, it looks difficult to associate the energies of the asymmetric shapes of equilibrium to the actual fission thresholds because of the character of the energy surfaces in the neighborhood of the asymmetric equilibrium configurations. The situation is illustrated in Fig. 3, where two surfaces of constant energy are shown for $x = 0.74$. One of these surfaces ($\Delta E/E_s = 0.03$) has an energy equal to that of the asymmetric equilibrium shape. It appears that the connection between the regions of lower energy does not occur through a «funnel» in representative space centered on the equilibrium configuration. On the contrary, surface $\Delta E/E_s = 0.03$ has a «hump», which is rather unlikely to be climbed by the representative point of the system while going from the origin of the co-ordinate towards fission.

However, the existence of such asymmetric shapes of equilibrium for $x > x_{\text{crit}}$ may perhaps have some significance in the frame of the unified model picture of fission ⁽⁶⁾, as transition states of odd parity.

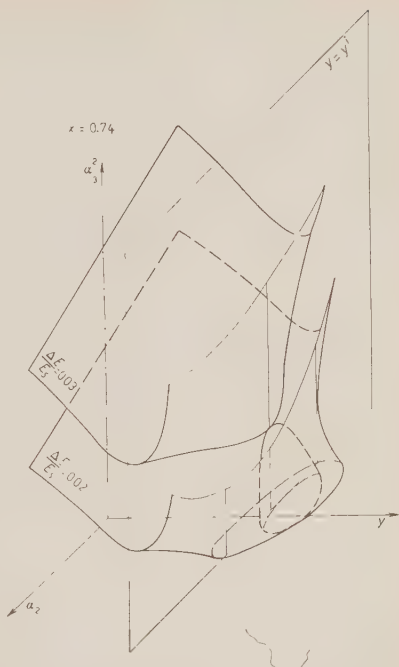


Fig. 3. - Two surfaces of constant energy are shown for $x = 0.74$. One of these surfaces ($\Delta E/E_s = 0.03$) has an energy equal to that of the asymmetric equilibrium shape. The dashed plane is the plane of «inversion», $y = y^i$.

⁽⁵⁾ R. O. L'ESSENT and J. K. KNIPP: *Phys. Rev.*, **57**, 751, 1188 (1940).

⁽⁶⁾ A. BOHR: *Proceedings of the International Conference on the Peaceful Uses of Atomic Energy*, **2**, 151 (Geneva, 1955).

On the Sign of the Real Central Part of the Neutron-Nucleus Complex Potential.

A. KIND

Istituto di Fisica dell'Università - Padova
Istituto Nazionale di Fisica Nucleare - Sezione di Padova

(Ricevuto il 5 Dicembre 1956)

Since the paper of TAYLOR on the optical model of the nucleus ⁽¹⁾ appeared in 1953, it has usually been admitted that the real central part of the complex potential which enters into the description of the neutron-nucleus interaction, is a function of the energy E of the incoming neutron, as is given by curve V_I in Fig. 1.

However, there are some arguments which make this assumption doubtful

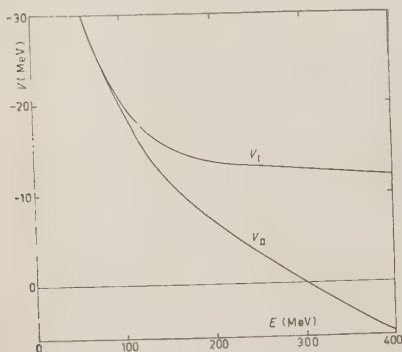


Fig. 1.

and which appear to support the idea that the correct dependence of V on E , for $E > 150$ MeV, could be markedly different from that given by curve V_I , and instead might correspond to a curve such as V_{II} in the same figure.

These arguments are the following:

1) Before the paper of TAYLOR appeared, DE JUREN ⁽²⁾ had deduced from the analysis of the neutron-nuclei total cross-sections for $E = 270$ MeV, that an accord between the optical model and the experimental data could only be reached if it was assumed that, for this energy, V is of the order of zero. This seems to have been confirmed recently by the work of FERNBACH, HECKROTTE and LEPORE ⁽³⁾ for $E = 290$ MeV.

2) TAYLOR has compared the calculated and measured cross-sections only for $E < 150$ MeV and for $E = 400$ MeV: the curves given by him in the energy

⁽²⁾ J. DE JUREN: *Phys. Rev.*, **80**, 27 (1950).

⁽³⁾ S. FERNBACH, W. HECKROTTE and J. V. LEPORE: *Phys. Rev.*, **97**, 1059 (1955).

⁽¹⁾ T. B. TAYLOR, *Phys. Rev.*, **92**, 831 (1953).

region between these two values have been obtained by joining smoothly the curves determined for $E < 150$ MeV with the values calculated for $E = 400$ MeV. From the analysis of the total cross-sections at 400 MeV it is possible to determine the value of V , but not its sign. TAYLOR has assumed that this is negative and has formed his curves accordingly. However, the possibility must be taken into account that the potential V is in fact positive. This would allow agreement between TAYLOR's results and those for the intermediate energies given in references (2) and (3), since the curve for V would then pass through 0 for $E \approx 300$ MeV, and would reach a value of the order of $-V_I$ for $E = 400$ MeV.

To analyse this possibility, it must first be pointed out that curve K_I of Fig. 2, which according to TAYLOR re-

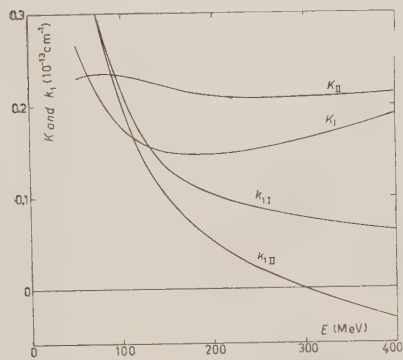


Fig. 2.

presents the energy dependence of the absorption coefficient K , is appreciably different from those values of K which one would expect starting from the known cross-sections for free nucleons. This becomes apparent from the comparison of curve K_I with curve K_{II} , which has been calculated from formula

$$(1) \quad K_{II} = \epsilon_{II}(E') \frac{3}{4\pi r_0 A} \cdot [(A - Z)\sigma_{nn}(E') + Z\sigma_{np}(E')],$$

where $E' = E - V$, $\sigma_{nn}(E') = \sigma_{pp}(E')$ and $\sigma_{np}(E')$ are the proton-proton and neutron-proton experimental total cross-sections, A and Z are respectively the numbers of nucleons and protons in the nucleus and $r_0 = 1.4 \cdot 10^{-13}$ cm. The factor $\epsilon_{II}(E')$, which takes account of the momentum distribution in the nucleus, has been determined from the calculation of KIND and PATERGNANI (4). In Fig. 3

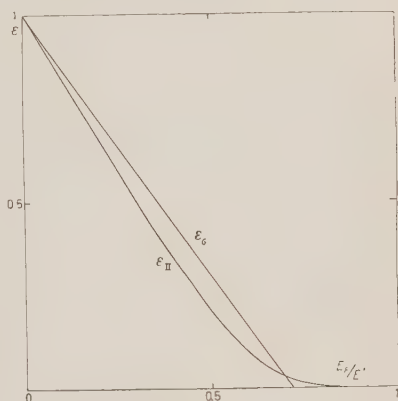


Fig. 3.

the curve ϵ_{II} is drawn together with curve ϵ_G which represents the same factor as given in the more rough approximation of GOLDBERGER (5)

$$(2) \quad \epsilon_G = 1 - \frac{7}{5} \frac{E_F}{E'}.$$

(4) A. KIND and G. PATERGNANI: *Nuovo Cimento*, **10**, 1375 (1953). English translation: CERN-T/5601 and 5602, N. Bohr Institut, Copenhagen. Subsequently the same model has also been used by E. CLEMENTEL and C. VILLI: *Nuovo Cimento*, **2**, 176 (1955) and by A. M. LANE and C. F. WANDEL: *Phys. Rev.*, **98**, 1524 (1955) for the same calculation of K , neglecting, however, the anisotropy of the neutron-proton cross-section, which has been taken into account in the calculation of KIND and PATERGNANI.

(5) M. L. GOLDBERGER: *Phys. Rev.*, **74**, 1268 (1948).

Here, E_F is the energy of the Fermi sphere.

If the optical model has to give correct values for the neutron-nuclei cross-sections using K_{II} instead of K_I , a change in V also becomes necessary.

To make a rough estimation in this sense, a new curve V_{II} for V has been determined by imposing the condition

$$(3) \quad \exp \left[-\frac{K_{II}R}{2} \right] \cos(k_{III}R) = \\ = \exp \left[-\frac{K_I R}{2} \right] \cos(k_{II}R),$$

where k_I is the change in the wave vector of the incoming neutron when it enters

the nucleus. For R the value $7 \cdot 10^{-13}$ cm has been chosen.

The curves k_{III} and V_{II} obtained in this way are given in Fig. 1 and Fig. 2 respectively. They seem to give quite interesting support to the idea of a change in the sign of V for $E \approx 300$ MeV.

A decision on this point would give a considerable insight into the problem of the nucleon-nucleon interaction, by providing an answer to the question of the sign of the scattering phase shifts in this energy region ⁽⁶⁾.

⁽⁶⁾ W. B. RIESENFELD and K. W. WATSON: *Phys. Rev.*, **102**, 1157 (1956).

LIBRI RICEVUTI E RECENSIONI

J. R. MENTZER - *Scattering and Diffraction of Radio Waves*, (Pergamon Press Ltd., London and New York, 1955), pgg. 134, \$ 4,50.

Questo libretto comprende una raccolta di metodi e risultati relativi alla diffrazione elettromagnetica, con particolare riguardo alle sezioni efficaci per il radar.

In un primo capitolo vengono trattati i metodi generali. Viene illustrato l'uso della funzione di Green e dimostrata l'unicità della soluzione per i problemi di diffrazione. Quindi vengono esposti i metodi approssimati dell'ottica geometrica, dell'ottica fisica e dei principi variazionali. Viene anche trattato il principio di Babinet nella formulazione moderna.

Si passa poi alla soluzione di problemi particolari. Prima di tutti quelli bidimensionali: cilindro circolare, cilindro ellittico, semipiano conduttore. Quindi i problemi tridimensionali: sfera, cono, cilindro finito, foro circolare, paraboloide, ellissoide.

Seguono poi alcune utili considerazioni per la misura delle sezioni efficaci per il radar.

In complesso un libro utile e aggiornato. Forse un po' troppo sintetico e, qua e là, di difficile lettura per chi non sia già abbastanza familiare con l'argomento. Si sarebbe desiderato un po' più di cautela nel trattare gli integrali im-

propri divergenti e le singolarità ai bordi degli schermi. Nel caso poi del semipiano riflettente non sarebbe stato male almeno nominare Sommerfeld.

Queste e altre pecche minori non tolgono interesse al libro, che raccoglie cose molto interessanti e di attualità.

G. TORALDO DI FRANCA

ALBERT EINSTEIN - *The Meaning of Relativity*. Fifth edition, pp. 170, in-16°, Princeton University Press, Princeton, 1955.

Per questa quinta edizione del noto volume di EINSTEIN, già apparso in italiano nel 1950 e 1953 presso Einaudi, è stata rifatta completamente l'appendice sulla teoria generalizzata della gravitazione, con le relative correzioni ed integrazioni del 1954, dandole il titolo di « Teoria relativistica del campo non simmetrico ». EINSTEIN era infatti riuscito nel frattempo, con la collaborazione dell'assistente B. KAUFMANN, a semplificare sia la forma delle sue equazioni di campo che la loro derivazione.

Dopo aver definito la « forza » di un sistema di equazioni di campo come all'incirca inversamente proporzionale al numero di dati lasciati liberi dal sistema stesso per determinare le sue possibili soluzioni, egli deduce le nuove equazioni

da un principio variazionale opportunamente scelto, in modo che il sistema di esse risulti dotato di forza massima, alla stregua degli altri sistemi in uso nella fisica, in particolare le equazioni di Maxwell per il campo elettromagnetico e quelle della relatività generale per il campo gravitazionale nello spazio vuoto.

Uno dei vantaggi di questa scelta consiste nel fatto che le equazioni così ottenute obbediscono automaticamente anche al postulato di «invarianza per trasposizione» introdotto dall'Autore in parte per ragioni formali ed in parte in omaggio all'esigenza che le cariche positive e negative entrino simmetricamente nelle leggi della fisica.

Rimane comunque affidato ad un futuro progresso dei metodi matematici, ripete per l'ultima volta lo stesso EINSTEIN, il compito di controllare se una teoria di questo tipo si presti ad inquadrare i fenomeni atomistici e quantistici senza perdere il suo carattere di teoria di campo, escludente per principio ogni genere di «singolarità».

V. SOMENZI

Process Chemistry, Vol. I; Editors F. R. BRUCE, J. M. FLETCHER, H. H. HYMAN, J. J. KATZ; Pergamon Press Ltd., London, 1956, 84 s.

Questo volume della collana *Progress in Nuclear Energy* è dedicato ai processi chimici adoperati o studiati per trattare il combustibile nucleare irradiato, con l'aggiunta dei metodi di produzione dell'uranio e del torio dai rispettivi minerali.

Il materiale è raccolto sotto forma di articoli in parte inediti, in parte relazioni di comunicazioni presentate alla Conferenza di Ginevra. Di norma ogni capitolo è aperto da una monografia a carattere generale che, pur senza essere una vera e propria rassegna, illustra numerosi problemi di dato argomento,

problemi che vengono successivamente esaminati in modo specifico dalle comunicazioni che seguono.

Dopo alcune considerazioni generali circa le difficoltà che si presentano nel trattamento chimico di sostanze intensamente radioattive, vengono esaminati i metodi di dissoluzione del combustibile nucleare irradiato. Due capitoli sono quindi dedicati alla separazione dell'uranio e del plutonio dai prodotti di fissione mediante estrazione con solvente e co-precipitazione.

Differenti metodi di attacco del combustibile irradiato sono trattati nei capitoli seguenti: i processi di volatilizzazione con formazione di fluoruri e quelli pirometallurgici per scorificazione.

Nell'ultimo capitolo viene esaminata la separazione ed il recupero di numerosi radioisotopi prodotti dalla fissione o dalla cattura neutronica e contenuti nel combustibile irradiato.

Le informazioni presentate sotto forma di tabelle e di grafici tendono a concretizzarsi, in senso industriale ed applicativo, nei numerosi diagrammi di lavorazione, alcuni schematici, altri più dettagliati fino ad indicare le quantità di sostanze presenti nelle varie fasi del processo. Per questa ragione il libro si indirizza oltre che al chimico che deve affrontare un nuovo problema, anche all'ingegnere chimico destinato all'effettiva realizzazione del processo su scala industriale.

M. MARAGHINI

A. MÜNSTER - *Statistische Thermodynamik*. Springer-Verlag, Berlin, Göttingen, Heidelberg 1956, pagine 852, D.M. 126.

Si tratta di un ottimo libro, il cui unico difetto è quello di essere troppo esteso e quindi troppo costoso. L'autore è ben conosciuto in questo campo, specialmente per i suoi lavori sulla trasfor-

mazioni di fase e sulla teoria delle fluttuazioni, ed ha improntato questo trattato ad una discussione completa degli stati di aggregazione della materia.

La prima parte, circa 300 pagine, è una trattazione generale del metodo meccanico-statistico, con una elaborazione particolare delle tecniche analitiche più moderne usate nella teoria dei liquidi. In particolare viene ampiamente usato il metodo della funzione di distribuzione molecolare, e quindi le equazioni integrali del tipo Mayer Kirkwood-Born e Green. Ancora da segnalare, sempre in questa parte generale, un capitolo sulla statistica quantistica ed un altro sulla grande funzione di ripartizione.

La seconda parte, di 170 pagine, tratta la teoria dei gas, tanto dei gas ideali con gradi interni di libertà, quanto dei gas reali fino al punto critico. Forse sono questi gli argomenti più noti, ed anche più ampiamente trattati in altri libri.

La terza parte, di circa 200 pagine, tratta la teoria dei cristalli, ed è davvero la parte più pregevole. Dopo due buoni capitoli che trattano in modo consueto il cristallo ideale, ci sono ben tre capitoli sui fenomeni cooperativi, un primo di carattere elementare (metodi di Bragg-Williams, Bethe, ecc.), un secondo di carattere teorico assai elevato (discussione del modello di Ising con il metodo delle matrici, ultimi lavori di Onsager, ecc.) ed un terzo sulle applicazioni alle soluzioni solide ed alle trasformazioni di rotazione nei solidi (FUCHS, MÜNSTER, KIKUCHI, YANG, etc.). Non conosciamo oggi altro libro in cui questi argomenti vengano trattati con tanta ampiezza; di per sé essi costituirebbero una monografia di valore.

L'ultima parte, circa 150 pagine, è dedicata ai liquidi. Forse qui l'autore è stato preso dal suo desiderio di fare troppo, e perciò ha trattato tanto i liquidi puri, che le soluzioni di non elettroliti forti e le soluzioni di micromolecole.

Riassumendo si può dire che il libro ha il massimo pregio di offrire una trattazione modernissima ed approfondita delle trasformazioni ordine-disordine, ed una trattazione quasi completa della teoria statistica degli stati di aggregazione.

G. CARERI

R. HAASE - *Thermodynamik der Mischphasen*, Springer - Verlag, Berlin - Göttingen - Heidelberg, 1956, pag. 597; D.M. 69.

L'autore ha voluto scrivere un trattato completo sulla termodinamica dei sistemi costituiti da più componenti e da più fasi. Le basi sono classiche, e si possono trovare su tutti i trattati classici di termodinamica, mentre le applicazioni riguardano sostanzialmente la chimica fisica. Ad un fisico questo libro non può dir niente di nuovo ed interessante, perchè viene omessa ogni trattazione statistica, ed ancora più, ogni descrizione dei fatti in termini molecolari. Tutto il libro ha insomma un certo sapore di vecchio e di rigidamente formale, ma di indubbia coerenza ed unità, quale può appunto provenirgli da un punto di vista solamente termodinamico.

G. CARERI

E. BODEWIG - *Matrix Calculus*, North-Holland Publishing Company, Amsterdam, 1956, pagine XI + 324.

Diamo un breve cenno del contenuto di questo volume. La parte prima riporta gli elementi di calcolo con matrici. Sono compresi dei teoremi che forniscono delle limitazioni per gli autovalori, utili in parecchi casi. La parte seconda insegna a risolvere i sistemi di equazioni lineari. La parte terza è dedicata alla inversione di matrici. La quarta tratta i problemi

ad autovalori. In queste ultime tre parti sono riportati i più svariati metodi per ottenere soluzioni approssimate. Alcuni di questi metodi sono noti ai fisici e di uso corrente: ad esempio i metodi di interazione e quelli variazionali. Altri sono stati proposti da vari autori e sono più adatti quando si disponga di particolari mezzi di calcolo, per esempio di calcolatrici elettroniche.

L'utilità di questo libro è, riteniamo, soprattutto limitata a chi debba risolvere problemi numerici con matrici e voglia suggerita la particolare procedura da seguire. In questo senso il libro è molto dettagliato e riporta anche metodi recenti interessandosi a confrontare per i vari metodi i numeri totali di operazioni richieste.

R. GATTO

PROPRIETÀ LETTERARIA RISERVATA
